ORGANOCATALYZED AND PHOTOINDUCED SYNTHETIC STRATEGIES FOR THE FORMATION OF DIVERSE C–C and C–HETEROATOM BONDS

A Thesis Submitted

In Partial Fulfillment of the Requirements

for the Degree of

Doctor of Philosophy

by

Sourav Roy

2018CYZ0013



DEPARTMENT OF CHEMISTRY

INDIAN INSTITUTE OF TECHNOLOGY ROPAR

July, 2023

Sourav Roy

Organocatalyzed and Photoinduced Synthetic Strategies for the Formation of Diverse C–C and C–Heteroatom Bonds

Copyright © 2023 by Indian Institute of Technology Ropar

Dedicated

To My

Parents

and

all loved ones

DECLARATION

I declare that this work entitled "**Organocatalyzed and Photoinduced Synthetic Strategies for the Formation of Diverse C–C and C–Heteroatom Bonds**" has not previously been accepted in substance for any degree and is not being simultaneously submitted in candidature for any other degree. This thesis is being submitted in partial fulfilment of the requirements for the degree of PhD in Chemistry. This thesis is the result of my own independent investigation, except where otherwise stated. I have acknowledged all the other sources by stating the references explicitly. I declare that any idea/data/fact/source stated in my thesis has not been fabricated/falsified/misrepresented. All the principles of academic honesty and integrity have been followed. I understand that any violation of the above will be cause for disciplinary action by the Institute and can also evoke penal action from the sources which have thus not been properly cited or from whom proper permission has not been taken when needed. I hereby give consent for my thesis, if accepted, to be available online in the Institute's Open Access repository and for inter-library loan, and for the title and abstract to be made available to outside organizations.

Sourav Roy 30/8/23

Signature

Name: **Sourav Roy**

Entry Number: 2018CYZ0013

Program: PhD

Department: Chemistry

Indian Institute of Technology Ropar

Rupnagar, Punjab 140001

Date: 04/07/2023

ACKNOWLEDGMENTS

I would like to take this opportunity for acknowledging some very special people who are integral parts of my journey this far.

At the very outset, I want to express my deepest gratitude to my supervisor **Dr. Indranil Chatterjee**, for his inspiring guidance, insightful advice, and constant encouragement throughout the present investigations. I am thankful to him for being supportive in the tough times during my Ph.D. journey and believing in me to accomplish my work. It was indeed an incredible journey all together as a Ph.D. student with the ups and downs of organic synthesis. It has been a great privilege and honor to be associated with him.

Besides my supervisor, I am thankful to my doctoral committee members **Dr. Prabal Banerjee, Dr. Avijit Goswami, and Dr. Srivatsava Naidu,** for spending their valuable time and offering useful suggestions during the half-yearly assessment of my thesis work.

It is my privilege to thank the present director of IIT Ropar, **Prof. Rajeev Ahuja**, and former director of IIT Ropar, **Prof. Sarit K. Das**, for providing world-class research infrastructures.

I acknowledge the NMR, X-ray, and HRMS facilities of IIT Ropar. I want to thank the convenor of the NMR facility **Dr. Manoj Kumar Pandey, for his cooperation**. I am grateful to **Dr. Debaprasad Mondal** and **Dr. C. M. Nagaraja** for their cooperation in recording SCX-ray data of my samples. Next, I sincerely thank HRMS facility committee members **Dr. Avijit Goswami** and **Dr. Anupam Bandyopadhyay**. I am grateful to the current head of the department **Dr. Tharamani C.N.**, former head of the department **Dr. T. J. Dhilip Kumar** and other faculty members of Chemistry Department for facilitating the use of various departmental instruments and their valuable suggestions.

My extraordinary lab-mates deserve special thanks for their friendly cooperation and invaluable helps whenever required. I cannot express in words how much fortunate I am to have talented former and current lab members **Suman da, Soumen da, Gautam, Sandeep, Naveen, Sangay, Vishali, Krishan, Hrishikesh, Biprajit, Gourav, Arijit, Surajit, Parag, Sampurna, Debkanta, Apurba, and Ariyan** for maintaining healthy environment and useful discussions in the lab which helped me in learning and understanding various aspects of research. It was great to work and spend times with all of them being full enjoyment package in the busy lab schedule. And I will always relish these memories throughout my life. I wish them great success in every aspect of their life. I am grateful to my co-authors for their contribution to my work. I also thank all the summer trainees and project students who worked on short-time projects in our lab.

It is an excellent privilege to express my sincere regards to all my teachers and lecturers, especially **Prof. Kamal Kanta Sarkar, Prof. Shubhankar Samata, Dr. Jaydeep Saha**, for their direct or indirect support and motivation to understand the organic chemistry in a better way and inspiring me to do research in this field which have guided me to reach this far.

I am thankful to my friends and brothers in IIT Ropar, **Prasoon Raj Singh, Debarshi Saha, Irshad Tally Maajid, Hemonta, Priyank, Himanshu, Manisha, Diksha, Moumita** for their heartily support throughout my PhD carrier in IIT Ropar. Special thanks to my best pal **Debarshi** and **Suman da** for stay alongside me in my difficult times and help me in many perspectives.

I am also thankful to my college and school friends, especially **Rakesh, Hansmin, Arnav, Shubhankar, Gargi, Sangita, Hena, Arpan, Biswajit, Dipvendu, Pradip**, and especially **Tanmay** for their friendship and affection throughout my educational journey.

I acknowledge the help and support provided by the technical stuff especially **Mr. Manish, Mr. Kamlesh, Mr. Nazre, Mr. Surya, Dr. Nilotpal Singha** for their timely help with HRMS and NMR data, and non-teaching staff especially, **Mr. Nagendra, Mr. Sushil, Mrs. Poonam, Mrs. Samita** of the department of Chemistry.

I am grateful to IIT Ropar for providing my doctoral fellowship.

As we went through a global pandemic (COVID-19), I have a special mention to all the health workers, professionals, and researchers fighting at the forefront and risking their lives.

Finally, I would like to express my heartfelt gratitude to my grand-parents, parents (**Ganesh Roy and Shefali Roy**), uncles, aunts, adored sister (**Tanisha Roy**), and my lovely wife (**Moumita Halder**) for their eternal blessing, unconditional love, unwavering support, and encouragement for accomplishing my dream. Any word of appreciation will fall short for them.

Sourav Roy

CERTIFICATE

It is certified that the work contained in the thesis titled "**Organocatalyzed and Photoinduced Synthetic Strategies for the Formation of Diverse C–C and C–Heteroatom Bonds**" by **Sourav Roy**" has been carried out under my/our supervision and that this work has not been submitted elsewhere for the award of any degree.

I Chatterjee, 30/08/23

Signature of the Supervisor

Dr. Indranil Chatterjee

Department of Chemistry

IIT Ropar

LAY SUMMARY

A full introduction to the designed work and pertinent literatures were provided in chapter 1. This review gave me the motivation to carry out the research programme and informed me of the difficulties and opportunities related to the planned work.

In chapter 2, an asymmetric organocatalyzed double 1,6 addition has been explored under chiral secondary amine catalysis to furnish enantioenriched chiral chromans with exclusive δ-selectivity.

Chapter 3 demonstrates a versatile reactivity of nitosoarenes with a different class of diazo compounds to deliver α-ketoesters and oxazetidine derivatives either via oxygen transfer or formal [2+2] cycloaddition reaction under light harvesting conditions without using any catalyst or transition-metal.

Carbene chemistry was once again explored in chapter 4, where by reacting both nucleophilic and electrophilic carbene precursor with *N*-sulfinylamine, a diverse range of amides and α-iminoesters were achieved using visible light as an only promoter.

In chapter 5, the *N*-terminal electrophilic character of diazo compounds and azodicarboxylates was documented in an EDA-complex guided (*sp3*)Cα–H functionalization of ethers under visible light irradiation. This technique remained equally potent over allylation and arylation reactions to construct C–C bonds.

ABSTRACT

One of the main focuses of the present thesis is to construct valuable motifs utilizing C–C and C–heteroatom bond formation in a metal-free, organocatalytic or photocatalytic fashion.

Keywords: Organocatalysis; Light-promoted; Transition-metal-free; EDA complex; Chiral Chromans; Carbenes; Wolff Rearrangement; Oxygenation; C–H Amination; Amidation.

Chapter 1: Introduction

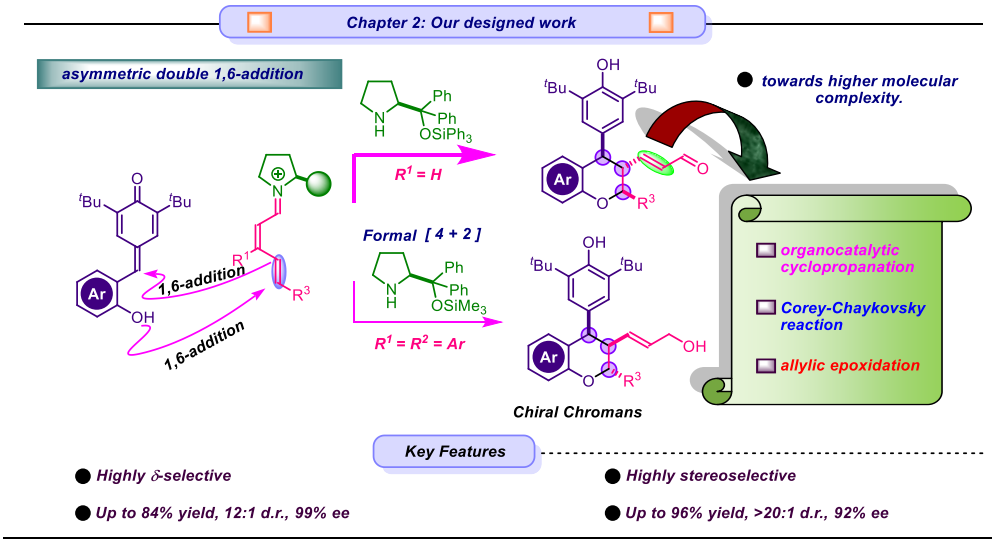
To pursue the above thought process, a detailed literature studies on organocatalysis and photocatalysis was carried out in chapter 1, introduction part.

Over the years, organocatalysis remained a main pillar in organic synthesis to achieve various enantioenriched products promptly and efficiently. Various organocatalysts have been developed over the year, amidst chiral secondary amine-based Hayashi-Jørgensen catalyst is a prime member. They can integrate orthogonal activation of carbonyls via HOMO-raising and the LUMO-lowering technique to access valuable building blocks and new scaffolds.

In recent times, visible light has gained tremendous attention from the synthetic community as a renewable source, and its robustness promotes versatile synthetic strategies. Photoexcitation of organic molecules can drive noteworthy transformation, usually inaccessible via traditional thermal routes, leading to the construction of several important cyclic and acyclic structural motifs.

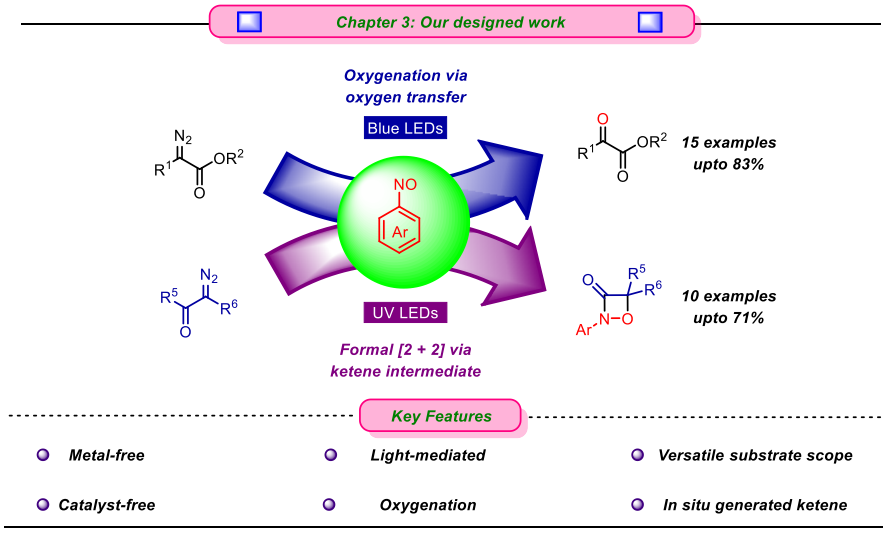
Chapter 2: Asymmetric Organocatalytic Double 1,6-Addition: Rapid Access to Chiral Chromans with Molecular Complexity

In this chapter, we have disclosed an organocatalytic asymmetric route for the synthesis of chroman derivatives with remarkable selectivity (up to >20:1 d.r., >99% *ee*) and moderate to good yield (up to 96%). The reaction starts with an oxa-Michael (1,6-addition) with exclusive δ-site selectivity took place to a vinylogous unbiased iminium-ion, followed by a vinylogous dienamine based another 1,6-addition to the *p*-QMs. This work illustrates a rare example of double 1,6-addition under Jørgensen–Hayashi catalysts. The sluggish reactivity of δ-aryl substituted unbiased 2,4-dienals was dramatically influenced by using β, δ- aryl-substituted 2,4-dienals. The α, β-unsaturated enal functionality present in the chiral chroman moiety gave an opportunity to introduce molecular complexity with high reactivity and stereoselectivity.



Chapter 3: Photoinduced Diverse Reactivity of Diazo Compounds with Nitrosoarenes

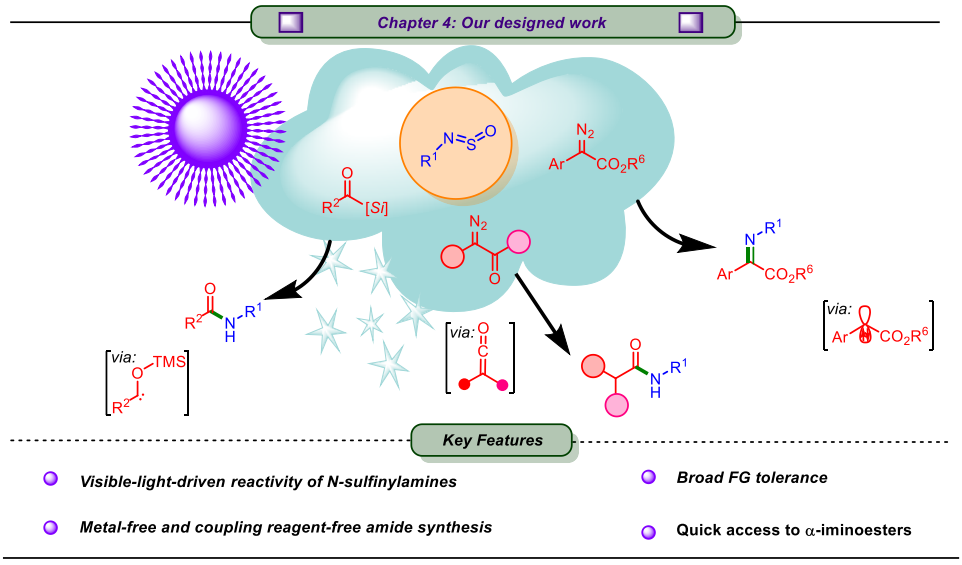
This chapter showcases the divergent role of a different class of photoexcited diazo compounds towards nitrosoarenes to deliver a wide range of α-ketoester and 1,2-oxazetidin-3-one derivatives in the absence of transition metal, catalyst using milder reaction conditions. The reaction was facilitated by the generation of carbene intermediate and *in situ* formation of ketene intermediate under light harvesting conditions. A versatile substrate scope was tolerated under the developed reaction conditions to deliver the desired product in moderate to good yield (up to 83%). Finally, the synthetic applicability of the developed protocol illustrates a one-pot synthesis of α-ketoester and transformation of cycloadduct to deliver synthetically beneficial compounds.



Chapter 4: Introducing *N*-Sulfinylamines into Visible-Light-Induced Carbene Chemistry for the Synthesis of Diverse Amides and α-Iminoesters

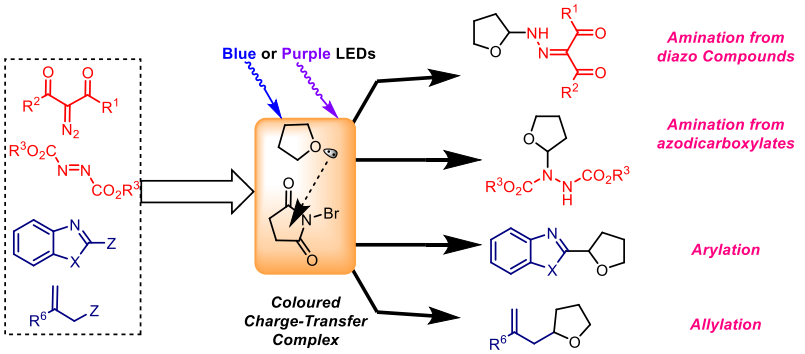
Alike previous chapter, this chapter demonstrates another exciting result on carbene chemistry, where different kinds of carbene precursors are brought into play with rarely explored reactivities of

N-sulfinylamine chemistry, through a visible-light-induced manifold to render versatile amide and α-iminoester derivatives The reaction conditions are mild, benign, easy to set up and scalable. The collective data, including UV-visible spectra, light on/off experiments, and other mechanistic studies, support the proposed mechanism. Further efforts for portraying the synthetic applicability of the developed protocol were carried out by late-stage functionalization of diazo esters derived from naturally occurring secondary alcohols and direct installation of unprotected amines and imines over diazo compounds by utilizing the sporadically explored reactivity of *N*-silylsulfinylamine.



Chapter 5: Visible-Light-Mediated (sp^3)Cα–H Functionalization of Ethers Enabled by Electron Donor-Acceptor Complex

In order to explore more reactivities of diazo compounds in this last chapter, we have developed a modular method for C(*sp*2)–H and C(*sp*3)–H functionalization to render a series of amines with various ethers. Visible lights were vital for this metal-free, oxidant-free C–N and C–C bond construction. The formation and characterization of catalytic NBS-THF electron donor-acceptor (EDA) complex were crucial, permitting direct and selective (*sp*3)Cα–H amination event. Based on the literature and our experimental evidence a radical chain mechanism was proposed. The developed methodology overcomes the major disadvantages like long reaction time and harsh reaction conditions connected with previously reported (*sp*3)Cα–H bond functionalization methods.



Key Features

- Selective (sp^3)C-H functionalization
- Metal-free
- Light-promoted
- Newly identified EDA complex-guided
- Catalytic EDA complex
- Versatile reaction

LIST OF PUBLICATIONS

Journal papers

1. Pradhan. S.; **Roy, S.**; Ghosh, S.; Chatterjee, I. Regiodivergent Aromatic Electrophilic Substitution Using Nitrosoarenes in Hexafluoroisopropanol: A Gateway for Diarylamines and *p*-Iminoquinone Synthesis. *Adv. Synth. Catal*, **2019**, *361*, 4294-4301.

2. **Roy, S.**; Pradhan. S.; Chatterjee, I. Asymmetric Organocatalytic Double 1,6-Addition: Rapid Access to Chiral Chromans with Molecular Complexity. *Org. Chem. Front.*, **2020**, *7*, 1388-1394.

3. Pradhan. S.‡; **Roy, S.**‡; Sahoo, B.; Chatterjee, I. Utilization of CO_2 Feedstock for Organic Synthesis by Visible-Light Photoredox Catalysis. *Chem. Eur. J.* **2020**, *7*, 2254-2269. ‡ Equal contributors.

4. Kumar, G., **Roy, S.**, Chatterjee. I. Tris(pentafluorophenyl)borane catalyzed C–C and C–heteroatom bond formation. *Org. Biomol. Chem*. **2021**, *19*, 1230-1267.

5. **Roy, S**., Kumar, G., Chatterjee I. Photoinduced Diverse Reactivity of Diazo Compounds with Nitrosoarenes *Org. Lett.* **2021**, *23*, 6709–6713.

6. **Roy, S.**, Chatterjee I. Visible-Light-Mediated (*sp3*)Cα–H Functionalization of Ethers Enabled by Electron Donor–Acceptor Complex *ACS Org. Inorg. Au* **2022**, *2*, 306–311.

7. **Roy, S.** ‡, Paul, H. ‡, Chatterjee I., Light-Mediated Aminocatalysis: The Dual-Catalytic Ability Enabling New Enantioselective Route *Eur. J. Org. Chem.* **2022**, *25*, e202203428. ‡ Equal contributors.

8. Ghosh, S.; Qu, Z.-W.; **Roy, S.**; Grimme, S.; Chatterjee, I. Photoredox Catalyzed Single C–F Bond Activation of Trifluoromethyl Ketones: A Solvent Controlled Divergent Access of gem-Difluoromethylene Containing Scaffolds. *Chem. Eur. J.* **2022**, *2022*, e202200446.

9. **Roy, S.** ‡; Biswas, A. ‡; Paul, H.; Ariyan S.; Chatterjee I. Introducing N-Sulfinylamines into Visible-Light-Induced Carbene Chemistry for the Synthesis of Diverse Amides and α-Iminoesters. ‡ Equal contributors. *(Manuscript Submitted for Publication)*

10. **Roy, S.**; Krishnapriya, A. U., Chakraborty, A.; Kuniyil, R.; Chatterjee, I. Exploiting *N*-Centered Umpolung Reactivity of α-Iminomalonates for the Synthesis of a New Class of *N*-Sulfenylimines and Sulfonamides. *(Manuscript Submitted for Publication)*.

TABLE OF CONTENTS

Declaration iv

Acknowledgement v

Certificate vii

Lay Summary viii

Abstract ix

List of Publications xiii

List of Figures xvi

List of Schemes xvi

List of Tables xix

Notations and Abbreviations xxi

Chapter 1: Introduction 23

1.1. Introduction 24

1.1.1 Organocatalysis in the Domain of Constructing Several Complex Molecular Architectures 24

1.1.2. Photocatalysis as an Important Gadget for Synthesizing Valuable Cyclic and Acyclic Structural Motifs 31

1.2 Objectives 37

1.3 Motivation and Scope 37

1.3.1 Organocatalytic Vinylogous Reactivity 37

1.3.2. Carbenes as a Key Intermediate in Visible Light Induced Transformations 41

1.3.3. Generation of Siloxycarbenes from Acylsilanes and Its Reactivity Under Visible-light-driven Conditions. 45

1.3.4. Employment of Catalytic Donors or Acceptors in Light-mediated Electron Donor−Acceptor Complex 48

1.4. Summary 50

Chapter 2: Asymmetric Organocatalytic Double 1,6-Addition: Rapid Access to Chiral Chromans with Molecular Complexity **56**

2. Abstract 57

2.1. Introduction 57

2.2. Result and Discussion 62

2.2.1 Optimization of the Reaction Condition 62

2.2.2 Substrate Scope Evaluation for Chiral Chromans 65

2.2.4 Proposed Mechanism 69

2.2.5 Synthetic transformations of the cascade product. 71

2.3 Conclusion 71

2.4. Experimental Section 72

2.5. References 99

2.6. NMR Spectra 105

2.7. HPLC Traces 136

Chapter 3: Photoinduced Diverse Reactivity of Diazo Compounds with Nitrosoarenes **155**

3: Abstract 156

3.1: Introduction 156

3.2. Result and Discussion 160

3.2.1 Optimization of the Reaction Condition for α-ketoesters 160

3.2.2. Substrate Scope Evaluation for α-ketoesters 163

3.2.3. Optimization of the Reaction Condition for [2+2] Cycloaddition Reaction 164

3.2.4. Substrate Scope Evaluation for oxazetidine derivatives 165

3.2.5. Control Experiments for the Oxygen Transfer Process 167

3.2.6. UV-Visible Spectra for diazo compounds 167

3.2.7. Mechanistic Proposal for oxygen transfer process and formal [2+2] cycloaddition reaction 168

3.2.8. Characterization of Reaction Intermediates 169

3.2.9. Synthetic Applications 172

3.3 Conclusion 173

3.4. Experimental Section 174

3.5. References 197

3.6. NMR Spectra 201

Chapter 4: Introducing *N*-Sulfinylamines into Visible-Light-Induced Carbene Chemistry for the Synthesis of Diverse Amides and α-Iminoesters 231

4. Abstract 232

4.1: Introduction 232

4.2. Result and Discussion 237

4.2.1 Optimization of the Reaction Condition for Amide 5 237

4.2.2 Substrate Scope Evaluation for Amide 5 239

4.2.3 Optimization of the Reaction Condition for Amide 6 240

4.2.4. Substrate Scope Evaluation for Amide 6 242

4.2.5. Optimization of the Reaction Condition for amide 7 242

4.2.6. Substrate Scope Evaluation for Amides 7 243

4.2.7. Optimization of the Reaction Condition for α-iminoester 9 244

4.2.8. Substrate Scope Evaluation for α-iminoesters 9 246

4.2.9. Mechanistic Studies: Experimental 246

4.2.10. Proposed Mechanistic Pathway 249

4.2.11. Synthetic Applications 253

4.3 Conclusion 254

4.4. Experimental Section 255

4.5. References 295

4.6. NMR Spectra 302

Chapter 5: Visible-Light-Mediated (*sp3*)C*α*–H Functionalization of Ethers Enabled by Electron Donor-Acceptor Complex 353

5: Abstract 354

5.1. Introduction 354

5.2. Result and Discussion 359

5.2.1 Optimization of the Reaction Condition for Amination from Diazo Compounds. 359

5.2.2 Substrate Scope Evaluation for Amination from Diazo Compounds. 361

5.2.3. Optimization of the Reaction Condition for Amination from Azodicarboxylates. 363

5.2.4. Substrate Scope Evaluation for Amination from Azodicarboxylates. 363

5.2.5. Synthetic Application: Arylation and Allylation reactions. 364

5.2.7. Substrate Scope Evaluation for Arylation and Allylation Reaction**.** 365

5.2.8. Mechanistic Studies: Experimental 366

5.2.9. Determination of Quantum Yield 370

5.2.10. Mechanistic Proposal for the Developed Protocol 378

5.3 Conclusion 380

5.4. Experimental Section 382

5.5. References 406

5.6. NMR Spectra 411

Chapter 6: Conclusion **442**

Curriculum Vitae (CV) of the Author **446**

LIST OF FIGURES

S. No.	Figure Caption	Page No.
1.3.2.1	Electronic Structure of Bent (sp^2) Singlet and Triplet Carbene.	41
1.3.3.1	Orbital Diagram for Siloxy Carbenes	46
3.2.6.1	Chapter 3: UV-Visible absorption spectra of compound 1a, 4a, and 4h	167
4.2.9.1	Chapter 4: UV-visible Spectra for different reaction partners.	246
4.2.9.2	Chapter4: Light On/Off Experiment.	247
4.2.10.1	HRMS data for intermediate triphenyl-1,2-thiazetidin-3-one 1-oxide (IXa)	250
4.2.10.2	HRMS data for intermediate ethyl-3-oxo-2-phenyl-4-(p-tolyl)-1,2-thiazetidine-4-carboxylate 1-oxide (IXb)	250
4.2.10.3	GC-MS data for methyl C,N-diphenylglycinate 1-oxide (XVa).	252
5.2.8.1	HRMS Data for TEMPO-adduct.	367
5.2.8.2	UV-Visible absorption spectra for NBS in CH3CN and THF.	368
5.2.8.3	UV-Visible absorption spectra for compound 2a and DIAD.	369
5.2.8.4	UV-Visible absorption spectra for compound 6a and 7a.	369

LIST OF SCHEMES

S. No.	Caption	Page No.
1.1.1.1	First Asymmetric Example Using an Organocatalyst.	24
1.1.1.2	Benzoin Condensation Using Chiral Carbenes.	24
1.1.1.3	First Use of Proline as an organocatalyst.	25
1.1.1.4	Development of Organocatalysis.	26
1.1.1.5	Classification of Organocatalyts.	26
1.1.1.6	Examples for Commonly Used Organocatalyst.	27
1.1.1.7	Activation Mode of Substrates by Primary and Secondary Amine Catalyst.	28
1.1.1.8	Activation Mode of Substrates by NHC Catalyst.	29
1.1.1.9	Activation Mode of Substrates by (Thio)urea Catalyst.	29
1.1.1.10	Activation Mode of Chiral Phosphoric Acid Catalyst.	30
1.1.2.1	General Representation of Photoinduced Transformations.	32
1.1.2.2	General Catalytic Cycle and Activation Modes of Photoredox Catalysis.	32
1.1.2.3	Basic Working Principle for EDA Chemistry.	34
1.1.2.4	Example for Commonly Used Donor and Acceptor Molecules.	35
1.1.2.5	General Representation of Photoinduced Transformations.	35
1.3.1.1:	Vinylogous Reactivity.	37
1.3.1.2	First organocatalytic asymmetric 1,6-addition	38
1.3.1.3	1,6 Addition Toward Various π-Conjugated Systems.	39
1.3.1.4	Amine Catalyzed Vinylogous Reactivity of Enals.	40
1.3.2.1	Structure of Singlet and Triplet Carbenes.	40
1.3.2.2	Different Class of Diazo Compounds with Light Absorption Properties.	42
1.3.2.3	Reactivity of Carbenes Upon Photolysis.	43

1.3.2.4	Possible Pathways for Carbene Generation Under Photolysis.	44
1.3.3.1	Formation of Siloxycarbenes Under Photochemical/Thermal Conditions.	45
1.3.3.2	Different Reactivities of Siloxycarbenes.	47
1.3.4.1	General Mechanism for Catalytic EDA-Guided Transformation.	48
1.3.4.2	Selected Examples for Catalytic EDA-Complex	48
2.1.1	Chiral Chromans Containing Bio-active Molecules	56
2.1.2	Fan's 1,6-Conjugate Addition to *para*-Quinone Methides.	57
2.1.3	Jørgensen's strategy for the addition of enamine-activated aldehydes to *p*-quinone methides.	57
2.1.4	Ender's Asymmetric Synthesis of Chromans Bearing Oxindole Scaffolds.	58
2.1.5	Jørgensen's 1,6 addition of Olefinic Lactones with 2,4-Dienals.	58
2.1.6	Jørgensen's 1,6-Friedel–Crafts/1,4-*oxa*-Michael Cascade Strategy.	59
2.1.7	Melchiorre's Strategy for the Synthesis of Tetrahydrofuran Spirooxindole Derivatives via Selective 1,6 Addition.	59
2.1.8	Melchiorre's Triple Cascade Strategy Forging Six Stereocenter Containing Spiro-Oxindolic Cyclohexanes the via Selective 1,6 Addition.	60
2.1.9	Challenges Associated with Double 1,6 Addition.	60
2.1.10	Chapter 2: Our Proposed Working Hypothesis.	59
2.1.11	Chapter-2 Substrate Scope of Chiral Chromans by Varing *para*-Quinone Methides.	61
2.1.12	Chapter-2 Substrate Scope of Chiral Chromans by Varing 2,4-dienals.	66
2.1.13	Asymmetric double 1,6-addition of β, δ-aryl substituted 2,4-dienals.	68
2.1.14	Chapter 2: Plausible Mechanism and Transition state-1.	69
2.1.15	Chapter 2: Plausible Mechanism and Transition state-2.	69
2.1.16	Chapter 2: Synthetic Applications.	70
3.1.1:	Versatile Reactivity of Diazo Compounds.	156
3.1.2	Chang's Copper-Catalyzed Oxygen Atom Transfer Using Diazo Compounds	157
3.1.3	3.1.3: Doyle's Hydroarylation of Olefins	157
3.1.4	Stoltz's Oxidation of Electron-Rich Diazo Compounds to Ketones	157
3.1.5	3.1.5: Fu's Enantioselective [2+2] Cycloadditions of Ketenes and Nitrosoarene.	158
3.1.6	Studer's Enantioselective [2+2] Cycloadditions of Ketenes and Nitrosoarene.	158
3.1.7	Ye's NHC catalyzed [2+2] Cycloadditions of Ketenes and Nitrosoarenes.	159
3.1.8	Chapter 3: Our Proposed Working Hypothesis	159
3.2.2.1	Substrate Scope for α-ketoesters.	163
3.2.4.1	Substrate Scope for oxazetidine derivatives.	165
3.2.5.1	Control Experiments for the Oxygen Transfer Process.	166
3.2.7.1	Chapter-3 Mechanistic Proposal for Both Oxygen Transfer and [2+2] Cycloaddition reaction.	168
3.2.9.1	Chapter-3: Synthetic Applications.	172
4.1.1	Traditional Reactivity of N-sulfinylamine Compounds.	231
4.1.2	Bolm's Reactivity of Aryldiazonium Salts with Trityl Substituted N-sulfinylamine.	232
4.1.3	Willis's One-Pot Synthesis of Sulfoximines and Sulfonimidamides Using N-sulfinylamines Compounds.	232
4.1.4.	Willis's One-Pot Three-Component Sulfonimidamides Using N-sulfinylamines Compounds.	233

4.1.5	Tamber's Catalytic Oxidation of Internal Alkenes Using N-Sulfinylbenzenesulfonamide.	233
4.1.6	Wertz's [3+2] and [4+2] Cycloaddition Using N-Sulfinylanilines, Cyclopropane and Cyclobutates.	233
4.1.7	Li's introduction of Photoredox Chemistry into N-sulfinylamine Compounds.	234
4.1.8	Reactivity of Siloxycarbenes Under Visible Light.	235
4.1.9	Amide Functionality in Different Valuable Motifs.	235
4.1.10	Chapter 4: Our Proposed Working Hypothesis	236
4.2.2.1	Substrate Scope Evaluation for Amide 5.	239
4.2.4.1	Substrate Scope Evaluation for Amide 6.	241
4.2.6.1	Substrate Scope Evaluation for Amide 7.	243
4.2.8.1	Substrate Scope Evaluation for α-iminoester 9.	245
4.2.9.1	Chapter 4: Dark Experiments.	247
4.2.9.2	Radical Trapping Experiments.	248
4.2.9.3	Detection of Singlet/Triplet Experiments.	248
4.2.10.1	Mechanism for Amide Formation from Acylsilanes 2.	249
4.2.10.2	Mechanism for Amide Formation from Diazo Compounds 3 or 4.	249
4.2.10.3	Mechanism for α-Iminoester Formation from Diazo Compounds 8.	251
4.2.10.4	Chapter 4: Synthetic Applications.	252
4.2.11.1	Mechanism for Amine 10 Formation.	253
4.2.12.1	Mechanism for Imine 11 Formation.	253
5.1.1	Hemiaminal Ethers Present in Different Bio-active Molecules.	353
5.1.2	Nikolaev's Photochemical Reaction of Diazoketones.	354
5.1.3	Yu's Diversified Synthesis of Functionalized N-Alkyl Hydrazones.	354
5.1.4	Lu's α-C(sp3)–H amination of ethereal compounds.	355
5.1.5	Lu's Radical Hydroamination of Olefins.	355
5.1.6	XU's Protocol to Construct C(sp2)–N bonds via dual Ni/photoredox-catalysis.	356
5.1.7	Chudasama's α-C(sp3)–H Amination of Ethereal Compounds.	356
5.1.8	Kokotos's Phenylglyoxylic acid Catalyzed C–H Functionalization of Heterocycles.	357
5.1.9	Laulhé's Visible-light-promoted Selective C(sp3)–H	357
5.1.10	Chapter 5: Our Hypothesis.	358
5.2.2.1	Substrate scope for amination from diazo compounds.	361
5.2.4.1	Substrate scope for amination from azodicarboxylates	363
5.2.7.1	Substrate scope for amination from azodicarboxylates	365
5.2.8.1	Chapter 5: Control Experiments 1.	366
5.2.8.2	Chapter 5: Control Experiments 2 and 3.	367
5.2.10.1	Chapter 5: Plausible Mechanism.	378

LIST OF TABLES

S. No.	Table Caption	Page No.
2.2.1.	Chapter 2: Table 1: Screening of Various Additives.	61
2.2.2.	Chapter 2: Table 2: Screening of Various Solvents.	62
2.2.3.	Chapter 2: Table 3: Miscellaneous Optimization-1.	63
2.2.4.	Chapter 2: Table 4. Miscellaneous Optimization-2	66
3.2.1.1.	Chapter 3: Table 1. Optimization Study: Miscellaneous Optimization	160
3.2.1.2.	Chapter 3: Table 2. Optimization Study: Screening of Solvents	160
3.2.1.3.	Chapter 3: Table 3. Optimization Study: Screening of Different Light Sources	161
3.2.1.4.	Chapter 3: Table 4. Optimization Study: Screening of	162

	Nitrosoarenes	
3.2.1.5.	Chapter 3: Table 5. Optimization Study: Miscellaneous Optimization 2	164
4.2.1.1.	Chapter 4: Table 1: Miscellaneous Optimization-1	236
4.2.1.2.	Chapter 4: Table 2: Screening of Different Light Sources-1	237
4.2.1.3.	Chapter 4: Table 3: Screening of Different Solvents-1	237
4.2.3.1.	Chapter 4: Table 5: Screening of Different Light Source-2	239
4.2.3.2.	Chapter 4: Table 6: Miscellaneous Optimization-2	240
4.2.5.1.	Chapter 4: Table 7: Screening of Different Light Source-3	241
4.2.5.2.	Chapter 4: Table 8: Miscellaneous Optimization-3	241
4.2.7.1.	Chapter 4: Table 9: Miscellaneous Optimization-4	243
4.2.7.2.	Chapter 4: Table 10: Screening of Different Light Source-4	244
5.2.1.1.	Chapter 5: Table 1: Screening of Radical Initiator	358
5.2.1.2.	Chapter 5: Table 2: Miscellaneous Optimization	358
5.2.1.3.	Chapte 5: Table 3: Screening of Different Light Source 1	360
5.2.3.1.	Chapter 5: Table 4: Screening of Different Light Source 2	362
5.2.6.1.	Chapter 5: Table 5: Screening of Different Light Source 3	363
5.2.6.2.	Chapter 5: Table 6: Screening of Different Light Source 4	364

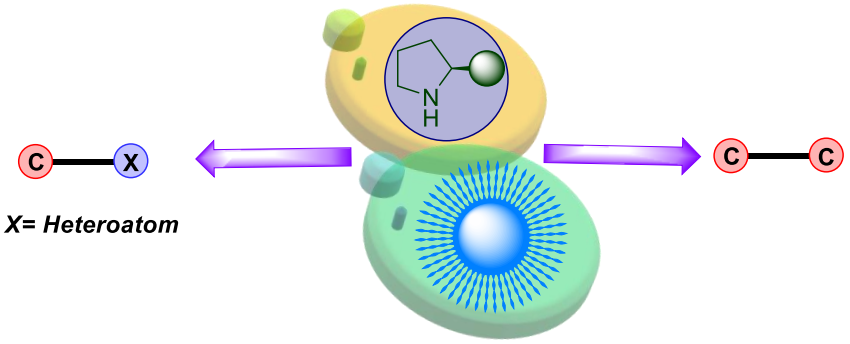
NOTATIONS AND ABBREVIATIONS

Ac	acetyl
ACN/MeCN	acetonitrile
aq	aqueous
atm	atmospheric
BINOL	1,1′-binaphthalene-2,2′-diol
Bn	benzyl
Boc	*tert*-butyloxycarbonyl
brs	broad singlet
^{n}Bu	butyl
^{t}Bu	*tert*-butyl
calcd	calculated
CPA	chiral phosphoric acid
Cy	cyclohexyl
d	doublet
DABCO	1,4-diazabicyclo[2.2.2]octane
DBU	1,8-diazabicyclo[5.4.0]undec-7-ene
DCE	1,2-dichloroethane
DCM	dichloromethane
dd	doublet of a doublet
DKR	dynamic kinetic resolution
DMAP	4-dimethylaminopyridine
DME	1,2-dimethoxyethane
DMF	*N,N'*-dimethyl formamide
DMSO	dimethyl sulfoxide
dq	doublet of a quartet
dr	diastereomeric ratio
dt	doublet of a triplet
ee	enantiomeric excess
equiv	equivalents
ESI	electron spray ionization
FT-IR	Fourier-transform infrared spectroscopy
Gem	geminal
h	hour(s)
HFIP	1,1,1,3,3,3-hexafluoroisopropanol
HPLC	high-performance liquid chromatography
HRMS	high-resolution mass spectrum
Hz	Hertz
IBX	2-iodoxybenzoic acid

J	coupling constant
LDA	lithium diisopropylamide
m	multiplet
mg	milligram(s)
MHz	megahertz
min	minute(s)
mL	milliliter(s)
mmol	millimole(s)
M.P	melting point
MS	molecular sieves
m/z	mass/charge
NMF	N-methylformamide
NMR	Nuclear Magnetic Resonance
ppm	parts per million
^{n}Pr	*n*-propyl
^{i}Pr	isopropyl
p-TSA	*para*-toluenesulfonic acid
q	quartet
rt	room temperature
s	singlet
sept	septet
t	triplet
td	triplet of a doublet
tert	tertiary
TFE	2,2,2-trifluoroethanol
THF	tetrahydrofuran
TMS	trimethylsilyl
TLC	thin layer chromatography

Chapter 1

Introduction



1. Abstract

Organocatalysis has emerged during the past few decades as a powerful method for quickly building various complex molecular architectures, frequently through inducing chirality. On the other hand, chemists have incorporated visible light into the synthetic organic chemistry domain in an effort to discover a viable modern synthesis method. Additionally, this chemistry has a solid track record in academic labs and industrial settings to trigger numerous transformations.

1.1. Introduction

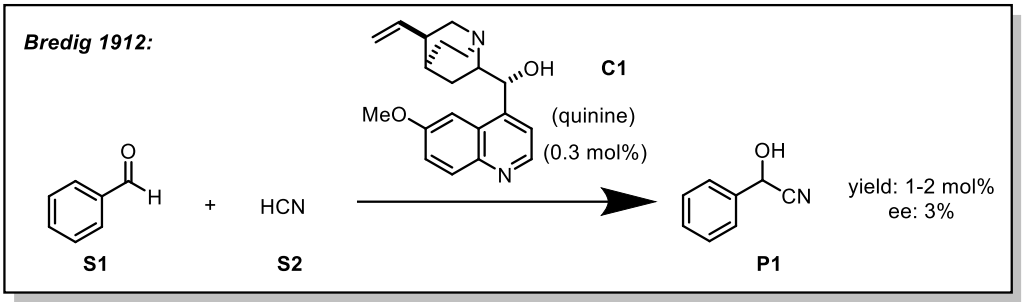
1.1.1 Organocatalysis in the Domain of Constructing Several Complex Molecular Architectures

Organocatalysis: According to David W. C. MacMillan organocatalysis can be termed as-"*The use of organic molecules with low molecular weight as catalysts in organic reactions*."[1] Similarly Benjamin List portrayed organocatalysis as-"*The catalysis with small organic molecules, where an inorganic element is not part of the active principle, has become a highly dynamic area in chemical research.*"[2]

In organocatalysis, small organic molecules are used as catalysts, often derived from natural products, has been well established as a key promoter and attractive tool to synthesize enantiomerically enriched molecules. This process is generally straightforward, non-toxic, and affordable, and in most cases, it does not require any fancy reaction conditions.

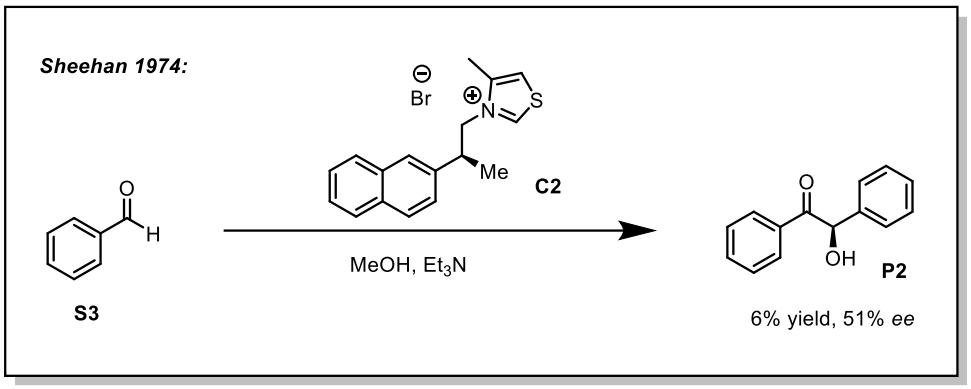
History of Organocatalysis: The historical background of organocatalysis started in 1860 when Justus von Liebig discovered that an aqueous solution of acetaldehyde was able to catalyze the hydrolysis of dicyan into oxamide.[3] To explain this phenomenon later in 1929, Langenbeck used the German term "*Organische Katalysatoren*", which reveals the actual role of acetaldehyde in Liebig's dicyan hydrolysis.[4] In 1896, Knoevenagel disclosed a secondary amine-catalyzed condensation reaction between acetoacetate and benzaldehyde via in situ iminium ion generation.[5]

A few years later, in 1912, asymmetric organocatalysis was introduced by Bredig when naturally occurring Cinchona alkaloids **C1** were able to catalyze HCN **S2** addition to benzaldehyde **S1** with traces amount of chirality induction (<10%) (Scheme 1.1.1.1). Prelog then carried out a detailed investigation in 1950s.[6]



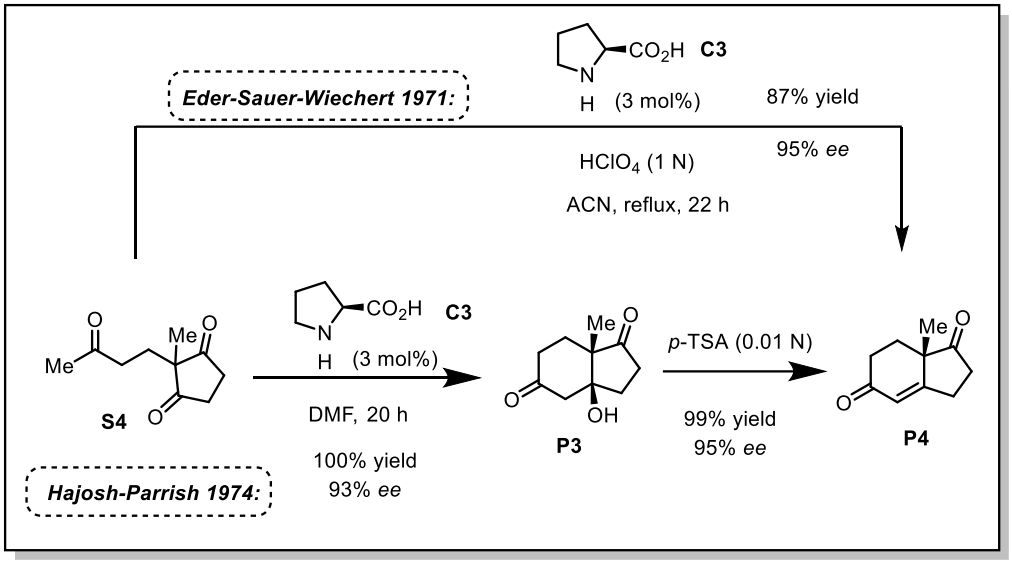
Scheme 1.1.1.1: First Asymmetric Example Using an Organocatalyst.

After that, Pracejus reported the first highly enantioselective reaction by reacting methanol with methyl phenyl ketene in the presence of *O*-acetylquinine. Following this, in 1974, Sheehan carried out a benzoin condensation reaction by using chiral carbene **C2** as catalysts, furnishing the product **P2** with moderate enantioselectivity (Scheme 1.1.1.2).[7]



Scheme 1.1.1.2: Benzoin Condensation Using Chiral Carbenes.

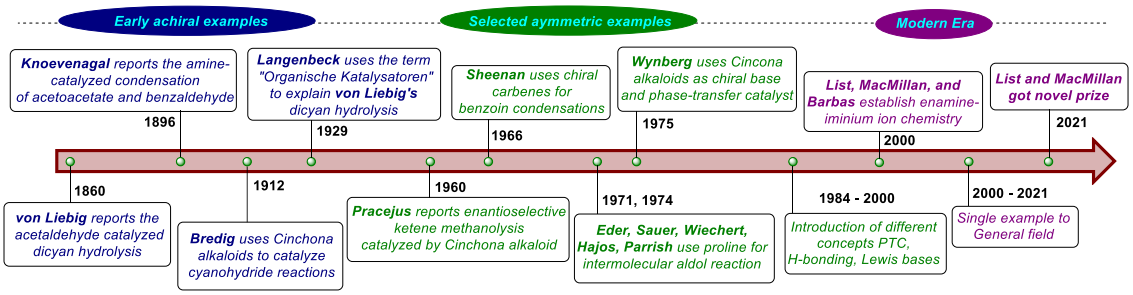
Modern-day asymmetric organocatalysis majorly relies on two milestones in the early 1970s achieved by Eder, Sauer, and Wiechert at Schering[8] and Hajos and Parrish at Hoffmann-La Roche[9] independently published two works on intramolecular aldol cyclization en route to advanced steroid precursors **P4**, using naturally occurring proline **C3** as a catalyst (Scheme 1.1.1.3).



Scheme 1.1.1.3: First Use of Proline as an organocatalyst.

Thereafter several mechanistically different strategies came across in 1970's and 1980's.[10,11] Some prominent examples were then reported in 1990's e. g. Jacobsen's chiral thiourea-catalyzed Strecker reaction,[12] Miller's small peptides catalysis,[13] Fu's use of chiral DMAP derivatives[14] Shi's and Yang's chiral ketone-based oxidation catalysts,[15] Denmark's introduction of chiral phosphoramides,[16] and Maruoka's utilization of quaternary ammonium salt as a catalyst.[17]

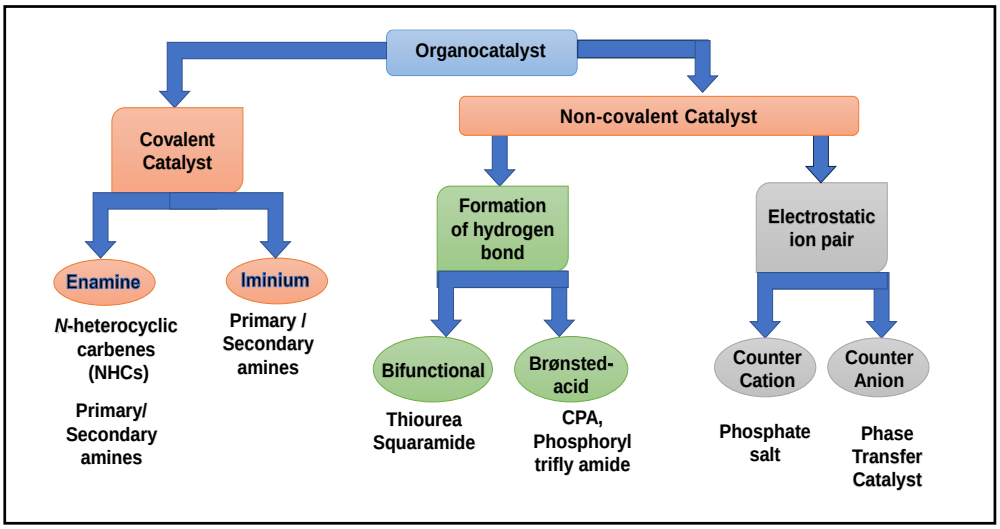
The above-mentioned reports demonstrated the catalytic prowess of organocatalysts to trigger valuable asymmetric transformations. However, they were restricted to their individual fields. Later, in the early 20th century, a new era of organocatalysis began when MacMillan, List, Jørgensen, and Barbas applied simple proline and its derivatives as secondary amine catalysts in various asymmetric reactions via its enamine and iminium-ion activation.[18] Thus, generalization of this field was established. After that, several research groups worked in this direction, and a sudden boom was observed with a huge number of publications.[19] As a result, in 2021, List and MacMillan were awarded the "Novel Prize" for their significant contribution and "the development of asymmetric organocatalysis" (Scheme 1.1.1.4). To date, this benign field is still growing alone or sometimes by merging with photochemistry, electro-organic chemistry, or metal catalysis in the quest for novel methodologies.[20]



Scheme 1.1.1.4: Development of Organocatalysis.

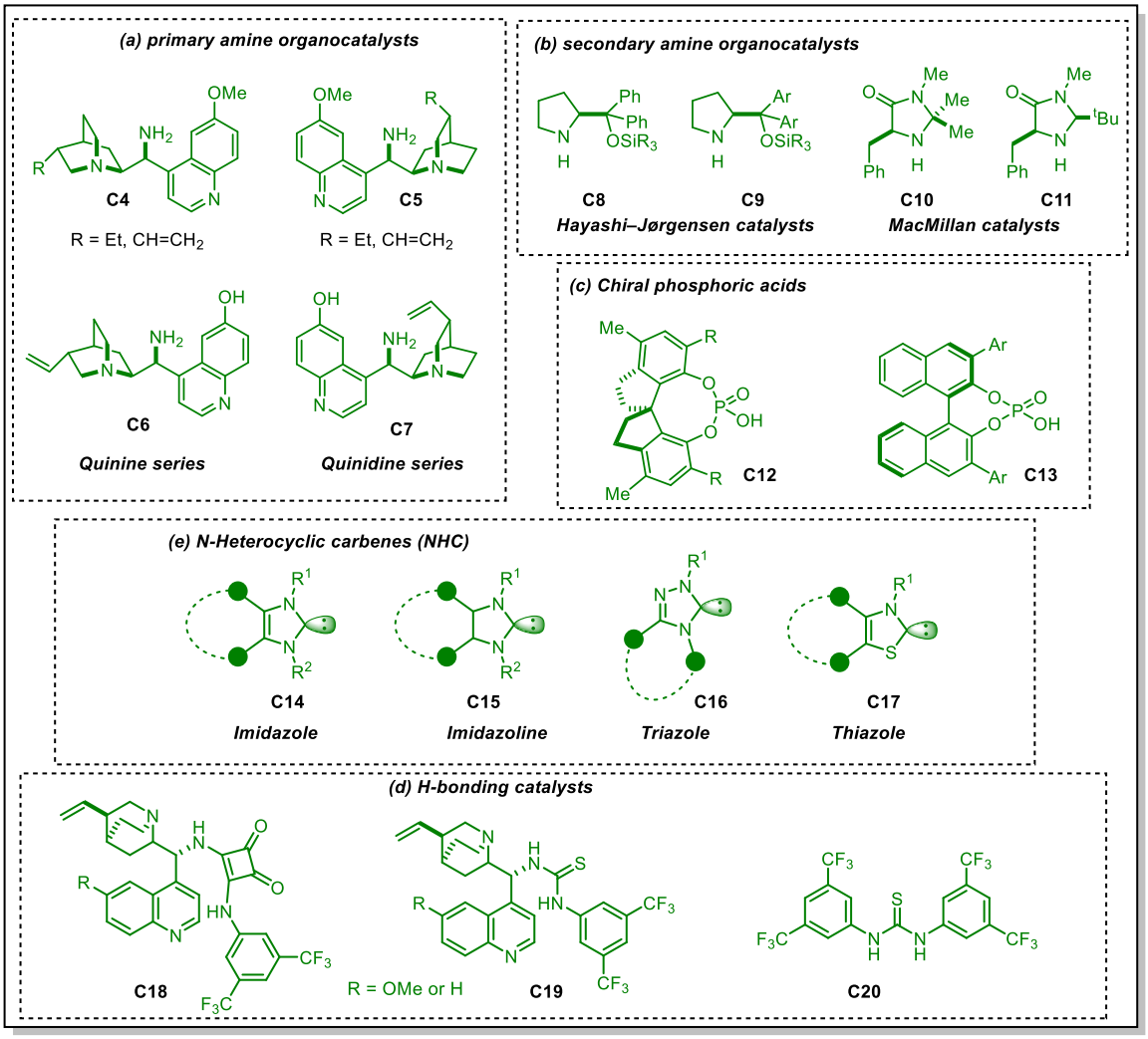
Classification of Organocatalysts: The organocatalysts can be majorly divided into three segments depending upon mode of activation provided to the substrates: i) electrophilic activation; ii) nucleophilic activation; or iii) bifunctional activation. Alternatively, they can also produce an asymmetric environment which ensures the chirality induction of the product.

The above-mentioned activations classify the organocatalysts into either covalent or non-covalent catalysts (Scheme 1.1.5). Covalent catalysis relies on the formation of a covalent bond between the organocatalyst and the substrate. Primary and secondary amine catalysts, N-heterocyclic carbenes (NHCs), are included in this category. On the other hand, non-covalent catalysis is based on non-covalent interactions between catalyst and substrate. The activation of the substrate takes place either via hydrogen bonds (e.g., thioureas, squaramides, and chiral phosphoric acids) or ionic interactions (e.g., phase-transfer catalysts, phosphate salt, and chiral bases such as cinchona alkaloids). These activation modes represent a portfolio of organocatalysts together, which triggers a variety of enantioselective transformations. Recently, it is a well-established concept that has found widespread use for both academic and industrial applications.[21]



Scheme 1.1.1.5: Classification of Organocatalyts.

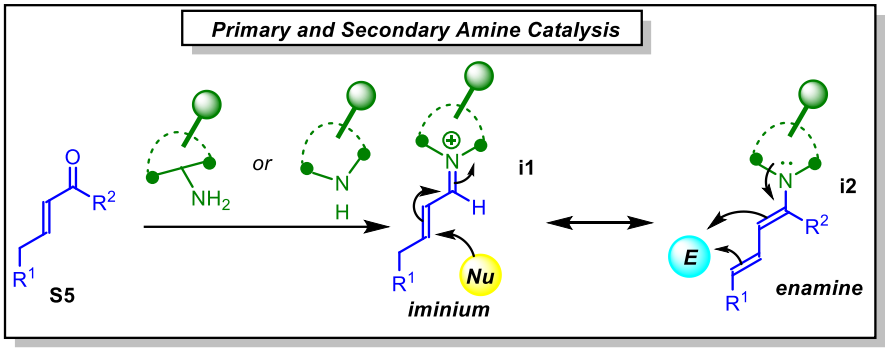
Scheme 1.1.1.6 represents some organocatalysts which are commonly used in research laboratories. Most of the organocatalysts are easily available or derived from easily available starting materials.[21]



Scheme 1.1.1.6: Examples for Commonly Used Organocatalyst.

Primary and secondary amines have contributed a widespread part in the organocatalytic arena. Aminocatalysis is mainly governed by iminium and enamine activations of the carbonyl compounds. The iminium activation of carbonyl compounds lowers its LUMO, enhancing its vulnerability to the nucleophilic attack from an incoming nucleophile. In contrast, via an enamine activation, HOMO is generally raised, thus it become susceptible for an electrophilic attack.[22]

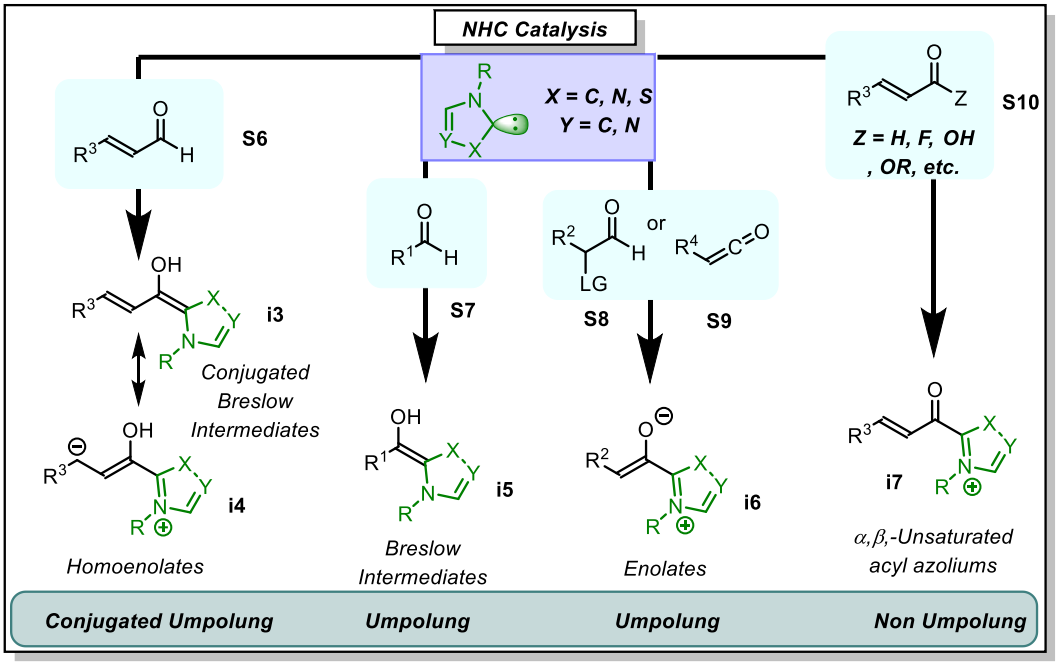
A general model is shown in scheme 1.1.1.7 iminium and enamine activations. If we take an α,β-unsaturated carbonyl compound **S5**, it binds with primary and secondary amines (**C4-C11**) to form an iminium intermediate **i1**. In the presence of a γ-proton, it readily converts enamine intermediate **i2** and remains in equilibrium with the iminium ion. The bulkiness present in the catalyst governs the stereoselectivity of the reaction (Scheme 1.1.1.7).



Scheme 1.1.1.7: Activation Mode of Substrates by Primary and Secondary Amine Catalyst.

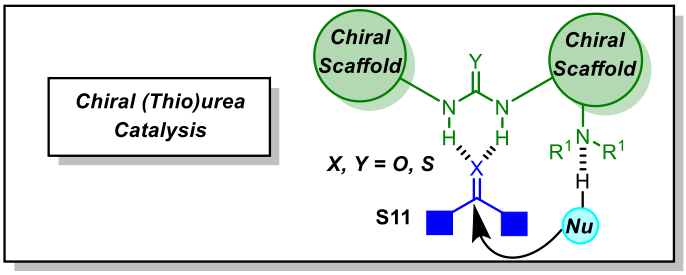
Another type of amine catalyst i. e. *N*-heterocyclic carbenes (NHCs) are frequently employed as p-block elements, ligands for transition metals, and as organocatalysts in numerous chemical transformations. As an organocatalyst, it is operative via umpolung and non-umpolung mechanisms. NHC-catalyzed reactions typically proceed via four species: (i) homoenolates **i4**; (ii) Breslow (enaminol-type) intermediates **i5**; (iii) enolates **i6**; and (iv) α,β-unsaturated unsaturated acyl azoliums **i7** (Scheme 1.1.1.8).[23]

In the presence of a NHC catalyst, α,β-unsaturated aldehydes **S6** form a conjugated Breslow intermediate which is also known as homoenolate **i4**. The reaction between aldehyde and NHC via deprotonation/ reprotonation leads to a crucial Breslow intermediate **i5**. Similarly, an enolate intermediate can be formed when the NHCs are allowed to react with α-functionalized aldehydes or ketenes (**S8** or **S9**). These three intermediates display umpolung reactivity of the aldehyde. On the other hand, substrates like α,β-unsaturated acyl compounds, 2-bromoenals, and ynals **S10** do not participate in umpolung processes after binding with NHC, exhibiting non-umpolung reactivity (Scheme 1.1.1.8).



Scheme 1.1.1.8: Activation Mode of Substrates by NHC Catalyst.

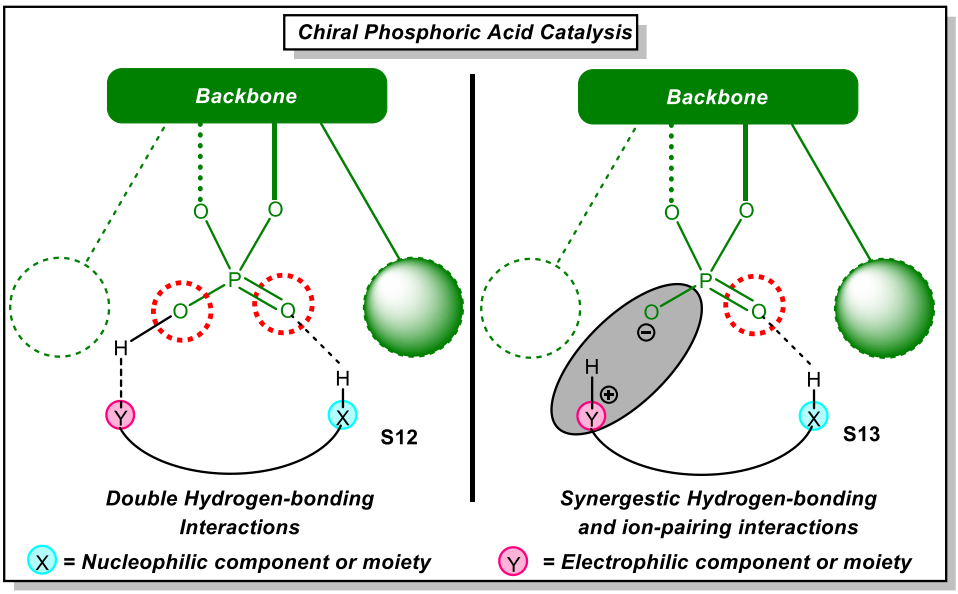
Besides the above-mentioned covalent organocatalysts, thio(urea)-based organocatalysts encompass unique advancements due to their non-covalent catalytic character. Chiral thiourea-amine organocatalysts generally comprise three components: i) the basicity and nucleophilicity of the amine group help to initiate the reaction; ii) the formation of hydrogen bond between the thio(urea) group and substrate which activates the substrate; iii) the chiral skeleton is the linker of the amine group and thiourea group and establishes a chiral environment. The thiourea group plays a pivotal role as a Brønsted acid to activate the substrate and acts as a linker to make a strong connection between catalyst and substrate **S11**.[24] The formation of extra hydrogen bonds between the thiourea catalyst and substrate provides additional stability to some key transition states, decreasing the reaction energy barrier and enhancing its efficacy (Scheme 1.1.1.9).



Scheme 1.1.1.9: Activation Mode of Substrates by (Thio)urea Catalyst.

In the same line, chiral phosphoric acids can activate both the nucleophilic and the electrophilic substrates via the utilization of the basic property of the P=O moiety and, concurrently, by employing hydrogen bond interactions. The conventional model for a CPA-

catalyzed reaction is based on dual hydrogen-bonding interaction between the substrates **S12** and the catalyst. In addition, other approaches dealt with the complementary existence of noncovalent interactions (e.g., CH/π, π-stacking) or ionic interaction between the substrates **S13** and catalyst substituents or their anionic part. In these transformations, stereochemistry is guided by the axial chirality of the BINOL structure, while the size and nature of the aromatic substituents can control the level of asymmetric induction and reactivity (Scheme 1.1.1.10).[25]



Scheme 1.1.1.10: Activation Mode of Chiral Phosphoric Acid Catalyst.

Alike organocatalysis, modern days have witnessed several sustainable techniques to drive synthetic chemistry in a greener way, amidst photochemistry and electrochemistry are two potential candidates due to their wide range of applicability. Photochemistry was later merged with electrocatalysis or organocatalysis to develop photoelectrochemistry or photo-driven organocatalysis, respectively. Apart from these techniques, scientists are using other sustainable methods like ball milling, microwave, sonochemistry, flow chemistry, etc. Recently, our group has been devoted to exploring various reactivity using visible light as an abundant, clean, and renewable energy source to carry out organic transformations. Therefore, I will discuss more in the domain of photochemistry in the next section.

1.1.2. Photocatalysis as an Important Gadget for Synthesizing Valuable Cyclic and Acyclic Structural Motifs

Over last few decades, the utilization of photocatalysis remained a frontrunner due to its efficacy in the construction of traditional and nontraditional bonds in organic chemistry. Although there are numerous advantages associated with this technique, the primary obstacle related to photochemistry is the maximum number of organic molecules that cannot absorb light effectively.

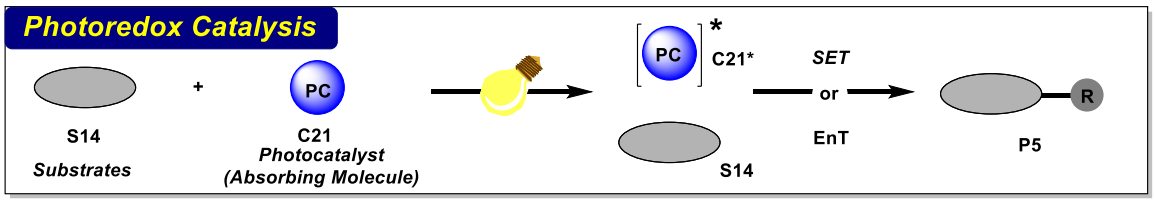
Sunlight itself can be used as a light source, still is complex to control its accuracy in the reaction vessel. Artificial light sources like white lamps are very incompetent, specifically because, in most cases, only specific wavelength ranges are required. Some widely used sources are incandescent, excimer lamp, low- and high-pressure mercury lamps, which illustrated their great potential over the years to trigger numerous organic transformations. However, the main disadvantages are: i) emission of light took place from extended surfaces, therefore, the light collected efficiently to the reaction site, ii) the light output must be filtered out, causing poor energy efficiency, iii) the toxicity associated with mercury, iv) moreover they have very short self-life 500-1000 h, thus hampers the cost-effectiveness.[26]

To overcome the challenges mentioned above, visible light photochemistry was evolved, which can provide light energy with specific wavelengths. Other specifications associated with these techniques are: i) can be used in excess and leaves no trace, ii) easy to generate and set up the reaction, iii) renewable energy source, iv) operative under exceptionally mild conditions, thus visible light, is considered as a sustainable energy source to carry out organic transformations.[27]

In recent times, this progressive field has undergone a substantial renaissance, and a series of new activation modes have been discovered to establish new methodologies. The most common working principle by which visible lights can be used to convert light into chemical energy is divided into three segments: i) Photoredox catalysis, ii) EDA-guided transformations, and iii) photoinduced transformations.

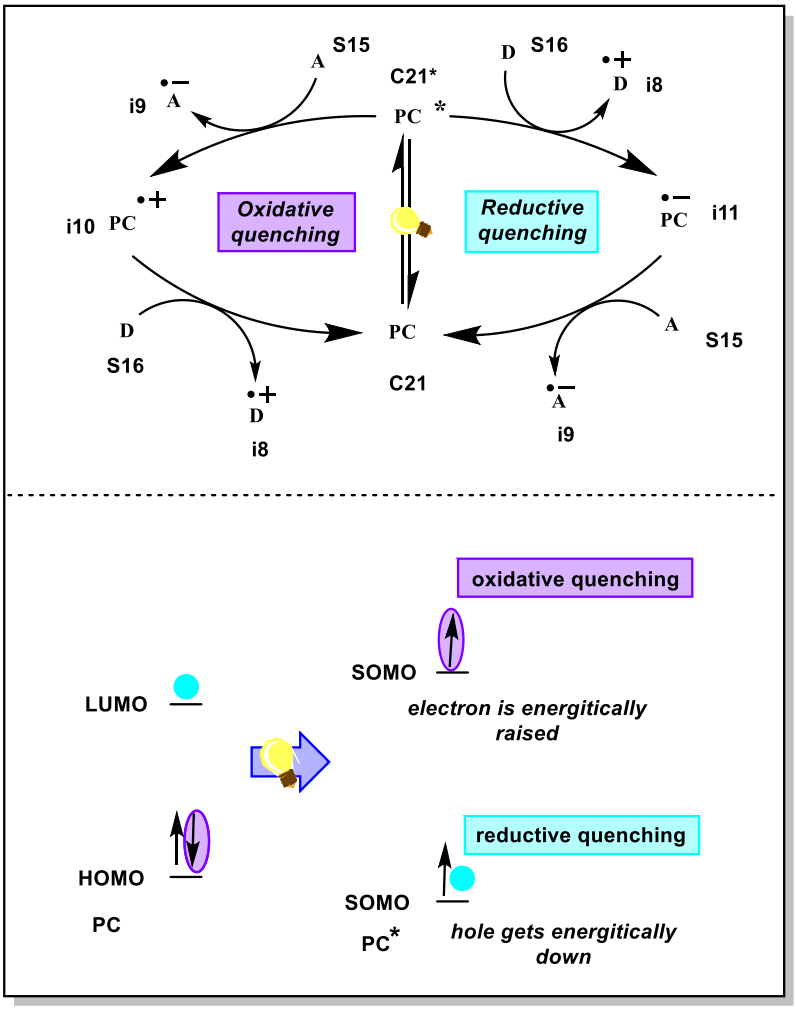
Photoredox Catalysis: From a historical point of view the first application of photoredox catalysis in organic synthesis was bought into play in 1978 by Kellogg et al. to demonstrate photomediated reduction of sulfonium ions to the corresponding alkanes and thioethers using of $[Ru(bpy)_3]Cl_2$ as a photocatalyst and *N*-substituted 1,4-dihydropyridines as a reductant.[28]

Photoredox catalysis was employed where common organic molecules **S14** cannot absorb light, thus requiring a specifically designed photonabsorbing catalyst or photocatalyst **C21** (organic or organometallic) which can be excited with a specific wavelength. The resultant photoexcited species **C21*** can simultaneously behave as both a strong reductant and a strong oxidant, induce an associated substrate via single electron transfer (SET) or energy transfer (EnT), and unlocks unique reaction pathways, which are generally unreachable under traditional thermal methods (Scheme 1.1.2.1).[29]



Scheme 1.1.2.1: General Representation of Photoinduced Transformations.

Working Principle of a Photocatalyst: Upon excitation, a ground-state photocatalyst (PC, **C21**) gets converted into its excited state PC* (**C21***), the active state of any photocatalyst. However, the steady-state concentration in PC* remains minimal amount. After excitation, one electron jumps from its HOMO to LUMO, thereby opening two opportunities, and can be operative via either oxidative quenching or reductive quenching cycle. In the case of oxidative quenching, PC* donates its unpaired electron to an acceptor substrate (A, **S15**), furnishing $A^{\bullet-}$ (**i9)** and converted into its oxidized form $PC^{\bullet+}$ (**i10**). Alternatively, in presence of a donor species (D, **S16**), PC* can operate via a reductive quenching cycle where the photocatalyst gets reduced to form $PC^{\bullet-}$ (**i11**). along with its radical cationic partner $D^{\bullet+}$ (**i8**). These open-shell reactive species then involved in a single-electron transfer (SET) process to fabricate new chemical bonds (Scheme 1.1.2.2).



Scheme 1.1.2.2: General Catalytic Cycle and Activation Modes of Photoredox Catalysis.

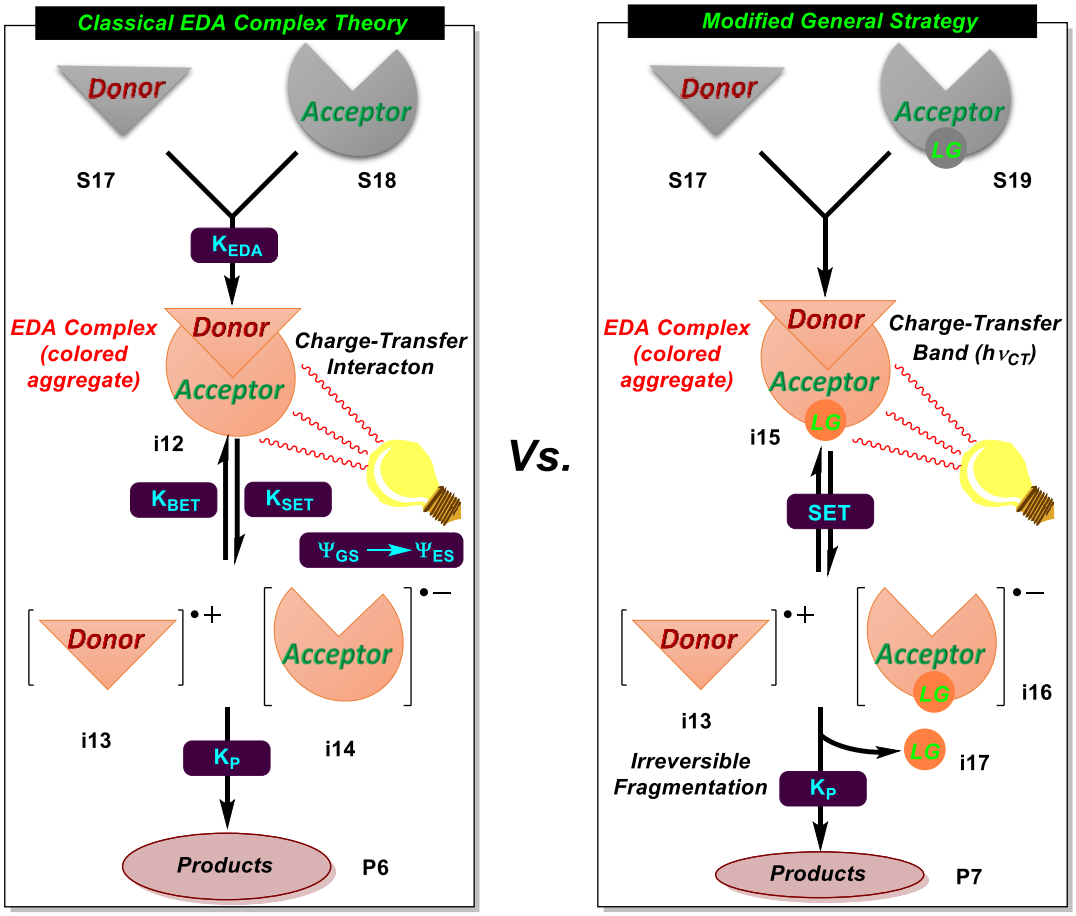
EDA-Guided Transformations: Another division of photochemistry relies on the electron donor-acceptor complex or EDA chemistry, where the two reacting substrates are generally non-

absorbing molecules. The electron-rich substrate is a donor, and the electron-demanding substrate can be termed an acceptor.

The EDA concept was first introduced by Dr. Robert Mulliken in 1952 to define a new type of noncovalent interaction.[30] According to Dr. Mulliken, the donor **S17** and acceptor **S18** molecule can come together to form a charge transfer complex **i12**, where K_{EDA} represents the association constant of the complex formation. This complex can be characterized by the occurrence of a new absorption band, often within the visible range. Hence, upon photoexcitation, the wavefunction of excited EDA complex (Ψ_{ES}) gets populated, which renders in an intracomplex electron transfer from donor to acceptor site to deliver the corresponding radial ion pair (**i13** and **i14**). This radical ion pair enables C-C or C-heteroatom bond formation (Scheme 1.1.2.3, left part).

The major drawback associated with this model is the back electron transfer (BET) from the radical ion pair (**i13** and **i14**), which can be restored into the ground-state EDA complex **i12**. If there is another possibility leading to reactive radicals and, ultimately, products **P6** are kinetically not competitive with the BET (i.e. if $Kp < K_{BET}$), then the photoexcitation of the EDA complex remains synthetically unproductive (Scheme 1.1.2.3, left part).

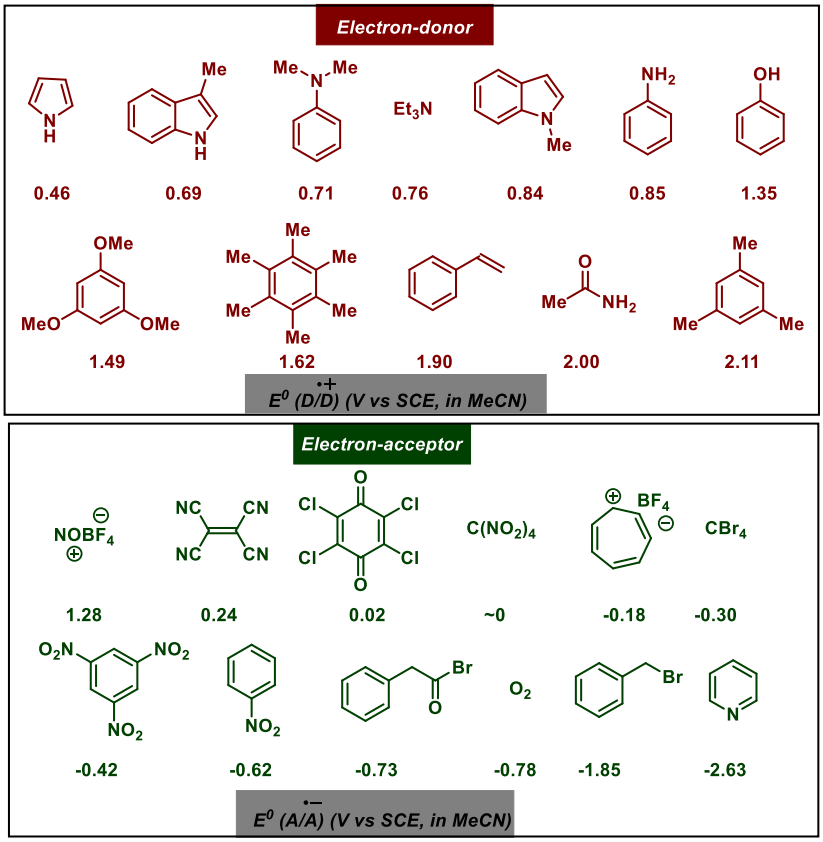
To overcome this limitation, in the early 1970s, Cantacuzene, Bunnett, Russell, Kornblum, Kochi, and others proposed a general model which renovated EDA complex activation into a fruitful synthetic approach. According to their proposal, the EDA complex photochemistry can rely on the existence of a labile leaving group (LG) embedded into the acceptor part **S19**. After photoexcitation, the acceptor part got converted into the radical anion **i16**, which triggers the detachment of irreversible fragmentation (LG, **i17**) in a rapid way, having the sufficient potential to compete with the BET step. This process thus becomes synthetically useful to initiate several radical-based transformations (Scheme 1.1.2.3, right part).[31]



Scheme 1.1.2.3: Basic Working Principle for EDA Chemistry.

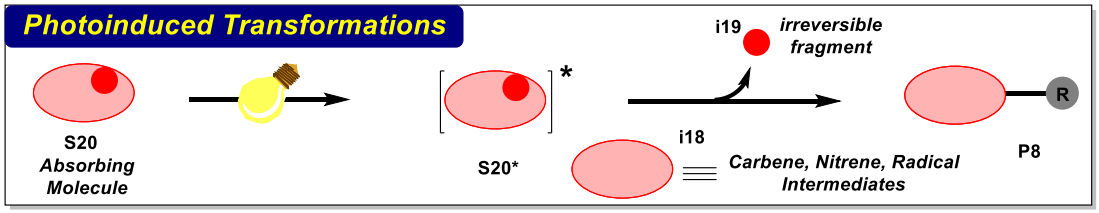
The key features associated with associated with EDA complex are: i) association of donor and acceptor molecule are less robust and less directional as compared to other weak interactions, such as H-bonding; ii) they have sensitivity towards temperature, solvent, and its concentrations, iii) after formation they exhibits a bathochromic shift at the UV-Vis absorption with respects to the spectra for individual components, often shifted towards visible region and forms a colored reaction mixture.[32]

Scheme 1.1.2.4 represents some common donor and acceptor molecules, frequently used in various research laboratory.



Scheme 1.1.2.4: Example for Commonly Used Donor and Acceptor Molecules.

As opposed to the above-mentioned frameworks, some organic compounds (**S20**) have the ability to absorb light directly in the visible spectrum (or close to the visible region). Thus, after excitation, the molecules get excited and facile cleavage of a fragment occurs (or occurs via an intramolecular rearrangement), leading to the formation of highly reactive intermediates like carbenes, nitrenes, and radicals **i18** (Scheme 15). These intermediates **i18** can be employed over various convenient synthetic transformations. Classic examples that can undergo mild photolysis include dithiocarbonates, pyridotriazoles, hypervalent iodine compounds, organometallic complexes, phosphonium salts, acylsilanes, and diazo compounds, etc.[33] Surprisingly, the number of various types of organic compounds known to undergo direct photolysis under visible light irradiation was very rare until recently, it has dramatically increased during the past ten years.



Scheme 1.1.2.5: General Representation of Photoinduced Transformations.

1.2 Objectives

- Development of novel methodologies under organocatalytic and photoinduced synthetic techniques.
- Exploration of the catalytic reactivity of Jørgensen-Hayashi organocatalyst.
- Utilization of visible light to carry out several synthetic transformations under metal-free conditions.
- Synthesis of enantioenriched chiral chroman via double 1,6 addition.
- Diverse reactivity of carbenes with nitrosoarenes and *N*-sulfinylamines under visible light.
- Identification and utilization of NBS-THF electron donor-acceptor (EDA) over radical-based amination reaction using diazo compounds.

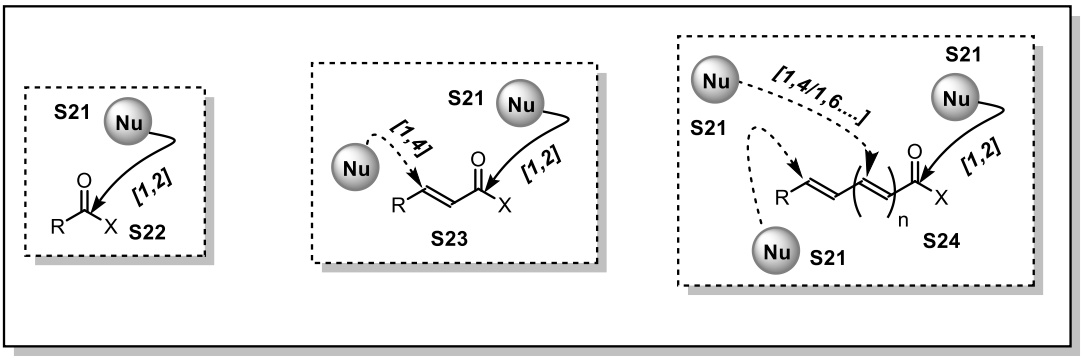
1.3 Motivation and Scope

1.3.1 Organocatalytic Vinylogous Reactivity

Asymmetric synthesis has grown exponentially since the early 20th century after the revitalization of organocatalysis field. Since then, this benign field has been explored in various asymmetric transformations, alone or by sometimes merging with transition-metal catalysis, photocatalysis, and electrocatalysis to fabricate a wide range of carbon-carbon and carbon-heteroatom bonds by participating in numerous complex cascade sequences and conjugate addition reactions. Unquestionably, different organocatalysts were also able to trigger the enantioselective 1,4-conjugate addition reactions and the domino sequences. As an extension to the 1,4-conjugate additions, 1,6-addition reactions are more challenging in asymmetric catalysis. The major task associated with the 1,6-addition reactions is to control the site selectivity, i.e. β vs. δ-position.[34] This reactivity differential mainly arises due to the poor transmission of the electronic effect through the π-conjugated system, leading to the regioselectivity issue. Another great challenge is getting control over the asymmetric induction at the remote stereogenic center since it is less favourable to induce a chiral environment at the δ-position, which is far from the catalyst binding site. This type of electronic transmission by moving along the chain of a carbonyl substrate is termed vinylogous reactivity, which was originally defined in R. C. Fuson in 1935 (Scheme 1.3.1.1).[35]

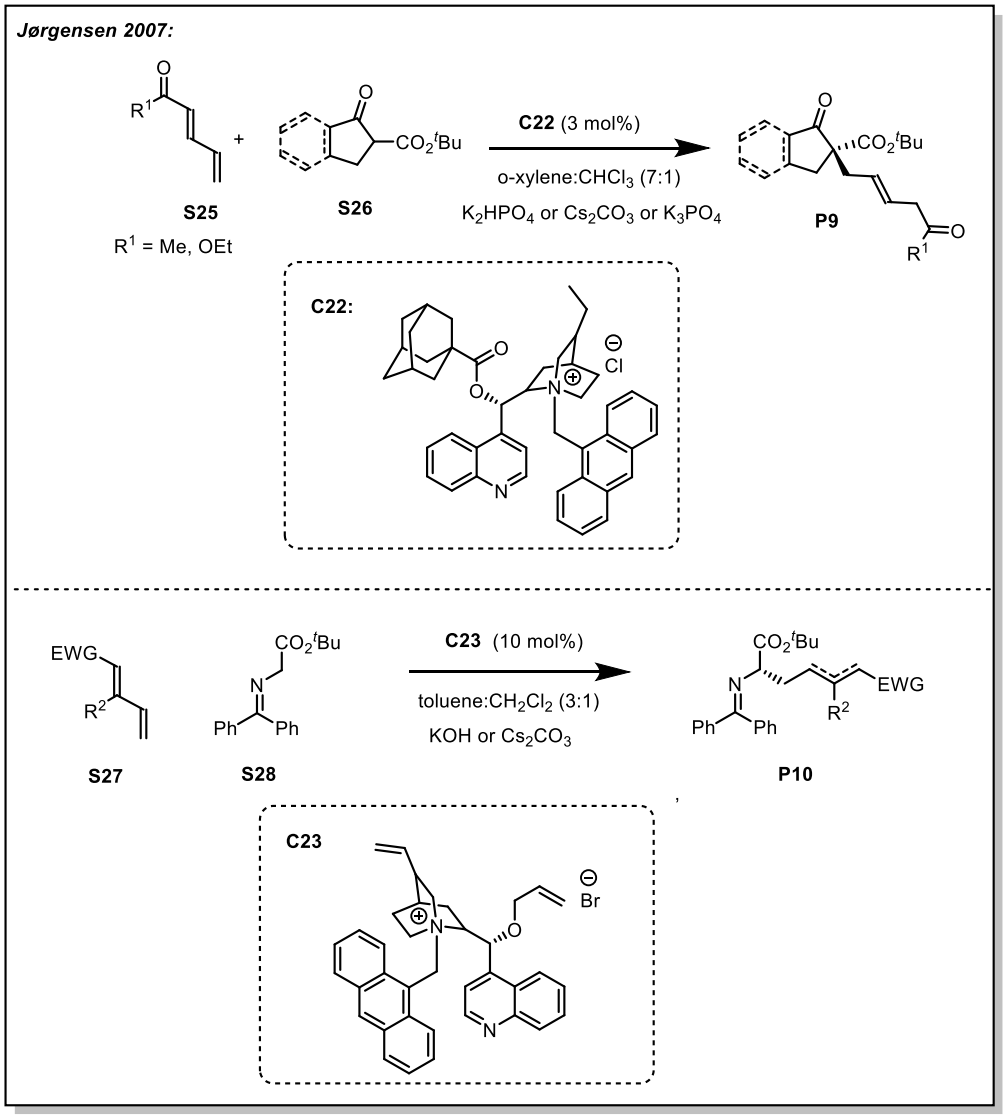
In the last few years, small chiral organic molecules have proven themselves as key promoter in various 1,6-nucleophilic addition reactions by activating δ-position to fabricate remote stereogenic centers. In order to perform an enantioselective 1,6-addition reaction, the basic requirement is careful design of the substrates and the catalysts since it is well proved by experimental and computational studies that an organocatalytic 1,4-addition is preferably favoured over the 1,6-addition.[36] The 1,4 reactivity can be strategically suppressed either by

increasing the steric bulk at the β-position of the substrate or via sketching a mode that can make remote positions more electrophilic through electrostatic interactions or hydrogen bonding with the catalyst. Sometimes, the steric bulk present in the catalyst can also govern the reactivity towards remote positions.



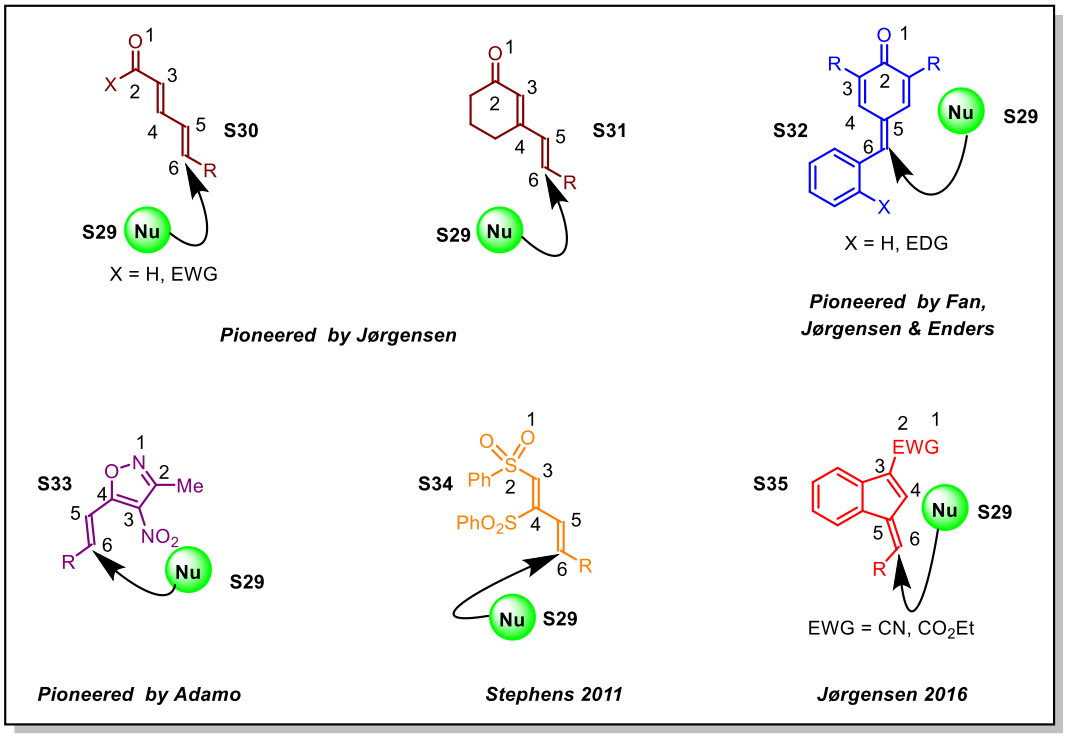
Scheme 1.3.1.1: Vinylogous Reactivity.

The first example of an organocatalytic asymmetric 1,6-addition reaction was reported by the Jørgensen group in 2007.[37] In this protocol, β-ketoesters **S26** and benzophenone imine **S28** were allowed to react with electron-deficient δ-unsubstituted dienes substituted with ketones, esters, and sulfones (**S25** and **S27**) to furnish corresponding enantioenriched products (**P9** and **P10**) in good yields and high enantioselectivities under chiral phase-transfer catalysts. The transformation was also applied over enantioselective 1,6-addition for various cyclic β-ketoesters having different ring systems, ring sizes, and substituents to furnish the desired products (Scheme 1.3.1.2).



Scheme 1.3.1.2: First organocatalytic asymmetric 1,6-addition

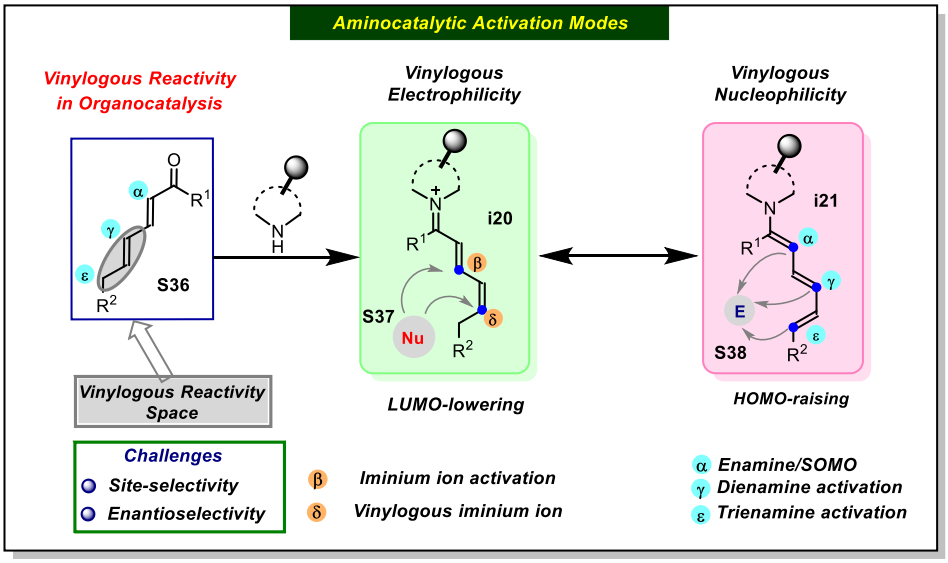
The major thrust in organocatalytic 1,6 addition arena was generated by different research groups in the last ten years. To generate a remote stereogenic center via 1,6-addition reactions, logically designed substrates such as dienones (**S30** or **S31**), dienals **S30**, *para*-quinone methides **S32**, unsaturated esters **S35**, 3-methyl-4-nitro-5-alkenylisoxazoles **S33**, benzofulvenes **S35**, and 1,3-bis(sulfonyl)butadienes **S34** were introduced. Vinylogous iminium ions and enamines are two common intermediates to perform a remote functionalization over the dienal and dienone systems (**S30** or **S31**) secondary or primary amine organocatalysis. A bifunctional hydrogen bonding catalyst or a phase-transfer catalyst can activate the *para*-quinone methides **S32** and alkenylisoxazoles **S33** (Scheme **1.3.1.3**).[34]



Scheme 1.3.1.3: 1,6 Addition Toward Various π-Conjugated Systems.

Aminocatalysis has added great value to the vinylogous reactivity of unsaturated compounds. This technique has been successfully utilized to induce vinylogous nucleophilicity in extended enamines as well as electrophilicity of extended iminium ions, resulting in direct functionalization of unsaturated carbonyl substrates **S36** at its γ, δ, and ε positions with excellent site and stereoselectivity.

The aminocatalytic mode relies on the ability of a chiral amine to bind reversibly with carbonyls or poly conjugated carbonyls **S36**, thus, enhancing its electrophilicity for a nucleophilic attack by lowering the LUMO energy. In contrast, enamine activation provides the nucleophilic character by HOMO energy-raising effect to the enamine intermediate **i21**, which is generally formed in presence of an enolizable proton present in the iminium ion intermediate **i20**. These two activation modes have rendered a crucial synthetic platform to functionalize remote γ, δ, and ε positions with high levels of enantiocontrol and recognized as 'vinylogous enamine-iminium ion catalysis', triggering rare examples of asymmetric catalytic 1,6-addition (Scheme 1.3.1.4).[36]

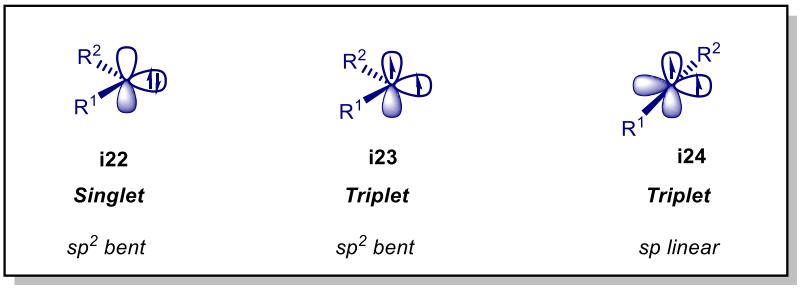


Scheme 1.3.1.4: Amine Catalyzed Vinylogous Reactivity of Enals.

1.3.2. Carbenes as a Key Intermediate in Visible Light Induced Transformations

Carbenes are imperative intermediates in synthetic organic chemistry to install various functionalities and engender molecular architectures in a rapid way.[38] Conventionally, carbenes intermediates can be generated through thermal, photolytic, or transition metal-catalyzed decomposition of diazo compounds. Rhodium and copper are two metal catalysts that are frequently used to facilitate the dinitrogen extrusion process from diazo compounds, resulting in valuable metal carbenoids.[39] Alternatively, the Bamford-Stevens reaction can produce carbene intermediates in polar aprotic solvents.[40]

Carbene species have two valence electrons dispersed between two nonbonding orbitals, considered to be a divalent compound, and the central carbon atom is covalently bonded to two other groups. They present either in a singlet state when the two electrons are spin-paired or in a triplet state with the parallel spin of the electrons. Singlet carbenes are generally present in bent sp^2 hybrid structures **i22**. In contrast, triplet carbenes may occur in either bent sp^2 hybrid **i23** or linear *sp* hybrid structure **i24**, with each electron occupying a different unoccupied orbital. Singlet methylene has a bond angle of 100-110°, whereas triplet methylene has a bond angle of 135-150° (Scheme 1.3.2.1).



Scheme 1.3.2.1: Structure of Singlet and Triplet Carbenes.

Most of the carbenes remain in a bent form. However, few carbenes have a linear structure. Bent carbenes possessing bond angles between 100° and 150° signifying a trigonal (sp^2) hybridization state. There are three lower energy sp^2 orbitals, and one high energy p orbital associated with carbene structures, among which the six electrons are distributed. In the case of singlet carbenes, all six electrons remain paired, situated in the sp^2 orbitals. On the other hand, triplet carbenes have two unpaired electrons, with one electron each in one of the sp^2 orbitals and in the p orbitals. The formation of singlet or triplet carbenes is greatly affected by the types of substituents present in it. Therefore, all carbenes have the potential to exist in either the singlet or the triplet state, depending upon the energy of that particular state. Suppose we consider a carbene intermediate such as $:CH_2$, it remains in its 'triplet state' as for this carbene, triplet energy is lower in energy than the singlet state, whereas the reverse is true for $:CCl_2$. Most of the triplet state carbenes are stable as the required energy for bringing the electron from the p orbital down into its sp^2 orbital is inadequate to overcome the repulsion associated with two electrons in a single orbital (Figure 1.3.2.1).

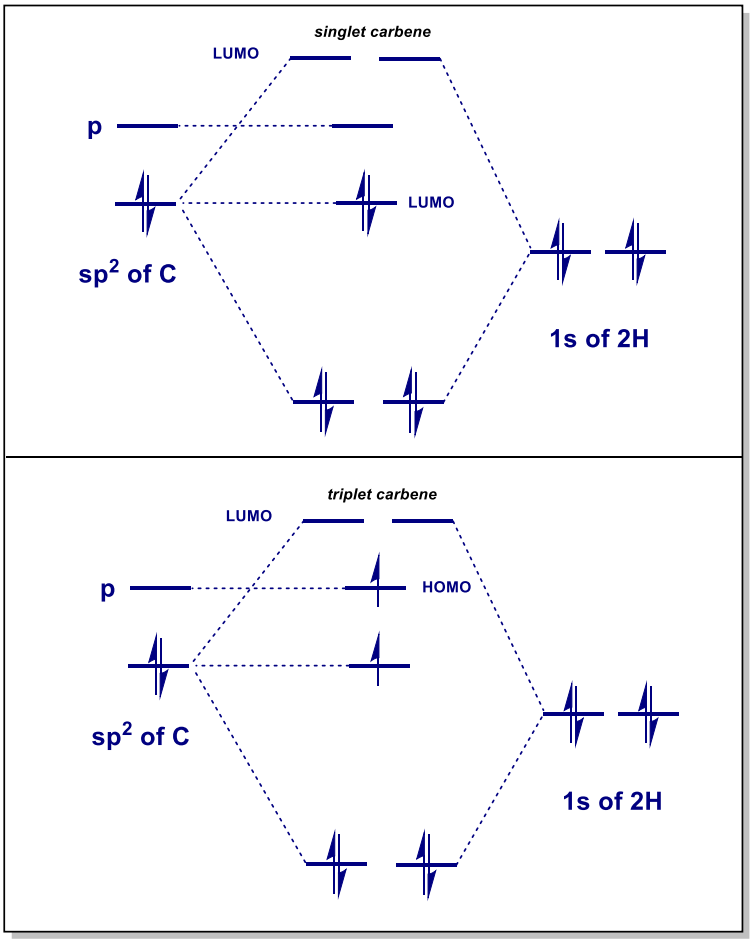
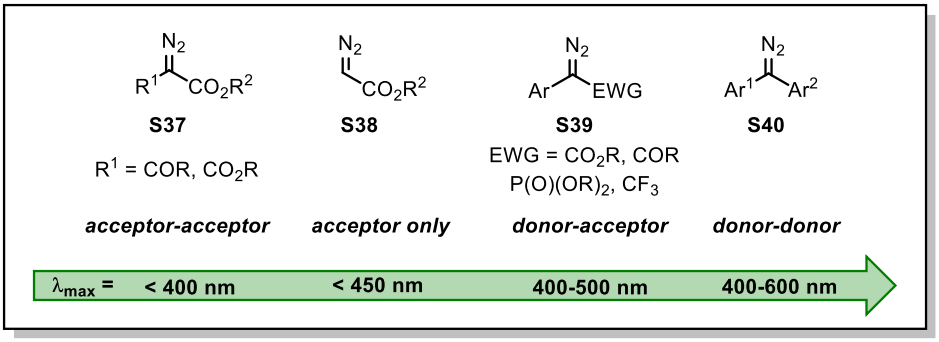


Figure 1.3.2.1: Electronic Structure of Bent (sp^2) Singlet and Triplet Carbene.

Over the years diazo compounds remained as a potent candidate to deliver carbene intermediates. Transition metal-catalyzed carbene generation from diazo compounds has drawn leading attention from the synthetic community due to their excellent efficiency and selectivity. However, in modern days, visible-light-induced generation of carbene intermediates and their utilization has witnessed an exponentially growing interest due to their ability to introduce various functionalities and engender molecular complexity. Due to its operational simplicity and mild reaction condition, several groups adapted this technique to perform various insertion, cycloaddition, and epoxidation reactions.

Diazo compounds can absorb light to some extent in the region of the electromagnetic spectrum. The diazo compounds substituted with mono or di electron demanding group exhibits λmax value below 450 nm (**S38** or **S39**). However, the presence of a donor group (most commonly an aryl ring) attached to the carbon atom carrying the diazo functionality leads to a redshift in an absorption band of its UV-Vis absorbance spectrum. It falls into the blue region (λmax = 440–485 nm), probably due to the n-π* electronic transition. A donor-donor substituted diazo compound shows a more bathochromic shift in the UV-Vis absorbance spectrum (λmax = 400-600 nm) (Scheme 1.3.2.2).[41]



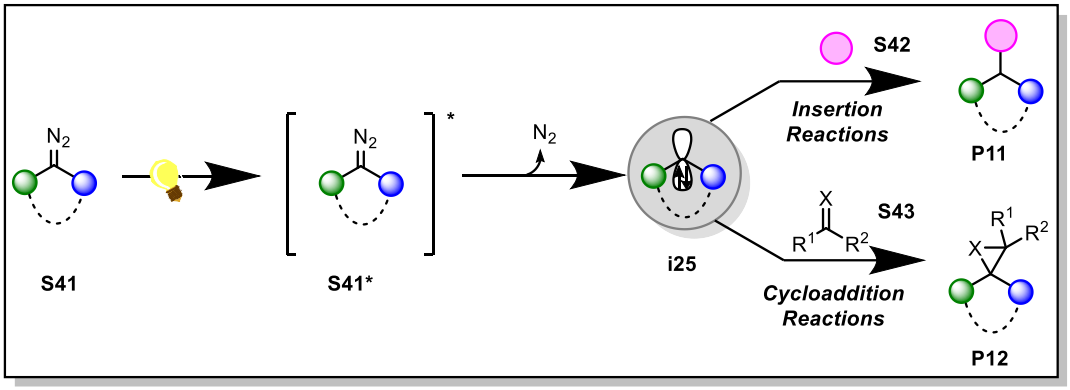
Scheme 1.3.2.2: Different Class of Diazo Compounds with Light Absorption Properties.

Due to its light absorption property, diazo compounds **S41** got excited upon irradiation by low-energy lights, e.g., blue, purple, white, or sometimes in the presence of low-energy UV light. Then, these photoexcited diazo compounds **S41*** facilitate the dinitrogen extrusion process to produce a highly unstable and reactive free carbene intermediate **i25**, which can be used to perform several insertion and cycloaddition reactions (Scheme 1.3.2.3).

Donor-acceptor diazo compounds **S39** are good precursors to generate singlet carbenes. In contrast, some triplet carbenes are produced from donor–donor diazo compounds. Nevertheless, photolysis α-diazo ketones also can produce free carbene, which upon a Wolff rearrangement, leads to a ketene intermediate.

The reactions involving singlet carbenes are easy to handle as they are typically insensitive to oxygen or moisture, being possibly performed under aerobic conditions, and thus do not require

any fancy reaction condition. In contrast, the reaction proceeds via triplet carbenes require specialized treatment like an inert atmosphere and anhydrous conditions, as oxygen or moisture can readily intercept such a diradical intermediate as they are supposed to be long-lived and highly reactive. On the other hand, in situ generated ketenes are also unstable in nature, which can readily be trapped by a nucleophile (NuH) or participates in a formal [n+2]-cyclization.

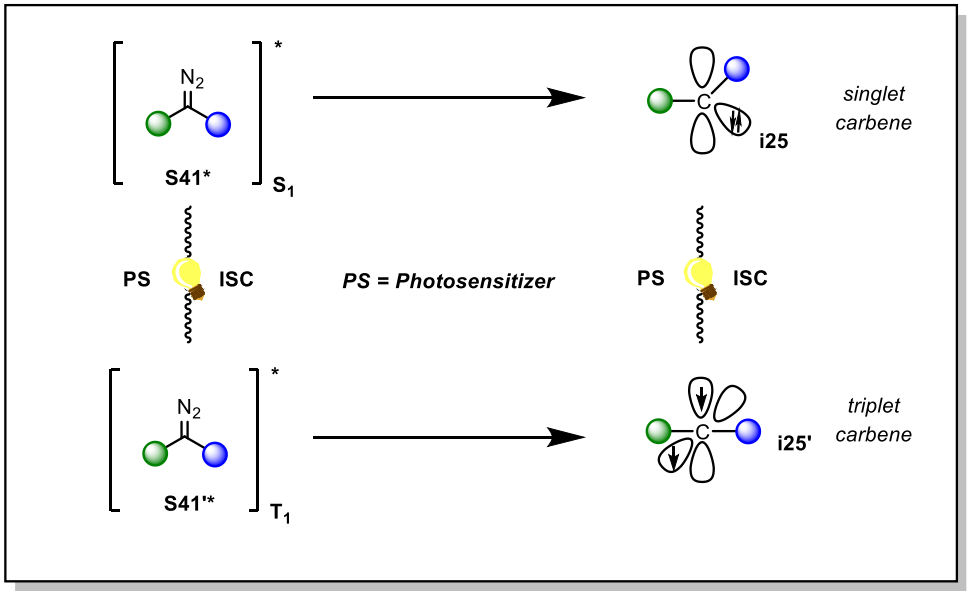


Scheme 1.3.2.3: Reactivity of Carbenes Upon Photolysis.

The reactivity of carbenes is greatly influenced by their spin state. Upon light irradiation, the photoexcited diazo compounds remain in the singlet state. From this point, different pathways lead to carbenes in either singlet or triplet states.

Primarily, the photolysis of excited diazo compound **S41*** leads to a singlet carbene **i25**. Here, two nonbonding electrons remain situated on the divalent carbon atom with antiparallel spins, reside in one hybridized orbital, and thus one p-orbital remain vacant. As a result, singlet carbenes can act as both electrophiles and nucleophiles depending upon the character of substituents. Therefore, they can be engaged in many transformations, such as C–H and X–H insertion reactions, as well as stereospecific addition to olefins.

On the other hand, the generation of the triplet carbene **i25´** may happen in two ways: i) either the singlet carbene **i25** produced from the excited diazo compound **S41*** can directly convert into its triplet state **i25´** via an intersystem crossing (ISC), ii) or the excited diazo compound **S41*** can be transformed from its singlet to triplet state **S41´***, afterward decomposition to the triplet carbene. Thus, both pathways can furnish triplet carbenes **i25´**, usually facilitated by energy transfer from an externally added photosensitizer (PS). In the case of triplet carbenes, two unpaired nonbonding electrons with parallel spins are distributed into two different orbitals (Scheme 1.3.2.4). Therefore, triplet carbenes **i25´** are generally considered diradicals and get involved in the hydrogen atom abstraction or nonstereospecific addition to olefins.



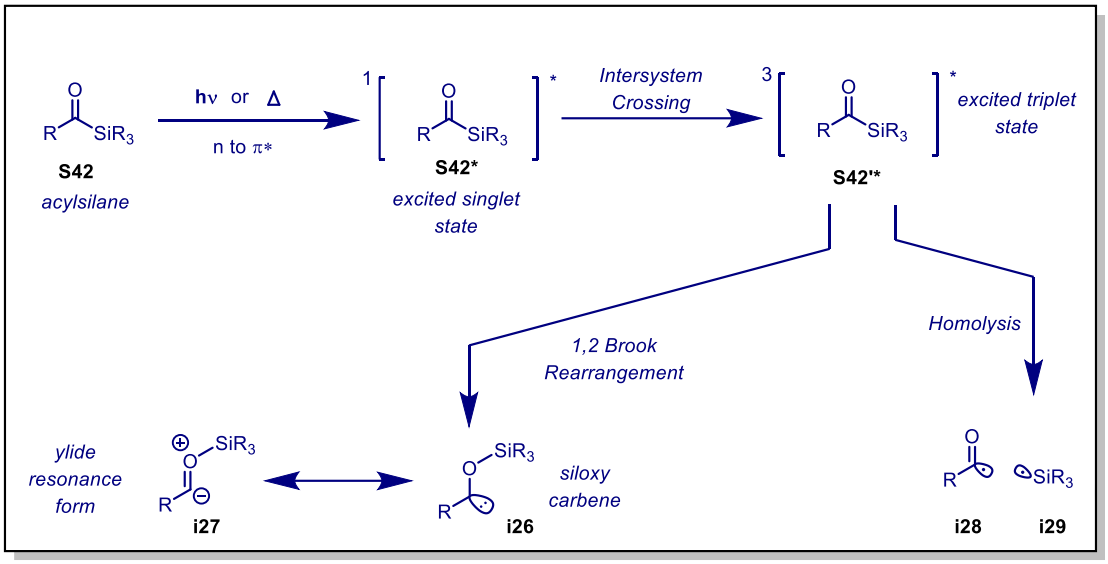
Scheme 1.3.2.4: Possible Pathways for Carbene Generation Under Photolysis.

1.3.3. Generation of Siloxycarbenes from Acylsilanes and Its Reactivity Under Visible-light-driven Conditions.

Alike diazo compounds, acylsilanes **S42** are an important class of molecules to produce siloxycarbenes **i26** was first described in 1957 by Brook et al.[42] Acylsilanes **S42** are a class of carbonyl compounds where the silicon atom is attached to the carbonyl carbon, demonstrating exciting chemical and physical properties. According to spectroscopic studies, acylsilanes absorb light near ultraviolet and visible regions, and ^{13}C NMR spectra indicate the shipment of carbonyl carbon toward the downfield region. These results suggest that the inductive effect of silicon atom affect the characteristics of the acylsilane carbonyl than their carbon counterparts. In addition, the X-ray crystallographic analysis of triphenylsilyl phenyl ketone showcases a longer C–Si bond length of 1.93 Å compared to a normal C–Si bond with a bond length of 1.86 Å.[43]

Siloxycarbenes **i26** are generally achieved from corresponding acylsilanes **S42** upon 1,2-Brook rearrangement of the silicon motif under thermal or photochemical conditions. Acyl silanes have unique properties as they can release electrons from the silicon atom to the carbonyl moiety. Photochemically (under visible or near-UV irradiation) or thermally activated acylsilanes participate in an n–π* transition involving the transfer of an electron from oxygen non-bonding orbital to the anti-bonding orbital of π-carbonyl moiety. This transition results in the generation of an excited singlet state **S42*** of acyl silane, which via an intersystem crossing (ISC), converts into its triplet state **S42′***. Finally, the 1,2-Brook rearrangement occurs from the excited triplet state of acylsilane **S42′*** to generate the siloxycarbene **i26**. Similarly, homolysis of the carbon–silicon bond can deliver two radical species **i28** and **i29** (Scheme 1.3.3.1). The singlet siloxycarbene

intermediate can also remain in its ylide resonance form **i27** and can act as a nucleophile in various transformations.[44]



Scheme 1.3.3.1: Formation of Siloxycarbenes Under Photochemical/Thermal Conditions.

Since its first report siloxycarbenes has been utilized over a wide range of organic transformations, by exploring its facile conversion from acylsilanes and benign reactivity profiles of these nucleophilic singlet carbenes. The stability of these singlet nucleophilic carbenes arises from the donation of electron pair from oxygen non-bonding valence electrons to the vacant 2p-orbital of carbene nucleus, thus, also facilitates the ylide formation.

Due to the interaction mentioned above, the energy of the unoccupied molecular orbital got raised, and thus ΔE_{nb} increases, causing a preferred singlet state and making such carbenes nucleophilic in nature. In general, all singlet nucleophilic carbene (SNCs) comprises at least one adjacent heteroatom capable of releasing π-electron into the carbene center, raising the energy of the LUMO, resulting decrease in the electrophilic property of these substrates (Figure 1.3.3.1).

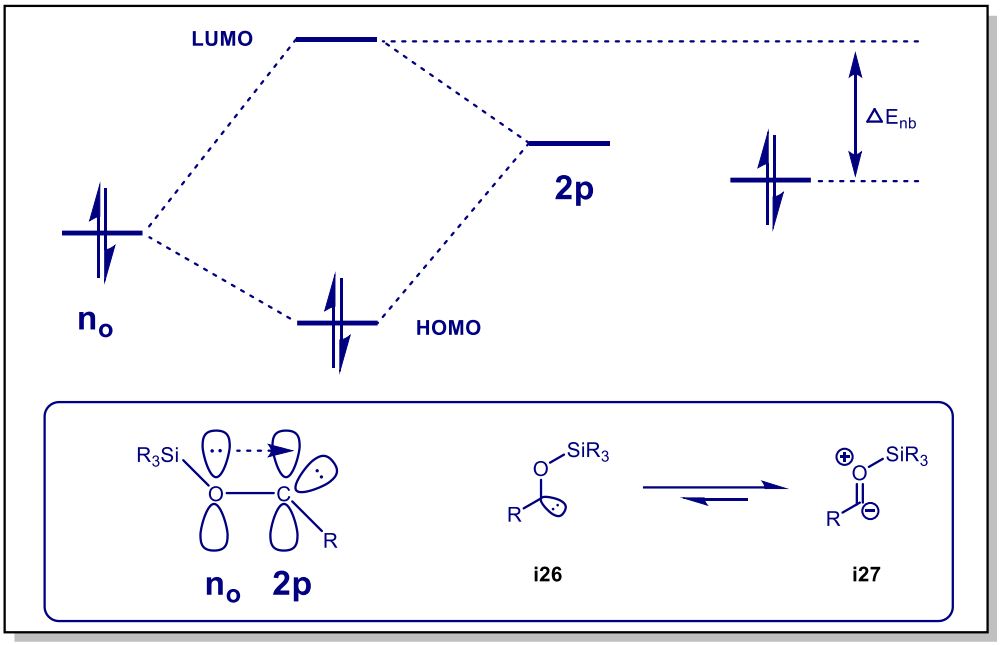
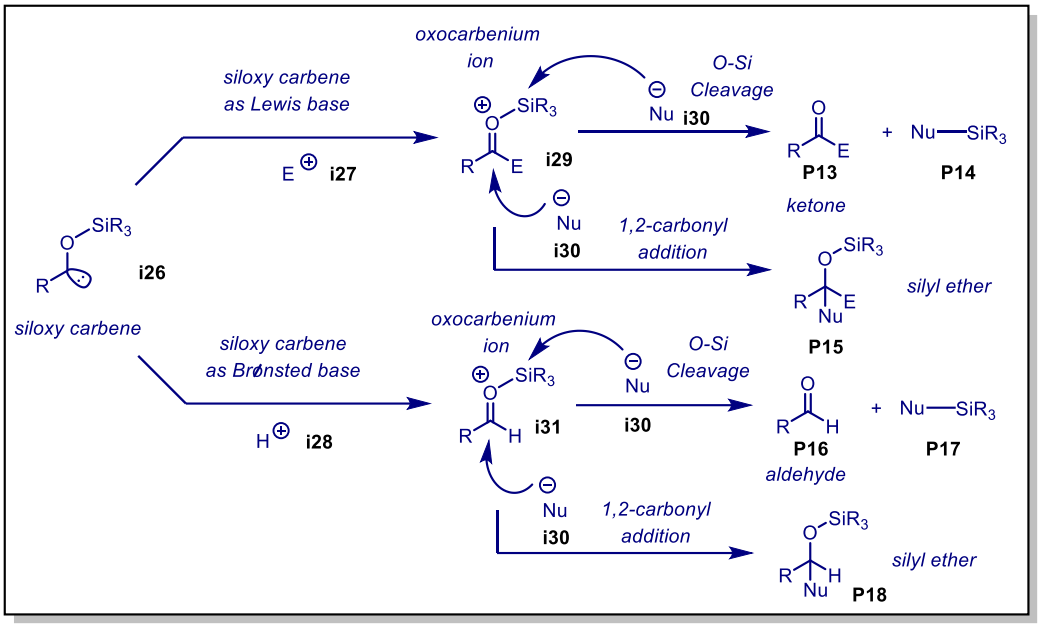


Figure 1.3.3.1: Orbital Diagram for Siloxy Carbenes.

These silicon-derived carbene intermediates possess both Lewis and Brønsted basic characters based on the parent acylsilane structure, reagents, and choice of solvents.

In 1991, Arduengo et al. calculated the proton affinity (approximately 250 kcal/mol) of nucleophilic carbenes, typically known as the Arduengo-type carbenes.[45] The calculation of ΔHacid value for alkyl, aryl, and amino siloxycarbenes reveals the basicity of siloxy carbenes. The siloxy carbenes have much ΔH_{acid} higher values (ΔH_{acid} = 259–270 kcal/mol for the alkyl siloxy carbenes, around 265 kcal/mol for the amino siloxy carbenes, and 260–275 kcal/mol for the aryl siloxy carbenes) as compared to methylidene with ΔH_{acid} = 208 kcal/mol.

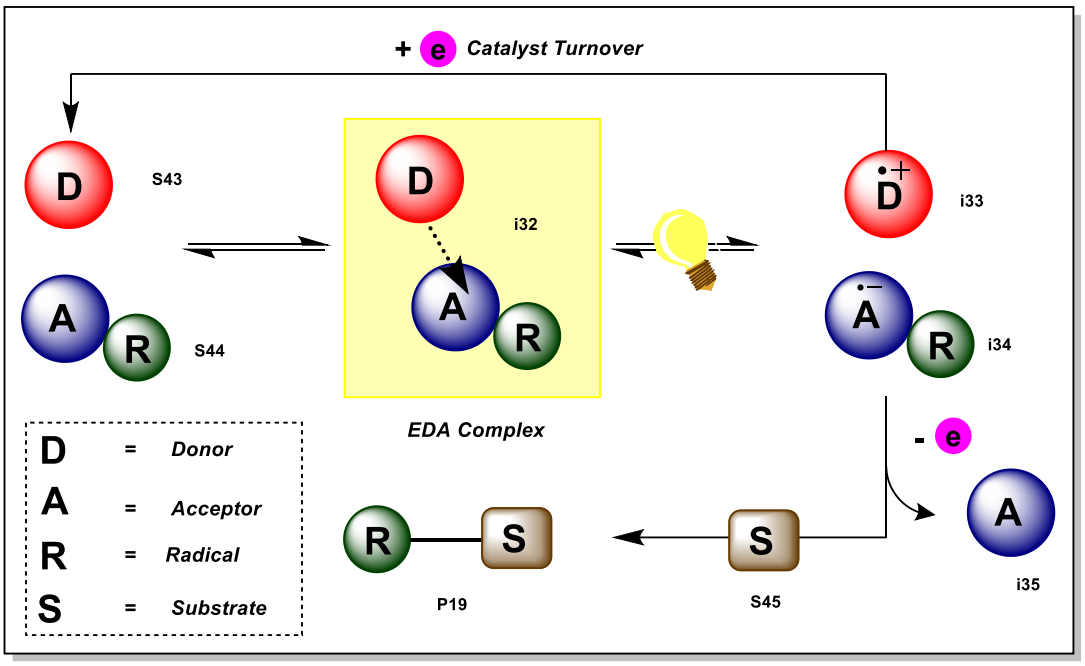
The characteristics of the corresponding oxocarbenium intermediate, which is produced after the initial reaction of the carbene **i26** with a proton or electrophile (**i27** or **i28**), have an impact on the structure of the final product synthesized, regardless of whether the siloxycarbene **i26** reacts as a base or nucleophile **i30**. The oxocarbenium resonance form over the carbonium ion (**i29** or **i31**) is preferable for the cation generated after protonation or addition to an electrophile since all atoms still have a full octet. By examining the oxocarbenium ion intermediate (**i29** or **i31**), which undergoes nucleophilic attack at one of two electrophilic sites (i) either the carbonyl carbon to form silyl ether **P15** as a product or (ii) at the silicon atom to cause the oxygen-silicon bond to be broken and the regeneration of the carbonyl system (**P13** or **P16**), it is possible to reconcile the structures of the products formed by reactions of siloxycarbenes (Scheme 1.3.3.2).



Scheme 1.3.3.2: Different Reactivities of Siloxycarbenes.

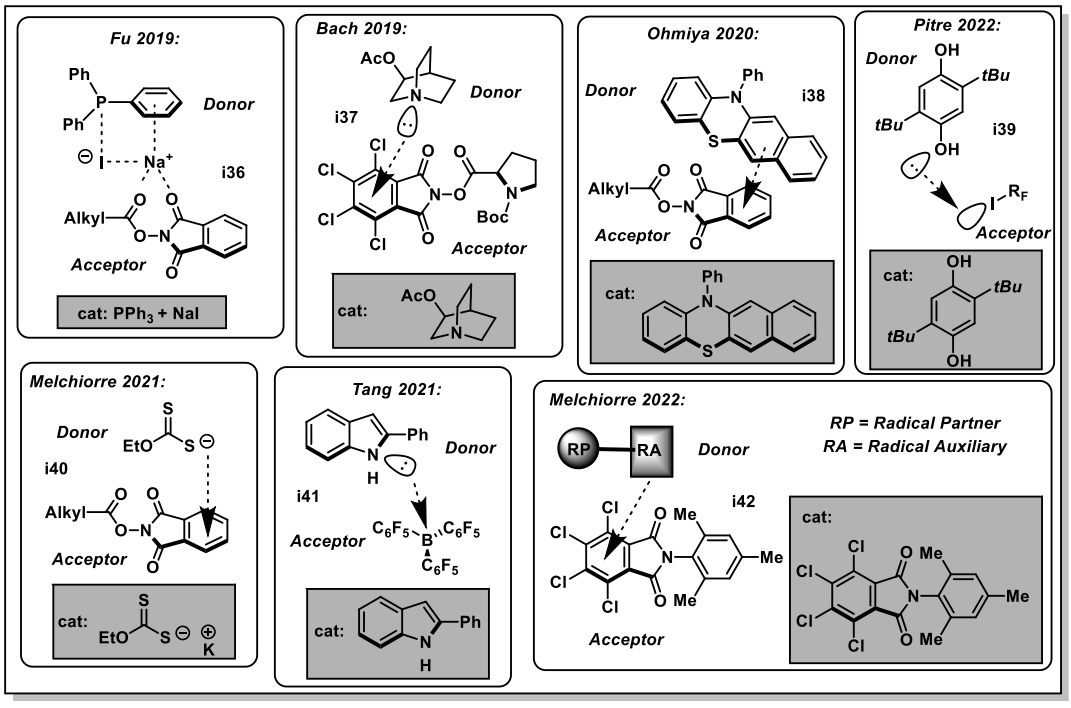
1.3.4. Employment of Catalytic Donors or Acceptors in Light-mediated Electron Donor−Acceptor Complex

Modern-day EDA complex photochemistry explores myriad ways to trigger the reactivity of compounds that generally do not absorb light in the visible region. The execution of donor and acceptor strategies has expanded the scope of radical reactivity, that might be inaccessible via thermal or other traditional methods. However, the main limitations of conventional EDA-guided synthetic transformations are the requirement of stoichiometric amounts of specially tailored donor and acceptor moiety, delimiting the overall scope of these techniques. A catalytic version of EDA complex formation, where either the donor or acceptor is used in a catalytic amount, is an ideal strategy to overcome the limitations associated with the previous EDA concept. Thus, substrates are no longer limited to structures embedded with specific moieties required for the complex formation, influencing the versatility of EDA-guided transformations. A general mechanism illustrates that this process starts with an EDA complex **i32** formation, which breaks down into reactive species like radical cations **i33** and radical anions **i34**. If the donor molecule **S43** is acting as a catalyst, it takes one electron from the reaction medium, which is released during the liberation of radical intermediate R from anionic species **i34**, and thus radical cation **i33** comes back into its initial D (**S43**) form. Finally, the in situ-generated radical species R can react with a substrate to deliver the product **P19** (Scheme 1.3.4.1).[46]



Scheme 1.3.4.1.: General Mechanism for Catalytic EDA-Guided Transformation.

Starting from the first catalytic EDA complex formation report from the Fu group in 2019,[47] this emerging field helped design several novel techniques by using free radical chemistry to construct value-added motifs (Scheme 1.3.4.2).[47] Apart from these methods, catalytic intermediates in EDA complex production, such as organocatalytically produced intermediates based on enamine or iminium ions or intermediates formed from *N*-heterocyclic carbene catalysts served as potent candidates to enrich the synthetic chemistry arena.[48]



Scheme 1.3.4.2: Selected Examples for Catalytic EDA-Complex.

1.4. Summary

Based on precedence literature, this chapter provides a brief introduction about the historical background, category, and the activation mode associated with asymmetric organocatalysis as well as modern-day photochemistry. Asymmetric organocatalysis area produced highly enantioselective compounds of therapeutic and biological significance. The logical design of catalysts from naturally occurring molecules and their steric bulkiness have remained key features of these techniques. Most of the organocatalysis reactions follow a polar pathway. However, some method also deals with radical species to achieve molecular complexity. On the other hand, a modernized technique such as visible-light-driven photochemistry has gathered increasing research interest from the synthetic community due to its great advantages under user-friendly conditions. This field majorly deals with highly reactive species like radicals, carbene, nitrenes, etc., to participate in numerous unconventional bond-forming events.

1.5. References:

1. Ahrendt, K. A.; Borths, C. J.; MacMillan, D. W. C. New Strategies for Organic Catalysis: The First Highly Enantioselective Organocatalytic Diels−Alder Reaction. *J. Am. Chem. Soc.* **2000**, *122*, 4243–4244.
2. List, B. Introduction: Organocatalysis *Chem. Rev.* **2007**, *107*, 5413–5415.
3. Liebig, J. von On the formation of oxamide from cyanide. *Ann. Pharm.* **1860**, *113*, 246–247.
4. Langenbeck, W. About organic catalysts. III. The formation of oxamide from cyanogen in the presence of aldehydes. *Liebigs Ann. Chem.* **1929**, *469*, 16–25.
5. Knoevenagel, E. On a method of preparation of the benzylidene acetoacetic ester. *Ber. Dtsch. Chem. Ges.* **1896**, *29*, 172–174.
6. Bredig, G.; Fiske, P. S. Catalyst-mediated asymmetric synthesis. *Biochem. Z.* **1912**, *46*, 7–23.
7. Pracejus, H. Organic Catalysts, LXI. Asymmetric syntheses with ketenes, I. Alkaloid-catalyzed asymmetric syntheses of α-phenylpropionic acid esters. *Liebigs Ann. Chem.* **1960**, *634*, 9–22.
8. Eder, U.; Sauer, G.; Wiechert, R. New Type of Asymmetric Cyclization to Optically Active Steroid CD Partial Structures. *Angew. Chem. Int. Ed.* **1971**, *10*, 496–497.
9. Hajos, Z. G.; Parrish, D. R. Asymmetric synthesis of bicyclic intermediates of natural product chemistry. *J. Org. Chem.* **1974**, *39*, 1615–1621.
10. a) Wynberg, H.; Helder, R. Asymmetric induction in the alkaloid-catalysed Michael reaction. *Tetrahedron Lett.* **1975**, *16*, 4057–4060; b) Helder, R.; Hummelen, J.; Laane, R. W. P. M.; Wiering, J. S.; Wynberg, H. Catalytic asymmetric induction in oxidation reactions. The synthesis of optically active epoxides. *Tetrahedron Lett.* **1976**, *17*, 1831–1834; c) Hiemstra, H.; Wynberg, H. Addition of aromatic thiols to conjugated cycloalkenones, catalyzed by chiral .beta.-hydroxy amines. A mechanistic study of homogeneous catalytic asymmetric synthesis. *J. Am. Chem. Soc.* **1981**, *103*, 417–430.
11. a) Dolling, U. H.; Davis, P.; Grabowski, E. J. J. Efficient catalytic asymmetric alkylations. 1. Enantioselective synthesis of (+)-indacrinone via chiral phase-transfer catalysis. *J. Am. Chem. Soc.* **1984**, *106*, 446–447; b) O'Donnell, M. J.; Bennett, W.; Wu, D S. The stereoselective synthesis of. alpha.-amino acids by phase-transfer catalysis. *J. Am. Chem. Soc.* **1989**, *111*, 2353–2355.
12. Sigman, M. S.; Jacobsen, E. N. Schiff Base Catalysts for the Asymmetric Strecker Reaction Identified and Optimized from Parallel Synthetic Libraries. *J. Am. Chem. Soc.* **1998**, *120*, 4901–4902.

13. Miller, S. J.; Copeland, G. T.; Papaioannou, N.; Horstmann, T. E.; Ruel, E. M. Kinetic Resolution of Alcohols Catalyzed by Tripeptides Containing the N-Alkylimidazole Substructure. *J. Am. Chem. Soc.* **1998**, *120*, 1629–1630.
14. Ruble, J. C.; Latham, H. A.; Fu, G. C. Effective Kinetic Resolution of Secondary Alcohols with a Planar−Chiral Analogue of 4-(Dimethylamino)pyridine. Use of the Fe(C_5Ph_5) Group in Asymmetric Catalysis. *J. Am. Chem. Soc.* **1997**, *119*, 1492–1493.
15. a) Tu, Y.; Wang, Z.-X.; Shi, Y. An Efficient Asymmetric Epoxidation Method for trans-Olefins Mediated by a Fructose-Derived Ketone*J. Am. Chem. Soc.* **1996**, *118*, 9806–9807; b) Yang, D.; Yip, Y.-C.; Tang, M.-W.; Wong, M.-K.; Zheng, J.-H.; Cheung, K.-K. A C2 Symmetric Chiral Ketone for Catalytic Asymmetric Epoxidation of Unfunctionalized Olefins. *J. Am. Chem. Soc.* **1996**, *118*, 491–492.
16. Denmark, S. E.; Winter, S. B. D.; Su, X.; Wong, K.-T. Chemistry of Trichlorosilyl Enolates. 1. New Reagents for Catalytic, Asymmetric Aldol Additions. *J. Am. Chem. Soc.* **1996**, *118*, 7404–7405.
17. Ooi, T.; Kameda, M.; Maruoka, K. Molecular Design of a C2-Symmetric Chiral Phase-Transfer Catalyst for Practical Asymmetric Synthesis of α-Amino Acids. *J. Am. Chem. Soc*. **1999**, *121*, 6519–6520.
18. a) List, B.; Lerner, R. A.; Barbas III, C. F. Proline-Catalyzed Direct Asymmetric Aldol Reactions. *J. Am. Chem. Soc*. **2000**, *122*, 2395–2396; b) Ahrendt, K. A.; Borths, C. J.; MacMillan, D. W. C. New Strategies for Organic Catalysis: The First Highly Enantioselective Organocatalytic Diels−Alder Reaction. *J. Am. Chem. Soc.* **2000**, *122*, 4243–4244; c) Bøgevig, A.; Kumaragurubaran, N.; Jørgensen, K. A. Direct catalytic asymmetric aldol reactions of aldehydes. *Chem. Commun.*, **2002**, 620-621.
19. a) Mancheño, O. G.; Waser, M. Recent Developments and Trends in Asymmetric Organocatalysis. *Eur. J. Org. Chem.* **2023**, *26*, e202200950; b) Alema´n, J.; Cabrera, S. *Chem. Soc. Rev.*, **2013**, *42*, 774--793
20. a) Chen, D.-F.; Han, Z.-Y.; Zhou, X.-L.; Gong, L.-Z. Asymmetric Organocatalysis Combined with Metal Catalysis: Concept, Proof of Concept, and Beyond. *Acc. Chem. Res.* **2014**, *47*, 2365–2377; b) Chen, D.-F.; Gong, L.-Z. Molecular Design of a C2-Symmetric Chiral Phase-Transfer Catalyst for Practical Asymmetric Synthesis of α-Amino Acids. *J. Am. Chem. Soc.* **2022**, *144*, 2415–2437; c) Roy, S., Paul, H., Chatterjee I., Light-Mediated Aminocatalysis: The Dual-Catalytic Ability Enabling New Enantioselective Route *Eur. J. Org. Chem.* **2022**, *25*, e202203428; d) Jiao, K.-J.; Wang, Z.-H.; Ma, C.; Liu, H.-L.; Cheng, B., Mei, T.-S. The Applications of Electrochemical Synthesis in Asymmetric Catalysis, *Chem. Catal*., **2022**, *2*, 3019–3047.
21. Seayada, J.; List, B. Asymmetric organocatalysis. *Org. Biomol. Chem.*, **2005**, *3*, 719-724.

22. Melchiorre, P.; Marigo, M.; Carlone, A.; Bartoli, G. Asymmetric Aminocatalysis—Gold Rush in OrganicChemistry. *Angew. Chem. Int. Ed.* **2008**, *47*, 6138–6171.
23. Que, Y.; He, H. Advances in N-Heterocyclic Carbene Catalysis for Natural Product Synthesis. *Eur. J. Org. Chem.* **2020**, *2020*, 5917–5925.
24. Parvin, T.; Yadava, R.; Choudhury, L. H. Recent applications of thiourea-based organocatalysts in asymmetric multicomponent reactions (AMCRs) *Org. Biomol. Chem.*, **2020**, *18*, 5513–5532.
25. Corte, X. d.; Marigorta, E. M. d.; Palacios, F.; Vicario, J.; Maestro, A. An overview of the applications of chiral phosphoric acid organocatalysts in enantioselective additions to C=O and C=N bonds. *Org. Chem. Front.*, **2022**, *9*, 6331.
26. Hölz, K.; Lietard, J.; Somoza, M. M. *ACS Sustainable Chem. Eng.* **2017**, *5*, 828−834.
27. Marzo, L.; Pagire, S. K.; Reiser, O.; König, B. Visible-Light Photocatalysis: Does It Make a Difference in Organic Synthesis? *Angew. Chem. Int. Ed.* **2018**, *57*, 10034–10072.
28. Hedstrand, D. M.; Kruizinga, W. M.; Kellogg, R. M. Light induced and dye accelerated reductions of phenacyl onium salts by 1,4-dihydropyridines. *Tetrahedron Lett.* **1978**, *19*, 1255−1258.
29. Romero, N. A.; Nicewicz, D. A. Organic Photoredox Catalysis. *Chem. Rev*. **2016**, *116*, 10075−10166.
30. a) Mulliken, R. S. Structures of Complexes Formed by Halogen Molecules with Aromatic and with Oxygenated Solvents. *J. Am. Chem. Soc.* **1950**, *72*, 600−608; b) Mulliken, R. S. Molecular Compounds and their Spectra. II. *J. Am. Chem. Soc.* **1952**, *74*, 811−824; c) Mulliken, R. S. Molecular Compounds and their Spectra. III. The Interaction of Electron Donors and Acceptors. *J. Phys. Chem.* **1952**, *56*, 801−822.
31. a) Rathore, R.; Kochi, J. K. Donor/Acceptor Organizations and the Electron-Transfer Paradigm for Organic Reactivity. *Adv. Phys. Org. Chem.* **2000**, *35*, 193−318; b) Cantacuzene, D.; Wakselman, C.; Dorme, R. Condensation of` Perfluoroalkyl Iodides with Unsaturated Nitrogen Compounds. *J. Chem. Soc., Perkin Trans. 1* **1977**, 1365−1371; c) Bunnett, J. F. Aromatic Substitution by the SRN1 Mechanism. *Acc. Chem. Res.* **1978**, *11*, 413−420; d) Russell, G. A.; Wang, K. Homolytic Alkylation of Enamines by Electrophilic Radicals. *J. Org. Chem.* **1991**, *56*, 3475−3479; e) Wade, P. A.; Morrison, H. A.; Kornblum, N. The Effect of Light on Electron-Transfer Substitution at a Saturated Carbon Atom. *J. Org. Chem*. **1987**, *52*, 3102−3107.
32. a) Lima, C. G. S.; Lima, T. d. M.; Duarte, M.; Jurberg, I. D.; Paixaõ M. W. Organic Synthesis Enabled by Light-Irradiation of EDA Complexes: Theoretical Background and Synthetic Applications. *ACS Catal.* **2016**, *6*, 1389–1407; b) Crisenza, G. E. M.; Mazzarella, D.; Melchiorre, P. Synthetic Methods Driven by the Photoactivity of Electron Donor–Acceptor Complexes *J. Am. Chem. Soc*. **2020**, *142*, 5461−5476.

33. Gallo, R. D. C.; Cariello, G.; Goulart, T. A. C.; Jurberg, I. D. Visible light-mediated photolysis of organic molecules: the case study of diazo compounds. *Chem. Commun.* **2023**, *59*, 7346–7360.

34. Chauhan, P.; Kaya, U.; Enders, D. Advances in Organocatalytic 1,6-Addition Reactions: Enantioselective Construction of Remote Stereogenic Centers, *Adv. Synth. Catal.* **2017**, *359*, 888–912.

35. Fuson, R. C. The Principle of Vinylogy. *Chem. Rev.*, **1935**, *16*, 1.

36. Jurberg, I. D.; Chatterjee, I. Tannert, R.; Melchiorre, P. When asymmetric aminocatalysis meets the vinylogy principle. *Chem. Commun.*, **2013**, *49*, 4869-4883.

37. Bernardi, L.; Cantarero, J. L.; Niess, B.; Jørgensen, K. A. Organocatalytic Asymmetric 1,6-Additions of β-Ketoesters and Glycine Imine *J. Am. Chem. Soc.* **2007**, *129*, 5772–5778.

38. (a) Ren, Y.-Y.; Zhu, S.-F.; Zhou, Q.-L. Chiral proton-transfer shuttle catalysts for carbene insertion reactions. *Org. Biomol. Chem.* **2018**, *16*, 3087–3094. (b) Empel, C.; Koenigs, R. M. Sustainable Carbene Transfer Reactions with Iron and Light. *Synlett* **2020**, 1929–1934.

39. (a) Doyle, M. P.; Duffy, R.; Ratnikov, M.; Zhou, L. Catalytic carbene insertion into C−H bonds. *Chem. Rev.* **2010**, *110*, 704. (b) Ford, A.; Miel, H.; Ring, A.; Slattery, C. N.; Maguire, A. R.; McKervey, M. A. Modern Organic Synthesis with α-Diazocarbonyl Compounds. *Chem. Rev.*, **2015**, *115*, 9981.

40.) Bamford, W. R.; Stevens, T. S. The Decomposition of Toluene-p-sulphonylhydrazones by Alkali. *J. Chem. Soc.* **1952**, 4735.

41. a) Ciszewski, Ł. W.; Rybicka-Jasińska, K.; Gryko, D. Recent developments in photochemical reactions of diazo compounds. *Org. Biomol. Chem.*, **2019**, *17*, 432–448; b) Yang, Z.; Stivanin, M. L.; Jurberg, I. D.; Koenigs R. M. Visible light-promoted reactions with diazo compounds: a mild and practical strategy towards free carbene intermediates. *Chem. Soc. Rev.*, **2020**, *49*, 6833–6847; c) Durka, J.; Turkowska, J.; Gryko, D.; Lightening Diazo Compounds? *ACS Sustainable Chem. Eng.*, **2021**, *9*, 8895−8918.

42. Brook, A. G.; Triphenylsilyl Phenyl Ketone, *J. Am. Chem. Soc.*, **1957**, *79*, 4373–4375.

43. Priebbenowa, D. L. Silicon-Derived Singlet Nucleophilic Carbene Reagents in Organic Synthesis. *Adv. Synth. Catal.* **2020**, *362*, 1927–1946.

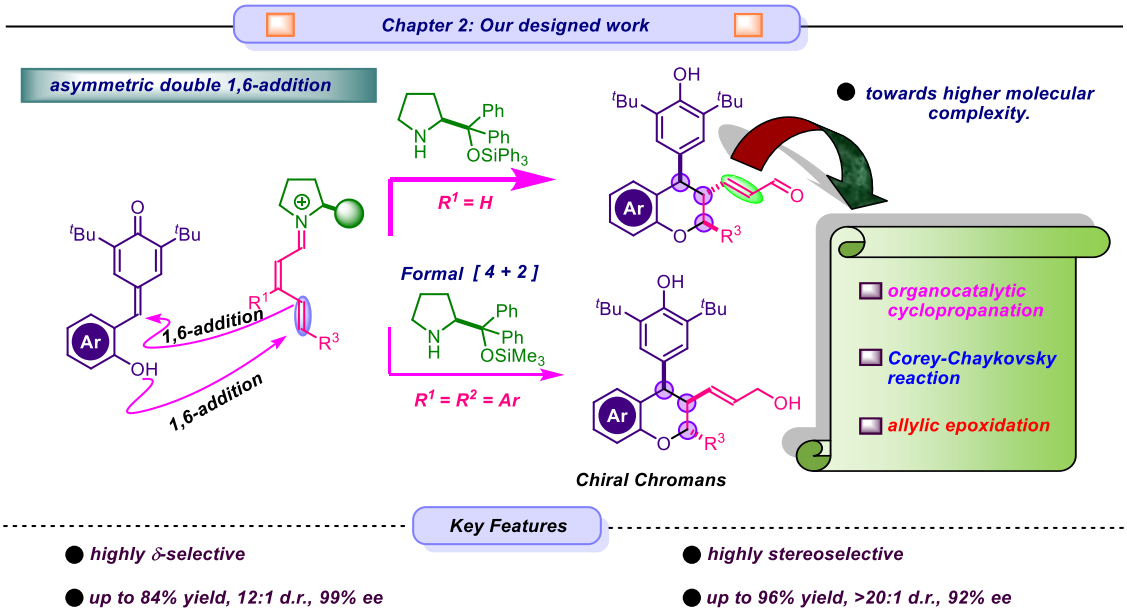
44. Hong, W. P.; Lim, H. N.; Shin, I. Recent progress and perspectives in photo-induced organic reactions of acylsilanes. *Org. Chem. Front.*, **2023**, *10*, 819–836.

45. Arduengo, A. J.; Harlow, R. L.; Kline, M. A stable crystalline carbene. *J. Am. Chem. Soc.* **1991**, *113*, 361–363.

46. Tasnim, T.; Ayodele, M. J.; Pitre, S. P. Recent Advances in Employing Catalytic Donors and Acceptors in Electron Donor−Acceptor Complex Photochemistry *J. Org. Chem.* **2022**, *87*, 10555−10563.
47. Fu, M.-C.; Shang, R.; Zhao, B.; Wang, B.; Fu, Y. Photocatalytic Decarboxylative Alkylations Mediated by Triphenylphosphine and Sodium Iodide. *Science* **2019**, *363*, 1429−1434.
48. a) Arceo, E.; Bahamonde, A.; Bergonzini, G.; Melchiorre, P. Enantioselective Direct *α*-Alkylation of Cyclic Ketones by Means of Photo-organocatalysis. *Chem. Sci.* **2014**, *5*, 2438−2442; b) Morack, T.; Mück-Lichtenfeld, C.; Gilmour, R. Bioinspired Radical Stetter Reaction: Radical Umpolung Enabled by Ion-Pair Photocatalysis. *Angew. Chem., Int. Ed.* **2019**, *58*, 1208−1212; c) Cao, Z.-Y.; Ghosh, T.; Melchiorre, P. Enantioselective Radical Conjugate Additions Driven by a Photoactive Intramolecular Iminiumion-based EDA Complex. *Nat. Commun.* **2018**, *9*, 3274; d) Goti, G.; Bieszczad, B.; Vega-Peñaloza, A.; Melchiorre, P. Stereocontrolled Synthesis of 1,4-Dicarbonyl Compounds by Photochemical Organocatalytic Acyl Radical Addition to Enals. *Angew. Chem., Int. Ed.* **2019**, *58*, 1213−1217; e) Rodriguez, R. I.; Sicignano, M.; Aleman, J. Fluorinated Sulfinates as Source of Alkyl Radicals in the Photo-Enantiocontrolled *β*-Functionalization of Enals. *Angew. Chem., Int. Ed.* **2022**, *61*, e202112632; f) Jin, S.; Sui, X.; Haug, G. C.; Nguyen, V. D.; Dang, H. T.; Arman, H. D.; Larionov, O. V. N-Heterocyclic Carbene-Photocatalyzed Tricomponent Regioselective 1,2-Diacylation of Alkenes Illuminates the Mechanistic Details of the Electron Donor−Acceptor Complex-Mediated Radical Relay Processes. *ACS Catal.* **2022**, *12*, 285−294.

Chapter 2

Asymmetric Organocatalytic Double 1,6-Addition: Rapid Access to Chiral Chromans with Molecular Complexity



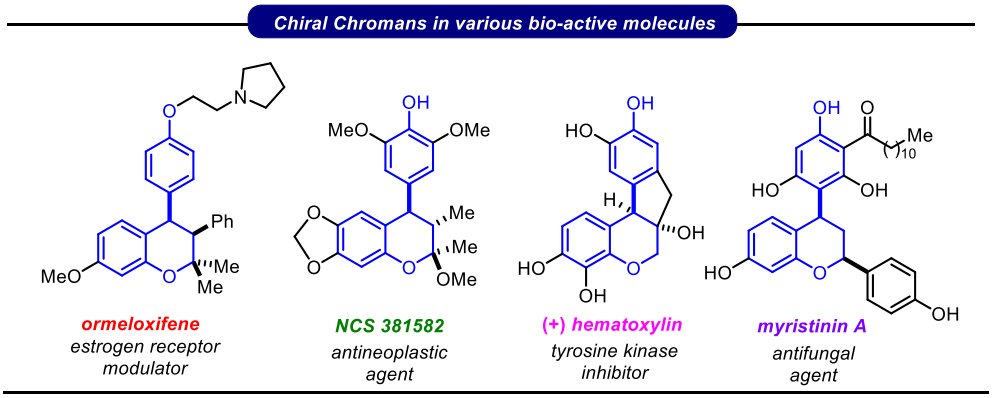
❖ This work was published in Organic Chemistry Frontiers (a journal of RSC). Please see the citation as: "Roy, S.; Pradhan, S.; Kumar, K.; Chatterjee, I. *Org. Chem. Front.*, **2020**, *7*, 1388–1394.

2. Abstract

In this chapter, an organocatalytic cascade vinylogous double 1,6-addition strategy for the synthesis of chiral chroman derivatives is reported. The cascade reaction follows *oxa*-Michael/1,6-addition reactions between *ortho*-hydroxyphenyl-substituted *para*-quinone methides and 2,4-dienal derivatives to deliver chroman derivatives with excellent yields (up to 96%) and stereoselectivities (up to >20:1 d.r., >99% *ee*). The chiral secondary amine-based Jørgensen-Hayashi organocatalysts are shown to catalyze the transformation of unbiased 2,4-dienals under mild reaction conditions with exclusive *δ*-site selectivity and high control over enantioselectivity at a remote position. The synthetic transformations of the products ensure molecular complexity with a great level of enantio control.

2.1. Introduction

As discussed in chapter 1, asymmetric organocatalytic cascade reactions in recent years have drawn immense attention due to its ability to generate molecular complexity in a rapid and atom-economical fashion. The utilization of this strategy for the generation of chiral molecules is an essential goal in modern synthetic chemistry.[1] Chromans are such an imperative target molecule exhibiting in various natural products and biologically active molecules (Scheme 2.1.1).[2] Targeting such a privileged scaffold, we envisioned to design the possibility of an organocatalytic cascade reaction between unbiased α,β,γ,δ-unsaturated enals and *ortho*-hydroxyphenyl-substituted *para*-quinone methides (*p*-QMs).

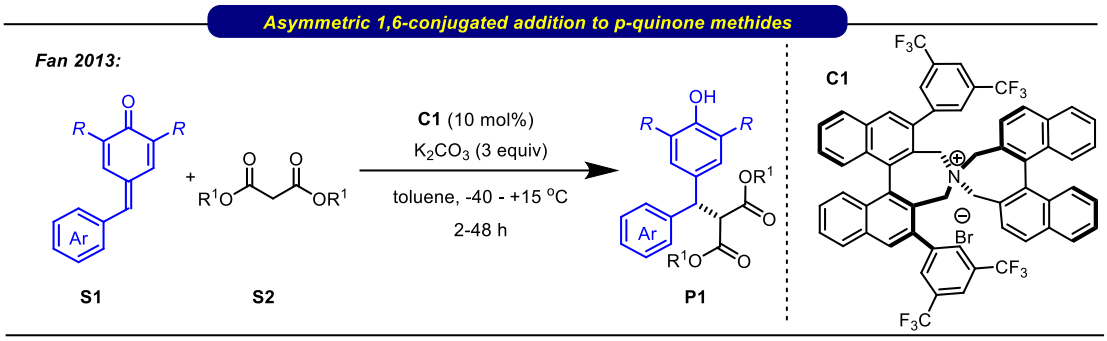


Scheme 2.1.1: Chiral Chromans Containing Bio-active Molecules

p-QMs in recent years have immerged as a potential Michael acceptor for developing various 1,6-addition protocols using different nucleophiles.

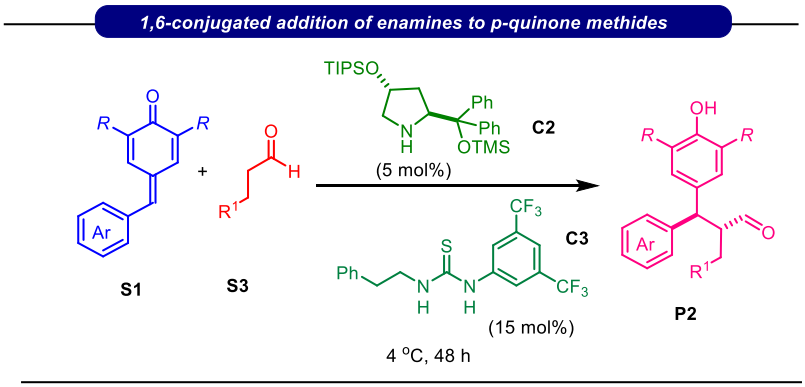
In 2013, the group of Fan developed the first asymmetric 1,6-addition of malonates **S2** to *p*-QMs **S1** under phase-transfer catalysis.[3] A series of synthetically beneficial, functionalized diarylalkanes **P1** were accomplished with good yields and stereocontrol, thus providing an

alternative method to synthesize enantioselective, functionalized diarylmethine stereogenic centers (Scheme 2.1.2).



Scheme 2.1.2: Fan's 1,6-Conjugate Addition to *para*-Quinone Methides.

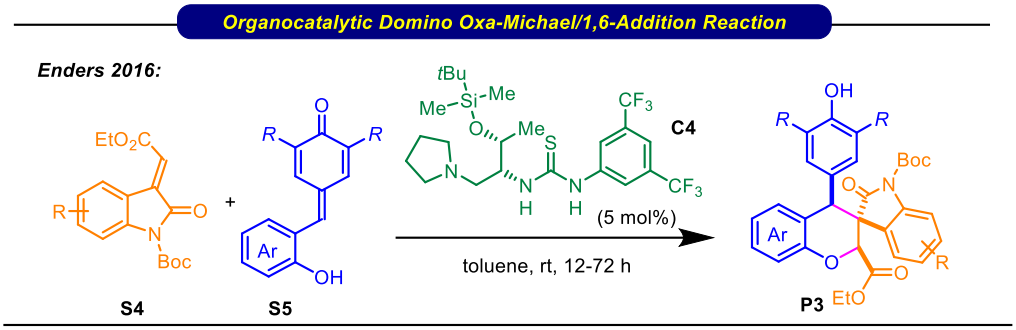
Following this, the Jørgensen group elegantly described a secondary amine-catalyzed α-alkylation of aldehydes **S3**.[4] For the first time, they utilized enamine-activated aldehydes for a 1,6-addition to *p*-quinone methides **S1**, furnishing α-diarylmethine-substituted aldehydes **P2** having two contiguous stereocenters. By employing new chiral secondary amine catalyst **C2** and a **C3** as a co-catalyst, a broad range of substrates were synthesized with a good level of diastereo- and enantio- control (Scheme 2.1.3).



Scheme 2.1.3: Jørgensen's strategy for the addition of enamine-activated aldehydes to *p*-quinone methides.

From then onwards, various metal and metal-free strategies were developed based on 1,6-addition to *p*-QMs.[5] Comparatively, *ortho*-hydroxyphenyl-substituted *p*-QMs have been less-explored for developing catalytic cascade approaches.

In 2016, Enders and co-workers developed an asymmetric cascade oxa-Michael/1,6-addition protocol using *ortho*-hydroxyphenyl-substituted *p*-QMs **S5** and isatin derivatives **S4** to synthesize chroman derivatives **P3** in the presence of bifunctional thiourea organocatalyst **C4**.[6] This process fabricates three vicinal stereogenic centers containing chroman derivatives in excellent yields and stereo-selectivity (Scheme 2.1.4).

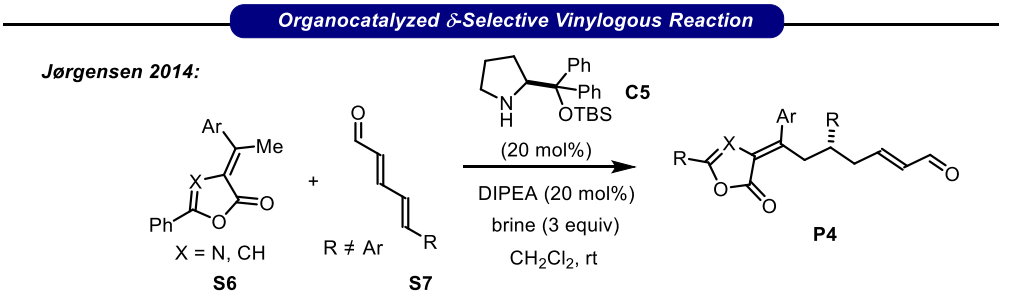


Scheme 2.1.4: Ender's Asymmetric Synthesis of Chromans Bearing Oxindole Scaffolds.

Later, several groups integrated this strategy to develop numerous cascade reactions.[7] Despite this progress in this venture, there are still rooms to design molecular complexity.

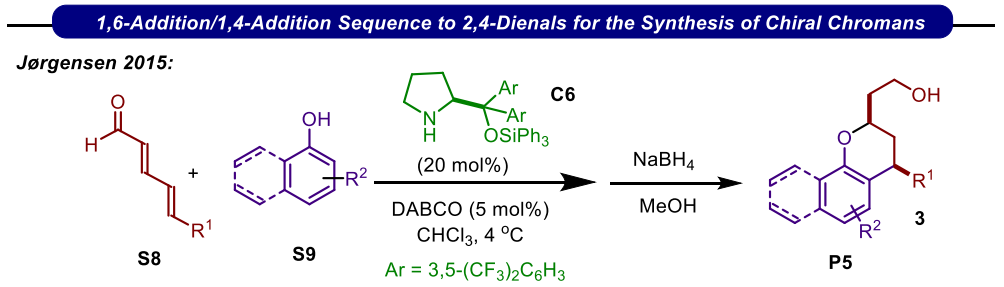
The ability of chiral secondary amines to integrate orthogonal activation of carbonyls has been successfully used to functionalize α- and β- position of carbonyls.[8] To translate this reactivity towards vinylogous direction has always been a challenging task.[9] Our thought process comprises of 1,6-addition by the hydroxyl group with exclusive δ-site selectivity to vinylogous iminium ion generated by the condensation of chiral secondary amine and 2,4-dienal followed by a cascade intramolecular vinylogous dienamine based 1,6-addition to *p*-QMs for constructing the chroman scaffolds.[10]

In 2013, the Jørgensen group investigated the reactivity of linear unbiased 2,4-dienals **S7** with unsaturated γ-butyrolactams **S6** under secondary amine catalysis to perform a vinylogous 1,6-addition. The resultant products **P4** have a remote stereogenic center that is six bonds away from the stereocenter of the catalyst, resulting in high enantiocontrol and complete control of the double bond configuration (Scheme 2.1.5).



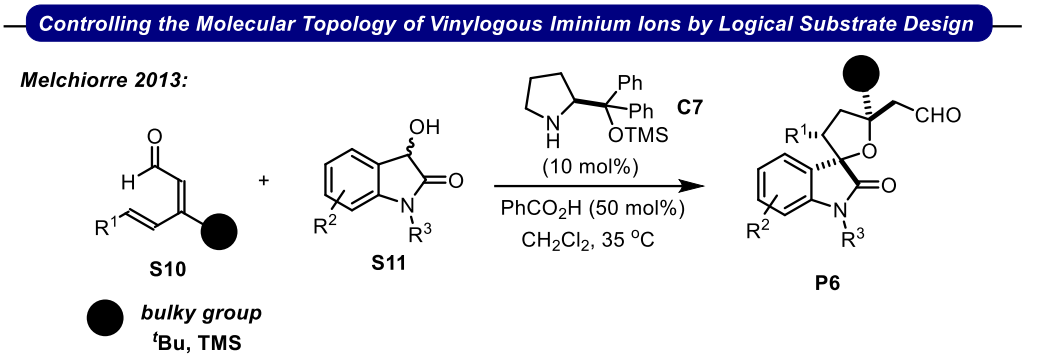
Scheme 2.1.5: Jørgensen's 1,6 addition of Olefinic Lactones with 2,4-Dienals.

Later in 2015, same group discovered a novel asymmetric 1,6-addition/1,4-addition domino sequence of 2,4-dienals **S8** with various phenols **S9** in the presence of a modified Jørgensen-Hayashi catalyst **C6**. According to DFT calculation, the Friedel-Crafts addition step is under thermodynamic control and drives the domino sequence, leading to a wide range of chiral chroman derivatives with excellent enantiocontrol (Scheme 2.1.6).



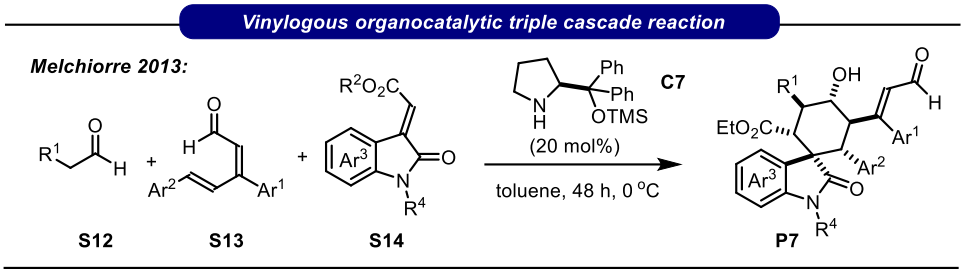
Scheme 2.1.6: Jørgensen's 1,6-Friedel–Crafts/1,4-*oxa*-Michael Cascade Strategy.

Apart from these reports, in 2013, Melchiorre et al. reported an aminocatalytic asymmetric 1,6-addition to linear β,δ-substituted 2,4-dienals **S10** by using 3-hydroxy-2-oxindole **S11** as a reacting partner to fabricate valuable tetrahydrofuran spirooxindole derivatives **P6**. The presence of a bulky group at β-position of the 2,4-dienals **S10** caused a significant amount of asymmetric induction in the synthesis of spirooxindole **P6** by increasing repulsive interactions with the catalyst framework (Scheme 2.1.7).



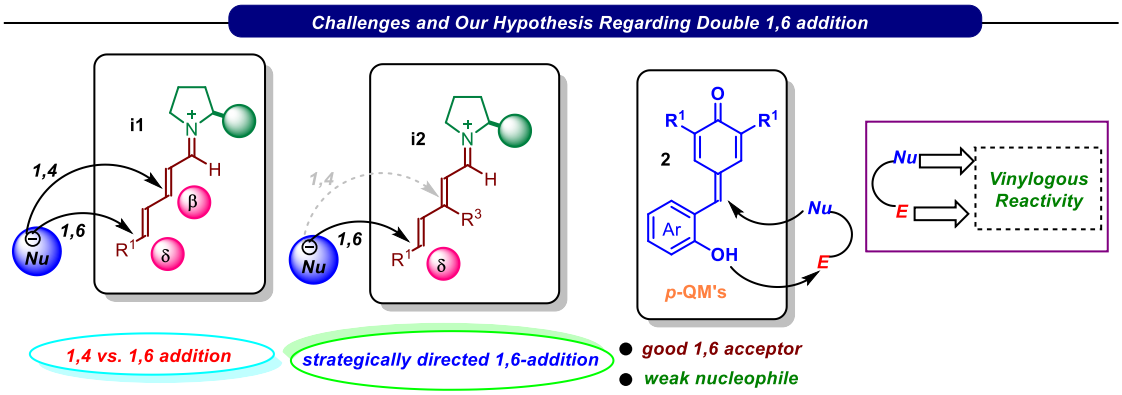
Scheme 2.1.7: Melchiorre's Strategy for the Synthesis of Tetrahydrofuran Spirooxindole Derivatives via Selective 1,6 Addition.

Following this, the same group demonstrated an aminocatalytic triple cascade reaction, by using linear α,β,γ,δ-unsaturated aldehydes **S13**, oxindole derivatives **S14**, and aliphatic aldehydes **S12** as reacting partners, resulting spiro-oxindolic cyclohexane derivatives **P7**. This domino process proceeds via amino-catalyzed Michael addition/1,6-addition/vinylogous aldolization sequence with a combination of two intermolecular and one intramolecular bond formation, leading to six contiguous stereogenic centers with high efficiency (Scheme 2.1.8).



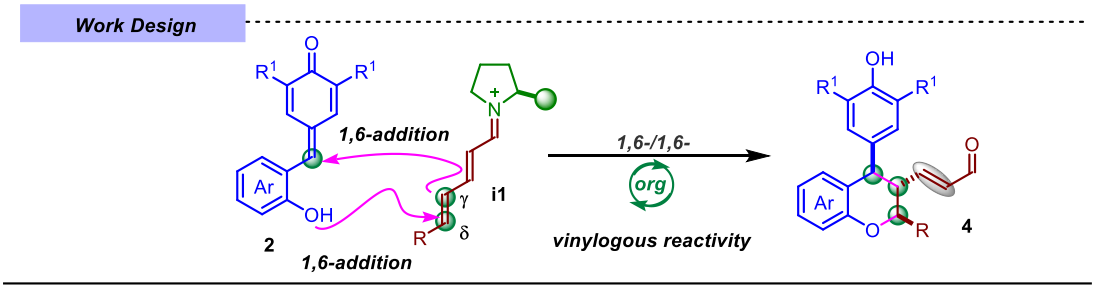
Scheme 2.1.8: Melchiorre's Triple Cascade Strategy Forging Six Stereocenter Containing Spiro-Oxindolic Cyclohexanes the via Selective 1,6 Addition.

From the above-discussed literature reports, it is well evident that there are certain number of challenges associated with envisaged double 1,6-addition process: (1) site-selectivity: β-vs δ-, as organocatalytic 1,4-addition is generally favouring over 1,6-addition. Except for a couple of examples from the group of Jørgensen where linear unbiased 2,4-dienals were used (Scheme 1c),[11] in most of the cases, 1,6-addition is strategically directed by suppressing the 1,4-addition using β-substituted 2,4-dienals;[12] (2) control over enantioselectivity at a remote δ-position, far from the catalyst binding site; (3) control over the geometry of vinylogous dienamine based 2nd 1,6-addition; (4) to overcome the low nucleophilicity of *ortho*-hydroxyphenyl-substituted *p*-QMs. (Scheme 2.1.9).



Scheme 2.1.9: Challenges Associated with Double 1,6 Addition.

Keeping in mind all the challenges, possibilities, and previous reports we hypnotised that first 1,6-addition by the hydroxyl group with exclusive δ-site selectivity to vinylogous iminium ion **i1** generated by the condensation of chiral secondary amine and 2,4-dienal followed by a cascade intramolecular vinylogous dienamine based second 1,6-addition to *p*-QMs **2** can construct the chroman scaffolds **4** (Scheme 2.1.10).



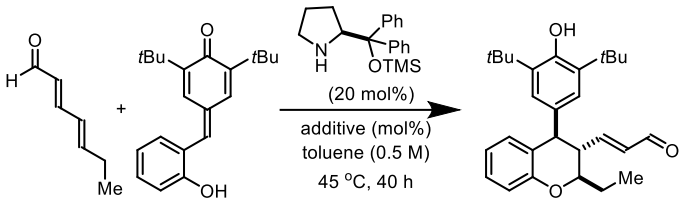
Scheme 2.1.10: Chapter 2: Our Proposed Working Hypothesis.

2.2. Result and Discussion

2.2.1 Optimization of the Reaction Condition

We commenced our study by reacting (2*E*,4*E*)-hepta-2,4-dienal **1a** as the model substrate with *ortho*-hydroxyphenyl-substituted *p*-QM **2a** in toluene (0.5 M) in the presence of **3a** as catalyst[13] at 45 °C for 40 h (Table 1). In the presence of various additives (20 mol%), irrespective of the nature of the base, we observed the product formation with moderate to good yield but with poor diastereo- and enantioselectivity. Increasing the additive loading (40 mol% Et_3N) did not improve much the reaction outcome (Table 1, entry 18).

2.2.1. Chapter 2: Table 1: Screening of Various Additives.



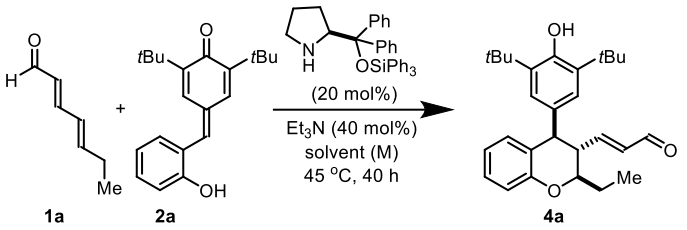
1a **2a** **4a**

Entry	1a/2a	Additive (mol%)	Yield (%)[b]	d.r.[c]	*ee* (%)[d]
1	1/2	$PhCO_2H$ (20)	42	2:1	-
2	1/1.2	$PhCO_2H$ (20)	23	2:1	71
3	2/1	$PhCO_2H$ (20)	28	2.5:1	67
4	2/1	4-NO_2-BA (20)	24	3:1	-
5	1/2	DABCO (20)	39	1.5:1	70
6	2/1	DABCO (20)	23	1.2:1	65
7	2/1	DABCO (40)	47	2:1	-
8	2/1	DIPEA (20)	58	1.2:1	71
9	1/1	DIPEA (40)	60	1:1	64
10	1/1.2	DIPEA (40)	53	1.1:1	61
11	1/1.5	DBU (20)	52	1.2:1	-
12	1/1.5	DBU (40)	60	1.5:1	62
13	1/1	DBU (40)	27	1.6:1	67
14	2/1	Et_3N (20)	44	1.4:1	60
15	1/1	Et_3N (40)	60	1.2:1	81
16	1/1	Et_3N (20)	68	1.2:1	-
17	1/1.5	Et_3N (40)	98	1:1:1	-
18	**2/1**	**Et_3N (40)**	**52**	**1.4:1**	**81**
19	1/1	Et_3N (100)	54	1:1	-

[a] unless untill mentioned all reactions were carried out in a 0.1 mmol scale by taking 1a (2.0 equiv) & 2a (1.0 equiv). [b] yield was measured by 1H-NMR analysis of the crude reaction mixture. [c] diastereomeric mixture measured by 1H-NMR analysis of the crude reaction mixture. [d] enantiomeric excess was measured by HPLC on a chiral stationary phase.

However, the reaction in the presence of catalyst **3c** having bulkier -$SiPh_3$ as protecting group resulted in a drastic improvement of the reactivity and selectivity as well delivering **4a** in 69% yield, 3:1 d.r. and 85% *ee* (Table 2, entry 1). To our delight, the variation of different solvents revealed that *o*-xylene worked as the best solvent to deliver the desired product **4a** in good yield and excellent diastereo- and enantioselectivity (Table 2, entry 12).

2.2.2. Chapter 2: Table 2: Screening of Various Solvents.

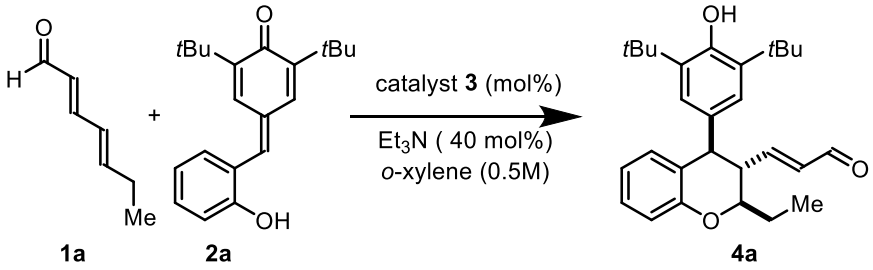


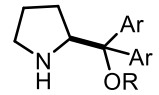
Entry	Solvent (M)	Yield (%)[b]	d.r.[c]	*ee* (%)[d]
1	toluene (0.5)	69	3:1	85
2	CH_2Cl_2 (0.5)	54	3.5:1	94
3	$CHCl_3$ (0.5)	60	2.5:1	85
4	CH_3CN (0.5)	42	1.2:1	-
5	THF (0.5)	63	1.8:1	92
6	Et_2O (0.5)	23	2.2:1	92
7	IPA (0.5)	21	4:1	-
8	benzene (0.5)	68	3:1	94
9	*p*-xylene (0.5)	74	2.5:1	92
10	*m*-xylene (0.5)	71	2.4:1	-
11	mesitylene (0.5)	69	2.5:1	-
12	***o*-xylene (0.5)**	**63**	**4.5:1**	**94**
13	*o*-xylene (0.25)	69	3:1	85
14	*o*-xylene (0.1)	68	3:1	85
15	*o*-xylene (0.5) brine (3 equiv.)	67	3.5:1	90

[a] unless untill mentioned all reactions were carried out in a 0.1 mmol scale by taking 1a (2.0 equiv) & 2a (1.0 equiv). [b] yield was measured by 1H-NMR analysis of the crude reaction mixture. [c] diastereomeric mixture measured by 1H-NMR analysis of the crude reaction mixture. [d] enantiomeric excess was measured by HPLC on a chiral stationary phase.

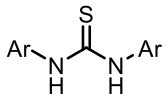
Lowering the reaction temperature to 10 ºC and prolonging reaction time further improved the reaction outcome (Table 3, entries 1-5). The catalyst loading and altering different other secondary amines as catalyst did not significantly improve the outcome (Table 3, entries 7–13). We choose Table 3, entry 8, as our optimized reaction condition for further screening of substrates.

2.2.3. Chapter 2: Table 3: Miscellaneous Optimization-1.



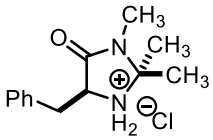


3a: Ar = Ph, R = $SiMe_3$
3b: Ar = 3,5-$(CF_3)_2$-C_6H_3, R = $SiMe_3$
3c: Ar = Ph, R = $SiPh_3$
3d: Ar = Ph, R = $Si(Me)_2{}^tBu$



3e

Ar = 3,5-$(CF_3)_2$-C_6H_3



3f

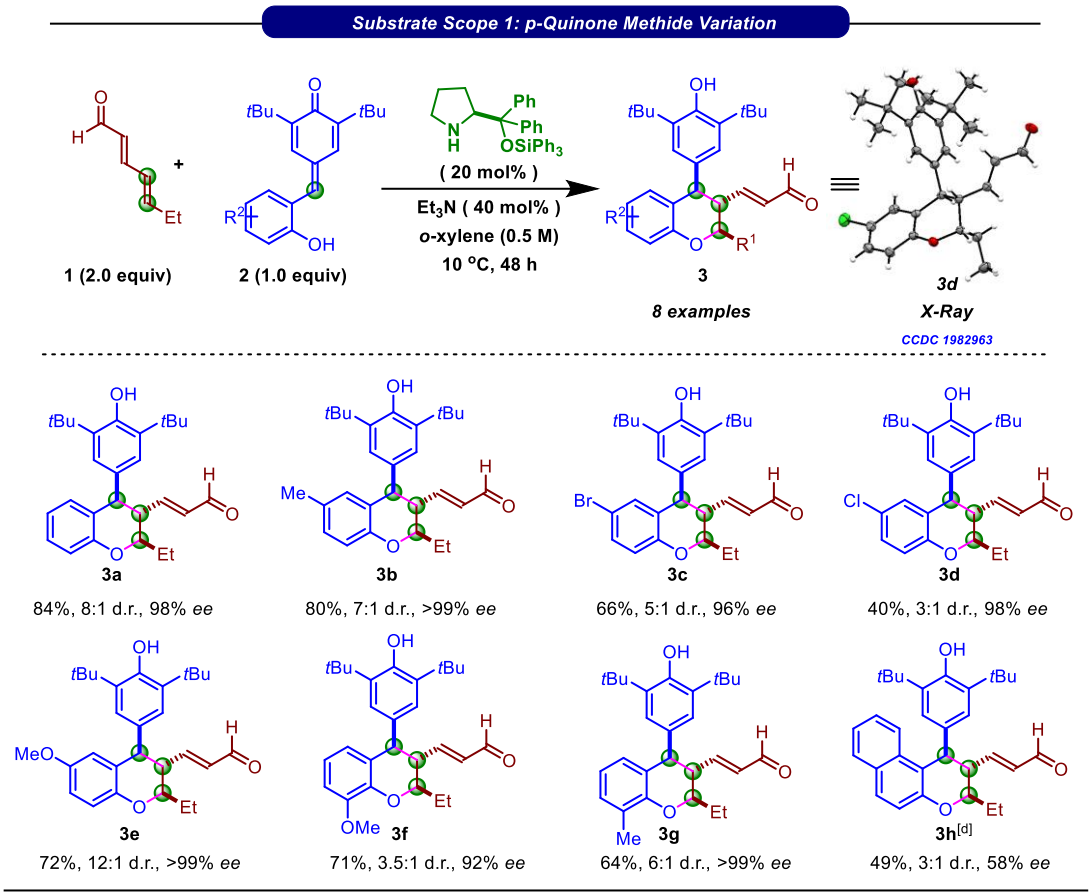
Entry	catalyst (mol%)	Temp. (°C)	Time (h)	Yield (%)[b]	d.r.[c]	*ee* (%)[d]
1	3c (20)	rt	40	67	2.5:1	88
2	3c (10)	10	40	68	2:1	93
3[e]	3c (10)	10	40	57	3.5:1	85
4	3c (20)	10	24	62	2.5:1	85
5	3c (20)	10	14	56	3:1	87
6	3a (20)	10	48	90	1.1:1	67
7[f]	3b (20)	10	48	36	-	-
8	**3c (20)**	**10**	**48**	**92(84)**	**8:1**	**98**
9	3d (20)	10	48	73	1.3:1	75
10	3e (20)	10	48	n.r	-	-
11	3f (20)	10	48	n.r	-	-
12	3c (20)	10	40	72	5:1	94
13	3c + 3e (20+30)	10	48	14	1:1	-

[a] unless untill mentioned all reactions were carried out in a 0.1 mmol scale by taking 1a (2.0 equiv) & 2a (1.0 equiv). [b] yield was measured by 1H-NMR analysis of the crude reaction mixture, isolated yield in parentheses. [c] diastereomeric mixture measured by 1H-NMR analysis of the crude reaction mixture. [d] enantiomeric excess was measured by HPLC on a chiral stationary phase. [e] 20 mol% Et_3N was used as an additive. [f] mixture of several isomers were found from 1H NMR analysis of crude reaction mixture.

2.2.2 Substrate Scope Evaluation for Chiral Chromans

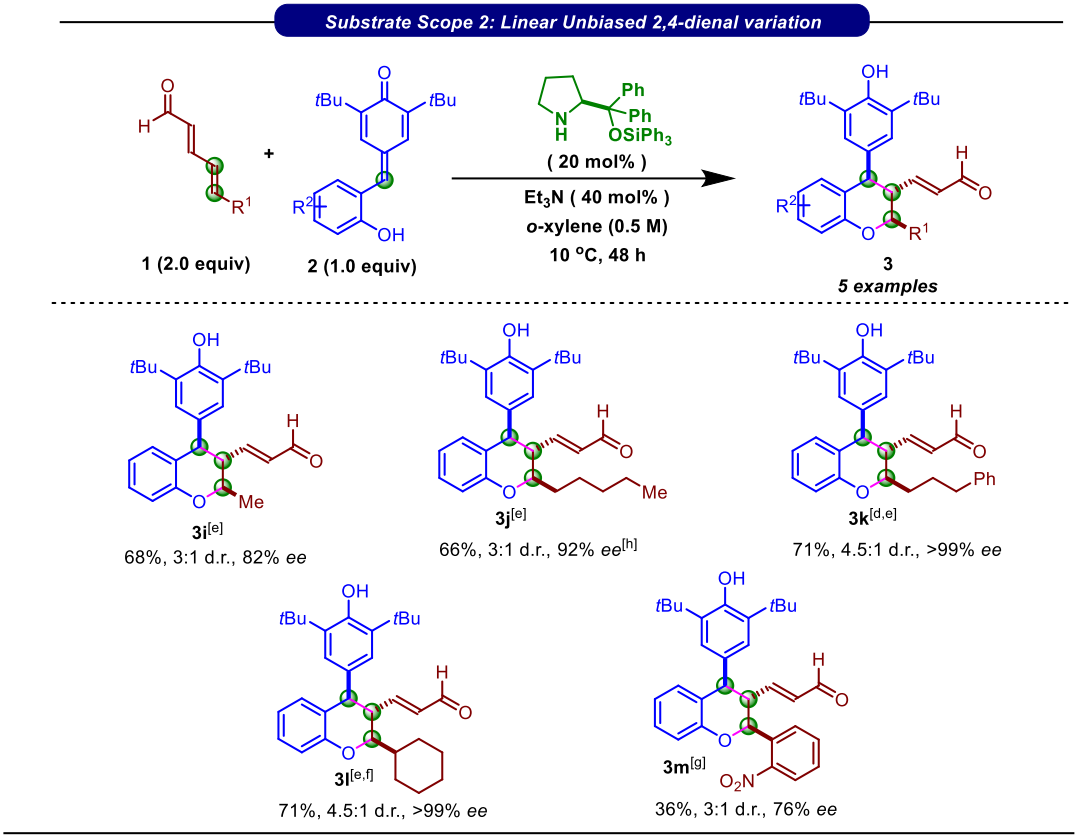
Variation of ortho-hydroxyphenyl-substituted p-QMs: The optimized reaction condition (Table 3, entry 8) was applied to test the reactivity of (2*E*,4*E*)-hepta-2,4-dienal **1a** with *ortho*-hydroxyphenyl-substituted *p*-QMs **2**. *p*-QMs and its derivatives having alkyl, halogen and methoxy group as a substituent at the *ortho* or *para*-position of the hydroxy group worked well in the presence of chiral secondary amine **3c** to furnish chromans **4b**–**4g** in high yields, good to excellent diastereoselectivity and excellent enantioselectivity (Scheme 11). In the case of 4-Cl substituted *p*-QM, low yield and moderate diastereoslectivity of **4d** was observed. The absolute

configuration of the chroman derivatives was unambiguously assigned by X-ray analysis of **4d** derivative (Scheme 2.1.11).



Scheme 2.1.11: Chapter-2 Substrate Scope of Chiral Chromans by Varing *para*-Quinone Methides.[a,b,c] [a] Unless otherwise mentioned all reactions were carried out in a 0.1 mmol scale by taking **1** (2.0 equiv.) and **2** (1.0 equiv.). Yields refer to isolated yield unless otherwise specify. [b] Diastereomeric mixture measured by ^{1}H NMR analysis of the crude reaction mixture. [c] Enantiomeric excess was measured by HPLC on a chiral stationary phase. [d] 20 mol% Et_3N was used as an additive.

Variation of linear unbiased 2,4-dienals: Next scope for various 2,4-dienals having aliphatic substituent like methyl, n-pentyl, -CH_2CH_2Ph and cyclohexyl group at the δ-position was investigated, which reacted smoothly to provide products **4h–4k** in good yields with excellent enantioselectivity and moderate to good diastereoselectivity (Scheme 12). Unfortunately, phenyl substituent at the δ-position of 2,4-dienal remained less reactive. Inserting an electron-withdrawing -NO_2 group at the aromatic ring moderately increased the reactivity to provide **4l** with low yield and moderate selectivity. A naphthyl substituted *p*-QM also furnished desired chroman product **4m** with moderate yield and selectivity (Scheme 2.1.12).

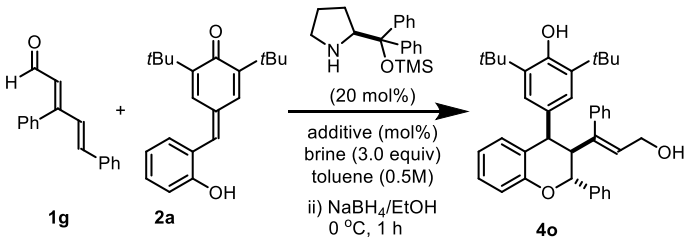


Scheme 2.1.12: Chapter-2 Substrate Scope of Chiral Chromans by Varing 2,4-dienals.[a,b,c] [a] Unless otherwise mentioned all reactions were carried out in a 0.1 mmol scale by taking **1** (2.0 equiv.) and **2** (1.0 equiv.). Yields refer to isolated yield unless otherwise specify. [b] Diastereomeric mixture measured by ^{1}H NMR analysis of the crude reaction mixture. [c] Enantiomeric excess was measured by HPLC on a chiral stationary phase. [e] 20 mol% Et_3N was used as an additive. [e] Reactions were performed at 45 °C for 40 h. [f] Reaction was performed at 10 °C for 48 h gives better *ee* (96%) but lower yield (40%). [g] Reactions were carried out in a 0.1 mmol scale by taking **1** (1.0 equiv.) and **2** (4.0 equiv.) at 45 °C for 7 days by using $CHCl_3$ (0.1 M) as a solvent. [h] *ee* measured by converting the aldehyde to alcohol.

Sluggish reactivity of the δ-aryl substituted 2,4-dienals prompted us to test the reactivity of β,δ- aryl-substituted 2,4-dienal.

Optimization for chroman synthesis from β, δ- aryl-substituted 2,4-dienals: Here, 2,4-dienal **1g** and *ortho*-hydroxyphenyl-substituted *p*-QM **2a** were chosen as the model substrates in toluene (0.5 M) in the presence of **3a** as a catalyst. Next, several additives, reaction time, temperature, and other parameters were varied to find the best-fitted one (Table 4). This screening reveals that triethyl amine was the suitable additive to form chroman **4o** at rt for 12 h (Table 4, entry 13, d.r. 45:1, *ee* 90%).

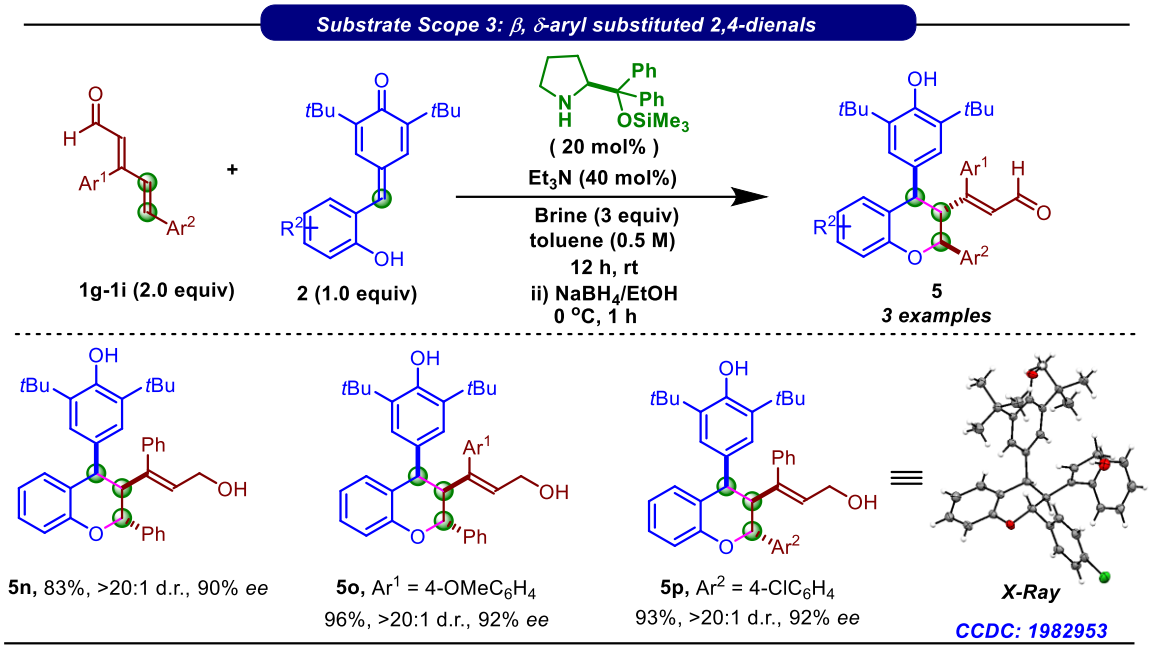
2.2.4. Chapter 2: Table 4. Miscellaneous Optimization-2



Entry	1g/2a	Additive (mol%)	Temp. (°C)	Time (h)	Yield (%)[b]	d.r.[c]	*ee* (%)[d]
1[g]	2/1	Et_3N (20)	rt	12	64	5:1	82
2	2/1	$PhCO_2H$ (20)	rt	12	20	9:1	81
3	2/1	Et_3N (20)	rt	12	70	6:1	83
4	2/1	NaOAc (20)	rt	12	54	10:1	75
5	2/1	DIPEA (20)	rt	12	67	5:1	79
6	2/1	K_2CO_3 (20)	rt	12	40	5:1	55
7[h]	2/1	Et_3N (20)	rt	12	69	90:1	76
8	2/1	Et_3N (20)	rt	40	45	30:1	70
9	2/1	Et_3N (20)	80	12	37	10:1	33
10	1/1	Et_3N (20)	rt	12	47	46:1	-
11	1/1.5	Et_3N (20)	rt	12	44	20:1	-
12	4/1	Et_3N (20)	rt	12	71	10:1	63
13	**2/1**	**Et_3N (40)**	**rt**	**12**	**92(83)**	**45:1**	**90**

[a] unless untill mentioned all reactions were carried out in a 0.1 mmol scale by taking 1g (2.0 equiv) & 2a (1.0 equiv). [b] yield was measured by 1H-NMR analysis of the crude reaction mixture, isolated yield in parentheses. [c] diastereomeric mixture measured by 1H-NMR analysis of the crude reaction mixture. [d] enantiomeric excess was measured by HPLC on a chiral stationary phase. [g] reaction performed without brine. [h] reaction carried out by taking 3c instead of 3a.

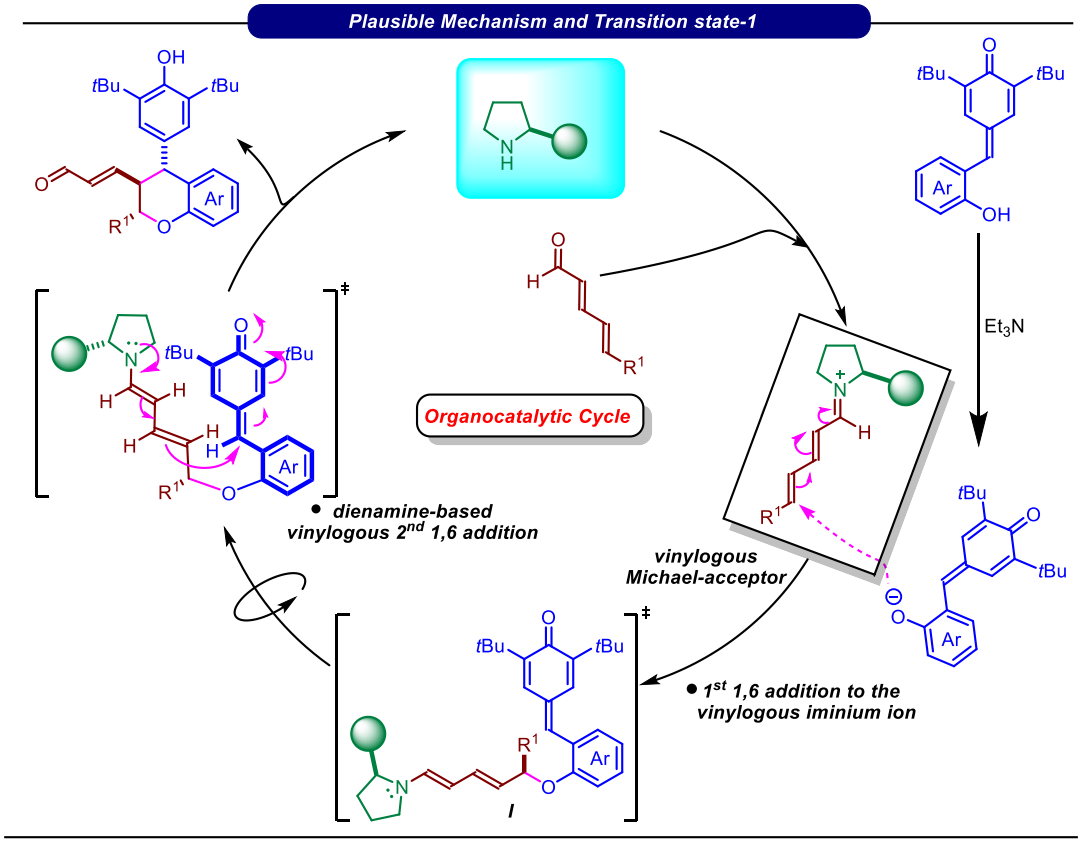
Substrate Scope for Chroman Synthesis from β, δ- aryl-substituted 2,4-dienals: The optimal reaction condition (Table 4, entry 13) was applied to evaluate the substrate scope for chroman **4** by reacting β,δ- aryl-substituted 2,4-dienal **1g** with different *ortho*-hydroxyphenyl-substituted *p*-QM **2**. To our delight, we were able to synthesize aryl-substituted chromans **4n-4p** (Scheme 3) with excellent yields, excellent diastereoselectivity and good enantioslectivity using catalyst **3a**. The absolute configuration of the diaryl-substituted chromans were unambiguously assigned by X-ray analysis of the **4p** derivative (Scheme 2.1.13).



Scheme 2.1.13: Asymmetric double 1,6-addition of β, δ-aryl substituted 2,4-dienals.[a] [a] Unless otherwise mentioned all reactions were carried out in a 0.1 mmol scale by taking **1** (2.0 equiv.) and **2** (1.0 equiv.), yields refer to isolated yield unless otherwise specify, diastereomeric mixture measured by ^{1}H NMR analysis of the crude reaction mixture, enantiomeric excess was measured by HPLC on a chiral stationary phase.

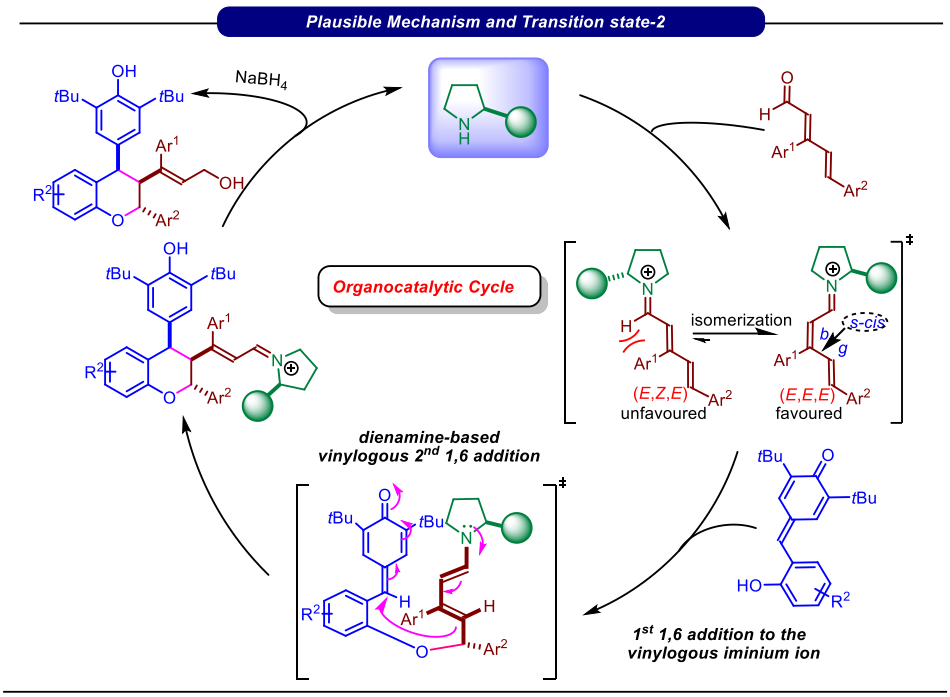
2.2.4 Proposed Mechanism

Plausible mechanism and transition state for double 1,6-addition of linear unbiased 2,4-dienal and p-QMs: Based on the X-ray structure analysis and literature evidences,[11a] we proposed a plausible mechanistic pathway for the formation of chroman derivatives. This cascade reaction triggers by the intermolecular vinylogous iminium-ion based 1,6-addition (*oxa*-Michael) of the deprotonated nucleophile to the linear unbiased 2,4-dienal to produce intermediate **4I**. Intermediate **4I** then undergoes an intramoleculer vinylogous dienamine-based another 1,6-addition to the *p*-QM to construct chromane derivative (Scheme 2.1.14). The vinylogous deprotonated nucleophile prefers selectively *oxa*-Michael at δ-position rather than the β-position, which is opposite to the observation by Jørgensen et. al.[11a,11f]



Scheme 2.1.14: Chapter 2: Plausible Mechanism and Transition state-1.

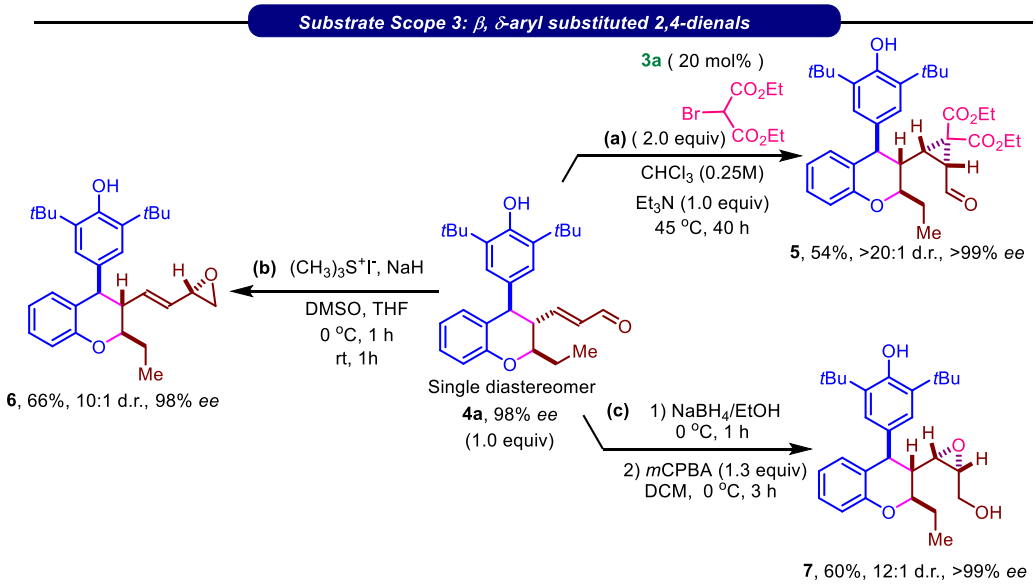
Plausible mechanism and transition state for double 1,6-addition of β, δ- aryl-substituted 2,4-dienals and p-QMs: Based on the X-ray analysis and literature evidences, we proposed a plausible transition state for the formation of products **4n-p**.[12b,12c] This organocascade reaction proceeds by way of a vinylogous iminium-ion/dienamine activation sequence of linear 2,4-dienals (Scheme 2.1.15).



Scheme 2.1.15: Chapter 2: Plausible Mechanism and Transition state-2.

2.2.5 Synthetic transformations of the cascade product.

The presence of an α, β-unsaturated system unlocks an opportunity to renovate these chroman derivatives into more complex molecular scaffolds. The compound **4a** can be cyclopropanated by using **3a** as a catalyst to obtain **5** with excellent d.r. and enantioselectivity (Scheme 2.1.16a).[14] Corey Chaykovsky reaction quickly converted **4a** to allylic epoxide **6** (Scheme 2.1.16b).[15] Simple epoxidation of allylic alcohol also readily furnished epoxide **7** having five continuous chiral centers with high yield and diastereo- as well as enantioselectivity (Scheme 2.1.16c).



Scheme 2.1.16: Chapter 2: Synthetic Applications.

2.3 Conclusion

We disclose here an organocatalytic asymmetric synthesis of chroman derivatives with high selectivity (up to >20:1 d.r., >99% *ee*) and high yield (up to 96%). The reaction is initiated by an oxa-Michael (1,6-addition) with exclusive δ-site selectivity to a vinylogous unbiased iminium-ion and concluded with a vinylogous dienamine based another 1,6-addition to the *p*-QMs. This work constitutes a rare example of asymmetric double 1,6-addition. The low reactivity of δ-aryl substituted unbiased 2,4-dienals can be dramatically influenced by using β, δ- aryl-substituted 2,4-dienals. The remaining α, β-unsaturated enal functionality is employed to introduce molecular complexity to the chiral chroman derivatives with high reactivity and stereoselectivity.

2.4. Experimental Section

2.4.1. General Information

All reactions were performed in flame-dried glassware under argon atmosphere unless otherwise stated. Liquids and solutions were transferred with syringes. Solvents used were dried and purified by following standard procedures.

Technical grade solvents for extraction or chromatography (ethyl acetate, and petroleum ether) were distilled prior to use. $CDCl_3$ was stored over 4A^o molecular sieves. Used chemicals were purchased from Sigma-Aldrich, TCI, Alfa-Aesar and Sisco Research Laboratories (SRL) used without further purification. All the liquid chemicals distilled freshly prior to use.

Analytical thin-layer chromatography (TLC) was performed on using pre-coated aluminium-backed plates (Merck Kieselgel 60 F254) and visualized by UV radiation, basic aqueous potassium permangante ($KMnO_4$), *p*-anisaldehyde stains and heat as developing agents. Flash column chromatography was performed on silica gel 60 (40–63 μm, 230–400 mesh, ASTM) from Merck using the indicated solvents. Organic solutions were concentrated under reduced pressure on Heidolph rotary evaporator.

NMR spectra were acquired on a JEOL JNM ECS-400 instrument running at 400 MHz for ^{1}H, 101 MHz ^{13}C and 376 MHz for ^{19}F respectively. Chemical shifts (δ) are reported in ppm relative to residual solvent signals ($CHCl_3$, 7.26 ppm for ^{1}H NMR, $CDCl_3$, 77.0 ppm for ^{13}C NMR). Data are reported as follows: chemical shift, multiplicity (br = broad singlet, s = singlet, d = doublet, dd = doublet of doublets, t = triplet, q = quartet, ddd = doublet of doublet of doublet, td = triplet of doublet, m = multiplet), coupling constants (Hz), and integration.

1,2-Dibromomethane was used as an internal standard to calculate NMR yields & diastereomeric ratio (dr) of products by ^{1}H NMR analysis of the crude mixture.

Optical rotations were measured on a Anton Paar MCP 200, $[\alpha]_D$ values are given in $deg \cdot cm^3 \cdot g^{-1} \cdot dm^{-1}$; concentration (c) in g $(100\ mL)^{-1}$.

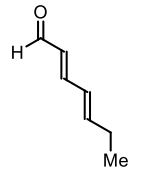
The enantiomeric excess (*ee*) of products was determined by High Performance liquid Chromatography (Waters modular system.) using Daicel Chiralpak IA, IB, IC, ODH, and ADH columns as chiral stationary phases. All the HRMS data were recorded on XEVO G2-XS QTOF. All the X-ray data were recorded on Bruker D8 venture instrument.

Dienals **1a, 1b, 1c** and amines **3a, 3b, 3g** has been obtained from commercial sources. Dienals **1d-1f** [11f], **1g-1i** [12c], *p*-QM's **2a-2k** [6] and Amines **3c-3f** [16-18] were synthesized according to the procedure in the literature.

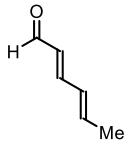
2.4.2. List of Substrates used.

The list of substrates for GP-1 and GP-2 are given bellow.

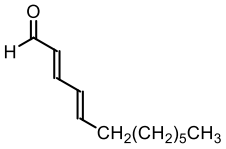
2.4.2.1 List of 2,4 dienals.



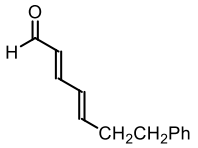
1a



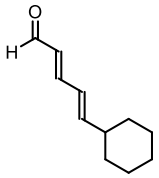
1b



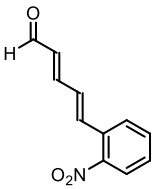
1c



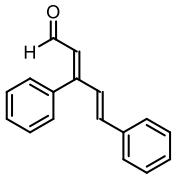
1d



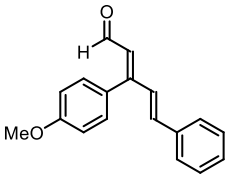
1e



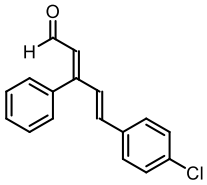
1f



1g

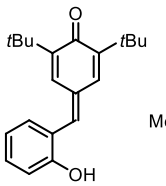


1h

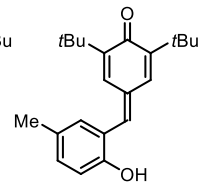


1i

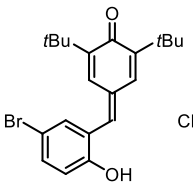
2.4.2.2 List of *p*-QM's.



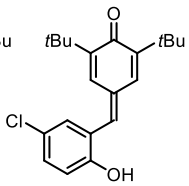
2a



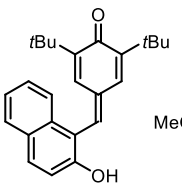
2b



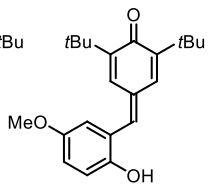
2c



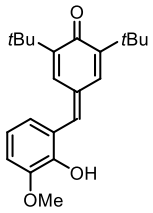
2d



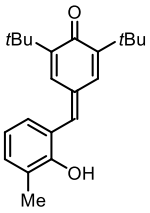
2e



2f



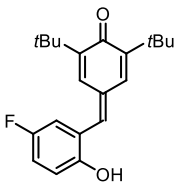
2g



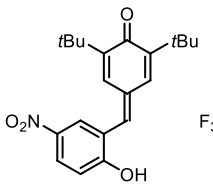
2h

2.4.2.3 List of unreacted *p*-QM's.

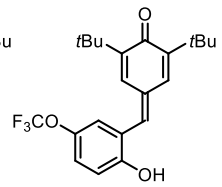
Following substrates remains un-reacted according to GP-1 and GP-2.



2i

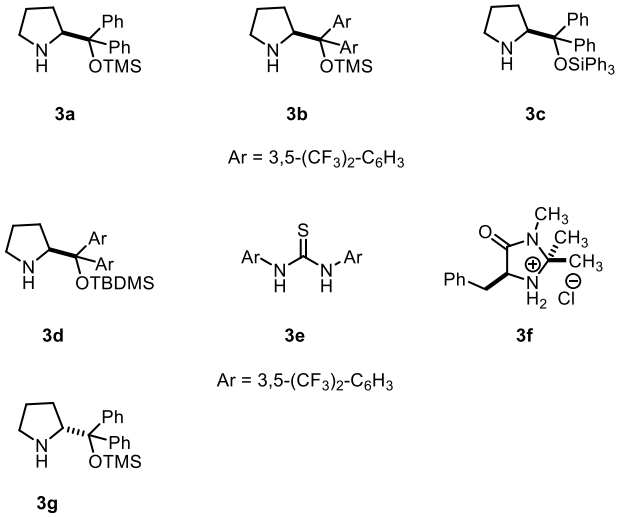


2j



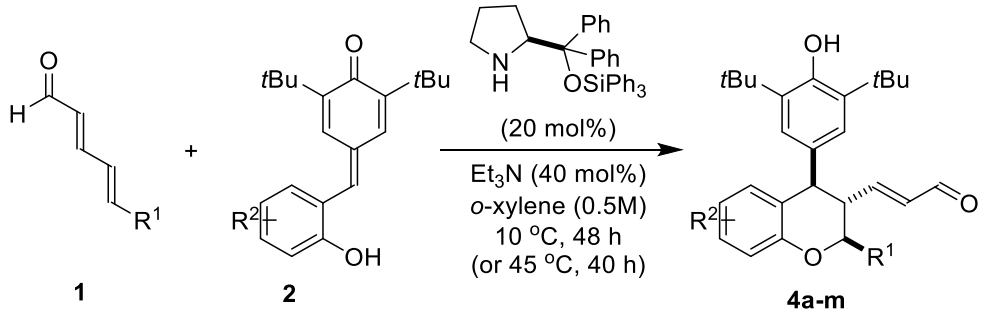
2k

2.4.2.4. List of amines.



2.4.3. Asymmetric Organocatalytic Double 1,6-Addition: Synthesis of Chiral Chromans.

2.4.3.1. General Procedure for formation of chroman derivatives from linear 2,4 dienals (GP-1)



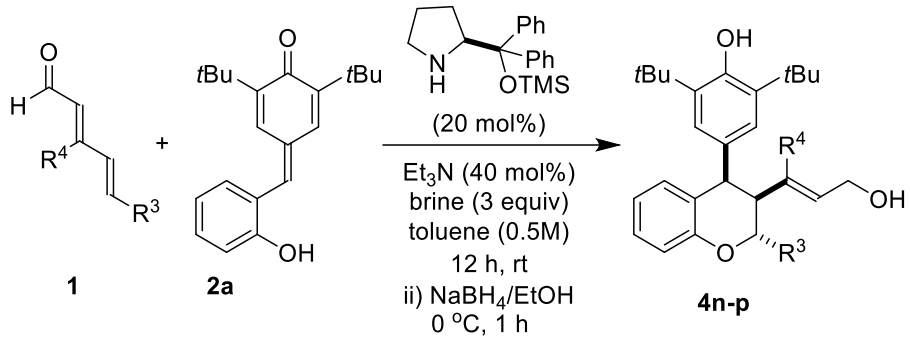
All the reactions were carried out in *o*-xylene (synthesis grade, >98%), without any precaution to exclude air and moisture (open air chemistry on the benchtop). An ordinary vial equipped with a Teflon-coated stir bar and a plastic screw cap was charged with amine **3c** (0.02 mmol, 10.2 mg, 0.2 equiv). Then *o*-xylene (0.2 mL, 0.5 M) and the additive triethylamine (0.04 mmol, 6.0 µL, 0.4 equiv) were sequentially added. The reaction mixture was stirred in a cooling bath maintained at 10 °C (or 45 °C) for 5 minutes to let the mixture reaching a uniform temperature. The reaction was started by the addition of α,β,γ,δ-unsaturated aldehyde (2.0 equiv, 0.2 mmol) and the reaction mixture was stirred at 10 °C (or 45 °C) for 15 min. After that, *p*-QM derivative (1.0 equiv, 0.1 mmol) was added and purged with argon then the vial was sealed and immerged in the cooling bath again maintained at 10 °C (or 45 °C). Stirring was continued over 48 h.

The progress of the reaction was monitored by TLC and by ^{1}H NMR analysis of the aliquot taken from the crude mixture using CH_2Br_2 as internal standard. The analytically pure product is

obtained by column chromatography on silica gel using petroleum ether and ethyl acetate as eluent.

Racemic samples were prepared according to **GP-1** by using mixture of amine **3a** (0.010 mmol, 3.4 mg, 0.1 equiv) and amine **3g** (0.010 mmol, 3.4 mg, 0.1 equiv) instead of amine **3c.**

2.4.3.2. General Procedure for formation of chroman derivatives from branched 2,4 dienals (GP-2).

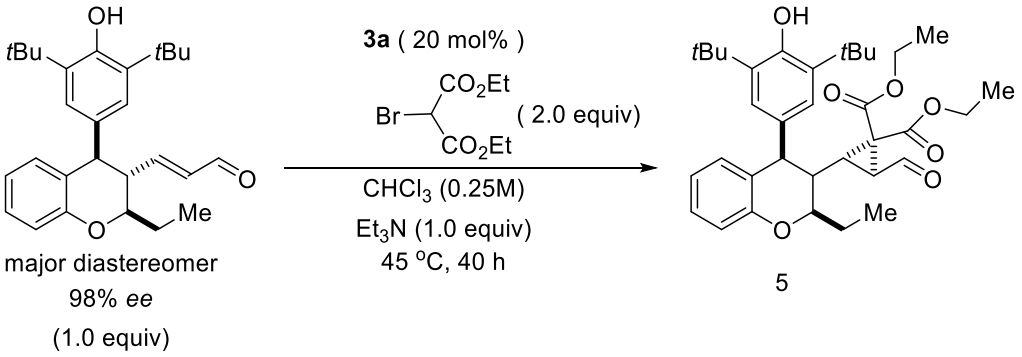


All the reactions were carried out in toluene (HPLC grade, >98%), without any precaution to exclude air and moisture (open air chemistry on the benchtop). An ordinary vial equipped with a Teflon-coated stir bar and a plastic screw cap was charged with amine **3a** (0.02 mmol, 6.5 mg, 0.2 equiv). Then toluene (0.2 mL, 0.5 M), the additive triethylamine (0.04 mmol, 6.0 µL, 0.4 equiv) and brine (0.6 mmol, 3.0 equiv) were sequentially added. The reaction mixture was stirred at room temperature for 5 minutes to let the mixture reaching a uniform temperature. The reaction was started by the addition of α,β,γ,δ-unsaturated aldehyde (2.0 equiv, 0.2 mmol) and the reaction mixture was stirred at room temperature for 15 min. After that, *p*-QM derivative (1.0 equiv, 0.1 mmol) was added and purged with argon then the vial was sealed and kept at room temperature. Stirring was continued over 12 h. Upon completion of the reaction the reaction mixture was diluted with 1.0 mL of ethanol and solid $NaBH_4$ (0.4 mmol, 4.0 equiv) were added and kept at 0 ^oC for 60 minutes. The reaction was quenched by adding few drops of water. Brine (5 mL) was added and resulted mixture was extracted with DCM (3 X 10 mL), dried over $MgSO_4$, filtered and concentrated *in vacuo*.

The progress of the reaction was monitored by TLC and by ^1H NMR analysis of the aliquot taken from the crude mixture using CH_2Br_2 as internal standard. The analytically pure product is obtained by column chromatography on silica gel using petroleum ether and ethyl acetate as eluent.

Racemic samples were prepared according to **GP-2** by using mixture of amine **3a** (0.010 mmol, 3.4 mg, 0.1 equiv) and amine **3g** (0.010 mmol, 3.4 mg, 0.1 equiv) instead of amine **3a.**

2.4.3.3. General Procedure for asymmetric synthesis of cyclopropane derivative from α,β-unsaturated Aldehyde (4a) (GP-3).[14]

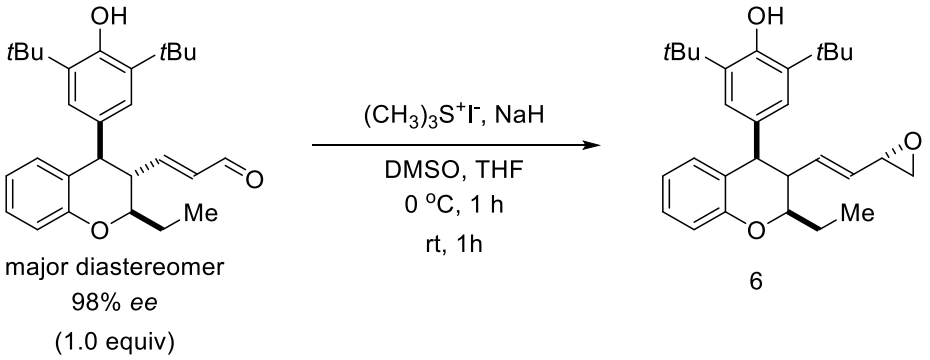


All the reactions were carried out in chloroform (HPLC grade, >98%), without any precaution to exclude air and moisture (open air chemistry on the benchtop). An ordinary vial equipped with a Teflon-coated stir bar and a plastic screw cap was charged with amine **3a** (0.02 mmol, 6.5 mg, 0.2 equiv). Then chloroform (0.4 mL, 0.25 M) and the additive triethylamine (0.1 mmol, 14.0 µL, 1.0 equiv) were sequentially added. The reaction mixture was stirred in a heating bath maintained at 45 °C for 5 minutes to let the mixture reaching a uniform temperature. The reaction was started by the addition of α,β-unsaturated aldehyde (0.1 mmol, 42.0 mg, 1.0 equiv) and the reaction mixture was stirred at 45 °C for 15 min. After that, diethyl bromomalonate (0.2 mmol, 35.0 µL, 2.0 equiv) was added and purged with argon then the vial was sealed and immerged in the heating bath again 45 °C. Stirring was continued over 40 h.

The progress of the reaction was monitored by TLC and by ^{1}H NMR analysis of the aliquot taken from the crude mixture using CH_2Br_2 as internal standard. The analytically pure product is obtained by column chromatography on silica gel using petroleum ether and ethyl acetate as eluent.

Racemic samples were prepared according to **GP-3** by using mixture of amine **3a** (0.010 mmol, 3.4 mg, 0.1equiv) and amine **3g** (0.010 mmol, 3.4 mg, 0.1 equiv) instead of amine **3a.**

2.4.3.4. General Procedure for Corey-Chaykovsky reaction of α,β-unsaturated Aldehyde (4a) (GP-4).[15]



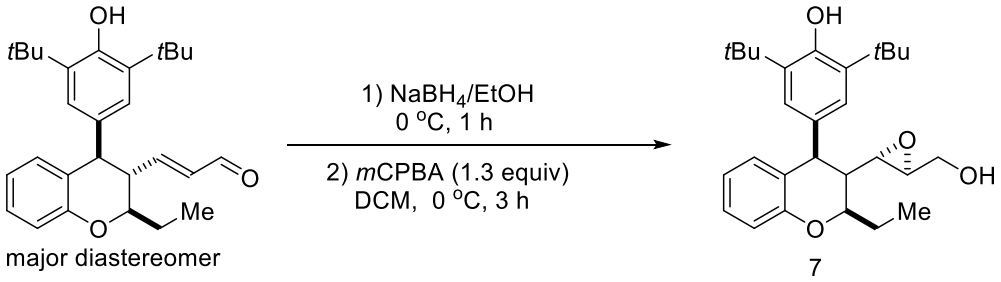
A 5 mL oven-dried Schlenk flask was charged with NaH (60 % dispersion in oil, washed hexanes (5 x 5 mL) and dried under vacuum, 12.0 mg, 0.31 mmol, 3.1 equiv). Dry THF (0.15 mL) and DMSO (0.15 mL) were added to the flask and the resulting slurry solution was cooled to 0 °C.

Trimethylsulfonium iodide (61.0 mg, 0.3 mmol, 3.0 equiv) and DMSO (0.25 mL) were added to a separate oven-dried Schlenk flask. The solution was transferred slowly to the NaH solution via cannula. After the transfer was complete, α,β-unsaturated aldehyde **4a** (0.1 mmol, 42.0 mg, 1.0 equiv) was then added to the reaction mixture in one portion. The resulting mixture was stirred at 0 °C for 1 h, then at room temperature for another 1 h and quenched with distilled water (1 mL). The resulting mixture was then diluted with diethyl ether (5 mL) and brine (10 mL). The two layers were separated, and the aqueous layer was back extracted with diethyl ether (2 X 20 mL). The combined organic layer was dried with $MgSO_4$, filtered, and concentrated *in vacuo*.

The progress of the reaction was monitored by TLC and by ^1H NMR analysis of the aliquot taken from the crude mixture using CH_2Br_2 as internal standard. The analytically pure product is obtained by column chromatography on silica gel using petroleum ether and ethyl acetate as eluent.

Racemic sample was prepared according to **GP-4** by taking *rac*-**4a** instead of **4a.**

2.4.3.5. General Procedure for formation of epoxide ring from α,β-unsaturated aldehyde (GP-5).[17]



In an oven dried ordinary vial equipped with a Teflon-coated stir bar and a plastic screw cap α,β-unsaturated aldehyde **4a** (0.1 mmol, 42.0 mg, 1.0 equiv) was taken and diluted with 1.0 mL of ethanol. Then to this mixture solid $NaBH_4$ (0.4 mmol, 4.0 equiv) were added and kept at 0 °C for 60 minutes. The reaction was quenched by adding few drops of water. Brine (5 mL) was added and resulted mixture was extracted with DCM (3 X 10 mL), dried over $MgSO_4$, filtered and concentrated *in vacuo*.

The analytically pure product was obtained by column chromatography on silica gel using petroleum ether and ethyl acetate as eluent.

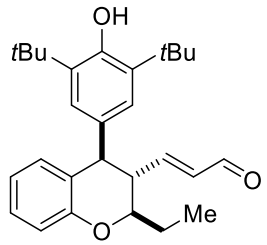
Allyllic alcohol (36.0 mg, 0.085 mmol) obtained from above procedure was placed in a round bottom flask and dissolved in DCM (0.2 mL) at 0 °C. *meta*-Chloroperoxybenzoic acid (*m*CPBA, 1.3 equiv, 0.11 mmol) was added and the reaction mixture stirred for 3 h. Then the reaction was diluted with 10 mL of DCM and washed with $NaHCO_3$ solution (2 times) and brine. The organic phase was dried over Na_2SO_4 and filtered. Solvent was evaporated in vacuo and the crude reaction

mixture purified by column chromatography on silica gel using petroleum ether and ethyl acetate as eluent.

Racemic sample was prepared according to **GP-5** by taking *rac*-**4a** instead of **4a.**

2.4.4. Results & Characterization.

2.4.4.1. (*E*)-3-((2R,3S,4R)-4-(3,5-di-*tert*-butyl-4-hydroxyphenyl)-2-ethylchroman-3-yl)acrylaldehyde (4a).



4a

$C_{28}H_{36}O_3$

M = 420.59 g/mol

According to **GP-1** compound **(4a)** was prepared by using **1a** (22.0 µL, 0.2 mmol, 2.0 equiv) **2a** (31.0 mg, 0.1 mmol, 1.0 equiv), triethylamine (6.0 µL, 0.04 mmol, 0.4 equiv) and **Amine 3c** (10.2 mg, 0.02 mmol) in *o*-xylene for 48 h at 10 °C.

Column chromatographic purification (petroleum ether/EtOAc 99:1 to 97:3) afforded **4a** (major diastereomer) as pale yellow solid (35.5 mg, 84%).

Melting Point: 108-110 °C

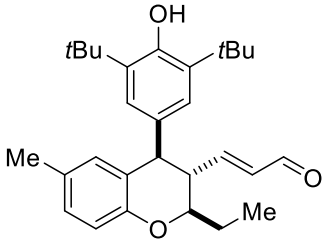
$[\alpha]_D^{20}$ = +16.0 (c = 0.4, CH_2Cl_2).

HPLC: Daicel CHIRALPAK IC column; *n*-hexane/*i*PrOH = 200/1; flow rate = 0.2 mL/min; T = 25 °C; retention time: 46.24 min (major), 52.66 min (minor), *ee*: 98 %.

HRMS (ESI): *m/z* $[M-H]^+$ Calculated for **$C_{28}H_{35}O_3^+$:** 419.2586; Found 419.2588.

^{1}H NMR (400 MHz, $CDCl_3$) : δ 9.41 (d, *J* = 7.8 Hz, 1H), 7.13-70.9 (m, 1H), 6.88 (d, *J* = 8.2 Hz, 1H), 6.77 (d, *J* = 4.0 Hz, 2H), 6.74 (s, 2H), 6.52 (dd, *J* = 15.7, 9.8 Hz, 1H), 5.69 (dd, *J* = 15.7, 7.8 Hz, 1H), 5.08 (s, 1H), 4.03 (ddd, *J* = 10.6, 8.0, 2.9 Hz, 1H), 3.92 (d, *J* = 10.8 Hz, 1H), 2.76 (q, *J* = 10.1 Hz, 1H), 1.77 ((dqd, *J* = 14.4, 7.5, 7.0, 3.2 Hz, 1H), 1.64-1.60 (m, 1H), 1.34 (s, 18H), 1.08 (t, *J* = 7.4 Hz, 3H). **^{13}C NMR (101 MHz, $CDCl_3$):** δ 193.1, 155.7, 154.7, 152.7, 135.9, 135.2, 132.4, 130.2, 127.8, 125.6, 125.0, 120.7, 116.5, 78.7, 50.1, 48.6, 34.4, 30.5, 27.2, 9.2. **^{13}C NMR DEPT-135 (101 MHz, $CDCl_3$) :** δ 193.1, 155.8, 135.2, 130.2, 127.8, 125.6, 120.7, 116.5, 78.7, 50.1, 48.6, 30.5, 27.2, 9.2.

2.4.4.2. (*E*)-3-((2R,3S,4R)-4-(3,5-di-*tert*-butyl-4-hydroxyphenyl)-2-ethyl-6-methylchroman-3-yl)acrylaldehyde (4b).



4b
$C_{29}H_{38}O_3$
M = 434.62

According to **GP-1** compound **(4b)** was prepared by using **1a** (22.0 µL, 0.2 mmol, 2.0 equiv) **2b** (32.5 mg, 0.1 mmol, 1.0 equiv), triethylamine (6.0 µL, 0.04 mmol, 0.4equiv) and **Amine 3c** (10.2 mg, 0.02 mmol) in *o*-xylene for 48 h at 10 °C.

Column chromatographic purification (petroleum ether/EtOAc 99:1 to 97:3) afforded **4b** (major diastereomer) as pale yellow solid (35.0 mg, 80 %).

Melting Point: 128-130 °C

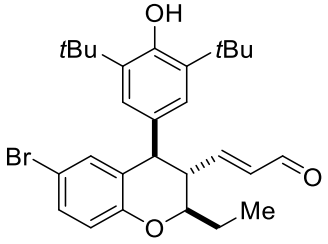
$[\alpha]_D^{20}$ = + 60.1. (c = 0.2, EtOH).

HPLC: Daicel CHIRALPAK ODH column; *n*-hexane/ *i*PrOH = 400/1; flow rate = 1.0 mL/min; T = 25 °C; retention time: 12.73 min (major), 17.58 min (minor) *ee*: > 99 %.

HRMS (ESI): *m/z* $[M+H]^+$ Calculated for **$C_{29}H_{39}O_3^+$:** 435.2899; Found 435.2882

^{1}H NMR (400 MHz, $CDCl_3$): δ 9.41 (d, *J* = 7.8 Hz, 1H), 6.91 (d, *J* = 8.2 Hz, 1H), 6.78 (d, *J* = 8.2 Hz, 1H), 6.73 (s, 2H), 6.58 (s, 1H), 6.51 (dd, *J* = 15.6, 9.8 Hz, 1H), 5.66 (dd, *J* = 15.5, 7.9 Hz, 1H), 5.08 (s, 1H), 3.97 (ddd, *J* = 10.2, 8.7, 2.7 Hz, 1H). , 3.87 (d, *J* = 10.8 Hz, 1H), 2.72 (q, *J* = 10.1 Hz, 1H), 2.13 (s, 3H), 1.74 (dqd, *J* = 14.7, 7.5, 2.9 Hz, 1H), 1.63-1.59 (m, 1H), 1.34 (s, 18H), 1.06 (t, *J* = 7.3 Hz, 3H). **^{13}C NMR (101 MHz, $CDCl_3$):** δ 193.1, 156.0, 152.7, 152.6, 135.8, 135.1, 132.5, 130.3, 129.9, 128.5, 125.6, 124.6, 116.2, 78.7, 50.6, 48.5, 34.4, 30.5, 27.2, 20.7, 9.2. **^{13}C NMR DEPT-135 (101 MHz, $CDCl_3$):** δ 193.1, 156.0, 135.1, 130.3, 128.5, 125.6, 116.2, 78.7, 50.6, 48.5, 30.5, 27.2, 20.7, 9.2.

2.4.4.3. (*E*)-3-((2R,3S,4R)-6-bromo-4-(3,5-di-*tert*-butyl-4-hydroxyphenyl)-2-ethylchroman-3-yl)acrylaldehyde (4c).



4c
$C_{28}H_{35}BrO_3$
M = 499.48

According to **GP-1** compound **(4c)** was prepared by using **1a** (22.0 µL, 0.2 mmol, 2.0 equiv) **2c** (39.0 mg, 0.1 mmol, 1.0 equiv) triethylamine (6.0 µL, 0.04 mmol, 0.4 equiv) and **Amine 3c** (10.2 mg, 0.02 mmol) in *o*-xylene for 48 h at 10 °C.

Column chromatographic purification (petroleum ether/EtOAc 99:1 to 97:3) afforded **4c** (major diastereomer) as yellow solid (33.0 mg, 66%).

Melting Point: 156-158 °C

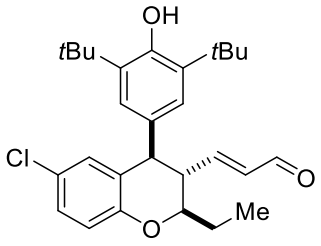
$[\alpha]_D^{20}$ = + 25.4. (c = 0.6, EtOH).

HPLC: Daicel CHIRALPAK ODH column; *n*-hexane/ *i*PrOH = 1000/1; flow rate = 1.0 mL/min; T = 25 °C; retention time: 16.57 min (major), 21.21 min (minor), *ee*: 96%.

HRMS (ESI): *m/z* $[M-H]^+$ Calculated for **$C_{28}H_{34}BrO_3^+$:** 497.1691; Found 497.1687.

^{1}H NMR (400 MHz, $CDCl_3$): δ 9.40 (d, *J* = 7.7 Hz, 1H), 7.22-7.19 (m, 1H), 6.90 (dd, *J* = 2.4, 1.1 Hz, 1H), 6.77 (d, *J* = 8.7 Hz, 1H), 6.71 (s, 2H), 6.47 (dd, *J* = 15.7, 9.8 Hz, 1H), 5.67 (dd, *J* = 15.5, 7.5 Hz, 1H), 5.11 (s, 1H), 3.99 (ddd, *J* = 10.1, 8.0, 3.0 Hz, 1H), 3.86 (d, *J* = 10.8 Hz, 1H), 2.71 (q, *J* = 10.1 Hz, 1H), 1.76 (dqd, *J* = 14.9, 7.5, 3.0 Hz, 1H), 1.64-1.60 (m, 1H), 1.35 (s, 18H), 1.06 (t, *J* = 7.4 Hz, 3H). **^{13}C NMR (101 MHz, $CDCl_3$):** δ 192.9, 155.0, 154.0, 152.9, 136.1, 135.4, 132.6, 131.5, 130.8, 127.3, 125.5, 118.5, 112.8, 79.0, 49.8, 48.4, 34.4, 30.4, 27.1, 9.1. **^{13}C NMR DEPT-135 (101 MHz, $CDCl_3$):** δ 192.9, 155.0, 135.4, 132.6, 130.8, 125.5, 118.5, 79.0, 49.8, 48.4, 30.4, 27.1, 9.1.

2.4.4.4. (*E*)-3-((2R,3S,4R)-6-chloro-4-(3,5-di-*tert*-butyl-4-hydroxyphenyl)-2-ethylchroman-3-yl)acrylaldehyde (4d).



4d
$C_{28}H_{35}ClO_3$
M: 455.03

According to **GP-1** compound **(4d)** was prepared by using **1a** (22.0 µL, 0.2 mmol, 2 equiv) **2d** (34.5 mg, 0.1 mmol, 1equiv) triethylamine (6.0 µL, 0.04 mmol, 0.4 equiv) and **Amine 3c** (10.2 mg, 0.02 mmol) in *o*-xylene for 48 h at 10 °C.

Column chromatographic purification (petroleum ether/EtOAc 99:1 to 97:3) afforded **4d** (major diastereomer) as yellow solid (18.0 mg, 40 %).

Melting Point: 150-152 °C

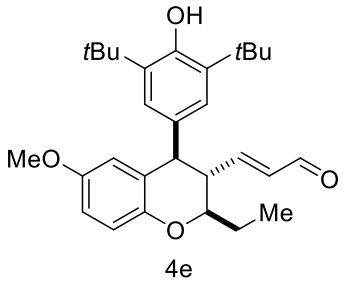
$[\alpha]_D^{20}$ = + 53.7. (c = 0.6., EtOH).

HPLC: Daicel Chiralpak ODH column; *n*-hexane/ *i*PrOH = 1000/1; flow rate = 1 mL/min; T = 25 °C; retention time: 13.80 min (major), 19.63 min (minor), *ee*: 98%.

HRMS (ESI): *m/z* $[M-H]^+$ Calculated for **$C_{28}H_{34}ClO_3^+$:** 453.2196; Found 453.2194.

^{1}H NMR (400 MHz, $CDCl_3$): δ 9.40 (d, *J* = 7.7 Hz, 1H), 7.06 (dd, *J* = 8.6, 2.7 Hz, 1H), 6.82 (d, *J* = 9.0 Hz, 1H), 6.75 (d, *J* = 2.5 Hz, 1H), 6.72 (s, 2H), 6.47 (dd, *J* = 15.7, 9.8 Hz, 1H), 5.67 (dd, *J* = 15.7, 7.7 Hz, 1H), 5.11 (s, 1H), 3.99 (ddd, *J* = 10.7, 8.0, 2.9 Hz, 1H), 3.85 (d, *J* = 10.8 Hz, 1H), 2.72 (q, *J* = 10.1 Hz, 1H), 1.76 (dqd, *J* = 14.7, 7.3, 3.1 Hz, 1H), 1.64-1.57 (m, 1H), 1.35 (s, 18H), 1.07 (t, *J* = 7.6 Hz, 3H). **^{13}C NMR (101 MHz, $CDCl_3$):** δ 192.9, 155.0, 153.4, 152.9, 136.1, 135.4, 131.5, 129.6, 127.9, 126.7, 125.5 (2C), 118.0, 79.1, 49.9, 48.5, 34.4, 30.5, 27.2, 9.2. **^{13}C NMR DEPT-135 (101 MHz, $CDCl_3$):** δ 192.9, 155.0, 135.4, 129.6, 127.9, 125.5, 118.0, 79.1, 49.9, 48.5, 30.5, 27.2, 9.2.

2.4.4.5. (*E*)-3-((2R,3S,4R)-4-(3,5-di-*tert*-butyl-4-hydroxyphenyl)-2-ethyl-6-methoxychroman-3-yl)acrylaldehyde (4e).



4e

$C_{29}H_{38}O_4$

M = 450.61

According to **GP-1** compound **(4e)** was prepared by using **1a** (22.0 µL, 0.2 mmol, 2.0 equiv) **2f** (34.0 mg, 0.1 mmol, 1.0 equiv) triethylamine (6.0 µL, 0.04 mmol, 0.4 equiv) and **Amine 3c** (10.2 mg, 0.02 mmol) in *o*-xylene for 48 h. at 10 °C.

Column Chromatographic purification (petroleum ether/EtOAc 99:1 to 95:5) afforded **4e** (major diastereomer) as light yellow gummy liquid (32.5 mg, 72%).

$[\alpha]_D^{20}$ = + 82.1 (c = 2.0, EtOH).

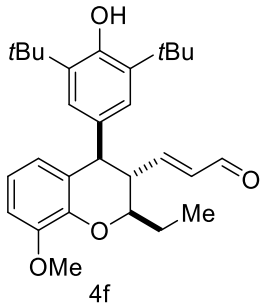
HPLC: Daicel CHIRALPAK IC column; *n*-hexane/ *i*PrOH = 95/5; flow rate = 1.0 mL/min; T = 25 °C; retention time: 26.77 min (major), 35.84 min (minor), *ee*: > 99%.

HRMS (ESI): *m/z* $[M-H]^+$ Calculated for **$C_{29}H_{37}O_4^+$:** 449.2692; Found 449.2705.

^{1}H NMR (400 MHz, $CDCl_3$): δ 9.41 (d, *J* = 7.8 Hz, 1H), 6.81 (d, *J* = 8.8 Hz, 1H), 6.73 (s, 2H), 6.69 (d, *J* = 8.0 Hz, 1H), 6.52 (dd, *J* = 15.6, 9.8 Hz, 1H), 6.29 (s, 1H), 5.70 (dd, *J* = 15.7, 7.8 Hz, 1H), 5.07 (s, 1H), 3.98-3.94 (m, 1H), 3.88 (d, *J* = 10.6 Hz, 1H), 3.60 (s, 3H), 2.75 (q, *J* = 9.9 Hz, 1H), 1.79-1.70 (m, 1H), 1.56-1.54 (m, 1H), 1.34 (s, 18H), 1.06 (t, *J* = 7.3 Hz, 3H).**^{13}C NMR (101 MHz, $CDCl_3$):** δ 193.1, 155.9, 153.5, 152.7, 149.0, 135.9, 135.2, 132.1, 125.8, 125.5, 117.1,

115.0, 113.8, 78.8, 55.9, 50.2, 48.8, 34.4, 30.5, 27.2, 9.2. **^{13}C NMR DEPT-135 (101 MHz, $CDCl_3$):** δ 193.1, 155.9, 135.2, 125.5, 117.1, 115.0, 113.8, 78.8, 55.9, 50.2, 48.8, 30.5, 27.2, 9.2.

2.4.4.6. (*E*)-3-((2R,3S,4R)-4-(3,5-di-*tert*-butyl-4-hydroxyphenyl)-2-ethyl-8-methoxychroman-3-yl)acrylaldehyde (4f).



4f

$C_{29}H_{38}O_4$
M = 450.61

According to **GP-1**compound **(4f)** was prepared by using **1a** (22.0 µL, 0.2 mmol, 2.0 equiv) **2g** (34.0 mg, 0.1 mmol, 1.0 equiv) triethylamine (6.0 µL, 0.04 mmol, 0.4 equiv) and **Amine 3c** (10.2 mg, 0.02 mmol) in *o*-xylene for 48 h at 10 °C.

Column Chromatographic purification (petroleum ether/EtOAc 99:1 to 90:10) afforded **4f** (d.r. 5:1) as light yellow gummy liquid (32.0 mg, 71 %).

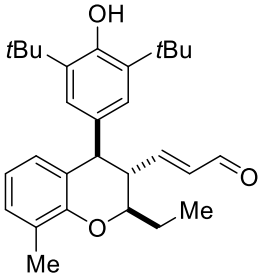
$[\alpha]_D^{20}$ = + 14.8 (c = 1.0, EtOH).

HPLC: Daicel CHIRALPAK IC column; *n*-hexane/ *i*PrOH = 95/5; flow rate = 0.5 mL/min; T = 25 °C; retention time: 13.71 min (major), 18.24 min (minor), *ee*: 92%.

HRMS (ESI): *m/z* $[M-H]^+$ Calculated for **$C_{29}H_{37}O_4^+$:** 449.2692; Found 449.2683.

^{1}H NMR (400 MHz, $CDCl_3$): δ 9.42 (d, *J* = 7.8 Hz, 1H), 6.81-6.76 (m, 1H), 6.72-6.71 (m, 3H), 6.53 (dd, *J* = 15.7, 9.9 Hz, 1H), 6.38 (dd, *J* = 6.3, 3.2 Hz, 1H), 5.69 (dd, *J* = 15.6, 7.8 Hz, 1H), 5.07 (s, 1H), 4.03 (ddd, *J* = 10.6, 7.9, 3.1 Hz, 1H), 3.90 (d, *J* = 3.6 Hz, 1H), 3.88 (s, 3H), 2.78 (q, *J* = 10.1 Hz, 1H), 1.82 (dtd, *J* = 14.8, 7.3, 3.0 Hz, 1H), 1.69 (dq, *J* = 14.7, 7.4 Hz, 1H), 1.33 (s, 18H), 1.11 (t, *J* = 7.4 Hz, 3H). **^{13}C NMR (101 MHz, $CDCl_3$):** δ 193.1, 155.7, 152.6, 148.2, 144.5, 135.8, 135.2, 132.5, 125.9, 125.5, 122.1, 120.1, 109.7, 79.1, 56.2, 50.2, 48.5, 34.4, 30.5, 27.2, 9.4. **^{13}C NMR DEPT-135 (101 MHz, $CDCl_3$):** δ 193.1, 155.7, 135.2, 125.5, 122.1, 120.1, 109.7, 79.1, 56.2, 50.2, 48.5, 30.4, 27.2, 9.4.

2.4.4.7. (*E*)-3-((2R,3S,4R)-4-(3,5-di-*tert*-butyl-4-hydroxyphenyl)-2-ethyl-8-methylchroman-3-yl)acrylaldehyde (4g).



4g
$C_{29}H_{38}O_3$
M = 434.62

According to **GP-1**compound **(4g)** was prepared by using **1a** (22.0 µL, 0.2 mmol, 2.0 equiv), **2h** (33.5 mg, 0.1 mmol, 1.0 equiv), triethylamine (6.0 µL, 0.04 mmol, 0.4 equiv) and **Amine 3c** (10.2 mg, 0.02 mmol) in *o*-xylene for 48 h at 10 °C.

Column Chromatographic purification (petroleum ether/EtOAc 99:1 to 97:3) afforded **4g** (major diastereomer) as pale yellow solid (28.0 mg, 64 %).

Melting Point: 134-136 °C

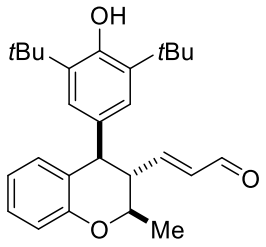
$[\alpha]_D^{20}$ = + 10.6 (c = 0.8, EtOH).

HPLC: Daicel CHIRALPAK IC column; *n*-hexane/ *i*PrOH = 400/1; flow rate = 0.2 mL/min; T = 25 °C; retention time: 64.66 min (major), 69.78 min (minor), *ee*: >99 %.

HRMS (ESI): *m/z* $[M-H]^+$ Calculated for **$C_{29}H_{37}O_3^+$:** 433.2743; Found 433.2729.

^{1}H NMR (400 MHz, $CDCl_3$): δ 9.41 (d, *J* = 7.8 Hz, 1H), 6.97 (d, *J* = 7.4 Hz, 1H), 6.74 (s, 2H), 6.67 (t, *J* = 7.0 Hz, 1H), 6.60 (d, *J* = 7.5 Hz, 1H), 6.52 (dd, *J* = 15.7, 9.8 Hz, 1H), 5.70 (dd, *J* = 15.6, 7.8 Hz, 1H), 5.07 (s, 1H), 3.99 (td, *J* = 8.9, 2.3 Hz, 1H), 3.92 (d, *J* = 10.8 Hz, 1H), 2.75 (q, *J* = 10.2 Hz, 1H), 2.25 (s, 3H), 1.80-1.71 (m, 1H), 1.67-1.59 (m, 1H), 1.34 (s, 18H), 1.11 (t, *J* = 7.0 Hz, 3H). **^{13}C NMR (101 MHz, $CDCl_3$):** δ 193.2, 156.1, 152.8, 152.6, 135.8, 135.1, 132.6, 128.8, 127.7, 125.7, 125.6, 124.5, 120.0, 78.7, 50.5, 48.8, 34.4, 30.5, 27.5, 16.1, 9.6. **^{13}C NMR DEPT-135 (101 MHz, $CDCl_3$):** δ 193.2, 156.1, 135.1, 128.8, 127.7, 125.6, 120.0, 78.7, 50.5, 48.8, 30.5, 27.5, 16.1, 9.6.

2.4.4.8. (*E*)-3-((2R,3S,4R)-4-(3,5-di-*tert*-butyl-4-hydroxyphenyl)-2-methylchroman-3-yl)acrylaldehyde (4h).



4h

$C_{27}H_{34}O_3$

M = 406.56

According to **GP-1** compound **(4h)** was prepared by using **1b** (22.0 µL, 0.2 mmol, 2.0 equiv) **2a** (31.0 mg, 0.1 mmol, 1.0 equiv) triethylamine (6.0 µL, 0.04 mmol, 0.4 equiv) and **Amine 3c** (10.2 mg, 0.02 mmol) in *o*-xylene for 40 h. at 45 °C.

Column Chromatographic purification (petroleum ether/EtOAc 99:1 to 97:3) afforded **4h** (major diastereomer) as light yellow gummy liquid (27.5 mg, 68 %).

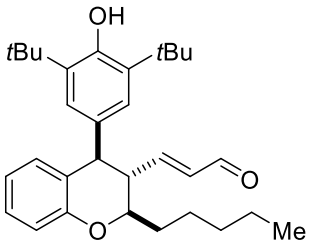
$[\alpha]_D^{20}$ = + 52.1 (c = 0.2, EtOH).

HPLC: Daicel Chiralpak IC column; *n*-hexane/ *i*PrOH = 400/1; flow rate = 1.0 mL/min; T = 25 °C; retention time: 17.56 min (major), 23.38 min (minor), *ee*: 82 %.

HRMS (ESI): *m/z* $[M-H]^+$ Calculated for **$C_{27}H_{33}O_3^+$:** 405.2430; Found 405.2425.

^{1}H NMR (400 MHz, $CDCl_3$): δ 9.42 (d, *J* = 7.8 Hz, 1H), 7.13-7.09 (m, 1H), 6.86 (d, *J* = 8.1 Hz, 1H), 6.78-6.77 (m, 2H), 6.74 (s, 2H), 6.51 (dd, *J* = 15.6, 9.7 Hz, 1H), 5.72 (dd, *J* = 15.7, 7.8 Hz, 1H), 5.08 (s, 1H), 4.23-4.16 (m, 1H), 3.92 (d, *J* = 10.9 Hz, 1H), 2.70 (q, *J* = 10.0 Hz, 1H), 1.38 (d, *J* = 6.3 Hz, 3H), 1.34 (s, 18H).**^{13}C NMR (101 MHz, $CDCl_3$):** δ 193.1, 155.7, 154.5, 152.7, 135.9, 135.3, 132.3, 130.3, 127.8, 125.6, 125.0, 120.8, 116.4, 74.2, 52.1, 48.4, 34.4, 30.5, 20.6. **^{13}C NMR DEPT-135 (101 MHz, $CDCl_3$):** δ 193.1, 155.7, 135.3, 130.3, 127.8, 125.6, 120.8, 116.4, 74.2, 52.1, 48.4, 20.6.

2.4.4.9. (*E*)-3-((2R,3S,4R)-4-(3,5-di-*tert*-butyl-4-hydroxyphenyl)-2-pentylchroman-3-yl)acrylaldehyde (4i).



4i

$C_{31}H_{42}O_3$

M = 462.67

According to **GP-1** compound **(4i)** was prepared by using **1c** (35.0 µL, 0.2 mmol, 2.0 equiv), **2a** (31.0 mg, 0.1 mmol, 1 equiv), triethylamine (6.0 µL, 0.04 mmol, 0.4 equiv) and **Amine 3c** (10.2 mg, 0.02 mmol) in *o*-xylene for 40 h at 45 °C.

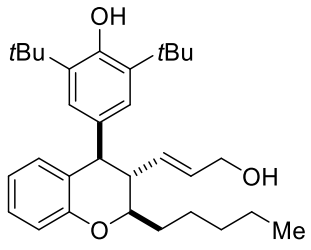
Column Chromatographic purification (petroleum ether/EtOAc 99:1 to 98:2) afforded **4i** (major diastereomer) as light yellow gummy liquid (30.5 mg, 66 %).

$[\alpha]_D^{20}$ = + 20.0 (c = 1.0, EtOH).

HRMS (ESI): *m/z* $[M-H]^+$ Calculated for **$C_{31}H_{41}O_3^+$:** 461.3056; Found 461.3050.

^{1}H NMR (400 MHz, $CDCl_3$) : δ 9.42 (d, *J* = 7.8 Hz, 1H), 7.13-7.09 (m, 1H), 6.87 (d, *J* = 8.1 Hz, 1H), 6.77 (d, *J* = 4.2 Hz, 2H), 6.73 (s, 2H), 6.51 (dd, *J* = 15.6, 9.8 Hz, 1H), 5.68 (dd, *J* = 15.7, 7.8 Hz, 1H), 5.08 (s, 1H), 4.09-4.06 (m, 1H), 3.91 (d, *J* = 10.8 Hz, 1H), 2.75 (q, *J* = 10.1 Hz, 1H), 1.67-1.59 (m, 3H), 1.49-1.41 (m, 5H), 1.34 (s, 18H), 0.89 (t, *J* = 6.2 Hz, 3H). **^{13}C NMR (101 MHz, $CDCl_3$):** δ 193.1, 155.9, 154.7, 152.7, 135.9, 135.2, 132.4, 130.3, 127.7, 125.6, 125.0, 120.7, 116.5, 77.7, 50.6, 48.6, 34.4, 34.3, 31.8, 30.5, 24.5, 22.7, 14.2. **^{13}C NMR DEPT-135 (101 MHz, $CDCl_3$):** δ 193.1, 155.9, 135.2, 130.3, 127.7, 125.6, 120.7, 116.5, 77.7, 50.6, 48.6, 34.3, 31.8, 30.5, 24.5, 22.7, 14.2.

2.4.4.10. 2,6-di-*tert*-butyl-4-((2R,3S,4R)-3-((*E*)-3-hydroxyprop-1-en-1-yl)-2-pentylchroman-4-yl)phenol (4i-1).



4i-1
$C_{31}H_{44}O_3$
M = 464.69

Compound **(4i-1)** was prepared by the reduction of **4i** (30.5 mg, 0.066 mmol, 1 equiv) using $NaBH_4$/EtOH at 0 °C for 1 h.

Column Chromatographic purification (petroleum ether/EtOAc 99:1 to 90:10) afforded **4j** as colourless gummy liquid (24.0 mg, 78 %).

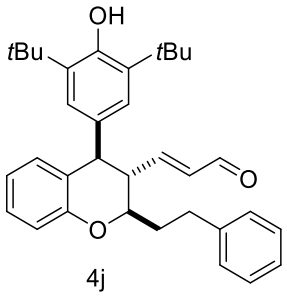
$[\alpha]_D^{20}$ = –14.0 (c = 0.2, EtOH).

HPLC: Daicel Chiralpak IC column; *n*-hexane/ *i*PrOH = 200/1; flow rate = 1.0 mL/min; T = 25 °C; retention time: 9.55 min (major), 10.49 min (minor), *ee*: 92 %.

HRMS (ESI): *m/z* $[M-H]^+$ Calculated for **$C_{31}H_{43}O_3$:** 463.3212; Found 463.3250.

^{1}H NMR (400 MHz, $CDCl_3$) : δ 7.09-7.05 (m, 1H), 6.84 (d, *J* = 8.0 Hz, 1H), 6.77-6.71 (m, 4H), 5.33 (dd, *J* = 15.7, 9.1 Hz, 1H), 5.23-5.16 (m, 1H), 5.04 (s, 1H), 3.97-3.91 (m, 3H), 3.75 (d, *J* = 10.7 Hz, 1H), 2.42 (q, *J* = 10.1 Hz, 1H), 1.75-1.68 (m, 1H), 1.62-1.57 (m, 1H), 1.44-1.40 (m, 1H), 1.36 (s, 18H), 1.35-1.28 (m, 5H), 0.89 (t, *J* = 6.8 Hz, 3H). **^{13}C NMR (101 MHz, $CDCl_3$):** δ 155.0, 152.2, 135.5, 133.7, 132.3, 131.1, 130.4, 127.4, 126.1, 126.0, 120.3, 116.3, 78.7, 63.5, 49.8, 49.0, 34.4, 34.1, 32.0, 30.5, 24.6, 22.8, 14.2. **^{13}C NMR DEPT-135 (101 MHz, $CDCl_3$):** δ 132.3, 131.1, 130.4, 127.4, 126.0, 120.3, 116.3, 78.7, 63.5, 49.8, 49.0, 34.1, 32.0, 24.6, 22.8, 14.2.

2.4.4.11. (*E*)-3-((2R,3S,4R)-4-(3,5-di-*tert*-butyl-4-hydroxyphenyl)-2-phenethylchroman-3-yl)acrylaldehyde (4j).



4j
$C_{34}H_{40}O_3$
M = 496.69

According to **GP-1** compound **(4j)** was prepared by using **1d** (37.0 mg, 0.2 mmol, 2.0 equiv) **2a** (31.0 mg, 0.1 mmol, 1.0 equiv) triethylamine (6.0 µL, 0.04 mmol, 0.4 equiv) and **Amine 3c** (10.2 mg, 0.02 mmol) in *o*-xylene for 40 h. at 45 °C.

Column Chromatographic purification (petroleum ether/EtOAc 99:1 to 97:3) afforded **4j** (major diastereomer) as pale yellow gummy liquid (35.5 mg, 71 %).

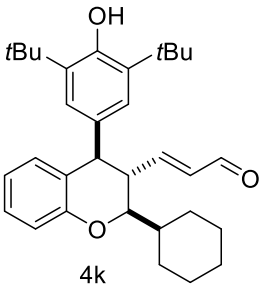
$[\alpha]_D^{20}$ = + 15.5 (c = 0.8, EtOH).

HPLC: Daicel CHIRALPAK IC column; *n*-hexane/ *i*PrOH = 200/1; flow rate = 1.0 mL/min; T = 25 °C; retention time: 16.55 min (major), 18.26 min (minor), *ee*: > 99%.

HRMS (ESI): *m/z* $[M-H]^+$ Calculated for **$C_{34}H_{39}O_3^+$:** 495.2899; Found 495.2887.

^{1}H NMR (400 MHz, $CDCl_3$): δ 9.38 (d, *J* = 7.8 Hz, 1H), 7.29-7.27 (m, 1H), 7.20-7.19 (m, 3H), 7.16-7.12 (m, 2H), 6.94 (d, *J* = 8.1 Hz, 1H), 6.79-6.78 (m, 2H), 6.72 (s, 2H), 6.44 (dd, *J* = 15.6, 9.9 Hz, 1H), 5.64 (dd, *J* = 15.6, 7.8 Hz, 1H), 5.08 (s, 1H), 4.07-4.02 (m, 1H), 3.88 (d, *J* = 10.8 Hz, 1H), 3.02-2.95 (m, 1H), 2.88-2.81 (m, 1H), 2.80-2.74 (m, 1H), 1.95-1.90 (m, 2H), 1.33 (s, 18H). **^{13}C NMR (101 MHz, $CDCl_3$):** δ 193.0, 155.4, 154.5, 152.7, 141.6, 135.9, 135.3, 132.3, 130.3, 128.7, 128.6, 127.8, 126.1, 125.6, 125.1, 120.9, 116.5, 76.5, 50.7, 48.5, 36.2, 34.4, 31.1, 30.4. **^{13}C NMR DEPT-135 (101 MHz, $CDCl_3$):** δ 193.0, 155.4, 135.3, 130.3, 128.7, 128.6, 127.8, 126.1, 125.6, 125.1, 120.9, 116.5, 76.5, 50.7, 48.5, 36.2, 31.1, 30.4.

2.4.4.12. (*E*)-3-((2R,3S,4R)-2-cyclohexyl-4-(3,5-di-*tert*-butyl-4-hydroxyphenyl)chroman-3-yl)acrylaldehyde (4k).



4k

$C_{32}H_{42}O_3$

M = 474.6850

According to **GP-1** compound **(4k)** was prepared by using **1e** (33.0 mg, 0.2 mmol, 2.0 equiv) **2a** (31.0 mg, 0.1 mmol, 1.0 equiv) triethylamine (6.0 µL, 0.04 mmol, 0.4 equiv) and **Amine 3c** (10.2 mg, 0.02 mmol) in *o*-xylene for 40 h. at 45 °C.

Column Chromatographic purification (petroleum ether/EtOAc 99:1 to 97:3) afforded **4k** (major diastereomer) as orange solid (28.5 mg, 60%).

Melting Point: 106-108 °C

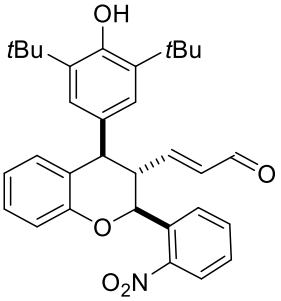
$[\alpha]_D^{20}$ = + 15.0 (c = 0.8, EtOH).

HPLC: Daicel CHIRALPAK IC column; *n*-hexane/ *i*PrOH = 200/1; flow rate = 1 mL/min; T = 25 °C; retention time: 8.60 min (minor), 10.15 min (major), *ee*: 92%.

HRMS (ESI): *m/z* $[M+H]^+$ Calculated for $C_{32}H_{43}O_3^+$ **:** 475.3212; Found 475.3188.

^{1}H NMR (400 MHz, $CDCl_3$): δ 9.42 (d, *J* = 7.7 Hz, 1H), 7.12-7.08 (m, 1H), 6.86 (d, *J* = 8.3 Hz, 1H), 6.76 (d, *J* = 4.3 Hz, 2H), 6.73 (s, 2H), 6.53 (dd, *J* = 15.6, 10.0 Hz, 1H), 5.68 (dd, *J* = 15.6, 7.8 Hz, 1H), 5.07 (s, 1H), 3.97-3.91 (m, 2H), 2.91 (q, *J* = 10.1 Hz, 1H), 1.77-1.73 (m, 3H), 1.69-1.63 (m, 3H), 1.42-1.38 (m, 2H), 1.34 (s, 18H), 1.14-1.08 (m, 3H). **^{13}C NMR (101 MHz, $CDCl_3$):** δ 193.2, 156.0, 155.0, 135.8, 134.8, 132.3, 130.2, 127.7, 125.6, 124.9, 120.5, 116.5, 81.8, 48.8, 47.6, 40.6, 34.4, 30.5, 30.2, 26.7, 26.4, 26.2, 24.7. **^{13}C NMR DEPT-135 (101 MHz, $CDCl_3$):** δ 193.2, 156.0, 134.8, 130.2, 127.7, 125.6, 120.5, 116.5, 81.8, 48.8, 47.6, 40.6, 30.5, 30.2, 26.7, 26.4, 26.2, 24.7.

2.4.4.13. (*E*)-3-((*2S,3S,4R*)-4-(3,5-di-*tert*-butyl-4-hydroxyphenyl)-2-(2-nitrophenyl)chroman-3-yl)acrylaldehyde (4l).



4l

$C_{32}H_{35}NO_5$

M = 513.63

According to **GP-1** compound **(4l)** was prepared by using **1f** (21.0 mg, 0.1 mmol, 1.0 equiv) **2a** (124.0 mg, 0.4 mmol, 4.0 equiv) triethylamine (6.0 µL, 0.04 mmol, 0.4 equiv) and **Amine 3c** (10.2 mg, 0.02 mmol) in chloroform (0.1 M) for 7 d. at 45 ºC.

Column Chromatographic purification (petroleum ether/EtOAc 99:1 to 90:10) afforded **4l** (major diastereomer) as yellow gummy liquid (18.0 mg, 35 %).

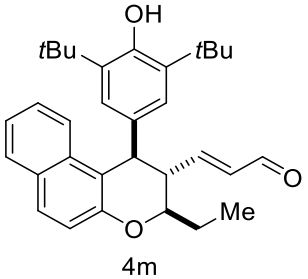
$[\alpha]_D^{20}$ = + 34.1 (c = 0.6, EtOH).

HPLC: Daicel CHIRALPAK IC column; *n*-hexane/ *i*PrOH = 95/5; flow rate = 1.0 mL/min; T = 25 ºC; retention time: 7.53min (major), 9.91min (minor), *ee*: 76 %.

HRMS (ESI): *m/z* $[M+H]^+$ Calculated for $C_{32}H_{36}NO_5^+$ **:** 514.2593; Found 514.2564.

^{1}H NMR (400 MHz, $CDCl_3$): δ 9.28 (d, *J* = 7.9 Hz, 1H), 8.11 (d, *J* = 7.6 Hz, 1H), 7.80 (d, *J* = 7.8 Hz, 1H), 7.67-7.63 (m, 1H), 7.49-7.45 (m, 1H), 7.22 (d, *J* = 7.7 Hz, 1H), 7.03 (dd, *J* = 12.9, 7.8 Hz, 2H), 6.95-6.91 (m, 1H), 6.88-6.81 (m, 3H), 6.15 (d, *J* = 8.0 Hz, 1H), 5.27 (dd, *J* = 15.7, 7.8 Hz, 1H), 5.11 (s, 1H), 4.89 (d, *J* = 5.3 Hz, 1H), 3.35 (dd, *J* = 10.9, 5.4 Hz, 1H), 1.34 (s, 18H). **^{13}C NMR (101 MHz, $CDCl_3$):** δ 192.8, 154.6, 152.9, 152.5, 137.4, 135.7, 135.0, 133.7, 130.7, 130.5, 128.9, 128.7, 128.3, 126.2, 125.2, 123.7, 121.8, 117.0, 76.8, 49.1, 48.3, 34.4, 30.4. **^{13}C NMR DEPT-135 (101 MHz, $CDCl_3$):** δ 192.8, 152.5, 137.4, 133.7, 130.7, 128.9, 128.7, 128.3, 126.2, 125.2, 121.8, 117.0, 76.8, 49.1, 48.3, 30.4.

2.4.4.14. (*E*)-3-((*1R,2S,3R*)-1-(3,5-di-*tert*-butyl-4-hydroxyphenyl)-3-ethyl-2,3-dihydro-1*H*-benzo[*f*]chromen-2-yl)acrylaldehyde (4m).



4m

$C_{32}H_{38}O_3$

M = 470.65

According to **GP-1** compound **(4m)** was prepared by using **1a** (22.0 µL, 0.2 mmol, 2.0 equiv) **2e** (36.0 mg, 0.1 mmol, 1.0 equiv) triethylamine (3.0 µL, 0.02 mmol, 0.2 equiv) and **Amine 3c** (10.2 mg, 0.02 mmol) in *o*-xylene for 48 h at 10 °C.

Column Chromatographic purification (petroleum ether/EtOAc 99:1 to 97:3) afforded **4m** as light yellow gummy liquid (23.0 mg, 49 %).

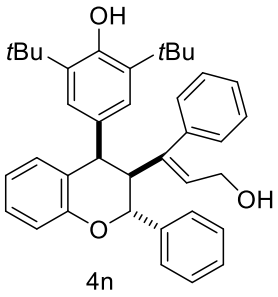
$[\alpha]_D^{20}$ = – 32.1 (c = 0.6, EtOH).

HPLC: Daicel Chiralpak IC column; *n*-hexane/ *i*PrOH = 95/5; flow rate = 1.0 mL/min; T = 25 °C; retention time: 7.15 min (minor), 10.53 min (major), *ee*: 58 %.

HRMS (ESI): *m/z* $[M-H]^+$ Calculated for **$C_{28}H_{37}O_3^+$:** 469.2743; Found 469.2739.

^{1}H NMR (400 MHz, $CDCl_3$) :δ 9.41 (d, *J* = 7.9 Hz, 1H), 7.76-7.68 (m, 2H), 7.44-7.42 (m, 1H), 7.30-7.26 (m, 2H), 7.16 (d, *J* = 9.0 Hz, 1H), 6.86 (s, 2H), 6.79 (dd, *J* = 15.7, 9.8 Hz, 1H), 6.30 (dd, *J* = 15.7, 7.9 Hz, 1H), 5.09 (s, 1H), 4.48-4.46 (m, 1H), 4.08 (ddd, *J* = 8.8, 4.9, 1.8 Hz, 1H), 2.88 (d, *J* = 9.7 Hz, 1H), 1.80-1.69 (m, 1H), 1.51-1.43 (m, 1H), 1.31 (s, 18H), 1.01 (t, *J* = 7.4 Hz, 3H). **^{13}C NMR (101 MHz, $CDCl_3$):** δ 194.0, 156.0, 152.5, 135.9, 134.9, 134.9, 133.3, 129.6, 129.3, 128.5, 126.6, 125.1, 123.4, 123.4, 118.7, 112.5, 77.3, 73.5, 48.2, 44.2, 34.4, 30.3, 26.7, 10.1. **^{13}C NMR DEPT-135 (101 MHz, $CDCl_3$):** δ 194.0, 156.0, 134.9, 129.3, 128.5, 126.6, 125.1, 123.4, 118.7, 77.3, 73.5, 48.2, 44.2, 30.3, 26.7, 10.1.

2.4.4.15. 2,6-di-*tert*-butyl-4-((*2R,3S,4R*)-3-((*Z*)-3-hydroxy-1-phenylprop-1-en-1-yl)-2-phenylchroman-4-yl)phenol (4n).



4n

$C_{38}H_{42}O_3$

M = 546.75

According to **GP-2** compound **(4n)** was prepared by using **1g** (46.0 mg, 0.2 mmol, 2.0 equiv) **2a** (31.0 mg, 0.1 mmol, 1.0 equiv) triethylamine (6.0 µL, 0.04 mmol, 0.4 equiv), brine (3.0 equiv) and **Amine 3a** (6.7 mg, 0.02 mmol) in toluene for 12 h. at room temperature.

Column Chromatographic purification (petroleum ether/EtOAc 99:1 to 85:15) afforded **4n** (major diastereomer) as white solid (45.0 mg, 83 %).

Melting Point: 166-168 ºC

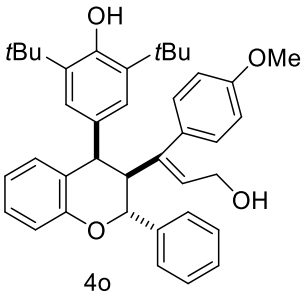
$[\alpha]_D^{20}$ = – 76.9 (c = 1.0, EtOH).

HPLC: Daicel CHIRALPAK IC column; *n*-hexane/ *i*PrOH = 200/1; flow rate = 1.0 mL/min; T = 25 ºC; retention time: 13.42 min (major), 15.84 min (minor), *ee*: 90%.

HRMS (ESI): *m/z* $[M+H]^+$ Calculated for **$C_{38}H_{43}O_3^+$:** 547.3212; Found 547.3239

^{1}H NMR (400 MHz, $CDCl_3$): δ 7.39-7.28 (m, 5H), 7.23-7.20 (m, 3H), 7.17-7.12 (m, 1H), 7.00-6.96 (m, 2H), 6.90 (s, 2H), 6.81 (td, *J* = 7.5, 1.2 Hz, 1H), 6.76-6.74 (m, 2H), 5.31 (d, *J* = 11.1 Hz, 1H), 5.15 (s, 1H), 4.57 (dd, *J* = 7.7, 6.0 Hz, 1H), 4.10 (d, *J* = 4.6 Hz, 1H), 3.73-3.62 (m, 2H), 3.39 (dd, *J* = 11.1, 4.7 Hz, 1H), 1.41 (s, 18H). **^{13}C NMR (101 MHz, $CDCl_3$):** δ 154.4, 152.6, 140.8, 140.3, 139.4, 135.0, 132.2, 131.1, 130.5, 128.4, 128.4, 128.3, 128.2, 128.1, 128.0, 127.4, 127.3, 125.6, 120.5, 116.5, 77.9, 60.3, 50.8, 45.6, 34.4, 30.5. **^{13}C NMR DEPT-135 (101 MHz, $CDCl_3$):** δ 131.1, 130.5, 128.4, 128.4, 128.3, 128.2, 128.1, 128.0, 127.4, 127.3, 120.5, 116.5, 77.9, 60.3, 50.8, 45.6, 30.5.

2.4.4.16. 2,6-di-*tert*-butyl-4-((*2R,3S,4R*)-3-((*Z*)-3-hydroxy-1-(4-methoxyphenyl)prop-1-en-1-yl)-2-phenylchroman-4-yl)phenol (4o).



4o

$C_{39}H_{44}O_4$

M = 576.78

According to **GP-2** compound **(4o)** was prepared by using **1h** (52.0 mg, 0.2 mmol, 2.0 equiv) **2a** (31.0 mg, 0.1 mmol, 1.0 equiv) triethylamine (6.0 µL, 0.04 mmol, 0.4 equiv), brine (3.0 equiv) and **Amine 3a** (6.7 mg, 0.02 mmol) in toluene for 12 h. at room temperature.

Column Chromatographic purification (petroleum ether/EtOAc 0199:1 to 85:15) afforded **4o** (major diastereomer) as colourless gummy liquid (55.0 mg, 96 %).

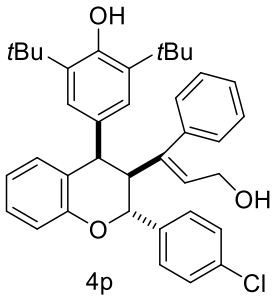
$[\alpha]_D^{20}$ = – 127.8 (c = 1.0, EtOH).

HPLC: Daicel Chiralpak IC column; *n*-hexane/ *i*PrOH = 200/1; flow rate = 1.0 mL/min; T = 25 °C; retention time: 22.78. min (major), 25.69 min (minor), *ee*: 92 %.

HRMS (ESI): *m/z* $[M+H]^+$ Calculated for **$C_{39}H_{45}O_4^+$:** 577.3318; Found 577.3289

^{1}H NMR (400 MHz, $CDCl_3$): δ 7.38-7.36 (m, 2H), 7.34-7.27 (m, 3H), 7.14 (ddd, *J* = 8.6, 7.4, 1.8 Hz, 1H), 6.98 (td, *J* = 7.3, 6.8, 1.1 Hz, 2H), 6.87 (s, 2H), 6.81 (td, *J* = 7.3, 1.1 Hz, 1H), 6.78-6.69 (m, 4H), 5.30 (d, *J* = 11.1 Hz, 1H), 5.14 (s, 1H), 4.54 (dd, *J* = 7.8, 5.9 Hz, 1H), 4.08 (d, *J* = 4.6 Hz, 1H), 3.76 (s, 3H), 3.69 (m, 2H), 3.39 (dd, *J* = 11.1, 4.7 Hz, 1H), 1.41 (s, 18H). **^{13}C NMR (101 MHz, $CDCl_3$):** δ 158.9, 154.4, 152.6, 140.4, 139.0, 135.0, 133.0, 132.3, 130.6, 130.5, 129.3, 128.4, 128.3, 128.0, 127.2, 125.6, 120.5, 116.5, 113.5, 77.9, 60.3, 55.4, 50.8, 45.7, 34.4, 30.5. **^{13}C NMR DEPT-135 (101 MHz, $CDCl_3$):** δ 130.6, 130.5, 129.3, 128.4, 128.3, 128.0, 127.2, 120.5, 116.5, 113.5, 77.9, 60.3, 55.4, 50.8, 45.7, 30.5.

2.4.4.17. 2,6-di-*tert*-butyl-4-((*2R,3S,4R*)-2-(4-chlorophenyl)-3-((*Z*)-3-hydroxy-1-phenylprop-1-en-1-yl)chroman-4-yl)phenol (4p).



4p

$C_{38}H_{41}ClO_3$

M = 581.19

According to **GP-2** compound **(4p)** was prepared by using **1i** (53.0 mg, 0.2 mmol, 2.0 equiv) **2a** (31.0 mg, 0.1 mmol, 1.0 equiv) triethylamine (6.0 µL, 0.04 mmol, 0.4 equiv), brine (3.0 equiv) and **Amine 3a** (6.7 mg, 0.02 mmol) in toluene for 12 h. at room temperature.

Column Chromatographic purification (petroleum ether/EtOAc 99:1 to 85:15) afforded **4p** (major diastereomer) as white solid (54.0 mg, 93 %).

Melting Point: 160-162 °C

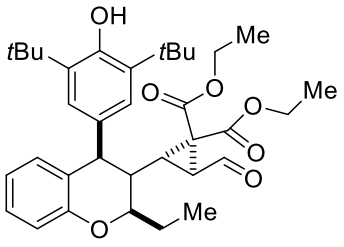
$[\alpha]_D^{20}$ = – 127.8 (c = 1.0, EtOH).

HPLC: Daicel Chiralpak IC column; *n*-hexane/ *i*PrOH = 200/1; flow rate = 1.0 mL/min; T = 25 °C; retention time: 11.69. min (minor), 13.36 min (major), *ee*: 92 %.

HRMS (ESI): *m/z* $[M-H]^+$ Calculated for **$C_{38}H_{40}ClO_3^+$:** 579.2666; Found 579.2660

^{1}H NMR (400 MHz, $CDCl_3$): δ 7.31-7.30 (m, 4H), 7.24-7.21 (m, 3H), 7.17-7.12 (m, 1H), 6.97 (dd, *J* = 15.5, 7.7 Hz, 2H), 6.88 (s, 2H), 6.82 (td, *J* = 7.5, 1.0 Hz, 1H), 6.74-6.72 (m, 2H), 5.28 (d, *J* = 11.2 Hz, 1H), 5.16 (s, 1H), 4.57 (dd, *J* = 7.5, 6.2 Hz, 1H), 4.10 (d, *J* = 4.5 Hz, 1H). 3.76-3.64 (m, 2H), 3.34 (dd, *J* = 11.2, 4.7 Hz, 1H), 1.41 (s, 18H). **^{13}C NMR (101 MHz, $CDCl_3$):** δ 154.1, 152.7, 140.6, 139.1, 139.0, 135.1, 134.0, 132.0, 131.2, 130.5, 129.7, 128.5, 128.3, 128.1, 128.0, 127.5, 127.2, 125.5, 120.7, 116.4, 77.2, 60.2, 50.8, 45.7, 34.4, 30.5. **^{13}C NMR DEPT-135 (101 MHz, $CDCl_3$):** δ 131.2, 130.5, 129.7, 128.5, 128.3, 128.1, 128.0, 127.5, 127.2, 120.7, 116.4, 77.2, 60.2, 50.8, 45.7, 30.5.

2.4.4.18. (*2S,3S*)-diethyl 2-((*2R,4R*)-4-(3,5-di-*tert*-butyl-4-hydroxyphenyl)-2-ethylchroman-3-yl)-3-formylcyclopropane-1,1-dicarboxylate (5).



5

$C_{35}H_{46}O_7$

M = 578.75

According to **GP-3** compound **(5)** was prepared by using **4a** (42.0 mg, 0.1 mmol, 1.0 equiv) **diethyl bromomalonate** (34 .0 µL, 0.2 mmol, 2.0 equiv) triethylamine (14.0 µL, 0.1 mmol, 1 equiv) and **Amine 3a** (6.7 mg, 0.02 mmol) in chloroform for 40 h. at 45 °C.

Column Chromatographic purification (petroleum ether/EtOAc 99:1 to 90:10) afforded **1a** as colourless gummy liquid (31.0 mg, 54 %).

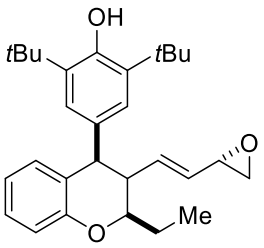
$[\alpha]_D^{20}$ = – 38.1 (c = 1.0, EtOH).

HPLC: Daicel CHIRALPAK IC column; *n*-hexane/*i*PrOH = 95/5; flow rate = 1.0 mL/min; T = 25 °C; retention time: 10.88 min (major), 11.79 min (minor), *ee*: > 99%.

HRMS (ESI): *m/z* $[M+H]^+$ Calculated for **$C_{35}H_{47}O_7^+$:** 579.3322; Found 579.3317

^{1}H NMR (400 MHz, $CDCl_3$): δ 9.18 (d, *J* = 4.8 Hz, 1H), 7.09-7.04 (m, 1H), 6.85 (d, *J* = 9.0 Hz, 1H), 6.83 (s, 2H), 6.79-6.74 (m, 1H), 6.70 (d, *J* = 6.7 Hz, 1H), 5.04 (s, 1H), 4.22-4.09 (m, 2H), 4.03-3.98 (m, 2H), 3.89 (q, *J* = 6.4 Hz, 1H), 3.66-3.58 (m, 1H), 2.81 (dd, *J* = 7.1, 4.8 Hz, 1H), 2.42-2.30 (m, 2H), 1.62-1.58 (m, 2H), 1.33 (s, 18H), 1.20 (t, *J* = 7.2 Hz, 3H), 1.09 (t, *J* = 7.1 Hz, 3H), 0.95 (t, *J* = 7.3 Hz, 3H). **^{13}C NMR (101 MHz, $CDCl_3$):** δ 196.4, 166.0, 165.8, 154.4, 152.3, 135.2, 133.9, 131.1, 127.4, 126.4, 125.5, 120.7, 116.7, 80.3, 77.3, 62.2, 62.0, 47.9, 42.2, 40.7, 40.2, 35.8, 34.4, 30.4, 26.4, 14.1, 9.7. **^{13}C NMR DEPT-135 (101 MHz, $CDCl_3$):** δ 196.4, 131.1, 127.4, 126.4, 120.7, 116.7, 80.3, 62.2, 62.0, 47.9, 40.7, 40.2, 35.8, 30.4, 26.4, 14.1, 9.7.

2.4.4.19. 2,6-di-*tert*-butyl-4-((*2R,4R*)-2-ethyl-3-((*E*)-2-((*S*)-oxiran-2-yl)vinyl)chroman-4-yl)phenol (6).



6

$C_{29}H_{38}O_3$

M = 434.62

According to **GP-4** compound **(6)** was prepared by using **4a** (42.0 mg, 0.1 mmol, 1.0 equiv), NaH (60 % dispersion in oil, 12.0 mg, 0.31 mmol, 3.1 equiv), Trimethylsulfonium iodide (61.0 mg, 0.3 mmol, 3.0 equiv) in a mixture of dry THF & dry DMSO at 0 °C for 1 h, then at room temperature for another 1 h.

Column Chromatographic purification (petroleum ether/EtOAc 99:1 to 95:5) afforded **6** (major diastereomer) as pale yellow solid (29.0 mg, 66 %).

Melting Point: 95-97 °C

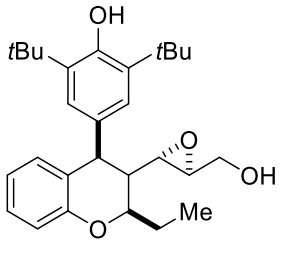
$[\alpha]_D^{20}$ = + 39.7 (c = 1.0, EtOH).

HPLC: Daicel CHIRALPAK ODH column; *n*-hexane/ *i*PrOH = 1000/1; flow rate = 1.0 mL/min; T = 25 °C; retention time: 7.46 min (minor), 9.25 min (major), *ee*: 98%.

HRMS (ESI): *m/z* $[M+H]^+$ Calculated for **$C_{29}H_{39}O_3^+$:** 435.2899; Found 435.2881

^{1}H NMR (400 MHz, $CDCl_3$): δ 7.10-7.06 (m, 1H), 6.85 (d, *J* = 8.1 Hz, 1H), 6.78-6.75 (m, 2H), 6.74 (s, 2H), 5.57 (dd, *J* = 15.5, 9.6 Hz, 1H), 5.03 (s, 1H), 4.66 (dd, *J* = 15.5, 8.1 Hz, 1H), 3.91 (ddd, *J* = 10.5, 8.0, 3.0 Hz, 1H), 3.75 (d, *J* = 10.9 Hz, 1H), 3.21-3.17 (m, 1H), 2.82-2.80 (m, 1H), 2.44 (q, *J* = 10.1 Hz, 1H), 2.30 (dd, *J* = 5.3, 2.6 Hz, 1H), 1.84 (dqd, *J* = 14.9, 7.4, 2.8 Hz, 1H), 1.64-1.59 (m, 1H), 1.36 (s, 18H), 1.06 (t, *J* = 7.4 Hz, 3H). **^{13}C NMR (101 MHz, $CDCl_3$):** δ 155.1, 152.2, 135.4, 134.2, 133.5, 131.1, 130.4, 127.4, 126.0, 125.9, 120.3, 116.3, 79.5, 52.1, 49.7, 48.9, 48.6, 34.3, 30.5, 27.0, 9.3. **^{13}C NMR DEPT-135 (101 MHz, $CDCl_3$):** δ 134.2, 133.5, 131.1, 130.4, 127.4, 125.9, 120.3, 116.3, 79.5, 52.1, 49.7, 48.9, 48.6, 30.5, 27.0, 9.3.

2.4.4.20. 2,6-di-*tert*-butyl-4-((*2R,4R*)-2-ethyl-3-((*2S,3S*)-3-(hydroxymethyl)oxiran-2-yl)chroman-4-yl)phenol (7).



7

$C_{28}H_{38}O_4$

M = 438.61

According to **GP-4** compound **(7)** was prepared by the reduction of **4a** (42.0 mg, 0.1 mmol, 1.0 equiv) using $NaBH_4$/EtOH at 0 °C for 1 h.

Allyllic alcohol obtained from above procedure dissolved in DCM (0.2 mL) at 0 °C. *meta*-Chloroperoxybenzoic acid (*m*CPBA, 1.3 equiv, 0.11 mmol) was added and the reaction mixture stirred for 3 h

Column Chromatographic purification (petroleum ether/EtOAc 90:10 to 70:30) afforded **7** (major diastereomer) as colourless gummy liquid (26.0 mg, 60 %).

$[\alpha]_D^{20}$ = – 16.5 (c = 0.8, EtOH).

HPLC: Daicel CHIRALPAK IC column; *n*-hexane/iPrOH = 95/5; flow rate = 0.2 mL/min; T = 25 °C; retention time: 7.46 min (minor), 9.25 min (major), *ee*: >99%.

HRMS (ESI): *m/z* $[M-H]^+$ Calculated for **$C_{28}H_{37}O_4^+$:** 437.2692; Found 437.2679

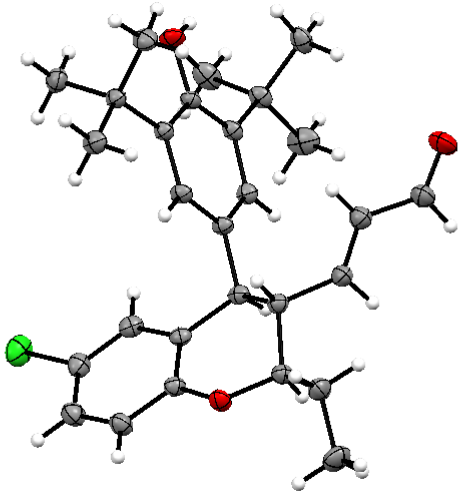
^{1}H NMR (400 MHz, $CDCl_3$): δ 7.10-7.06 (m, 1H), 6.88 (s, 2H), 6.85 (d, *J* = 8.7 Hz, 1H), 6.78-6.77 (m, 2H), 5.07 (s, 1H), 3.99 (d, *J* = 8.4 Hz, 1H), 3.92 (td, *J* = 8.2, 3.7 Hz, 1H), 3.82 (dd, *J* = 12.7, 2.2 Hz, 1H), 3.55 (dd, *J* = 12.7, 3.8 Hz, 1H), 3.03-3.02 (m, 1H), 2.96 (dd, *J* = 7.2, 2.0 Hz, 1H), 2.09 (q, *J* = 7.8 Hz, 1H), 1.79-1.73 (m, 1H), 1.71-1.64 (m, 1H), 1.37 (s, 18H), 1.01 (t, *J* = 7.3 Hz, 3H). **^{13}C NMR (101 MHz, $CDCl_3$):** δ 154.3, 152.3, 135.7, 134.3, 130.5, 127.5, 125.8, 125.6, 120.7, 116.6, 78.2, 61.3, 57.0, 56.8, 45.3, 45.2, 34.4, 30.5, 26.7, 9.8. **^{13}C NMR DEPT-135 (101 MHz, $CDCl_3$):** δ 130.5, 127.5, 125.6, 120.7, 116.6, 78.2, 61.3, 57.0, 56.8, 45.3, 45.2, 30.5, 26.7, 9.8.

2.4.5. X-ray data of 4d & 4p.

2.4.5.1. X-Ray data of 4d and 4p:

For the determination of X-ray crystal structures of **4d** and **4p** a single crystal was selected and mounted with paratone oil on a glass fiber using gum. The data was collected at 298K on a CMOS based Bruker D8 Venture PHOTON 100 diffractometer equipped with a INCOATEC micro-focus source with graphite monochromatic Mo Kα radiation (λ = 0.71073 Å) operation at 50 kV and 30 mA. For the integration of diffraction profiles SAINT program[19] was used. Absorption correction was done applying SADABS program.[20] The crystal structure was solved by SIR 92[21] and refined by full matrix least square method using SHELXL-97[22] WinGX system, Ver 1.70.01.[23] All the non-hydrogen atoms in the structure were located the Fourier map and refined anisotropically. The hydrogen atoms were fixed by HFIX in their ideal positions and refined using riding model with isotropic thermal parameters. The crystal structure (excluding structure factor) has been deposited to Cambridge Crystallographic Data Centre and allocated deposition number: **4d: CCDC 1982963** and **4p: CCDC 1982953**.[24]

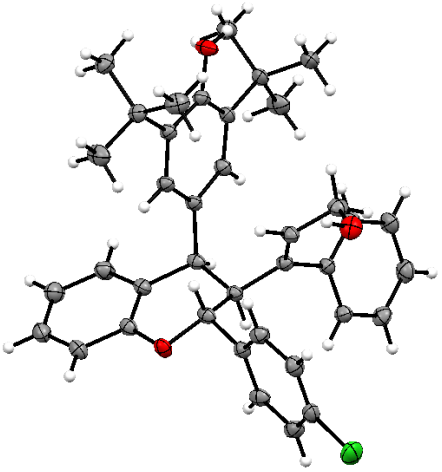
2.4.5.2. Crystal Data and Structure Refinement for Complex 4d (CCDC 1982963)



Atom color code: grey = carbon atom, white = hydrogen atom, green = chlorine atom and red = oxygen atom.

CCDC No.	CCDC 1982963
Formula	C28 H35 Cl O3
Formula weight	455.01
Crystal System	triclinic
Space group	P -1
a, b, c (Å)	10.335(3), 10.973(2), 14.104(3)
α, β, γ (°)	92.007(7), 109.843(8), 117.445(7)
V ($Å^3$)	1299.6(5)
Z	2
Calculated Density (g/cm^3)	1.163
Absorption coefficient (mm^{-1})	0.172
F(000)	488.0
Crystal Size (mm)	0.16 x 0.19 x 0.20
Theta range for data collection:	2.3° to 26.4°
Data set	-12: 12 ; -13: 13 ; -17: 17
R indices [I>=2σ (I)] (all data)	R1 = 0.0548, wR2 = 0.1583
Reflection	19227
Independent refl.	5299, [R(int) = 0.072]
S	1.035
Min. and Max. Resd. Dens. ($e/Å^3$)	-0.20 and 0.19
Npar	289

2.4.5.2. Crystal Data and Structure Refinement for Complex 4p (CCDC 1982953)



Atom color code: grey = carbon atom, white = hydrogen atom, green = chlorine atom and red = oxygen atom.

CCDC No.	CCDC 1982953
Formula	C38 H41 Cl O3
Formula weight	581.16
Crystal System	Orthorhombic
Space group	P212121
a, b, c (Å)	10.561(2), 16.603(3), 18.352(4)
α, β, γ (°)	90, 90, 90
V ($Å^3$)	3217.9(11)
Z	4
Calculated Density (g/cm^3)	1.200
Absorption coefficient (mm^{-1})	0.154
Crystal Size (mm)	0.26 x 0.30 x 0.31
F(000)	1240
Theta range for data collection:	2.2^o to 26.5^o
Data set	-13: 13 ; -20: 20 ; -22: 22
R indexes [I>=2σ (I)] (all data)	R1 = 0.0561, wR2 = 0.1641
Reflection	24944
Independent refl.	4189, [R(int) = 0.070]
S	1.04
Min. and Max. Resd. Dens. ($e/Å^3$)	-0.31 and 0.17
Npar	379

2.5. References:

1. (a) Grondal, C.; Hüttl, M. R. M.; Enders, D. Asymmetric Organocatalytic Domino Reactions. *Angew. Chem., Int. Ed.* **2007**, *46*, 1570-1581. (b) Walji, A. M.; MacMillan, D. W. C. Strategies to Bypass the Taxol Problem. Enantioselective Cascade Catalysis, a New Approach for the Efficient Construction of Molecular Complexity. *Synlett* **2007**, *10*, 1477–1489. (c) Grondal, C.; Jeanty, M.; Enders, D. Organocatalytic cascade reactions as a new tool in total synthesis. *Nat. Chem.* **2010**, *2*, 167-178. (d) Jones, S. P.; Simmons, B.; Mastracchio, A.; MacMillan, D. W. C. Collective synthesis of natural products by means of organocascade catalysis. *Nature* **2011**, *475*, 183-188. (e) Moyano, A.; Rios, R. Asymmetric Organocatalytic Cyclization and Cycloaddition Reactions. *Chem. Rev.* **2011**, *111*, 4703–4831. (f) Albrecht, Ł.; Jiang, H.; Jørgensen, A. K. A. Simple Recipe for Sophisticated Cocktails: Organocatalytic One-Pot Reactions—Concept, Nomenclature, and Future Perspectives. *Angew. Chem., Int. Ed*., **2011**, *50*, 8492–8509. (g) Pellissier, H. Recent Developments in Asymmetric Organocatalytic Domino Reactions. *Adv. Synth. Catal.* **2012**, *354*, 237-294. (h) Pellissier, H. Stereocontrolled Domino Reactions *Chemical Reviews*. **2012,** *113*, 442-524. (i) Grossmann, A.; Enders, D. Domino reactions catalyzed by N-heterocyclic carbenes. *Angew. Chem., Int. Ed.* **2012**, *51*, 314–325. (j) Lu, L.-Q.; Chen, J.-R; Xiao, W.-J. Development of Cascade Reactions for the Concise Construction of Diverse Heterocyclic Architectures. *Acc. Chem. Res.* **2012**, *45*, 1278–1293. (k) Goudedranche, S.; Raimondi, W.; Bugaut, X.; Constantieux, T.; Bonne, D.; Rodriguez, J. Enantioselective Organocatalyzed Domino Synthesis of Six-Membered Carbocycles. *Synthesis* **2013**, *45*, 1909–1930. (l) Volla, C. M. R.; Atodiresei, I.; Rueping, M. Catalytic C-C Bond Forming Multi-Component Cascade or Domino Reactions: Pushing the Boundaries of Complexity in Asymmetric Organocatalysis. *Chem. Rev.* **2014**, *114*, 2390−2431. (m) Chauhan, P.; Mahajan, S.; Kaya, U.; Hack, D.; Enders, D. Bifunctional Amine-Squaramides: Powerful Hydrogen-Bonding Organocatalysts for Asymmetric Domino/Cascade Reactions. *Adv. Synth. Catal.* **2015**, *357*, 253–281.
2. (a) Ellis, G. P. Chemistry of Heterocyclic Compounds, Chromenes, Chromanones, and Chromones. *Wiley-VCH: Weinheim*, **1977**, *31*, doi.org/10.1002/9780470187012.ch1. (b) Cannon, J. G. Comprehensive Heterocyclic Chemistry II, *J. Med. Chem.* **1997**, *40*, 4165-4166. (c) Shen, C. Asymmetric synthesis of chiral chromans. *Tetrahedron* **2009**, *65*, 3931-3952.
3. Chu, W.-D.; Zhang, L.-F.; Bao, X.; Zhao, X.-H.; Zeng, C.; Du, J.-Y.; Zhang, G.-B.; Wang, F.-X.; Ma, X.-Y.; Fan, C.-A. Asymmetric Catalytic 1,6-Conjugate Addition/Aromatization of *para*-Quinone Methides: Enantioselective Introduction of

Functionalized Diarylmethine Stereogenic Centers. *Angew. Chem., Int. Ed.* **2013**, 52, 9229−9233.

4. Caruana, L.; Kniep, F.; Johansen, T. K.; Poulsen, H. P.; Jørgensen, K. A. A New Organocatalytic Concept for Asymmetric α-Alkylation of Aldehydes. *J. Am. Chem. Soc.* **2014**, *136*, 15929−15932.
5. Selected examples: (a) Parra, A.; Tortosa, M.;. *para*-Quinone Methide: a New Player in Asymmetric Catalysis. *ChemCatChem* **2015**, *7*, 1524–1526. (b) Lou, Y.-Z.; Cao, P.; Jia, T.; Zhang, Y.-L.; Wang, M.; Liao, J. Copper-Catalyzed Enantioselective 1,6-Boration of *para*-Quinone Methides and Efficient Transformation of gem-Diarylmethine Boronates to Triarylmethanes. *Angew. Chem., Int. Ed.* **2015**, *54*, 12134−12138. (c) Wang, Z.-B.; Wong, Y. F.; Sun, J.-W. Catalytic Asymmetric 1,6-Conjugate Addition of *para*-Quinone Methides: Formation of All-Carbon Quaternary Stereocenters. *Angew. Chem., Int. Ed.* **2015**, *54*, 13711−13714. (d) Ramanjaneyulu, B. T.; Mahesh, S.; Anand, R. V. Bis(amino)-cyclopropenylidene-Catalyzed 1,6-Conjugate Addition of Aromatic Aldehydes to *para*-Quinone Methides: Expedient Access to α, α′-Diarylated Ketones. *Org. Lett.* **2015**, *17*, 3952−3955. (e) Zhao, K.; Zhi, Y.; Wang, A.; Enders, D. Asymmetric Organocatalytic Synthesis of 3-Diarylmethine-Substituted Oxindoles. Bearing a Quaternary Stereocenter via 1,6-Conjugate Addition to *para*-Quinone Methides. *ACS Catal.* **2016**, *6*, 657−660. (f) Deng, Y.-H.; Zhang, X.-Z.; Yu, K.-Y.; Yan, X.; Du, J.-Y.; Huang, H.; Fan, C.-A. Bifunctional tertiary amine-squaramide catalyzed asymmetric catalytic 1,6-conjugate addition/aromatization of *para*-quinone methides with oxindoles. *Chem. Commun*. **2016**, *52*, 4183−4186. (g) Jarava-Barrera, C.; Parra, A.; Lopez, A.; Cruz-Acosta, F.; Collado-Sanz, D.; Cárdenas, D. J.; Tortosa, M. Copper-Catalyzed Borylative Aromatization of *p*-Quinone Methides: Enantioselective Synthesis of Dibenzylic Boronates. *ACS Catal*. **2016**, *6*, 442−446. (h) Ma, C.; Huang, Y. Zhao, Y. Stereoselective 1,6-Conjugate Addition/Annulation of *para*-Quinone Methides with Vinyl Epoxides/Cyclopropanes. *ACS Catal*. **2016**, *6*, 6408−6412. (i) Dong, N.; Zhang, Z.-P.; Xue, X.-S.; Li, X.; Cheng, J.-P. Phosphoric Acid Catalyzed Asymmetric 1,6-Conjugate Addition of Thioacetic Acid to *para*-Quinone Methides. *Angew. Chem., Int. Ed.* **2016**, *55*, 1460−1464. (j) Arde, P.; Anand, R. V. Expedient access to unsymmetrical triarylmethanes through N-heterocyclic carbene catalysed 1,6-conjugate addition of 2-naphthols to *para*-quinone methides. *RSC Adv.* **2016**, *6*, 77111−77115. (k) Chen, M.; Sun, J.-W. How Understanding the Role of an Additive Can Lead to an Improved Synthetic Protocol without an Additive: Organocatalytic Synthesis of Chiral Diarylmethyl Alkynes. *Angew. Chem., Int. Ed*. **2017**, *56*, 11966−11970. (l) Chen, M.; Sun, J.-W. Catalytic Asymmetric N-Alkylation of Indoles and Carbazoles through 1,6-Conjugate Addition of Aza-*para*-quinone Methides. *Angew. Chem., Int. Ed*. **2017**, *56*, 4583-4587. (m) Goswami,

P.; Singh, G.; Anand, R. V. N-Heterocyclic Carbene Catalyzed 1,6-Conjugate Addition of Me3Si-CN to *para*-Quinone Methides and Fuchsones: Access to α-Arylated Nitriles. *Org. Lett.* **2017**, *19*, 1982−1985. (n) Li, S.-H.; Liu, Y.-Y.; Huang, B.; Zhou, T.; Tao, H.-M.; Xiao, Y.-J.; Liu, L.; Zhang, J.-L. Phosphine-Catalyzed Asymmetric Intermolecular Cross-Vinylogous Rauhut−Currier Reactions of Vinyl Ketones with *para*-Quinone Methides. *ACS Catal.* **2017**, 7, 2805−2809. (o) Zhang, X.-Z.; Gan, K.-J.; Liu, X.-X.; Deng, Y.-H.; Wang, F.-X.; Yu, K.-Y.; Zhang, J.; Fan, C.-A. Enantioselective Synthesis of Functionalized 4-Aryl Hydrocoumarins and 4-Aryl Hydroquinolin-2-ones via Intramolecular Vinylogous Rauhut−Currier Reaction of *para*-Quinone Methides. *Org. Lett.* **2017**, *19*, 3207−3210.

6. Zhao, K.; Zhi, Y.; Shu, T.; Valkonen, A.; Rissanen, K.; Enders, D. Organocatalytic Domino Oxa-Michael/1,6-Addition Reactions: Asymmetric Synthesis of Chromans Bearing Oxindole Scaffolds. *Angew. Chem., Int. Ed*. **2016**, *55*, 12104−12108.
7. Selected examples: (a) Zhang, L.-L.; Zhou, X.; Li, P.-F.; Liu, Z.-T.; Liu, Y.; Sun, Y.; Li, W.-J. Asymmetric synthesis of chromene skeletons via organocatalytic domino reactions of in situ generated ortho-quinone methide withmalononitrile and β-functionalized ketone. *RSC Adv.* **2017**, *7*, 39216−39220. (b) Li, W.-J.; Yuan, H.-J.; Liu, Z.-T.; Zhang, Z.-Y.; Cheng, Y.-Y.; Li, P.-F. NHC-Catalyzed Enantioselective [4+3] Cycloaddition of Ortho-Hydroxyphenyl Substituted *Para*-Quinone Methides with Isatin-Derived Enals. *Adv. Synth. Catal.* **2018**, *360*, 2460−2464. (c) Liu, Q.; Li, S.; Chen, X.-Y.; Rissanen, K.; Enders, D. Asymmetric Synthesis of Spiro-oxindole-ε-lactones through N-Heterocyclic Carbene Catalysis. *Org. Lett.* **2018**, *20*, 3622−3626. (d) Zhang, Z.-P.; Chen, L.; Li, X.; Cheng, J.-P. Organocatalytic Asymmetric Sequential 1,6-Addition/Acetalization of 1-Oxotetralin-2-carbaldehyde to ortho-Hydroxyphenyl-Substituted *para*-Quinone Methides for Synthesis of Spiro-3,4-dihydrocoumarins. *J. Org. Chem.* **2018**, *83*, 2714−2724. (e) Chen, X.-M.; Xie, K.-X.; Yue, D.-F.; Zhang, X.-M.; Xu, X.-Y.; Yuan, W.-C. Catalyst-free synthesis of 2,3 dihydrobenzofurans through [4+1] cycloaddition of ortho-hydroxyphenyl substituted *para*-quinone methides and sulfur ylides. *Tetrahedron* **2018**, *74*, 600−605. (f) Zhang, Z.-P.; Xie, K.-X.; Yang, C.; Li, M.; Li, X. Asymmetric Synthesis of Dihydrocoumarins through Chiral Phosphoric Acid-Catalyzed Cycloannulation of *para*-Quinone Methides and Azlactones. *J. Org. Chem.* **2018**, *83*, 364−373 (g) Zhi, Y.; Zhao, K.; von Essen, C.; Rissanen, K.; Enders, D. Synthesis of transdisubstituted-2,3-dihydrobenzofurans by a formal [4+1] annulations between *para*-quinone methides and sulfonium salts. *Org. Chem. Front.* **2018**, *5*, 1348−1351. (h) Liu, L.-N.; Yuan, Z.-B.; Pan, R.; Zeng, Y.-Y.; Lin, A.-J.; Yao, H.-Q.; Huang, Y. 1,6-Conjugated addition-mediated [4+1] annulation: an approach to 2,3-dihydrobenzofurans. *Org. Chem. Front.* **2018**, *5*, 623−628. (i) Wang, J.-W.; Pan, X.; Liu, J.; Zhao, L.; Zhi, Y.; Zhao, K.; Hu, L.-H.

Diastereoselective Synthesis of Tetrahydroquinolines via [4 +2] Annulation between in Situ Generated *p*-Quinone Methides and Nitroalkenes. *Org. Lett.* **2018**, *20*, 5995−5998. (j) Yang, G. H.; Zhao, Q.; Zhang, Z. P.; Zheng, H. L.; Chen, L.; Li., X. Asymmetric Cycloaddition of ortho-Hydroxyphenyl-Substituted para-Quinone Methides and Enamides Catalyzed by Chiral Phosphoric Acid. *J. Org. Chem.* **2019**, *84*, 7883−7893 (k) Singh, G.; Kumar, S.; Chowdhury, A.; Anand., R. V.; Base-Mediated One-pot Synthesis of Oxygen-Based Heterocycles from 2-Hydroxyphenyl-Substituted para-Quinone Methides. *J. Org. Chem.* **2019,** *84*, 15978-15989.

8. (a) Huang, *Y.*; Walji, A. M.; Larsen C. H.; MacMillan, D. W. C. Enantioselective Organo-Cascade Catalysis. *J. Am. Chem. Soc.* **2005**, *127*, 15051-15053. (b) Marigo, M.; Schulte, T.; Franzen, J.; Jørgensen, K. A. Asymmetric Multicomponent Domino Reactions and Highly Enantioselective Conjugated Addition of Thiols to α,β-Unsaturated Aldehydes. *J. Am. Chem. Soc.* **2005**, *127*, 15710-15711.

9. (a) Fuson, R. C. The Principle of Vinylogy. *Chem. Rev.* **1935**, *16*, 1. (b) Arceo E.*;* Melchiorre P. Extending the Aminocatalytic HOMO-Raising Activation Strategy: Where Is the Limit? *Angew. Chem., Int. Ed.* **2012**, *51*, 5290–5292. (c) Hayashi, H. Okamura, D. Umemiya, T.; Ucimaru, Organocatalytic 1,4-Addition Reaction of α,β,γ,δ Diunsaturated Aldehydes versus 1,6-Addition Reaction. *ChemCatChem.* **2012**, *4*, 959–962.

10. For reviews on vinylogous reactivity: a) Jurberg, I. D.; Chatterjee, I.; Tannert, R.; Melchiorre, P. When asymmetric aminocatalysis meets the vinylogy principle *Chem. Commun*. **2013**, *49*, 4869-4883. b) Jiang, H.; Albrecht, Ł.; Jørgensen, K. A. Aminocatalytic remote functionalization strategies. *Chem. Sci.* **2013**, *4*, 2287. c) Chauhan, P.; Kaya, U.; Enders, D. Advances in Organocatalytic 1,6-Addition Reactions: Enantioselective Construction of Remote Stereogenic Centers. *Adv. Synth. Catal.* **2017**, *359*, 888–912.

11. (a) Dell'Amico, L.; Albrecht, Ł.; Naicker, T.; Poulsen, H. P.; Jørgensen, A. K. Beyond Classical Reactivity Patterns: Shifting from 1,4- to 1,6-Additions in Regio- and Enantioselective Organocatalyzed Vinylogous Reactions of Olefinic Lactones with Enals and 2,4-Dienals. *J. Am. Chem. Soc*. **2013**, *135*, 8063-8070. (b) Akagawa, K.; Sen, J.; Kudo, K. Peptide-Catalyzed Regio- and Enantioselective Reduction of α,β,γ,δ-Unsaturated Aldehydes. *Angew. Chem., Int. Ed.* **2013**, *52*, 11585-11588. (c) Tian, X.; Melchiorre, P. Control of Remote Stereochemistry in the Synthesis of Spirocyclic Oxindoles: Vinylogous Organocascade Catalysis. *Angew. Chem., Int. Ed*. **2013**, *52*, 5360–5363. (d) Martin, J.; Lear, Hayashi, Y. Remote 1,6-Stereocontrol by Iminium-mediated Organocatalytic Events. *ChemCatChem*. **2013**, *5*, 3499–3501. (e) Akagawa, K.; Nishi, N.; Sen, J.; Kudo, K. Peptide-catalyzed consecutive 1,6- and 1,4-additions of thiols to α,β,γ,δ-unsaturated aldehydes. *Org. Biomol. Chem.* **2014**, *12*, 3581–3585. (f) Poulsen, H. P.; Feu,

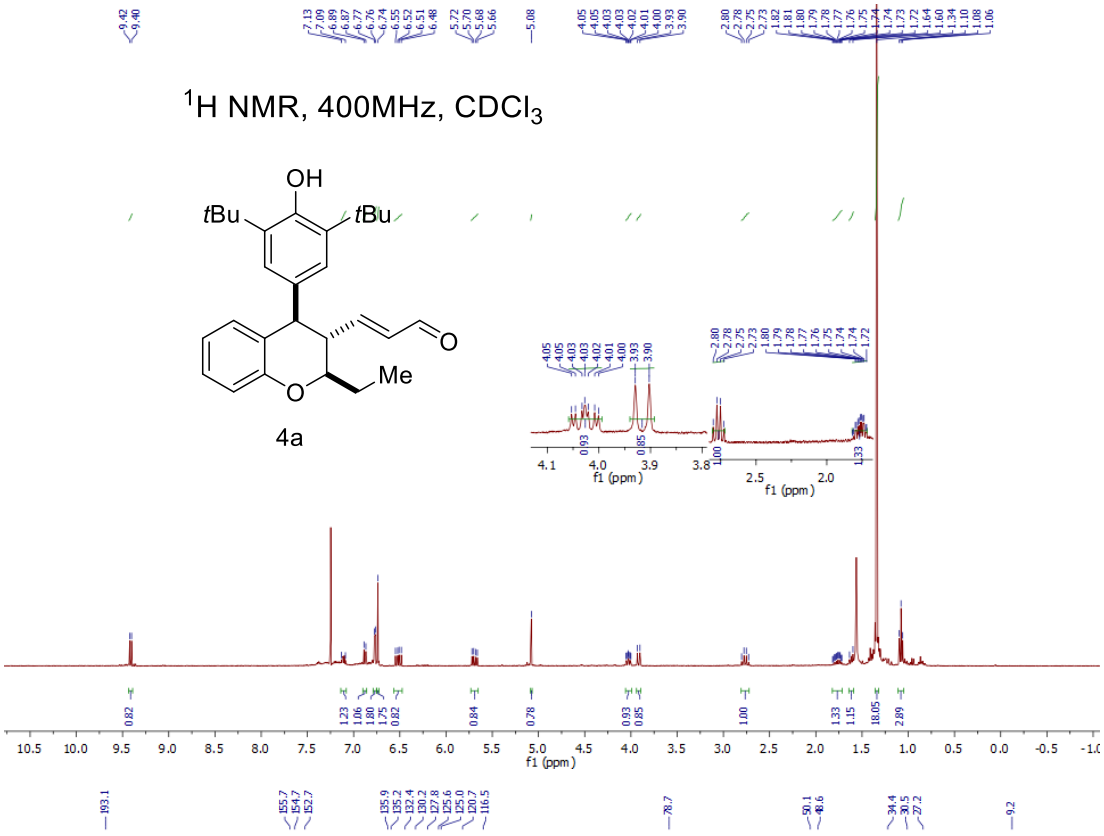
K. S.; Paz, B. M.; Jensen, F.; Jørgensen, A. K. Organocatalytic Asymmetric 1,6-Addition/1,4-Addition Sequence to 2,4-Dienals for the Synthesis of Chiral Chromans. *Angew. Chem., Int. Ed.* **2015**, *54*, 8203–8207.

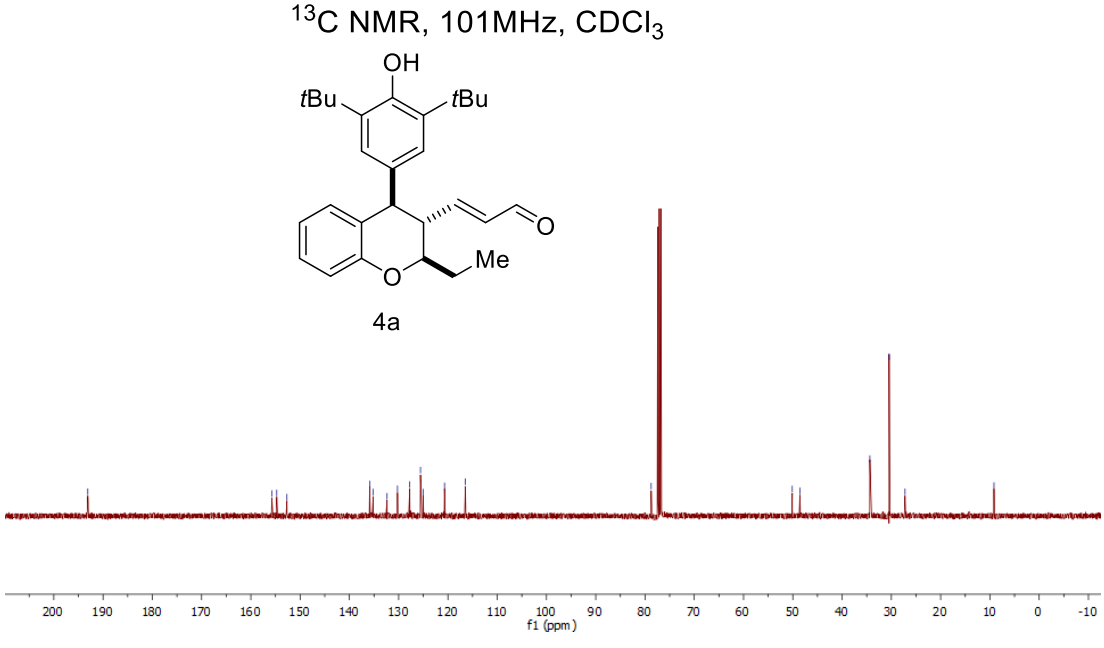
12. (a) Halskov, S. K.; Naicker, T.; Jensen, E. M.; Jørgensen, A. K. Organocatalytic asymmetric remote aziridination of 2,4-dienals. *Chem. Commun.* **2013**, *49*, 6382-6384. (b) Silvi, M.; Chatterjee, I.; Liu, Y.; Melchiorre, P. Controlling the Molecular Topology of Vinylogous Iminium Ions by Logical Substrate Design: Highly Regio- and Stereoselective Aminocatalytic 1,6-Addition to Linear 2,4-Dienals. *Angew. Chem., Int. Ed.* **2013**, *52*, 10780-10783. (c) Chatterjee, I.; Bastida, D.; Melchiorre, P. Vinylogous Organo-catalytic Triple Cascade Reaction: Forging Six Stereocenters in Complex Spiro-Oxindolic Cyclohexanes. *Adv. Synth. Catal*. **2013**, *355*, 3124−3130. (d) Silva, C., R.; Chatterjee, I.; Escudero-Adán, E.; Paixão, W., M.; Melchiorre, P. Synthesis of Cyclopropane Spirooxindoles by means of a Vinylogous Organocatalytic Cascade. *Asian J. Org. Chem.* **2014**, *3*, 466-469.
13. (a) Jensen, L. K.; Dickmeiss, G.; Jiang, H; Albrecht, L.; Jørgensen, A. K. The diarylprolinol silyl ether system: a general organocatalyst. *Acc. Chem. Res.* **2012**, *45*, 248–264. (b) Hayashi, Y.; Gotoh, Y.; Hayashi, T.; Shoji, M. Diphenylprolinol silyl ethers as efficient organocatalysts for the asymmetric Michael reaction of aldehydes and nitroalkenes. *Angew. Chem., Int. Ed.* **2005**, *44*, 4212-4215.
14. Rios, R.; Sundén, H.; Vesely, J.; Zhao, G.; Dziedzic, P.; Córdova, A. A Simple Organocatalytic Enantioselective Cyclopropanation of α, β-Unsaturated Aldehydes. *Adv. Synth. Catal.* **2007**, *349*, 1028–1032.
15. Zhang, Q.; Nguyen, M. H. Rhodium-catalyzed regioselective opening of vinyl epoxides with $Et_3N.3HF$ reagent-formation of allylic fluorohydrins. *Chem. Sci.* **2014**, *5*, 291-296.
16. Gómez-Bengoa, E.; Landa, A.; Lizarraga, A.; Mielgo, A.; Oiarbide, M.; Palomo, C. Catalytic Asymmetric α-Alkylation of Aldehydes via a $SN^{2'}$-type Addition-elimination Pathway, *Chem. Sci.*, 2011, **2**, 353–357.
17. Hçrmann, M., F.; Chung, T.; Rodriguez, S. E.; Jakob, M.; Bach, T. Evidence for Triplet Sensitization in the Visible-Light-Induced [2+2] Photocycloaddition of Eniminium Ions, *Angew. Chem. Int. Ed.*, **2018**, *57*, 827–831.
18. Liedtke, T.; Spannring, P.; Riccardi, L.; Gansäuer, A. Mechanism-Based Condition Screening for Sustainable Catalysis in Single-Electron Steps by Cyclic Voltammetry, *Angew. Chem., Int. Ed.*, **2018**, *57*, 5006–5010.
19. Bruker, *SAINT V7.68A*, Bruker AXS Inc., Madison (WI, USA), **2005**.
20. G. M. Sheldrick, *SADABS 2008/2*, Göttingen, **2008.**

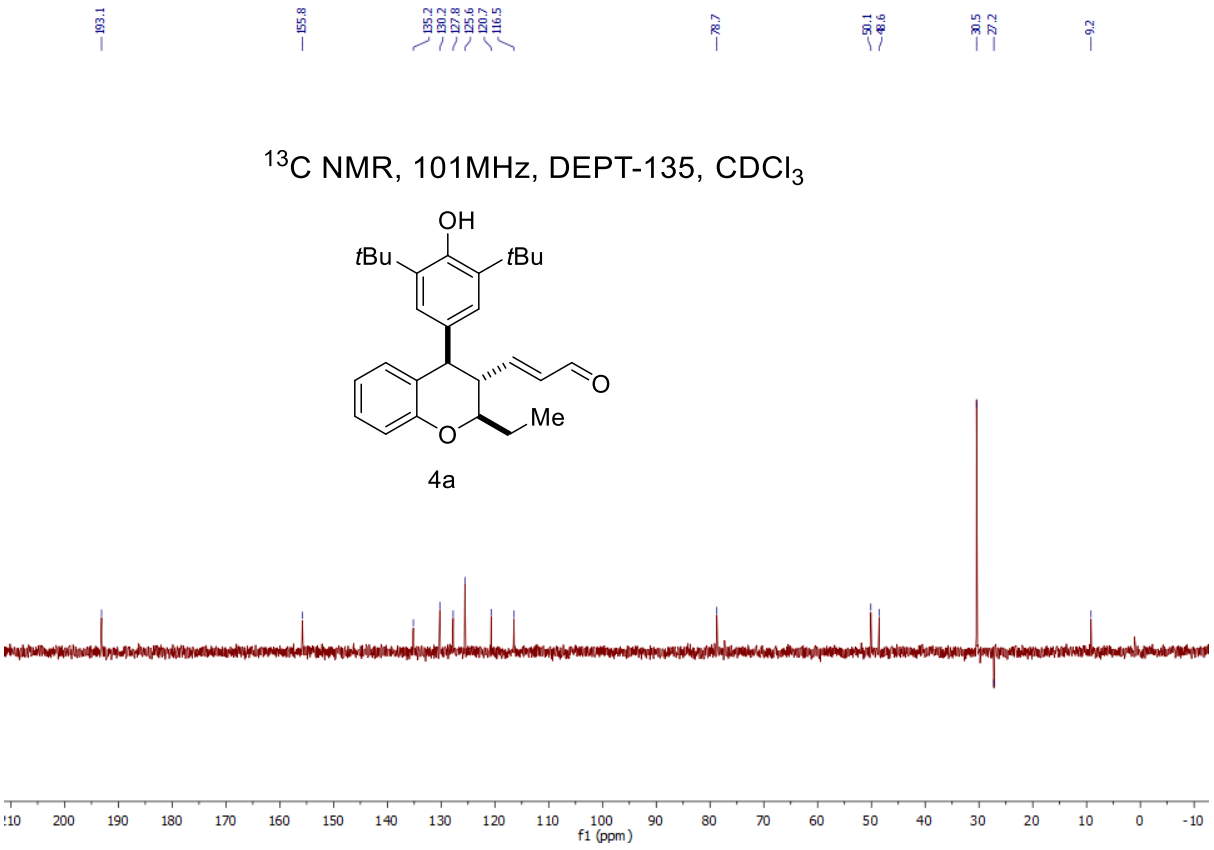
21. Altomare, A.; Cascarano, G.; Giacovazzo, C.; Guagliardi, A. *J. Appl. Cryst*., **1993,** *26*, 343–350.
22. Sheldrick, G. M. SHELXL-97, Program for Crystal Structure Solution and Refinement; University of Göttingen, Göttingen, Germany, **1997**.
23. Farrugia, L. J. WinGX-A Windows Program for Crystal Structure Analysis, *J. Appl. Cryst*., **1999**, *32*, 837–838.
24. CCDC **1982963** & CCDC **1982953** contain supplementary crystallographic data for the compound **4d** & **4p** respectively.

2.6. NMR Spectra:

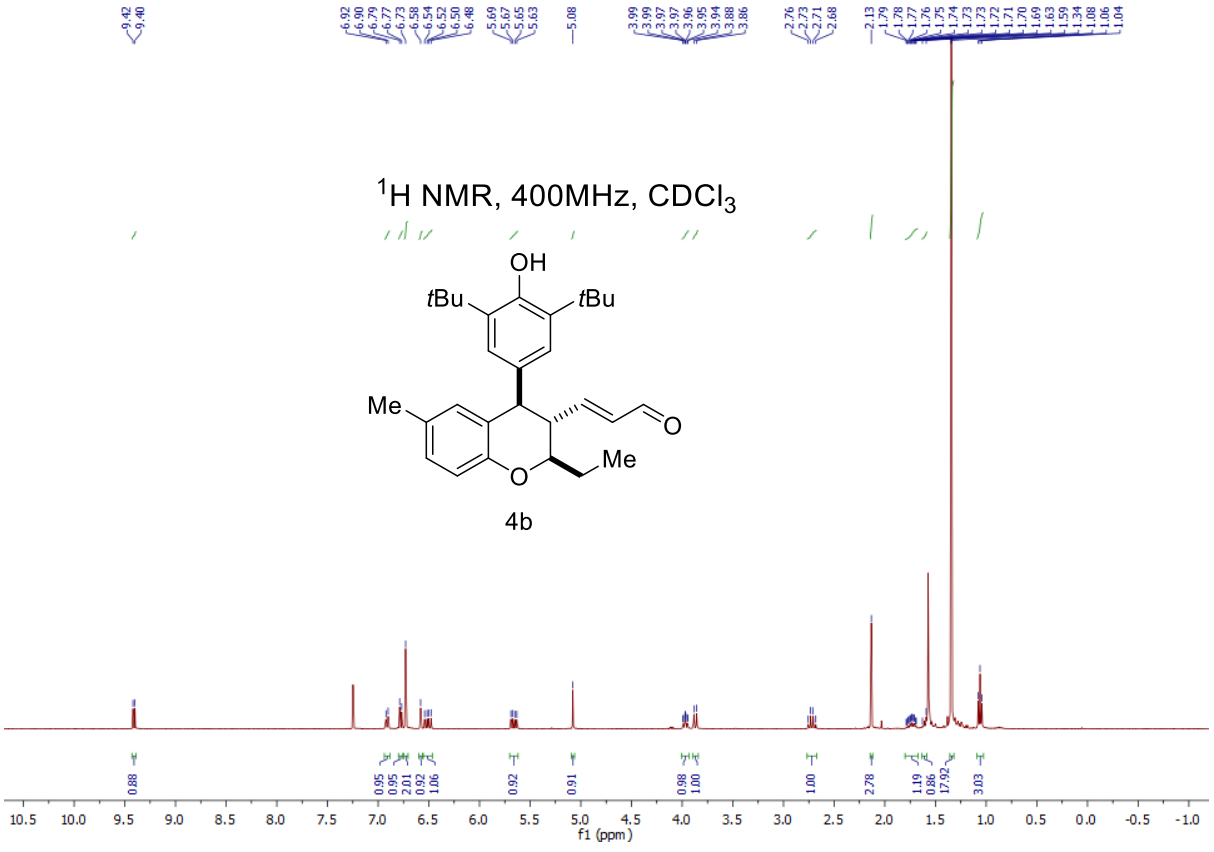
2.6.1. (*E*)-3-((2R,3S,4R)-4-(3,5-di-*tert*-butyl-4-hydroxyphenyl)-2-ethylchroman-3-yl)acrylaldehyde (4a)

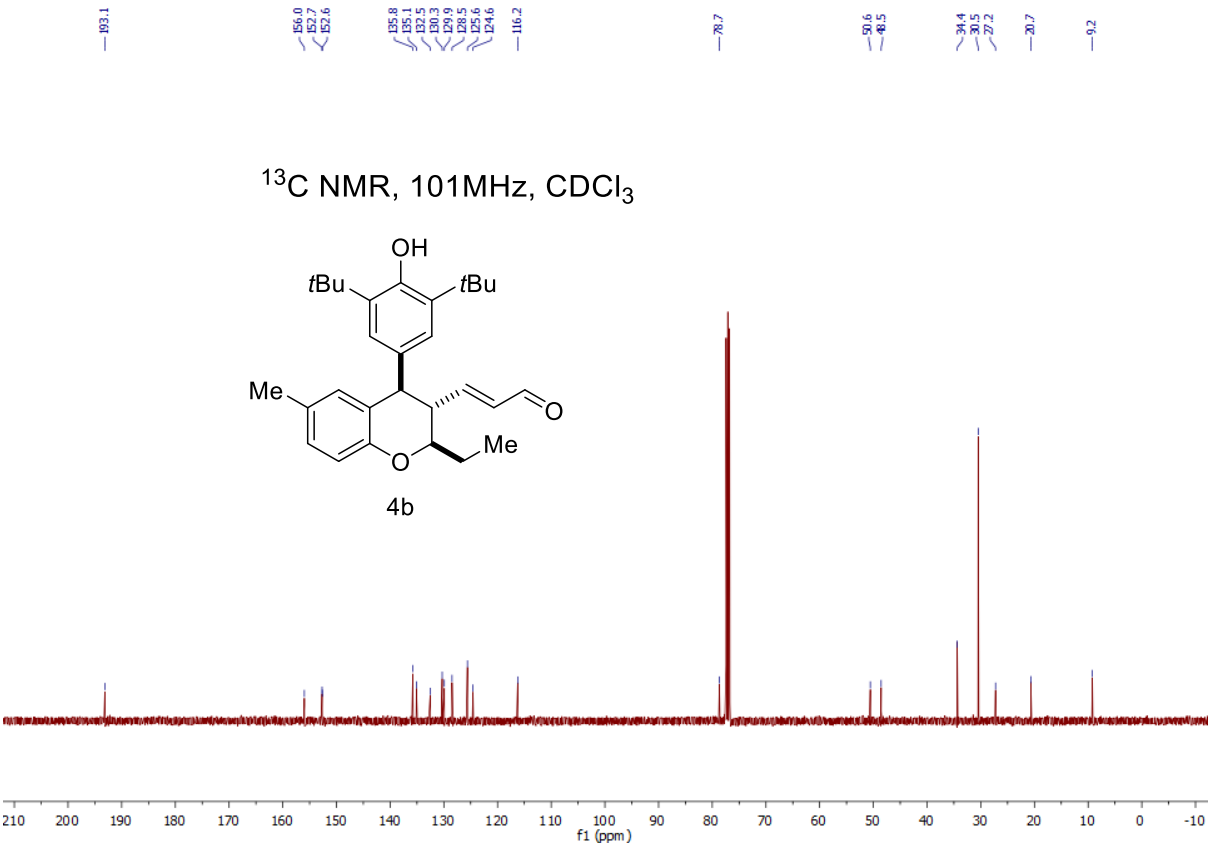




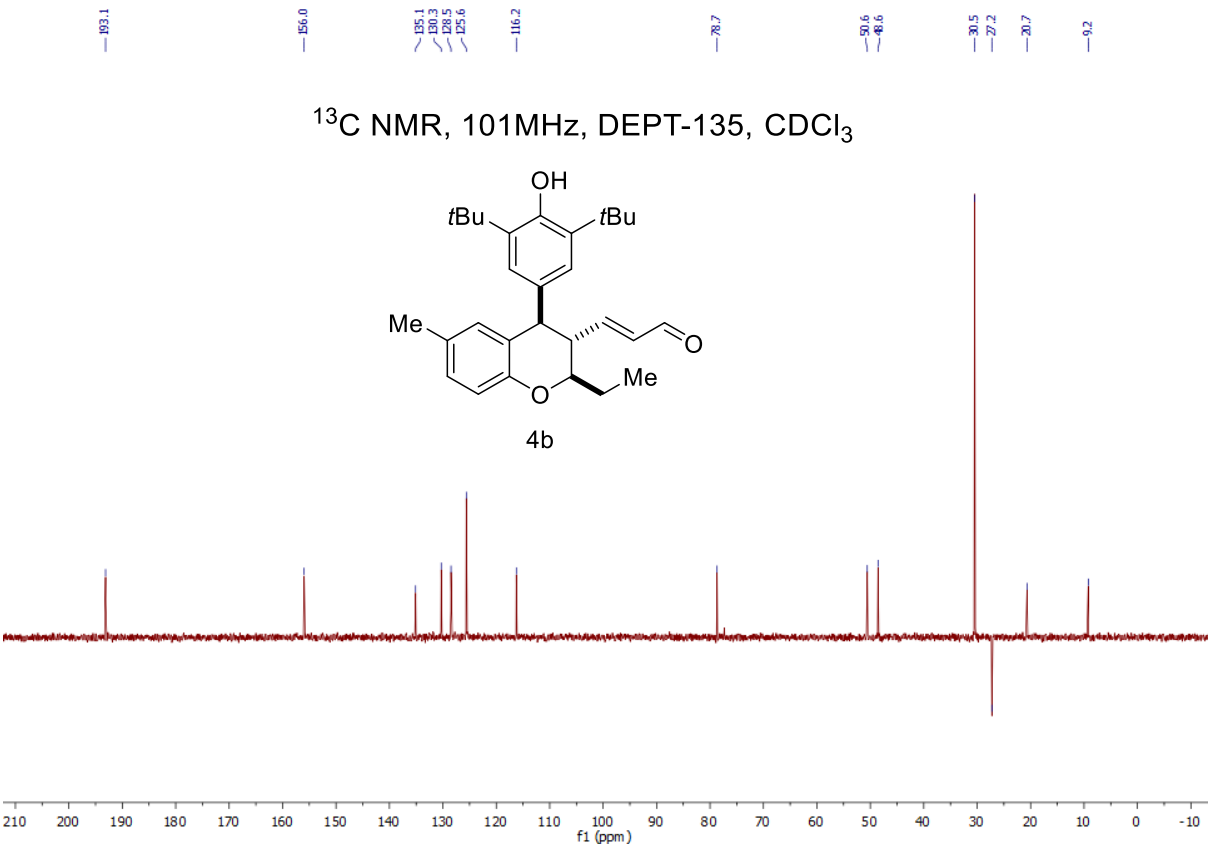


2.6.2. (*E*)-3-((2R,3S,4R)-4-(3,5-di-*tert*-butyl-4-hydroxyphenyl)-2-ethyl-6-methylchroman-3-yl)acrylaldehyde (4b).





^{13}C NMR, 101MHz, $CDCl_3$

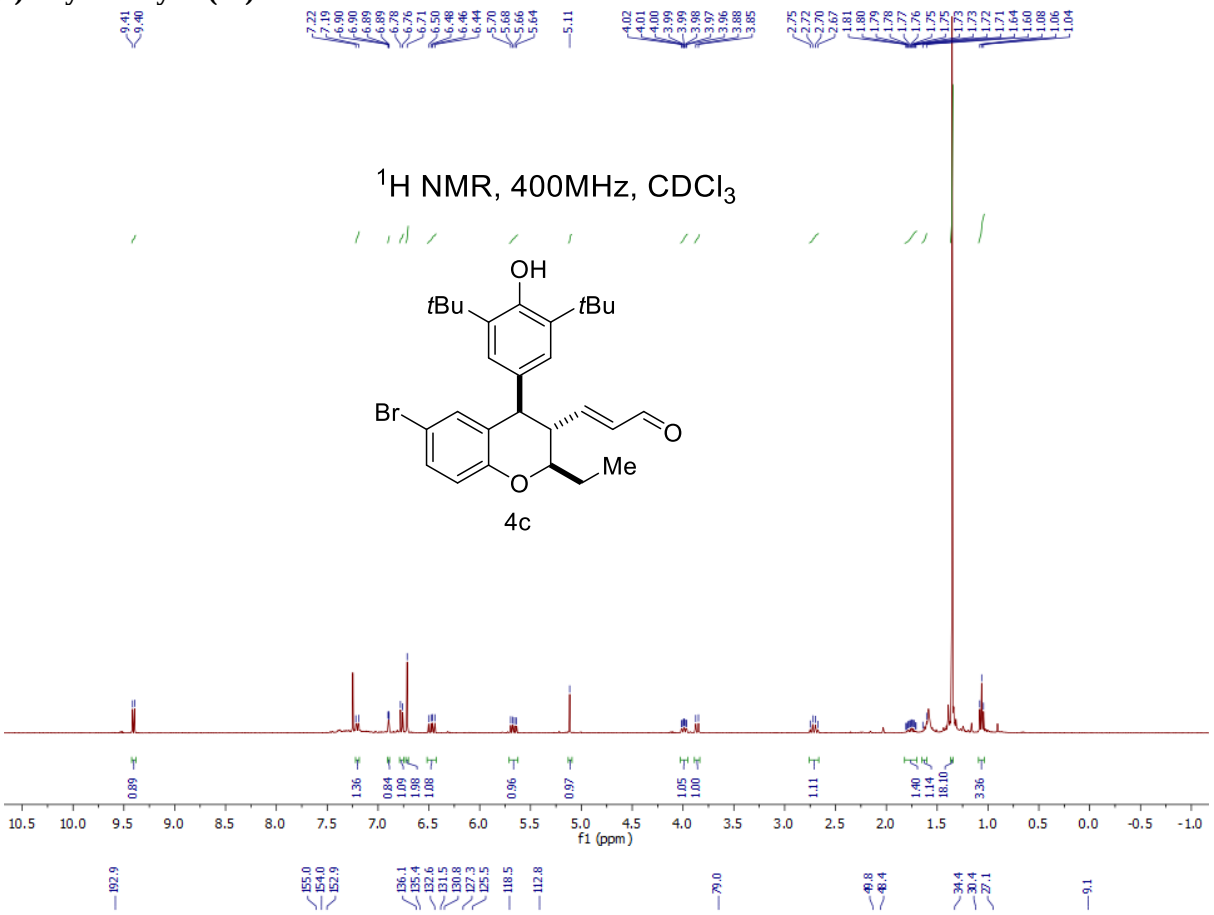


^{13}C NMR, 101MHz, DEPT-135, $CDCl_3$

2.6.3. (*E*)-3-((2R,3S,4R)-6-bromo-4-(3,5-di-*tert*-butyl-4-hydroxyphenyl)-2-ethylchroman-3-yl)acrylaldehyde (4c).

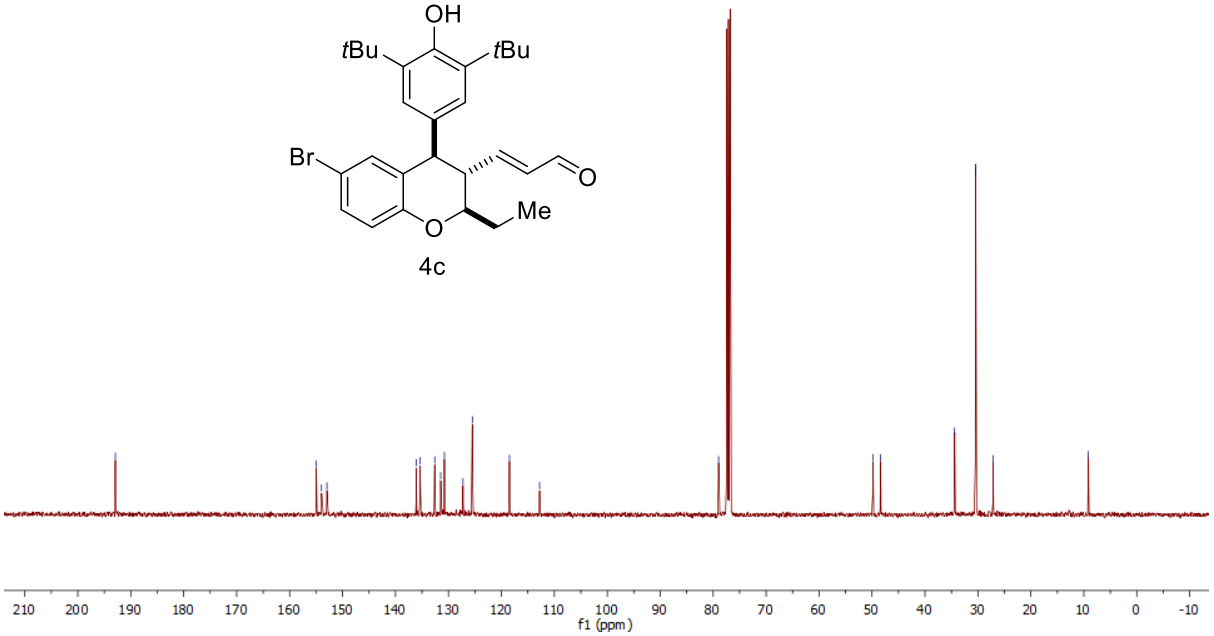
^{1}H NMR, 400MHz, $CDCl_3$

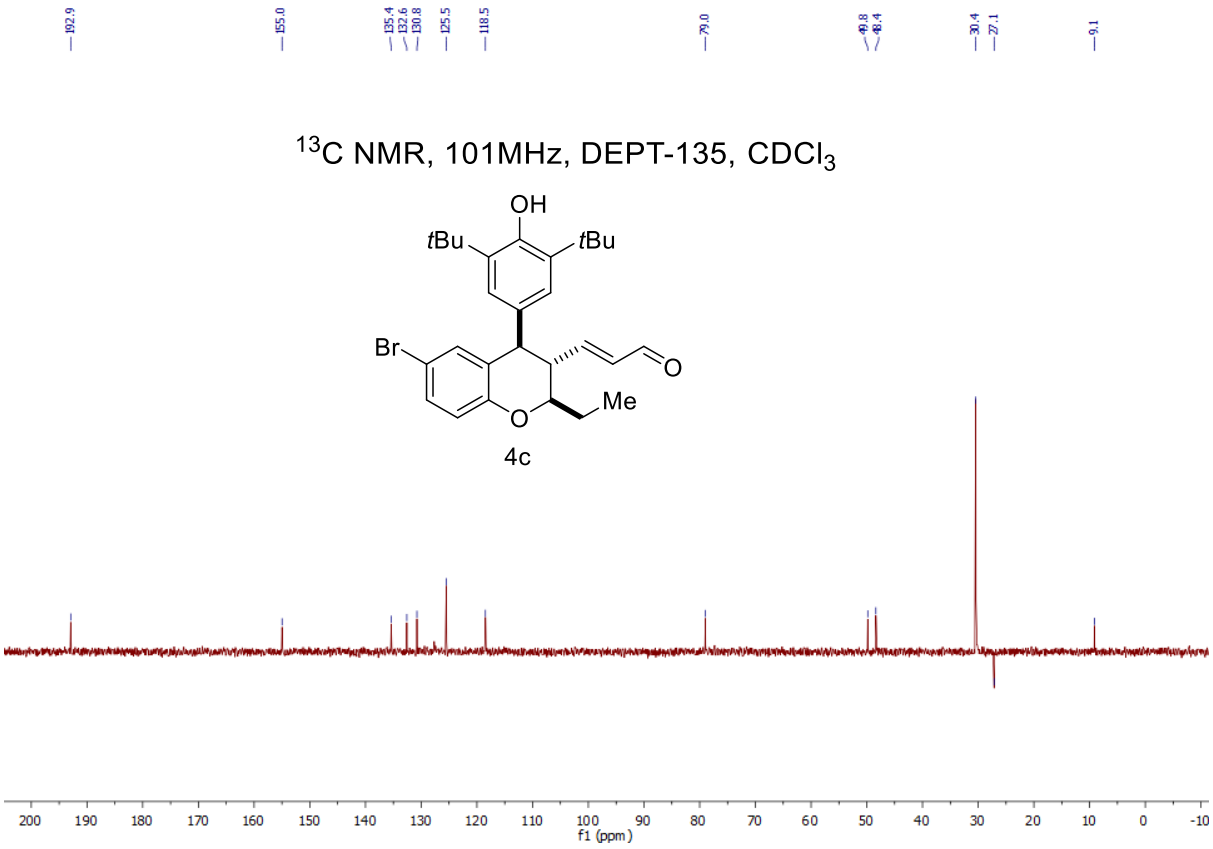
4c



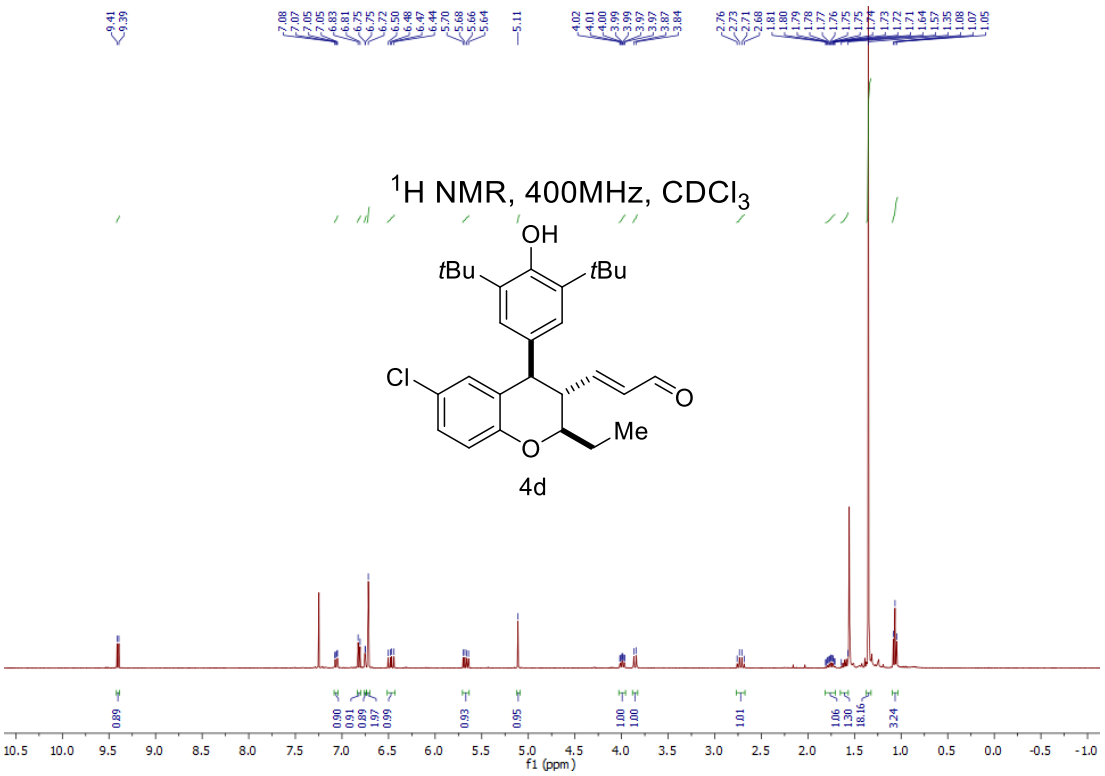
^{13}C NMR, 101MHz, $CDCl_3$

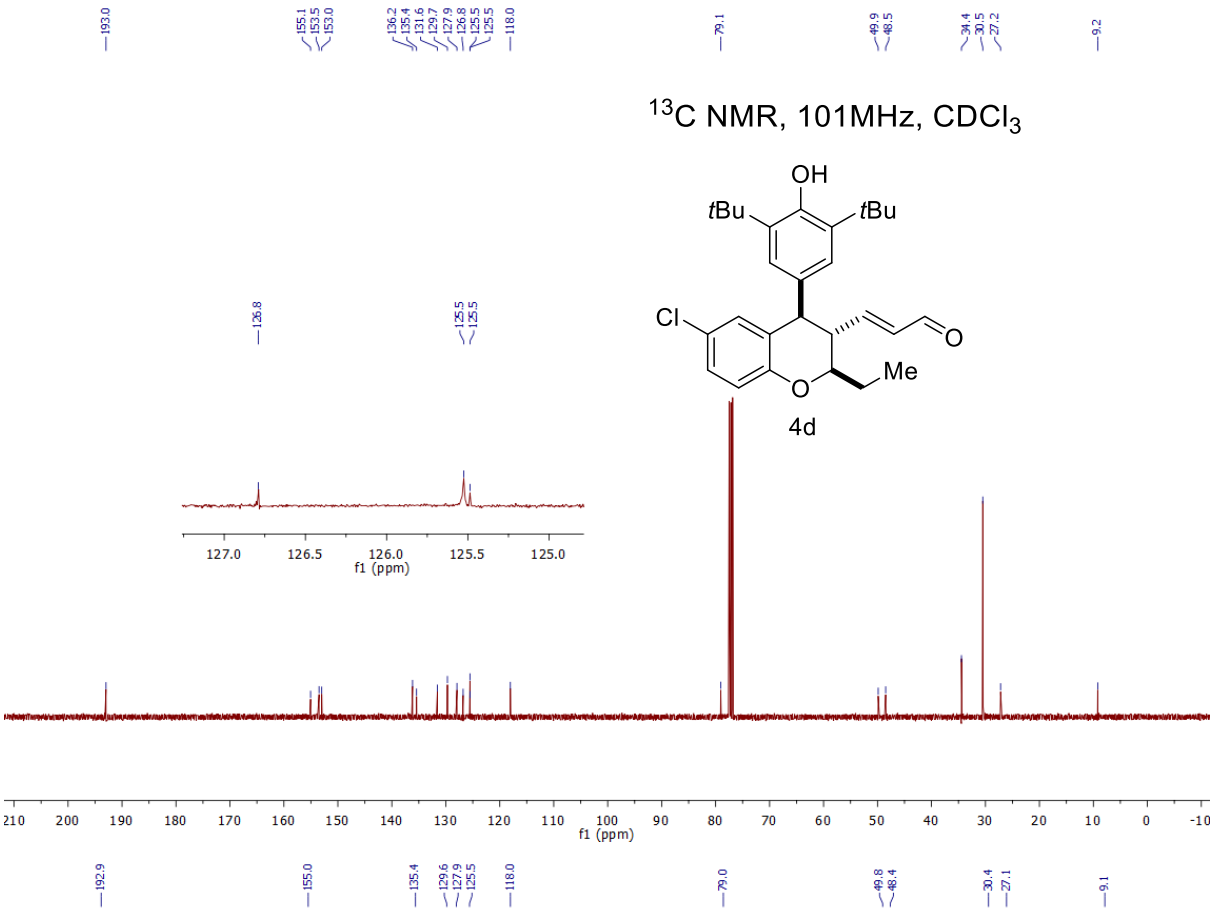
4c

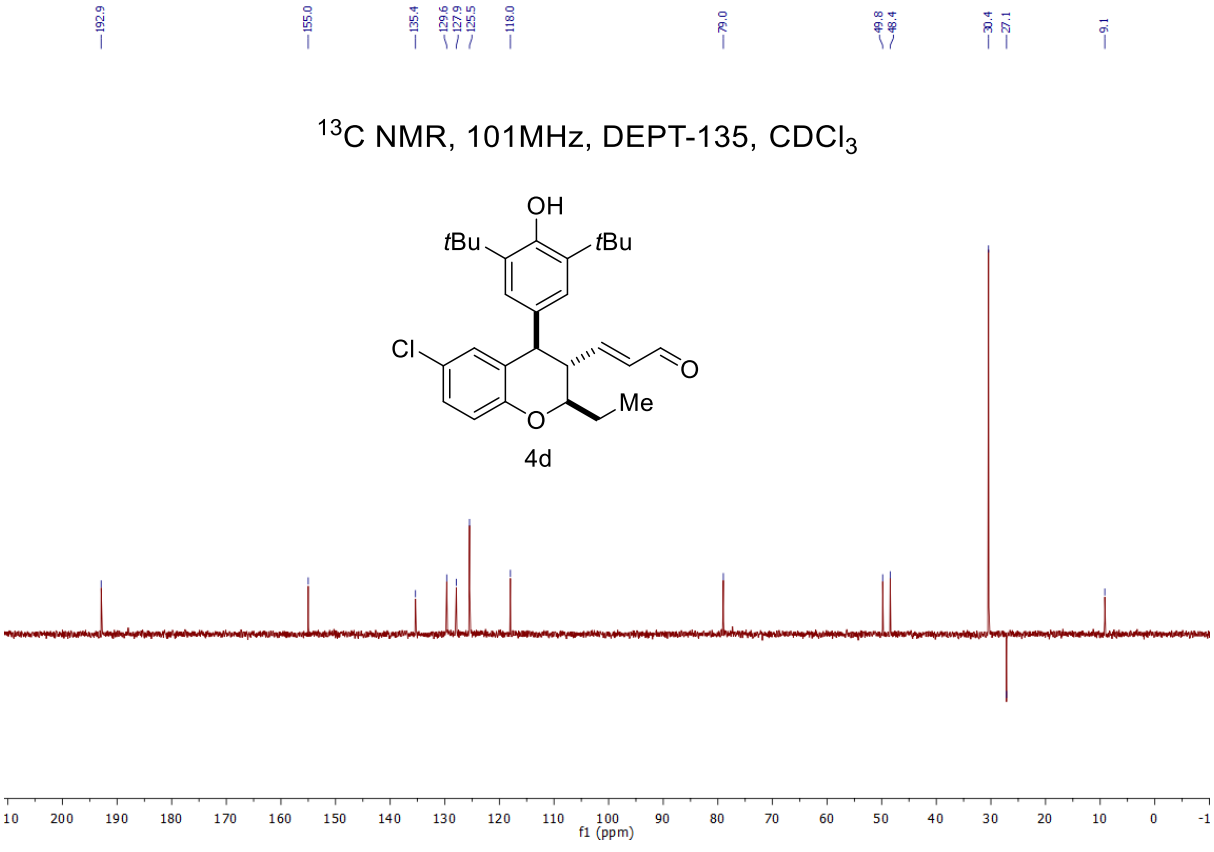




2.6.4. (*E*)-3-((2R,3S,4R)-6-chloro-4-(3,5-di-*tert*-butyl-4-hydroxyphenyl)-2-ethylchroman-3-yl)acrylaldehyde (4d)



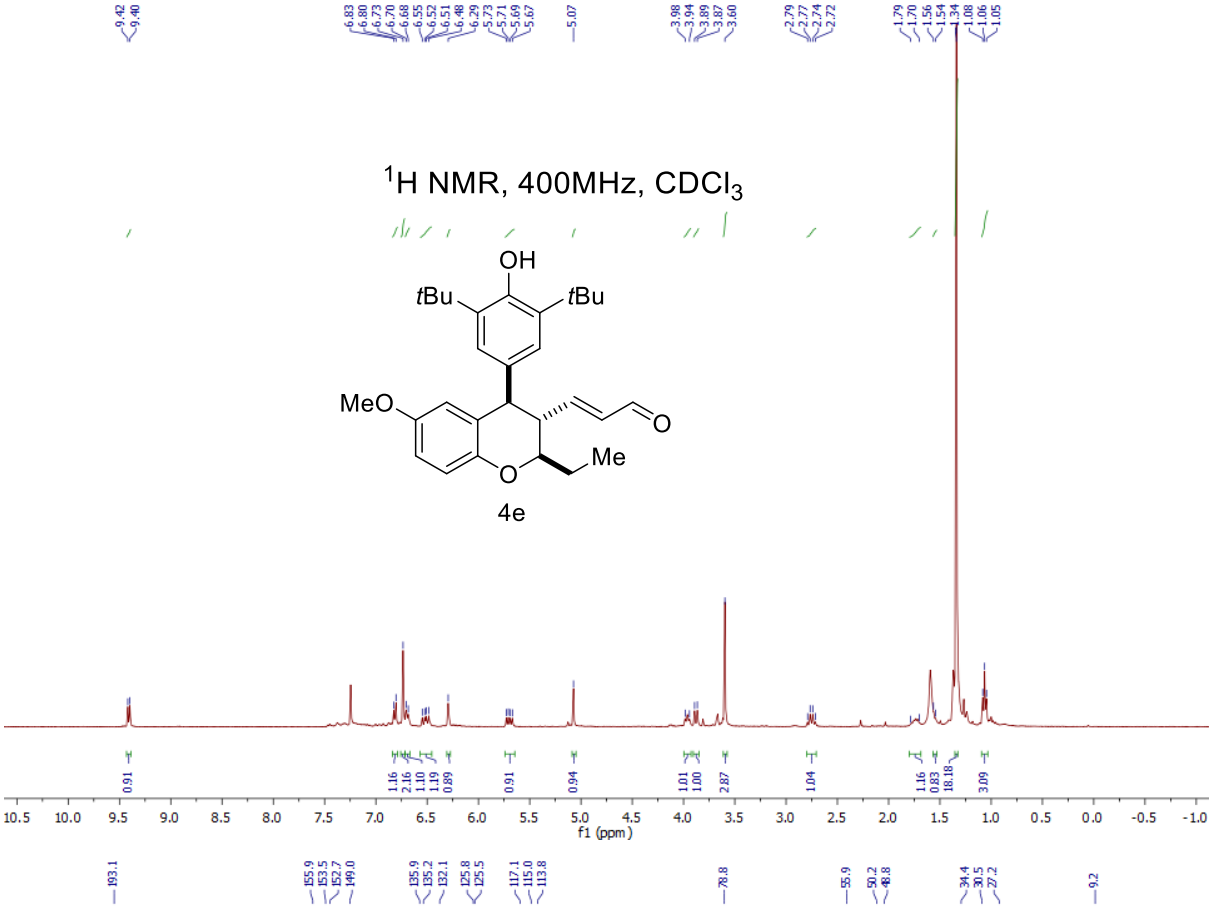

193.0
155.1
153.5
153.0
136.2
135.4
131.6
129.7
127.9
126.8
125.5
125.5
118.0
79.1
49.9
48.5
34.4
30.5
27.2
9.2
^{13}C NMR, 101MHz, CDCl$_3$
OH
tBu
tBu
Cl
O
Me
O
4d
126.8
125.5
125.5
127.0
126.5
126.0
125.5
125.0
f1 (ppm)
210
200
190
180
170
160
150
140
130
120
110
100
90
80
70
60
50
40
30
20
10
0
-10
f1 (ppm)


192.9
155.0
135.4
129.6
127.9
125.5
118.0
79.0
49.8
48.4
30.4
27.1
9.1
^{13}C NMR, 101MHz, DEPT-135, CDCl$_3$
OH
tBu
tBu
Cl
O
Me
O
4d
10
200
190
180
170
160
150
140
130
120
110
100
90
80
70
60
50
40
30
20
10
0
-1
f1 (ppm)

2.6.5. (*E*)-3-((2R,3S,4R)-4-(3,5-di-*tert*-butyl-4-hydroxyphenyl)-2-ethyl-6-methoxychroman-3-yl)acrylaldehyde (4e).

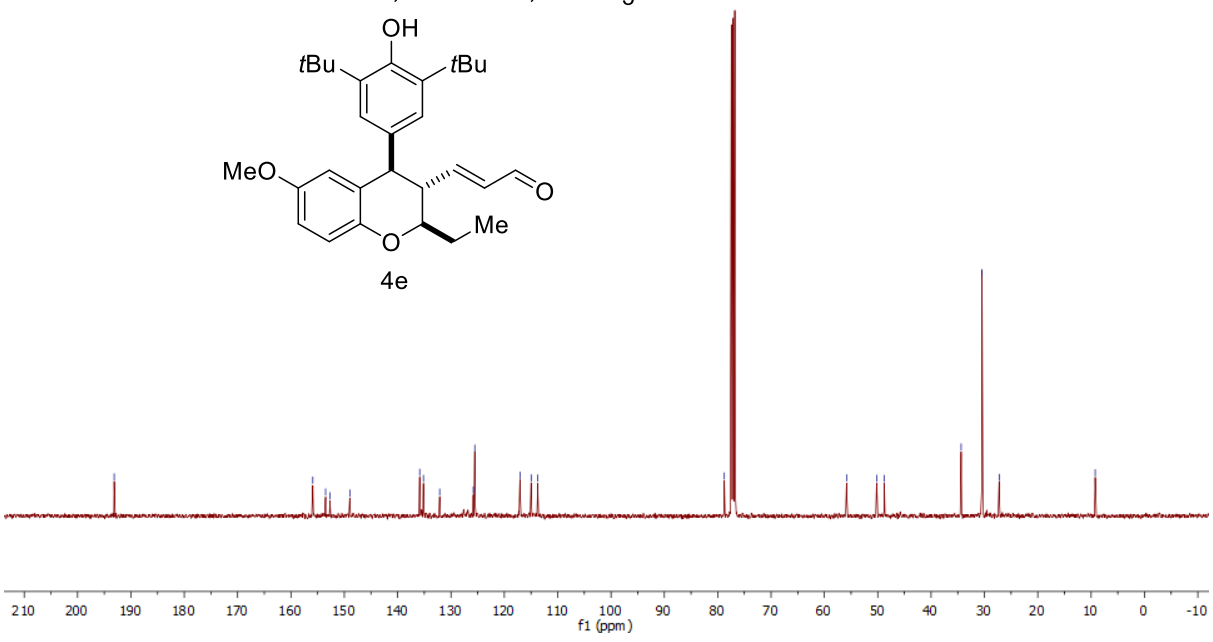
^{1}H NMR, 400MHz, $CDCl_3$

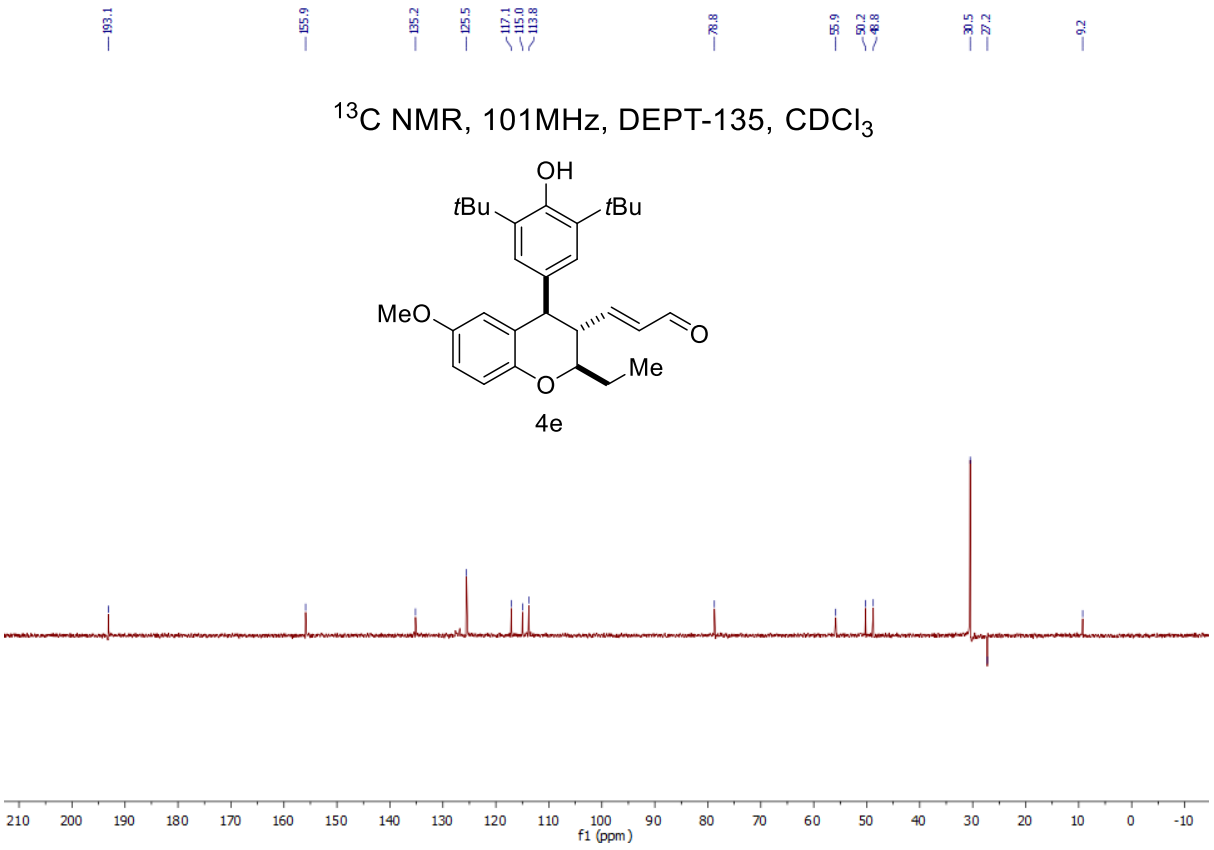
4e



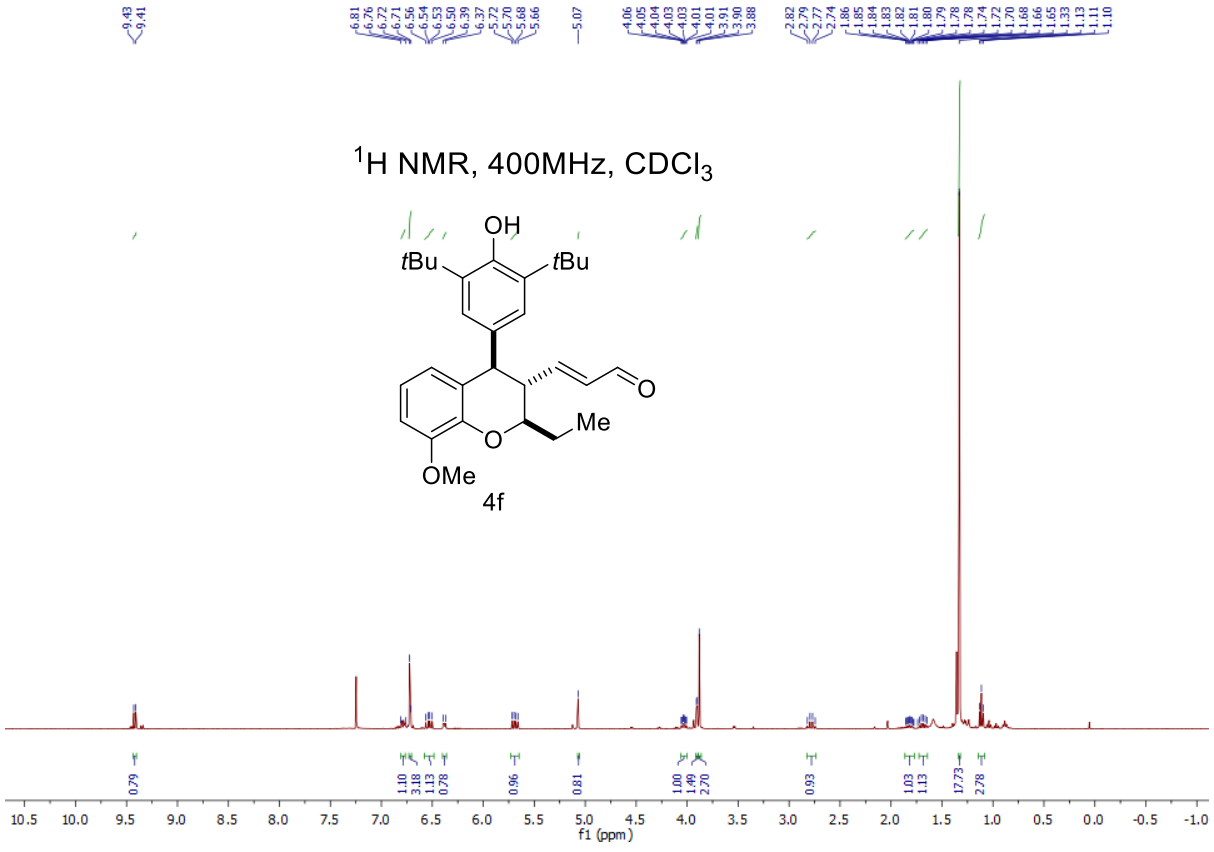
^{13}C NMR, 101MHz, $CDCl_3$

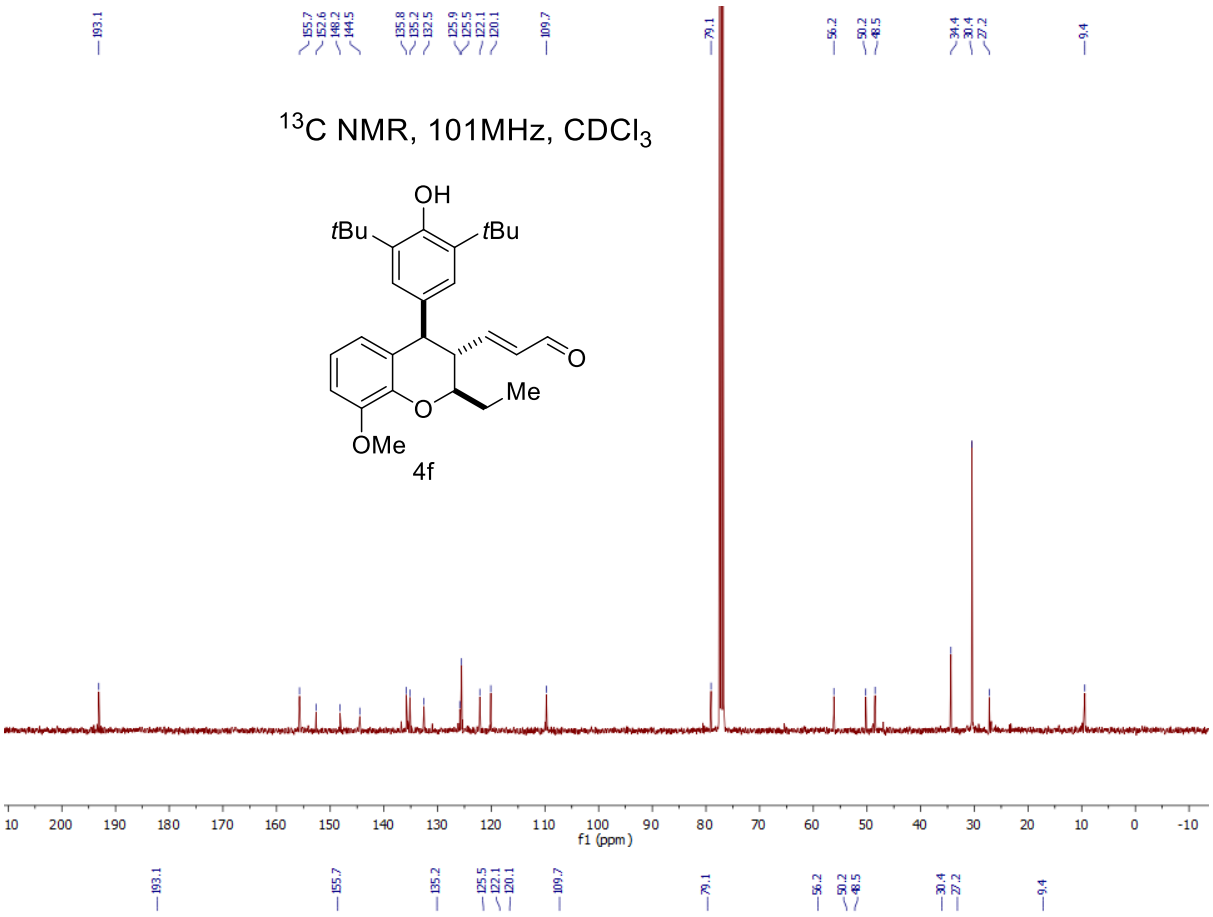
4e

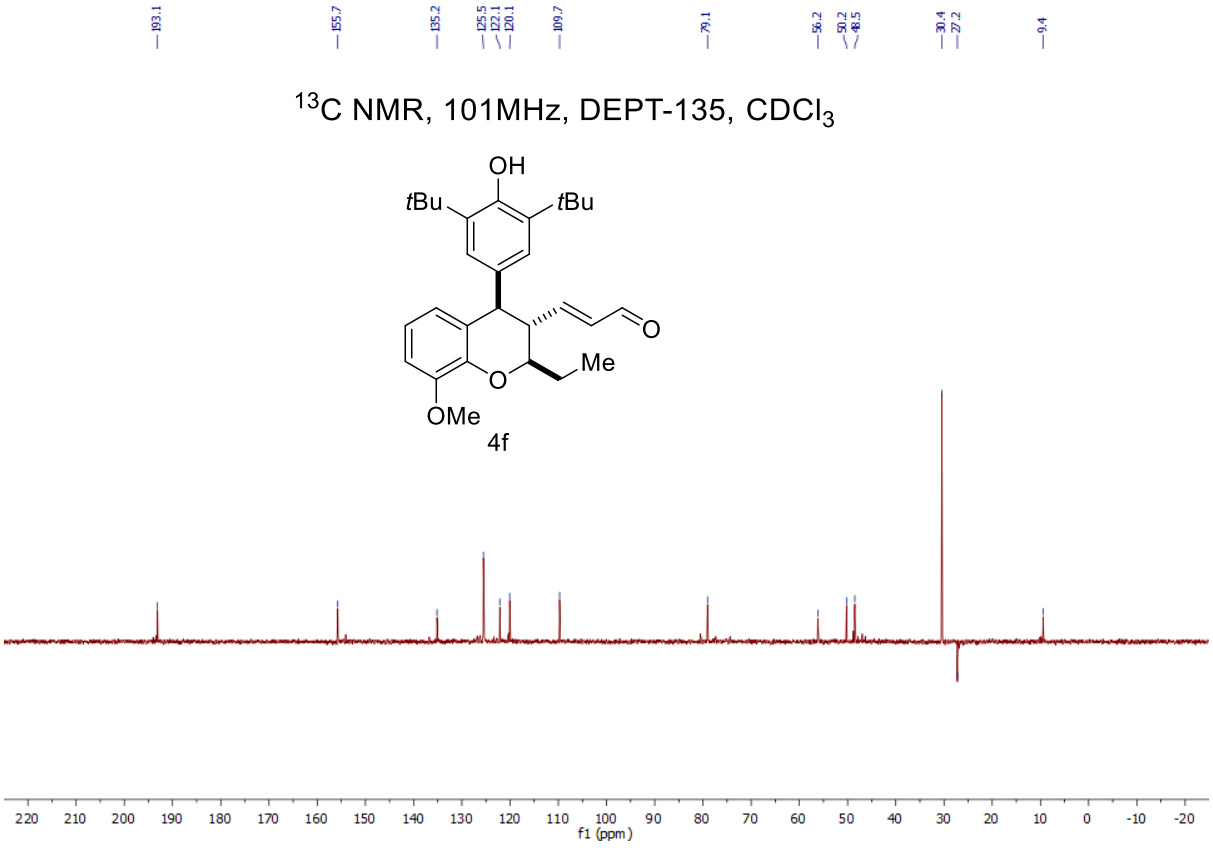




2.6.6. (*E*)-3-((2R,3S,4R)-4-(3,5-di-*tert*-butyl-4-hydroxyphenyl)-2-ethyl-8-methoxychroman-3-yl)acrylaldehyde (4f).

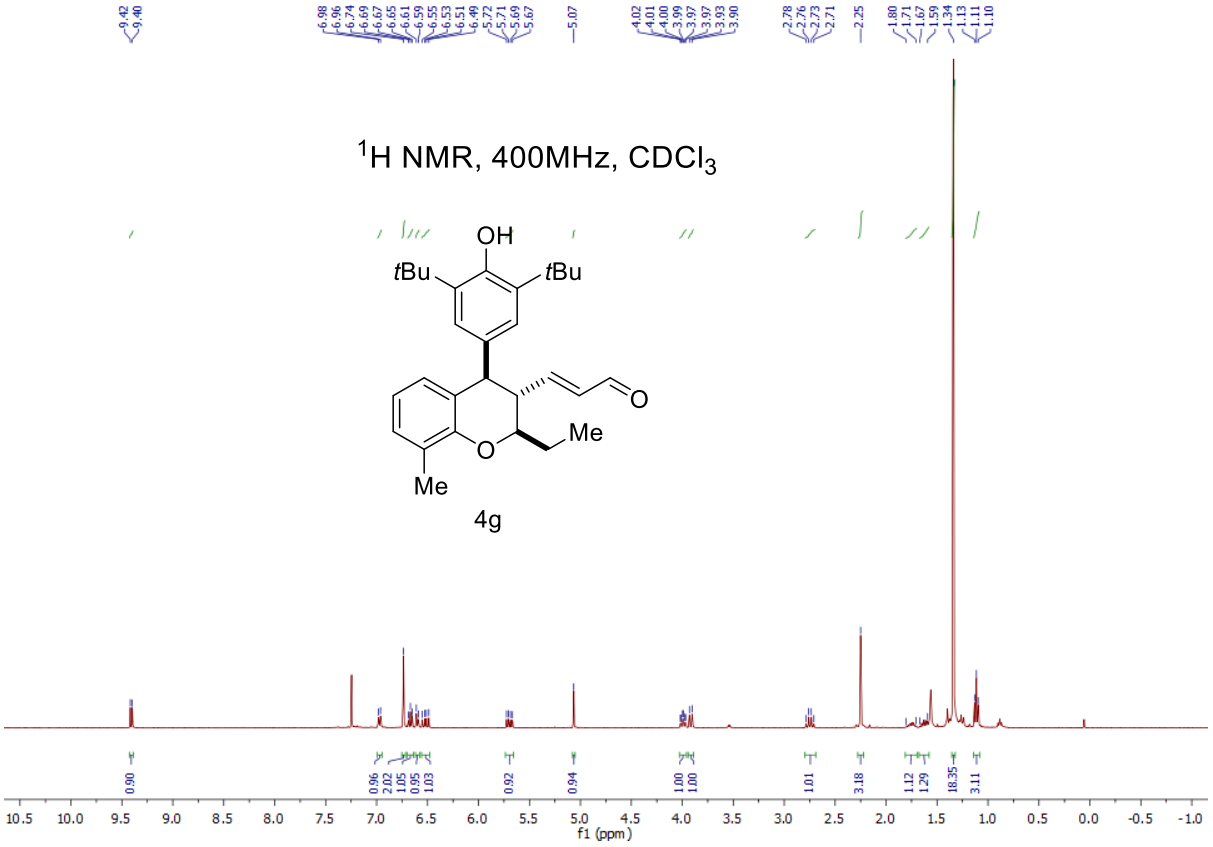



193.1
155.7
152.6
148.2
144.5
135.8
135.2
132.5
125.9
125.5
122.1
120.1
109.7
79.1
56.2
50.2
48.5
34.4
30.4
27.2
9.4
13C NMR, 101MHz, CDCl3
OH
tBu
tBu
O
Me
O
OMe
4f
f1 (ppm)

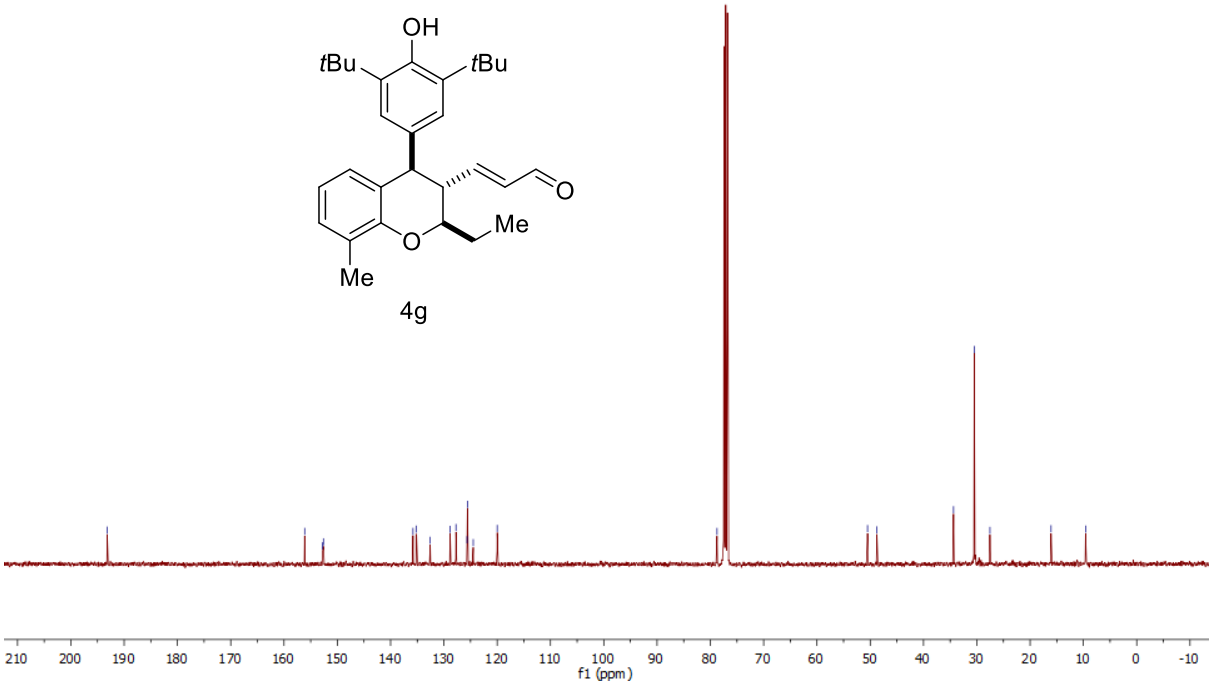

193.1
155.7
135.2
125.5
122.1
120.1
109.7
79.1
56.2
50.2
48.5
30.4
27.2
9.4
13C NMR, 101MHz, DEPT-135, CDCl3
OH
tBu
tBu
O
Me
O
OMe
4f
f1 (ppm)

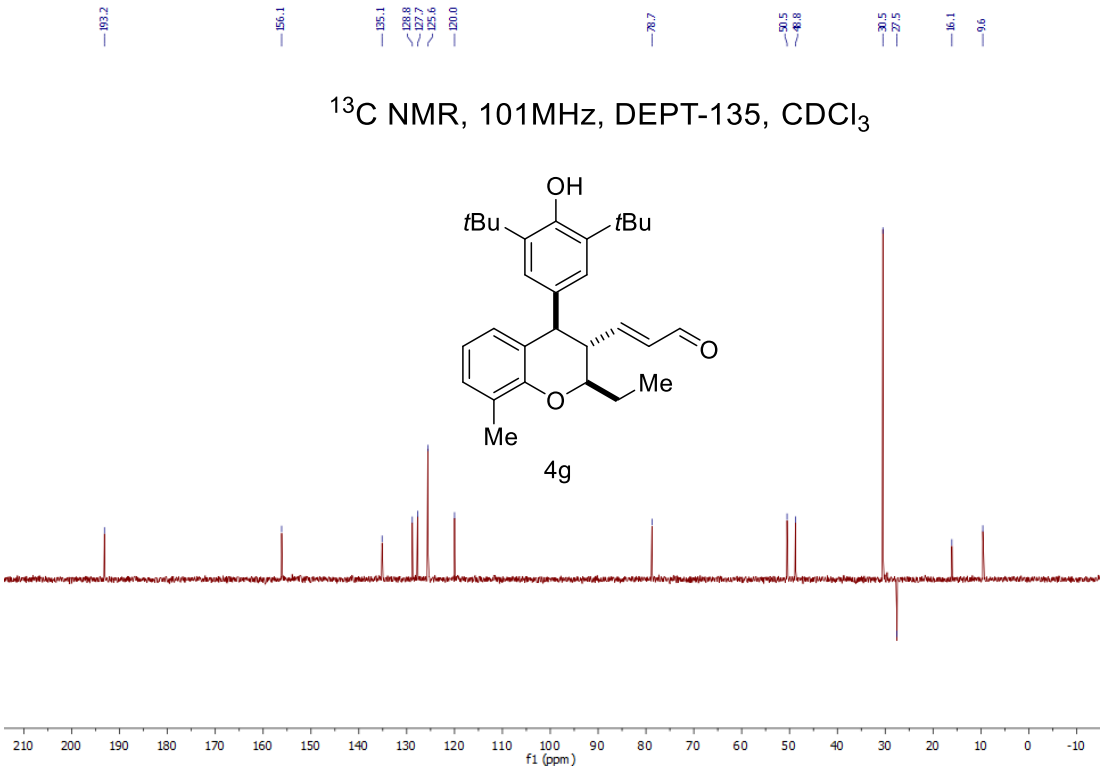
2.6.7. (*E*)-3-((2R,3S,4R)-4-(3,5-di-*tert*-butyl-4-hydroxyphenyl)-2-ethyl-8-methylchroman-3-yl)acrylaldehyde (4g).

^{1}H NMR, 400MHz, $CDCl_3$

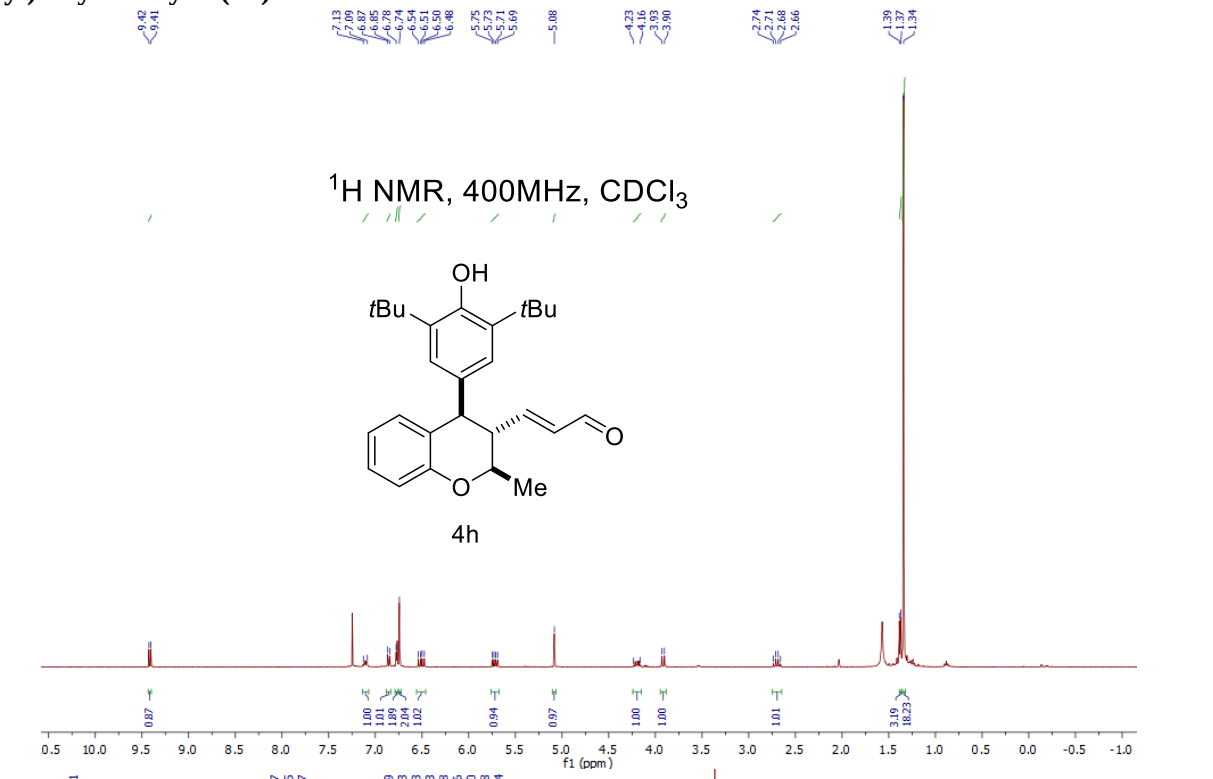


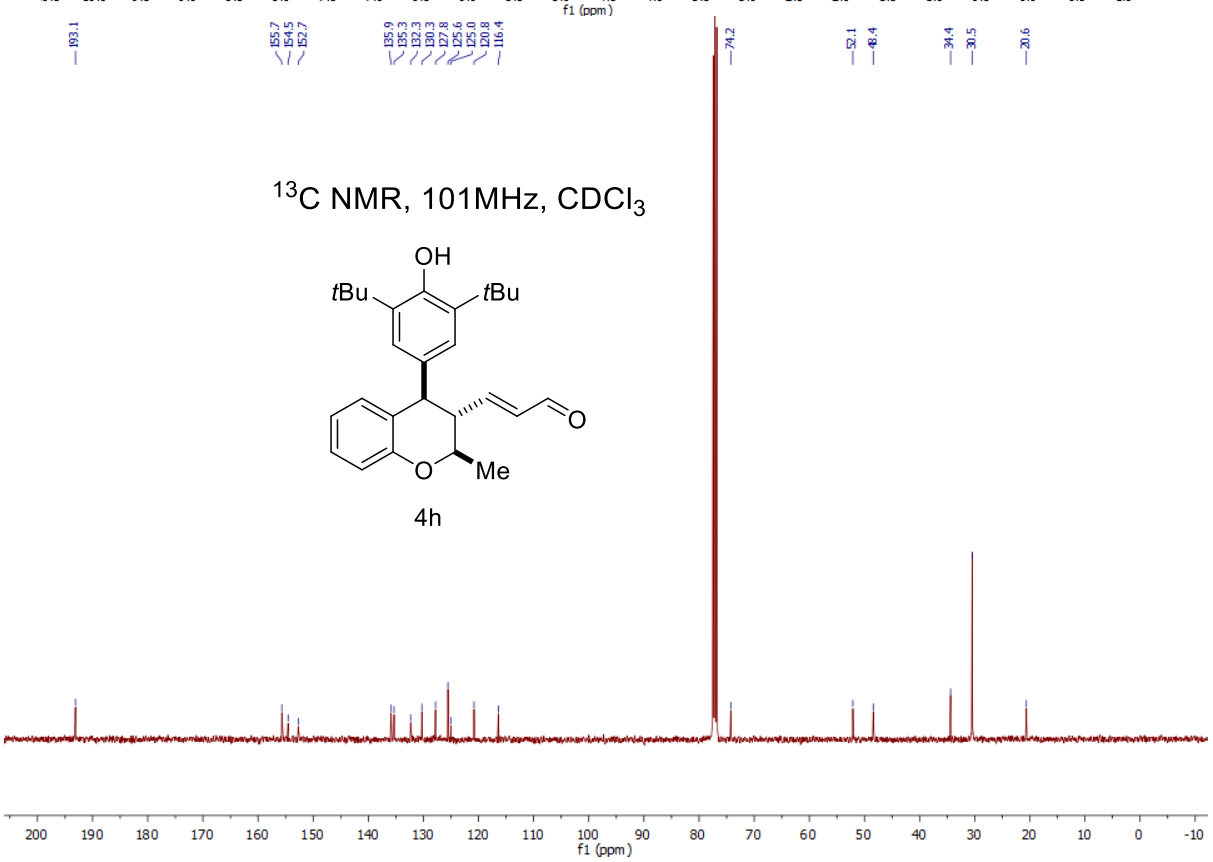
^{13}C NMR, 101MHz, $CDCl_3$

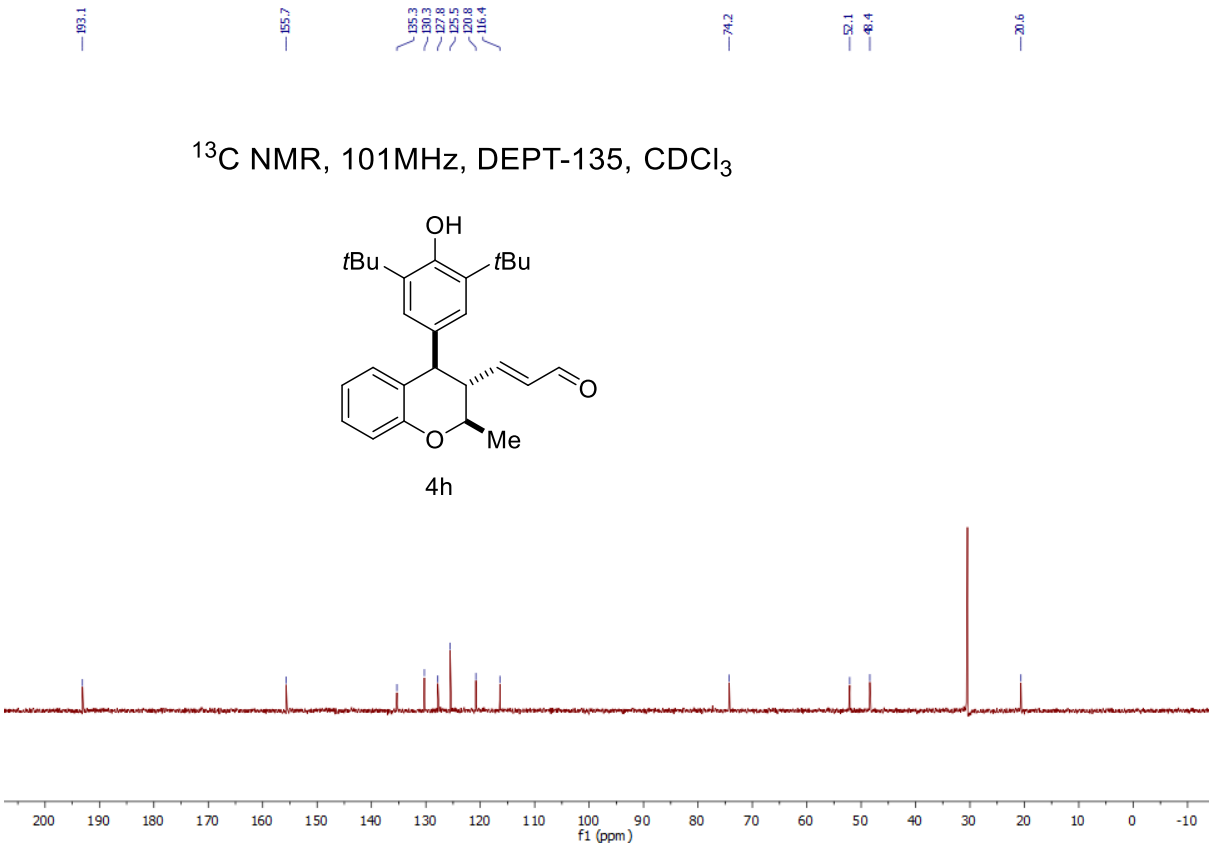



193.2
156.1
135.1
128.8
127.7
125.6
120.0
78.7
50.5
48.8
30.5
27.5
16.1
9.6
^{13}C NMR, 101MHz, DEPT-135, $CDCl_3$
OH
*t*Bu
*t*Bu
O
Me
O
Me
4g
210 200 190 180 170 160 150 140 130 120 110 100 90 80 70 60 50 40 30 20 10 0 -10
f1 (ppm)

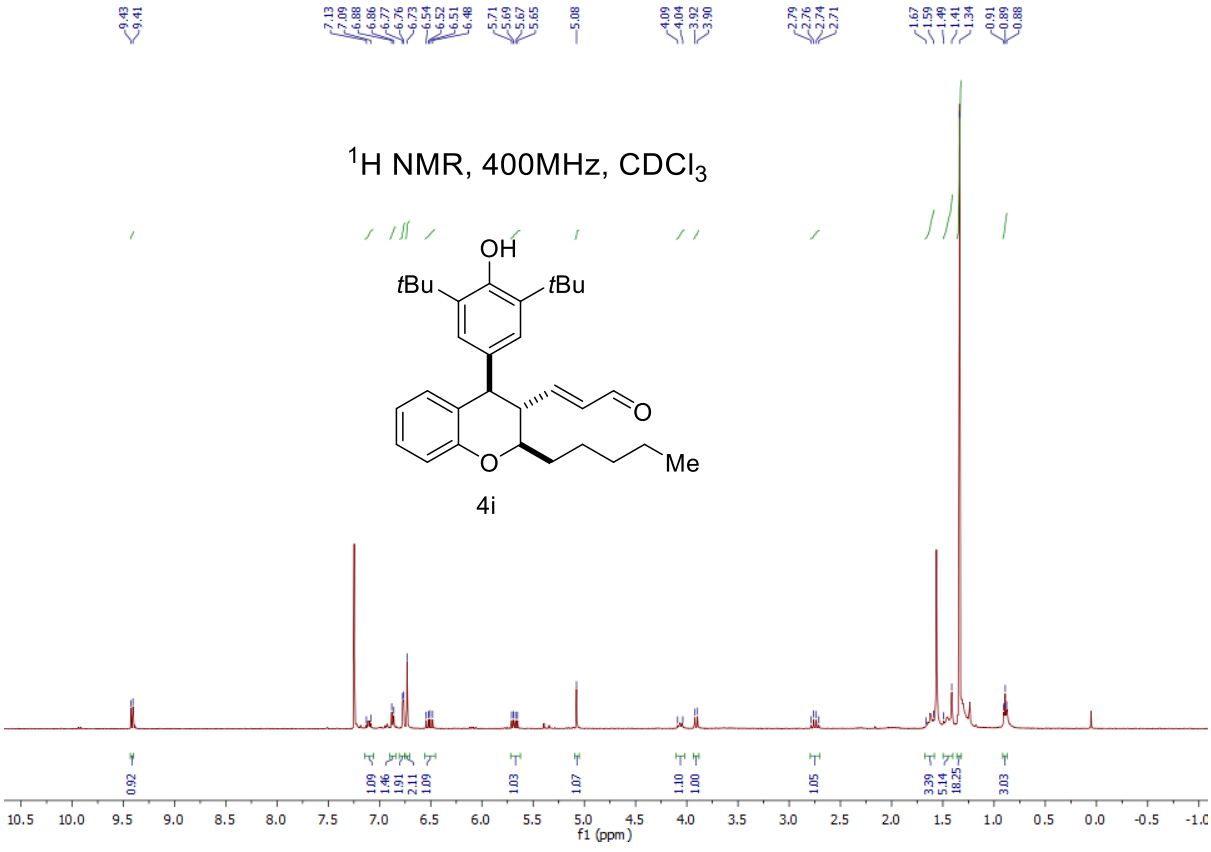
2.6.8. (*E*)-3-((2R,3S,4R)-4-(3,5-di-*tert*-butyl-4-hydroxyphenyl)-2-methylchroman-3-yl)acrylaldehyde (4h).

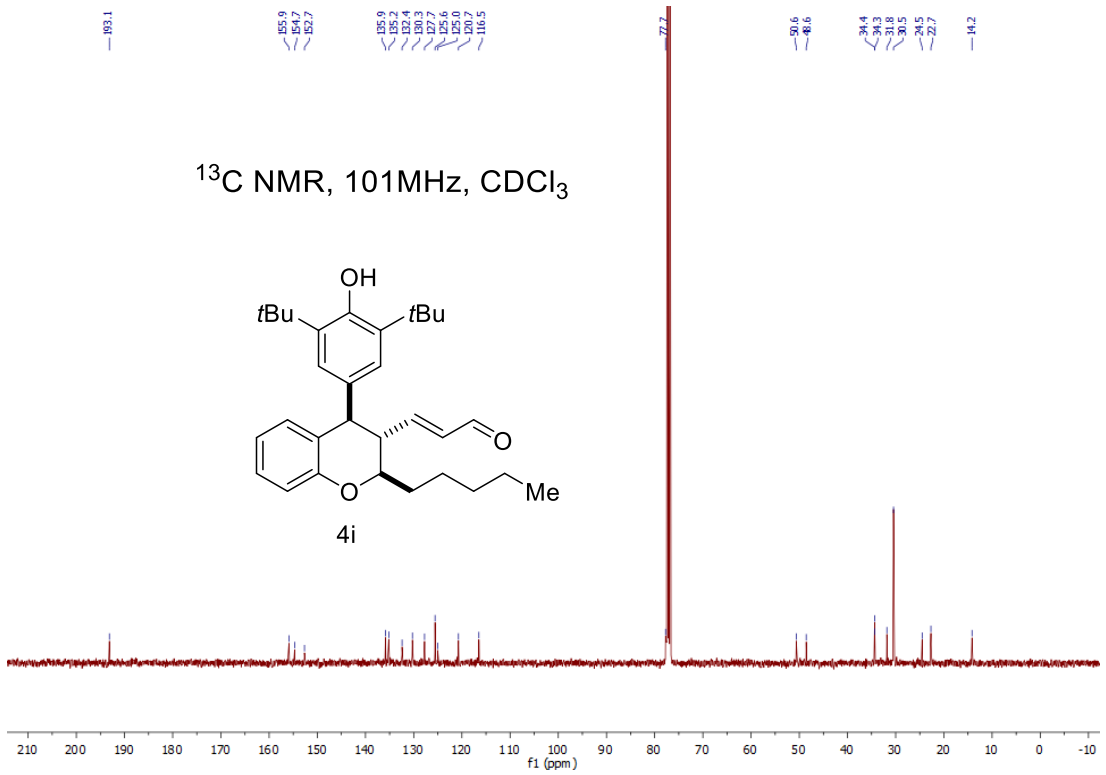


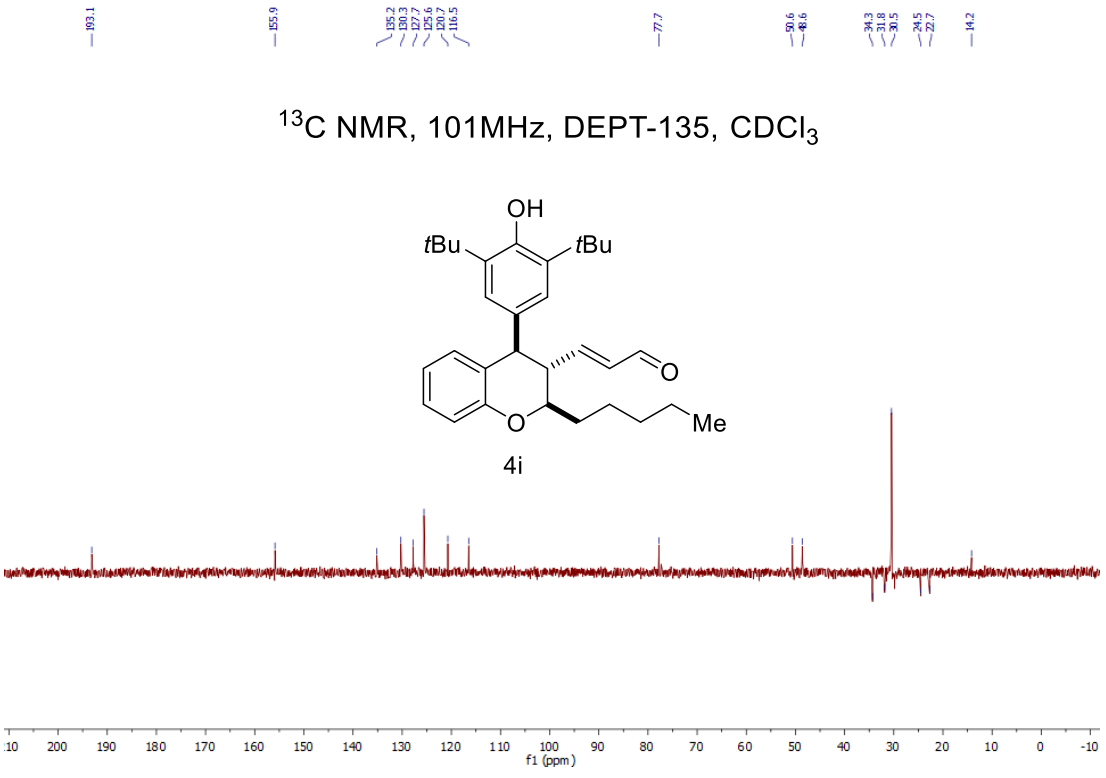




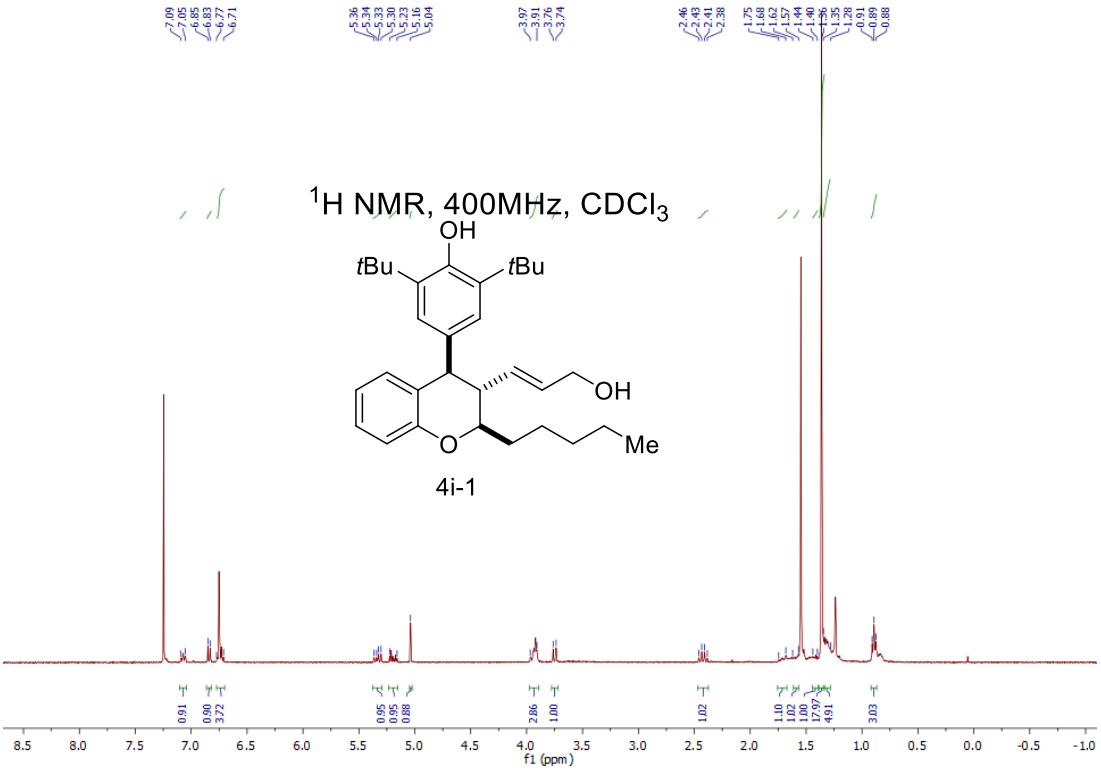
2.6.9. (*E*)-3-((2R,3S,4R)-4-(3,5-di-*tert*-butyl-4-hydroxyphenyl)-2-pentylchroman-3-yl)acrylaldehyde (4i).

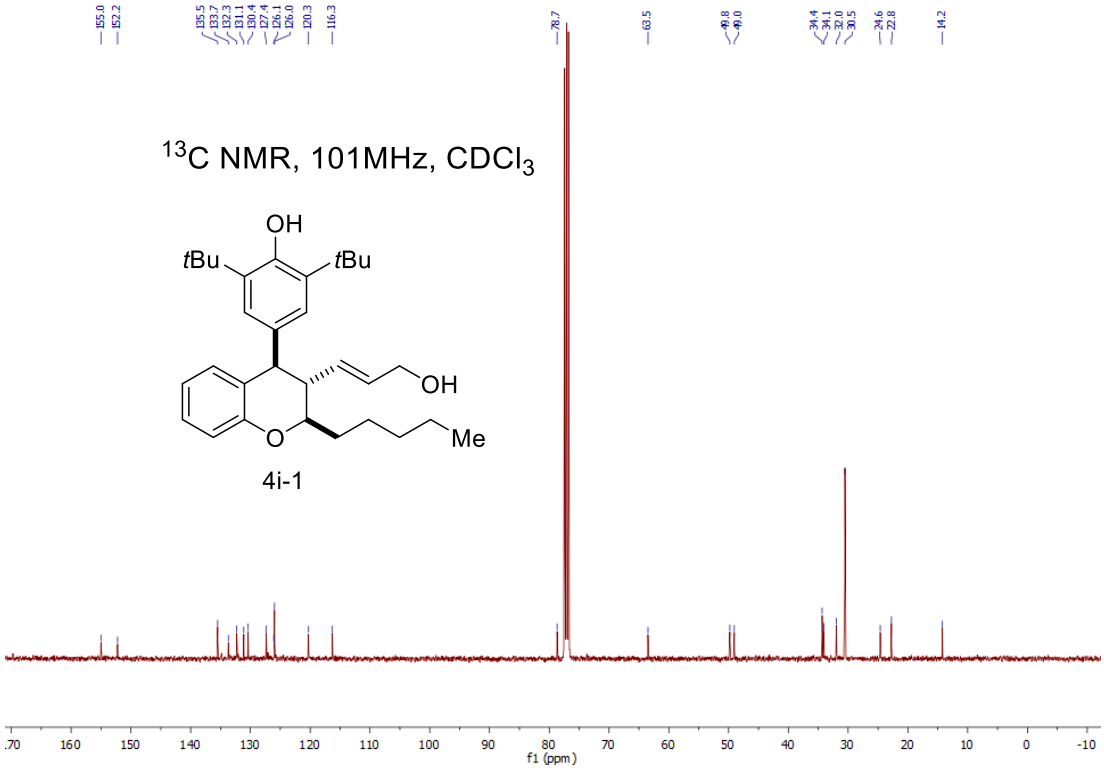


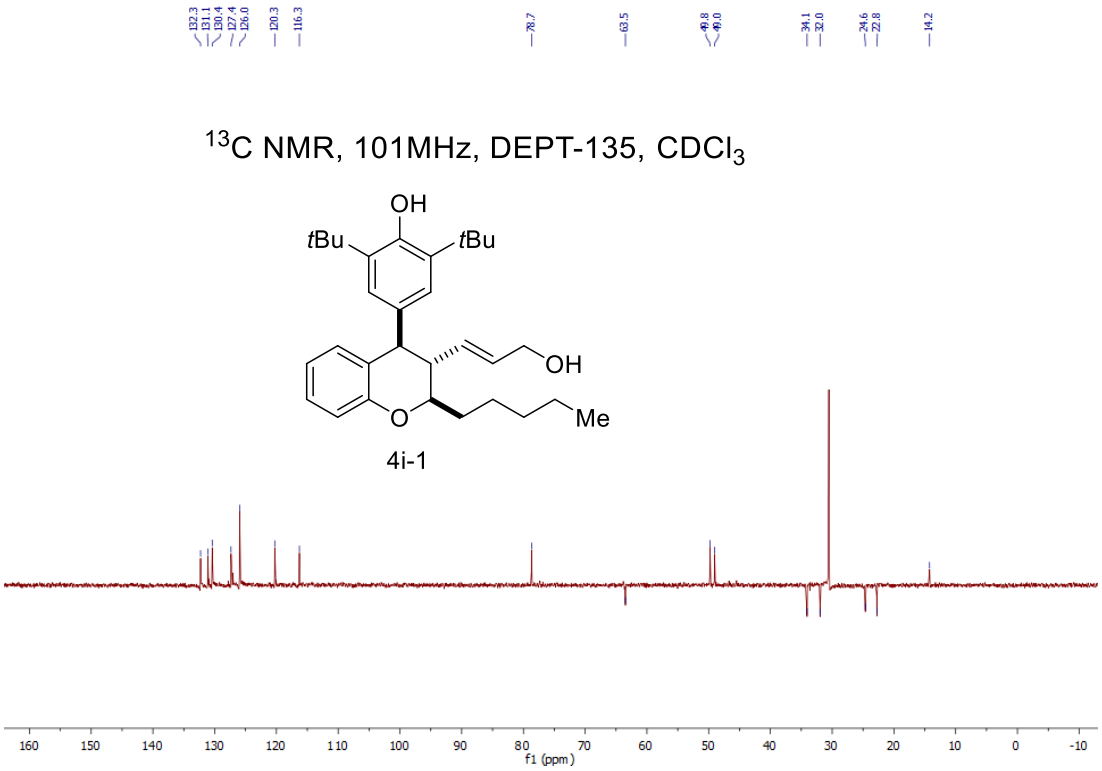




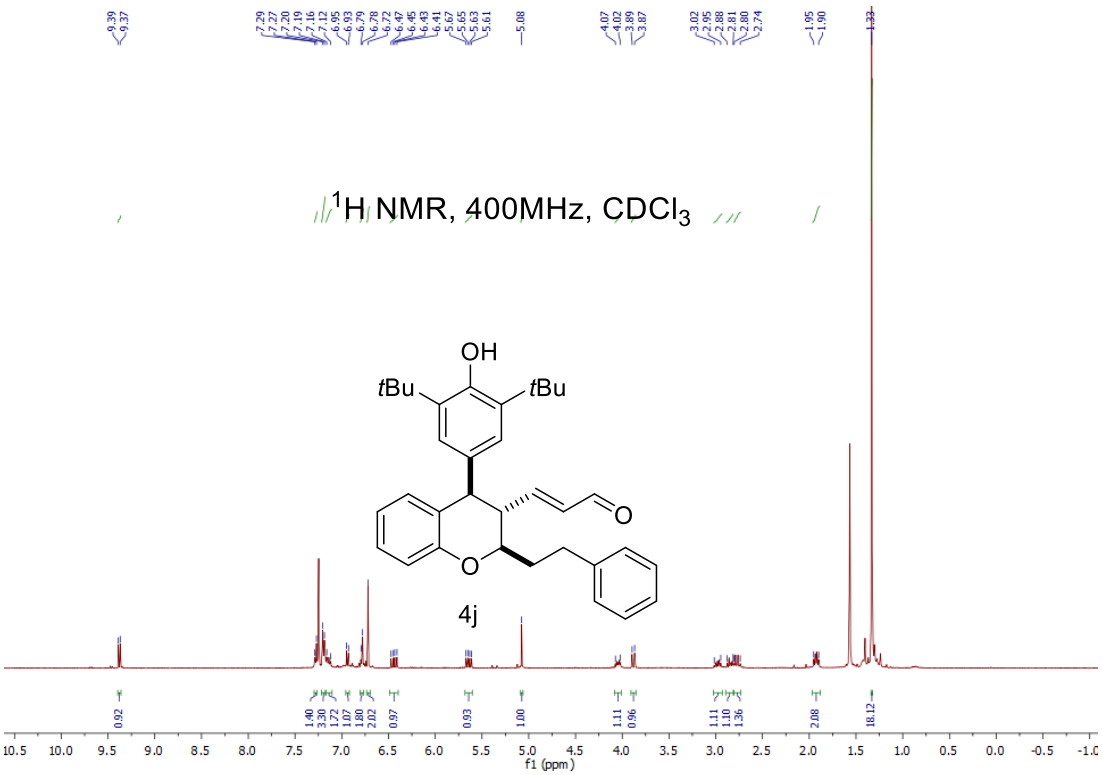
2.6.10. 2,6-di-*tert*-butyl-4-((2R,3S,4R)-3-((*E*)-3-hydroxyprop-1-en-1-yl)-2-pentylchroman-4-yl)phenol (4i-1).

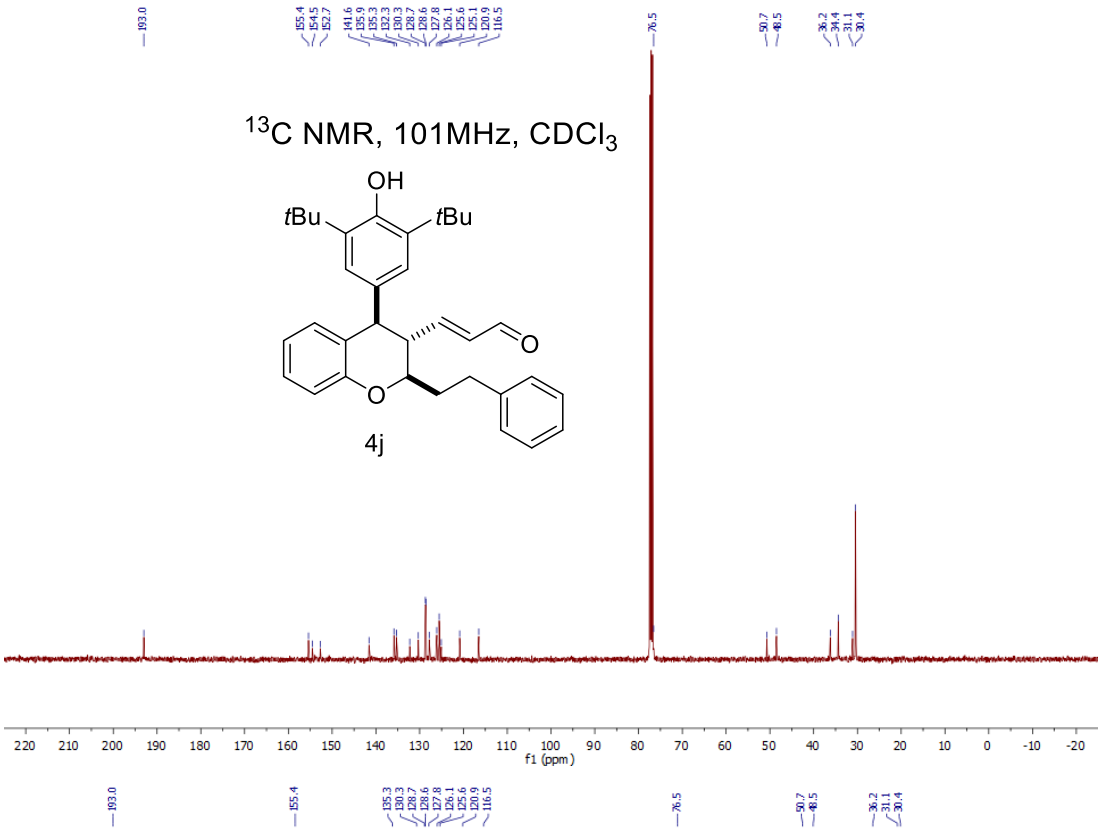

^{1}H NMR, 400MHz, CDCl$_3$
OH
tBu
tBu
OH
O
Me
4i-1
f1 (ppm)

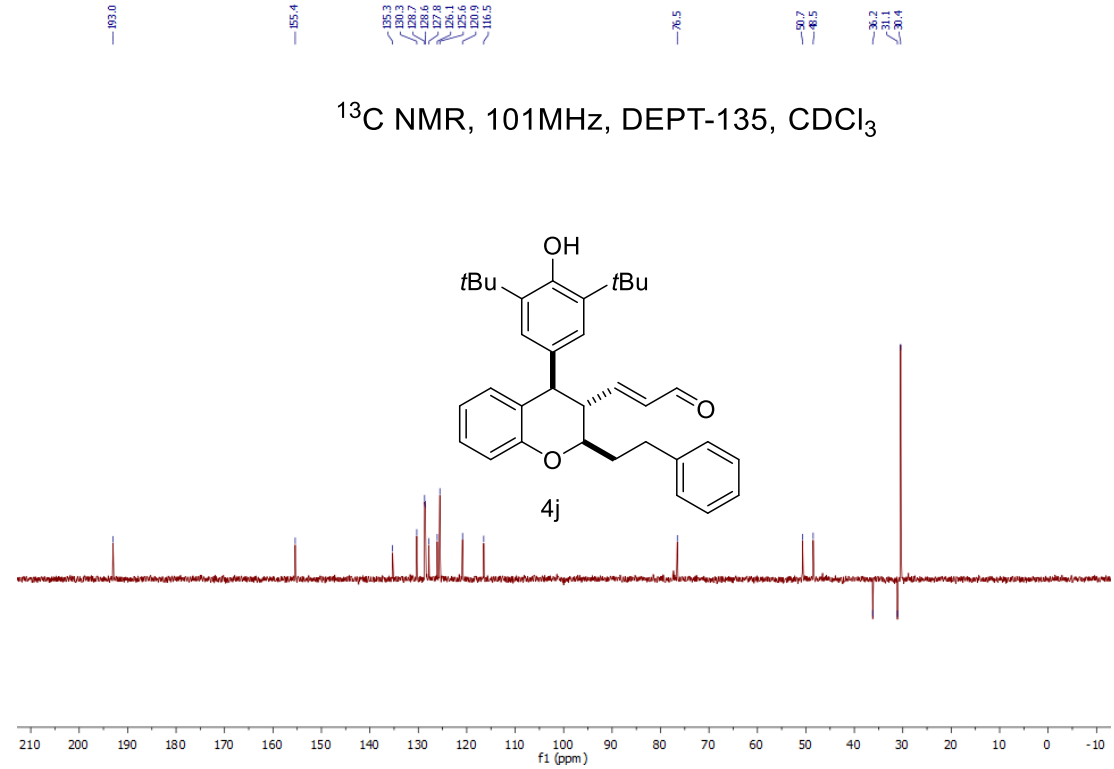

^{13}C NMR, 101MHz, CDCl$_3$
OH
tBu
tBu
OH
O
Me
4i-1
f1 (ppm)



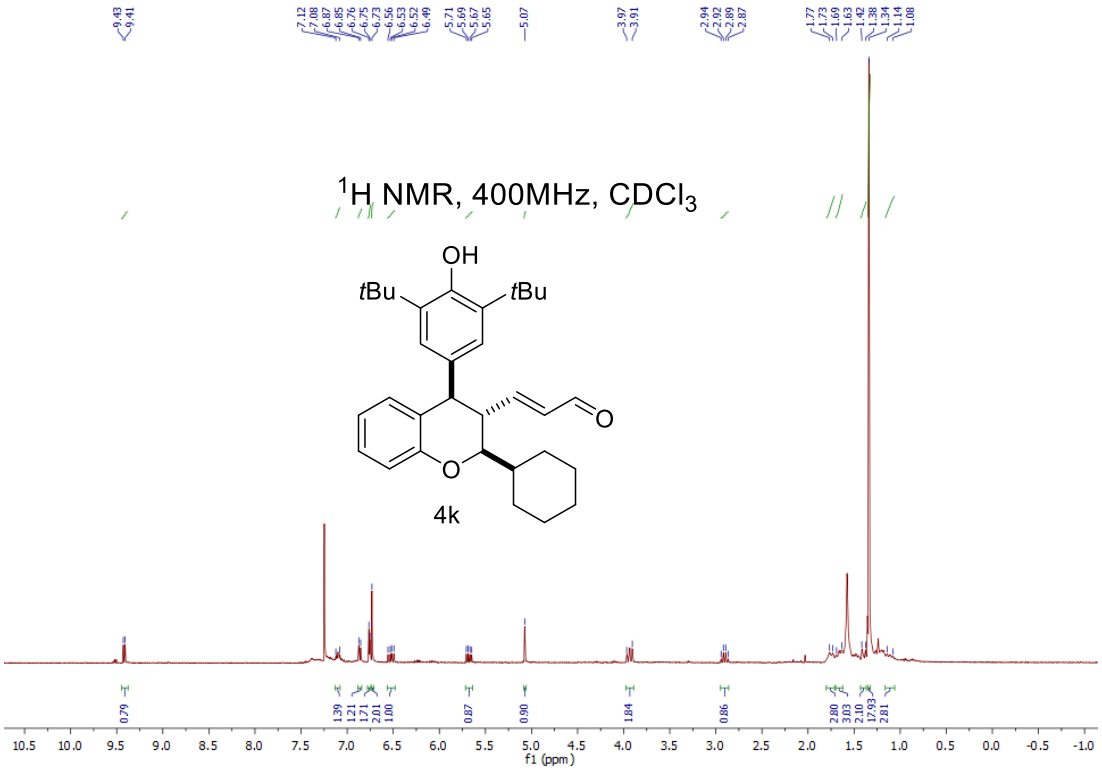
2.6.11. (*E*)-3-((2R,3S,4R)-4-(3,5-di-*tert*-butyl-4-hydroxyphenyl)-2-phenethylchroman-3-yl)acrylaldehyde (4j).

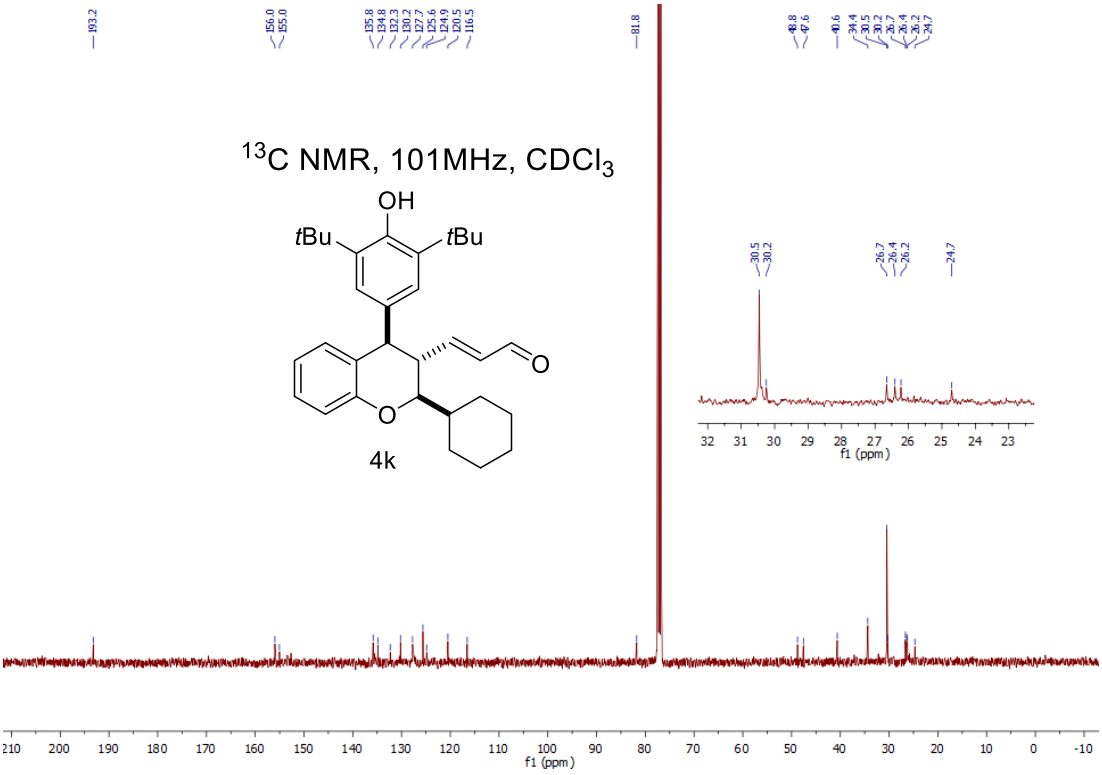


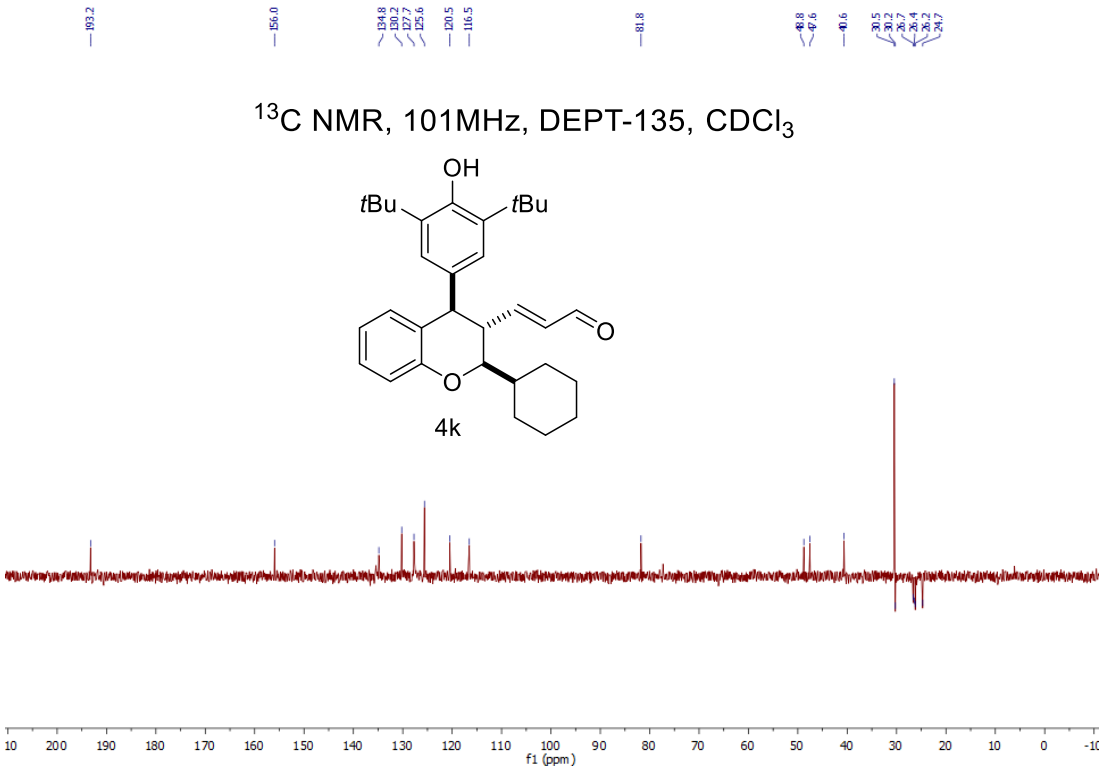




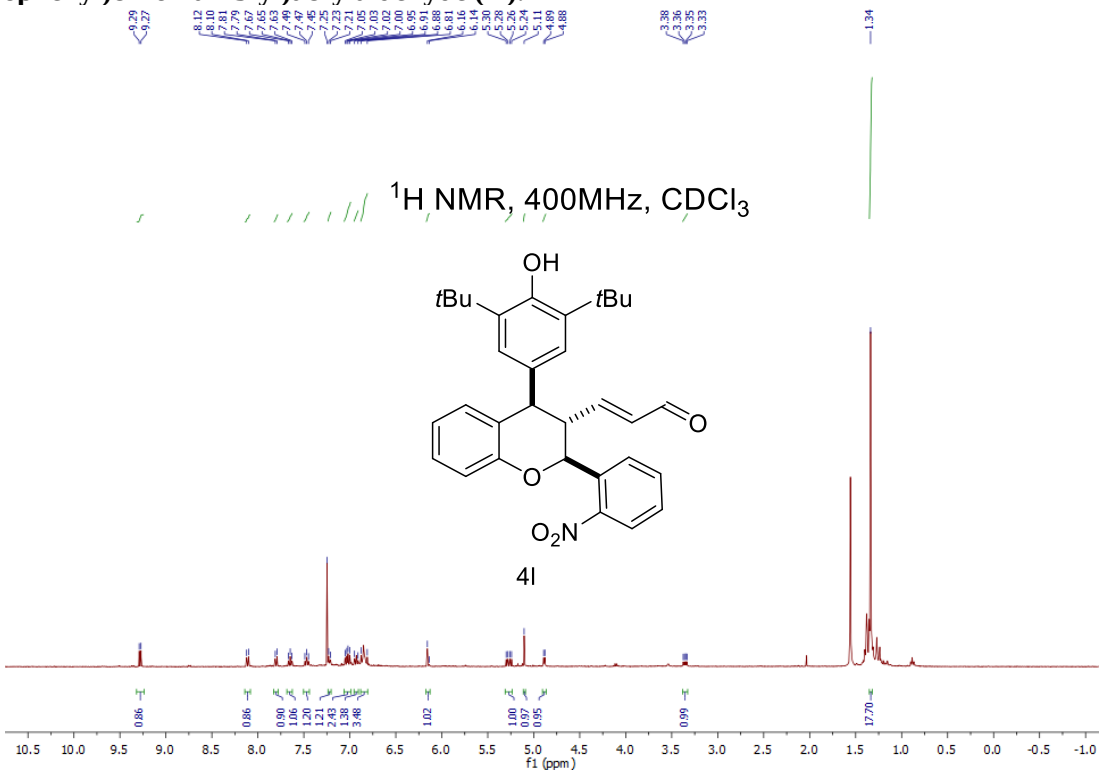
2.6.12. (*E*)-3-((2R,3S,4R)-2-cyclohexyl-4-(3,5-di-*tert*-butyl-4-hydroxyphenyl)chroman-3-yl)acrylaldehyde (4k).

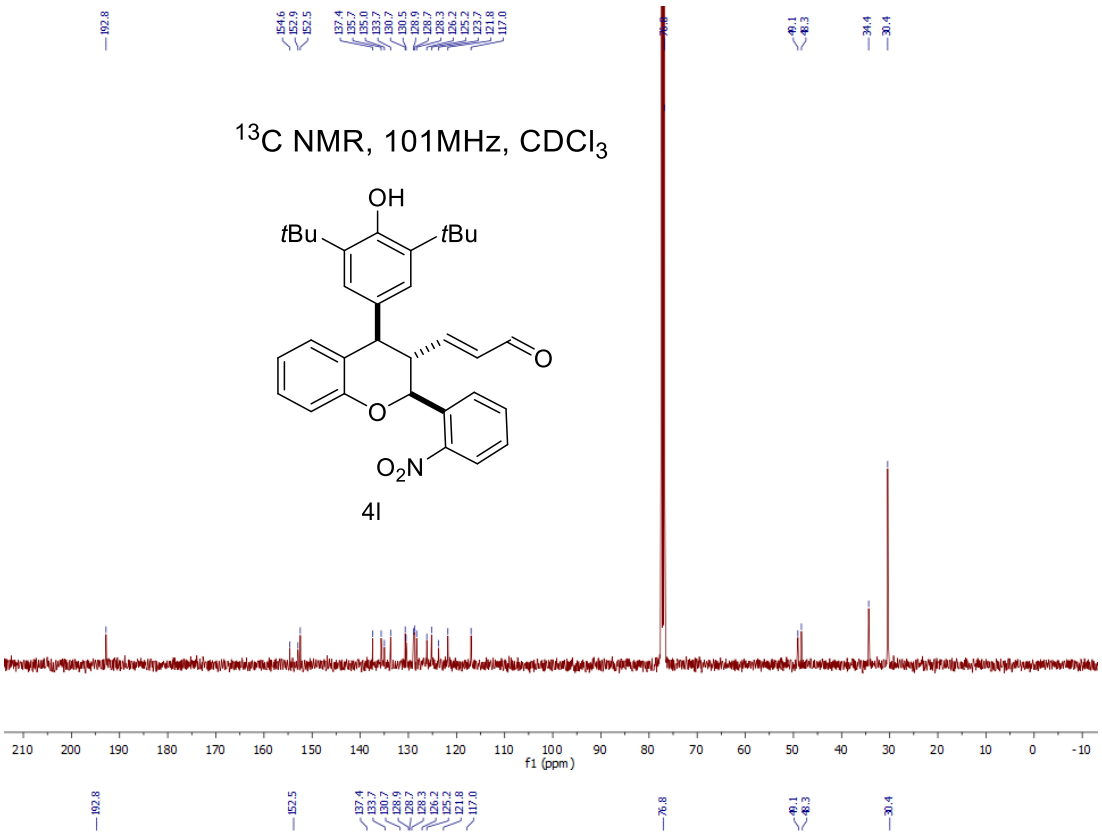

^{1}H NMR, 400MHz, $CDCl_3$
OH
tBu
tBu
O
O
4k
f1 (ppm)


^{13}C NMR, 101MHz, $CDCl_3$
OH
tBu
tBu
O
O
4k
f1 (ppm)
f1 (ppm)



2.6.13. (*E*)-3-((2S,3S,4R)-4-(3,5-di-*tert*-butyl-4-hydroxyphenyl)-2-(2-nitrophenyl)chroman-3-yl)acrylaldehyde (4l).

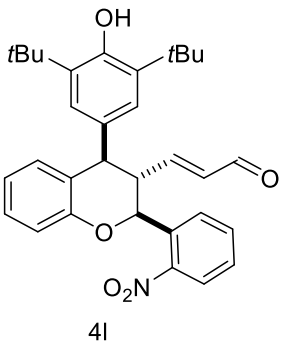




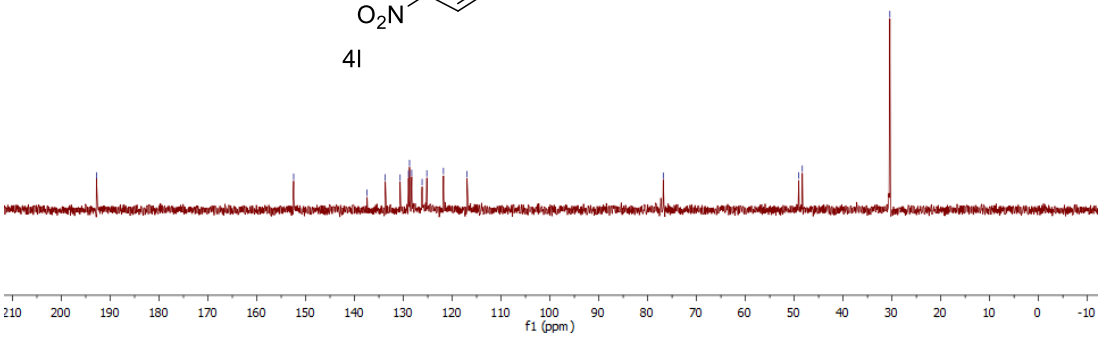
^{13}C NMR, 101MHz, $CDCl_3$

4l

^{13}C NMR, 101MHz, DEPT-135, $CDCl_3$

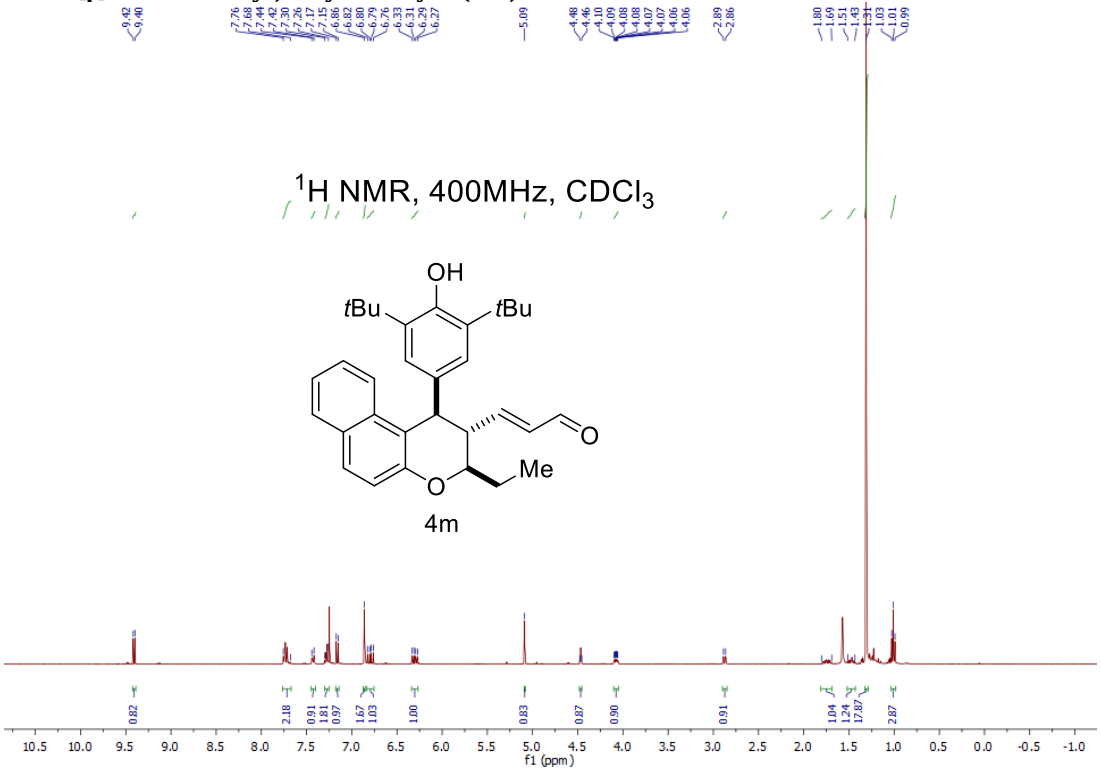


4l

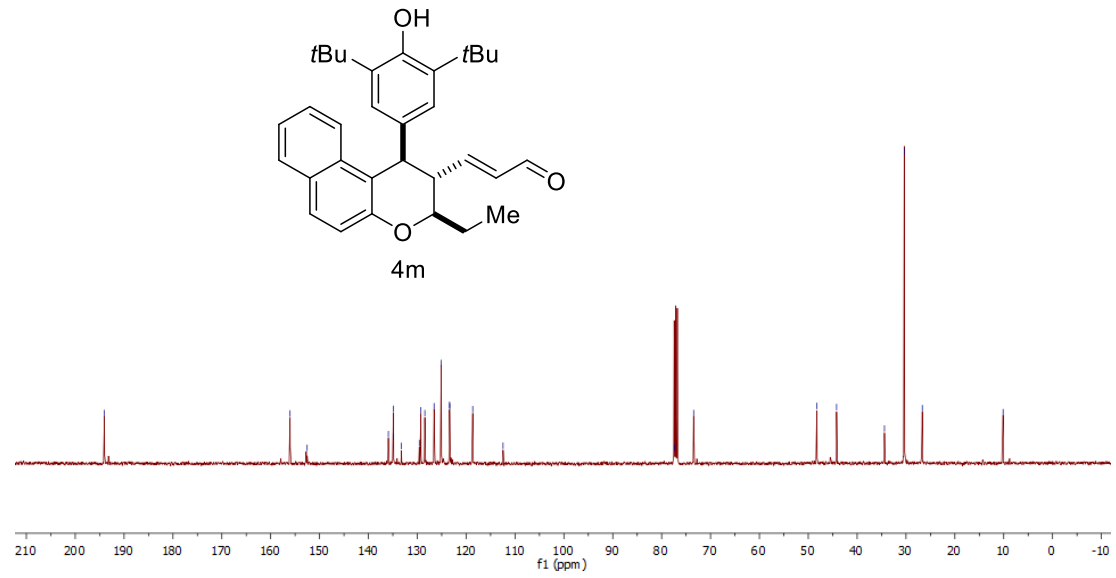


2.6.14. (*E*)-3-((1R,2S,3R)-1-(3,5-di-*tert*-butyl-4-hydroxyphenyl)-3-ethyl-2,3-dihydro-1*H*-benzo[*f*]chromen-2-yl)acrylaldehyde(4m).

^{1}H NMR, 400MHz, $CDCl_3$

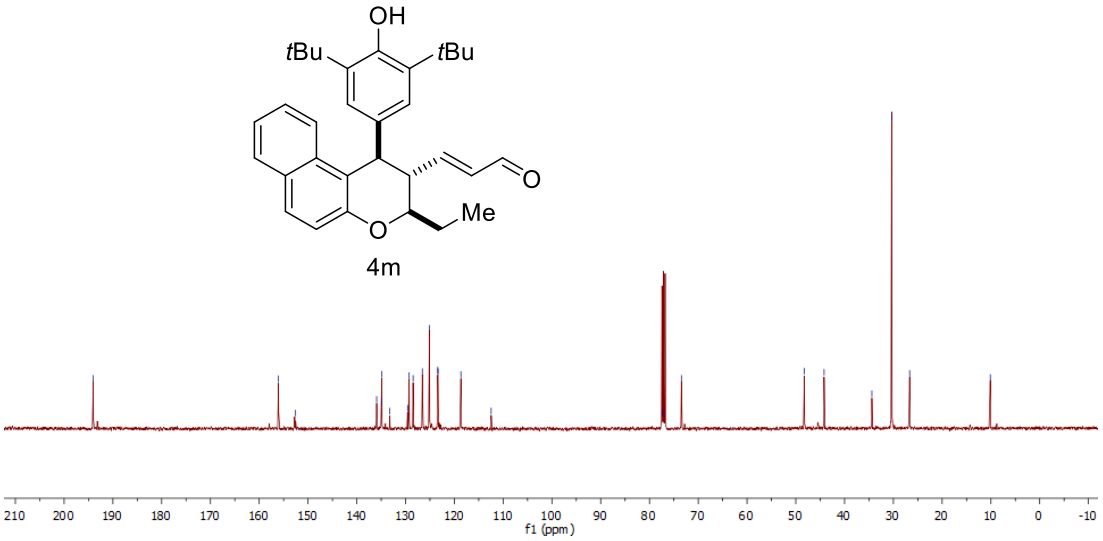


^{13}C NMR, 101MHz, $CDCl_3$

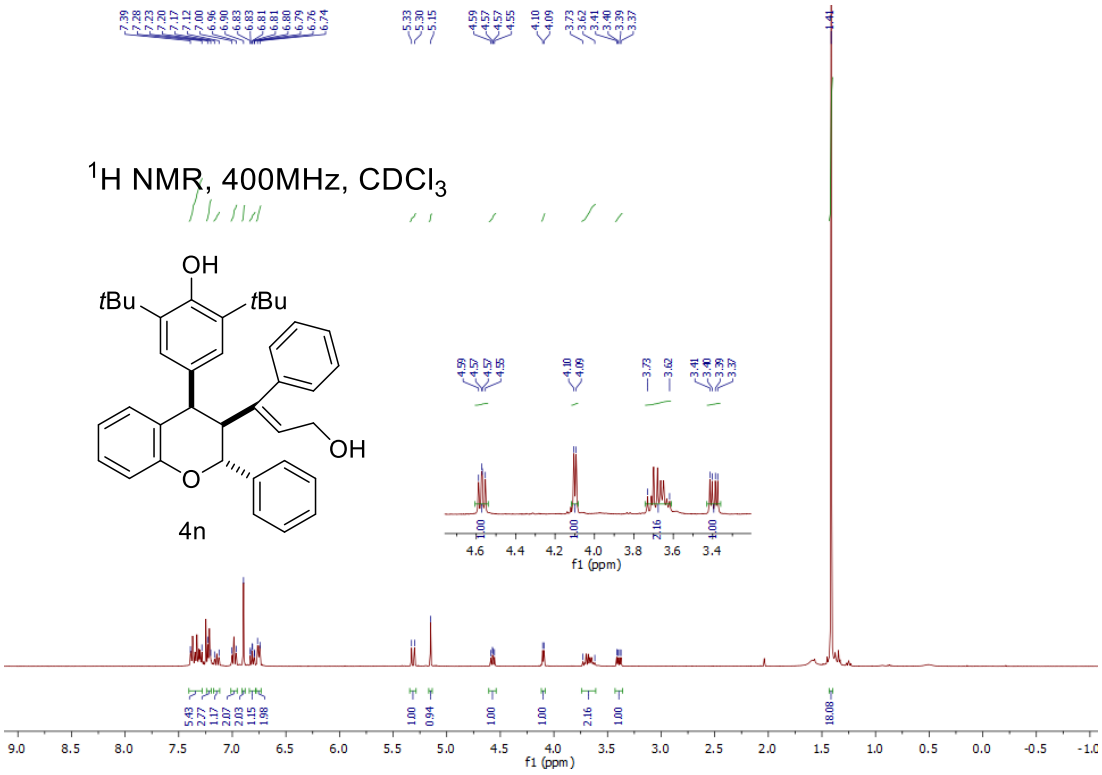


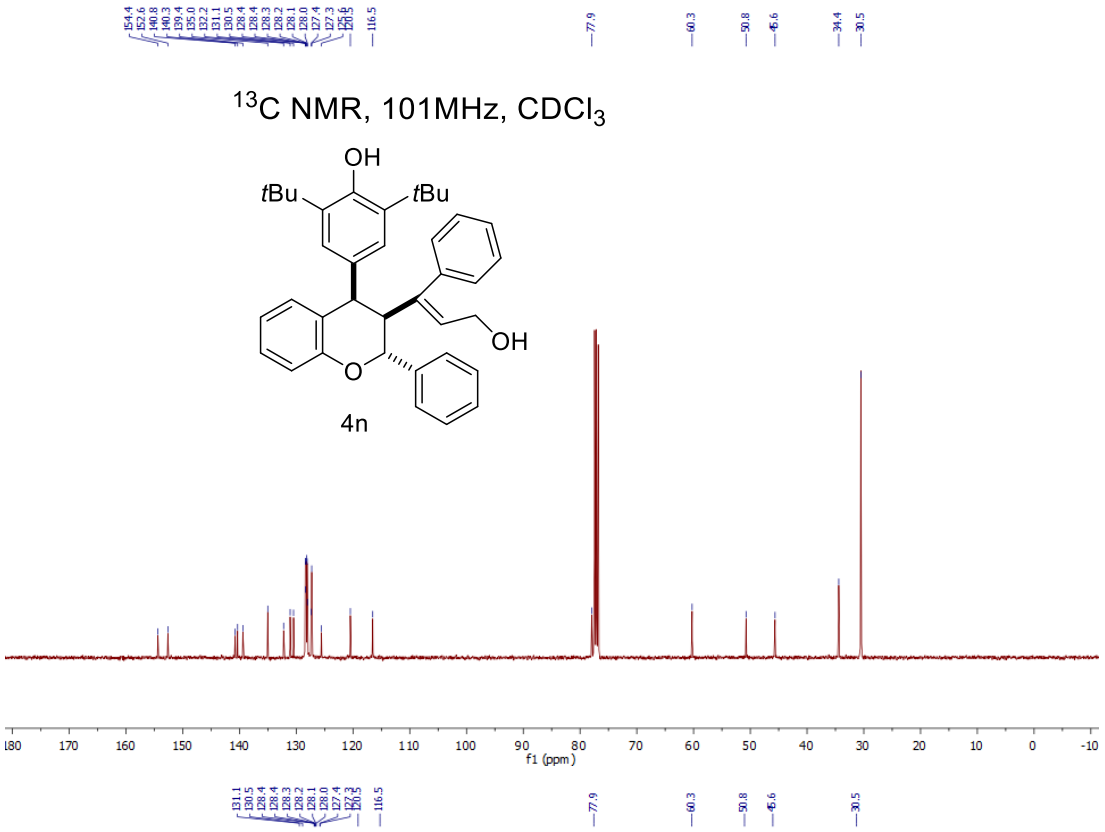


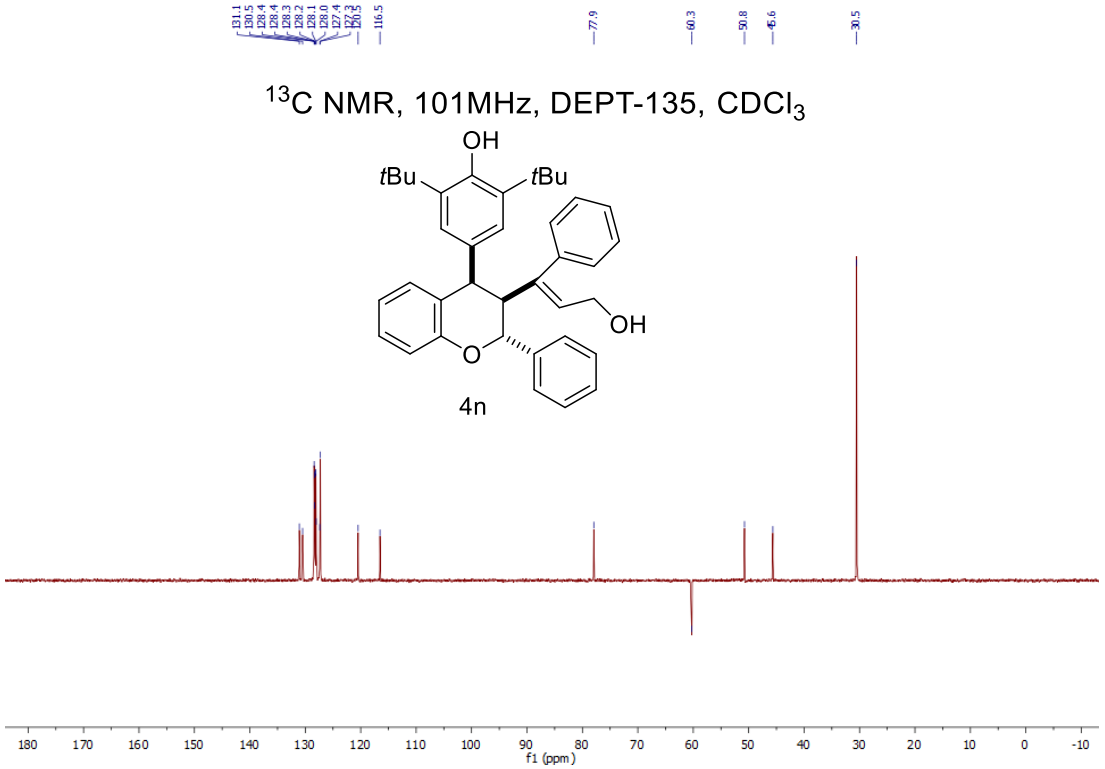
^{13}C NMR, 101MHz, DEPT-135, $CDCl_3$



2.6.15. 2,6-di-*tert*-butyl-4-((2R,3S,4R)-3-((*Z*)-3-hydroxy-1-phenylprop-1-en-1-yl)-2-phenylchroman-4-yl)phenol (4n).

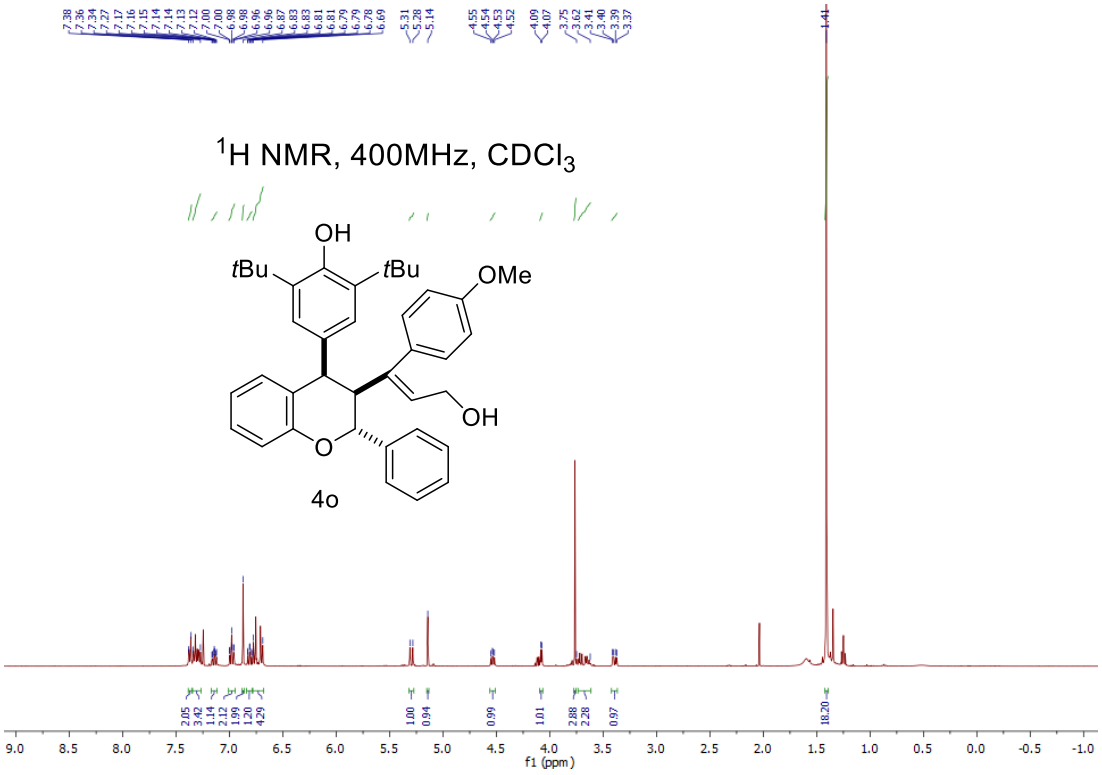



154.4
152.6
140.8
140.3
139.4
135.6
132.2
131.1
130.5
128.4
128.4
128.3
128.2
128.1
127.4
127.3
116.5
77.9
60.3
50.8
45.6
34.4
30.5
13C NMR, 101MHz, CDCl3
OH
tBu
tBu
OH
O
4n
180
170
160
150
140
130
120
110
100
90
80
70
60
50
40
30
20
10
0
-10
f1 (ppm)

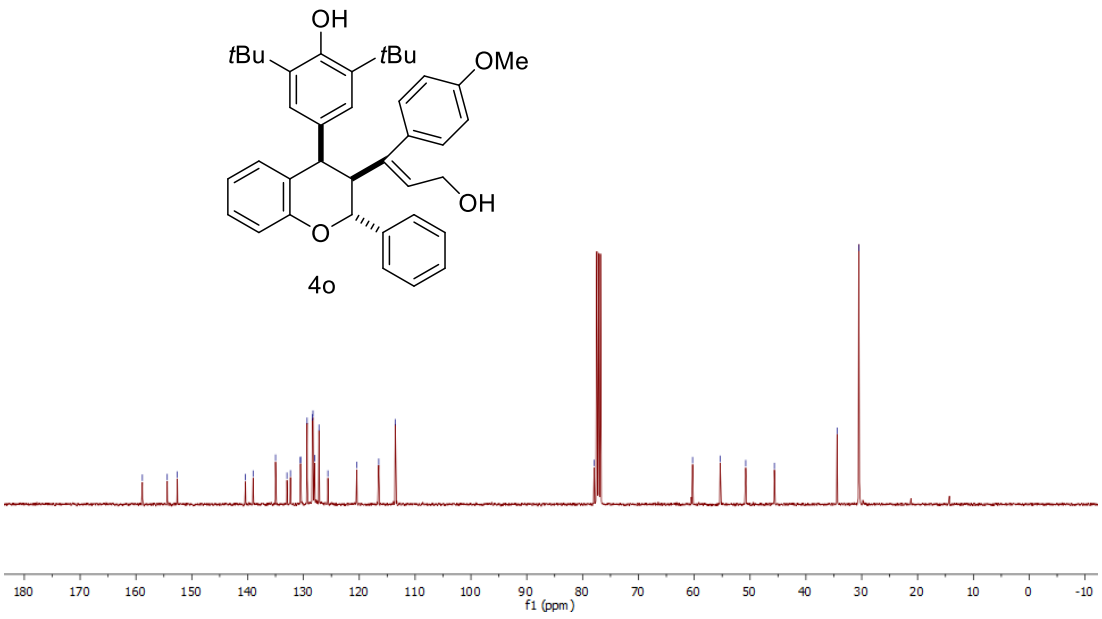

131.1
130.5
128.4
128.4
128.3
128.2
128.1
128.0
127.4
127.3
126.5
116.5
77.9
60.3
50.8
45.6
30.5
13C NMR, 101MHz, DEPT-135, CDCl3
OH
tBu
tBu
OH
O
4n
180
170
160
150
140
130
120
110
100
90
80
70
60
50
40
30
20
10
0
-10
f1 (ppm)

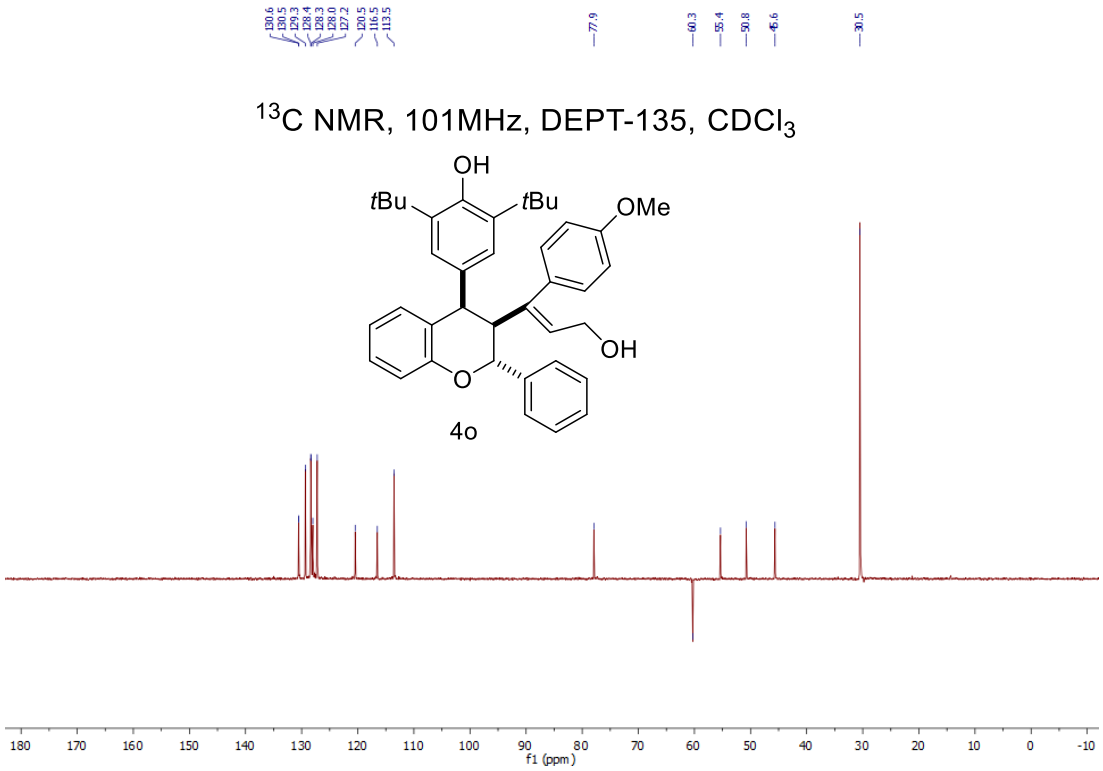
2.6.16. 2,6-di-*tert*-butyl-4-((2R,3S,4R)-3-((*Z*)-3-hydroxy-1-(4-methoxyphenyl)prop-1-en-1-yl)-2-phenylchroman-4-yl)phenol (4o).

^{1}H NMR, 400MHz, $CDCl_3$

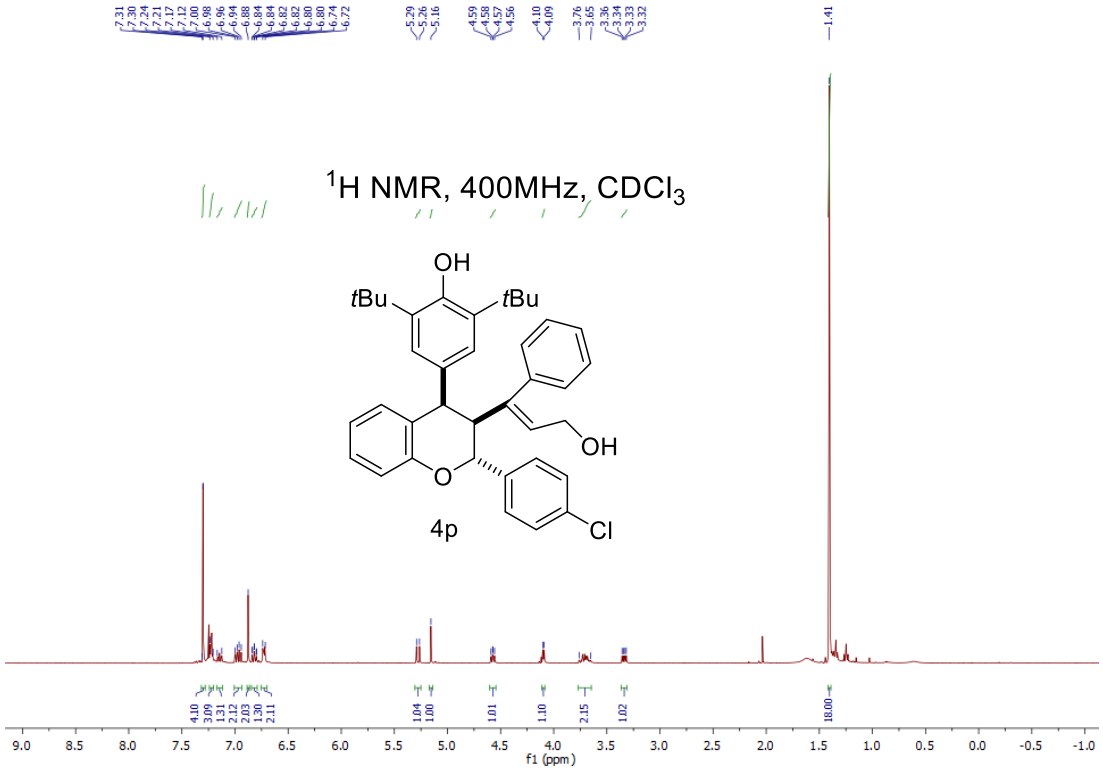


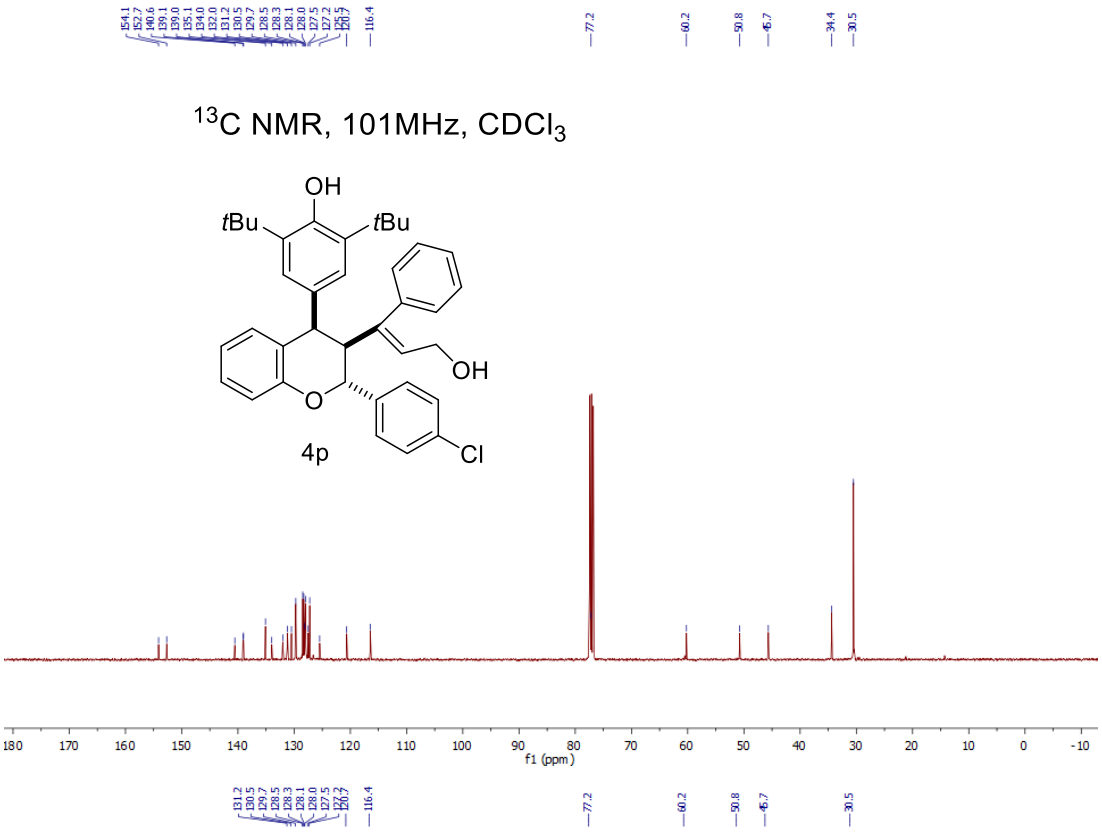
^{13}C NMR, 101MHz, $CDCl_3$



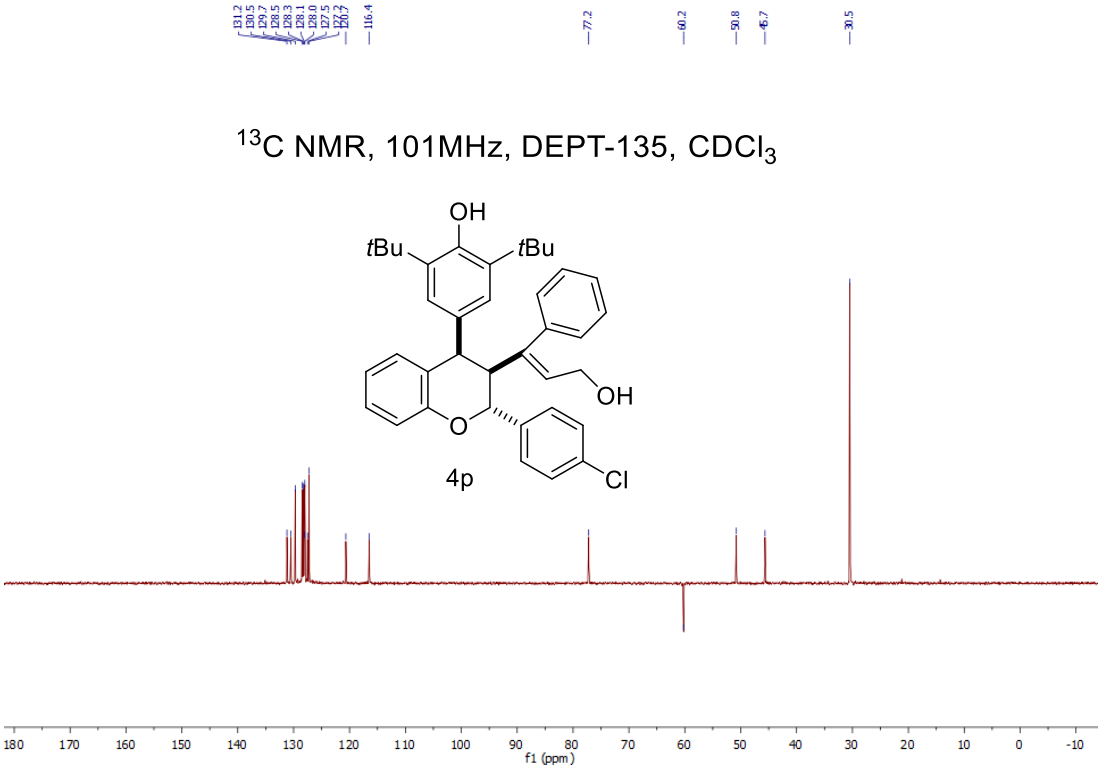


2.6.17. 2,6-di-*tert*-butyl-4-((2R,3S,4R)-2-(4-chlorophenyl)-3-((*Z*)-3-hydroxy-1-phenylprop-1-en-1-yl)chroman-4-yl)phenol (4p).



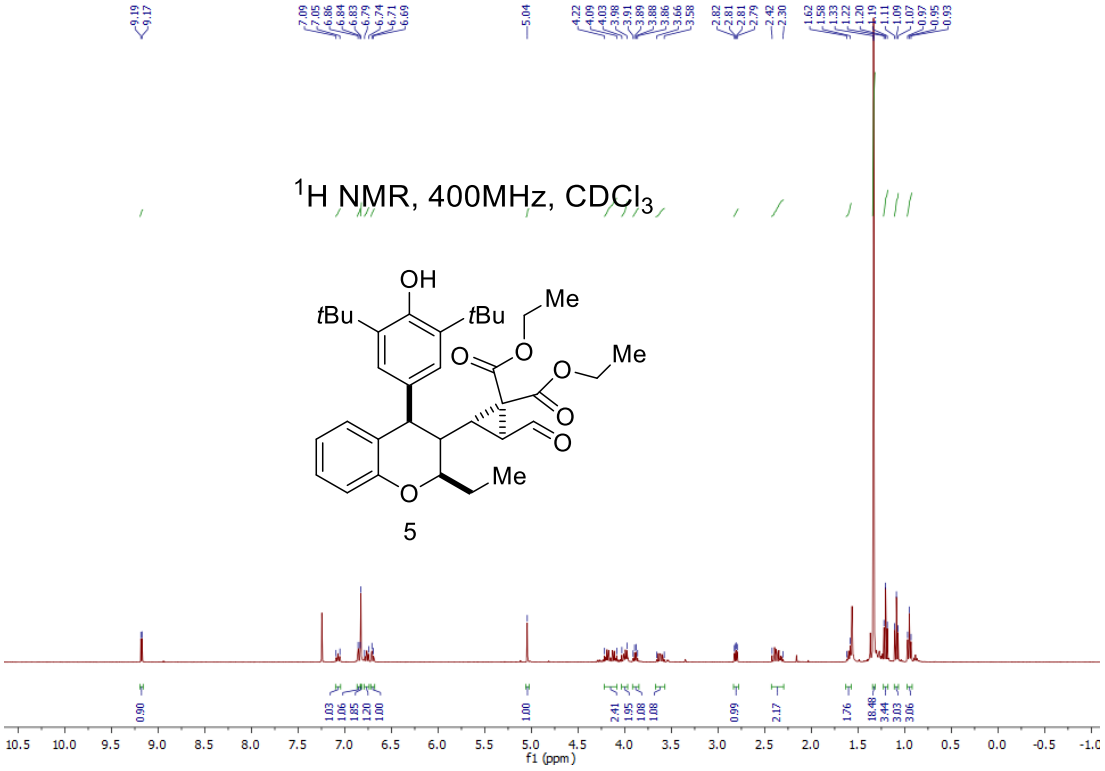


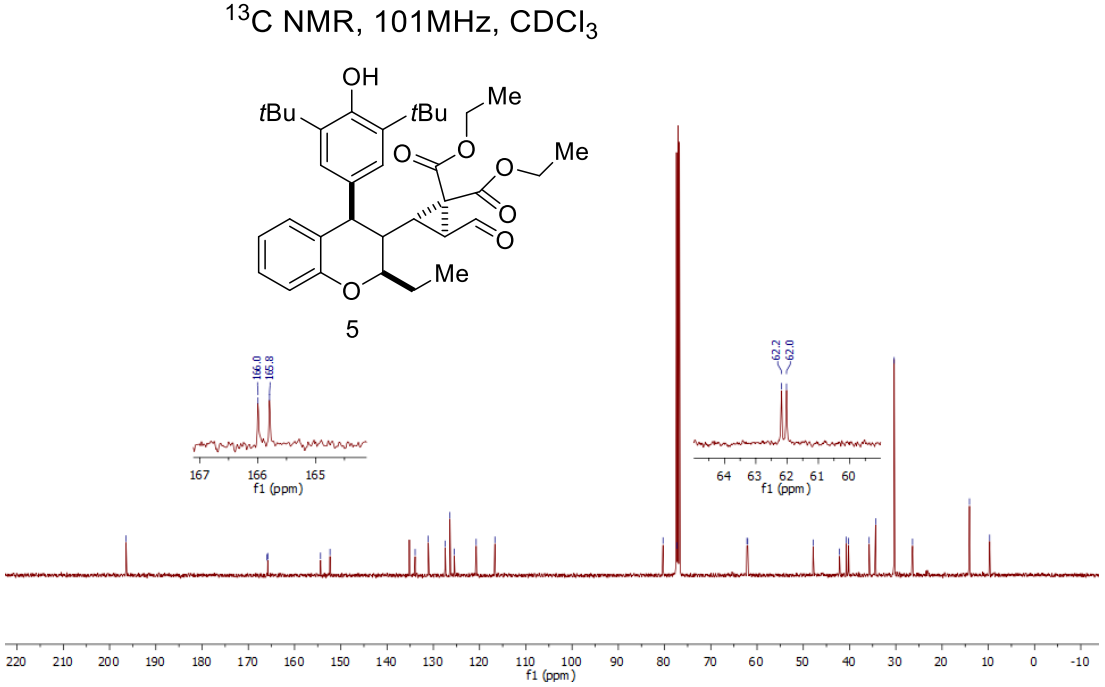
^{13}C NMR, 101MHz, $CDCl_3$

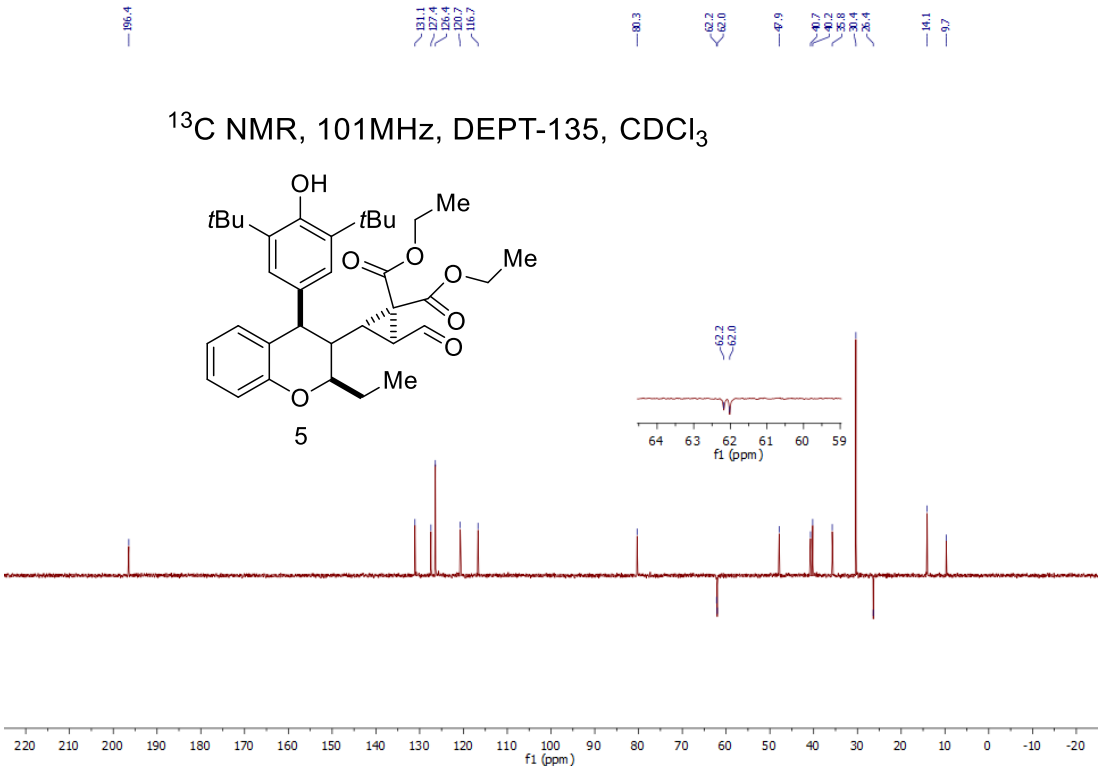


^{13}C NMR, 101MHz, DEPT-135, $CDCl_3$

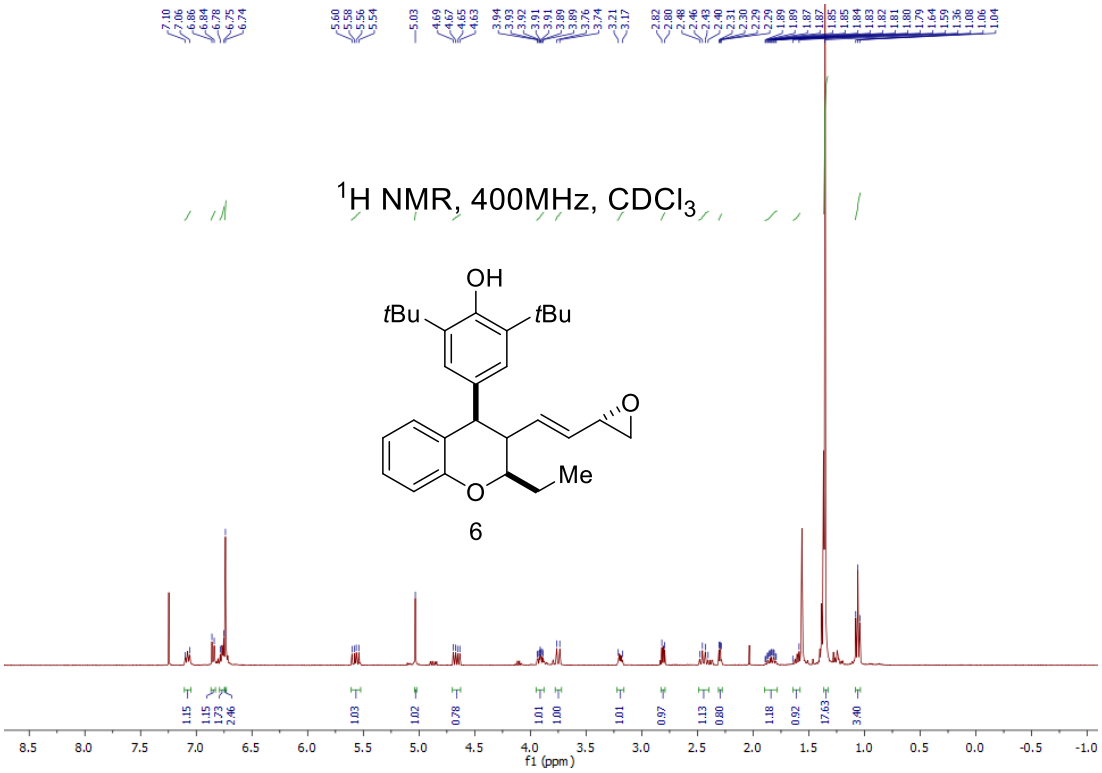
2.6.18. (2S,3S)-diethyl 2-((2R,4R)-4-(3,5-di-*tert*-butyl-4-hydroxyphenyl)-2-ethylchroman-3-yl)-3-formylcyclopropane-1,1-dicarboxylate (5).

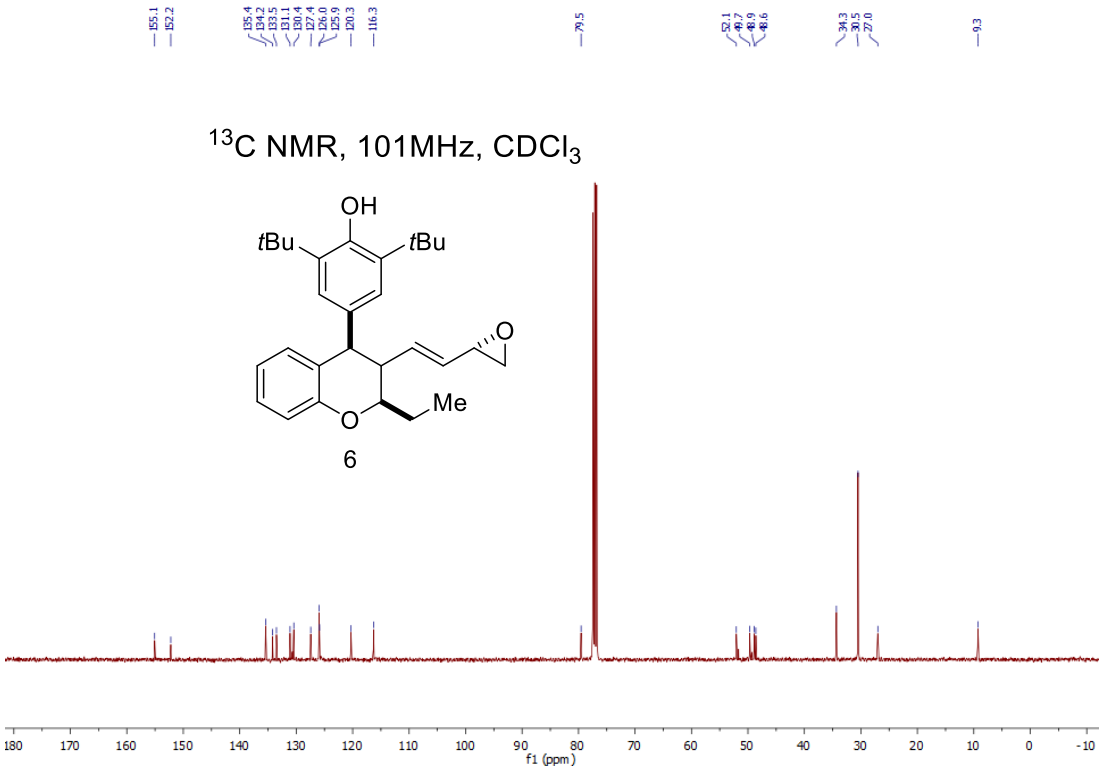


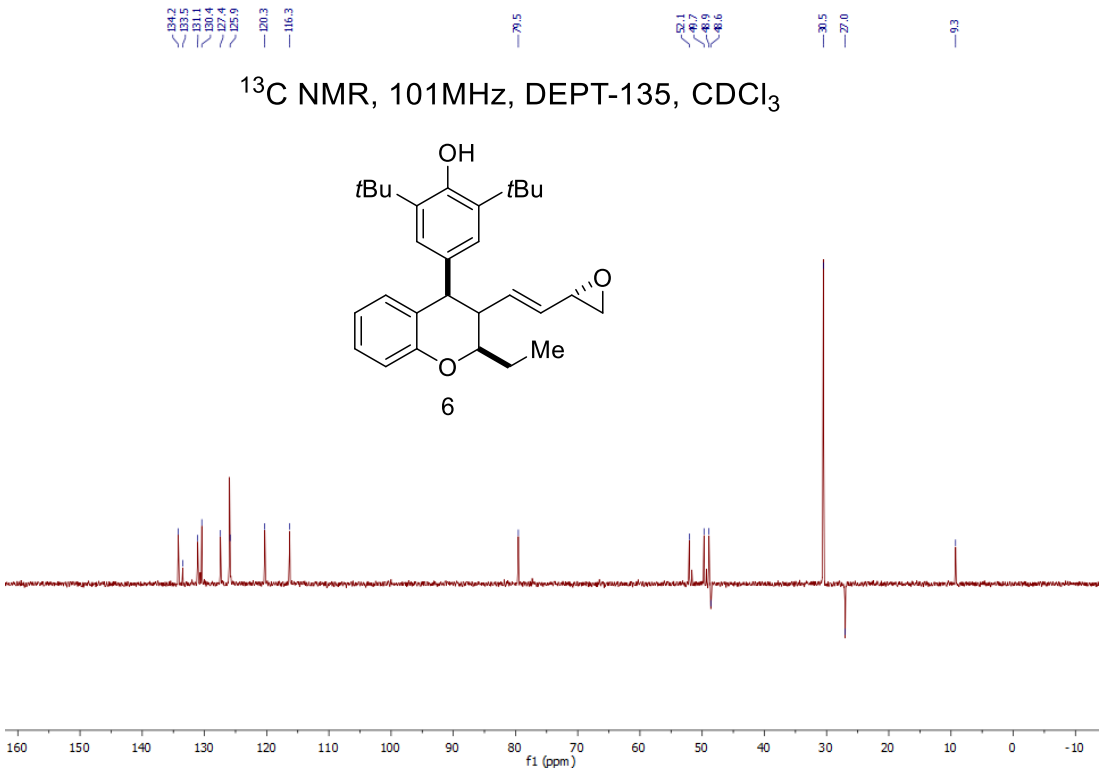




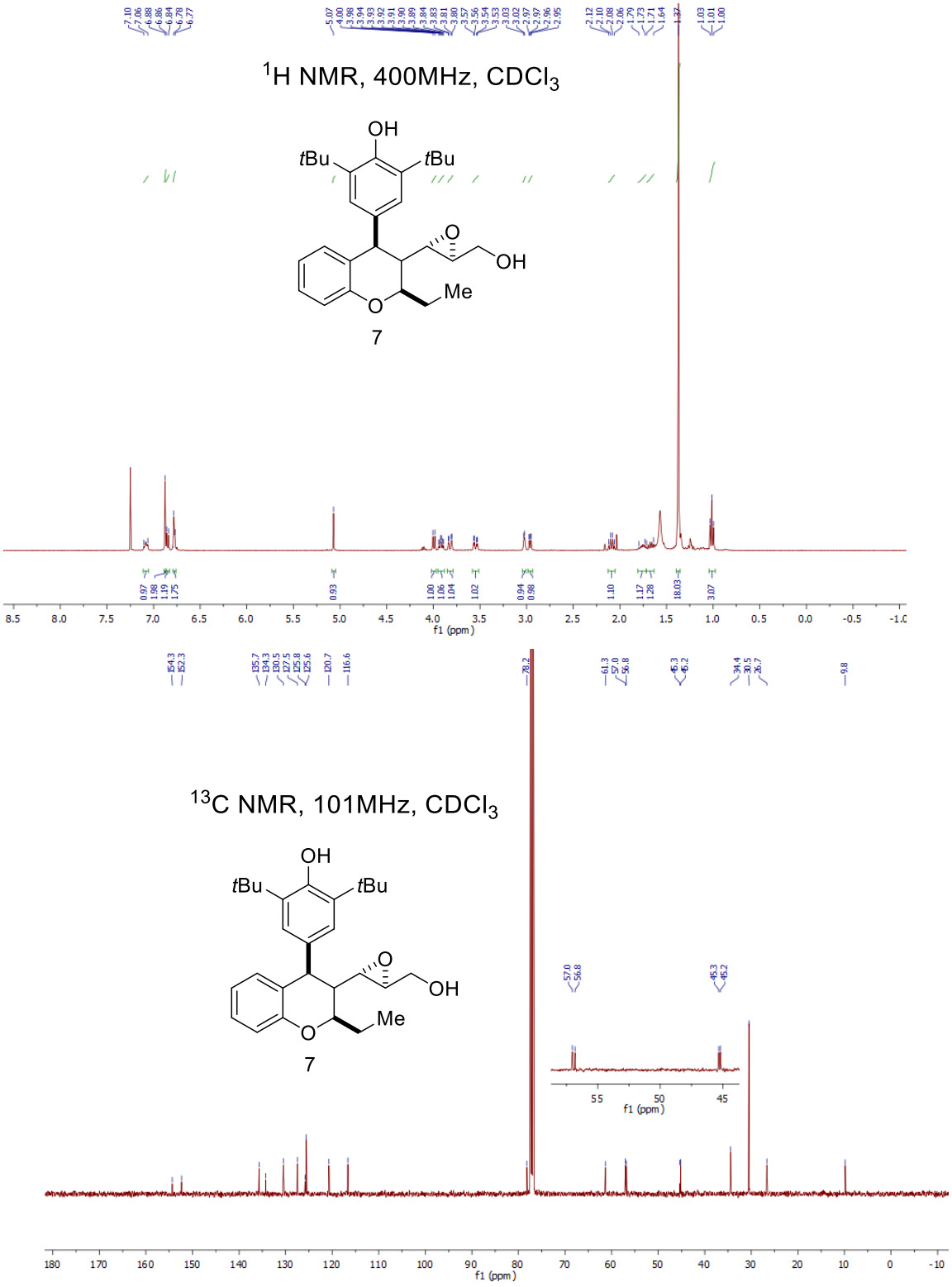
2.6.19. 2,6-di-*tert*-butyl-4-((2R,4R)-2-ethyl-3-((*E*)-2-((S)-oxiran-2-yl)vinyl)chroman-4-yl)phenol (6).

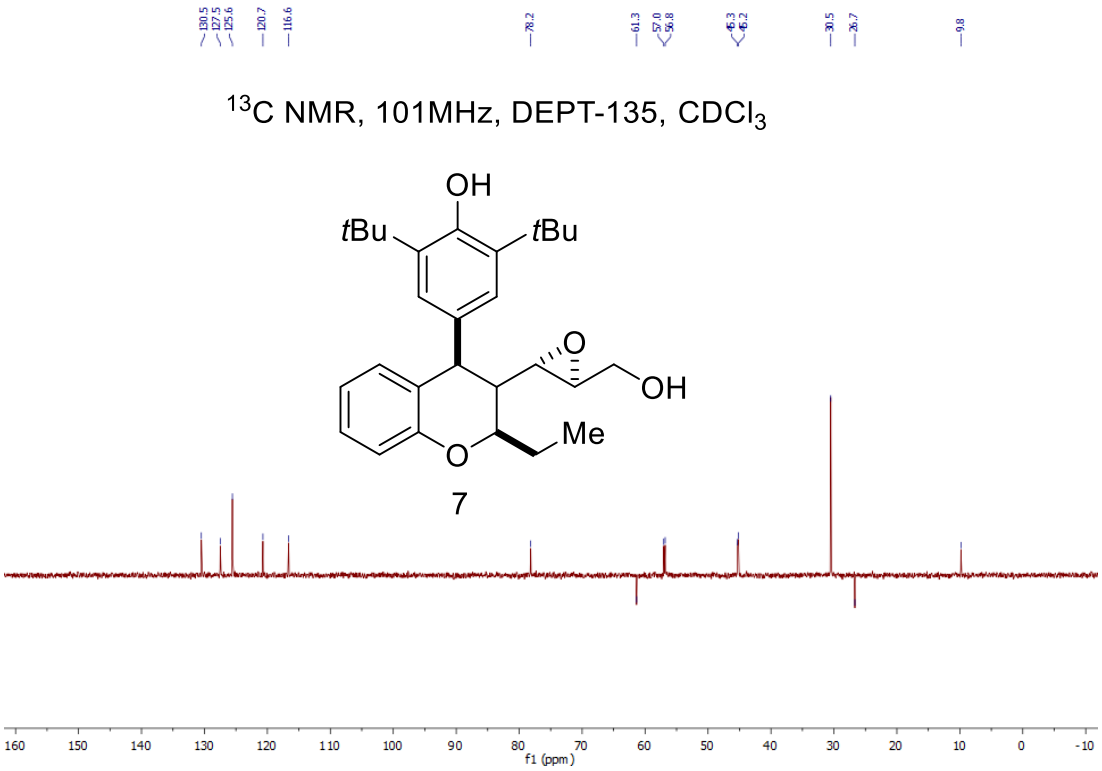



155.1
152.2
135.4
134.2
133.5
131.1
130.4
127.4
126.0
125.9
120.3
116.3
79.5
52.1
49.7
48.9
48.6
34.3
30.5
27.0
9.3
^{13}C NMR, 101MHz, $CDCl_3$
OH
*t*Bu
*t*Bu
O
Me
O
6
180 170 160 150 140 130 120 110 100 90 80 70 60 50 40 30 20 10 0 -10
f1 (ppm)

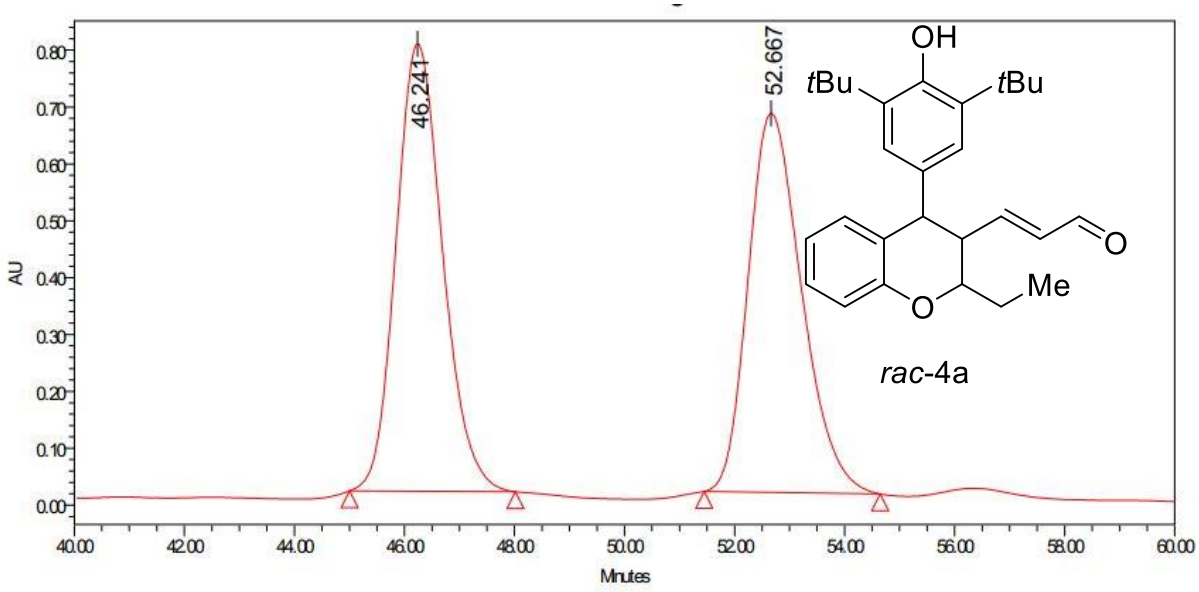

134.2
133.5
131.1
130.4
127.4
125.9
120.3
116.3
79.5
52.1
49.7
48.9
48.6
30.5
27.0
9.3
^{13}C NMR, 101MHz, DEPT-135, $CDCl_3$
OH
*t*Bu
*t*Bu
O
Me
O
6
160 150 140 130 120 110 100 90 80 70 60 50 40 30 20 10 0 -10
f1 (ppm)

2.6.21. 2,6-di-*tert*-butyl-4-((2R,4R)-2-ethyl-3-((2S,3S)-3-(hydroxymethyl)oxiran-2-yl)chroman-4-yl)phenol(7).



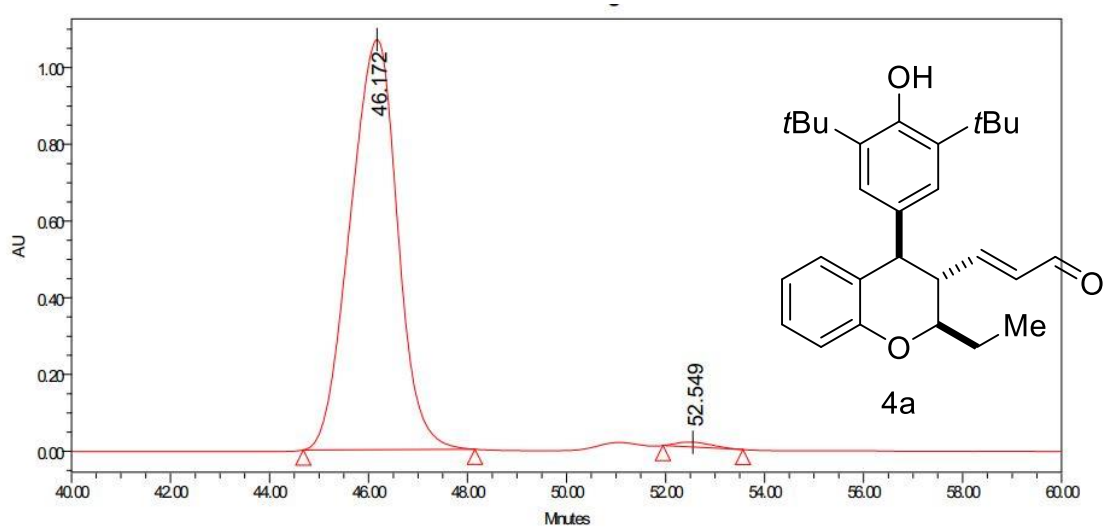

130.5
127.5
125.6
120.7
116.6
78.2
61.3
57.0
56.8
45.3
45.2
30.5
26.7
9.8
^{13}C NMR, 101MHz, DEPT-135, $CDCl_3$
OH
*t*Bu
*t*Bu
O
OH
Me
O
7
160
150
140
130
120
110
100
90
80
70
60
50
40
30
20
10
0
-10
f1 (ppm)

2.7. HPLC Traces:



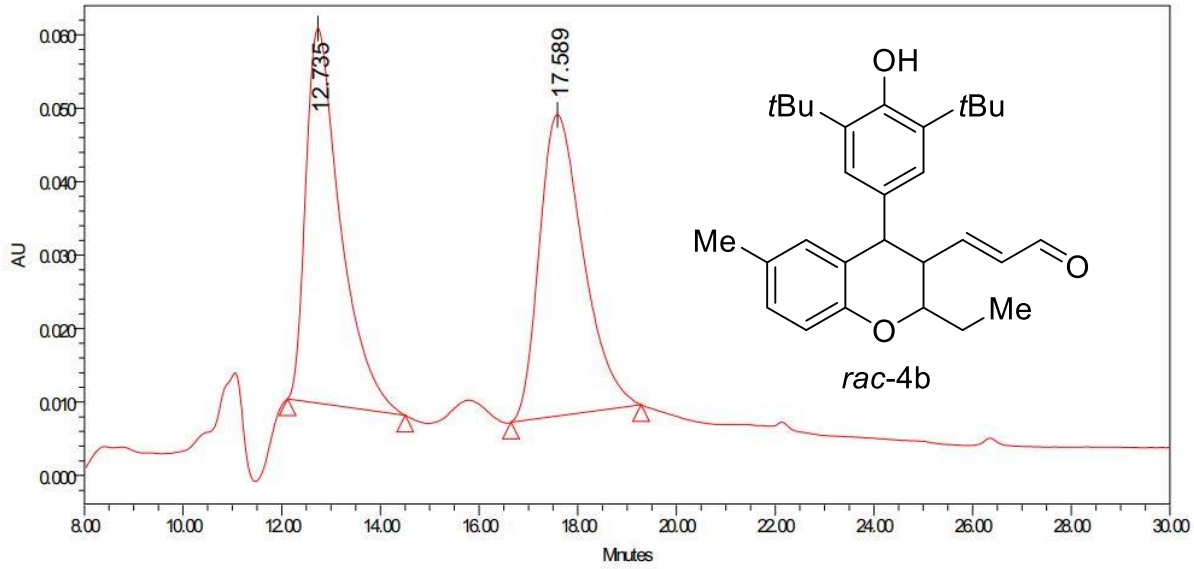
Peak Results

	RT	Area	%Area	Height
1	46.241	46411426	50.80	786866
2	52.667	44958509	49.20	666352



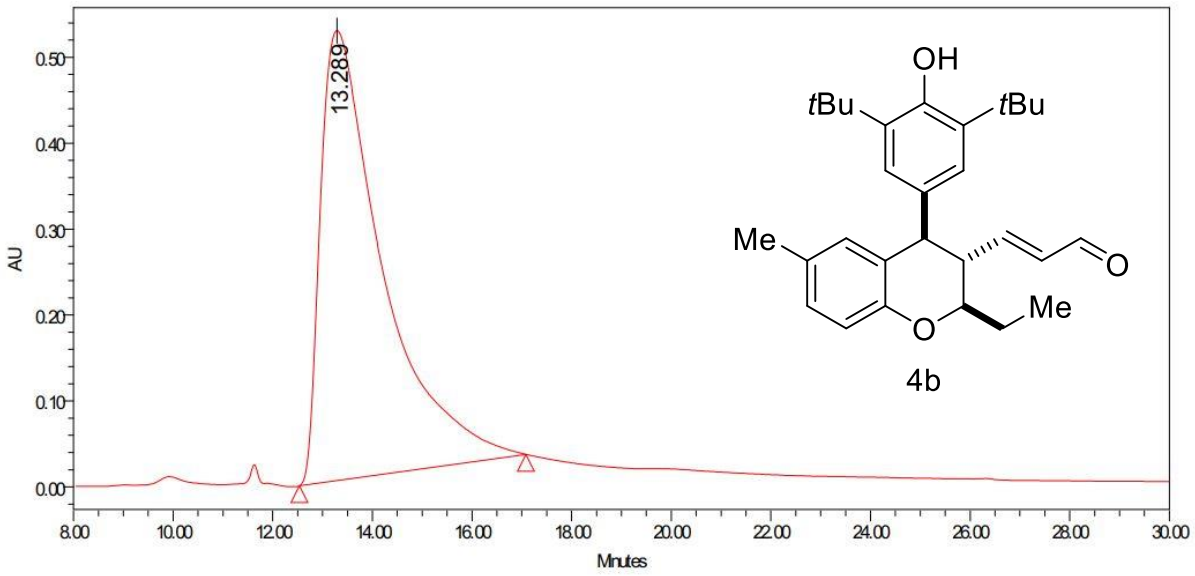
Peak Results

	RT	Area	%Area	Height
1	46.172	70964734	99.11	1068996
2	52.549	640833	0.89	12915



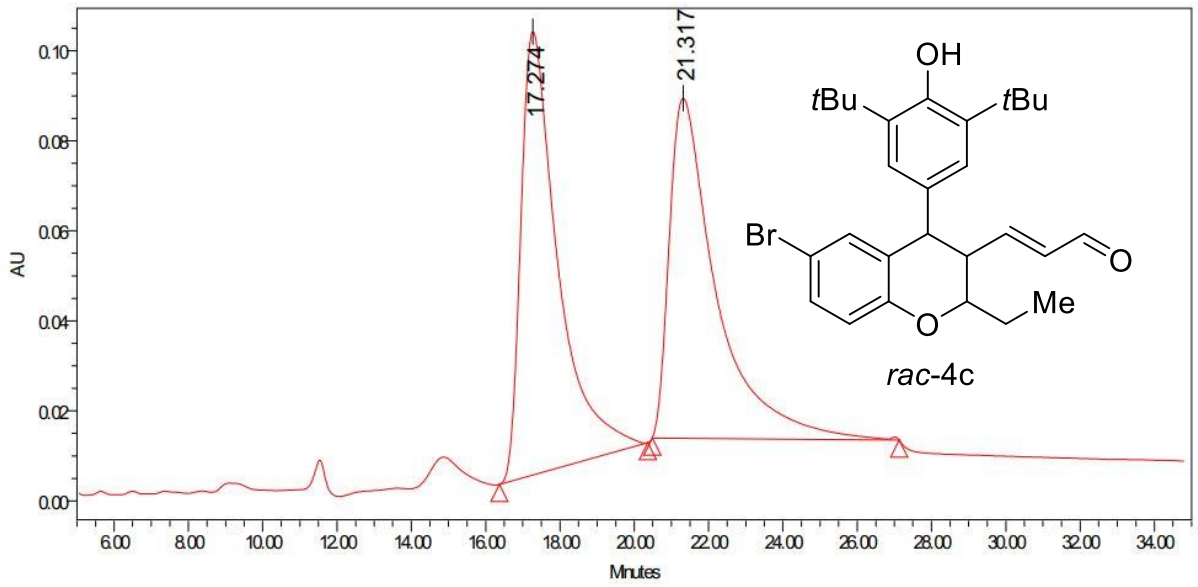
Peak Results

	RT	Area	%Area	Height
1	12.735	2487487	49.52	51000
2	17.589	2535264	50.48	41017



Peak Results

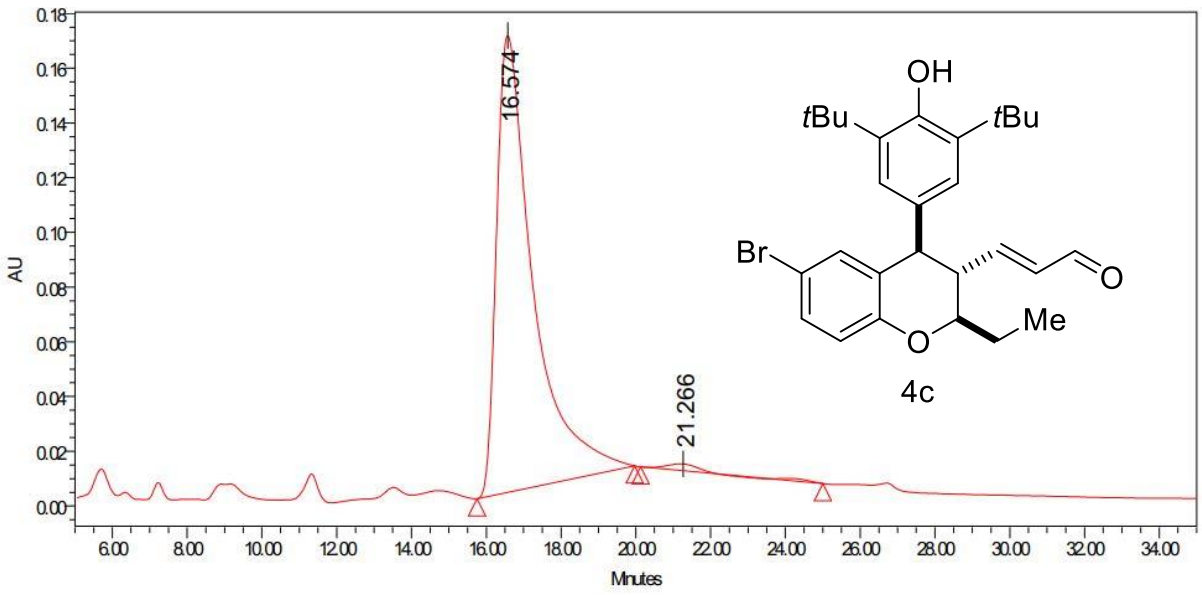
	RT	Area	%Area	Height
1	13.289	45311099	100.00	523829



rac-4c

Peak Results

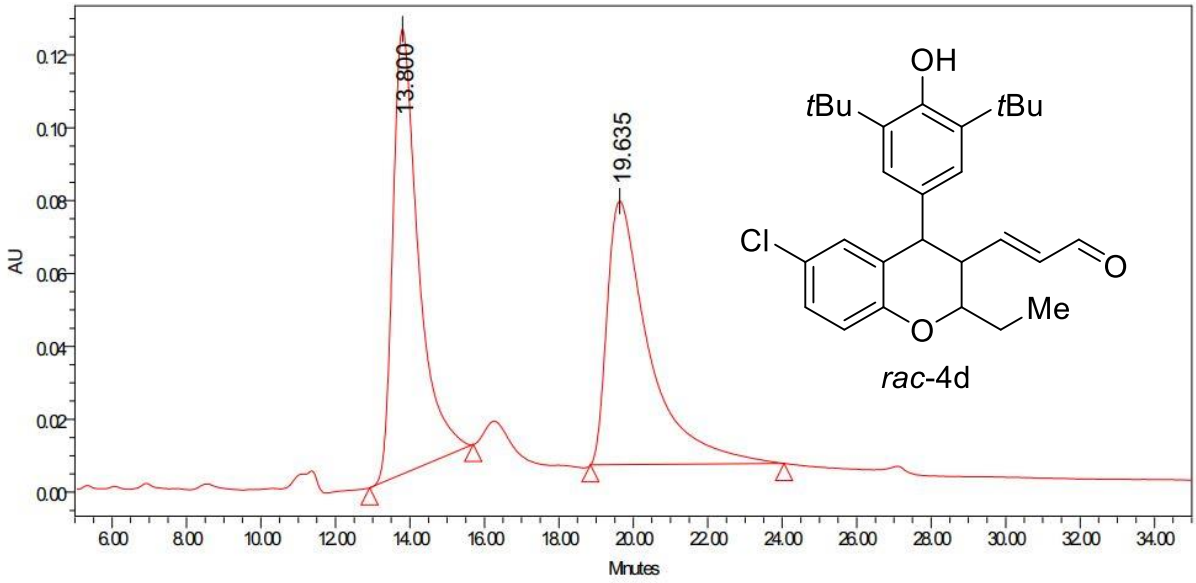
	RT	Area	%Area	Height
1	17.274	6841682	50.65	98554
2	21.317	6666945	49.35	75523



4c

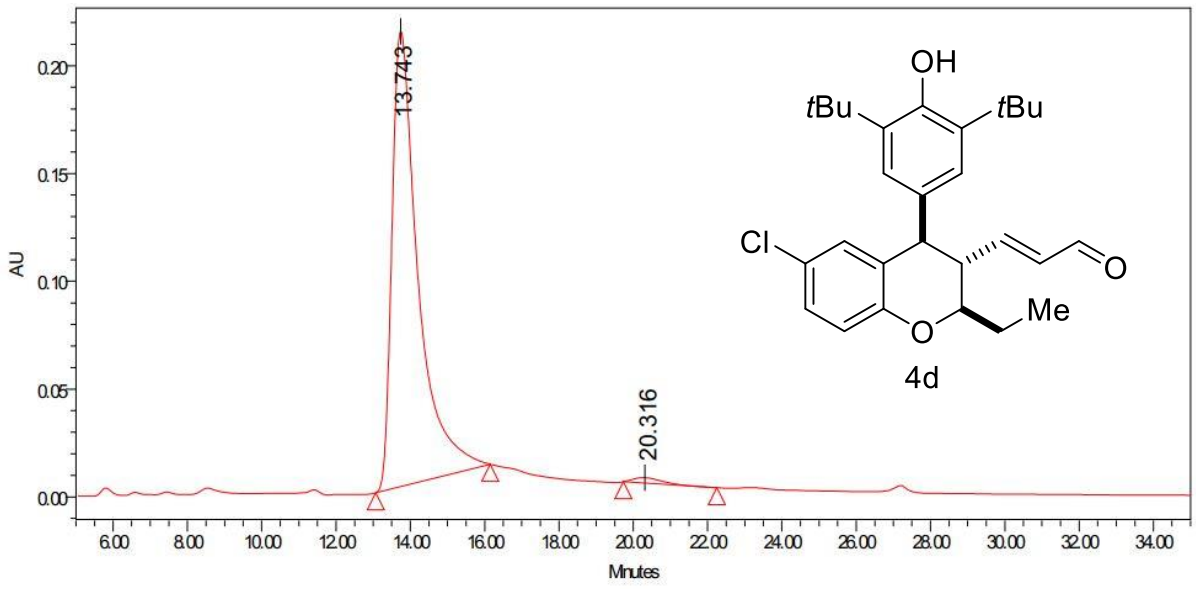
Peak Results

	RT	Area	%Area	Height
1	16.574	11361230	98.24	166951
2	21.266	203891	1.76	2504



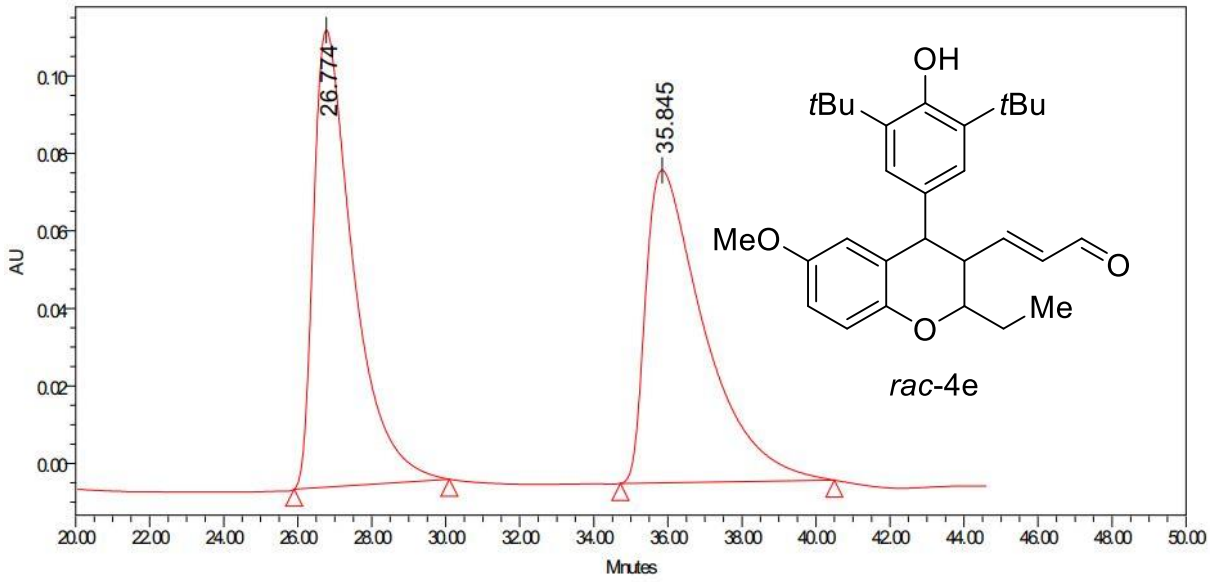
Peak Results

	RT	Area	%Area	Height
1	13.800	5816663	50.59	122158
2	19.635	5681789	49.41	72372



Peak Results

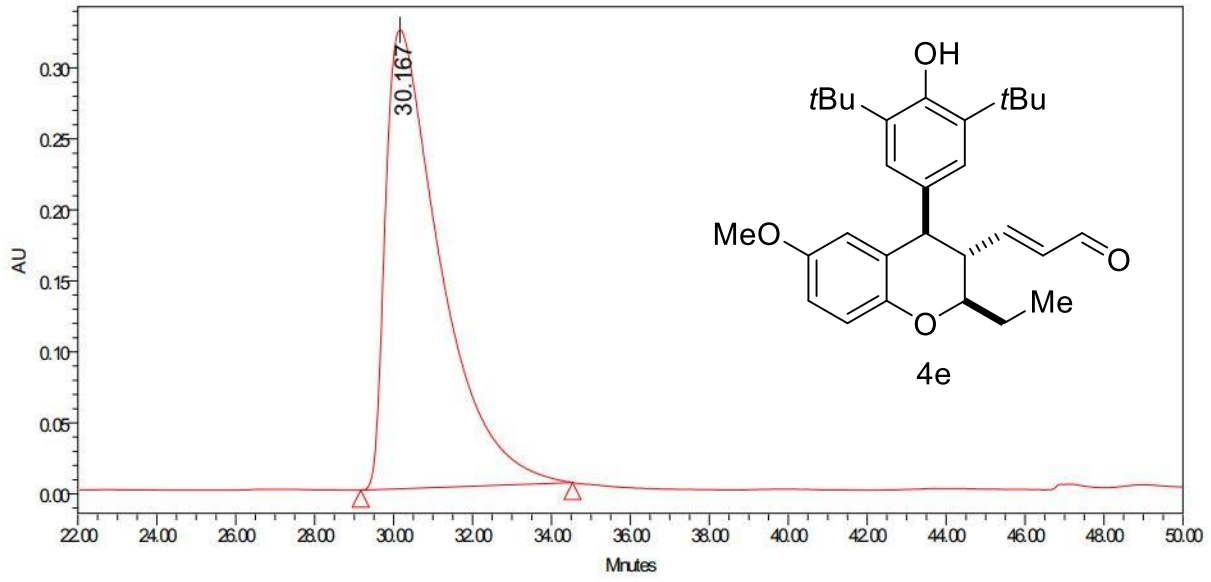
	RT	Area	%Area	Height
1	13.743	10338205	98.69	211233
2	20.316	136776	1.31	2517



rac-4e

Peak Results

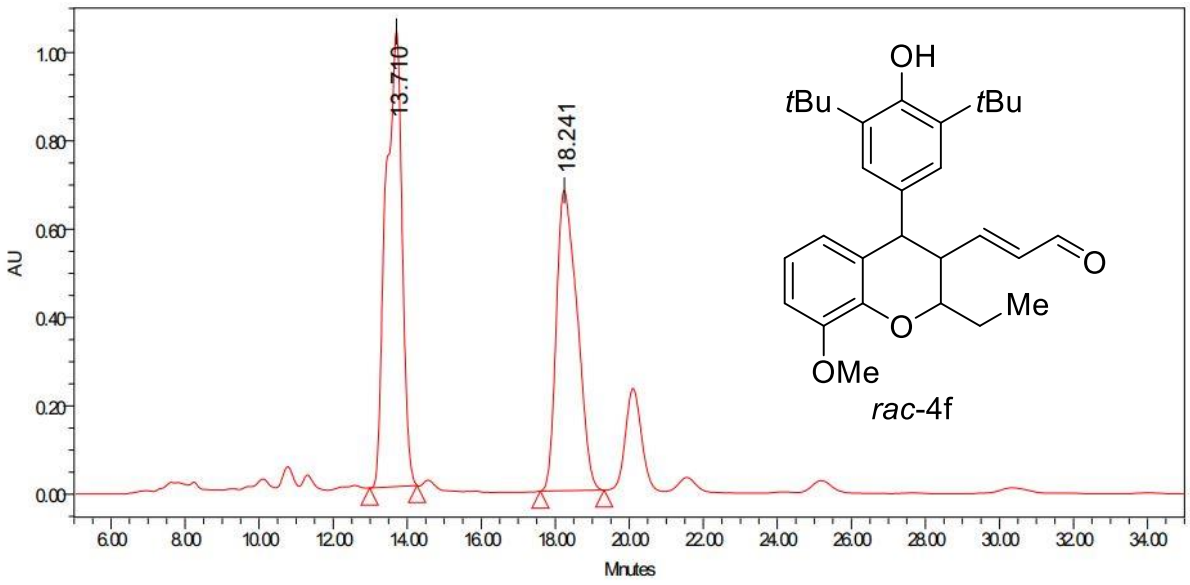
	RT	Area	%Area	Height
1	26.774	8775427	49.70	117932
2	35.845	8881871	50.30	80628



4e

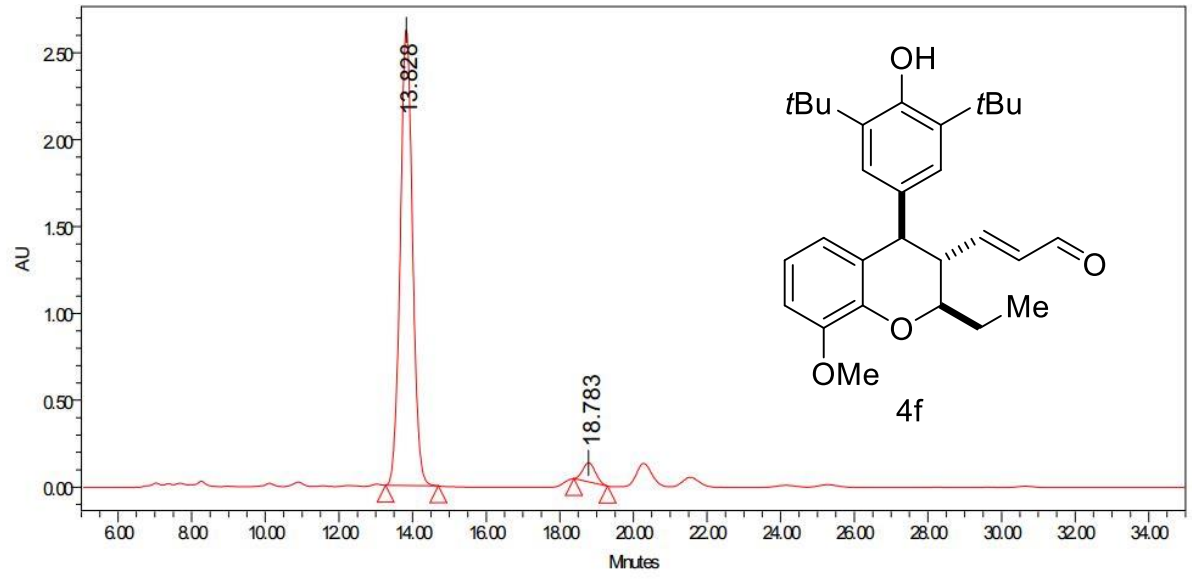
Peak Results

	RT	Area	%Area	Height
1	30.167	31254293	100.00	323256



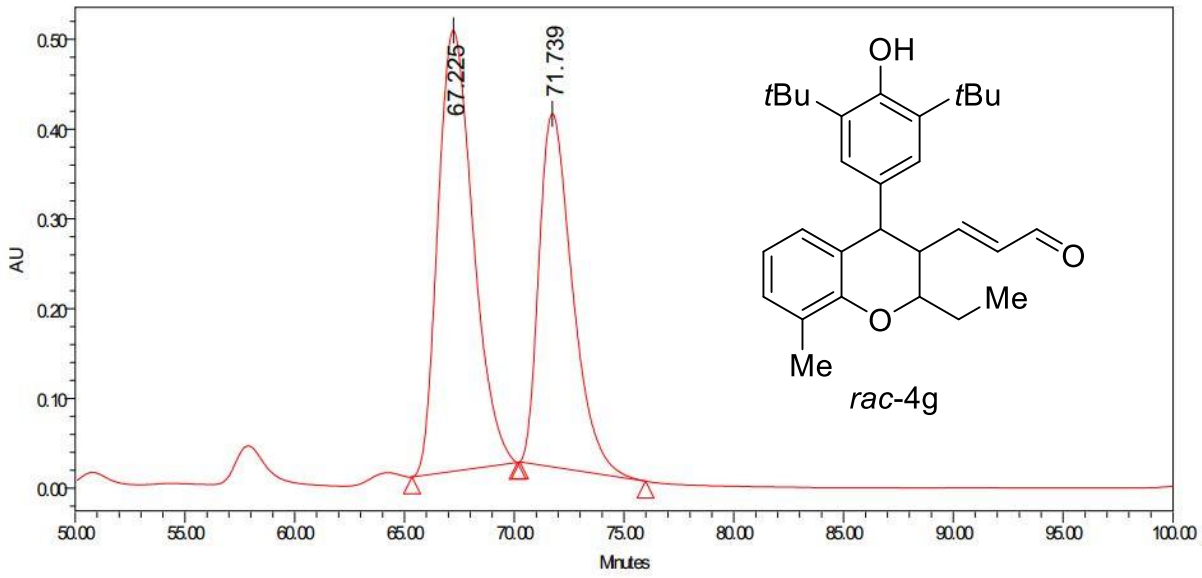
Peak Results

	RT	Area	%Area	Height
1	13.710	31338942	54.11	1032136
2	18.241	26582538	45.89	680307



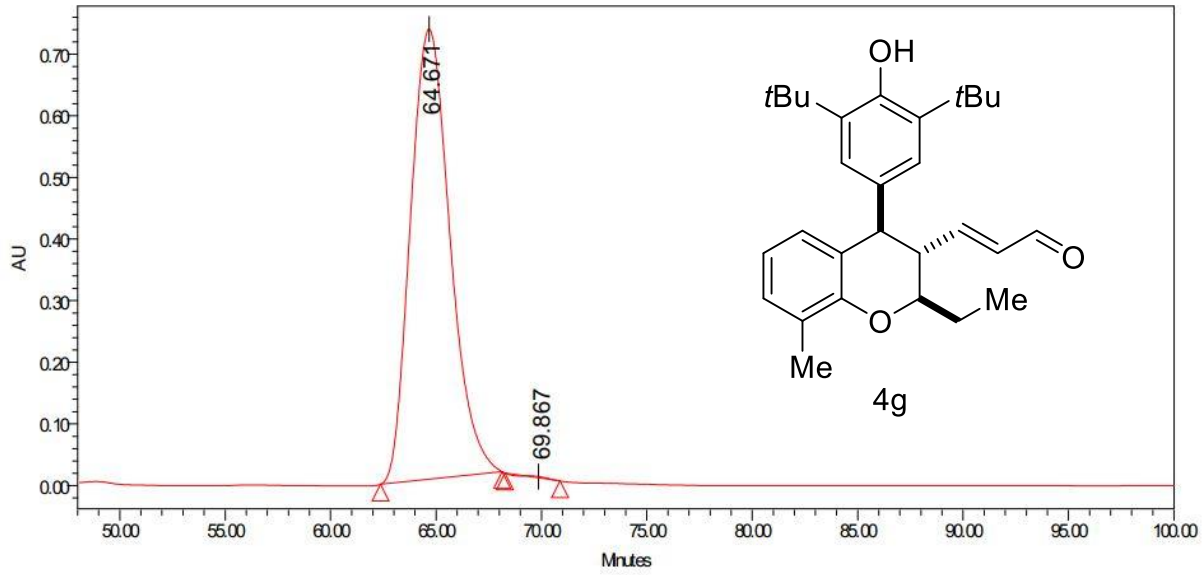
Peak Results

	RT	Area	%Area	Height
1	13.828	60807232	95.82	2625809
2	18.783	2651487	4.18	109872



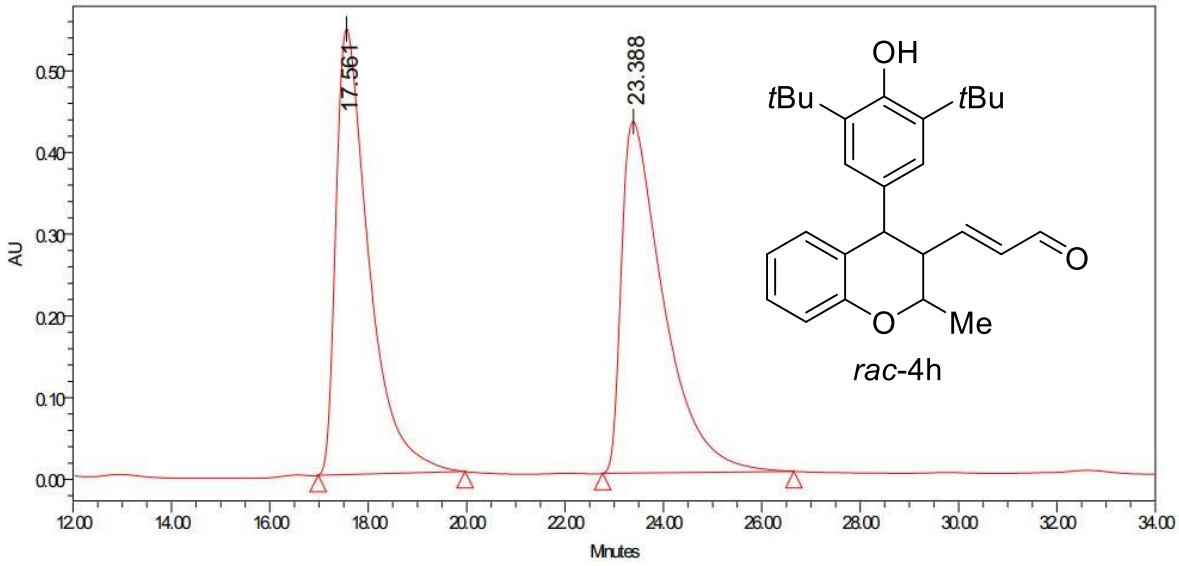
Peak Results

	RT	Area	%Area	Height
1	67.225	54627881	56.74	49111
2	71.739	41642560	43.26	393414



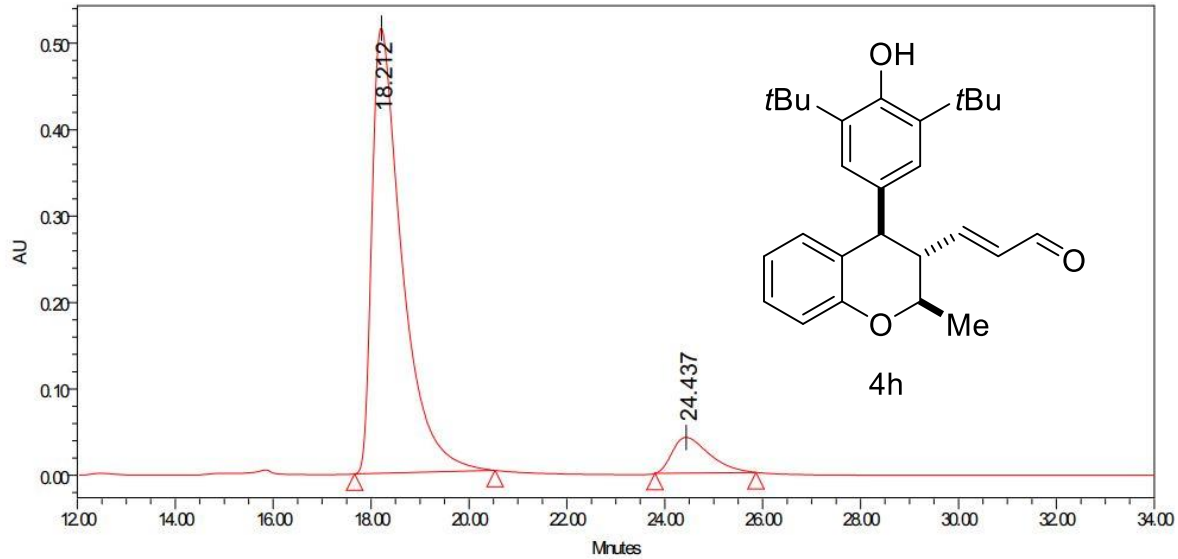
Peak Results

	RT	Area	%Area	Height
1	64.671	95373401	99.79	730588
2	69.867	198113	0.21	2138



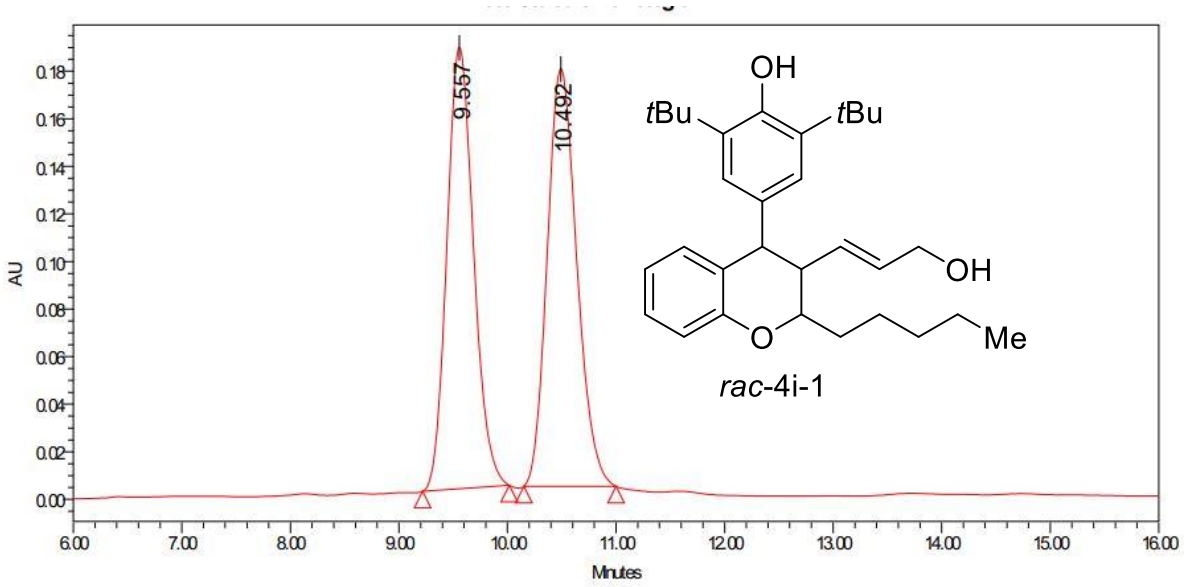
Peak Results

	RT	Area	%Area	Height
1	17.561	25436583	49.88	545363
2	23.388	25557150	50.12	429987



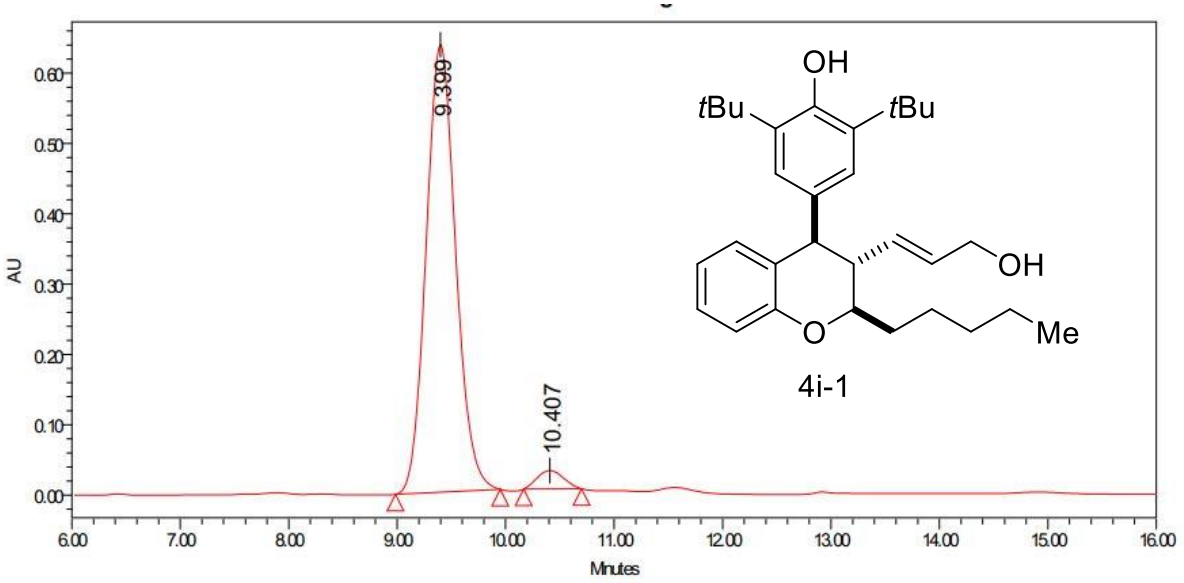
Peak Results

	RT	Area	%Area	Height
1	18.212	21997846	91.00	515188
2	24.437	2175667	9.00	41339



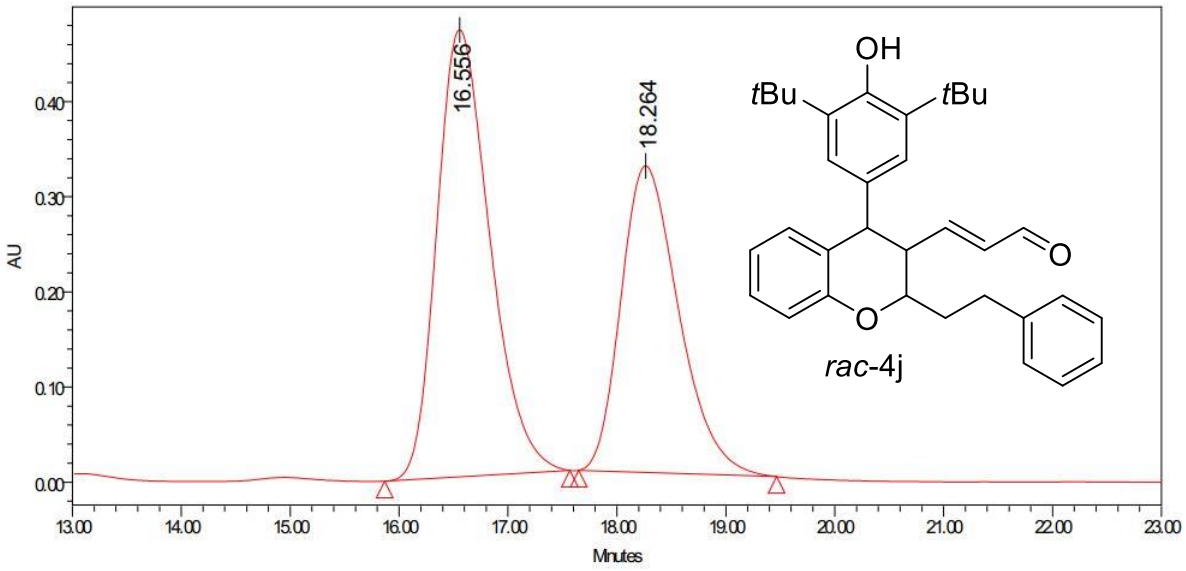
Peak Results

	RT	%Area	Area	Height
1	9.557	48.85	3175090	185903
2	10.492	51.15	3325226	175817



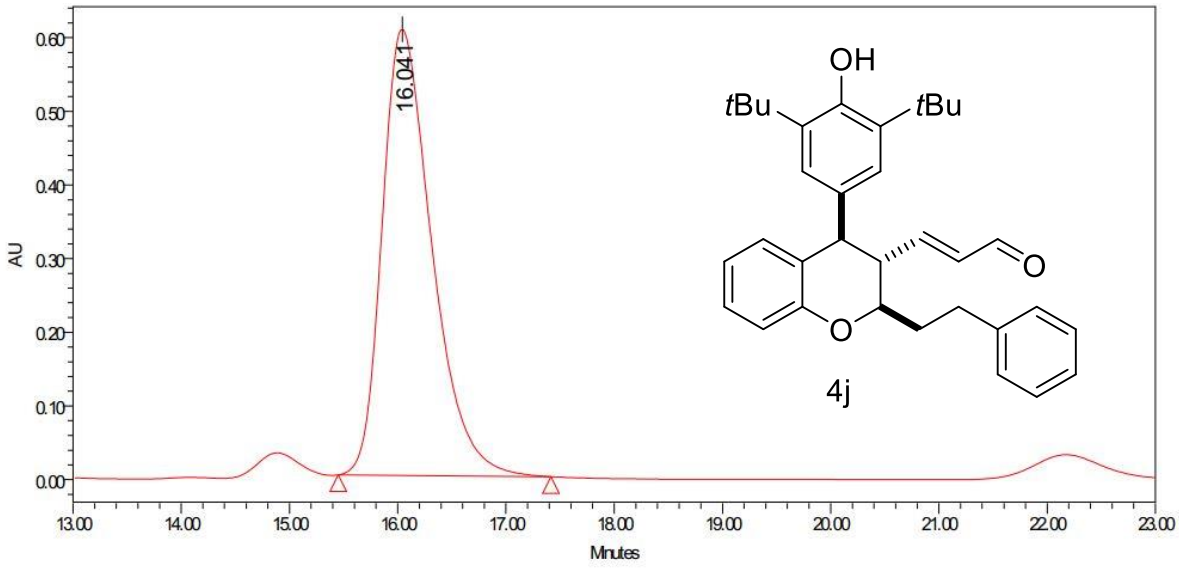
Peak Results

	RT	Area	%Area	Height
1	9.399	12036569	96.48	636516
2	10.407	438611	3.52	26048



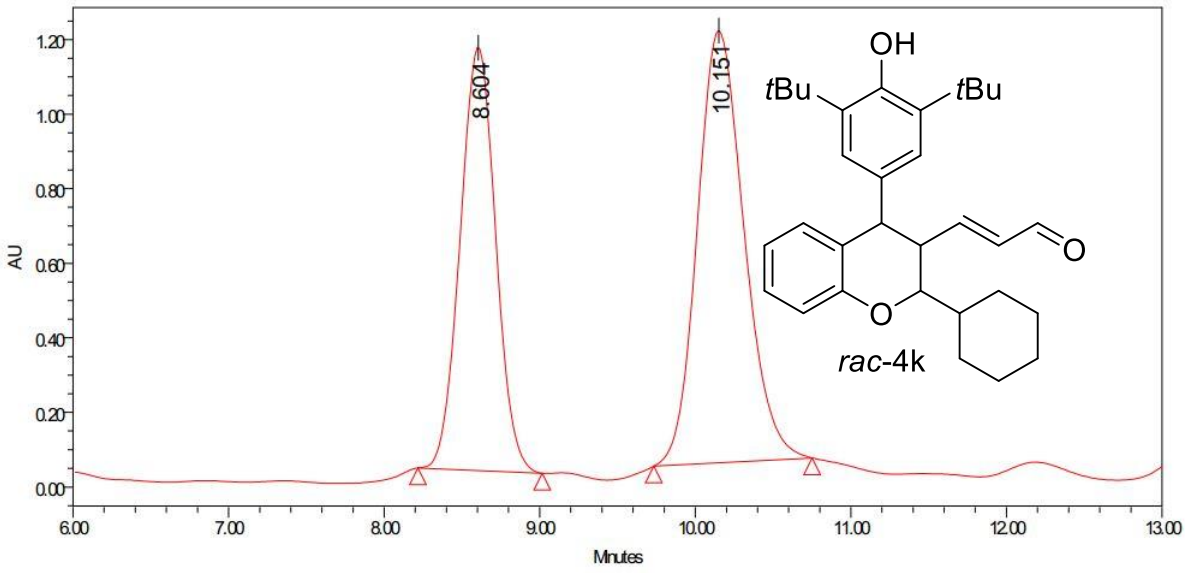
Peak Results

	RT	Area	%Area	Height
1	16.556	15877102	57.16	470235
2	18.264	1190133[illegible]	42.84	322307



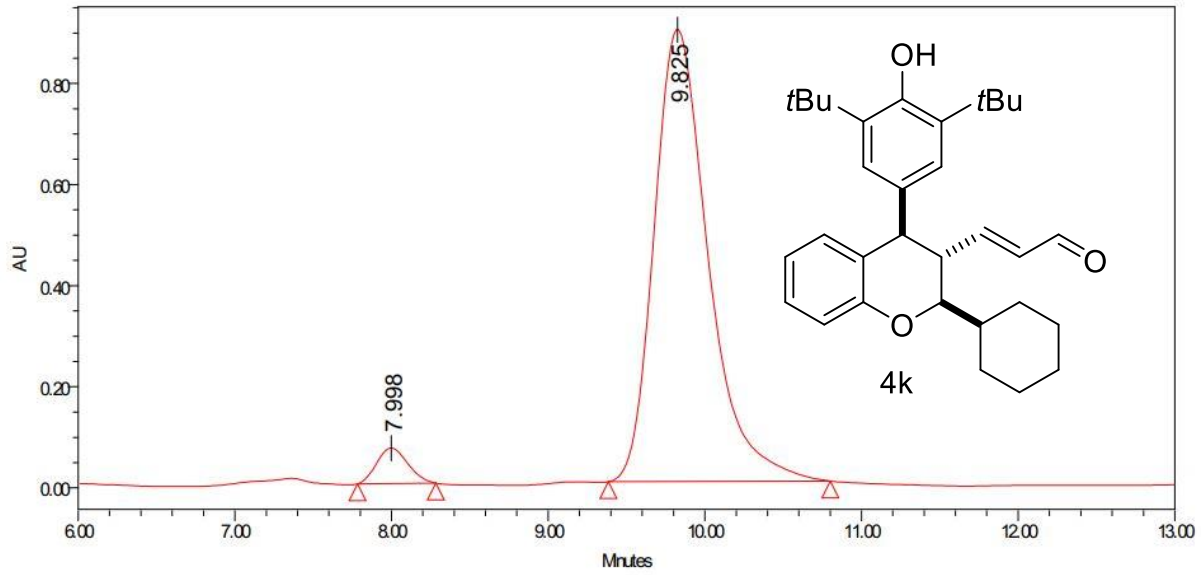
Peak Results

	RT	Area	%Area	Height
1	16.041	19343443	100.00	606172



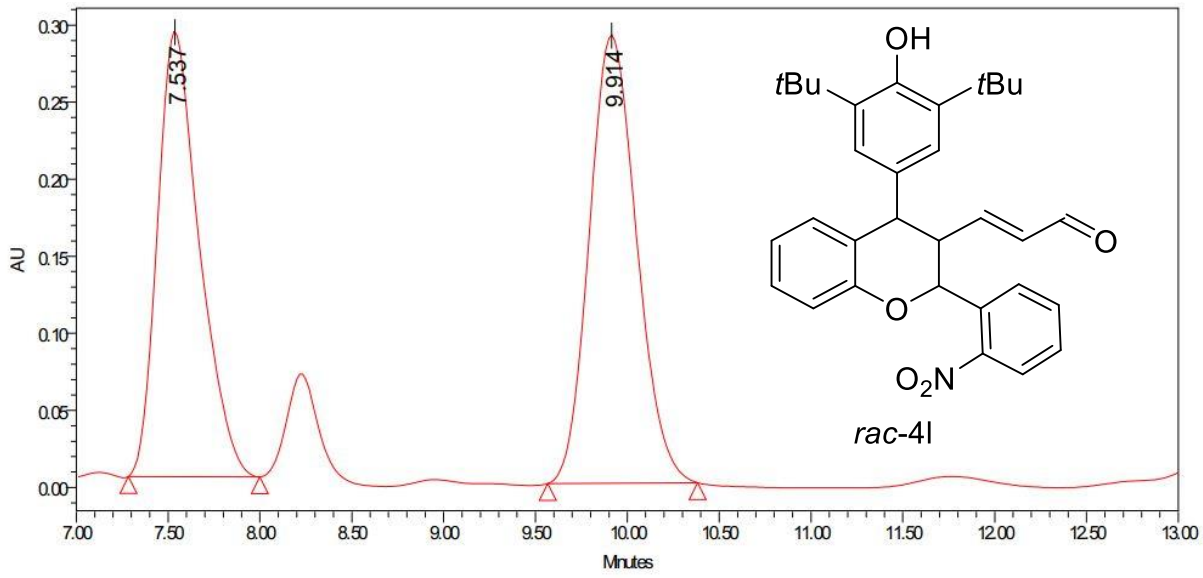
Peak Results

	RT	Area	%Area	Height
1	8.604	18047640	42.78	113618E
2	10.151	24138486	57.22	1159974



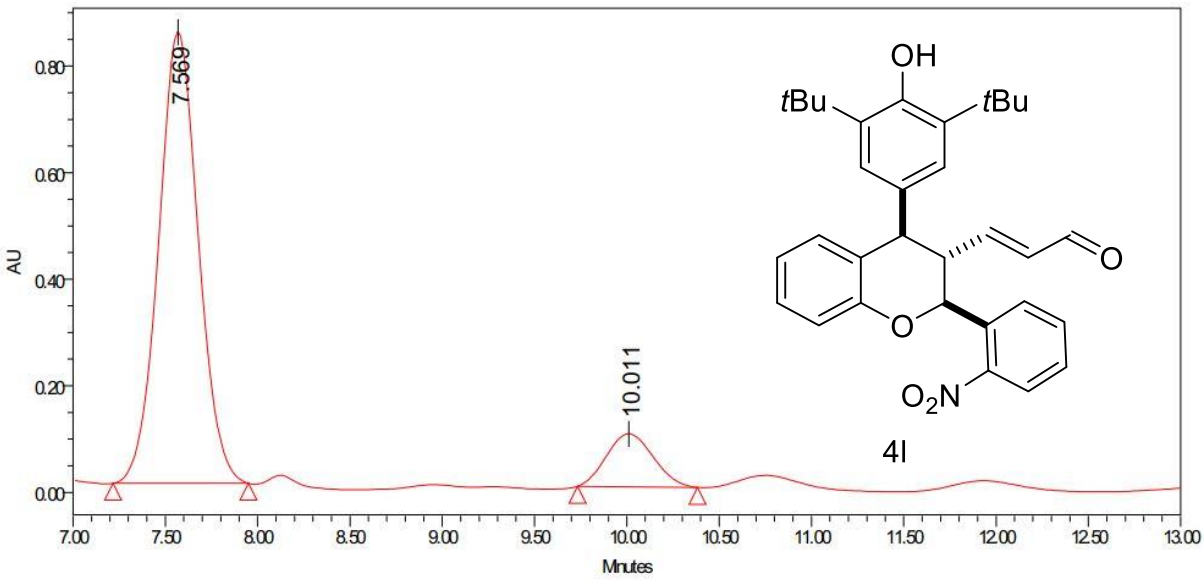
Peak Results

	RT	Area	%Area	Height
1	7.998	966673	4.32	70073
2	9.825	21428750	95.68	894827



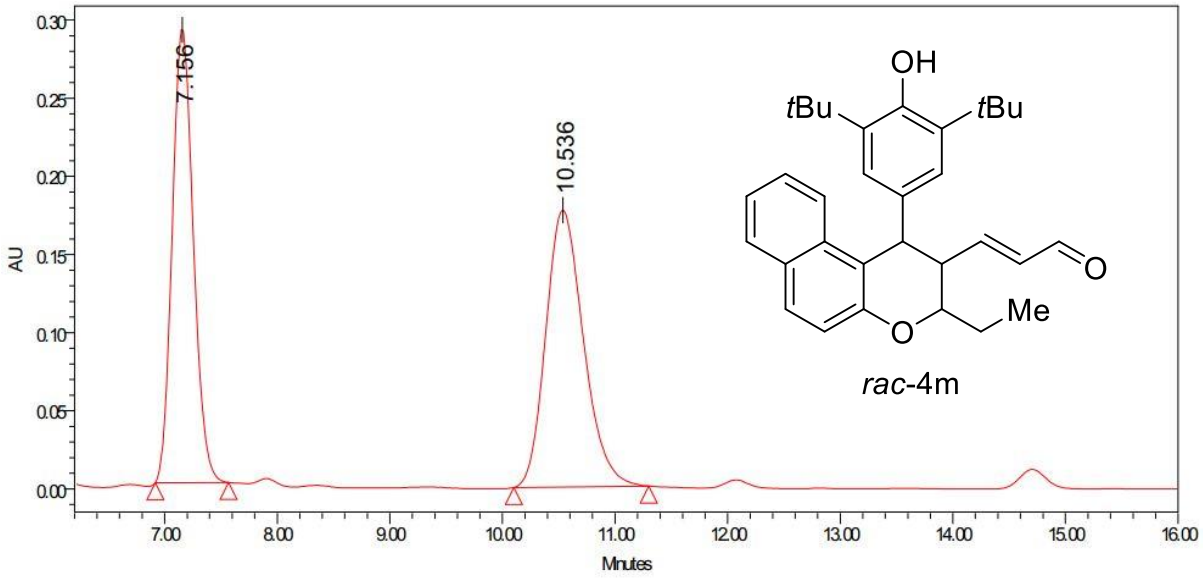
Peak Results

	RT	Area	%Area	Height
1	7.537	4581203	46.81	289251
2	9.914	5206123	53.19	290835



Peak Results

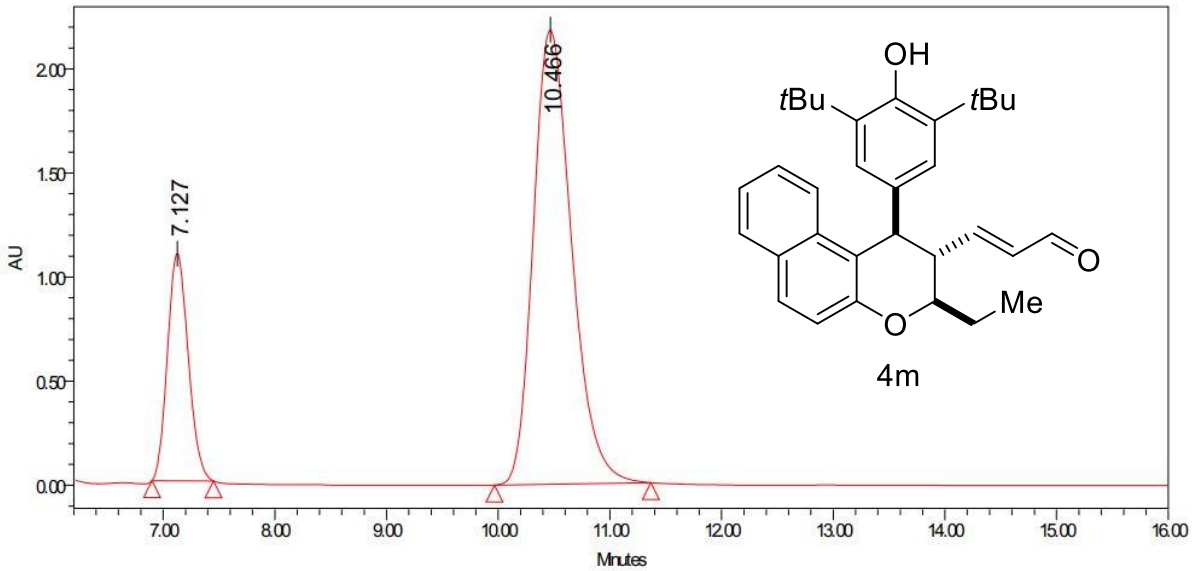
	RT	Area	%Area	Height
1	7.569	12655274	87.88	848422
2	10.011	1745815	12.12	99484



rac-4m

Peak Results

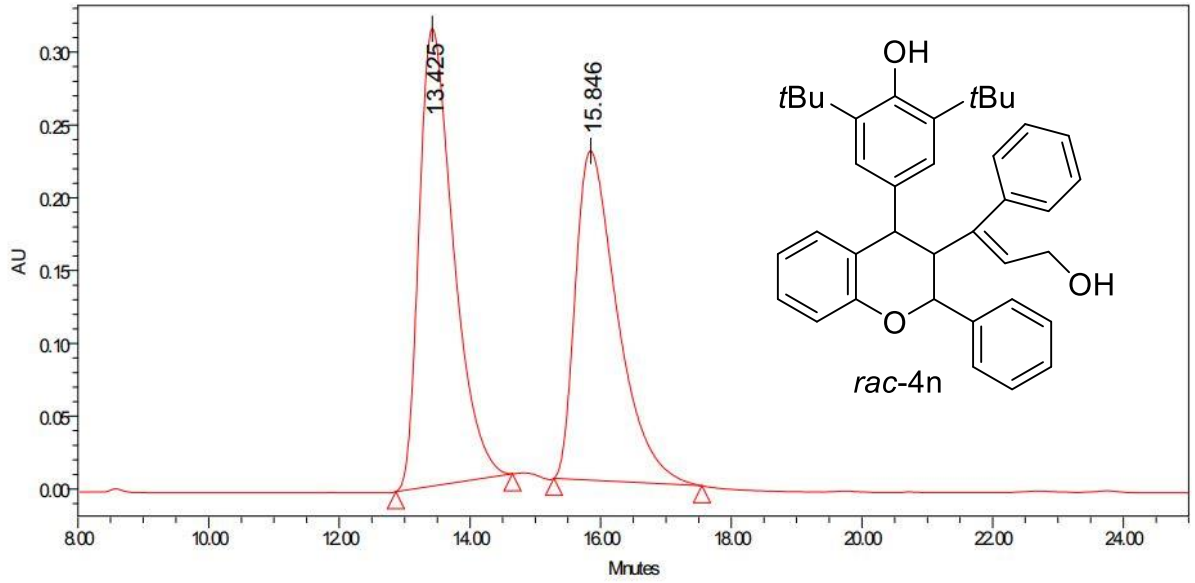
	RT	Area	%Area	Height
1	7.156	3775474	47.78	291083
2	10.536	4125680	52.22	177368



4m

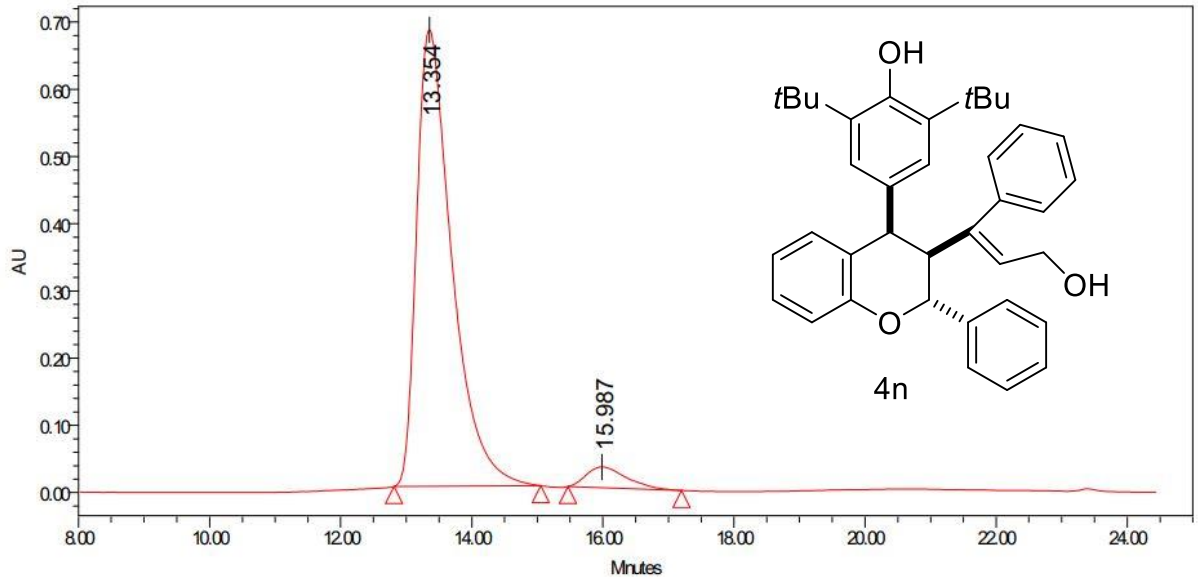
Peak Results

	RT	Area	%Area	Height
1	7.127	14121423	21.32	1094379
2	10.466	52102869	78.68	2183607



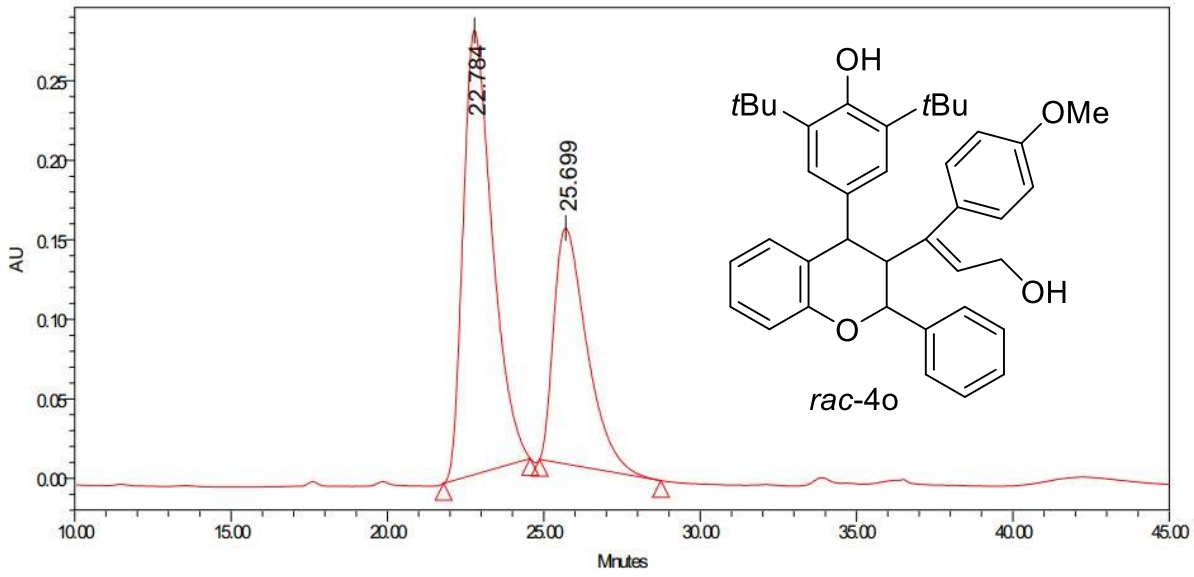
Peak Results

	RT	Area	%Area	Height
1	13.425	11472875	53.12	314156
2	15.846	10123394	46.88	226310



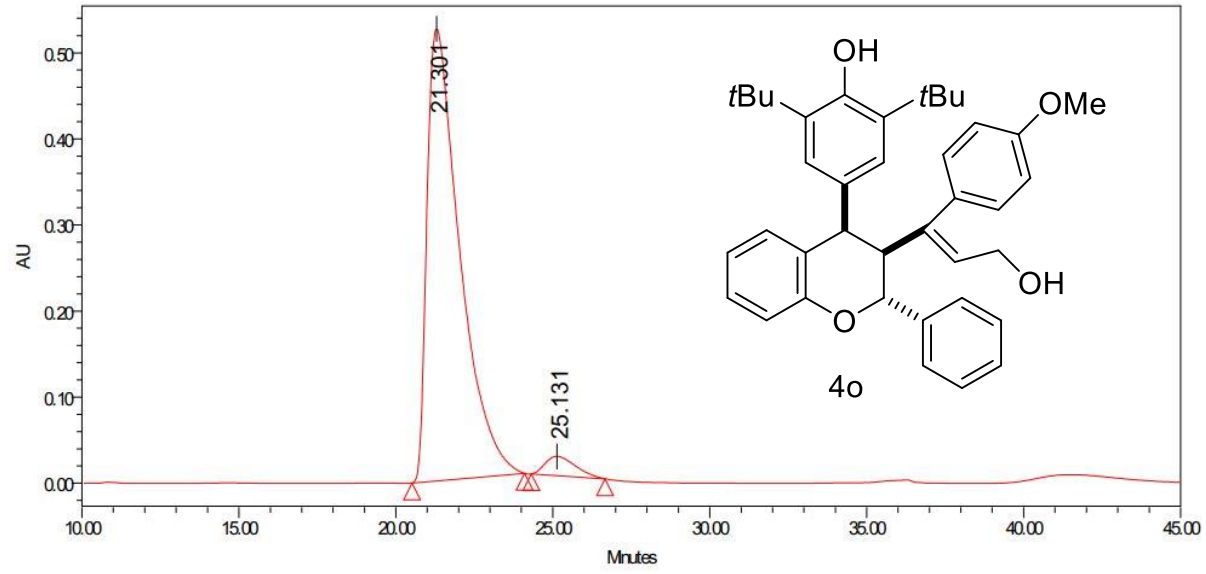
Peak Results

	RT	Area	%Area	Height
1	13.354	25357507	95.05	679443
2	15.987	1321790	4.95	30966



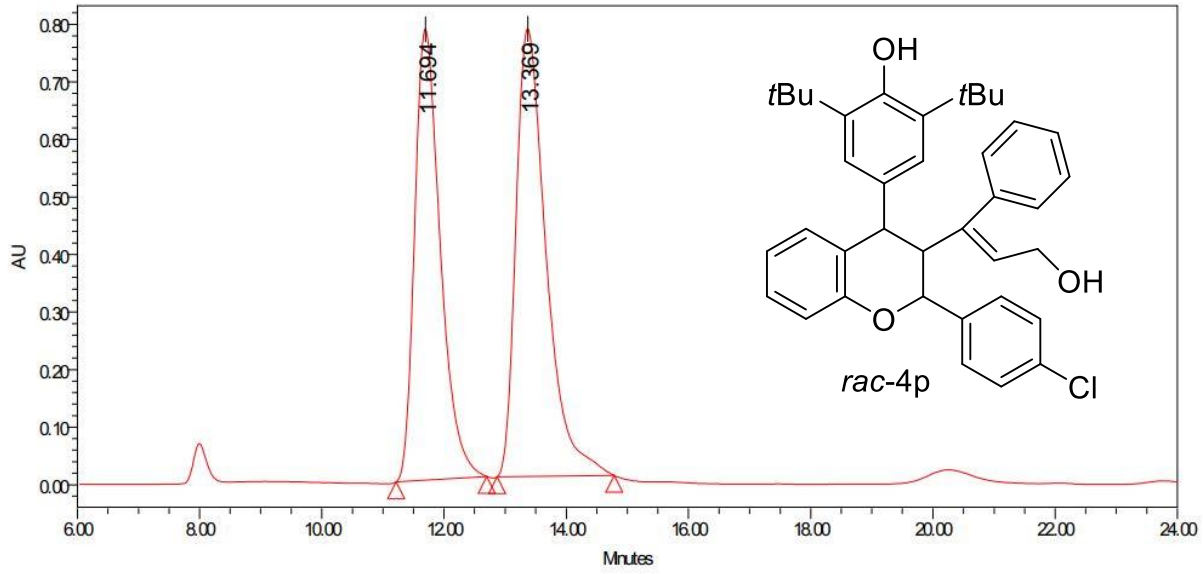
Peak Results

	RT	Area	%Area	Height
1	22.784	18071331	62.32	279198
2	25.699	10926306	37.68	148310



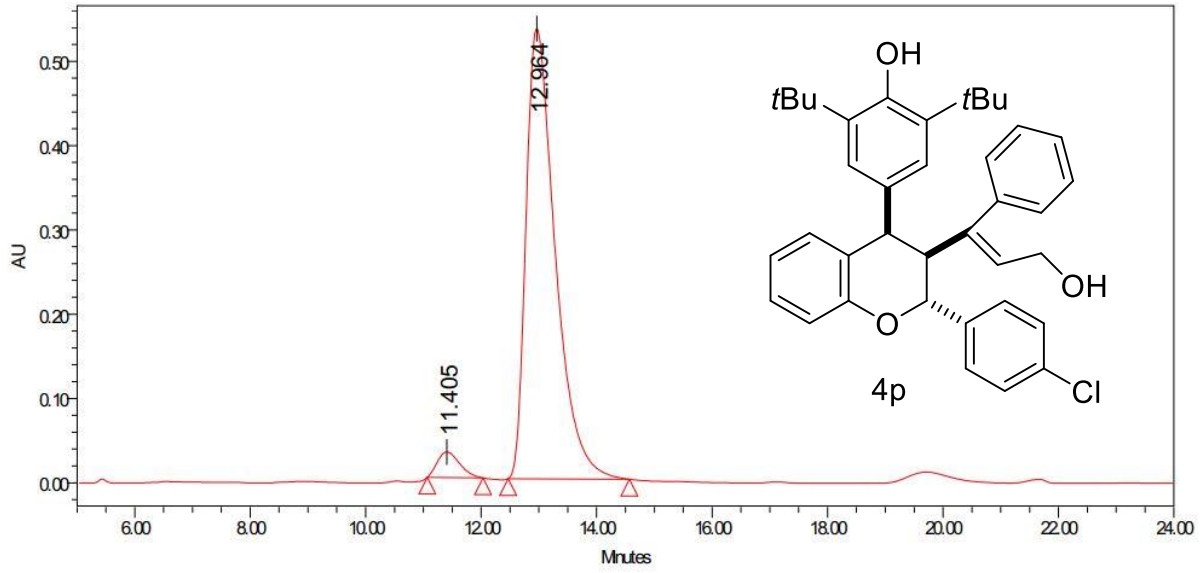
Peak Results

	RT	Area	%Area	Height
1	21.301	38056790	96.18	525207
2	25.131	1511703	3.82	22447



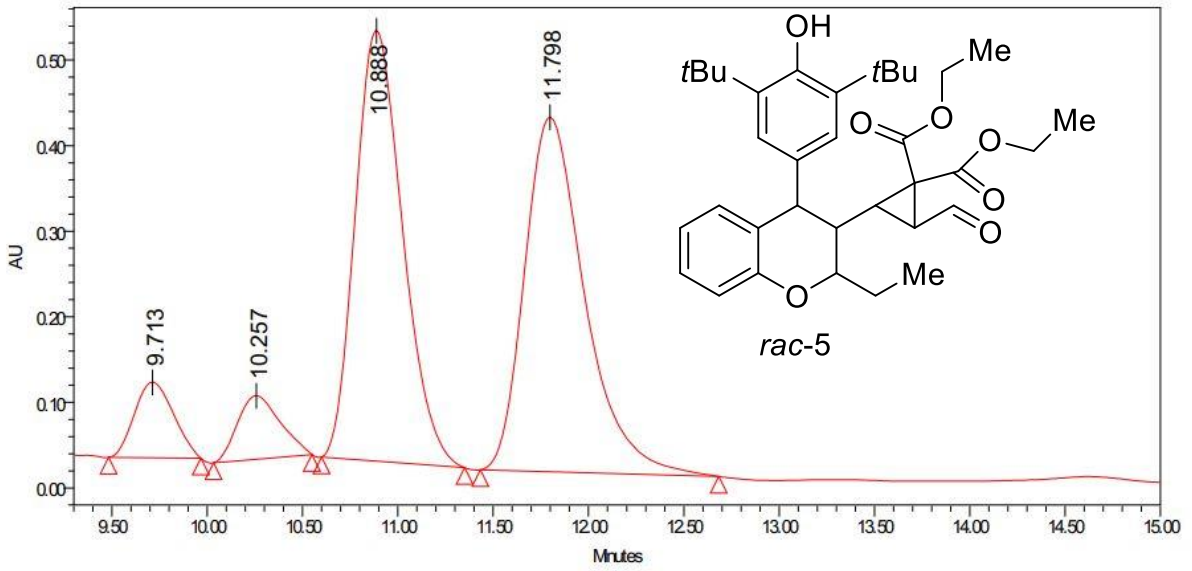
Peak Results

	RT	Area	%Area	Height
1	11.694	22842913	46.10	784212
2	13.369	26711098	53.90	778421



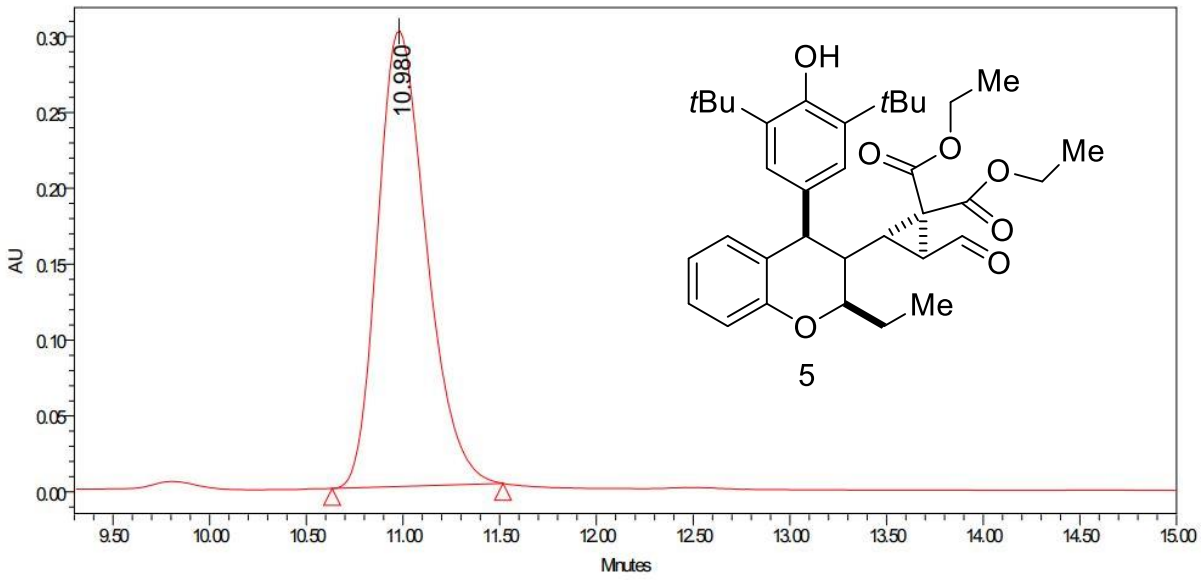
Peak Results

	RT	Area	%Area	Height
1	11.405	821942	4.19	30435
2	12.964	18807149	95.81	534160



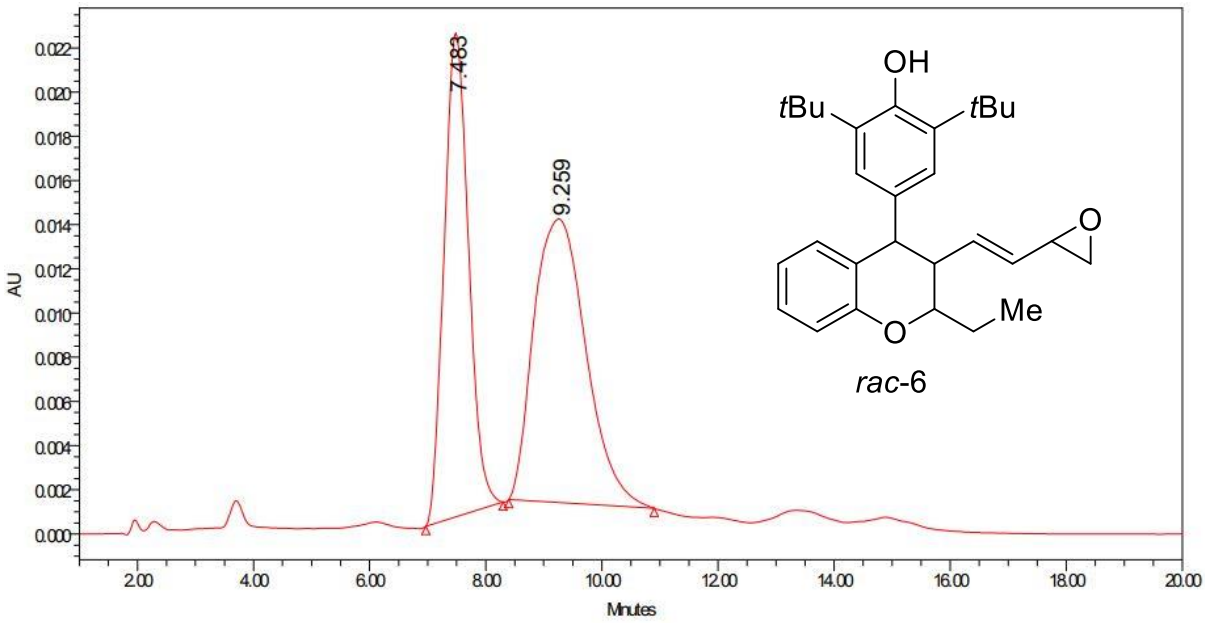
Peak Results

	RT	Area	%Area	Height
1	9.713	1255113	6.22	88455
2	10.257	1145709	5.68	74267
3	10.888	8710431	43.15	504041
4	11.798	9076166	44.96	414599

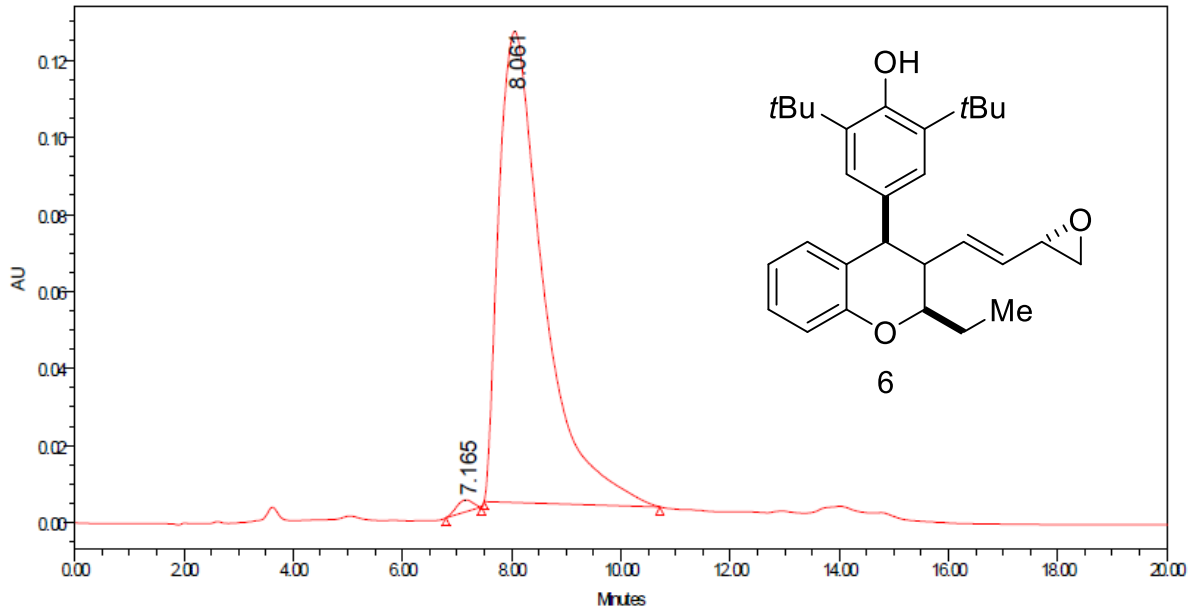


Peak Results

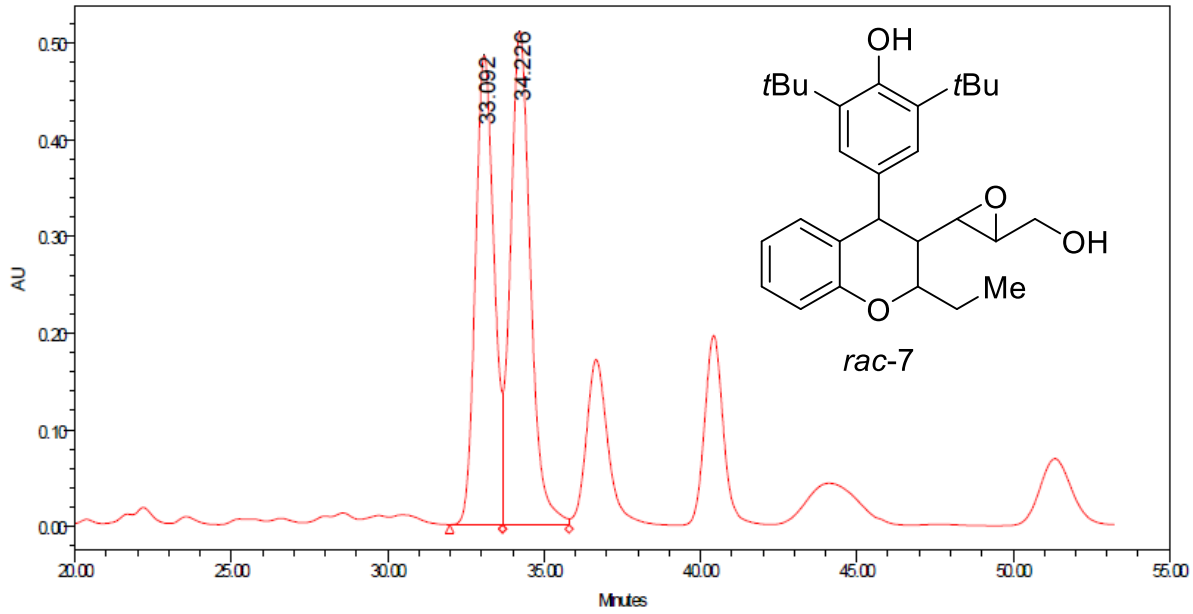
	RT	Area	%Area	Height
1	10.980	5271147	100.00	300489



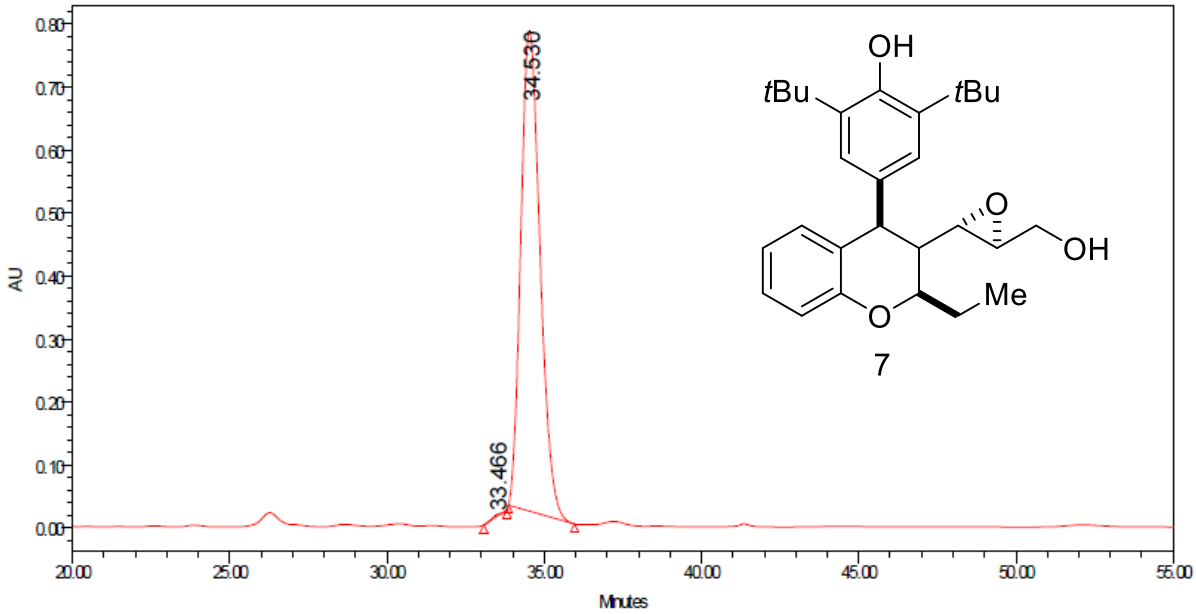
	RT	Area	%Area	Height
1	7.483	640791	44.40	21895
2	9.259	802472	55.60	12824



	RT	Area	%Area	Height
1	7.165	65017	0.92	3093
2	8.061	6973259	99.08	122343



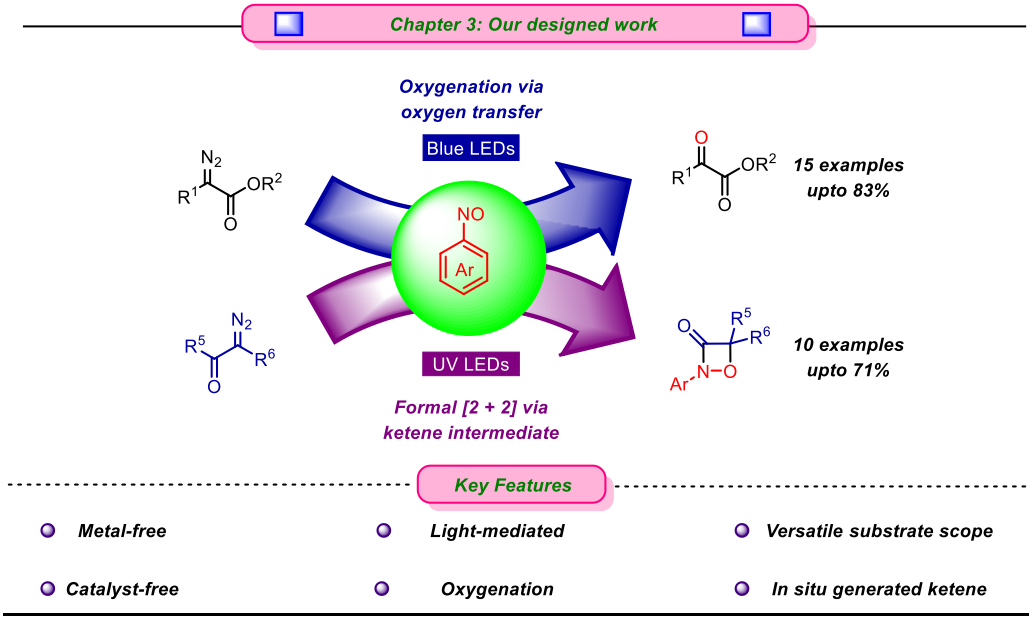
	RT	Area	%Area	Height
1	33.092	20085187	46.77	485792
2	34.226	22861993	53.23	510996



	RT	Area	%Area	Height
1	33.466	67028	0.21	3368
2	34.530	32388512	99.79	763008

Chapter 3

Photoinduced Diverse Reactivity of Diazo Compounds with Nitrosoarenes



This work was published in Organic Letters (a journal of ACS). Please see the citation as: "Roy, S.; Kumar, G.; Chatterjee, I. *Org. Lett.* **2021**, *23*, 6709–6713."

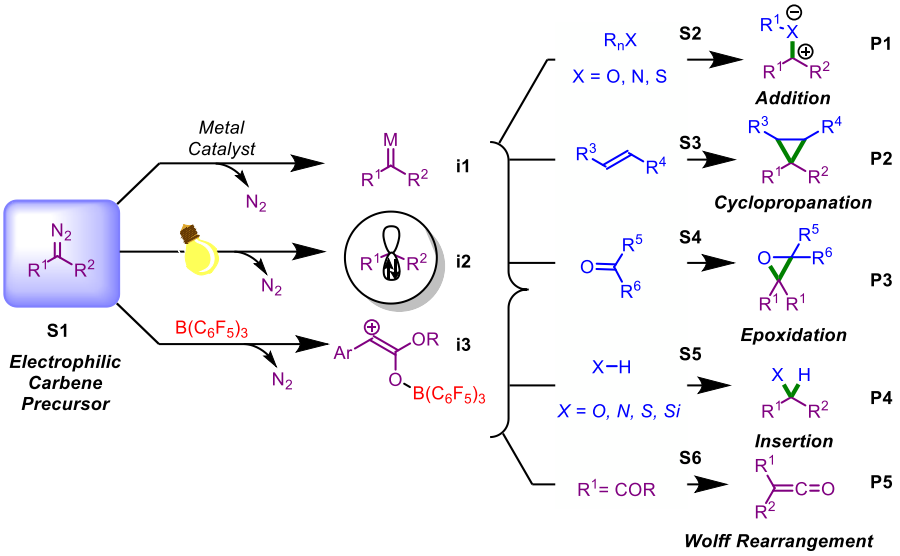
3. Abstract

A diverse reactivity of diazo compounds with nitrosoarene in an oxygen-transfer process and a formal [2 + 2] cycloaddition is reported. Nitrosoarene has been exploited as a mild oxygen source to oxidize an *in situ* generated carbene intermediate under visible-light irradiation. UV-light-mediated *in situ* generated ketenes react with nitosoarenes to deliver oxazetidine derivatives. These operationally simple processes exemplify a transition-metal-free and catalyst-free protocol to give structurally diverse α-ketoesters or oxazetidines.

3.1 Introduction

Carbenes are synthetically important intermediate to introduce various functionalities and engender molecular complexity rapidly and with high efficiency. Conventionally, diazo compounds are used as a carbene precursor as it undergoes a dinitrogen extrusion process. Diazo compound was first prepared by Curtius in 1883.[1] Since then, these were well exploited as a carbene forerunner in the presence of thermal, photochemical, or metal-catalyzed processes to deliver singlet and triplet carbene or metal carbenoids, resulting in numerous crucial organic transformations to deliver several value-added structural motifs.[2]

Over the decades, transition metal-catalyzed carbene generation gained prime attention from the synthetic community due to their high efficiency and selectivity.[3] However, recently, photochemical generation of carbene intermediates has become an alternative for transition-metal catalysis due to the use of simple operation, milder and/or greener reaction conditions. In classical organic chemistry, UV light is a common source to liberate carbenes from diazo compounds.[4] However, in recent days, visible-light has emerged as a green and sustainable source to enrich the synthetic organic photochemistry.[5] In 2018, Davis and Jurberg brought into play the diazo compounds under visible light irradiation and had demonstrated photolysis of aryldiazoacetates could be performed in the region of 400–500 nm to carry out cyclopropanation, O–H, N–H, and C–H insertions.[6] Afterward, various elegant methodologies have embellished by He, Jurberg, Koenigs, Zhou, and other groups to expand this blooming field of modern-day chemistry (Scheme 3.1.1).[7] Although various insights have been studied to date, the robustness of light-mediated carbene transfer reactions in the synthetic chemistry arena still remained underdeveloped.

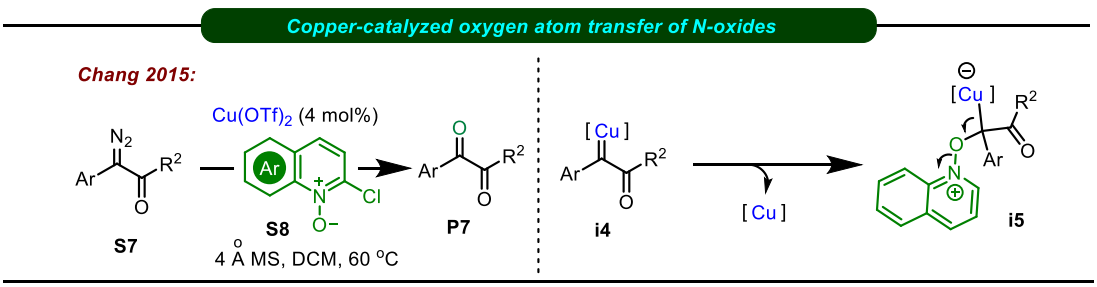


Scheme 3.1.1: Versatile Reactivity of Diazo Compounds.

For the last few years, our lab has engrossed in developing different kinds of reactivity of nitrosoarenes. Our preliminary thought process was to react a transiently formed carbene intermediate from diazo compound with nitrosoarene under light irradiation. Herein, we report a divergent reactivity of different kinds of diazo compounds with nitrosoarenes to deliver either α-ketoesters via oxygen transfer protocol or oxazetidine moieties via formal [2 + 2] cycloaddition.

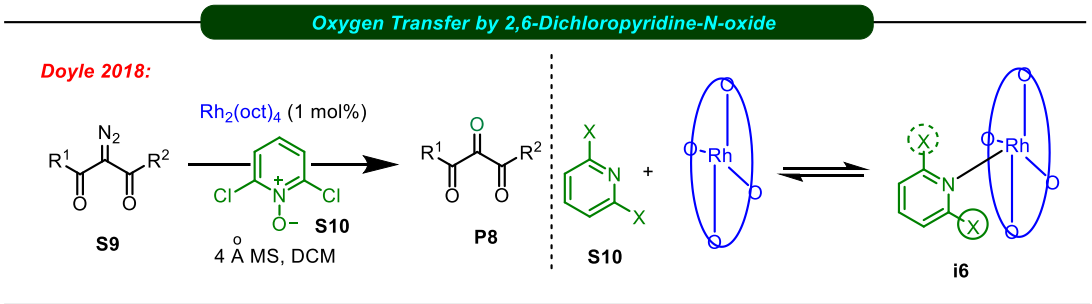
The oxygenation of organic molecules plays a significant role in organic transformations.[8] There are few reports in the literature which deal with oxidative dinitrogen extrusion event where diazo compounds act as an oxygen acceptor in the oxygen transfer process.

To fulfill this, in 2015, Chang et al. reported a copper-catalyzed oxygen atom transfer method, where diazo compounds **S7** act as oxygen atom acceptors and both heterocyclic and alkyl(aryl)amine *N*-oxide **S8** derivatives act as oxygen donors. The protocol shows broad functional group tolerance, and chemoselectivity under mild reaction conditions (Scheme 3.1.2).



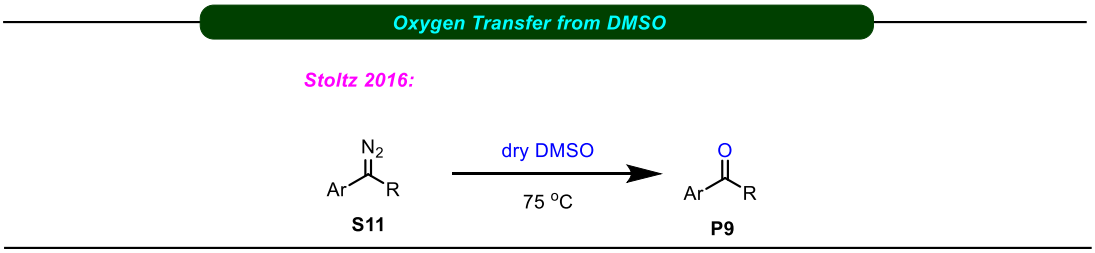
Scheme 3.1.2: Chang's Copper-Catalyzed Oxygen Atom Transfer Using Diazo Compounds as an Oxygen Acceptor

By following these works in 2018 Doyle et al. came with a modified strategy where dinitrogen extrusion from diazocarbonyl compounds **S9** took place by 2,6-dichloropyridine-*N*-oxide **S10** under dirhodium(II) catalysis to achieve ketocarbonyl compounds **P8**. Various pyridine-*N*-oxides were screened as an oxygen transfer reagent among which 2,6-dichloropyridine-*N*-oxide **S10** proved to be the most efficient one. The authors proposed that the weak coordination of the pyridine-N-oxide and the oxygen ligands present in rhodium(II) carboxylates provide a barrier to association by its pyridine product but the electron-rich chloride substituents at the ortho and para-positions can block this association, therefore facilitates the oxygen transfer process (Scheme 3.1.3).



Scheme 3.1.3: Doyle's Hydroarylation of Olefins

On the other hand, in 2016, Stoltz identified a highly chemoselective and simpler method for the oxidation of diazo compounds **S11** to form corresponding ketones **P9**. A wide range of aryl diazoacetates was compatible with the reaction, even those having other easily oxidizable functional groups. This straightforward synthetic strategy offered an alternate route to synthetically useful α-ketoesters from readily available aryl ddiazoacetates (Scheme 3.1.4).

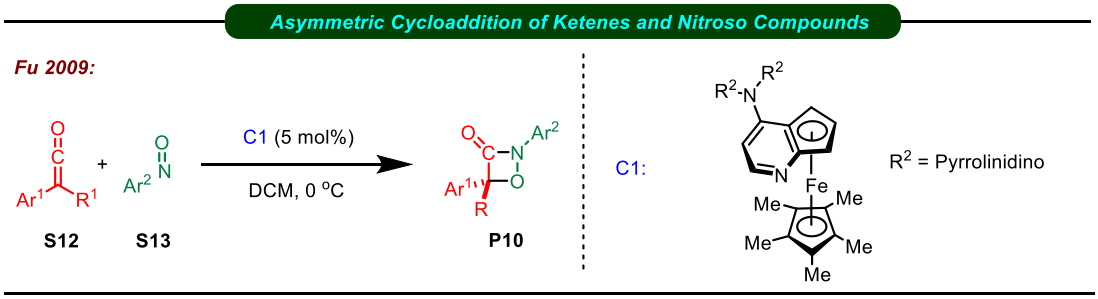


Scheme 3.1.4: Stoltz's Oxidation of Electron-Rich Diazo Compounds to Ketones

Effect of light on another classes of diazo compounds, α-diazoketones, can trigger photochemical Wolff rearrangement to generate ketene intermediate via 1,2-rearrangement.[10] This *in situ* generated ketene has been used to study various concerted or formal cycloaddition reactions to construct structurally divergent cyclic frameworks.[11] Alike, the unsaturated compounds, over the years, nitrosoarenes have vastly exploited as a reaction partner in various cycloaddition events.[12] Surprisingly, the *in situ* generation of ketenes from α-diazoketones and

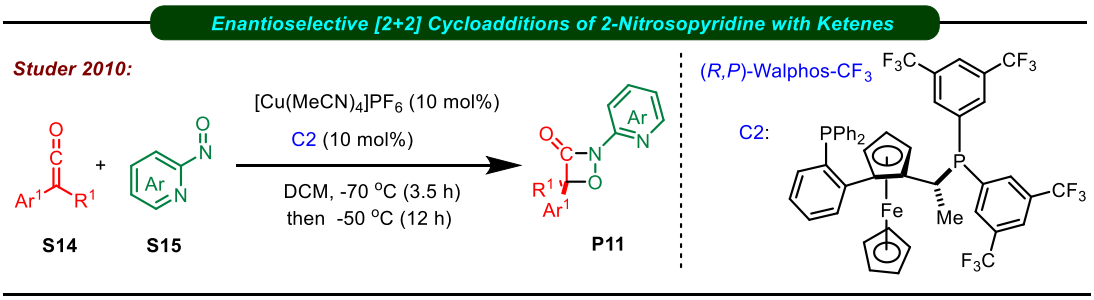
their reactivity with nitrosoarenes has not been studied before. To the best of our knowledge, there are only two reports, individually from the Fu and Studer group where transition-metal catalysis has been utilized, another from Ye group, which involves NHC catalysis to achieve oxazetidine moieties by reacting nitrosoarenes with ketenes which are described below.

In 2009, Fu et al. had provided the first example of cycloadditions of preformed ketenes **S12** with nitroso compounds **S13** to achieve 1,2-oxazetidin-3-ones **P10** under organometallic iron reagents. Diverse four-membered heterocycles were achieved with excellent regioselectivity and enantioselectivity. The synthesized potentially bioactive target molecules, 1,2-oxazetidin-3-ones **P10** were successfully transformed into other value-added compounds, such as α-hydroxycarboxylic acid derivatives (Scheme 3.1.5).



Scheme 3.1.5: Fu's Enantioselective [2+2] Cycloadditions of Ketenes and Nitrosoarene.

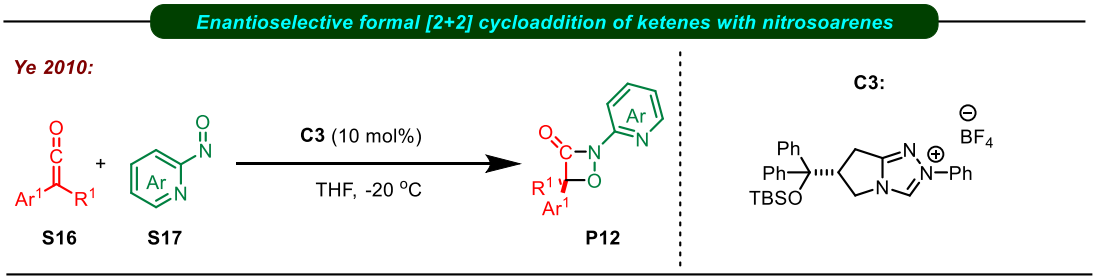
In the same line in 2010, Studer et al. represented an enantioselective [2+2] cycloadditions of 2-nitrosopyridine **S15** with various ketenes **S14** to achieve four-membered 1,2-oxazetidine-3-one **P11** rings under Cu(I)/Walphos-CF_3 catalysis in regio- and stereo- controlled manner. The products obtained were important for further synthetic manipulations. The authors proposed a DFT-supported mechanism that gave strong indications that reactions followed a concerted asynchronous [2+2] cycloaddition pathway (Scheme 3.1.6).



Scheme 3.1.6: Studer's Enantioselective [2+2] Cycloadditions of Ketenes and Nitrosoarene.

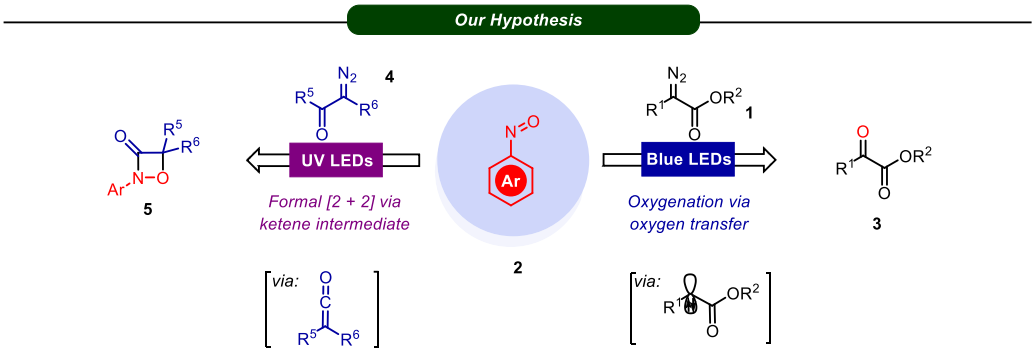
Following this, in the same year, Ye and coworkers disclosed a chiral *N*-heterocyclic carbene **C3** catalyzed to carry out a cycloaddition reaction between aryl(alkyl)ketenes **S16** and a nitroso

compound **S17**. Various ketenes with methyl, ethyl, n-propyl, and n-butyl substituent and different aryl substituted nitrosoarenes worked well to give the corresponding 1,2-oxazetidin-3-ones **P12** in high yield and enantioselectivities (Scheme 3.1.7).



Scheme 3.1.7: Ye's NHC catalyzed [2+2] Cycloadditions of Ketenes and Nitrosoarenes.

However, their strategies mainly deal with preformed ketenes and having limitations in the substrate scope. Thus, we hypotheses to react nitrosoarenes with an *in situ* generated ketene from diazo compounds under metal-free, catalyst-free, and mild reaction conditions, where light can be used as a crucial promoter (Scheme 3.1.8).



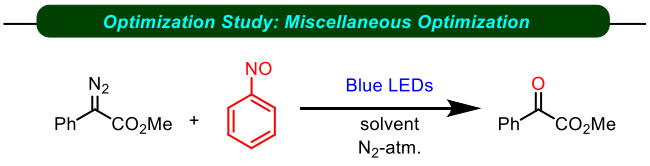
Scheme 3.1.8: Chapter 3: Our Proposed Working Hypothesis

3.2. Results and Discussion

3.2.1 Optimization of the Reaction Condition for α-ketoesters

We began our investigation by taking a donor/acceptor substituted diazo compound, α-arydiazoacetate **1a**, and nitrosobenzene **2a** as the model substrates in dichloromethane (DCM) solvent at 45 °C under blue light-emitting diode (LED) irradiation (Table 1, entry 1). Initially, we obtained the oxygen-transfer product α-ketoester **3a** in 31% yield along with the corresponding nitrone as a byproduct. We were pleased to find that this α-ketoester **3a** can be obtained in good yield by lowering the reaction temperature, increasing the equivalency of **1a**, and also increasing the reaction time (Table 3.2.1.1).

3.2.1.1. Chapter 3: Table 1. Optimization Study: Miscellaneous Optimization



1a **2a** **3a**

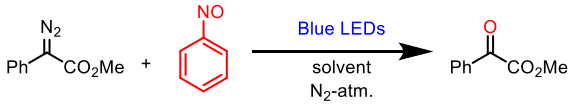
Entry	1a	2a	Solvent (M)	Time (h)	Temp. (°C)	Yield (%)[b]
1	1	1	DCM (0.1)	3	45	31
2	1	1	DCM (0.1)	5	45	33
3	1	1	DCM (0.1)	10	45	42
4	1	1	DCM (0.1)	10	0	49
5	1	1	DCM (0.1)	10	- 20	37
6	1	1	DCM (0.1)	10	rt	47
7	1	1.5	DCM (0.1)	10	rt	34
8	1.5	1	DCM (0.1)	10	rt	68
9	2	1	DCM (0.1)	10	rt	74
10	**2**	**1**	**DCM (0.2)**	**10**	**rt**	**81 (76)**
11	1	0	DCM (0.1)	10	rt	8
12[c]	1	0	DCM (0.2)	10	rt	10
13[c]	2	1	DCM (0.2)	10	rt	72
14[d]	2	1	DCM (0.2)	10	rt	89

[a] unless untill mentioned all reactions were carried out in 0.1 mmol scale in dry DCM. [b] yield was measured by ^{1}H-NMR analysis of the crude reaction mixture using CH_2Br_2 as an internal standard, isolated yield in parentheses. [c] reaction was carried out under O_2 atmosphere. [d] reaction was performed under aerobic conditions in non dried DCM.

Variation in the solvent concentration and screening of several other solvents (Table 3.2.1.2) suggested that DCM has superiority among other solvents to afford **3a** in 76% isolated yield.

3.2.1.2. Chapter 3: Table 2. Optimization Study: Scerrening of Solvents

Optimization Study: Screening of Solvents



1a **2a** **3a**

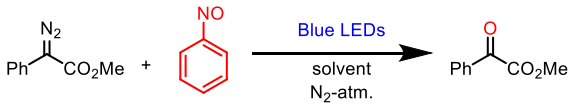
Entry	Solvent (M)	Time (h)	Temp. (°C)	Yield (%)[b]
1	**DCM (0.2)**	**10**	**rt**	**81 (76)**
2	$CHCl_3$ (0.2)	10	rt	46
3	Et_2O (0.2)	10	rt	75
4	CH_3CN (0.2)	10	rt	57
5	DCE (0.2)	10	rt	77
6	THF (0.2)	10	rt	64
7	benzene (0.2)	10	rt	73
8	toluene (0.2)	10	rt	75
9	DMSO (0.2)	10	rt	32
10	EtOH (0.2)	10	rt	17
11[c]	DMSO (0.2)	10	rt	20

[a] unless untill mentioned all reactions were carried out in 0.1 mmol scale by taking **1a** (2.0 equiv) & **2a** (1.0 equiv) in respective dry solvents. [b] yield was measured by ^{1}H-NMR analysis of the crude reaction mixture using CH_2Br_2 as an internal standard, isolated yield in parentheses. [c] Reaction was carried out in absence of **2a**.

The screening of different light sources reveals that blue LEDs irradiation was more potent over others (Table 3.2.1.3).

3.2.1.3. Chapter 3: Table 3. Optimization Study: Scerrening of Diffrent Light Sources

Optimization Study: Screening of Different Light Source



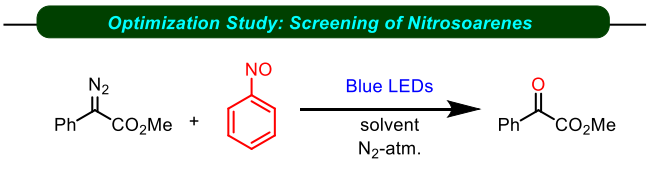
1a **2a** **3a**

Entry	Light Source	Time (h)	Temp. (°C)	Yield (%)[b]
1	**Blue LEDs (450 nm)**	**10**	**rt**	**81(76)**
2	Blue LEDs (425 nm)	10	rt	56
3	White LEDs	10	rt	52
4	UV LEDs	10	rt	37
5	Blue LEDs (strip)	10	rt	31
6	Green LEDs (strip)	10	rt	15
7	in dark	10	rt	0

[a] unless untill mentioned all reactions were carried out in 0.1 mmol scale by taking **1a** (2.0 equiv) & **2a** (1.0 equiv) in dry DCM. [b] yield was measured by ^{1}H-NMR analysis of the crude reaction mixture using CH_2Br_2 as an internal standard, isolated yield in parentheses.

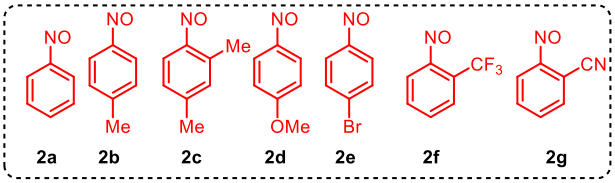
Next, different nitrosoarenes were screened as an oxygen source, which did not significantly improve the reaction yield (Table 3.2.1.4).

3.2.1.4. Chapter 3: Table 4. Optimization Study: Scerrening of Nitrosoarenes



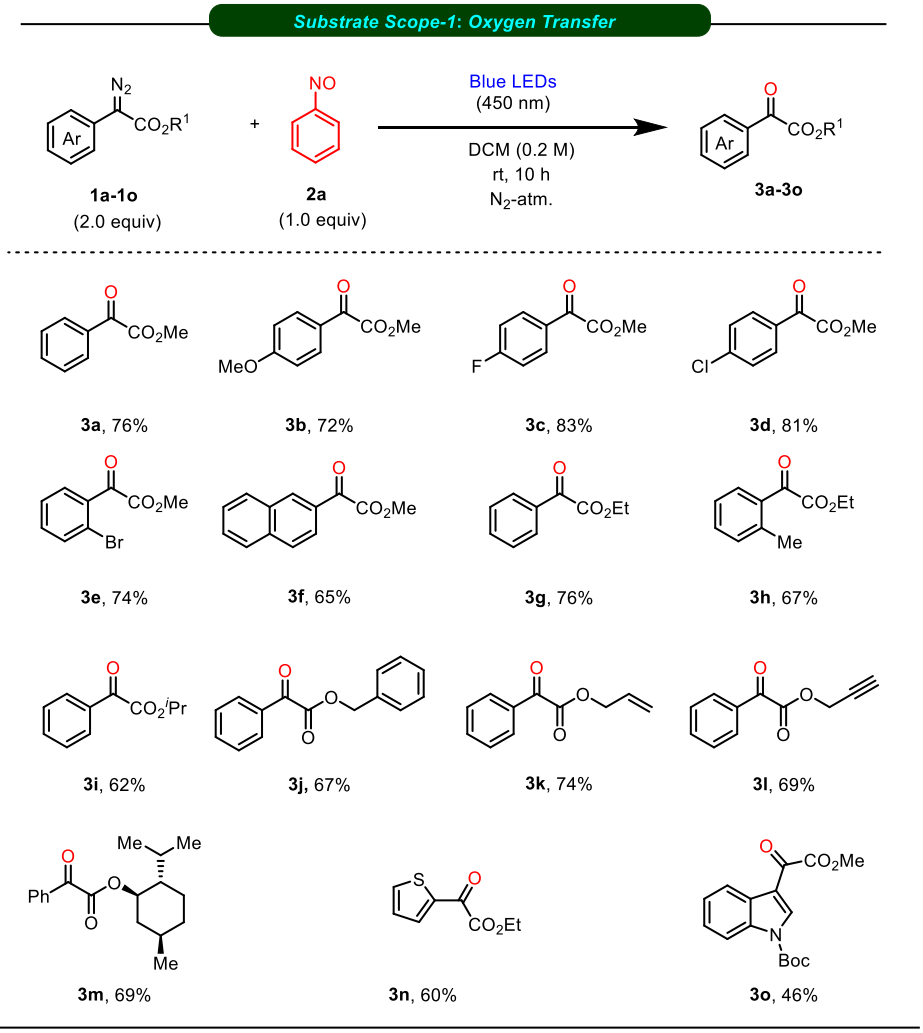
Entry	Nitrosoarene (2)	Time (h)	Temp. (°C)	Yield (%)[b]
1	**2a**	**10**	**rt**	**81(76)**
2	2b	10	rt	51
3	2c	10	rt	49
4	2d	10	rt	42
5	2e	10	rt	55
6	2f	10	rt	57

[a] unless untill mentioned all reactions were carried out in 0.1 mmol scale by taking **1a** (2.0 equiv) & **2** (1.0 equiv) in dry DCM. [b] yield was measured by ^{1}H-NMR analysis of the crude reaction mixture using CH_2Br_2 as an internal standard, isolated yield in parentheses.



3.2.2. Substrate Scope Evaluation for α-ketoesters

After validating Table 4, entry 1, as the optimal reaction condition, we assessed the robustness of the reaction first by varying different substituents on the aryl ring of α-aryldiazoacetate **1** (Scheme 9). Methoxy and halo-substituted ones in *para* position of the aromatic ring delivered the desired α-ketoesters **3** with moderate to good yield (Scheme 3.2.2.1, entries **3b**-**3d**). Sterically demanding substituents such as *o*-Br and *o*-Me were also able to furnish the corresponding product (Scheme 3.2.2.1, entries **3e** and **3h**). Moreover, methyl 2-naphthyldiazoacetate delivered product **3f** in 65% yield. Next, the variation on the ester part unfolds that this protocol is not only limited to linear, as branched, cyclic, bulky, unsaturated, and saturated chains were well tolerated under the reaction conditions (Scheme 3.2.2.1, entries **3g**-**3m**). To our delight, the analogous reaction of diazoesters containing heterocyclic moieties with mono and bicyclic heterocycles such as thiophene and indole led to a facile conversion to achieve the desired products in 60% and 46% yields respectively (Scheme 3.2.2.1, entries **3n** and **3o**).



Scheme 3.2.2.1: Substrate Scope for α-ketoesters. All reactions were carried out on a 0.1 mmol scale by taking **1** (2.0 equiv) and **2** (1.0 equiv). Yields refer to isolated yield. 1.0 mmol scale reaction provided 68% (112 mg) isolated yield of **3a**.

To check the versatility of the diazo compounds, we then moved from α-aryldiazoacetates (donor/acceptor) to α-diazo-β-keto esters (acceptor/acceptor), but unfortunately, no product was formed under the optimal reaction conditions. Based on previous literatures,[6,7,11] and UV-Visible spectra (Figure 1) we envisioned that blue LEDs might be ill-suited to generate the corresponding carbene intermediate from these types of diazo compounds.

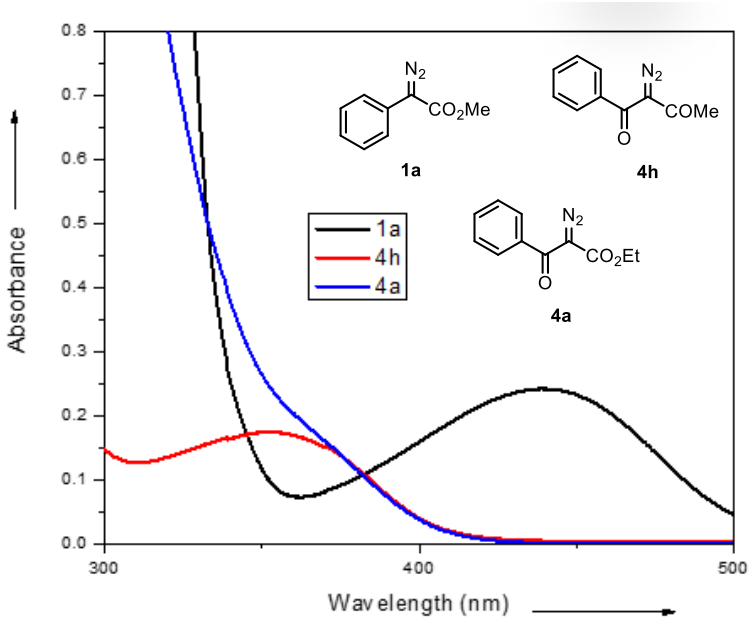


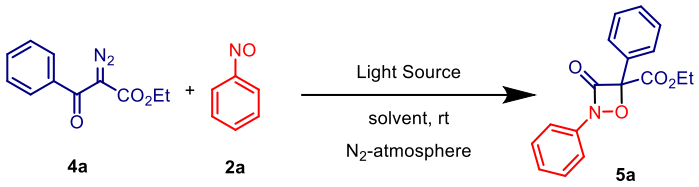
Figure 1: UV-Visible Spectra

3.2.3. Optimization of the Reaction Condition for [2+2] Cycloaddition Reaction

Here, several light sources and solvents were screened to find out the suitable one. Gratifyingly, UV LEDs irradiation facilitated carbene generation. However, surprisingly, with these types of substrates, nitrosoarene did not participates in the oxygen transfer process, instead, it underwent a formal [2 + 2] cycloaddition reaction with an *in situ* generated ketene (via Wolff Rearrangement) to furnish 1,2-oxazetidine-3-one 5a (Table 3.2.1.5). Under a modified reaction condition from the previous one, we went out to explore the substrate scope.

3.2.1.5. Chapter 3: Table 5. Optimization Study: Miscellaneous Optimization 2

Optimization Study: Miscellaneous Optimization-2



4a 2a 5a

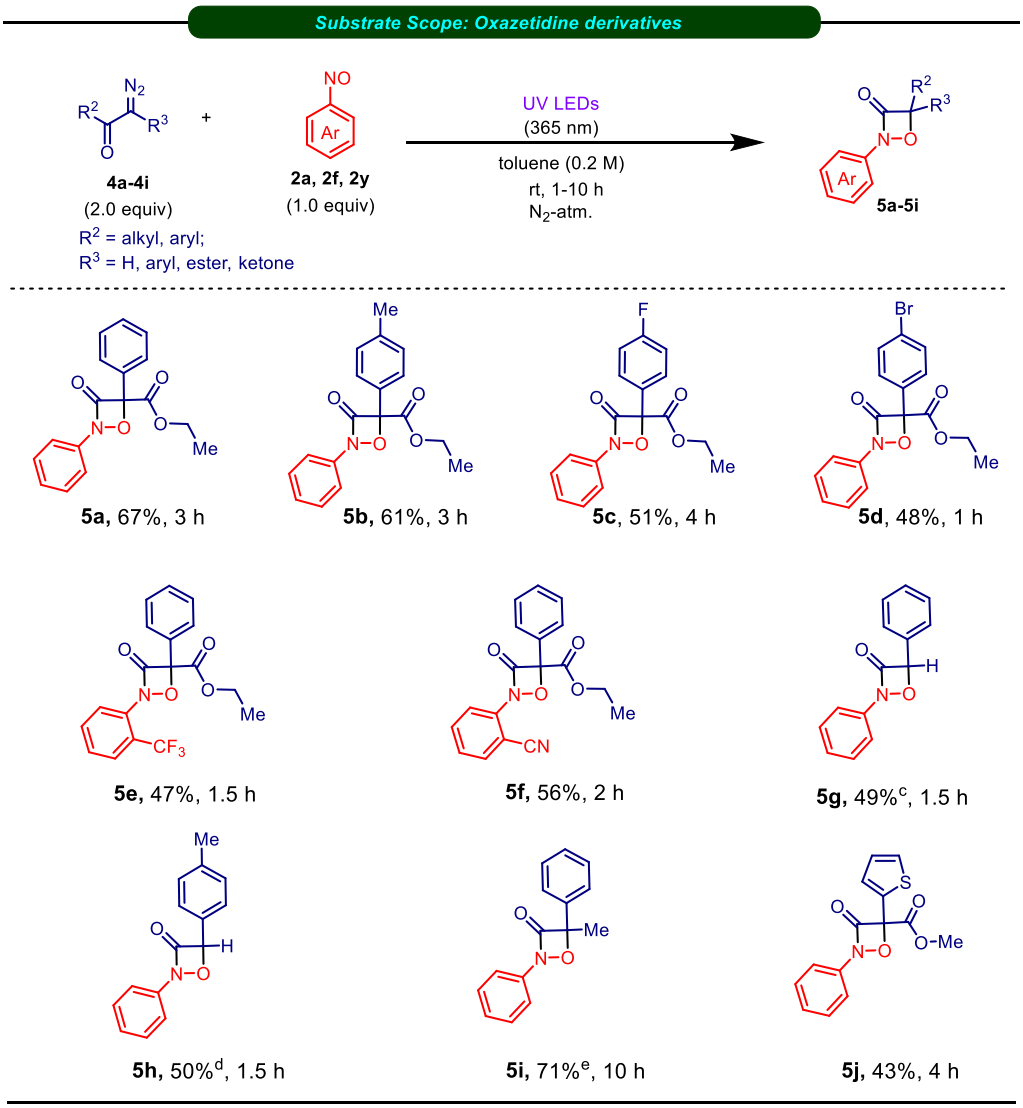
Entry	4a	2a	Solvent (M)	Time (h)	Light source (LEDs)	Yield (%)[b]
1	2	1	DCM (0.2)	10	450 nm	0
2	2	1	DCM (0.2)	10	420 nm	0
3	2	1	DCM (0.2)	10	365 nm	41
4	2	1	DCM (0.2)	3	365 nm	48
5	**2**	**1**	**toluene (0.2)**	**3**	**365 nm**	**75 (67)**
6	1	1	CH_3CN (0.2)	3	365 nm	0
7	2	1	Et_2O (0.2)	3	365 nm	0
8[c]	2	1	toluene (0.2)	3	365 nm	9
9	2	1	toluene (0.2)	3	in dark	0

[a] unless untill mentioned all reactions were carried out in 0.1 mmol scale in respective dry solvents. [b] yield was measured by ^{1}H-NMR analysis of the crude reaction mixture using CH_2Br_2 as an internal standard, isolated yield in parentheses. [c] UV strip was used as a light source instead of UV LEDs.

3.2.4. Substrate Scope Evaluation for oxazetidine derivatives

Here, a diversified range of oxazetidine derivatives were synthesized in moderate to good yield. A variety of α-diazo-β-keto esters containing electron releasing and demanding substituents in the aryl ring reacted smoothly for the product formation (Scheme 3.2.4.1, entries **5a-5d**). Nitrosoarenes decorated with functionality such as trifluoromethyl and cyano group were also well compatible with these reaction conditions (Scheme 3.2.4.1, entries **5e** and **5f**). However, nitrosoarene containing electron-donating group such as *p*-Me was unable to deliver the corresponding product, this may be due to the instability of the 1,2-oxazetidin-3-one cycloadduct, we observed the formation of ethyl 2-oxo-2-phenylacetate **3g** during the reaction as a major product (Scheme 3.2.4.1). Next, an acceptor diazo compound such as α-diazoaldehyde **4e** (R^2 = Ph, R^3 = H) was also examined, which reacted sluggishly to form compound **5g**. Interestingly, an α-diazo-β-keto compound **4f** (R^2 = Ph, R^3 = COMe) delivered the same product **5g** with moderate yield via a decarbonylation process (Scheme 3.2.4.1). Similarly, oxazetidine **5h** was prepared from **4g** (R^2 = 4-MeC_6H_4, R^3 = COMe) in 50% yield. A donor/acceptor–diazo compound such as α-aryldiazoketone **4h** (R^2 = Me, R^3 = Ph) reacted well under these reaction conditions. However, blue LEDs irradiation of α-aryldiazoketone **4h** improves its reactivity to furnish 1,2-oxazetidin-3-one **5i** in good yield. Moreover, a heteroaryl substituted diazo compound **4k** (R^2 = 2-thienyl, R^3 = CO_2Me) gives the corresponding oxazetidine **5h** in moderate yield. In few cases, we have

observed that the cycloadducts are relatively unstable and prone to generate corresponding α-ketoesters (Needs a quick isolation and data recording process).

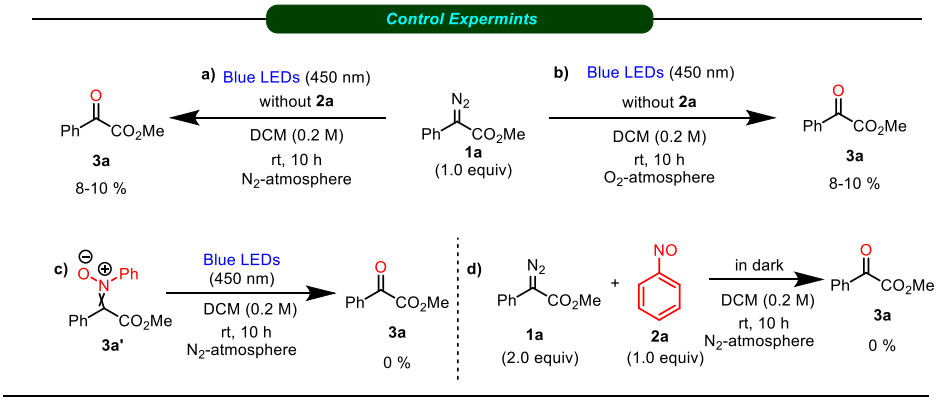


Scheme 3.2.4.1: Substrate Scope for oxazetidine derivatives.

[a] All reactions were carried out on a 0.1 mmol scale by taking **4** (2.0 equiv) and **2** (1.0 equiv). [b] Yields refer to isolated yield. [c] Prepared from **4h** (R^2 = Ph, R^3 = COMe) via decarbonylation (see experimental section). [d] Prepared from **4i** (R^2 = 4-MeC_6H_4, R^3 = COMe) via decarbonylation (see experimental section). [e] Reaction was carried out using DCM (0.2 M) as a solvent for 10 h under blue LEDs irradiation (optimized reaction condition gives 46% of isolated yield). [f] 1.0 mmol scale reaction provided 57% (170 mg) isolated yield of **5a**.

3.2.5. Control Experiments for the Oxygen Transfer Process.

To gain insight into the light-promoted oxygen transfer process, we carried out some control experiments. The reaction conducted in absence of nitrosobenzene **2a** leads to a trace amount (8-10%) of product formation (Scheme 3.2.5.1a). Then, we wanted to elucidate the origin of oxygen atoms for this oxygen transfer process. Hence, we carried the reaction under an oxygen atmosphere instead of nitrogen in the absence of **2a**; however, only a traces amount (8-10%) of product formation was observed (Scheme 3.2.5.1b). The above two experiments indicate that there is a minor amount of product formation, which may result from the dissolved oxygen present in the solvent or from the atmospheric oxygen. To further investigate whether nitrone is a potent intermediate or not, nitrone **3a'** was allowed to react under optimized reaction conditions in the absence of nitrosobenzene **2a** (Scheme 3.2.5.1c). No further product formation was detected, suggesting that nitrosoarene is acting as a potential oxygen donor in this oxygenation process and nitrone might not be the potent intermediate. In addition, no product formation was detected without light, indicating irradiation of light is required to assist this transformation (Scheme 3.2.5.1d). Addition of external water molecule only lead to the formation of traces amount of water (Scheme 3.2.5.1e).



Scheme 3.2.5.1: Control Experiments for the Oxygen Transfer Process.

3.2.6. UV-Visible Spectra for diazo compounds.

Next, in order to check the requirement of different light sources for different reaction UV-visible data was recorded for different diazo compounds. Donor acceptor diazo compound **1a** absorbs light near 450 nm, whereas acceptor-acceptor diazo compounds such as **4a** and **4h** provide the absorption band below 400 nm (Figure 3.2.6.1).

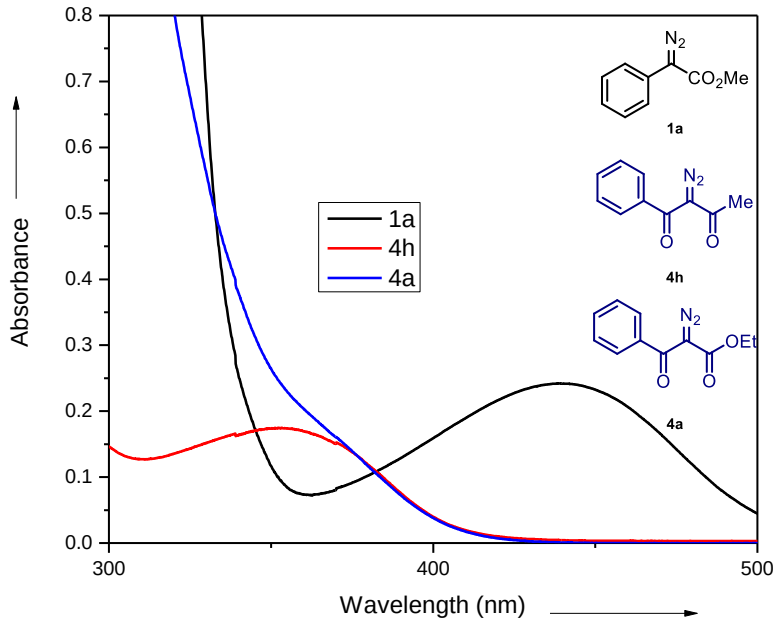


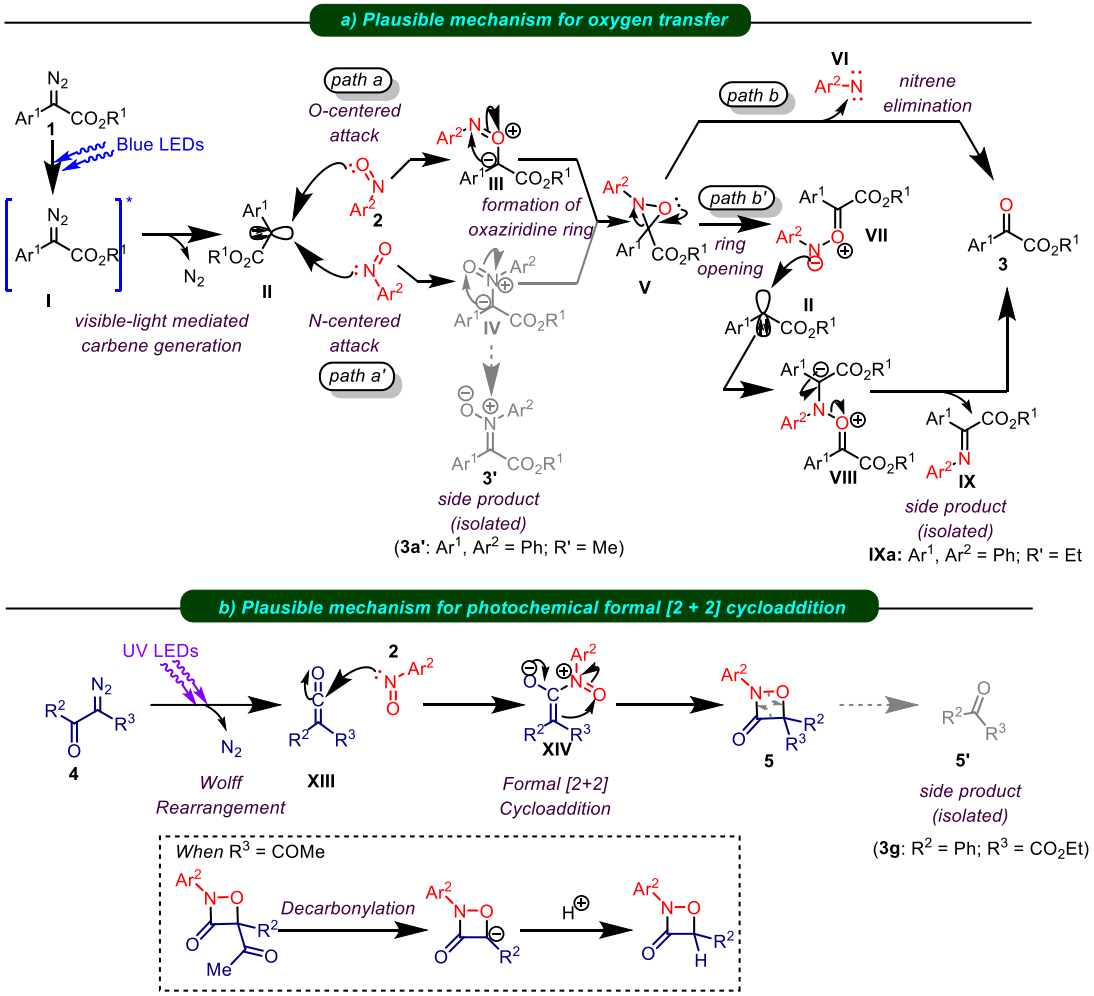
Figure 3.2.6.1: Chapter 3: UV-Visible absorption spectra of compound **1a**, **4a**, and **4h** (0.002 M in toluene).

3.2.7. Mechanistic Proposal for oxygen transfer process and formal [2+2] cycloaddition reaction.

Based on precedent literatures[6,7] and control experiments, in the case of oxygen transfer process, we have proposed that in the presence of Blue LEDs the diazo compound **1** was transformed into its excited state **I**. This excited intermediate **I** unshackle dinitrogen to furnish singlet carbene intermediate **II**. Then this transiently formed carbene intermediate **II** was readily attacked by nitrosoarene **2** either from its *O*-center (via path a) or *N*-center, leads to form intermediate **III** or **IV** respectively. The control experiment indicates that the nitrone **3'** cannot be a potent intermediate, so the path a' can only be a minor pathway for the decomposition process. Intermediate **III** then readily underwent cyclization to give oxaziridine intermediate **V**. Now, elimination of nitrene intermediate **VI** (we are unable to detect or trapped this nitrene intermediate) from the oxaziridine ring can lead to the product **3** formation via path b. On the other hand, path b' indicates the opening of oxaziridine ring, delivering intermediate **VII** which attacks another molecule of carbene **II** (diazo compound is used in excess) to give intermediate **VIII**. Finally, intermediate **VIII** releases imine **IX** to furnish desired product **3** (Scheme 3.2.7.1a).

Under UV light irradiation, the Wolff rearrangement of *in situ* generated carbene from diazo compound 4 leads to the formation of ketene X intermediate.[6,7,11] This ketene X intermediate then

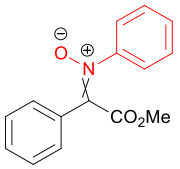
undergoes a formal [2 + 2] cycloaddition with nitrosoarene 2 to furnish product 5 via intermediate XI (Scheme 3.2.7.1b). However, in few cases, these oxazetidine rings 5 are unstable and leads to decomposition of the product and formation of aryl oxoacetate derivatives 5' was observed.



Scheme 3.2.7.1: Chapter-3 Mechanistic Proposal for Both Oxygen Transfer and [2+2] Cycloaddition reaction.

3.2.8. Characterization of Reaction Intermediates:

3.2.8.1. *N*-(2-methoxy-2-oxo-1-phenylethylidene)aniline oxide (3a'):



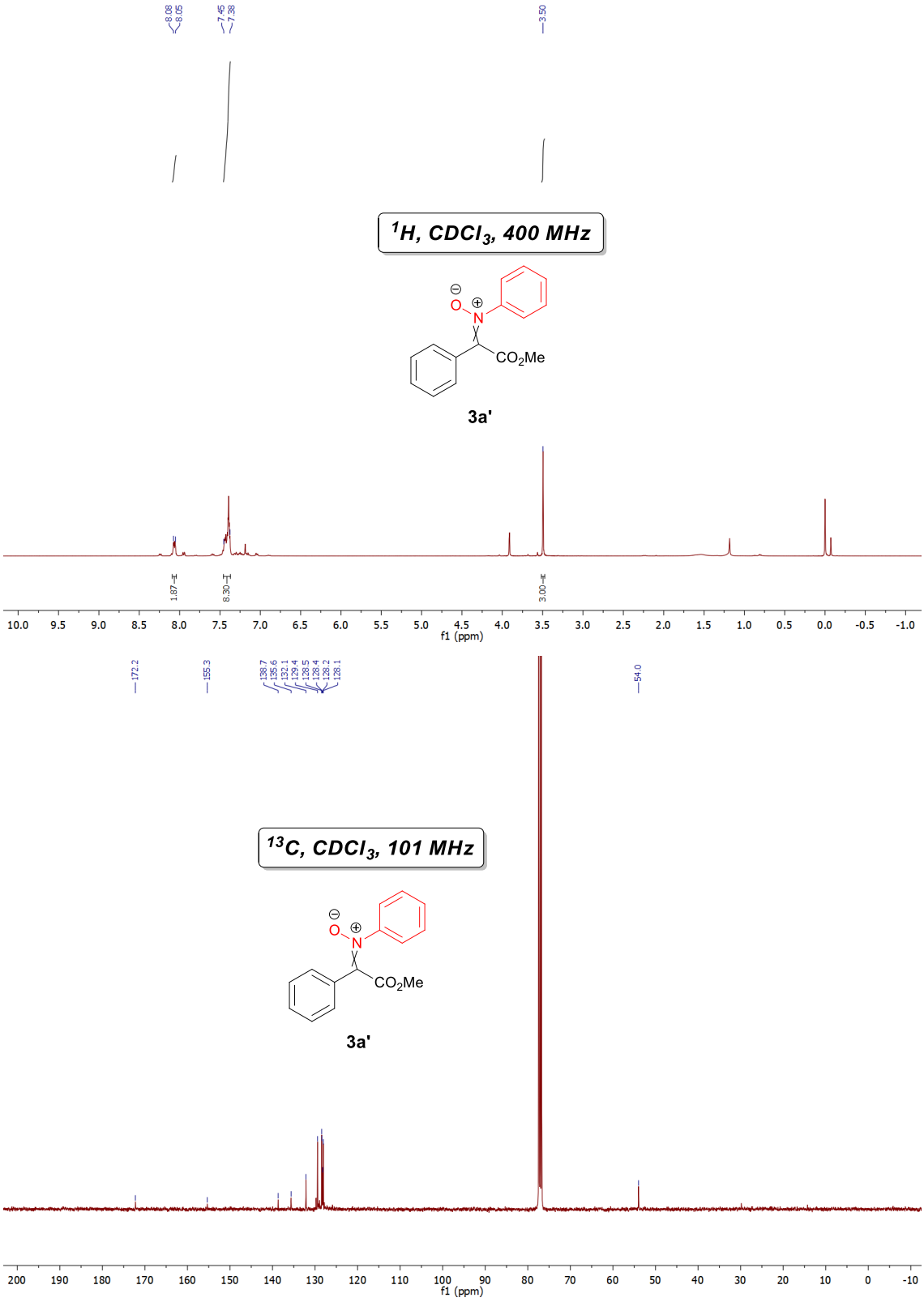
3a'

$C_{15}H_{13}NO_3$

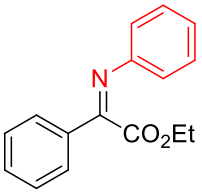
M. W. 255.27 g/mol

^{1}H NMR (400 MHz, $CDCl_3$): δ 8.08–8.06 (m, 2H), 7.45–7.38 (m, 8H), 3.50 (s, 3H). **^{13}C NMR (101 MHz, $CDCl_3$):** δ 172.2, 155.3, 138.7, 135.6, 132.1, 129.4, 128.5, 128.4, 128.2, 128.1, 54.0.

HRMS (ESI): m/z $[M+H]^+$ Calculated for $[C_{15}H_{14}NO_3]^+$: 256.0974; Found: 256.0970.



3.2.8.2. (*E*)-ethyl 2-phenyl-2-(phenylimino)acetate (IXa):



IXa

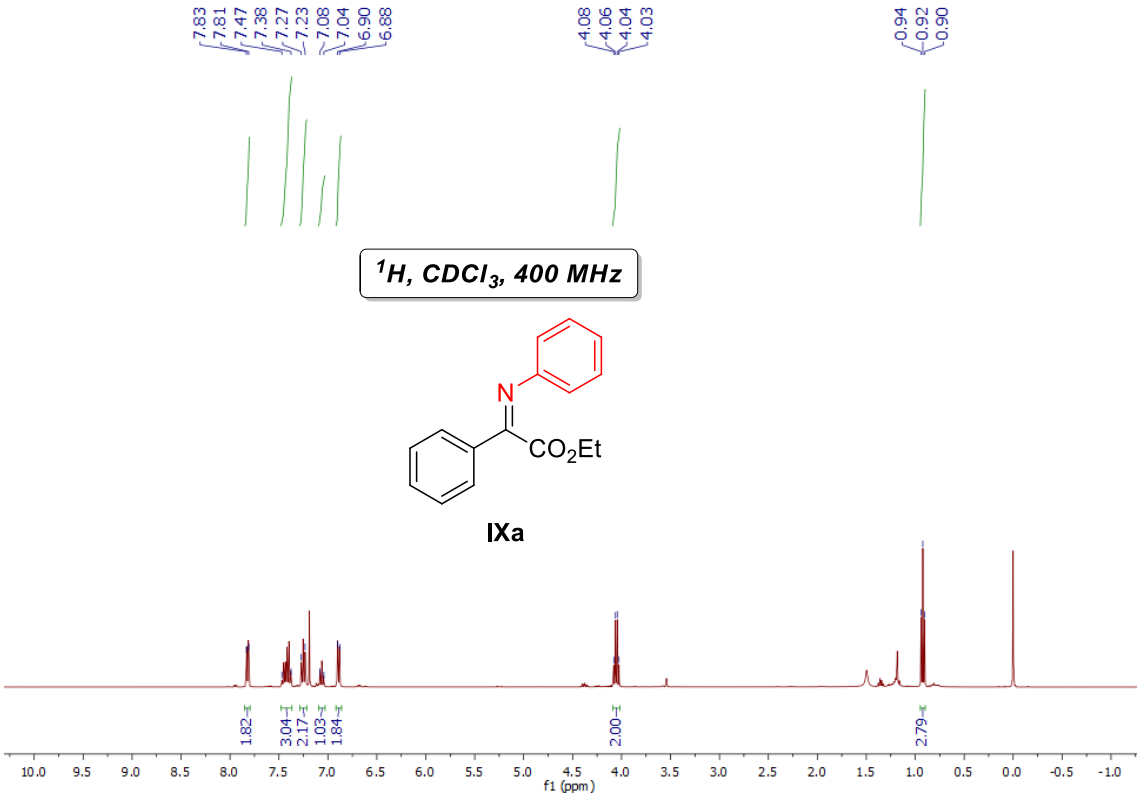
$C_{16}H_{15}NO_2$

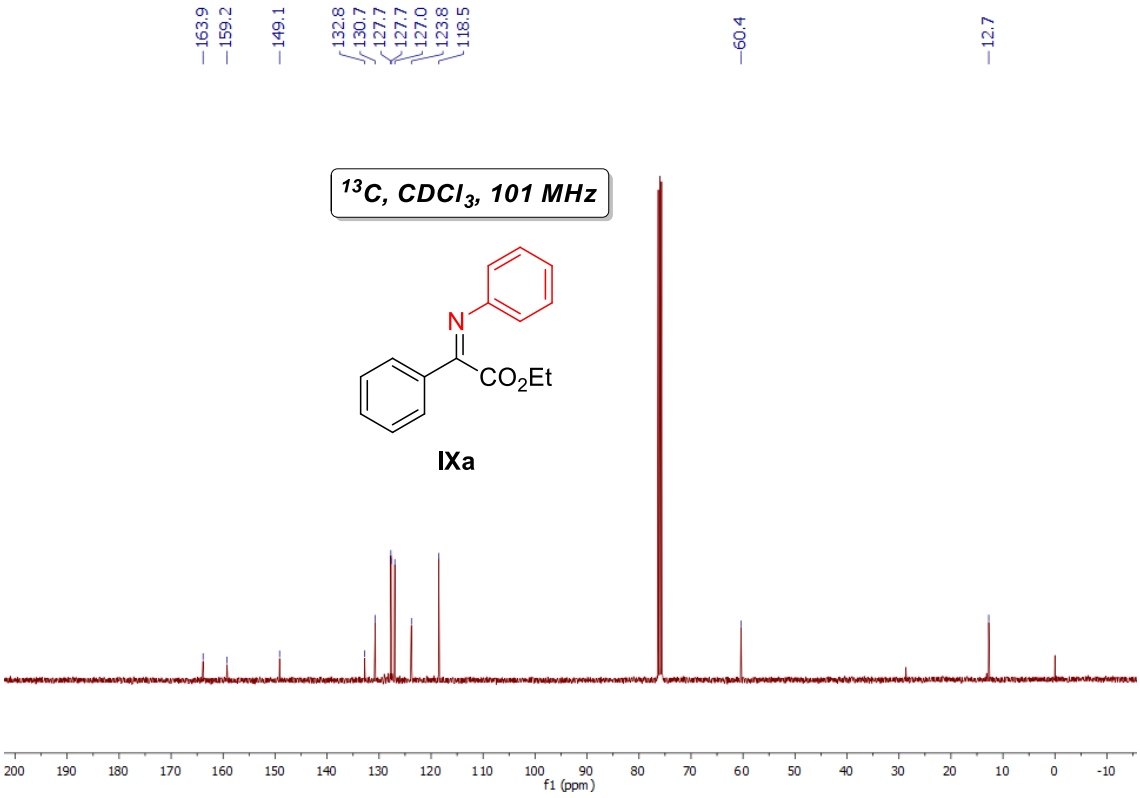
M. W. 253.29 g/mol

According to **GP-10** side product **IXa** was obtained while preparing compound **3g** by using **1g** (38.0 mg, 0.2 mmol, 2.0 equiv) and **2a** (11.0 mg, 0.1 mmol, 1.0 equiv) in CH_2Cl_2 for 10 h at rt. Column chromatographic purification (petroleum ether/EtOAc 99:1 to 95:5) afforded **IXa** (side product) as yellow oil (9.0 mg, 36%).

^{1}H NMR (400 MHz, $CDCl_3$): δ 7.83–7.81 (m, 2H), 7.47–7.38 (m, 3H), 7.27–7.23 (m, 2H), 7.08–7.04 (m, 1H), 6.90–6.88 (m, 2H), 4.05 (q, J = 7.1 Hz, 2H), 0.92 (t, *J* = 7.1 Hz, 3H). **^{13}C NMR (101 MHz, $CDCl_3$):** δ 163.9, 159.2, 149.1, 132.8, 130.7, 127.7, 127.7, 127.0, 123.8, 118.5, 60.4, 12.7.

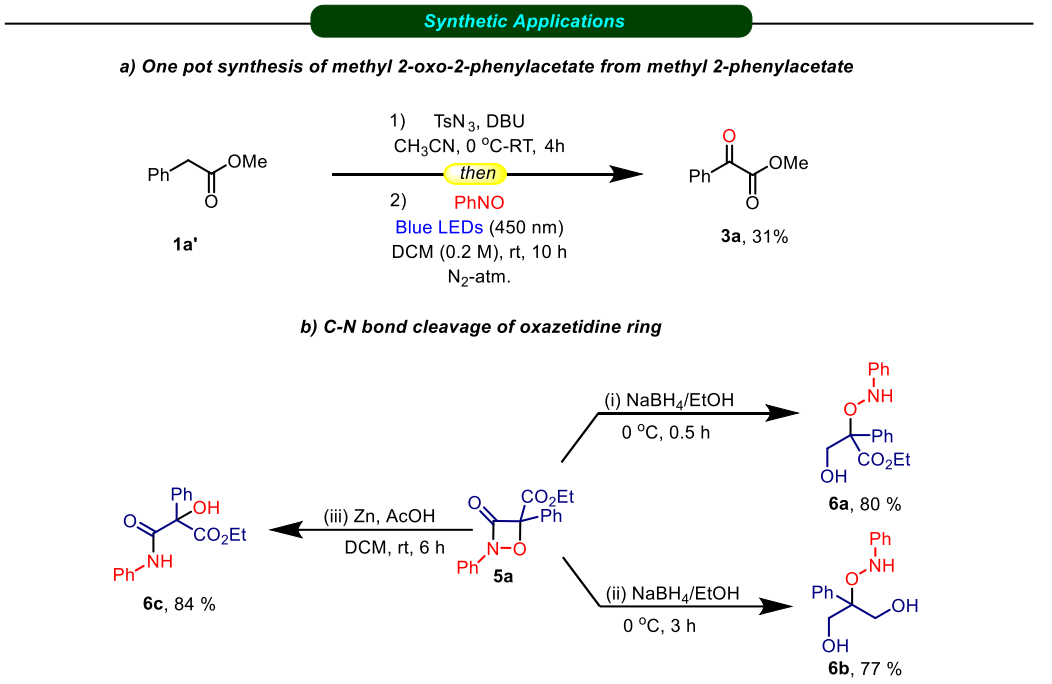
HRMS (ESI): m/z $[M+H]^+$ Calculated for $[C_{16}H_{16}NO_2]^+$: 254.1181; Found: 254.1141.





3.2.9. Synthetic Applications

As proof of applicability, a one-pot sequential operation was conducted, where α-arydiazoacetate **1a** was generated *in situ* from corresponding phenylacetate **1a'** and converted into the desired α-ketoester **3a** with moderate yield (Scheme 3.2.9.1a). Synthetic application of 1,2-oxazetidin-3-one **5a** has also been exemplified by borohydride reduction, furnishing aminoalcohol **6a**. Aminoalcohol **6a** is converted into the corresponding 1,3-diol **6b** under prolonged reaction time. Likewise, the reductive cleavage of N–O bond was also performed upon treatment of 1,2-oxazetidin-3-one **5a** with Zn/AcOH, furnishing α-hydroxy amide **6c** in good yield (Scheme 3.2.9.1b).



Scheme 3.2.9.1: Chapter-3: Synthetic Applications.

3.3 Conclusion

To conclude, this chapter showcases a divergent role of photoexcited diazo compounds towards nitrosoarenes to deliver a range of α-ketoester and 1,2-oxazetidin-3-one derivatives under transition-metal free, catalyst-free, simple, and mild reaction conditions. The key to the success was driven by a light-promoted generation of carbene intermediate and *in situ* formation of ketene intermediate. A versatile substrate scope was examined, which elegantly furnished the desired product in moderate to good yield (up to 83%). Furthermore, the synthetic applicability of the developed protocol was also verified, which illustrates one-pot synthesis of α-ketoester and transformation of cycloadduct to deliver synthetically useful compounds with good yields.

3.4. Experimental Section

3.4.1. General Information:

All reactions were performed in flame-dried glassware under argon atmosphere unless otherwise stated. Liquids and solutions were transferred with syringes. Solvents used were dried and purified by following standard procedures. Technical grade solvents for extraction or chromatography (ethyl acetate, and petroleum ether) were distilled prior to use. $CDCl_3$ was stored over 4Å molecular sieves. Used chemicals were purchased from Sigma-Aldrich, TCI, Alfa-Aesar and Sisco Research Laboratories (SRL) used without further purification. All the liquid chemicals distilled freshly prior to use. Analytical thin-layer chromatography (TLC) was performed on using pre-coated aluminium-backed plates (Merck Kieselgel 60 F254) and visualized by UV radiation, basic aqueous potassium permangante ($KMnO_4$), *p*-anisaldehyde stains and heat as developing agents.

Flash column chromatography was performed on silica gel 60 (40–63 μm, 230–400 mesh, ASTM) from Merck using the indicated solvents. Organic solutions were concentrated under reduced pressure on Heidolph rotary evaporator. NMR spectra were acquired on a JEOL JNM ECS-400, JEOL JNM ECS-500, Bruker AVANCE NEO 400 MHz FT-NMR and Bruker AVANCE NEO 500 MHz FT-NMR instrument running at 400 MHz for ^{1}H, 101 MHz ^{13}C and 376 MHz for ^{19}F and at 500MHz for ^{1}H, 126 MHz ^{13}C and 470 MHz for ^{19}F respectively. Chemical shifts (δ) are reported in ppm relative to residual solvent signals ($CHCl_3$, 7.26 ppm for ^{1}H NMR, $CDCl_3$, 77.0 ppm for ^{13}C NMR). Data are reported as follows: chemical shift, multiplicity (br = broad singlet, s = singlet, d = doublet, dd = doublet of doublets, t = triplet, q = quartet, ddd = doublet of doublet of doublet, td = triplet of doublet, m = multiplet), coupling constants (Hz), and integration. 1,2-Dibromomethane was used as an internal standard to calculate NMR yields of products by ^{1}H NMR analysis of the crude mixture.

3.4.2. Photoreactor Setup:

Photochemical reactions were carried out in bottom plane 5 ml bottom plane borosilicate glass vials in a Penn *Phd* Photoreactor m2 composed of cooling block and LED plate connected to AC/DC input 100 - 240 V AC, 50/60 Hz power supply (Figure 1). The instrument details are given by the manufacturer as follows-

AC/DC input 100 - 240 V AC, 50/60 Hz; feature thermocouple type K-Type Thermocouple (Touch Screen: 3.5” TFT LCD; 320 x 480 resolution); reaction suitability reaction type: Photocatalysis reagent type: catalyst parameter (Variable stir bar control 100 - 2000 RPM) 0-95% RH at 10-40 °C; W × H × D 11.4 cm × 27.2 cm × 27.9 cm 4.5 in. × 10.7 in. × 11.0 in. Filters used- 450nm, 420nm, and 365nm.



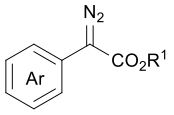
Figure S1: Photochemical reaction set up.

3.4.3. List of substrates prepared:

3.4.3.1. List of diazo compounds prepared:[14-24]

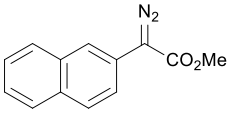
The lists of substrates prepared according to **GP-1–GP-7** are given bellow.

List of diazo compounds

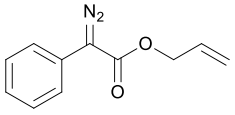


1

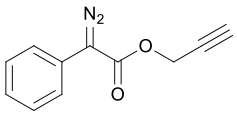
1a: Ar = Ph, R^1 = Me
1b: Ar = 4-$OMeC_6H_4$, R^1 = Me
1c: Ar = 4-FC_6H_4, R^1 = Me
1d: Ar = 4-ClC_6H_4, R^1 = Me
1e: Ar = 2-BrC_6H_4, R^1 = Me
1g: Ar = Ph, R^1 = Et
1h: Ar = 2-MeC_6H_4, R^1 = Et
1i: Ar = Ph, R^1 = ^{i}Pr
1j: Ar = Ph, R^1 = CH_2Ph



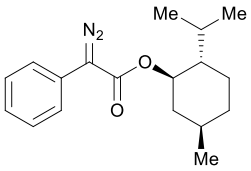
1f



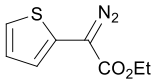
1k



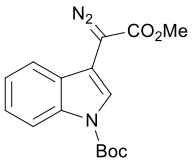
1l



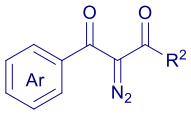
1m



1n

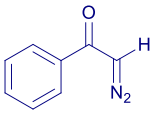


1o

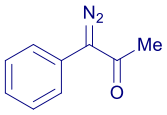


4

4a: Ar = Ph, R^2 = OEt
4b: Ar = 4-MeC_6H_4, R^2 = OEt
4c: Ar = 4-FC_6H_4, R^2 = OEt
4d: Ar = 4-BrC_6H_4, R^2 = OEt
4f: Ar = Ph, R^2 = Me
4g: Ar = 4-MeC_6H_4, R^2 = Me
4k: Ar = 2-thienyl, R^2 = OMe

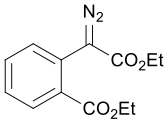


4e

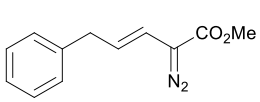


4h

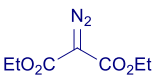
List of unsuccessful diazo compounds



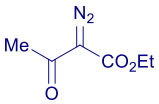
1p



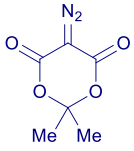
1q



4h



4i

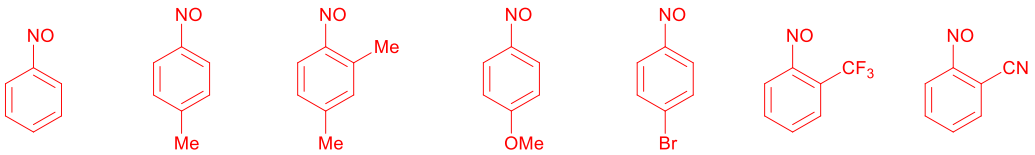


4j

3.4.3.2. List of nitrosoarenes prepared:

All nitrosoarenes were prepared according to the previous literatures.[25-32]

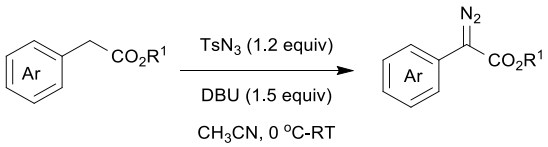
List of Nitrosoarenes



2a **2b** **2c** **2d** **2e** **2f** **2g**

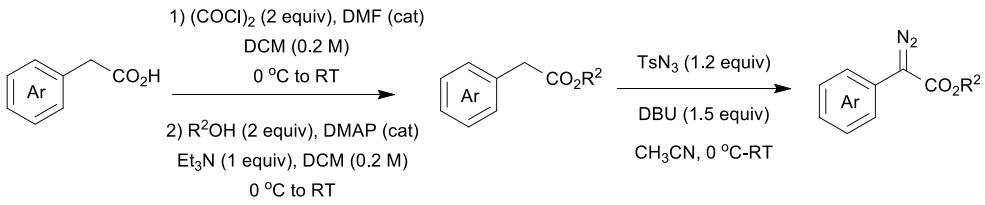
3.4.4. General Procedures:

3.4.4.1. General procedure for preparation of α-diazoesters (GP-1).[14]



According to previous literature,[14] α-diazoesters were prepared. To a mixture of ester (1 equiv, 10 mmol) and tosyl azide (1.2 equiv, 12 mmol) in anhydrous CH_3CN (15 mL) at 0 °C, 1,8-diazabicyclo[5.4.0]undec-7-ene (DBU) (1.5 equiv, 15 mmol) was added. The reaction mixture was then stirred at room temperature for overnight. Upon complete consumption of the starting materials, the reaction mixture was quenched with saturated aqueous solution of NH_4Cl (5 mL), extracted with CH_2Cl_2, washed with brine, dried over $MgSO_4$, and concentrated under reduced pressure to give the product. The residue was purified by coloumn chromatography (hexane/EtOAc, 9:1) to afford the α-diazoesters (**1a-1d)**.

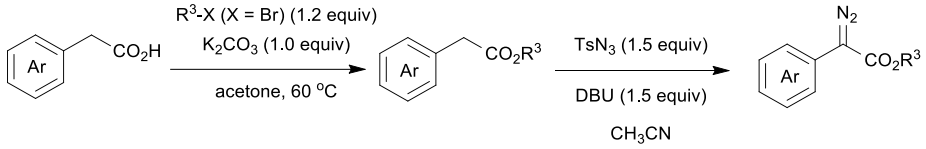
3.4.4.2. General procedure for preparation of α-diazoesters (GP-2).[15, 14]



According to previous literature,[14,15] α-diazoesters were prepared. At room temperature, under nitrogen, a round bottom flask is charged with 2-arylacetic acid (1 equiv, 15 mmol), DCM (0.2 M) and oxalyl chloride (2 equiv, 30 mmol). The temperature is cooled to 0 °C and DMF (1-2 drops) is added. The reaction temperature is allowed to warm up to room temperature and stirred at this temperature overnight. Then, the reaction mixture is concentrated under reduced pressure. Next, at room temperature, under nitrogen, the round bottom flask containing the previously prepared acyl chloride is charged with ROH (1.2 equiv, 18 mmol), DMAP (0.1 equiv, 0.15 mmol), Et_3N (1.0 equiv, 15 mmol) and DCM (0.2 M). The reaction is stirred at room temperature overnight. Then, the reaction is quenched with a saturated aqueous solution of

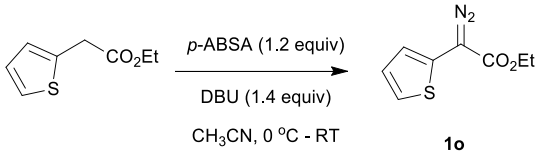
NH_4Cl, extracted with DCM, dried ($MgSO_4$), filtered and concentrated under reduced pressure. The obtained residue is purified by flash column chromatography to afford the corresponding esters. These esters then were converted into corresponding α-diazoesters (**3f**, **3g**, **3h**, **3i**, **3k**, **3m**) by following **GP-1**.

3.4.4.3. General procedure for preparation of α-diazoesters (GP-3).[15, 14]



According to previous literature,[14, 15] α-diazoesters were prepared. Under air, a round bottomed flask is charged with the carboxylic acid (1 equiv), acetone (0.5 M), alkyl halide (1.2 equiv) and K_2CO_3 (1 equiv). The reaction mixture is heated at reflux (60 °C) overnight. Then, the reaction is allowed to cool to room temperature and is concentrated under vacuum. The residue is dissolved in EtOAc, washed with H_2O, brine, dried ($MgSO_4$) and concentrated again under reduced pressure. Purification by flash column chromatography affords the corresponding esters. These esters then were converted into corresponding α-diazoesters (**3j**, **3l**) by following **GP-1**.

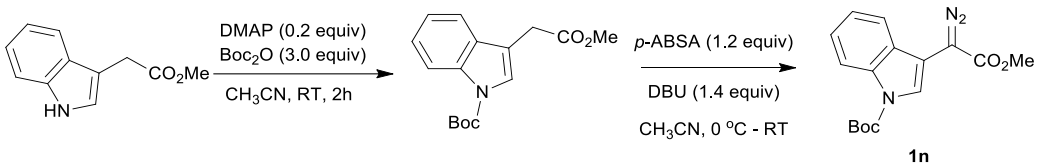
3.4.4.4. General procedure for preparation of ethyl 2-diazo-2-(thiophen-2-yl)acetate (GP-4).[16]



1o

According to previous literature,[16] α-diazoester was prepared. To a 100 mL round bottom flask equipped with a magnetic stir bar, α-arylacetate (10 mmol) and *p*-acetamidobencenesulfonylazide (12 mmol, 2.88 g) were added to prechilled CH_3CN (25 mL). DBU (14 mmol, 1.40 mL) was then added dropwise to the mixture. Upon complete consumption of the starting materials monitored by TLC, the reaction mixture was diluted with distilled water (20 mL) and extracted with diethyl ether (3 × 10 mL). The organic layer was then washed with 10% $NaHCO_3$ solution (3 X 10 mL) and brine (3 X 10 mL). The combined organic extracts were dried over anhydrous $MgSO_4$ and concentrated under reduced pressure. The aryl diazoacetate (**1o**) was purified by coloumn chromatography (eluent: Hexane/EtOAc, 20:1).

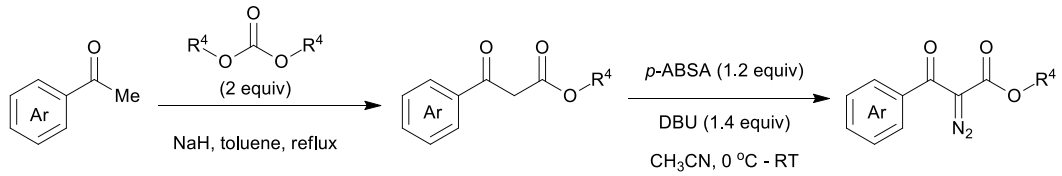
3.4.4.5. General procedure for preparation of *tert*-butyl 3-(1-diazo-2-methoxy-2-oxoethyl)-1*H*-indole-1-carboxylate (GP-5).[17]



1n

According to previous literature,[17] α-diazoester were prepared. Methyl 2-(1*H*-indol-3-yl)acetate (1.3 g, 6.39 mmol) was diluted in CH_3CN, then DMAP (0.16 g, 1.3 mmol) and Boc_2O (1.53 g, 7.03 mmol) were added. The reaction mixture was stirred at rt for 2 h then concentrated in vacuo, diluted in CH_2Cl_2 washed with water, brine, dried (Na_2SO_4) and concentrated in vacuo. Purification by silica gel chromatography (9:1 pentane:EtOAc) gave *tert*-butyl 3-(2-methoxy-2-oxoethyl)-1*H*-indole-1-carboxylate. In the next step, *p*-ABSA (2.72 g, 11.4 mmol) was added to a solution of *tert*-butyl 3-(2-methoxy-2-oxoethyl)-*1H*-indole-1-carboxylate (1.897g, 12.1 mmol) and DBU (5.75 g, 5.65 mL, 37.8 mmol) in CH_3CN (12 mL) at 0 °C. The reaction mixture was allowed to warm to rt over 3 h, then concentrated in vacuo and diluted in CH_2Cl_2. The organic phase was washed with 0.5 M pH7 sodium phosphate buffer solution, dried (Na_2SO_4) and concentrated in vacuo. Purification by silica gel chromatography (94:6 pentane:Et_2O) gave *tert*-butyl 3-(1-diazo-2-methoxy-2-oxoethyl)-1*H*-indole-1-carboxylate (**1n**) as pink solid.

3.4.4.6. General procedure for preparation of α-diazo-β-keto esters (GP-6).[18, 19, 39]



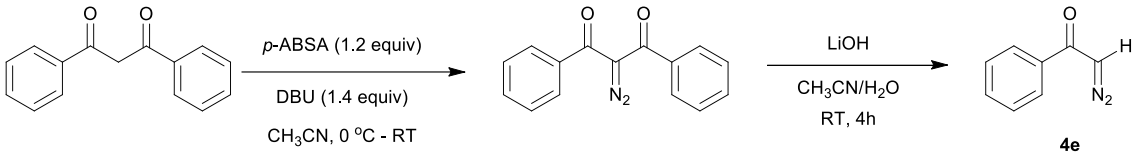
4a-4d, 4k

According to previous literature,[18] acetoacetate derivatives were prepared. To a dried 100 mL three-necked flask were added NaH (2.2 g, 60% w/w, 56 mmol), dimethyl carbonate or diethyl carbonate (40 mmol), and toluene (20 mL) under nitrogen. After the reaction mixture was heated to reflux in oil bath, a solution of acetophenone (20 mmol) in toluene (10 mL) was added dropwise over 0.5 h. After the evolution of hydrogen ceased (30-45 min), the reaction was cooled down to room temperature. Glacial acetic acid (6 mL) was added dropwise and a heavy pasty solid was separated. Ice-cold water was slowly added until the solid was dissolved completely. Then, the reaction system was diluted with EtOAc. The organic layer was separated, washed with water (20 mL) and then saturated brine (20 mL) and finally dried over anhydrous Na_2SO_4. After the solvent was evaporated with the aid of rotary evaporator, the residue was purified by flash chromatography on silica gel with EtOAc/hexanes.

In the next step, according to previous literature,[19, 39] α-diazoesters were prepared. To a solution of acetoacetate derivatives (1 equiv, 5 mmol) and *p*-acetamidobenzenesulfonyl azide (*p*-ABSA) (1.2 equiv, 6 mmol) in anhydrous CH_3CN at 0 °C, triethylamine (Et_3N) (3 equiv, 15 mmol) was added dropwise. After stirring at room temperature for 5 h the reaction mixture was concentrated in vacuo. Water (20 mL) was added. The resulting mixture was extracted with diethyl ether (2 X 20 mL). The combined organic layer

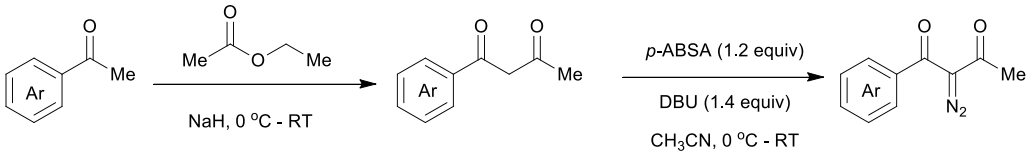
was washed with brine (20 mL) and dried over $MgSO_4$. The solvent was removed under reduced pressure, and the residue was purified by a silica gel column chromatography with petroleum ether/ethyl acetate as the eluent to give the entitled diazo compounds (**4a-4d, 4k**).

3.4.4.7. General procedure for preparation of diazoacetophenone (GP-7).[20]



According to previous literature,[20] to a solution of 1,3-diphenylpropanedione (896 mg, 4 mmol) and Et_3N (0.6 mL, 4.2 mmol) in acetonitrile (20 mL), a solution of *p*-ABSA (1200 mg, 5 mmol) in 20 mL acetonitrile was added dropwise with stirring. The reaction mixture was stirred at room temperature overnight. The compound 2-diazo-1,3-diphenylpropane-1,3-dione was purified by column chromatography (silica gel) using PE/EA 20:1 as eluent. The compound was then dissolved in acetonitrile (20 mL). Aqueous LiOH solution (8.5 mmol LiOH in 20 mL water) was added and the reaction mixture was stirred at room temperature for 4 h. After that, the reaction mixture was rotary evaporated at 30 °C under reduced pressure to remove most of acetonitrile. 20 mL water was added, and then the product was extracted by dichloromethane at least 3 times and finally purified by column chromatography (silica gel) using PE/EA 10:1 to give as a yellow solid (**4e**).

3.4.4.8. General procedure for preparation of α-diazoketones (GP-8):[21, 22]

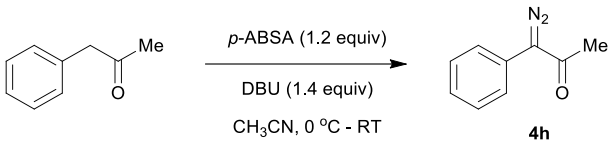


According to previous literature,[21] 1-arylbutane-1,3-diones were prepared. To an oven dried round-bottom flask, substituted aryl ketone (515 mg, 4.3 mmol) and ethyl acetate (20 mL) followed by NaH (17.2 mmol, 60% in dispersions oil) was added at 0 °C, The resultant reaction mixture was stirred at room temperature for 24 h. Then, it was quenched with saturated NH_4Cl solution, extracted with EtOAc (3 X 25 mL) and the combined layer was dried over Na_2SO_4. The evaporation of solvent under the reduced under pressure followed by purification using column chromatography afforded the products.

According to previous literature,[22]1-arylbutane-1,3-diones were converted into corresponding diazoketones. To an oven-dried round-bottom flask equipped with a magnetic stirring bar 1-arylbutane-1,3-dione (1 equiv, 10 mmol) and *p*-ABSA (1.2 equiv, 12 mmol) were added, and the system was filled with nitrogen. Acetonitrile was then added, and the reaction mixture was cooled to 0 °C using an ice-bath. Triethylamine (2 equiv, 20 mmol) was added dropwise within 2 min; the reaction mixture was slowly

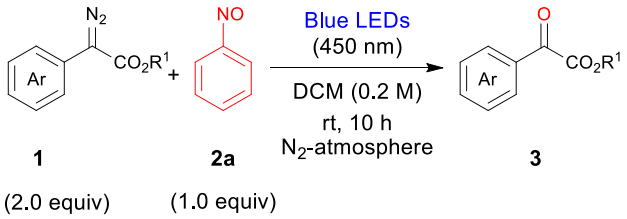
warmed to room temperature, and allowed to stir for 8 h. A white precipitate of *N*-(4-sulfamoylphenyl)acetamide was filtered and washed with dicloromethane (2 X 10 mL). Solvents were evaporated, and diazo compound (**4f**, **4g**) was purified by column chromatography on silica gel with a 9:1 to 4:1 (v/v) gradient of hexane:ethyl acetate as eluents.

3.4.4.9. General procedure for preparation of α-aryldiazoketone (GP-9):[23]



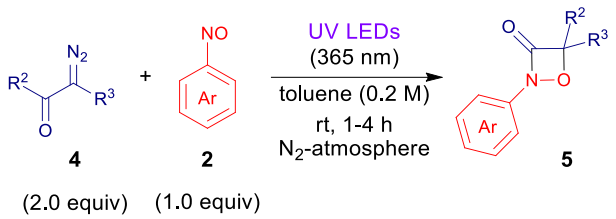
According to previous literature,[23] diazocompound **4g** was prepared. To a solution of 1-Phenylpropan-2-one (1.34 g, 10 mmol) and *p*-ABSA (2.88 g, 12 mmol) in dry CH_3CN (20 mL) was added DBU (1.94 mL, 13 mmol) drop wise at 0 °C. Then the mixture was stirred overnight at room temperature. The reaction was then quenched with 10 wt% NaOH (aq), followed by extraction with Et_2O (2×20 mL). The combined organic extracts were anhydrous $MgSO_4$, filtered and concentrated under reduced pressure. The yellow crude product was purified by silica gel column chromatography (petroleum ether:Et_2O = 10:1) to give the product as a yellow solid (**4h**).

3.4.4.10. General procedure for the preparation of oxoacetate derivatives (GP-10):



In an oven-dried vial equipped with a Teflon-coated stir bar, α-diazoesters **1** (0.2 mmol, 2 equiv) and nitrosobenzene **2a** (0.1 mmol, 1 equiv) were added. Dry DCM (0.2 M) was added to the reaction mixture under N_2 atmosphere. Then this reaction mixture was purged for at least 15 min by using a nitrogen balloon and was sealed. The reaction mixture was then irradiated under blue LEDs for 10 h. After completion, the solvent was evaporated under reduced pressure. Analytically pure products were obtained by column chromatography on silica gel using petroleum ether and ethyl acetate as eluents.

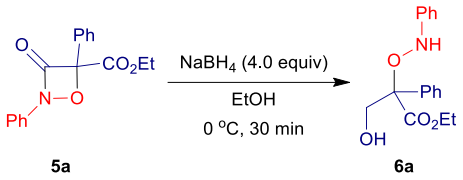
3.4.4.11. General procedure for the preparation of oxazetidine derivatives (GP-11):



In an oven-dried vial equipped with a Teflon-coated stir bar, α-diazoesters **1** (0.2 mmol, 2 equiv) and nitrosobenzene **2** (0.1 mmol, 1 equiv) were added. Dry Toluene (0.2 M) was added to the reaction mixture under N_2 atmosphere. Then this reaction mixture was purged for at least 15 min by using a nitrogen balloon and was sealed. The reaction mixture was then irradiated under UV LEDs for 1-4 h. After completion, the solvent was evaporated under reduced pressure. Analytically pure products were obtained by column chromatography on silica gel using petroleum ether and ethyl acetate as eluents.

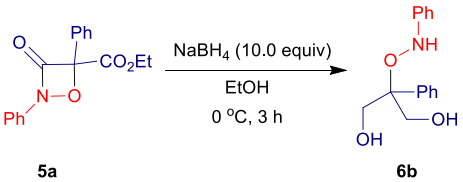
Note: These oxazetidine derivatives are unstable in nature, needs a quick isolation and data recording process.

3.4.4.12. General procedure for the reduction of oxazetidine derivative to prepare 6a (GP-12):



In an oven dried ordinary vial equipped with a Teflon-coated stir bar and a plastic screw cap compound **5a** (0.05 mmol, 15.0 mg, 1.0 equiv) was taken and diluted with 1.0 mL of ethanol. Then to this mixture solid $NaBH_4$ (0.2 mmol, 4.0 equiv) were added and kept at 0 °C for 30 minutes. The reaction was quenched by adding few drops of water. Brine (5 mL) was added and resulted mixture was extracted with DCM (3 X 10 mL), dried over $MgSO_4$, filtered and concentrated in vacuo. The analytically pure product was obtained by column chromatography on silica gel using petroleum ether and ethyl acetate as eluent.

3.4.4.13. General procedure for the reduction of oxazetidine derivative to prepare 6b (GP-13):



In an oven dried ordinary vial equipped with a Teflon-coated stir bar and a plastic screw cap compound **5a** (0.05 mmol, 15.0 mg, 1.0 equiv) was taken and diluted with 1.0 mL of ethanol. Then to this mixture solid $NaBH_4$ (0.5 mmol, 10.0 equiv) were added and kept at 0 °C for 3 h. The reaction was quenched by adding few drops of water. Brine (5 mL) was added and resulted mixture was extracted with DCM (3 X 10

mL), dried over $MgSO_4$, filtered and concentrated in vacuo. The analytically pure product was obtained by column chromatography on silica gel using petroleum ether and ethyl acetate as eluent.

3.4.4.14. General procedure for the reduction of oxazetidine derivative to prepare 6b (GP-14):

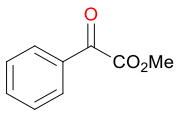


5a **6c**

To the suspension of 1,2-oxazetidin-3-one **5a** (15.0 mg, 0.05 mmol, 1.0 equiv) and zinc powder (16.0 mg, 0.25 mmol, 5 equiv) in DCM (1 mL) was added dropwise the solution of acetic acid (14 µL, 0.25 mmol, 5 equiv) in DCM (0.3 mL) in 3 h. The mixture was stirred for an additional 3 h at rt, and then the solids were removed by filtration through Celite. The filtrate was concentrated under reduced pressure. The analytically pure product was obtained by column chromatography on silica gel using petroleum ether and ethyl acetate as eluent.

3.4.5. Result & Characterization:

3.4.5.1. methyl 2-oxo-2-phenylacetate (3a):



3a

$C_9H_8O_3$

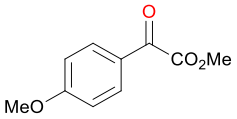
M. W. 164.16 g/mol

According to **GP-10** compound **3a** was prepared by using **1a** (35.0 mg, 0.2 mmol, 2.0 equiv) and **2a** (11.0 mg, 0.1 mmol, 1.0 equiv) in CH_2Cl_2 for 10 h at rt. Column chromatographic purification (petroleum ether/EtOAc 99:1 to 95:5) afforded **3a** as colourless oil (12.5 mg, 76%). For 1.0 mmol scale reaction: **1a** (352.0 mg, 1.0 mmol, 2.0 equiv), **2a** (1.0 equiv, 1 mmol, 107.0 mg), in dry DCM (5 mL, 0.2 M) was used and reaction was stirred for 15 h to get 68% isolated yield of **3a** (112.0 mg).

^{1}H NMR (400 MHz, $CDCl_3$): δ 8.02–8.00 (m, 2H), 7.68–7.64 (m, 1H), 7.53–7.49 (m, 2H), 3.97 (s, 3H). **^{13}C NMR (101 MHz, $CDCl_3$):** δ 186.1, 164.1, 135.1, 132.5, 130.2, 129.0, 52.9.

These data are in accordance with the previous report.[32]

3.4.5.2. methyl 2-(4-methoxyphenyl)-2-oxoacetate (3b):



3b

$C_{10}H_{10}O_4$

M. W. 194.18 g/mol

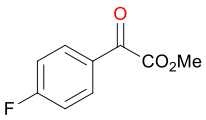
According to **GP-10** compound **3b** was prepared by using **1b** (41.0 mg, 0.2 mmol, 2.0 equiv) and **2a** (11.0 mg, 0.1 mmol, 1.0 equiv) in CH_2Cl_2 for 10 h at rt. Column chromatographic purification (petroleum ether/EtOAc 97:3 to 90:10) afforded **3b** as white solid (14.0 mg, 72%).

Melting Point: 48-50 ºC.

^{1}H NMR (400 MHz, $CDCl_3$): δ 8.02–7.98 (m, 2H), 6.98–6.94 (m, 2H), 3.95 (s, 3H), 3.88 (s, 3H). **^{13}C NMR (101 MHz, $CDCl_3$):** δ 184.5, 165.2, 164.4, 132.8, 125.5, 114.3, 55.8, 52.8.

These data are in accordance with the previous report.[33]

3.4.5.3. methyl 2-(4-fluorophenyl)-2-oxoacetate (3c):



3c

$C_9H_7FO_3$

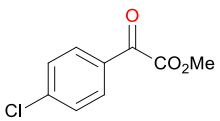
M. W. 182.15 g/mol

According to **GP-10** compound **3c** was prepared by using **1c** (39.0 mg, 0.2 mmol, 2.0 equiv) and **2a** (11.0 mg, 0.1 mmol, 1.0 equiv) in CH_2Cl_2 for 10 h at rt. Column chromatographic purification (petroleum ether/EtOAc 97:1 to 95:5) afforded **3c** as colourless oil (15.0 mg, 83%).

^{1}H NMR (400 MHz, $CDCl_3$): δ 8.10–8.06 (m, 2H), 7.20–7.16 (m, 2H), 3.97 (s, 3H). **^{13}C NMR (101 MHz, $CDCl_3$):** δ 184.2, 167.0 (d, *J* = 258.6 Hz), 163.7, 133.1 (d, *J* = 9.8 Hz), 129.0 (d, *J* = 3.4 Hz), 116.4 (d, *J* = 22.3 Hz), 53.0. **^{19}F NMR: (376 MHz, $CDCl_3$):** δ -100.9.

These data are in accordance with the previous report.[34]

3.4.5.4. methyl 2-(4-chlorophenyl)-2-oxoacetate (3d):



3d

$C_9H_7ClO_3$

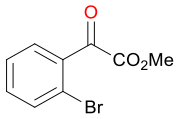
M. W. 198.60 g/mol

According to **GP-10** compound **3d** was prepared by using **1d** (42.0 mg, 0.2 mmol, 2.0 equiv) and **2a** (11.0 mg, 0.1 mmol, 1.0 equiv) in CH_2Cl_2 for 10 h at rt. Column chromatographic purification (petroleum ether/EtOAc 99:1 to 95:5) afforded **3d** as colourless oil (16.0 mg, 81%).

^{1}H NMR (400 MHz, $CDCl_3$): δ 8.00–7.97 (m, 2H), 7.50–7.46 (m, 2H), 3.97 (s, 3H). **^{13}C NMR (101 MHz, $CDCl_3$):** δ 184.6, 163.5, 141.9, 131.6, 130.9, 129.4, 53.1.

These data are in accordance with the previous report.[36]

3.4.5.5. methyl 2-(2-bromophenyl)-2-oxoacetate (3e):



3e

$C_9H_7BrO_3$

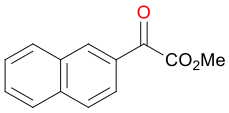
M. W. 243.05 g/mol

According to **GP-10** compound **3e** was prepared by using **1e** (51.0 mg, 0.2 mmol, 2.0 equiv) and **2a** (11.0 mg, 0.1 mmol, 1.0 equiv) in CH_2Cl_2 for 10 h at rt. Column chromatographic purification (petroleum ether/EtOAc 98:2 to 95:5) afforded **3e** as light yellow oil (18.0 mg, 74%).

^{1}H NMR (400 MHz, $CDCl_3$): δ 7.68–7.66 (m, 1H), 7.64–7.62 (m, 1H), 7.47–7.40 (m, 2H), 3.94 (s, 3H). **^{13}C NMR (101 MHz, $CDCl_3$):** δ 187.1, 162.9, 135.6, 134.2, 133.8, 131.9, 127.8, 121.7, 53.5.

These data are in accordance with the previous report.[35]

3.4.5.6. methyl 2-(naphthalen-2-yl)-2-oxoacetate (3f):



3f

$C_{13}H_{10}O_3$

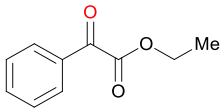
M. W. 214.22 g/mol

According to **GP-10** compound **3f** was prepared by using **1f** (45.0 mg, 0.2 mmol, 2.0 equiv) and **2a** (11.0 mg, 0.1 mmol, 1.0 equiv) in CH_2Cl_2 for 10 h at rt. Column chromatographic purification (petroleum ether/EtOAc 97:3 to 90:10) afforded **3f** as light yellow oil (14.0 mg, 65%).

^{1}H NMR (400 MHz, $CDCl_3$): δ 8.56 (s, 1H), 8.04 (dd, *J* = 8.7, 1.8 Hz, 1H), 7.98 (d, *J* = 8.2 Hz, 1H), 7.93 (d, *J* = 8.7 Hz, 1H), 7.89 (d, *J* = 8.3 Hz, 1H), 7.65 (ddd, *J* = 8.2, 7.0, 1.2 Hz, 1H), 7.58 (ddd, *J* = 8.1, 7.0, 1.2 Hz, 1H), 4.03 (s, 3H). **^{13}C NMR (101 MHz, $CDCl_3$):** δ 186.0, 164.2, 136.5, 133.7, 132.4, 130.1, 129.8, 129.7, 129.1, 128.0, 127.3, 124.1, 53.0.

These data are in accordance with the previous report.[36]

3.4.5.7. ethyl 2-oxo-2-phenylacetate (3g):



3g

$C_{10}H_{10}O_3$

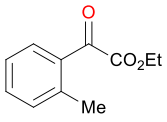
M. W. 178.18 g/mol

According to **GP-10** compound **3g** was prepared by using **1g** (38.0 mg, 0.2 mmol, 2.0 equiv) and **2a** (11.0 mg, 0.1 mmol, 1.0 equiv) in CH_2Cl_2 for 10 h at rt. Column chromatographic purification (petroleum ether/EtOAc 99:1 to 95:5) afforded **3g** as colourless oil (13.5 mg, 76%).

^{1}H NMR (400 MHz, $CDCl_3$): δ 8.01–7.98 (m, 2H), 7.67–7.63 (m, 1H), 7.52–7.48 (m, 2H), 4.44 (q, *J* = 7.1 Hz, 2H), 1.41 (t, *J* = 7.1 Hz, 3H). **^{13}C NMR (101 MHz, $CDCl_3$):** δ 186.5, 163.9, 135.0, 132.5, 130.1, 129.0, 62.5, 14.2.

These data are in accordance with the previous report.[32]

3.4.5.8. methyl 2-oxo-2-(*o*-tolyl)acetate (3h):



3h

$C_{11}H_{12}O_3$

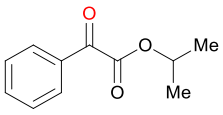
M. W. 192.21 g/mol

According to **GP-10** compound **3h** was prepared by using **1h** (38.0 mg, 0.2 mmol, 2.0 equiv) and **2a** (11.0 mg, 0.1 mmol, 1.0 equiv) in CH_2Cl_2 for 10 h at rt. Column chromatographic purification (petroleum ether/EtOAc 98:2 to 95:5) afforded **3h** as colourless oil (12.0 mg, 67%).

^{1}H NMR (400 MHz, $CDCl_3$): δ 7.69–7.67 (m, 1H), 7.50–7.46 (m, 1H), 7.33–7.29 (m, 2H), 4.42 (q, *J* = 7.1 Hz, 2H), 2.60 (s, 3H), 1.40 (t, *J* = 7.1 Hz, 3H). **^{13}C NMR (101 MHz, $CDCl_3$):** δ 188.9, 164.7, 141.5, 133.8, 132.4(2C), 131.3, 126.0, 62.4, 21.6, 14.2.

These data are in accordance with the previous report.[32]

3.4.5.9. isopropyl 2-oxo-2-phenylacetate (3i):



3i

$C_{11}H_{12}O_3$

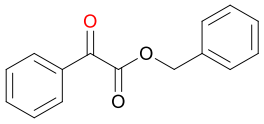
M. W. 192.21 g/mol

According to **GP-10** compound **3i** was prepared by using **1i** (38.0 mg, 0.2 mmol, 2.0 equiv) and **2a** (11.0 mg, 0.1 mmol, 1.0 equiv) in CH_2Cl_2 for 10 h at rt. Column chromatographic purification (petroleum ether/EtOAc 99:1 to 95:5) afforded **3i** as light yellow oil (12.0 mg, 62%).

^{1}H NMR (400 MHz, $CDCl_3$): δ 7.99–7.97 (m, 2H), 7.67–7.62 (m, 1H), 7.52–7.48 (m, 2H), 5.31 (dq, *J* = 12.7, 6.4 Hz, 1H), 1.40 (d, *J* = 6.1 Hz, 6H). **^{13}C NMR (101 MHz, $CDCl_3$):** δ 186.8, 163.7, 134.9, 132.6, 130.1, 129.0, 70.8, 21.8.

These data are in accordance with the previous report.[32]

3.4.5.10. benzyl 2-oxo-2-phenylacetate (3j):



3j

$C_{15}H_{12}O_3$

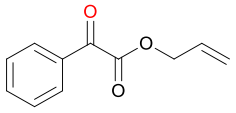
M. W. 240.25 g/mol

According to **GP-10** compound **3j** was prepared by using **1j** (50.0 mg, 0.2 mmol, 2.0 equiv) and **2a** (11.0 mg, 0.1 mmol, 1.0 equiv) in CH_2Cl_2 for 10 h at rt. Column chromatographic purification (petroleum ether/EtOAc 99:1 to 95:5) afforded **3j** as colourless oil (16.0 mg, 67%).

^{1}H NMR (400 MHz, $CDCl_3$): δ 7.97–7.94 (m, 2H), 7.66–7.62 (m, 1H), 7.50–7.35 (m, 7H), 5.41 (s, 2H). **^{13}C NMR (101 MHz, $CDCl_3$):** δ 186.2, 163.7, 135.1, 134.6, 132.5, 130.1, 129.0, 128.9 (2C), 128.7, 67.9.

These data are in accordance with the previous report.[33]

3.4.5.11. allyl 2-oxo-2-phenylacetate (3k):



3k

$C_{11}H_{10}O_3$

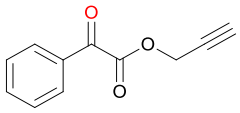
M. W. 190.20 g/mol

According to **GP-10** compound **3k** was prepared by using **1k** (40.0 mg, 0.2 mmol, 2.0 equiv) and **2a** (11.0 mg, 0.1 mmol, 1.0 equiv) in CH_2Cl_2 for 10 h at rt. Column chromatographic purification (petroleum ether/EtOAc 99:1 to 95:5) afforded **3k** as light yellow oil (14.0 mg, 74%).

^{1}H NMR (400 MHz, $CDCl_3$): δ 8.01–7.99 (m, 2H), 7.68–7.64 (m, 1H), 7.53–7.49 (m, 2H), 6.07–5.96 (m, 1H), 5.44 (dq, *J* = 17.3, 1.3 Hz, 1H), 5.34 (dq, *J* = 10.2, 0.9 Hz, 1H), 4.87 (dt, *J* = 5.9, 1.2 Hz, 2H). **^{13}C NMR (101 MHz, $CDCl_3$):** δ 186.2, 163.5, 135.1, 132.5, 130.8, 130.2, 129.0, 120.2, 66.7.

These data are in accordance with the previous report.[33]

3.4.5.12. prop-2-yn-1-yl 2-oxo-2-phenylacetate (3l):



3l

$C_{11}H_8O_3$

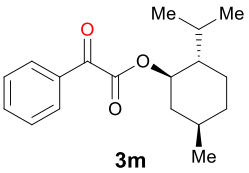
M. W. 188.18 g/mol

According to **GP-10** compound **3l** was prepared by using **1l** (40.0 mg, 0.2 mmol, 2.0 equiv) and **2a** (11.0 mg, 0.1 mmol, 1.0 equiv) in CH_2Cl_2 for 10 h at rt. Column chromatographic purification (petroleum ether/EtOAc 98:2 to 95:5) afforded **3l** as colourless oil (13.0 mg, 69%).

^{1}H NMR (400 MHz, $CDCl_3$): δ 8.02–8.01 (m, 2H), 7.69–7.65 (m, 1H), 7.54–7.50 (m, 2H), 4.96 (d, *J* = 2.5 Hz, 2H), 2.59 (t, *J* = 2.5 Hz, 1H). **^{13}C NMR (126 MHz, $CDCl_3$):** δ 185.2, 162.8, 135.2, 132.3, 130.1, 129.0, 77.2, 76.3, 53.3.

These data are in accordance with the previous report.[36]

3.4.5.13. (*1R,2S,5R*)-2-isopropyl-5-methylcyclohexyl 2-oxo-2-phenylacetate (3m):



3m

$C_{18}H_{24}O_3$

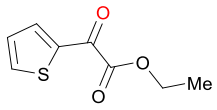
M. W. 288.38 g/mol

According to **GP-10** compound **3m** was prepared by using **1m** (60.0 mg, 0.2 mmol, 2.0 equiv) and **2a** (11.0 mg, 0.1 mmol, 1.0 equiv) in CH_2Cl_2 for 10 h at rt. Column chromatographic purification (petroleum ether/EtOAc 97:3 to 90:10) afforded **3m** as colourless oil (20.0 mg, 69%).

^{1}H NMR (400 MHz, $CDCl_3$): δ 7.98–7.95 (m, 2H), 7.67–7.63 (m, 1H), 7.53–7.49 (m, 2H), 4.99 (td, *J* = 11.0, 4.4 Hz, 1H), 2.17 (m, 1H), 1.94 (pd, *J* = 7.0, 2.7 Hz, 1H), 1.75–1.68 (m, 2H), 1.62–1.47 (m, 3H), 1.24–1.05 (m, 2H), 0.95 (d, *J* = 6.6 Hz, 3H), 0.89 (d, *J* = 7.0 Hz, 3H), 0.83 (d, *J* = 6.9 Hz, 3H). **^{13}C NMR (101 MHz, $CDCl_3$):** δ 186.9, 164.0, 134.9, 132.6, 130.0, 129.0, 46.9, 40.7, 34.1, 31.6, 26.2, 23.4, 22.1, 20.8, 16.2.

These data are in accordance with the previous report.[37]

3.4.5.14. ethyl 2-oxo-2-(thiophen-2-yl)acetate (3n):



3n

$C_8H_8O_3S$

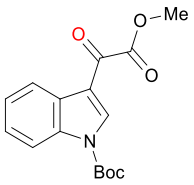
M. W. 184.21 g/mol

According to **GP-10** compound **3n** was prepared by using **1n** (39.0 mg, 0.2 mmol, 2.0 equiv) and **2a** (11.0 mg, 0.1 mmol, 1.0 equiv) in CH_2Cl_2 for 10 h at rt. Column chromatographic purification (petroleum ether/EtOAc 97:3 to 90:10) afforded **3n** as yellow oil (11.0 mg, 60%).

^{1}H NMR (400 MHz, $CDCl_3$): δ 8.13 (dd, *J* = 3.9, 1.2 Hz, 1H), 7.81 (dd, *J* = 4.9, 1.1 Hz, 1H), 7.19 (dd, *J* = 4.8, 4.0 Hz, 1H), 4.42 (q, *J* = 7.2 Hz, 2H), 1.42 (t, *J* = 7.2 Hz, 3H). **^{13}C NMR (101 MHz, $CDCl_3$):** δ 176.5, 161.7, 139.1, 137.6, 137.3, 128.7, 62.9, 14.1.

These data are in accordance with the previous report.[32]

3.4.5.15. *tert*-butyl 3-(2-methoxy-2-oxoacetyl)-1*H*-indole-1-carboxylate (3o):



3o

$C_{16}H_{17}NO_5$

M. W. 303.31 g/mol

According to **GP-10** compound **3o** was prepared by using **1o** (63.0 mg, 0.2 mmol, 2.0 equiv) and **2a** (11.0 mg, 0.1 mmol, 1.0 equiv) in CH_2Cl_2 for 10 h at rt. Column chromatographic purification (petroleum ether/EtOAc 97:3 to 90:10) afforded **3o** as colourless soild (14.0 mg, 46%).

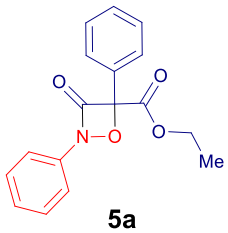
Melting Point: 128-130 ^oC

HRMS (ESI): m/z $[M+Na]^+$ Calculated for $[C_{16}H_{17}NO_5+Na]^+$: 326.1004; Found: 326.0997

^{1}H NMR (400 MHz, $CDCl_3$): δ 8.80 (s, 1H), 8.40–8.38 (m, 1H), 8.17–8.15 (m, 1H), 7.43–7.36 (m, 2H), 3.97 (s, 3H), 1.70 (s, 9H). **^{13}C NMR (101 MHz, $CDCl_3$):** δ 178.8, 162.4, 148.8, 137.3, 135.4, 127.5, 126.2, 125.0, 122.7, 116.3, 115.2, 86.0, 53.1, 28.1.

These data are in accordance with the previous report.[38]

3.4.5.16. ethyl 3-oxo-2,4-diphenyl-1,2-oxazetidine-4-carboxylate (5a):



5a

$C_{17}H_{15}NO_4$

M. W. 297.31 g/mol

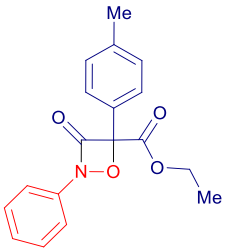
According to **GP-11** compound **5a** was prepared by using **4a** (44.0 mg, 0.2 mmol, 2.0 equiv) and **2a** (11.0 mg, 0.1 mmol, 1.0 equiv) in toluene for 3 h at rt. Column chromatographic purification (petroleum ether/EtOAc 99:1 to 95:5) afforded **5a** as light green oil (20.0 mg, 67%). For 1.0 mmol scale reaction: **1a** (436.0 mg, 1.0 mmol, 2.0 equiv), **2a** (1.0 equiv, 1 mmol, 107.0 mg), in dry toluene (5 mL, 0.2 M) was used and reaction was stirred for 5 h to get 57% isolated yield of **5a** (170.0 mg).

HRMS (ESI): m/z $[M+Na]^+$ Calculated for $[C_{17}H_{15}NNaO_4]^+$: 320.0899; Found: 320.0879.

^{1}H NMR (400 MHz, $CDCl_3$): δ 7.65–7.62 (m, 2H), 7.46–7.41 (m, 3H), 7.39–7.35 (m, 2H), 7.33–7.30 (m, 2H), 7.17–7.13 (m, 1H), 4.35 (qd, *J* = 7.1, 0.8 Hz, 2H), 1.31 (t, *J* = 7.1 Hz, 3H). **^{13}C**

NMR (101 MHz, $CDCl_3$): δ 164.6, 159.1, 137.0, 131.2, 130.1, 129.2, 129.0, 125.6, 125.5, 114.6, 97.0, 63.3, 14.1.

3.4.5.17. ethyl 3-oxo-2-phenyl-4-(*p*-tolyl)-1,2-oxazetidine-4-carboxylate (5b):



5b

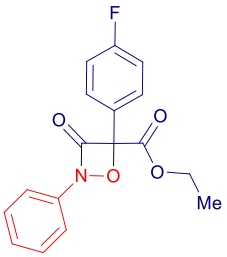
$C_{18}H_{17}NO_4$
M. W. 311.33 g/mol

According to **GP-11** compound **5b** was prepared by using **4b** (46.0 mg, 0.2 mmol, 2.0 equiv) and **2a** (11.0 mg, 0.1 mmol, 1.0 equiv) in toluene for 3 h at rt. Column chromatographic purification (petroleum ether/EtOAc 99:1 to 95:5) afforded **5b** as light green oil (19.0 mg, 61%).

HRMS (ESI): m/z $[M+Na]^+$ Calculated for $[C_{18}H_{17}NNaO_4]^+$: 334.1055; Found:.334.1016.

^{1}H NMR (400 MHz, $CDCl_3$): δ 7.55–7.45 (m, 2H), 7.40–7.34 (m, 2H), 7.32–7.28 (m, 2H), 7.25–7.23 (m, 2H), 7.17–7.12 (m, 1H), 4.34 (q, *J* = 7.2 Hz, 2H), 2.35 (s, 3H), 1.31 (t, *J* = 7.2 Hz, 3H). **^{13}C NMR (101 MHz, $CDCl_3$):** δ 164.8, 159.3, 140.3, 137.0, 129.7, 129.2, 128.3, 125.6, 125.4, 114.5, 97.1, 63.2, 21.4, 14.1.

3.4.5.18. ethyl 4-(4-fluorophenyl)-3-oxo-2-phenyl-1,2-oxazetidine-4-carboxylate (5c):



5c

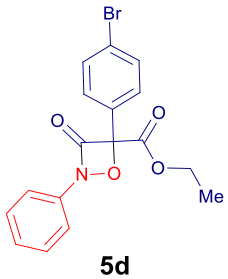
$C_{17}H_{14}FNO_4$
M. W. 315.30 g/mol

According to **GP-11** compound **5c** was prepared by using **4c** (47.0 mg, 0.2 mmol, 2.0 equiv) and **2a** (11.0 mg, 0.1 mmol, 1.0 equiv) in toluene for 4 h at rt. Column chromatographic purification (petroleum ether/EtOAc 99:1 to 95:5) afforded **5c** as light green oil (16.0 mg, 51%).

HRMS (ESI): m/z $[M+Na]^+$ Calculated for $[C_{17}H_{14}FNNaO_4]^+$: 338.0805; Found: 338.0799.

^{1}H NMR (400 MHz, $CDCl_3$): δ 7.65–7.61 (m, 2H), 7.40–7.36 (m, 2H), 7.32–7.29 (m, 2H), 7.18–7.11 (m, 3H), 4.35 (qd, *J*=7.1, 0.6 Hz, 2H), 1.31 (t, *J* = 7.1 Hz, 3H). **^{13}C NMR (126 MHz, $CDCl_3$):** δ 164.4, 163.7 (d, *J* = 249.6 Hz), 158.9, 136.9, 133.1 (d, *J* = 9.7 Hz), 129.3, 127.7 (d, *J* = 8.8 Hz), 125.6, 116.2 (d, *J* = 22.2 Hz), 114.6, 96.4, 63.4, 14.1. **^{19}F NMR: (376 MHz, $CDCl_3$):** δ -110.33.

3.4.5.19. ethyl 4-(4-bromophenyl)-3-oxo-2-phenyl-1,2-oxazetidine-4-carboxylate (5d):



5d

$C_{17}H_{14}BrNO_4$

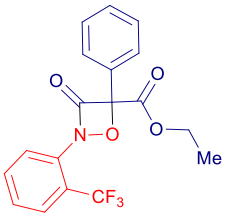
M. W. 376.20 g/mol

According to **GP-11** compound **5d** was prepared by using **4d** (47.0 mg, 0.2 mmol, 2.0 equiv) and **2a** (11.0 mg, 0.1 mmol, 1.0 equiv) in toluene for 1.5 h at rt. Column chromatographic purification (petroleum ether/EtOAc 99:1 to 90:10) afforded **5d** as light yellow oil (18.0 mg, 48%).

HRMS (ESI): m/z $[M+Na]^+$ Calculated for $[C_{17}H_{14}BrNNaO_4]^+$: 398.0004; Found:.398.0016.

^{1}H NMR (400 MHz, $CDCl_3$): δ 7.59–7.56 (m, 2H), 7.53–7.51 (m, 2H), 7.39–7.35 (m, 2H), 7.31–7.29 (m, 2H), 7.18–7.14 (m, 1H), 4.34 (qd, *J*=7.1, 0.8 Hz, 2H), 1.31 (t, *J* = 7.1 Hz, 3H) **^{13}C NMR (126 MHz, $CDCl_3$):** δ 164.2, 158.7, 136.9, 132.2, 130.2, 129.3, 127.2, 125.7, 124.5, 114.6, 96.4, 63.5, 14.1.

3.4.5.20. ethyl 3-oxo-4-phenyl-2-(2-(trifluoromethyl)phenyl)-1,2-oxazetidine-4-carboxylate (5e):



5e

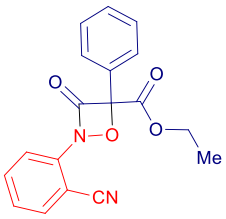
$C_{18}H_{14}F_3NO_4$
M. W. 365.30

According to **GP-11** compound **5e** was prepared by using **4a** (44.0 mg, 0.2 mmol, 2.0 equiv) and **2f** (17.5 mg, 0.1 mmol, 1.0 equiv) in toluene for 1.5 h at rt. Column chromatographic purification (petroleum ether/EtOAc 99:1 to 97:3) afforded **5e** as light green oil (17.0 mg, 47%).

HRMS (ESI): m/z $[M+Na]^+$ Calculated for $[C_{18}H_{14}NNaO_4]^+$: 388.0773; Found:.388.0762

^{1}H NMR (500 MHz, $CDCl_3$): δ 7.94–7.93 (m, 2H), 7.66–7.64 (m, 1H), 7.55–7.52 (m, 1H), 7.49–7.44 (m, 3H), 7.22–7.19 (m, 1H), 6.88–6.86 (m, 1H), 4.09 (q, *J* = 7.1 Hz, 2H), 0.93 (t, *J* = 7.1 Hz, 3H). **^{13}C NMR (126 MHz, $CDCl_3$):** δ 164.0, 160.7, 148.3, 133.5, 132.4, 132.3, 128.9, 128.5, 126.4 (q, *J* = 5.2 Hz), 124.9, 124.4, 119.6, 103.2, 61.6, 13.7. **^{19}F NMR: (376 MHz, $CDCl_3$):** δ -61.41.

3.4.5.21. ethyl 2-(2-cyanophenyl)-3-oxo-4-phenyl-1,2-oxazetidine-4-carboxylate (5f):



5f

$C_{18}H_{14}N_2O_4$
M. W. 322.31 g/mol

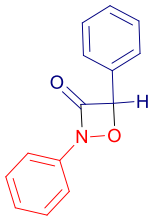
According to **GP-11** compound **5f** was prepared by using **4a** (44.0 mg, 0.2 mmol, 2.0 equiv) and **2g** (13.0 mg, 0.1 mmol, 1.0 equiv) in toluene for 2 h at rt. Column chromatographic purification (petroleum ether/EtOAc 99:1 to 85:15) afforded **5f** as light yellow oil (18.0 mg, 56%).

HRMS (ESI): m/z $[M+H]^+$ Calculated for $[C_{18}H_{15}N_2O_4]^+$: 323.1032; Found: 323.1019.

^{1}H NMR (400 MHz, $CDCl_3$): δ 7.70–7.63 (m, 3H), 7.62–7.57 (m, 2H), 7.50–7.44 (m, 3H), 7.33–7.29 (m, 1H), 4.36 (q, *J* = 7.1 Hz, 2H), 1.32 (t, *J* = 7.1 Hz, 3H). **^{13}C NMR (101 MHz,**

$CDCl_3$): δ 164.0, 160.1, 139.1, 134.2, 133.8, 130.7, 130.2, 129.1, 126.7, 125.5, 118.6, 115.9, 102.2, 98.3, 63.6, 14.1.

3.4.5.22. 2,4-diphenyl-1,2-oxazetidin-3-one (5g):



5g

$C_{14}H_{11}NO_2$

M. W. 225.24 g/mol

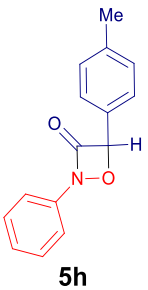
According to **GP-11** compound **5g** was prepared by using **4e** (29.0 mg, 0.2 mmol, 2.0 equiv) and **2a** (11.0 mg, 0.1 mmol, 1.0 equiv) in toluene for 1.5 h at rt. Column chromatographic purification (petroleum ether/EtOAc 99:1 to 95:5) afforded **5g** as colourless oil (7.0 mg, 31%).

Alternatively, compound **5g** was prepared according to **GP-11** by using **4f** (38.0 mg, 0.2 mmol, 2.0 equiv) and **2a** (11.0 mg, 0.1 mmol, 1.0 equiv) in toluene for 1.5 h at rt. Column chromatographic purification (petroleum ether/EtOAc 99:1 to 95:5) afforded **5g** as colourless oil (11.0 mg, 49%).

HRMS (ESI): m/z $[M+Na]^+$ Calculated for $[C_{14}H_{11}NNaO_2]^+$: 248.0687; Found:.248.0679.

^{1}H NMR (400 MHz, $CDCl_3$): δ 7.50–7.48 (m, 2H), 7.46–7.42 (m, 3H), 7.40–7.38 (m, 2H), 7.34–7.32 (m, 2H), 7.18–7.14 (m, 1H), 6.35 (s, 1H). **^{13}C NMR (126 MHz, $CDCl_3$):** δ 162.7, 137.3, 131.4, 130.2, 129.1, 129.1, 127.3, 124.9, 114.1, 92.7.

3.4.5.23. 2-phenyl-4-(*p*-tolyl)-1,2-oxazetidin-3-one (5h):



5h

$C_{15}H_{13}NO_2$

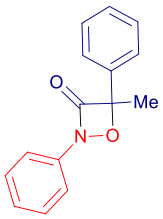
M. W. 239.27 g/mol

According to **GP-11** compound **5h** was prepared by using **4g** (40.0 mg, 0.2 mmol, 2.0 equiv) and **2a** (11.0 mg, 0.1 mmol, 1.0 equiv) in toluene for 1.5 h at rt. Column chromatographic purification (petroleum ether/EtOAc 99:1 to 95:5) afforded **5h** as colourless oil (12.0 mg, 50%).

HRMS (ESI): m/z $[M+Na]^+$ Calculated for $[C_{15}H_{13}NNaO_2]^+$: 262.0844; Found:.262.0858

^{1}H NMR (500 MHz, $CDCl_3$): δ 7.40–7.36 (m, 5H), 7.33–7.31 (m, 2H), 7.31–7.25 (m, 1H), 7.17–7.15 (m, 1H), 6.31 (s, 1H), 2.37 (s, 3H). **^{13}C NMR (126 MHz, $CDCl_3$):** δ 162.9, 140.6, 137.3, 129.9, 129.2, 128.5, 127.6, 124.8, 114.1, 92.8, 21.5.

3.4.5.24. 4-methyl-2,4-diphenyl-1,2-oxazetidin-3-one (5i):



5i

$C_{15}H_{13}NO_2$

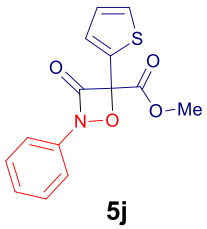
M. W. 239.27 g/mol

According to **GP-10** compound **5i** was prepared by using **4h** (32.0 mg, 0.2 mmol, 2.0 equiv) and **2a** (11.0 mg, 0.1 mmol, 1.0 equiv) in CH_2Cl_2 for 10 h at rt. Column chromatographic purification (petroleum ether/EtOAc 99:1 to 97:3) afforded **5i** as light yellow oil (17.0 mg, 71%).

HRMS (ESI): m/z $[M+H]^+$ Calculated for $[C_{15}H_{14}NO_2]^+$: 240.1025; Found: 240.1021.

^{1}H NMR (400 MHz, $CDCl_3$): δ 7.56–7.53 (m, 2H), 7.44–7.40 (m, 2H), 7.39–7.35 (m, 3H), 7.32–7.29 (m, 2H), 7.15–7.11 (m, 1H), 2.04 (s, 3H). **^{13}C NMR (101 MHz, $CDCl_3$):** δ 165.2, 137.4, 136.4, 129.2, 129.1, 128.9, 124.9, 124.7, 114.1, 98.5, 22.4.

3.4.5.25. methyl 3-oxo-2-phenyl-4-(thiophen-2-yl)-1,2-oxazetidine-4-carboxylate (5j):



5j

$C_{14}H_{11}NO_4S$

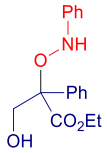
M. W. 289.3064 g/mol

According to **GP-11** compound **5j** was prepared by using **4k** (42.0 mg, 0.2 mmol, 2.0 equiv) and **2a** (11.0 mg, 0.1 mmol, 1.0 equiv) in toluene for 4 h at rt. Column chromatographic purification (petroleum ether/EtOAc 99:1 to 97:3) afforded **5j** as green oil (12.5 mg, 43%).

HRMS (ESI): m/z $[M+Na]^+$ Calculated for $[C_{14}H_{11}NNaO_4S]^+$: 312.0306; Found:.312.0311

^{1}H NMR (400 MHz, $CDCl_3$ δ 7.54 (dd, *J*=5.0, 0.9, 1H), 7.42 (dd, *J*=3.7, 0.9, 1H), 7.33–7.29 (m, 2H), 7.15–7.09 (m, 2H), 6.96–6.94 (m, 2H), 3.64 (s, 3H). **^{13}C NMR (101 MHz, $CDCl_3$):** δ 164.5, 154.0, 149.5, 140.6, 131.7, 131.6, 129.0, 128.0, 125.3, 119.9, 118.6, 52.4.

3.4.5.26. ethyl 3-hydroxy-2-phenyl-2-((phenylamino)oxy)propanoate (6a):



6a

$C_{17}H_{19}NO_4$

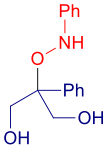
M. W. 301.34

According to **GP-12** compound **6a** was prepared by using **5a** (15.0 mg, 0.05 mmol, 1.0 equiv) and $NaBH_4$ (8.0 mg, 0.2 mmol, 4.0 equiv) in EtOH for 0.5 h at 0 °C. Column chromatographic purification (petroleum ether/EtOAc 97:3 to 85:15) afforded **6a** as colourless liquid (12.0 mg, 80%).

^{1}H NMR (500 MHz, $CDCl_3$): δ 7.70 (s, 1H), 7.56–7.54 (m, 2H), 7.40–7.37 (m, 2H), 7.36–7.34 (m, 1H), 7.29–7.26 (m, 2H), 7.11–7.09 (m, 2H), 7.03–7.00 (m, 1H), 4.45 (d, *J* = 12.4 Hz, 1H), 4.34 (d, *J* = 12.3 Hz, 1H), 4.29 (qd, *J* = 7.1, 3.3 Hz, 2H), 1.25 (t, *J* = 7.1 Hz, 3H). **^{13}C NMR (126 MHz, $CDCl_3$):** δ 171.2, 147.5, 136.0, 129.1, 128.8, 128.7, 126.1, 123.2, 115.9, 88.2, 67.8, 61.9, 14.1.

HRMS (ESI): m/z $[M+Na]^+$ Calculated for $[C_{17}H_{19}NNaO_4]^+$: 324.1212; Found: 324.1201.

3.4.5.27. 2-phenyl-2-((phenylamino)oxy)propane-1,3-diol (6b):



6b

$C_{15}H_{17}NO_3$

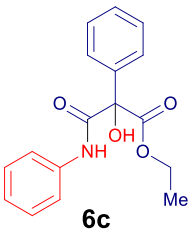
M. W. 259.30

According to **GP-13** compound **6b** was prepared by using **5a** (15.0 mg, 0.05 mmol, 1.0 equiv) and $NaBH_4$ (19.0 mg, 0.5 mmol, 10.0 equiv) in EtOH for 3 h at 0 °C. Column chromatographic purification (petroleum ether/EtOAc 97:3 to 80:20) afforded **6b** as colourless liquid (10.0 mg, 77%).

^{1}H NMR (500 MHz, $CDCl_3$): δ 7.55–7.53 (m, 2H), 7.45–7.41 (m, 2H), 7.37–7.33 (m, 1H), 7.31–7.28 (m, 2H), 7.11–7.10 (m, 2H), 7.04–7.01 (m, 1H), 6.95 (s, 1H), 4.18 (s, 4H), 2.62 (br s, 2H). **^{13}C NMR (126 MHz, $CDCl_3$):** δ 147.7, 138.7, 129.2, 129.0, 128.2, 126.5, 123.3, 115.8, 85.8, 67.2.

HRMS (ESI): m/z $[M+Na]^+$ Calculated for $[C_{15}H_{17}NNaO_3]^+$: 282.1106; Found: .282.1116.

3.4.5.28. ethyl 2-hydroxy-3-oxo-2-phenyl-3-(phenylamino)propanoate (6c):



6c

$C_{17}H_{17}NO_4$
M. W. 299.32 g/mol

According to **GP-14** compound **6c** was prepared by using **5a** (15.0 mg, 0.05 mmol, 1.0 equiv) and Zinc powder (16.0 mg, 0.25 mmol, 5 equiv) in DCM. To this suspension was added acetic acid (14 µL, 0.25 mmol, 5 equiv) portionwise over 3 h. The mixture was stirred for an additional 3 h at r.t., and then the solids were removed by filtration through Celite. The filtrate was concentrated under reduced pressure. Column chromatographic purification (petroleum ether/EtOAc 95:5 to 75:25) afforded **6c** as colourless liquid (12.5 mg, 84%).

^{1}H NMR (400 MHz, $CDCl_3$): δ 8.90 (br s, 1H), 7.77–7.75 (m, 2H), 7.55–7.53 (m, 2H), 7.41–7.30 (m, 5H), 7.14–7.10 (m, 1H), 4.98 (br s, 1H), 4.42–4.31 (m, 2H), 1.34 (t, J = 7.2 Hz, 4H). **^{13}C NMR (126 MHz, $CDCl_3$):** δ 171.3, 166.2, 137.3, 137.0, 129.1, 128.8, 128.4, 126.1, 124.9, 119.8, 80.0, 64.0, 14.0.

HRMS (ESI): m/z $[M+Na]^+$ Calculated for $[C_{17}H_{17}NNaO_4]^+$: 322.1055; Found: . 322.1064.

3.5. References:

1. Curtius, T. On the action of nitrous acid on hydrochloric acid glycocolla ether. *Ber. Dtsch. Chem. Ges.* **1883**, 16, 2230.
2. (a) Ren, Y.-Y.; Zhu, S.-F.; Zhou, Q.-L. Chiral proton-transfer shuttle catalysts for carbene insertion reactions. *Org. Biomol. Chem.* **2018**, *16*, 3087–3094. (b) Empel, C.; Koenigs, R. M. Sustainable Carbene Transfer Reactions with Iron and Light. *Synlett* **2020**, 1929–1934.
3. For reviews on metal catalyzed transformations of diazo compounds see: (a) Doyle, M. P.; Duffy, R.; Ratnikov, M.; Zhou, L. Catalytic carbene insertion into C−H bonds. *Chem. Rev.* **2010**, *110*, 704. (b) Ford, A.; Miel, H.; Ring, A.; Slattery, C. N.; Maguire, A. R.; McKervey, M. A. Modern Organic Synthesis with α-Diazocarbonyl Compounds. *Chem. Rev.*, **2015**, *115*, 9981.
4. (a) Wang, J.; Burdzinski, G.; Kubicki, J.; Platz, M. S. Ultrafast UV−Vis and IR Studies of *p*-Biphenylyl Acetyl and Carbomethoxy Carbenes. *J. Am. Chem. Soc.* **2008**, *130*, 11195–11209. (b) Galkina, O. S.; Rodina, L. L. Photochemical transformations of diazocarbonyl compounds: expected and novel reactions. *Russ. Chem. Rev.* **2016**, *85*, 537–555.
5. Selected reviews on visible-light-driven transformations and references therein. (a) Xuan, J.; He, X.-K.; Xiao, W.-J. Visible light-promoted ring-opening functionalization of three-membered carbo-and heterocycle. *Chem. Soc. Rev.*, **2020**, *49*, 2546–2556. (b) Yu, X.-Y.; Chen, J.-R.; Xiao, W.-J. Visible Light-Driven Radical-Mediated C–C Bond Cleavage/Functionalization in Organic Synthesis. *Chem. Rev.* **2021**, *121*, 506−561.
6. Jurberg I. D.; Davies, H. M. L. Blue light-promoted photolysis of aryldiazoacetates. *Chem. Sci.*, **2018**, *9*, 5112–5118.
7. Recent reviews on photochemical reactions of diazo compounds and references therein. (a) Ciszewski, Ł. W.; Rybicka-Jasińska, K.; Gryko, D. Recent developments in photochemical reactions of diazo compounds. *Org. Biomol. Chem.*, **2019**, *17*, 432–448. (b) Yang, Z.; Stivanin, M. L.; Jurberg, I. D.; Koenigs R. M. Visible light-promoted reactions with diazo compounds: a mild and practical strategy towards free carbene intermediates. *Chem. Soc. Rev.*, **2020**, *49*, 6833–6847. (c) Durka, J.; Turkowska, J.; Gryko, D.; Lightening Diazo Compounds? *ACS Sustainable Chem. Eng.*, **2021**, *9*, 8895−8918.
8. Selective reviews on oxygenation and oxygen transfer and references therein. (a) Melone, L.; Punta, C. Metal-free aerobic oxidations mediated by N-hydroxyphthalimide. A concise review. *Beilstein J. Org. Chem.* **2013**, *9*, 1296–1310. (b) Bian, C.; Singh, A. K.; Niu, L.; Yi, H.; Lei, A. Visible-Light-Mediated

Oxygenation Reactions using Molecular Oxygen. *Asian J. Org. Chem.* **2017**, *6*, 386–396. (c) Petrosyan, A.; Hauptmann, R.; Pospech, J. Heteroarene *N*-Oxides as Oxygen Source in Organic Reactions. *Eur. J. Org. Chem.* **2018**, 5237–5252.

9. (a) Jeong, J.; Lee, D.; Chang, S. Copper-catalyzed oxygen atom transfer of N-oxides leading to a facile deoxygenation procedure applicable to both heterocyclic and amine N-oxides. *Chem. Commun.*, **2015**, *51*, 7035–7038. (b) O'Connor, N. R.; Bolgar, P.; Stoltz, B. M. Development of a simple system for the oxidation of electron-rich diazo compounds to ketones. *Tetrahedron Lett.* **2016**, *57*, 849. (c) Yu, Y.; Sha, Q.; Cui, H.; Chandler, K. S.; Doyle, M. P. Displacement of Dinitrogen by Oxygen: A Methodology for the Catalytic Conversion of Diazocarbonyl Compounds to Ketocarbonyl Compounds by 2,6-Dichloropyridine-N-oxide. *Org. Lett.* **2018**, *20*, 776−779. (d) B. S., A.; Bhattacharjee, R.; Gupta, S.; Ahammad, S.; Datta, A.; Kundu, S. Deoxygenation of nitrosoarene by N-heterocyclic carbene (NHC): an elusive Breslow-type intermediate bridging carbene and nitrene. *Chem. Commun.*, **2020**, *56*, 12166-12169.
10. Wolff, L. About diazoanhydrides. *Justus Liebigs Ann. Chem.*, **1902**, *325*, 129.
11. Reviews on photochemical *in situ* generated ketene intermediate via Wolff rearrangement and its reactivity, references therein. (a) Kirmse, W. 100 Years of the Wolff Rearrangement. *Eur. J. Org. Chem.* **2002**, 2193−2256. (b) Hua, T.-B.; Yang, Q.-Q.; Zou, Y.-Q. Recent Advances in Enantioselective Photochemical Reactions of Stabilized Diazo Compounds. *Molecules* **2019**, *24*, 3191.
12. (a) Yamamoto, H.; Momiyama, N. Rich chemistry of nitroso compounds. *Chem. Commun.* **2005**, 3514–3525. (b) Bodnar, B. S.; Miller, M. J. The Nitrosocarbonyl Hetero-Diels–Alder Reaction as a Useful Tool for Organic Syntheses. *Angew. Chem., Int. Ed.*, **2011**, *50*, 5630–5647. (c) Carosso S.; Miller, M. J. Nitroso Diels–Alder (NDA) reaction as an efficient tool for the functionalization of diene-containing natural products. *Org. Biomol. Chem.*, **2014**, *12*, 7445–7468. (d) Huang, J.; Chen, Z.; Yuan J.; Peng, Y. Recent advances in highly selective applications of nitroso compounds. *Asian J. Org. Chem.*, **2016**, *5*, 951–960.
13. (a) Kerber R. C.; Cann M. C. Mechanism of Cycloaddition of Nitroso Compounds with Diphenylketene. *J. Org. Chem.* **1974**, *39*, 2552–2558; (b) Dochnahl, M.; Fu, G. C. Catalytic Asymmetric Cycloaddition of Ketenes and Nitroso Compounds: Enantioselective Synthesis of α-Hydroxycarboxylic Acid Derivatives. *Angew. Chem. Int. Ed.*, **2009**, *48*, 2391–2393. (c) Chatterjee, I.; Jana, C. K.; Steinmetz, M. S. Grimme, Studer A. Copper-Catalyzed Enantioselective [2+2] Cycloadditions of 2-Nitrosopyridine with Ketenes. *Adv. Synth. Catal.* **2010**, *352*, 945–948. (d) Wang, T.; Huang, X.-L.; Ye, S. Enantioselective formal [2+2] cycloaddition of ketenes with

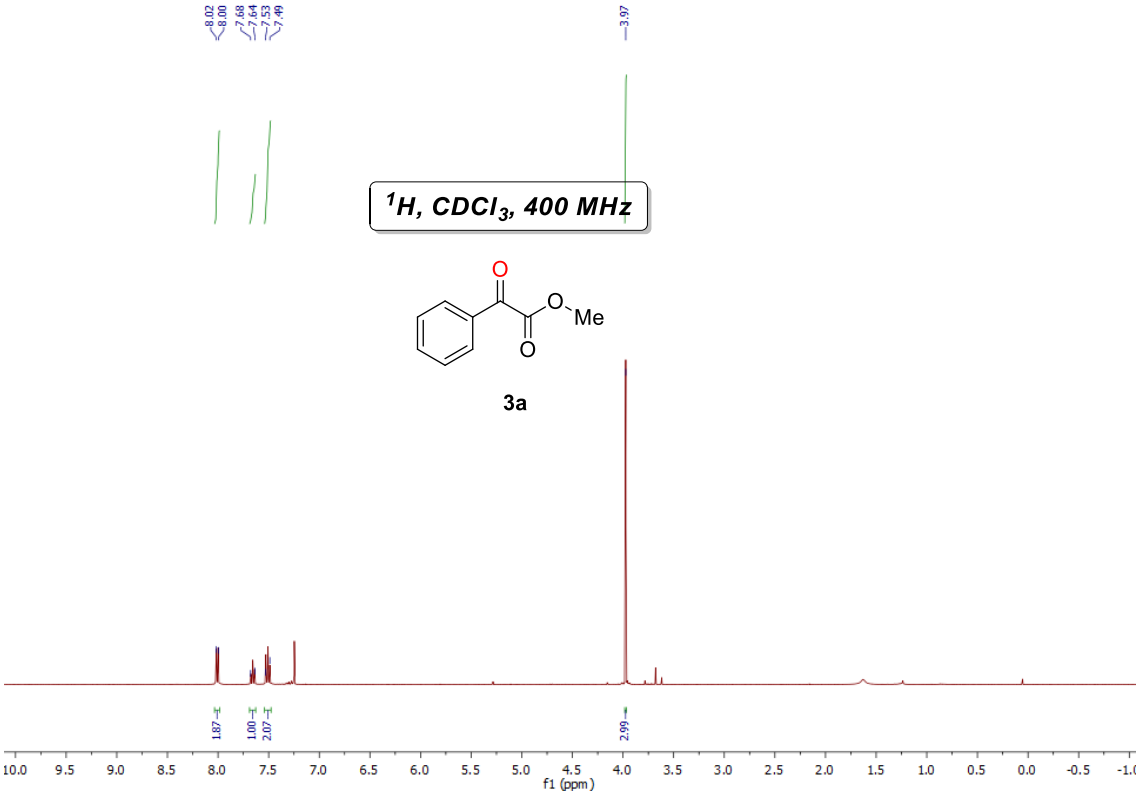
nitroso compounds catalyzed by N-heterocyclic carbenes. *Org. Biomol. Chem.* **2010**, *8*, 5007–5011.

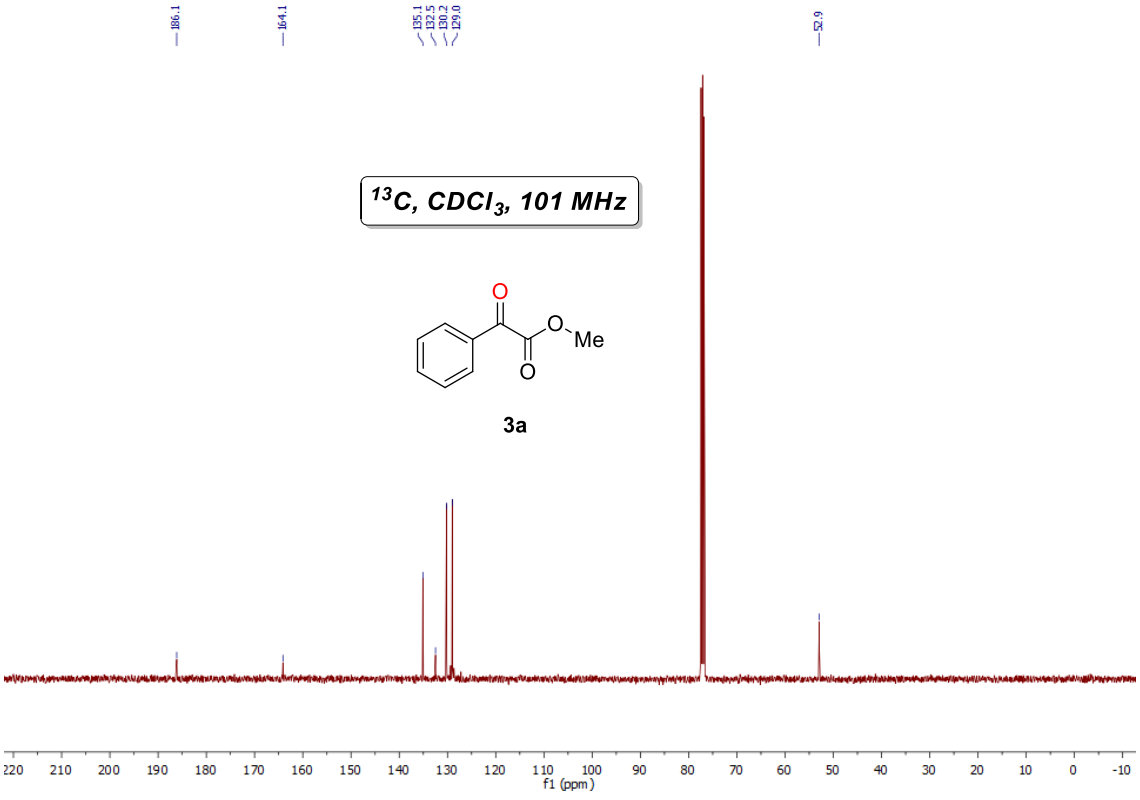
14. Keipour, H.; Ollevier T. Iron-Catalyzed Carbene Insertion Reactions of α-Diazoesters into Si–H Bonds. *Org. Lett.* **2017**, *19*, 5736–5739.
15. Thurow, S.; Fernandes, A. A. G.; Quevedo-Acosta, Y.; de Oliveira, M. F.; de Oliveira, M. G.; Jurberg, I. D. Preparation of Organic Nitrates from Aryldiazoacetates and $Fe(NO_3)_3{\cdot}9H_2O$ *Org. Lett.* **2019**, *21*, 6909–6913.
16. Chan, Q.; Xing, Y.-C.; Chow, S.-F.; Hung, Yu, W.-Y. Photoredox Decarboxylative C(*sp3*)–*N* Coupling of α-Diazoacetates with Alkyl *N*-Hydroxyphthalimide Esters for Diversified Synthesis of Functionalized N-Alkyl Hydrazones *Org. Lett.* **2019**, *21*, 8037–8043.
17. Davies, H. M. L.; Townsend, R. J. Catalytic Asymmetric Cyclopropanation of Heteroaryldiazoacetates *J. Org. Chem.* **2001**, *66*, 6595–6603.
18. Jiang, Y.; Chen, X.; Zheng, Y.; Xue, Z.; Shu, C.; Yuan, W.; Zhang, X. Highly Diastereoselective and Enantioselective Synthesis of α-Hydroxy β-Amino Acid Derivatives: Lewis Base Catalyzed Hydrosilylation of α-Acetoxy β-Enamino Esters *Angew. Chem. Int. Ed.* **2011**, *50*, 7304–7307.
19. Wang, J.; Wang, M.; Chen, K.; Zha, S.; Song, C.; Zhu, J. C–H Activation-Based Traceless Synthesis via Electrophilic Removal of a Directing Group. Rhodium(III)-Catalyzed Entry into Indoles from N-Nitroso and α-Diazo-β-keto Compounds *Org. Lett.* **2016**, *18*, 1178–1181.
20. Liu, Q.; Li, M.; Xiong, R.; Mo, F. Direct Carboxylation of the Diazo Group ipso-C(sp2)–H bond with Carbon Dioxide: Access to Unsymmetrical Diazomalonates and Derivatives *Org. Lett.* **2017**, *19*, 6756–6759.
21. Rajasekar, S.; Anbarasan, P. A General Proline-Catalyzed Synthesis of 4,5-Disubstituted N-Sulfonyl-1,2,3-Triazoles from 1,3-Dicarbonyl Compounds and Sulfonyl Azide *Chem. Asian J.* **2019**, *14*, 4563 –4567.
22. Marichev, K. O.; Wang, Y.; Carranco, A. M.; Garcia, E. C.; Yu, Z.-X.; Doyle, M. P. Rhodium(II)-catalysed generation of cycloprop-1-en-1-yl ketones and their rearrangement to 5-aryl-2-siloxyfurans *Chem. Commun.*, **2018**, *54*, 9513-9516.
23. Yang, J.; Ke, C.; Zhang, D.; Liu, X.; Feng, X. Enantioselective Synthesis of 2,2,3-Trisubstituted Indolines via Bimetallic Relay Catalysis of α-Diazoketones with Enones *Org. Lett.* **2018**, *20*, 4536–4539.
24. Lippincott, D. J.; Linstadt, R. T. H.; Maser, M. R.; Gallou, F.; Lipshutz, B. H. Synthesis of Functionalized 1,3-Butadienes via Pd-Catalyzed Cross-Couplings of Substituted Allenic Esters in Water at Room Temperature *Org. Lett.* **2018**, *20*, 4719–4722.
25. Tibiletti, F.; Simonetti, M.; Nicholas, K. M.; Palmisano, G.; Parravicini, M.; Imbesi, F.; Tollari, S.; Penoni, A. One-pot synthesis of meridianins and meridianin analogues via indolization of nitrosoarenes*Tetrahedron*, **2010**, *66*, 1280–1288.
26. Priewisch, B.; Braun, K. R. Efficient preparation of nitrosoarenes for the synthesis of azobenzenes *J. Org. Chem.*, **2005**, *70*, 2350–2352.

27. Jankowiak, A.; Obijalska, E.; Kaszynski, P.; Pieczonka, A.; Young, V. G. Synthesis and structural, spectroscopic, and electrochemical characterization of benzo[c] quinolizinium and its 5-aza-, 6-aza, and 5, 6-diaza analogues *Tetrahedron* **2011**, *67*, 3317–3327.
28. Arcadi, A.; Chiarini, M.; Vecchio, L. D.; Marinelli, F.; Michelet, V. Silver-versus gold-catalyzed sequential oxidative cyclization of unprotected 2-alkynylanilines with oxone *Chem. Commun.* **2016**, *52*, 1458–1461.
29. Defoin, A. Simple preparation of nitroso benzenes and nitro benzenes by oxidation of anilines with H_2O_2 catalysed with molybdenum salts *Synthesis*, **2004**, *5*, 706–710.
30. Min, G. M.; Bang, S.; Lee, H.; Yu, B. C. A photoswitchable methylene-spaced fluorinated aryl azobenzene monolayer grafted on silicon *Chem. Commun*. **2010**, *46*, 5232–5234.
31. Yu, Q.; Zhang, Y.; Wan, J.-P. Ambient and aerobic carbon–carbon bond cleavage toward α-ketoester synthesis by transition-metal-free photocatalysis *Green Chem.*, **2019**, *21*, 3436–3441.
32. Liu, R.; Liu, Q.; Meng, H.; Ding, H.; Hao, J.; Ji, Z.; Yue, H.; Wei, W. Metal-free visible-light-induced aerobic oxidation of α-diazoesters leading to α-ketoesters in air *Org. Chem. Front.*, **2021**, *8*, 1970−1975.
33. Wang, S. R.; Radosevich, A. T. $P(NMe_2)_3$-Mediated Umpolung Alkylation and Nonylidic Olefination of α-Keto Esters *Org. Lett.* **2015**, *17*, 3810−3813.
34. Battula, S.; Battini, N.; Singh, D.; Ahmed, Q. N. 2-Oxo promoted hydrophosphonylation & aerobic intramolecular nucleophilic displacement reaction *Org. Biomol. Chem.*, **2015**, *13*, 8637−8641.
35. Raghunadha, A.; Meruvaa, S. B.; Kumara, N. A.; Kumara, G. S.; Raob, L. V.; Kumar, U. K. S. An efficient and practical synthesis of aryl and hetaryl α-keto esters *Synthesis* **2012**, *2*, 283−289.
36. Luo, X.; He, R.; Liu, Q.; Gao, Y.; Li, J.; Chen, X.; Zhu, Z.; Huang, Y.; Li, Y. Metal-Free Oxidative Esterification of Ketones and Potassium Xanthates: Selective Synthesis of α-Ketoesters and Esters *J. Org. Chem.* **2020**, *85*, 5220−5230.
37. Markey, S. J.; Lewis, W.; Moody, C. J. A new route to α-carbolines based on 6π-electrocyclization of indole-3-alkenyl oximes *Org. Lett.* **2013**, *15*, 6306–6308.
38. Dochnahl, M.; Fu, G. C. Catalytic asymmetric cycloaddition of ketenes and nitroso compounds: enantioselective synthesis of α-hydroxycarboxylic acid derivatives *Angew. Chem. Int. Ed.*, **2009**, *48*, 2391–2393.
39. Long, Z.; Wang, Z.; Zhou, D.; Wan, D.; You, J. Rh(III)-Catalyzed Regio- and Chemoselective [4 + 1]-Annulation of Azoxy Compounds with Diazoesters for the Synthesis of 2*H*-Indazoles: Roles of the Azoxy Oxygen Atom *Org. Lett.* **2017**, *19*, 2777–2780.

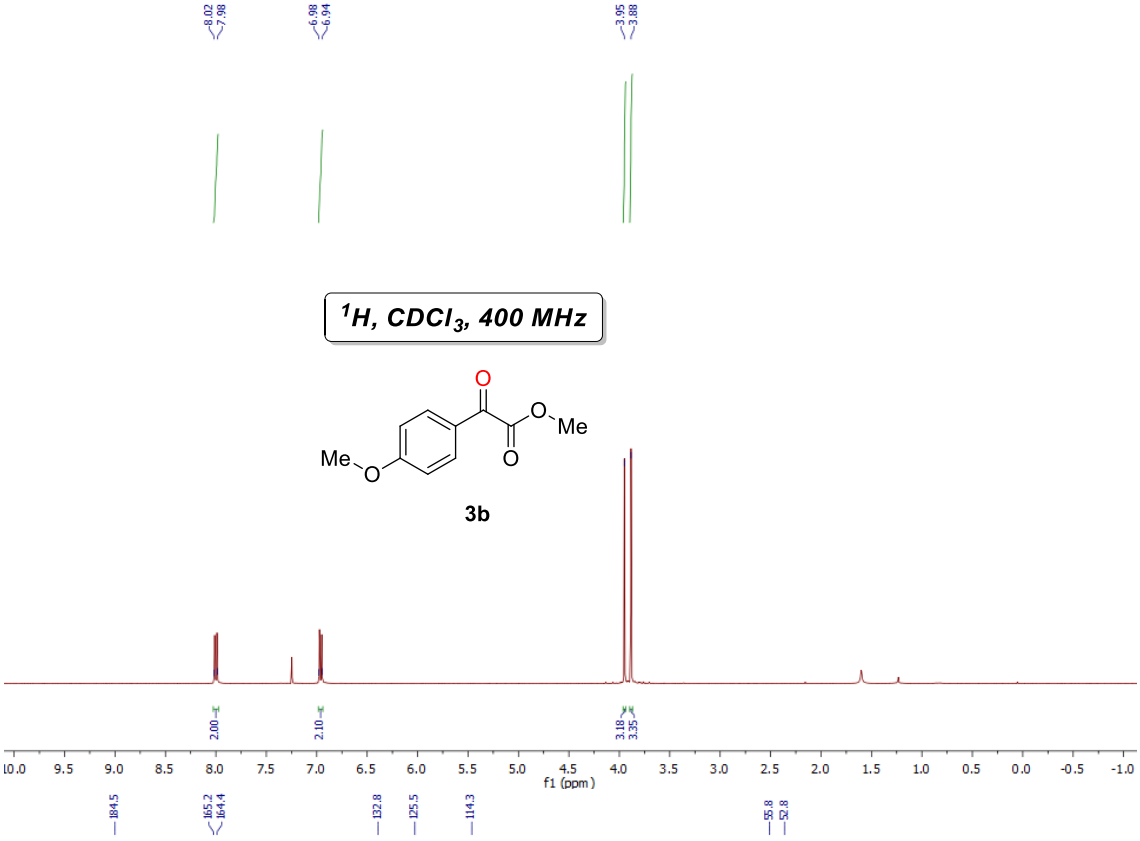
3.6. NMR Spectra:

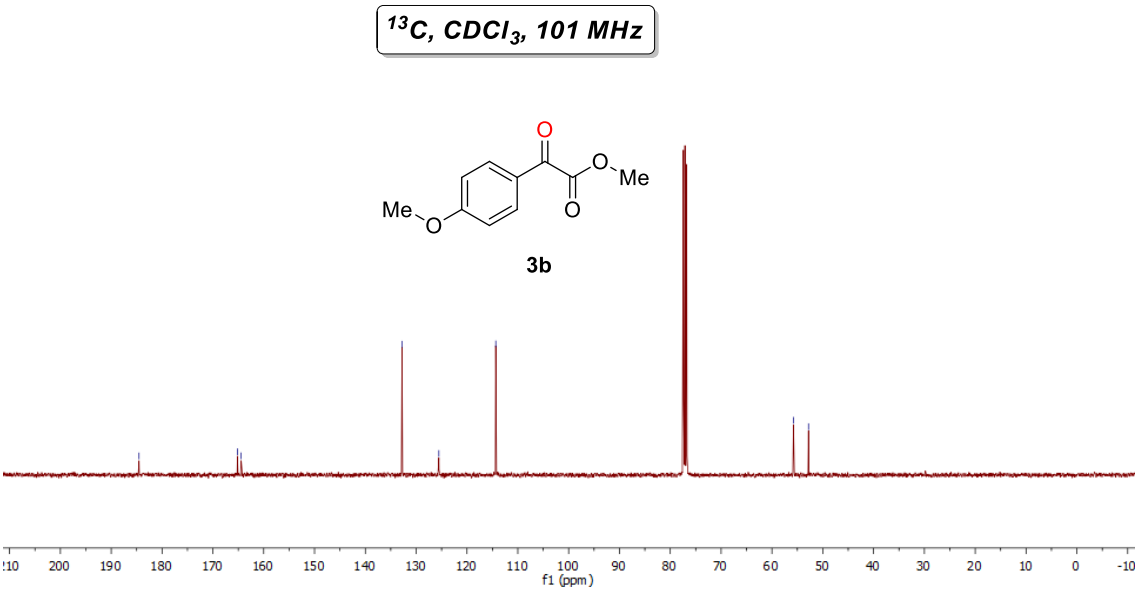
3.6.1. methyl 2-oxo-2-phenylacetate (3a):



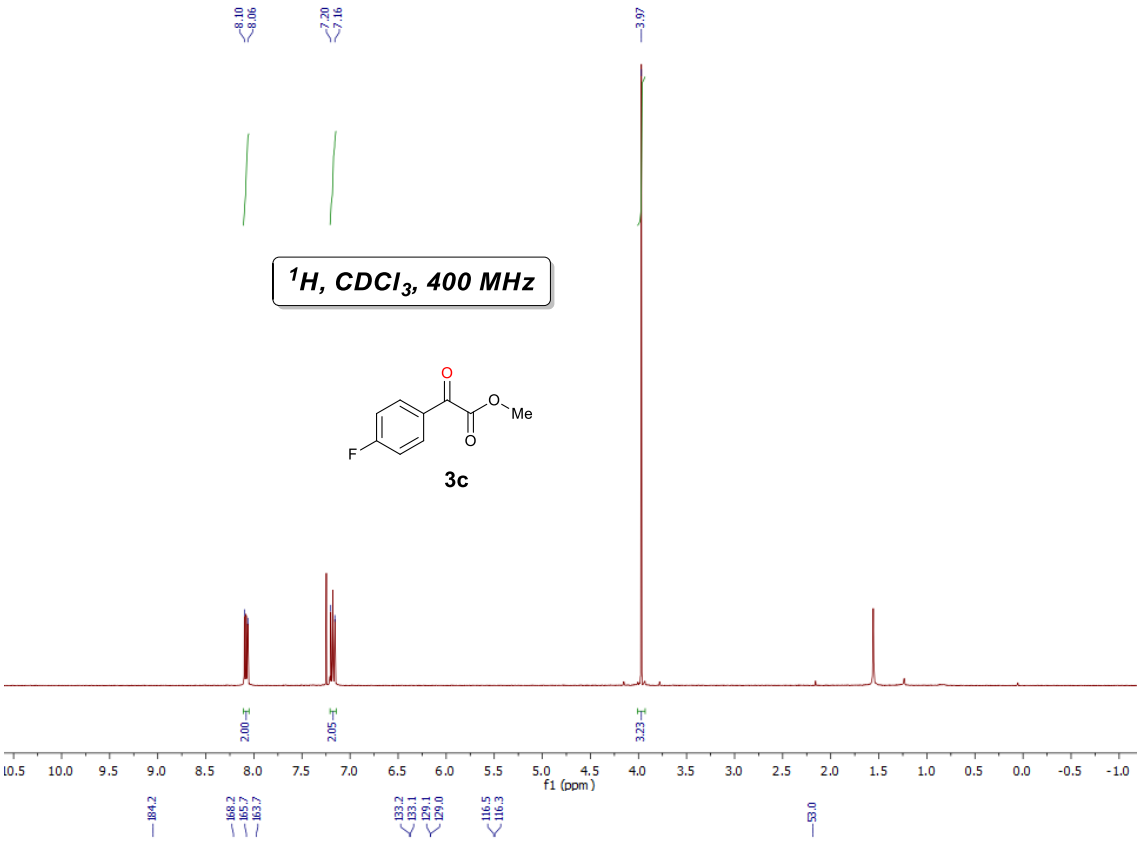


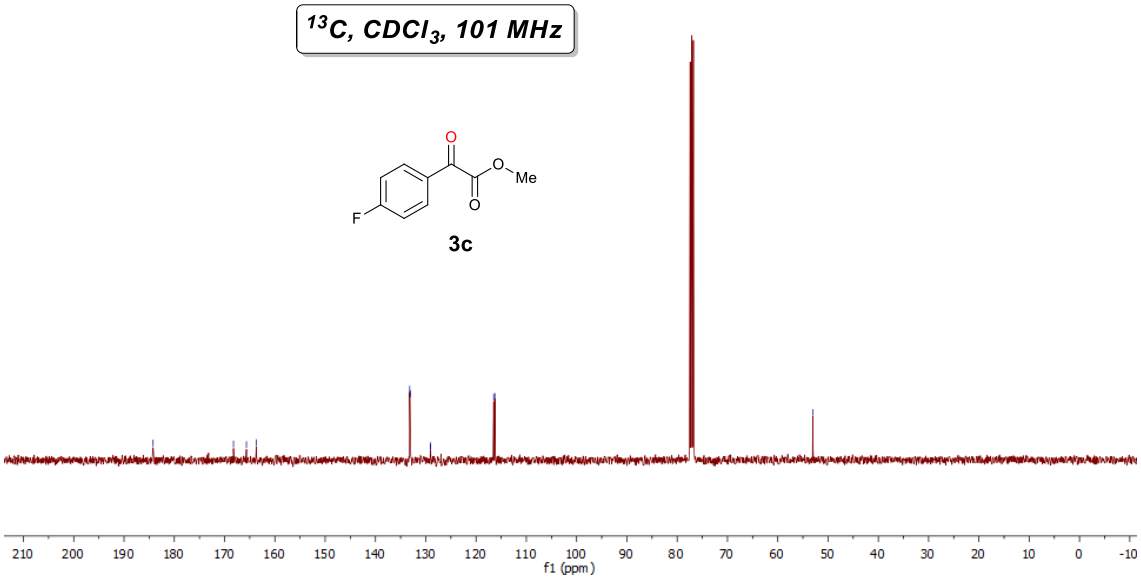
3.6.2. methyl 2-(4-methoxyphenyl)-2-oxoacetate (3b):

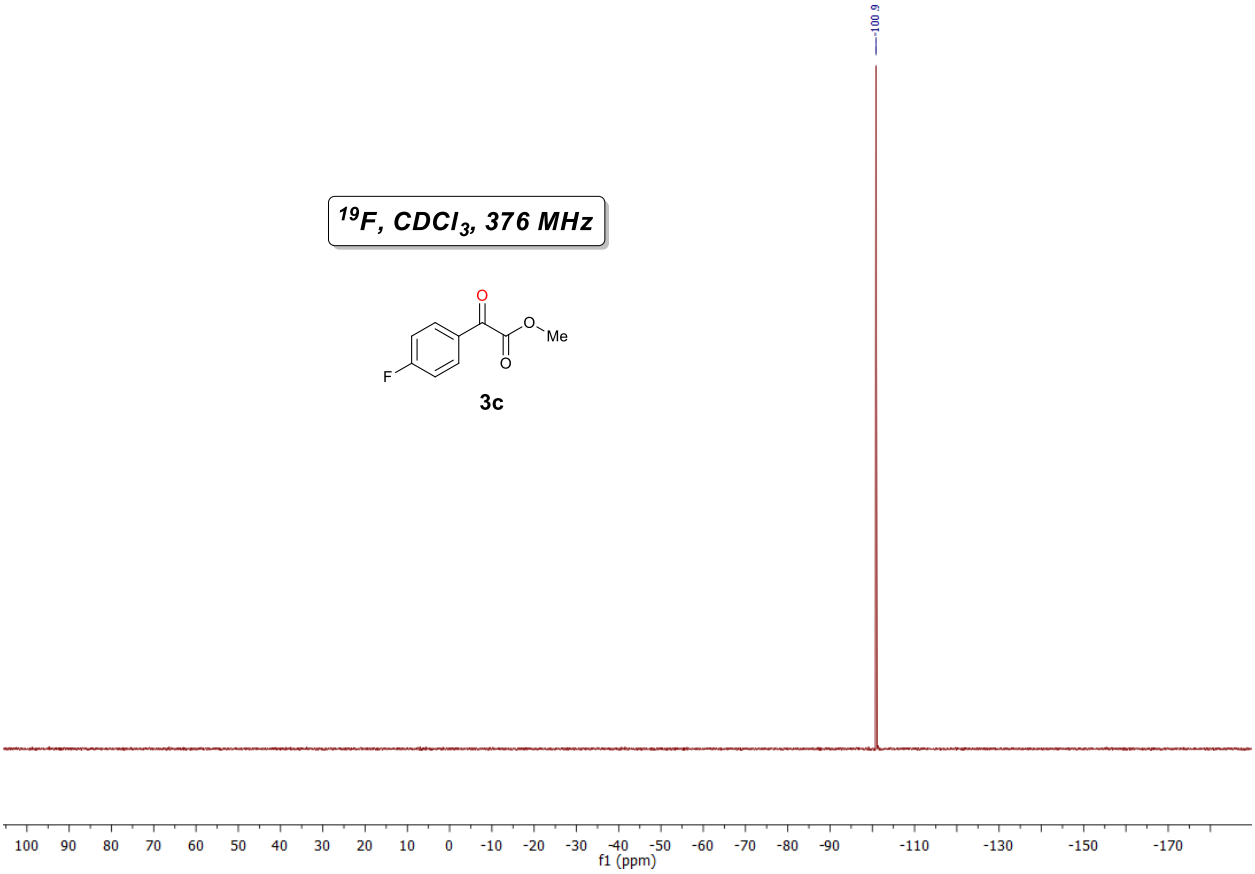




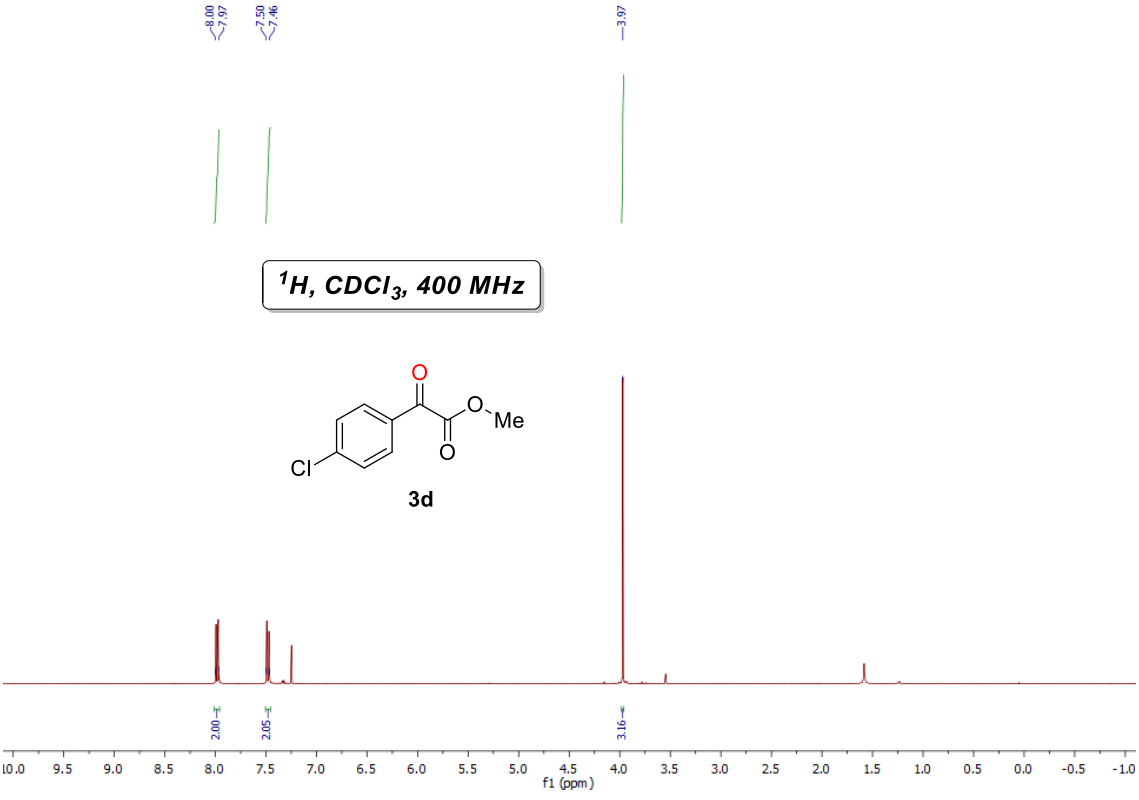
3.6.3. methyl 2-(4-fluorophenyl)-2-oxoacetate (3c):

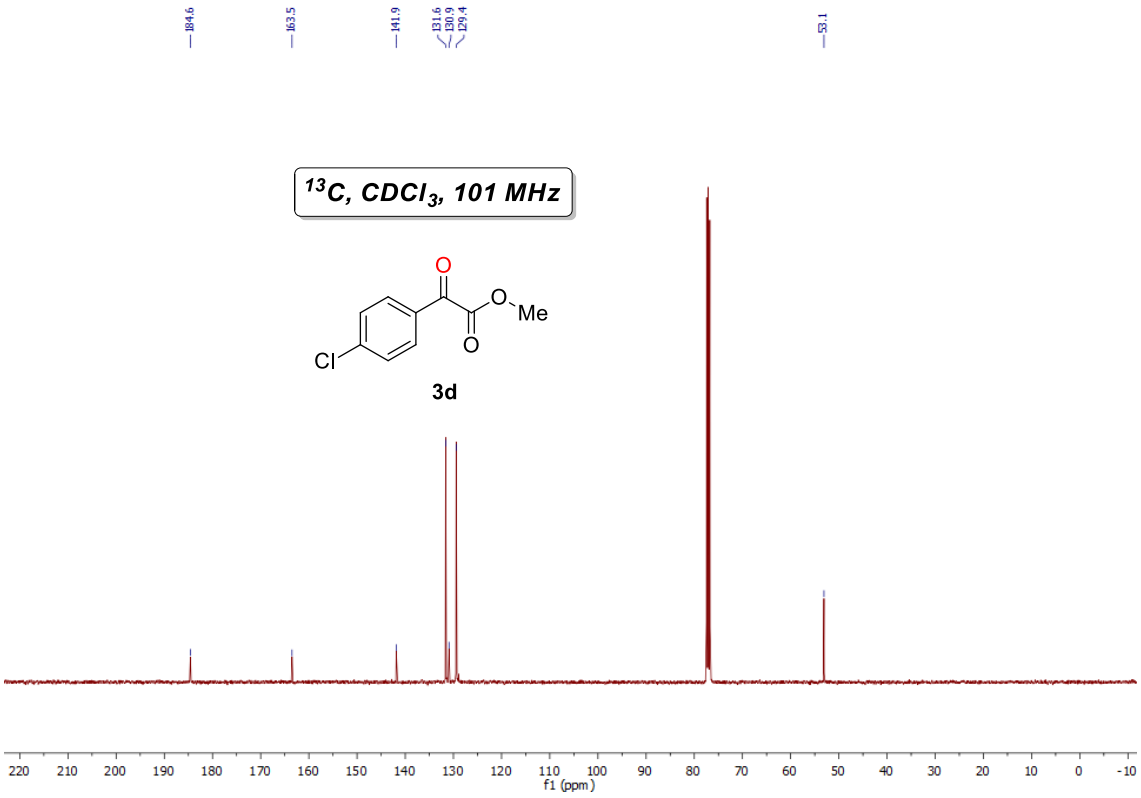

8.10
8.06
7.20
7.16
3.97
^{1}H, $CDCl_3$, 400 MHz
O
O
Me
F
O
3c
2.00
2.05
3.23
f1 (ppm)


184.2
168.2
165.7
163.7
133.2
133.1
129.1
129.0
116.5
116.3
53.0
^{13}C, $CDCl_3$, 101 MHz
O
O
Me
F
O
3c
f1 (ppm)

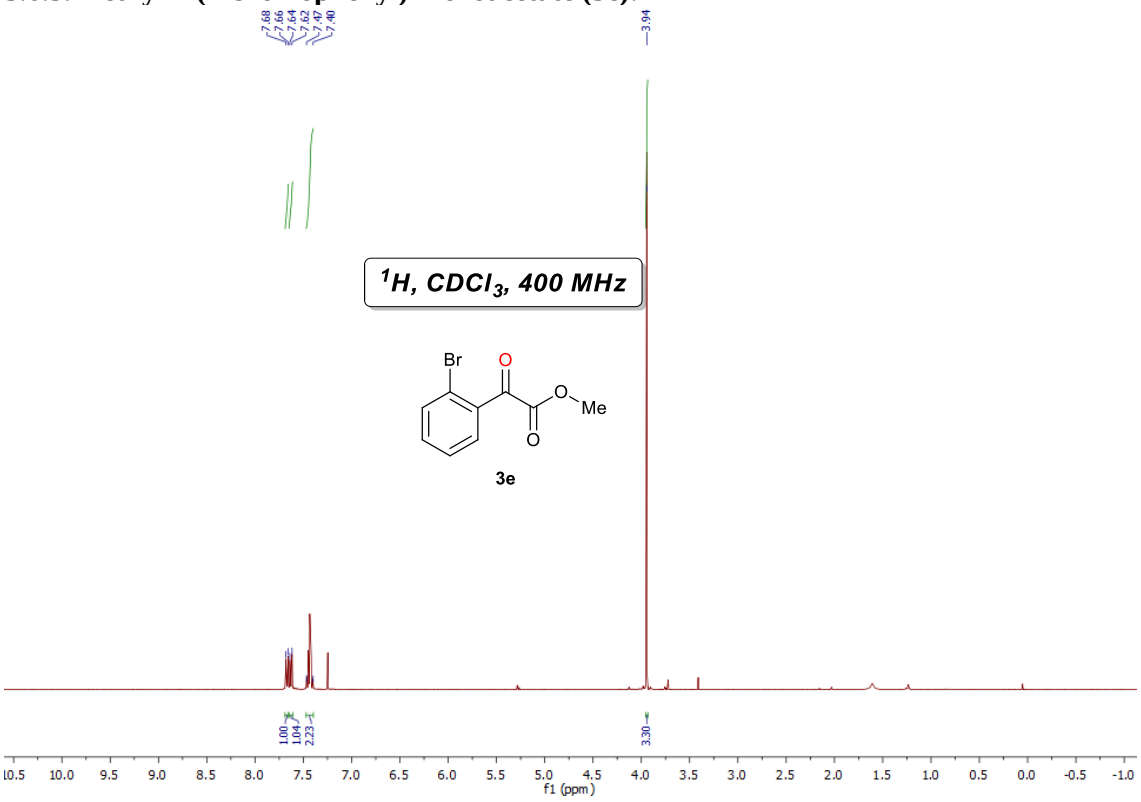


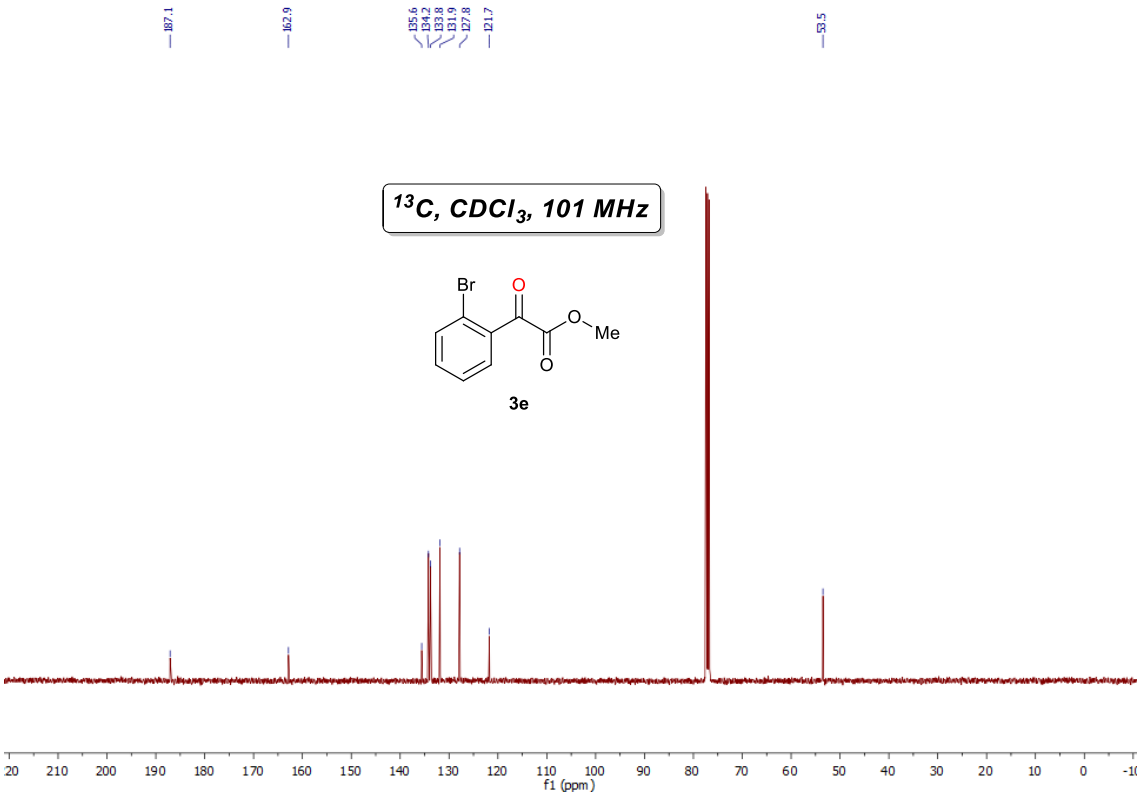
3.6.4. methyl 2-(4-chlorophenyl)-2-oxoacetate (3d):



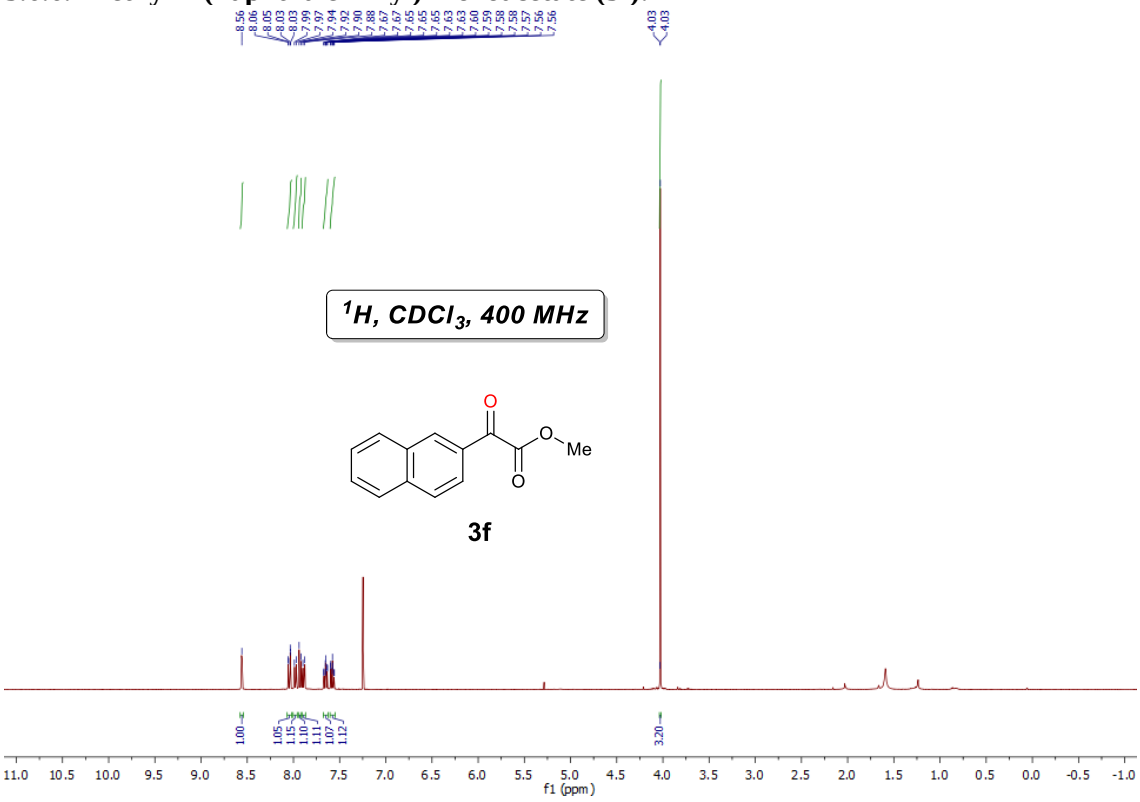


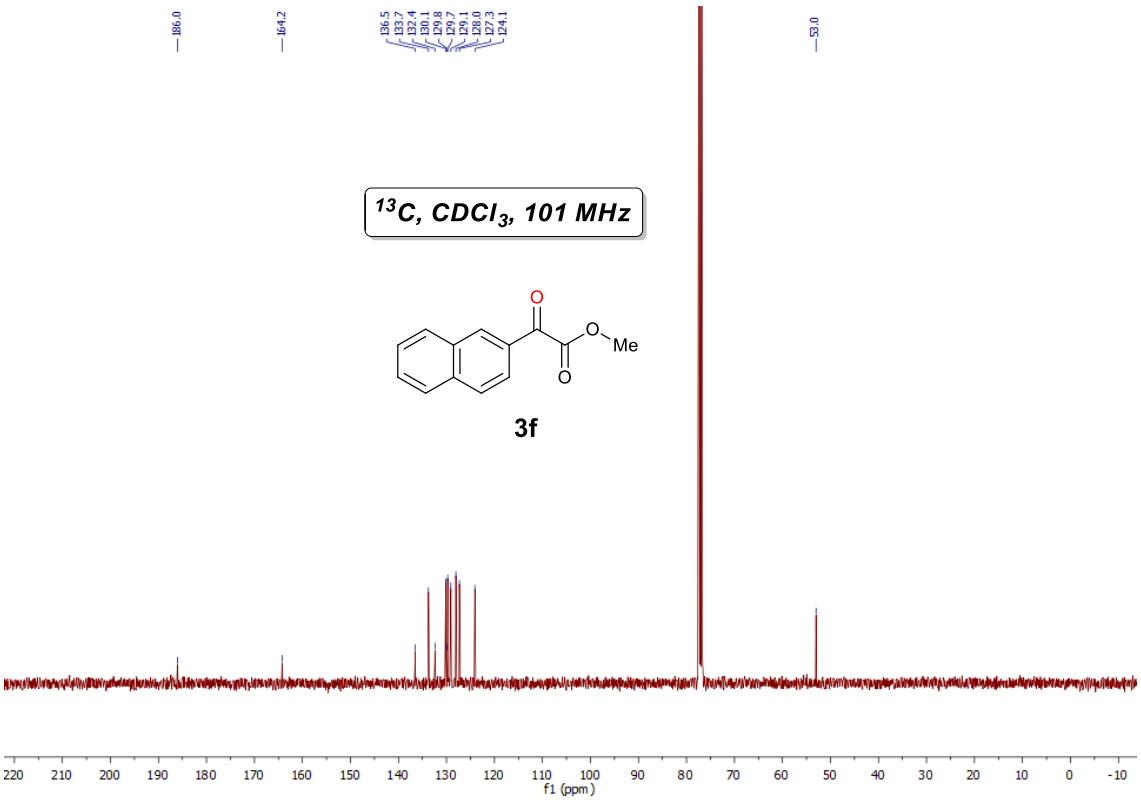
3.6.5. methyl 2-(2-bromophenyl)-2-oxoacetate (3e):



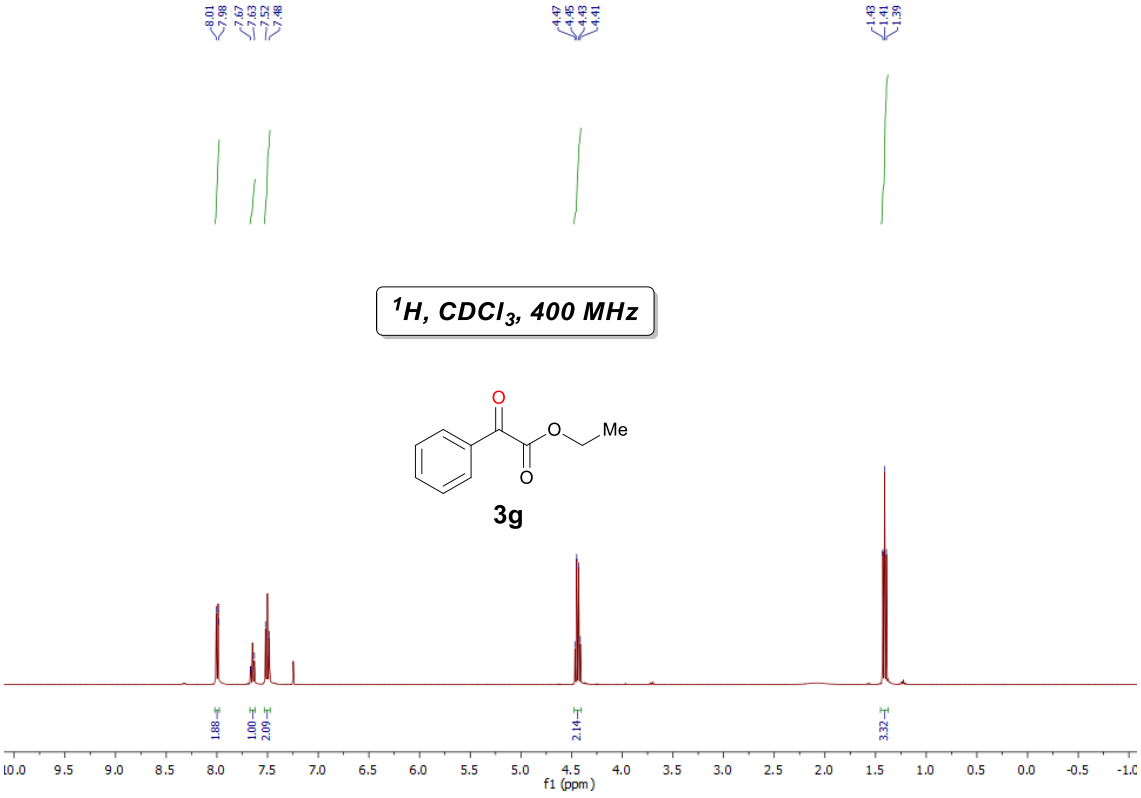


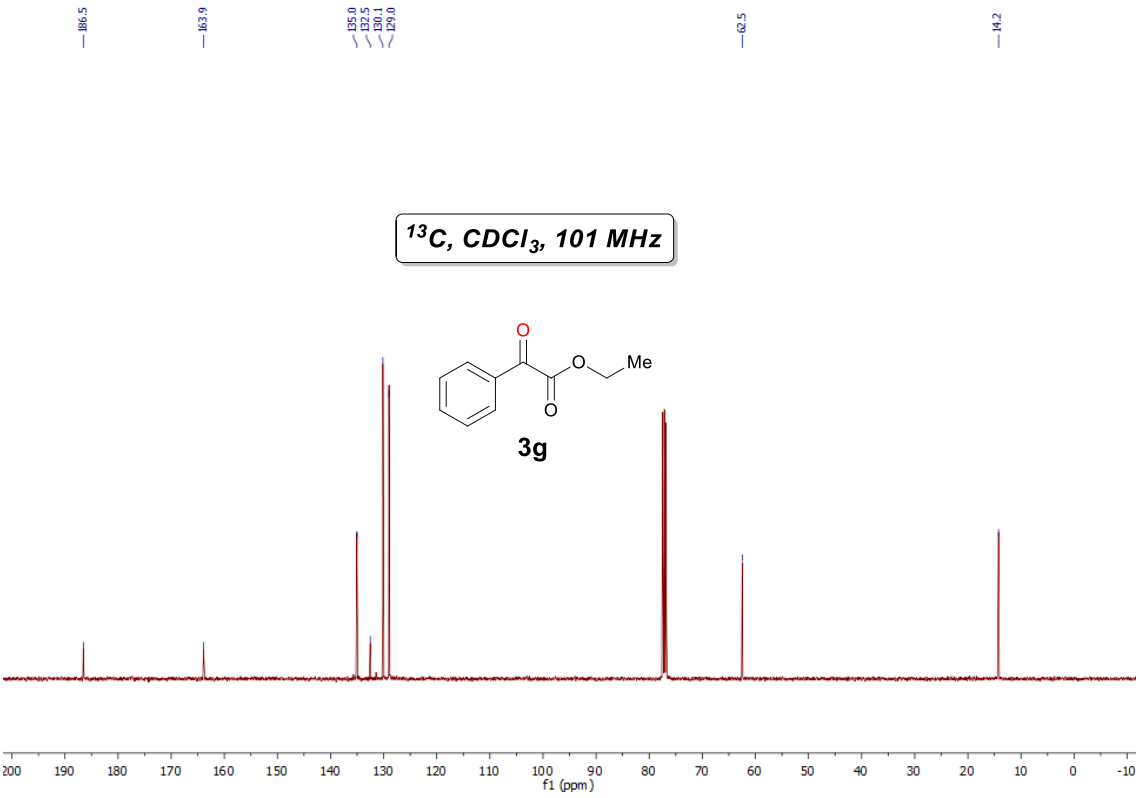
3.6.6. methyl 2-(naphthalen-2-yl)-2-oxoacetate (3f):



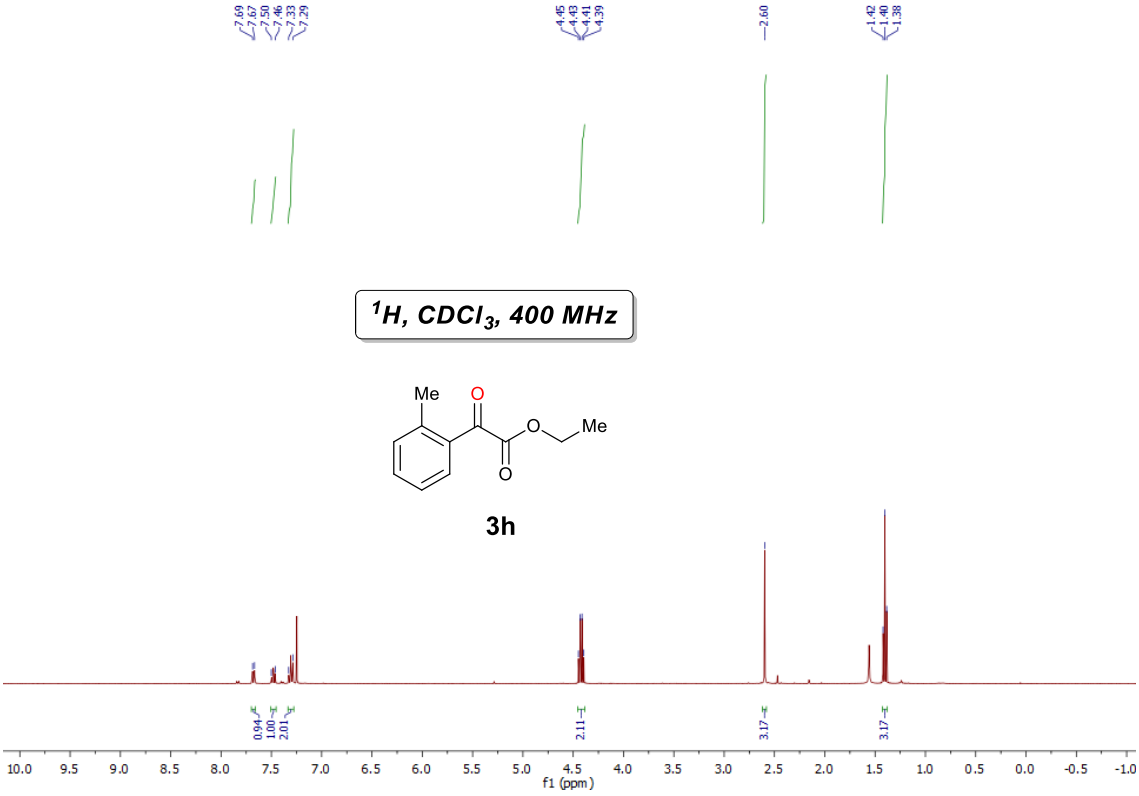


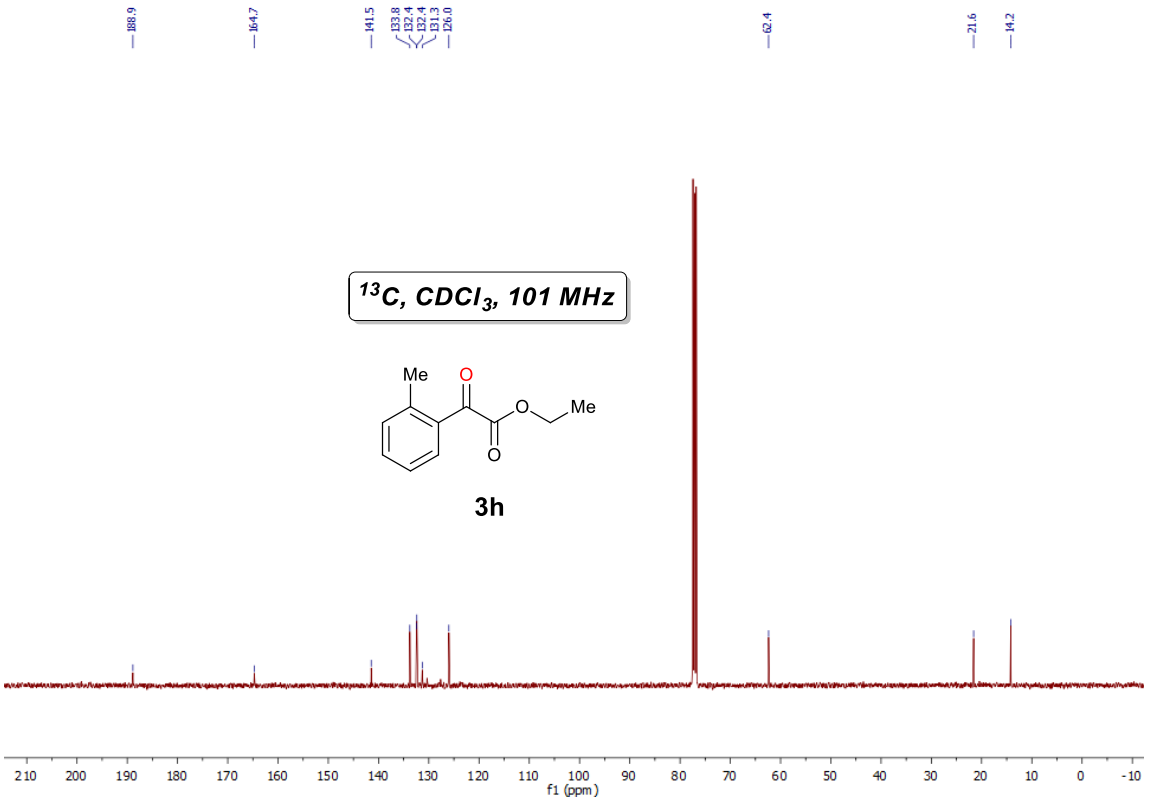
3.6.7. ethyl 2-oxo-2-phenylacetate (3g):



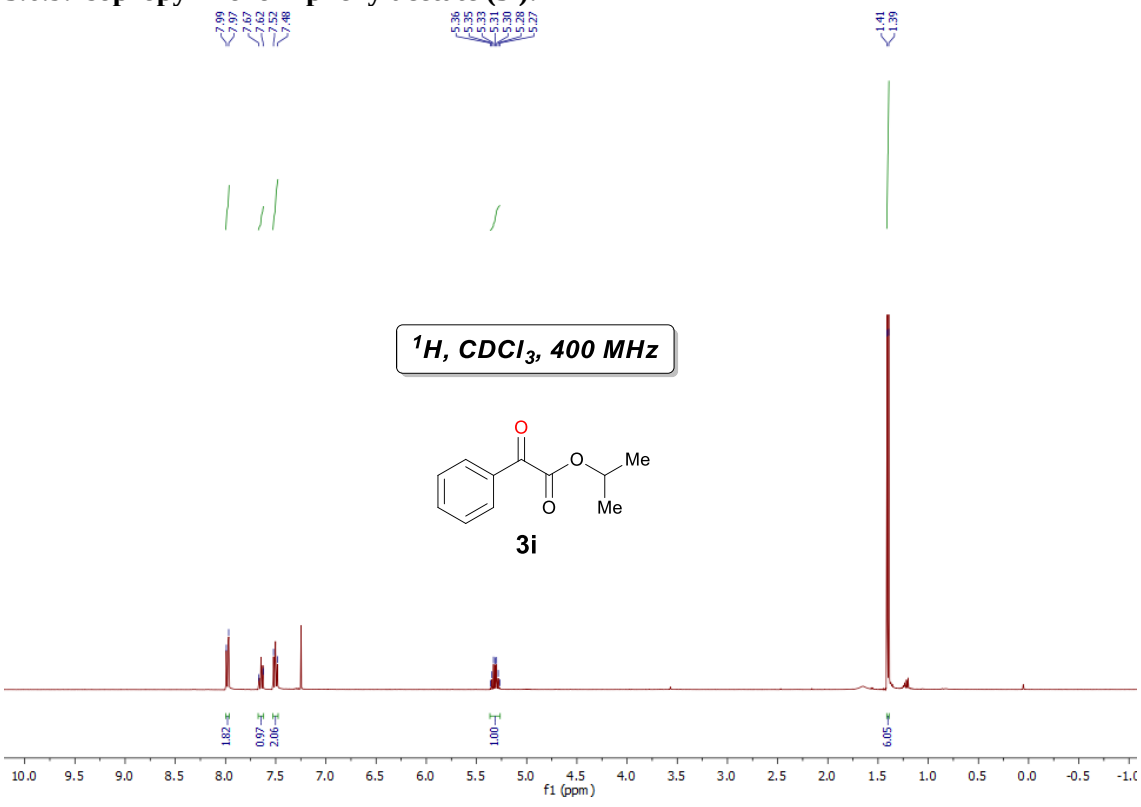


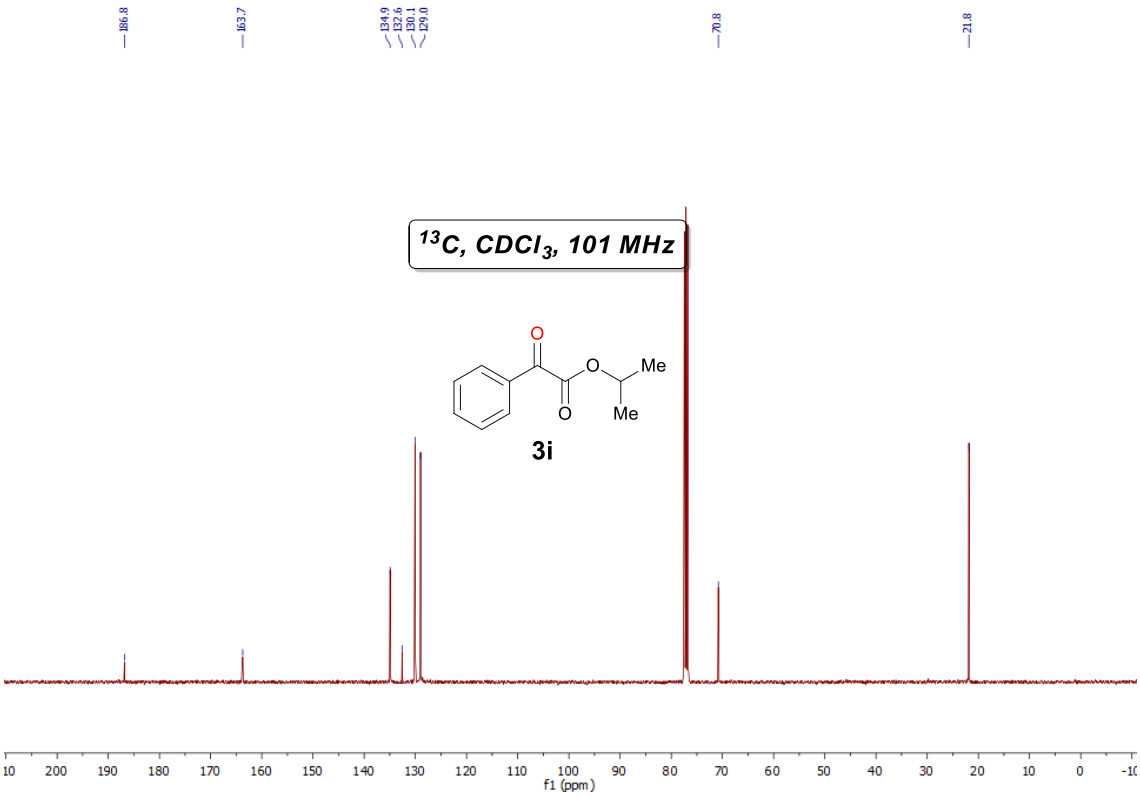
3.6.8. ethyl 2-oxo-2-(*o*-tolyl)acetate (3h):



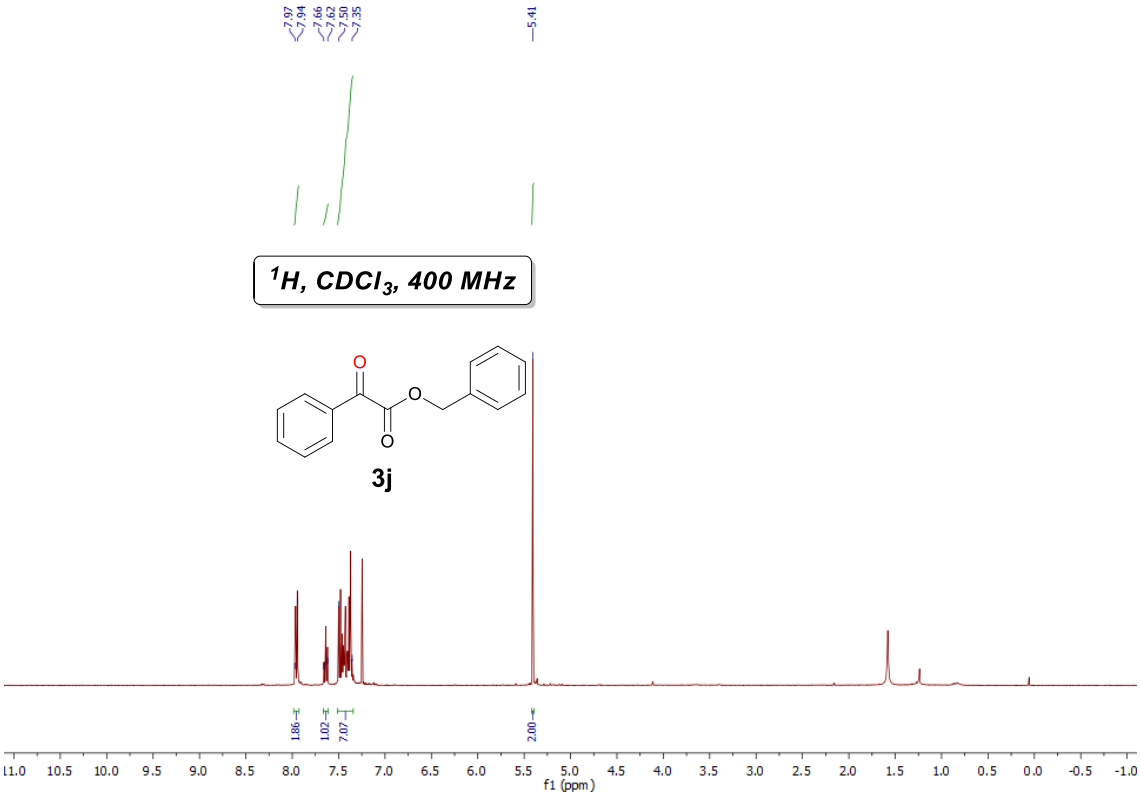


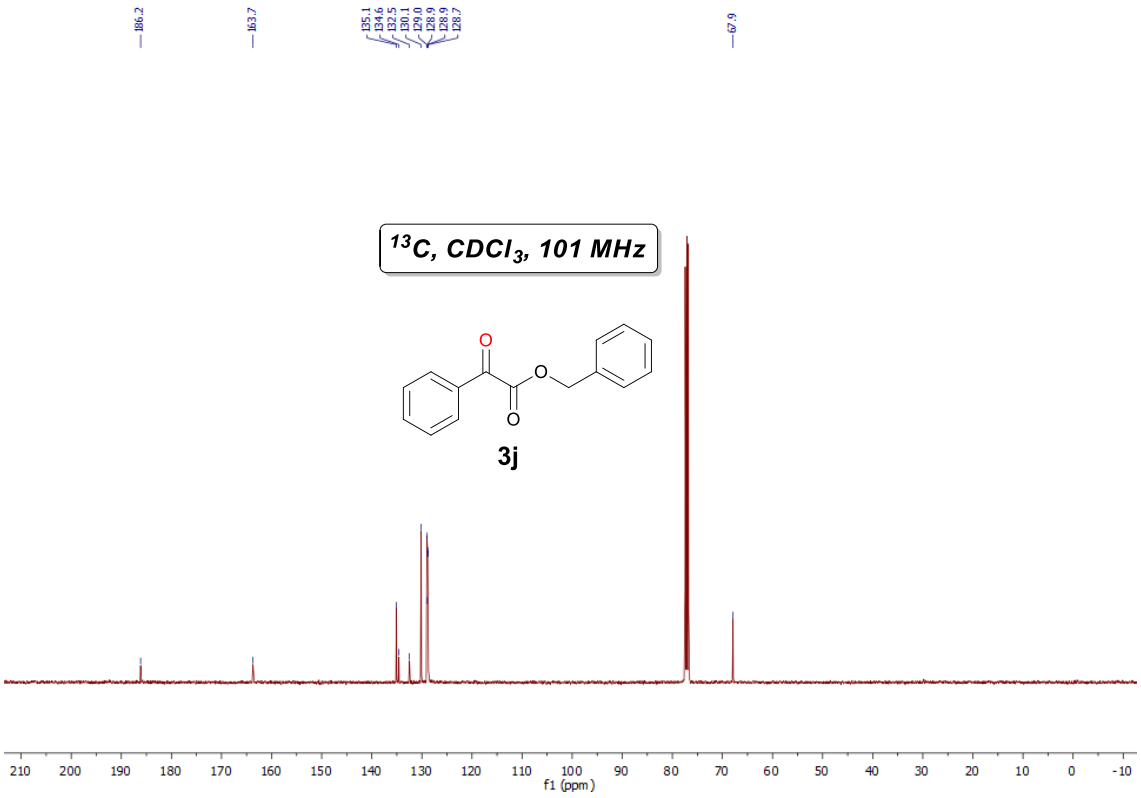
3.6.9. isopropyl 2-oxo-2-phenylacetate (3i):



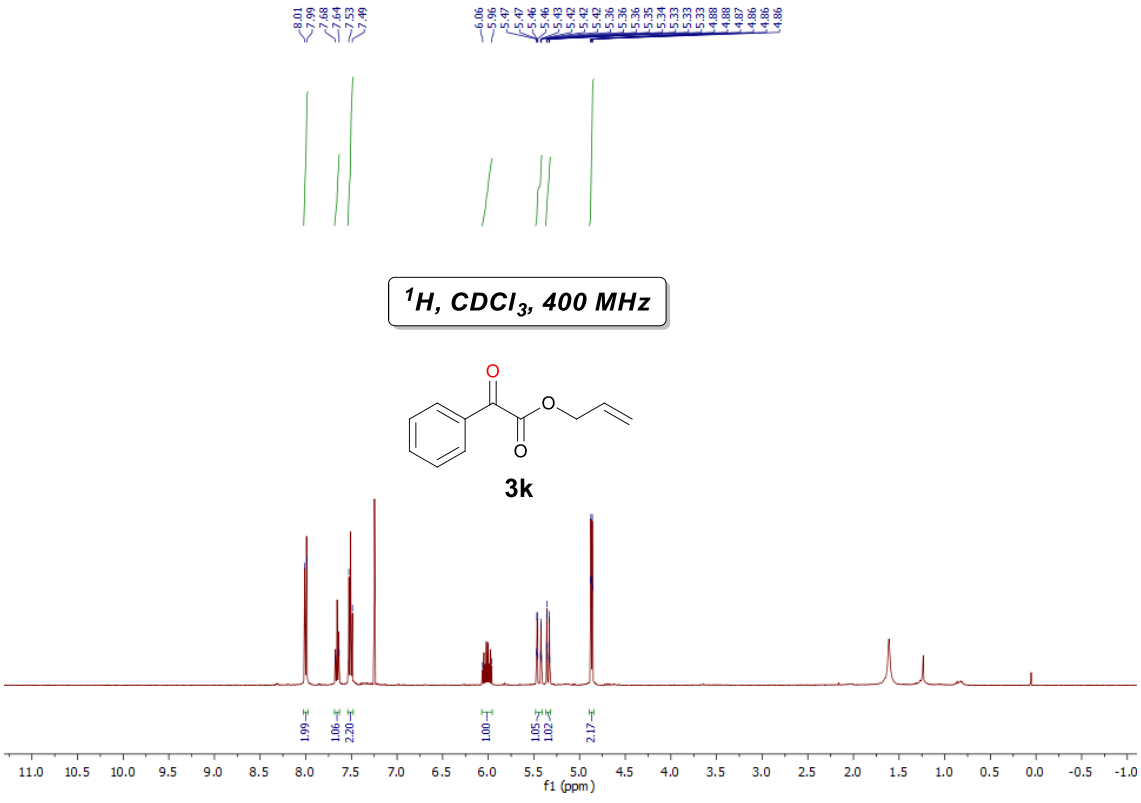


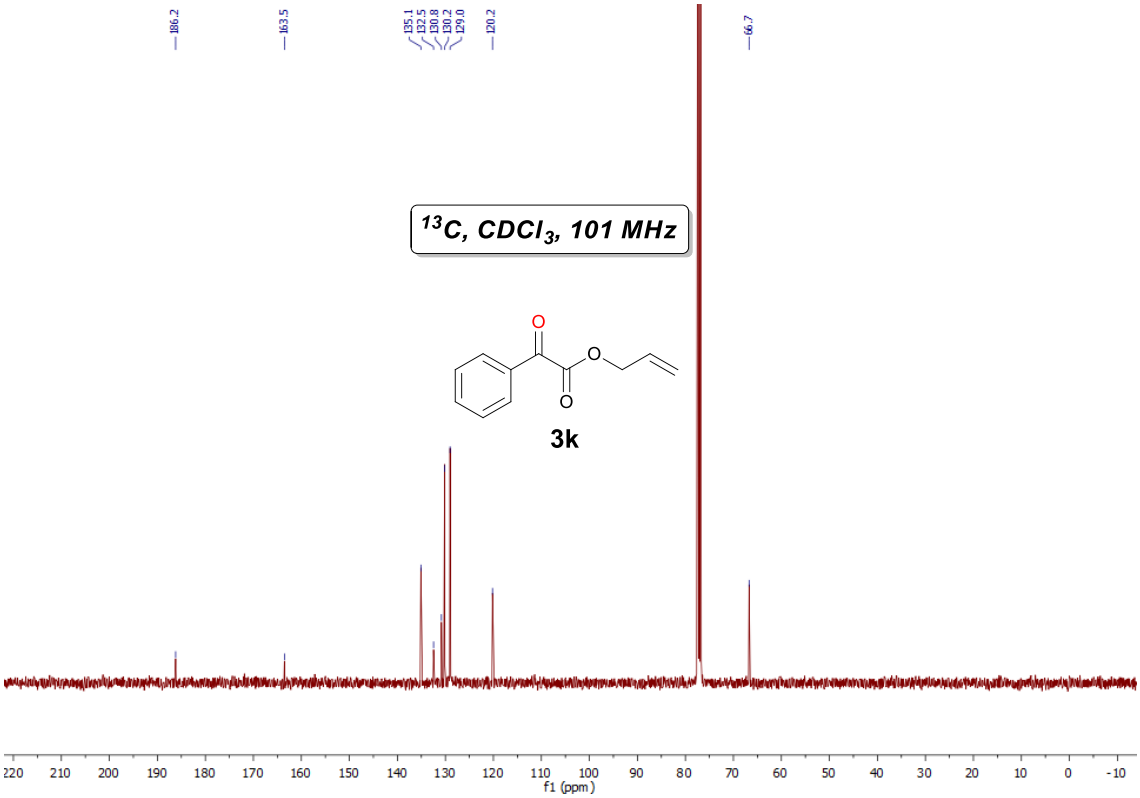
3.6.10. benzyl 2-oxo-2-phenylacetate (3j):



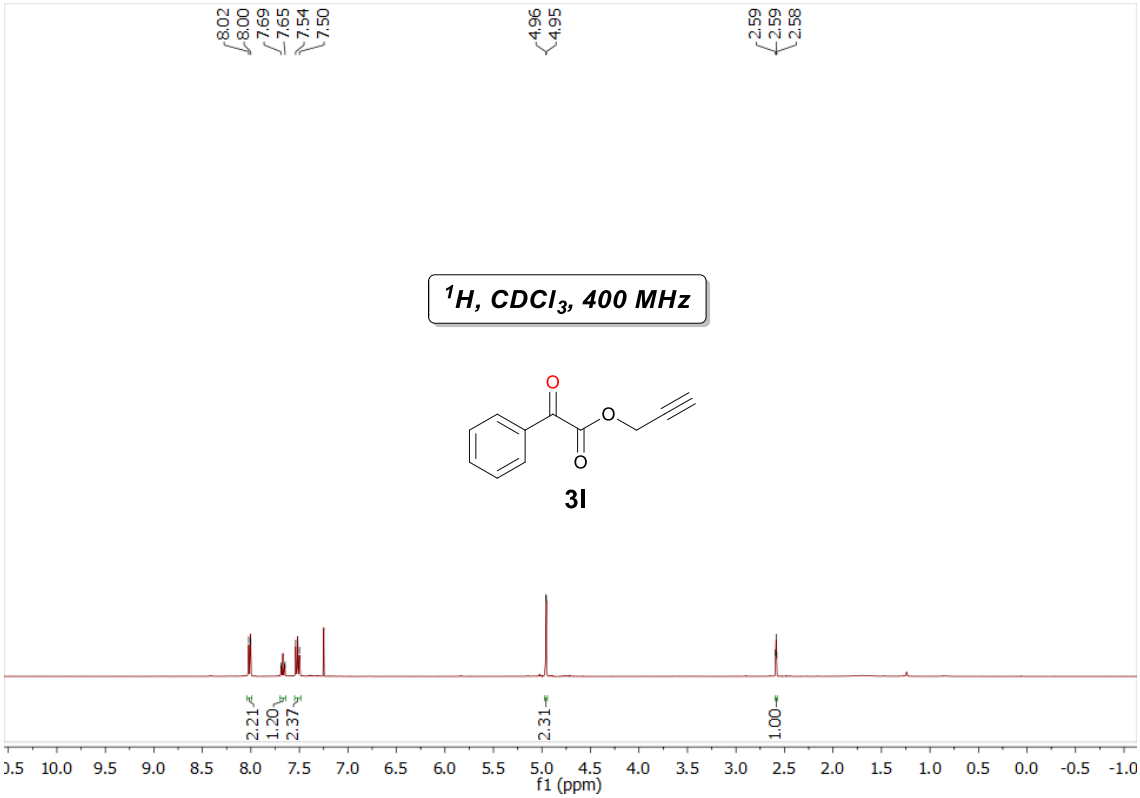


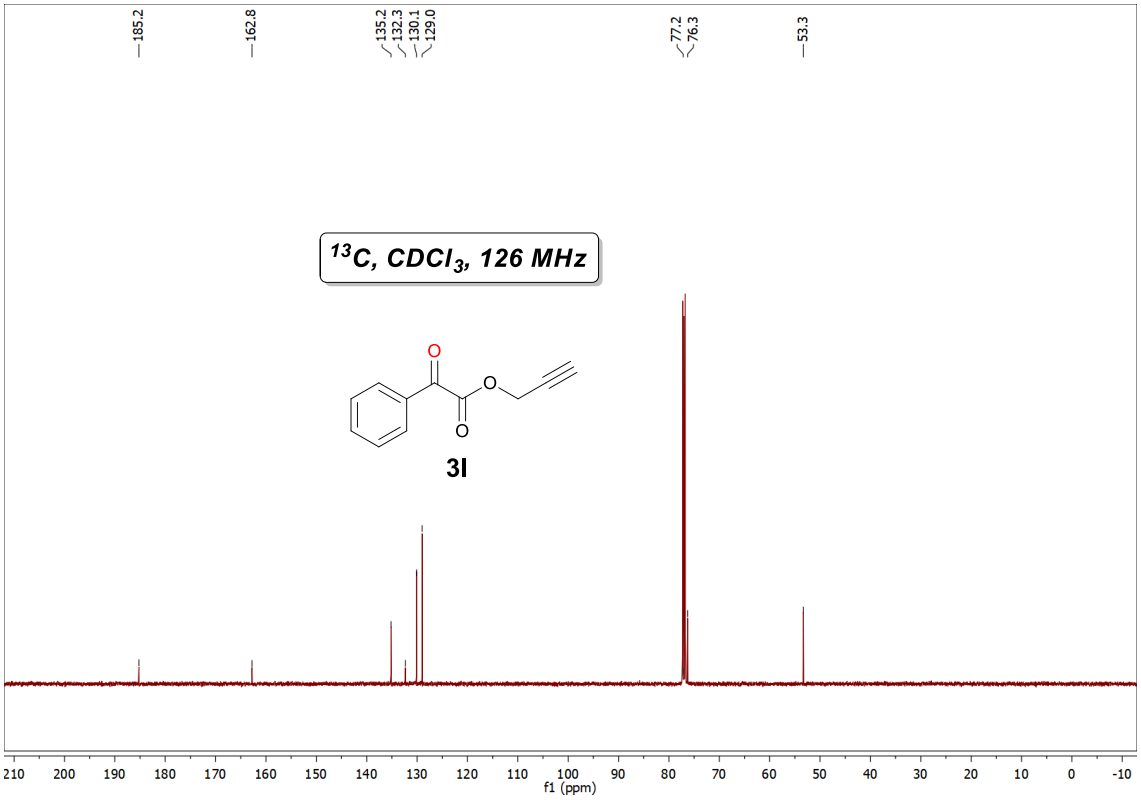
3.6.11. allyl 2-oxo-2-phenylacetate (3k):



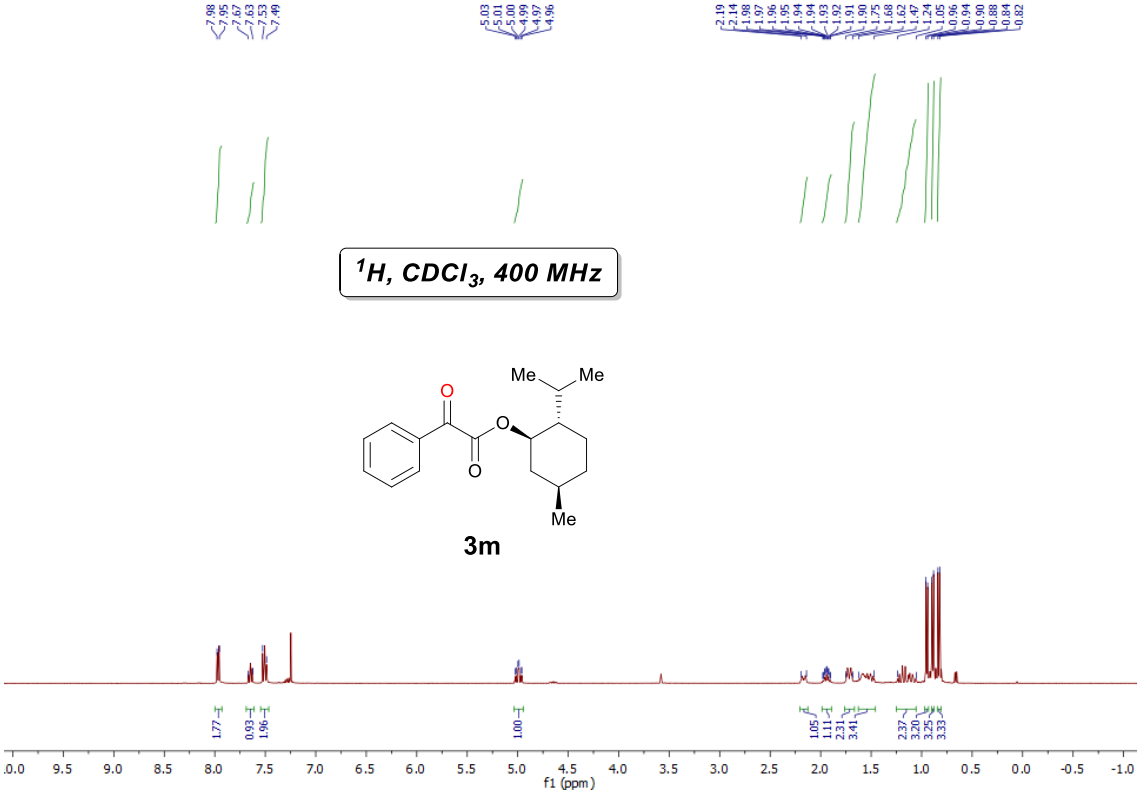


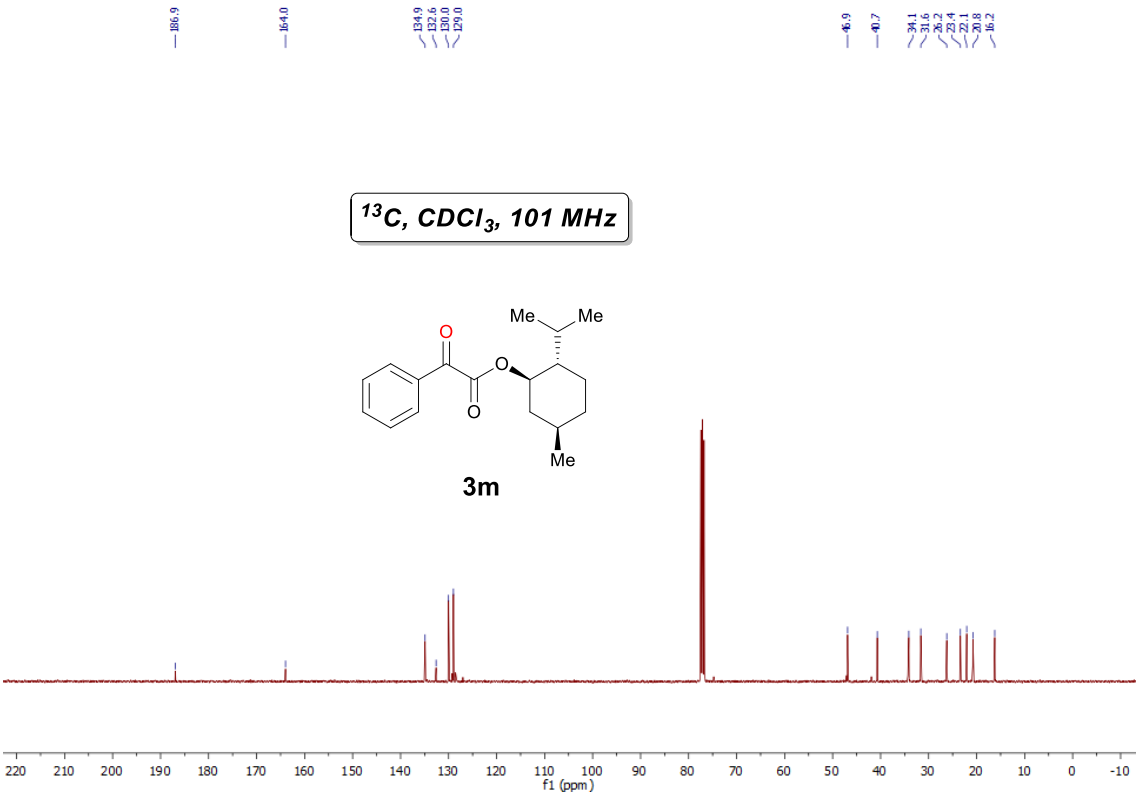
3.6.12. prop-2-yn-1-yl 2-oxo-2-phenylacetate (3l):



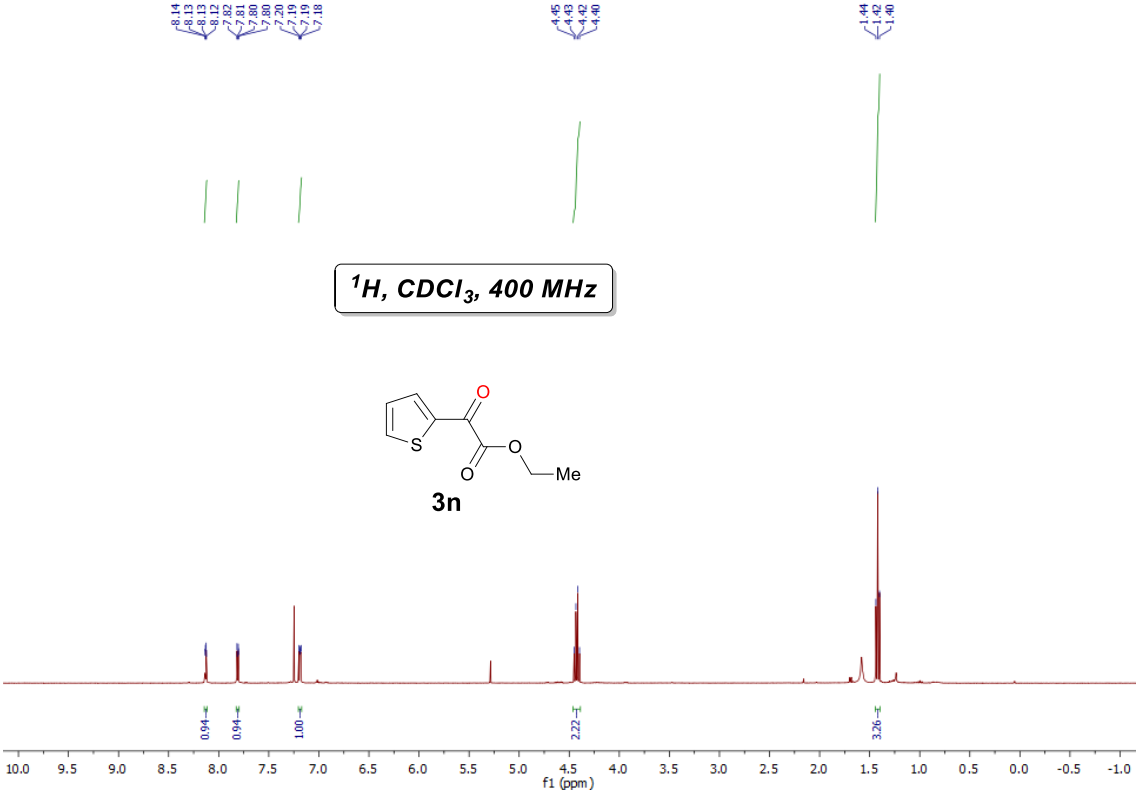


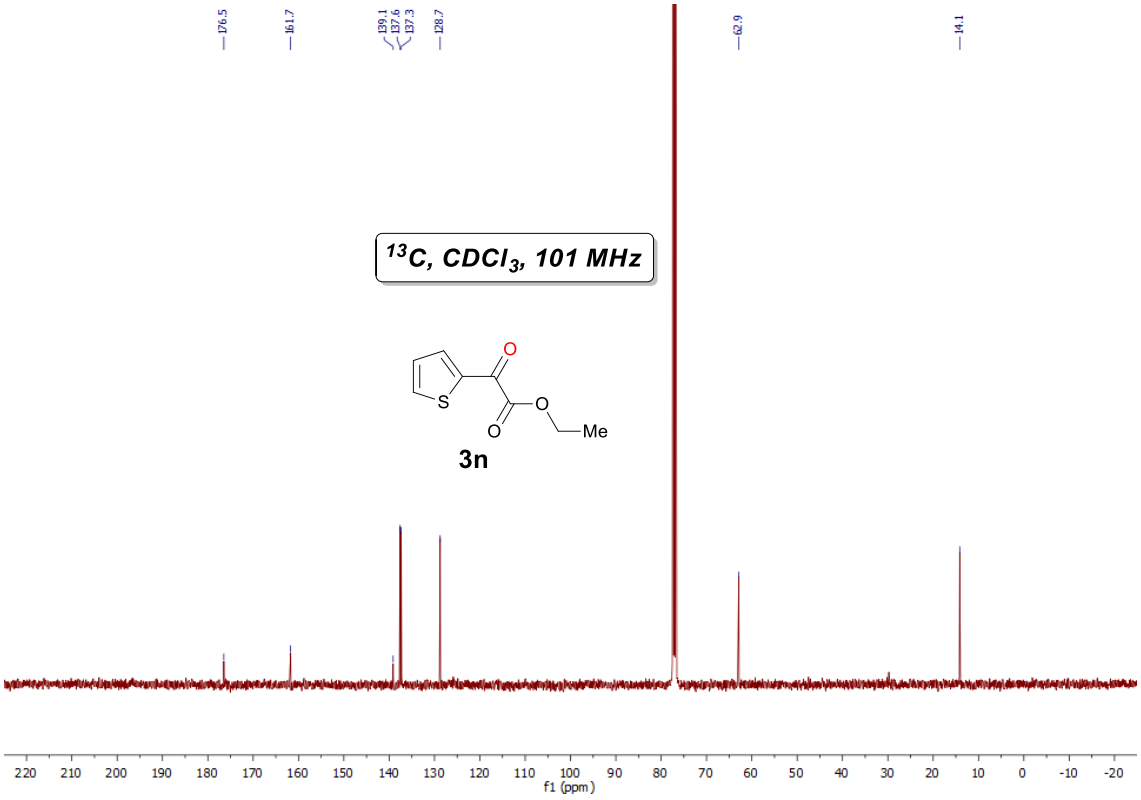
3.6.13. (*1R,2S,5R*)-2-isopropyl-5-methylcyclohexyl 2-oxo-2-phenylacetate (3m):



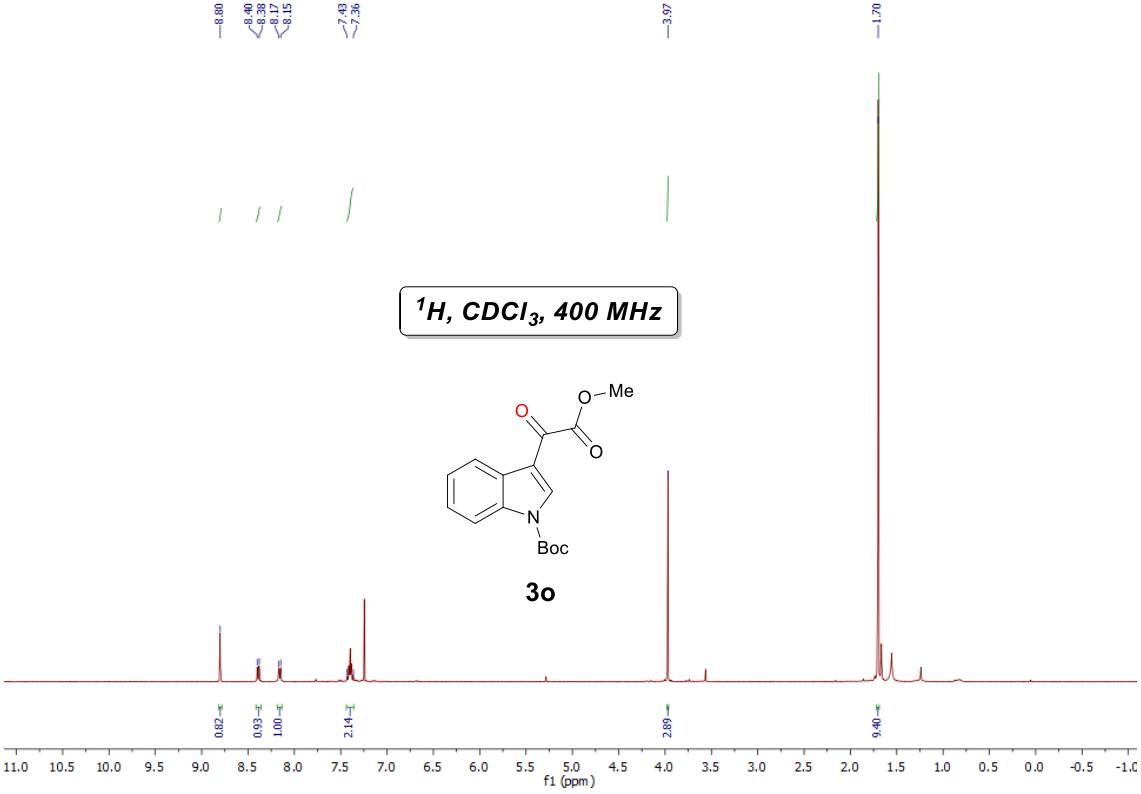


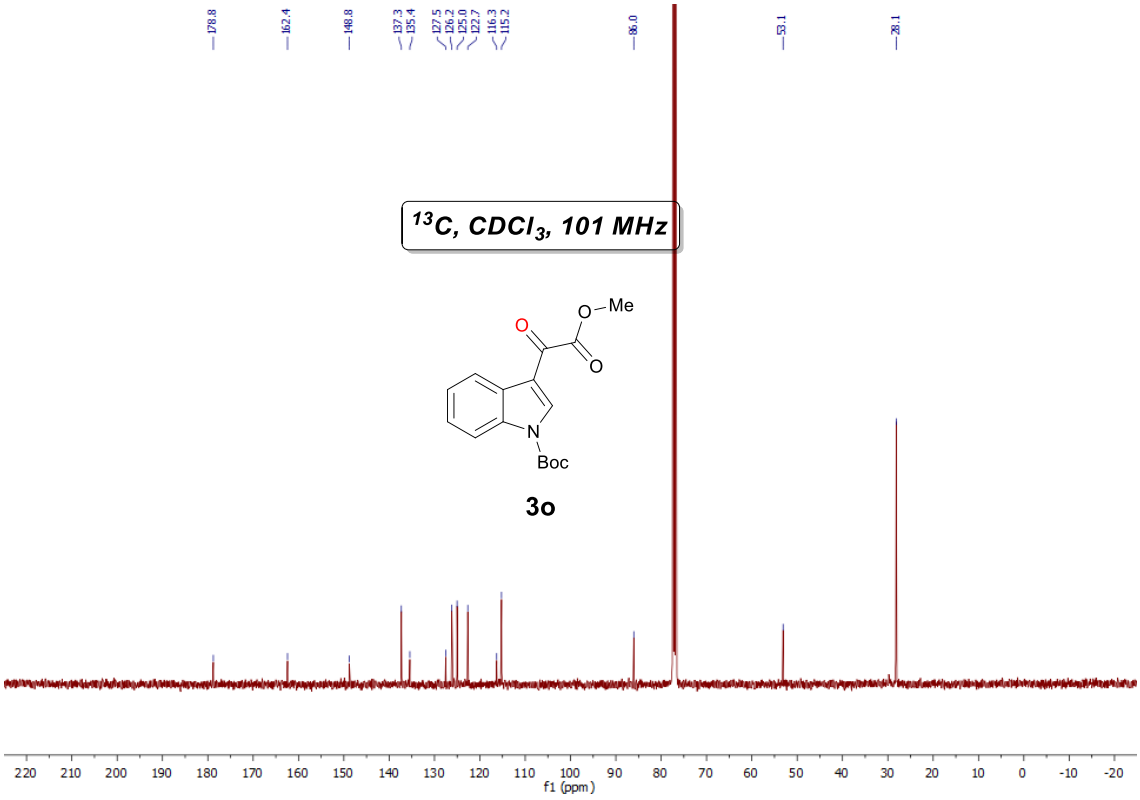
3.6.14. ethyl 2-oxo-2-(thiophen-2-yl)acetate (3n):



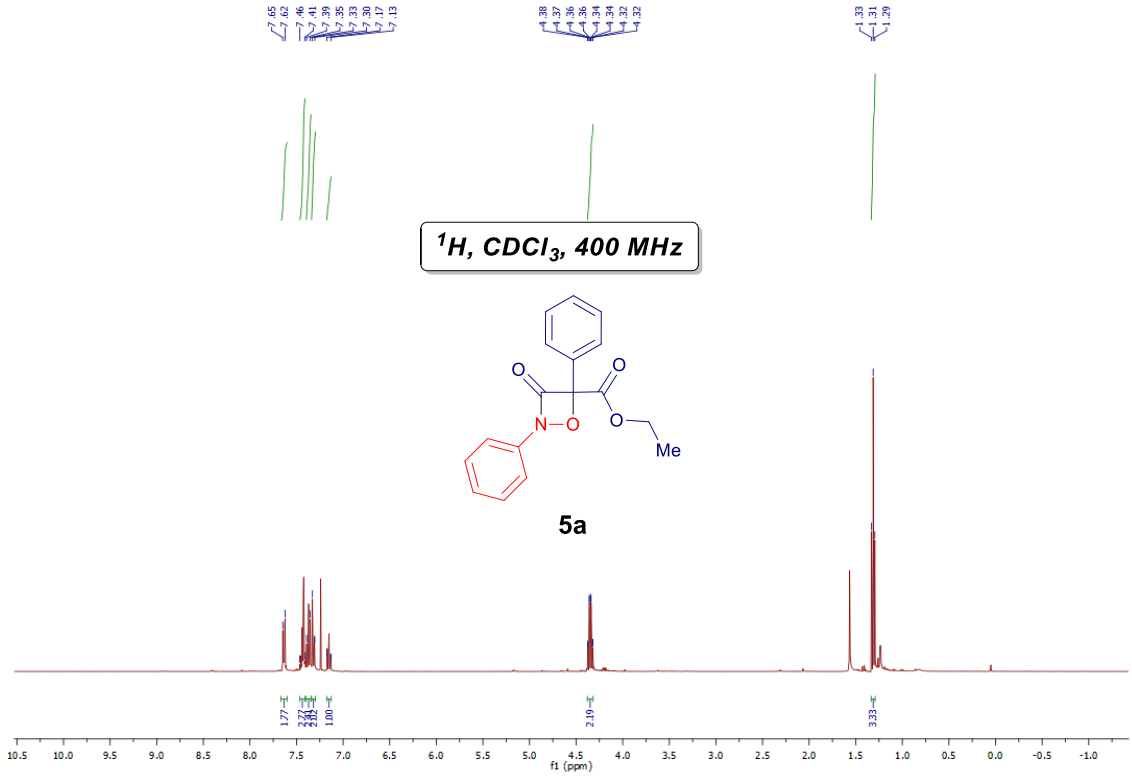


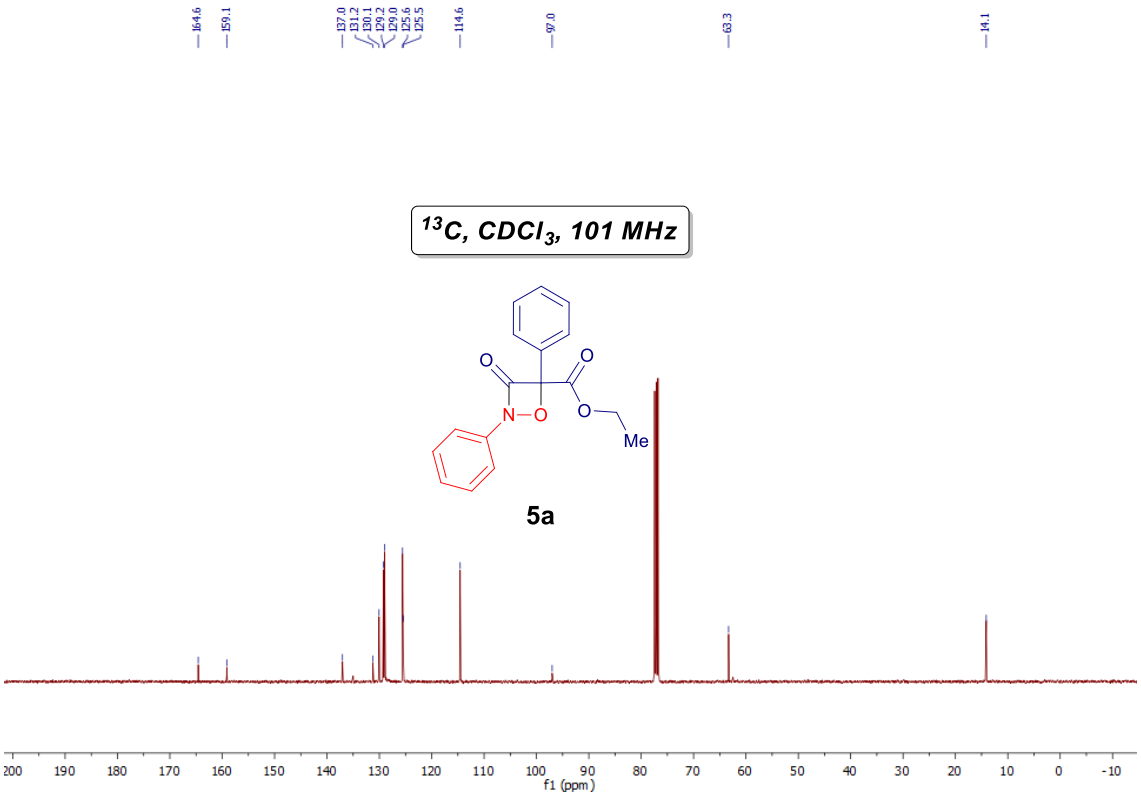
3.6.15. *tert*-butyl 3-(2-methoxy-2-oxoacetyl)-1*H*-indole-1-carboxylate (3o):



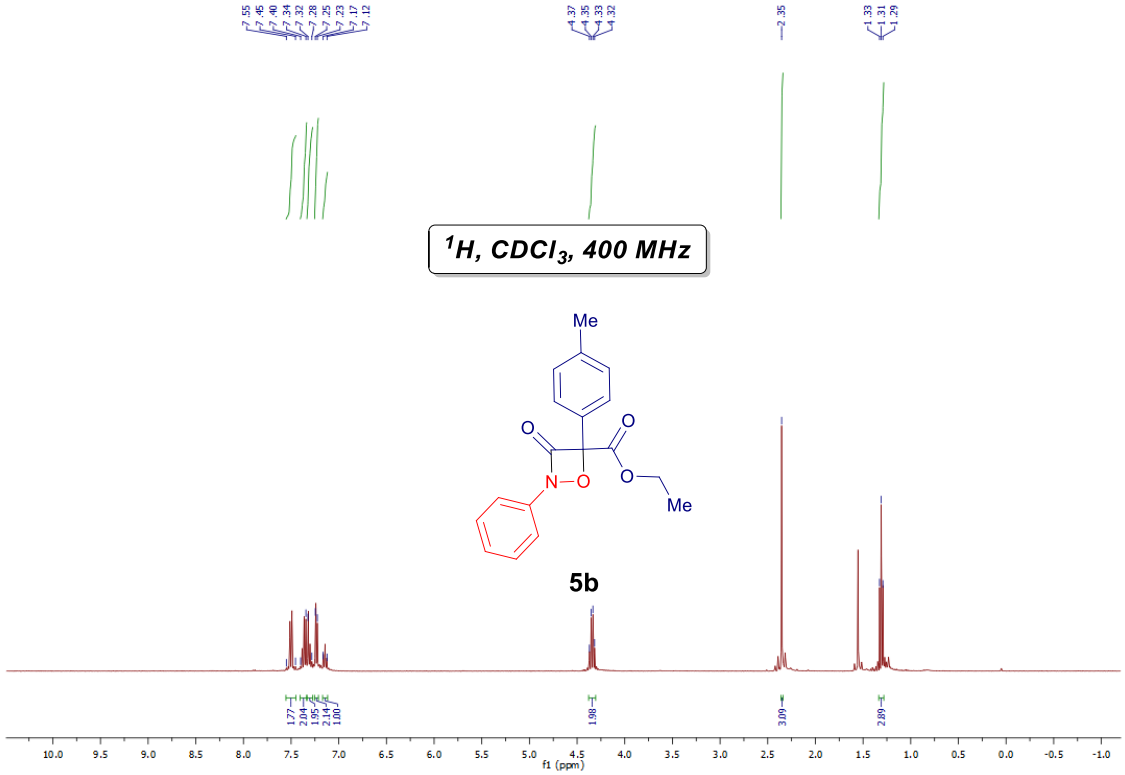


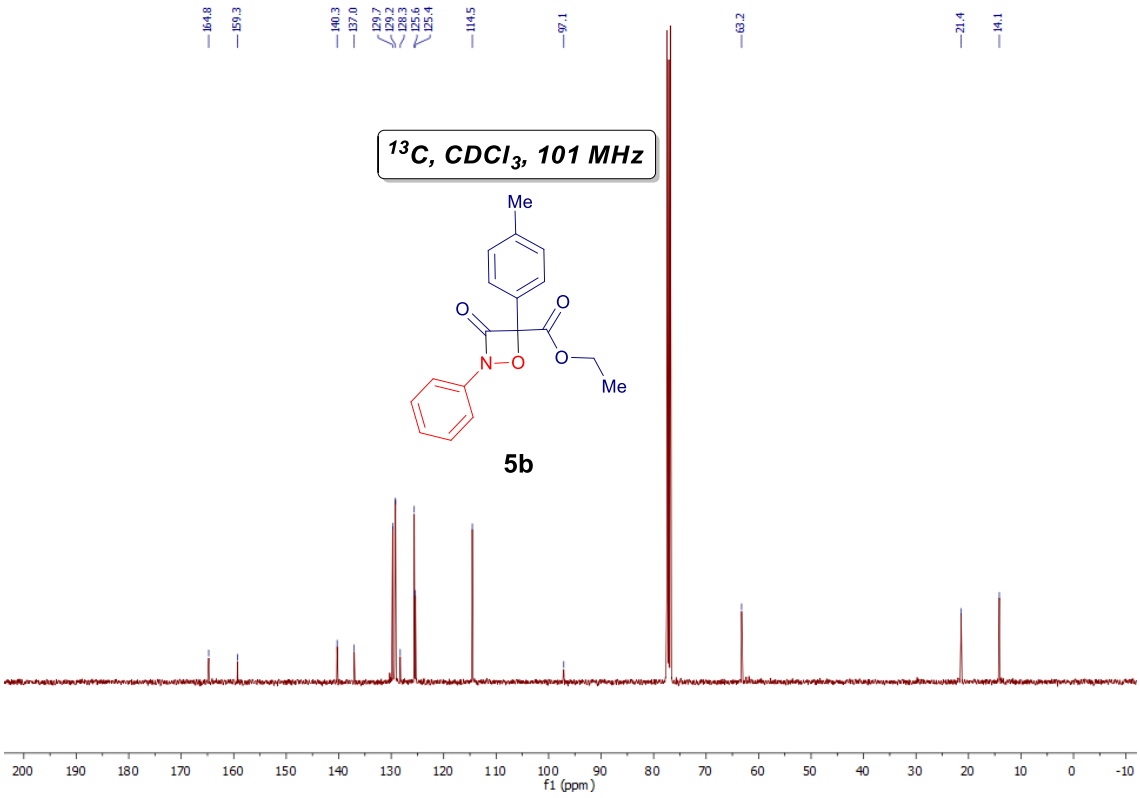
3.6.16. ethyl 3-oxo-2,4-diphenyl-1,2-oxazetidine-4-carboxylate (5a):



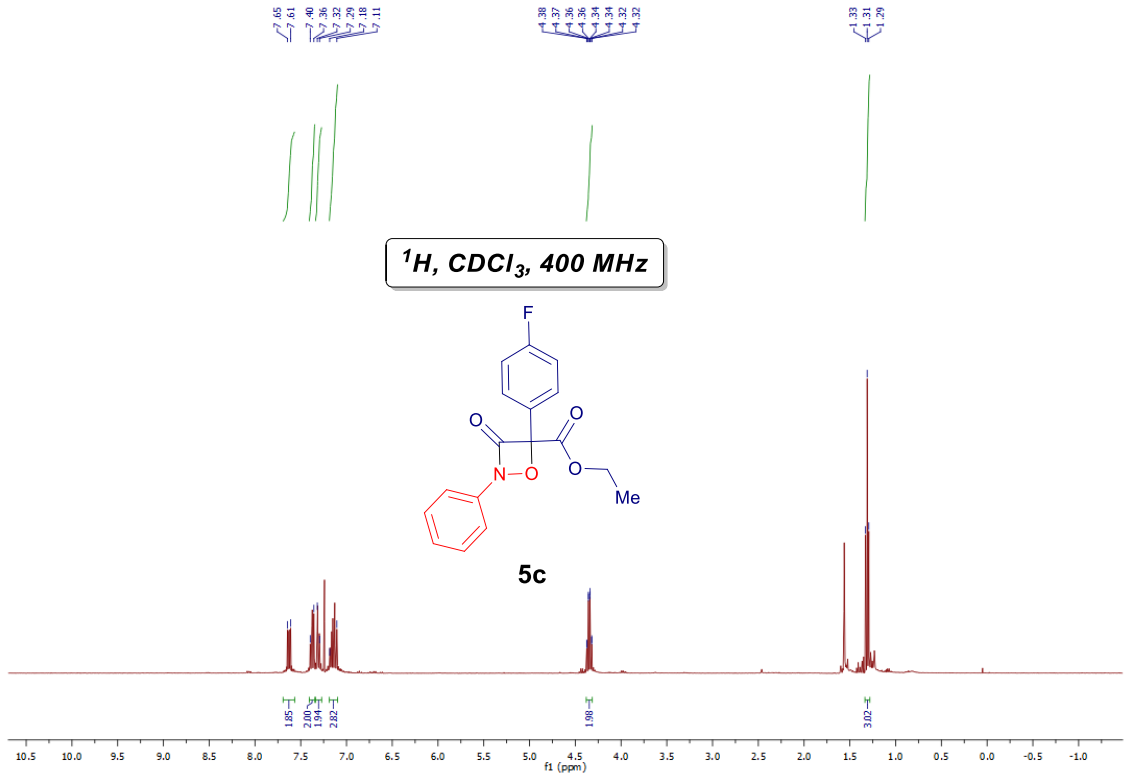


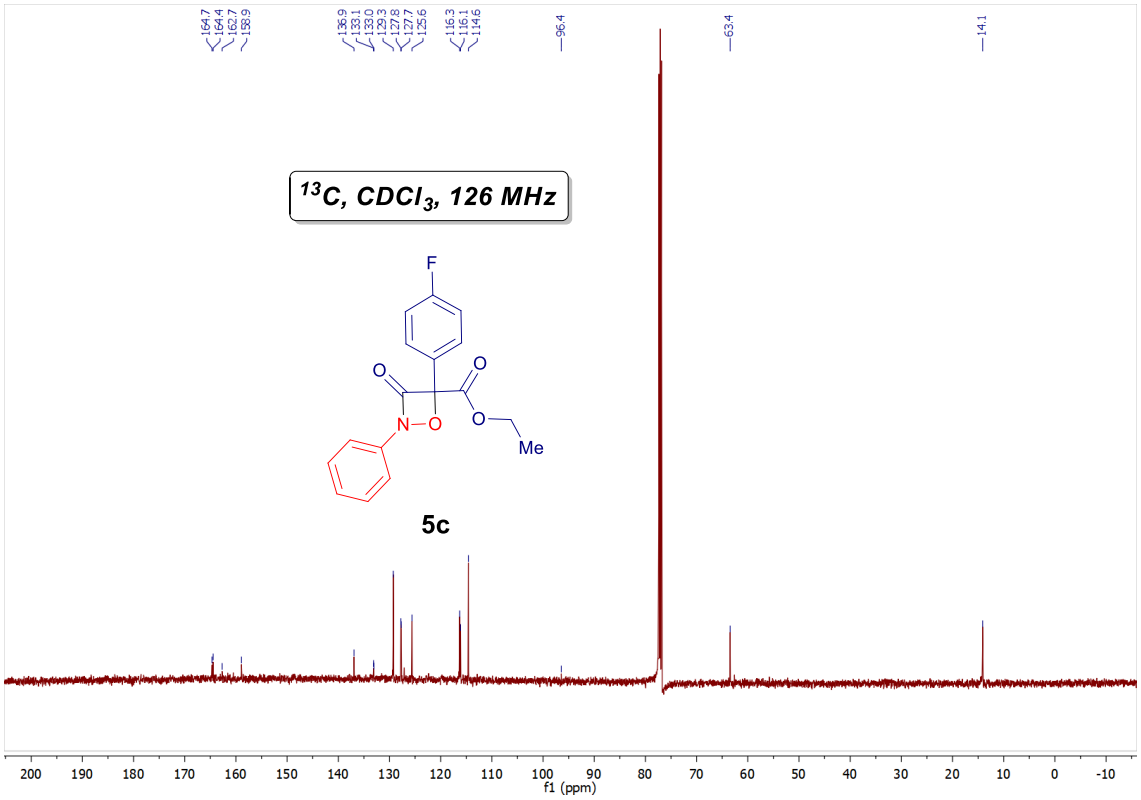
3.6.17. ethyl 3-oxo-2-phenyl-4-(*p*-tolyl)-1,2-oxazetidine-4-carboxylate (5b):

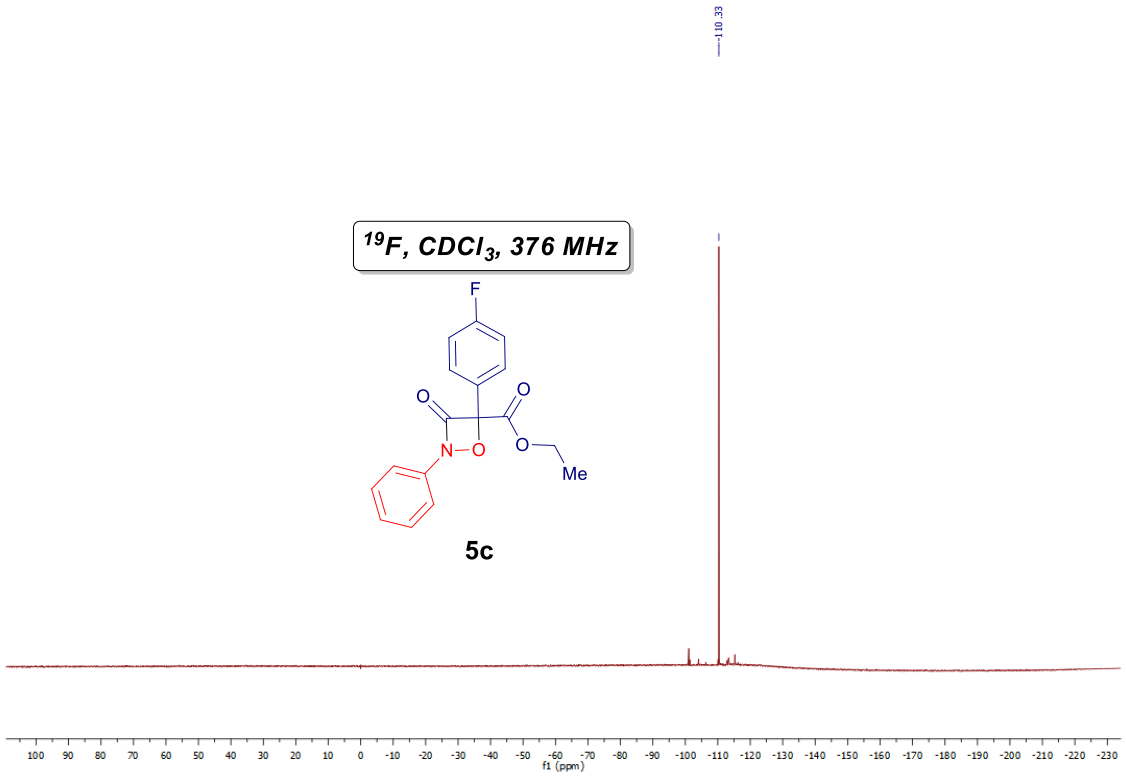




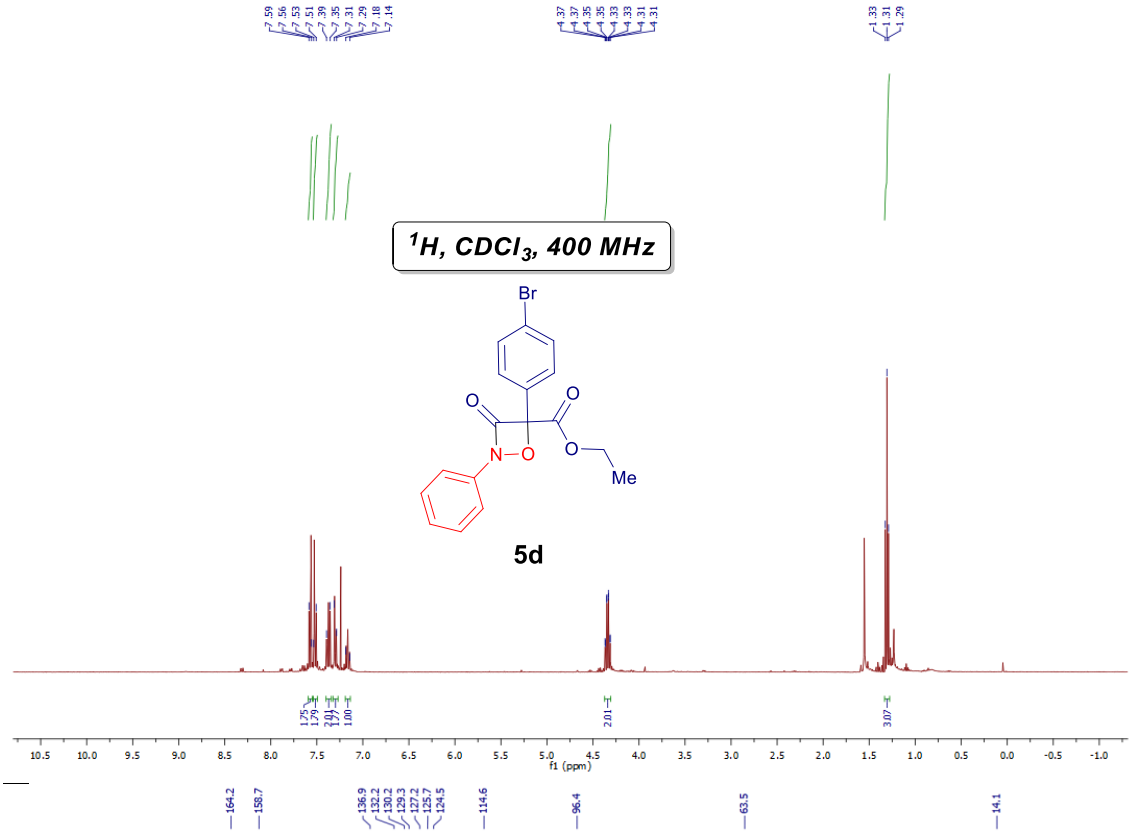
3.6.18. ethyl 4-(4-fluorophenyl)-3-oxo-2-phenyl-1,2-oxazetidine-4-carboxylate (5c):

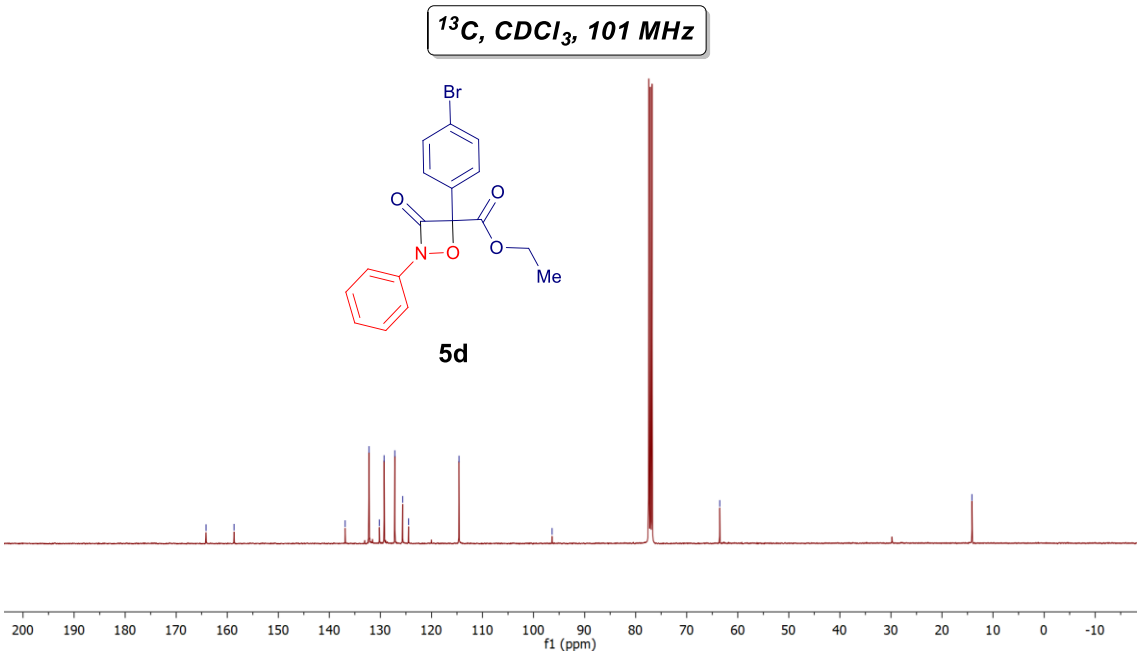



164.7
164.4
162.7
159.9
136.9
133.1
133.0
129.3
127.8
127.7
125.6
116.3
116.1
114.6
96.4
63.4
14.1
^{13}C, $CDCl_3$, 126 MHz
F
O
O
O
N—O
O
Me
5c
200 190 180 170 160 150 140 130 120 110 100 90 80 70 60 50 40 30 20 10 0 -10
f1 (ppm)

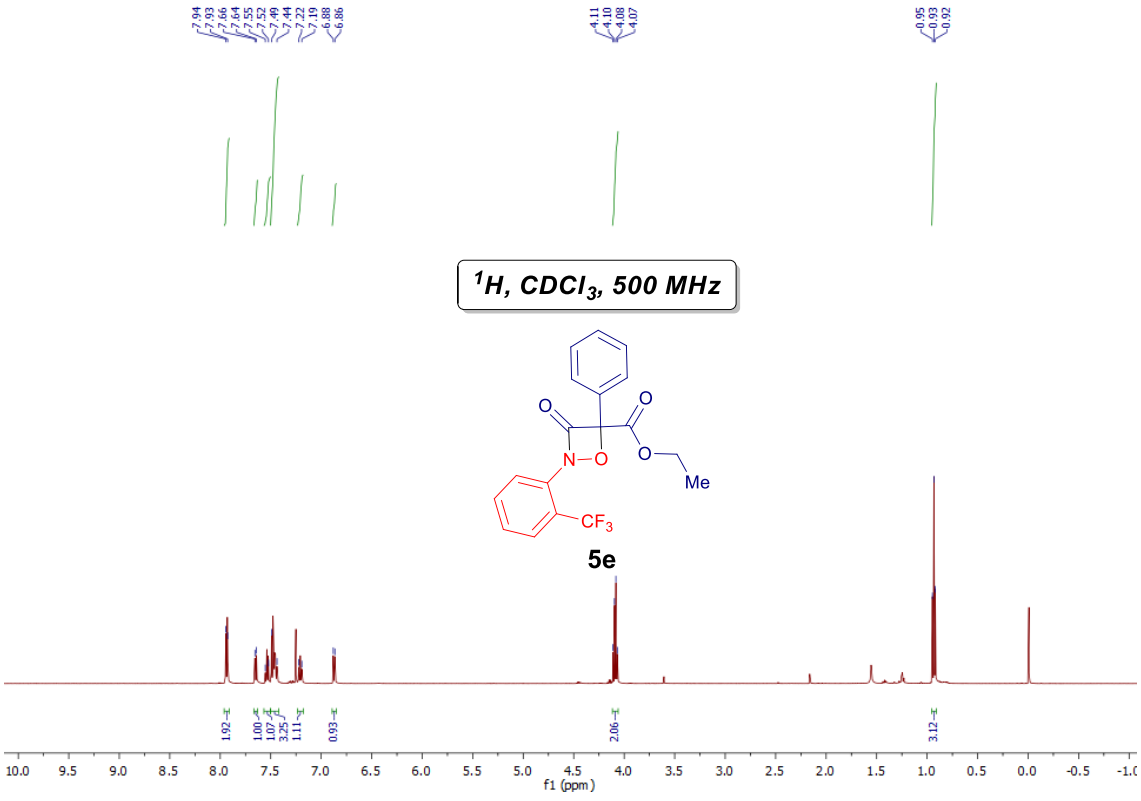

-110.33
^{19}F, $CDCl_3$, 376 MHz
F
O
O
O
N—O
O
Me
5c
100 90 80 70 60 50 40 30 20 10 0 -10 -20 -30 -40 -50 -60 -70 -80 -90 -100 -110 -120 -130 -140 -150 -160 -170 -180 -190 -200 -210 -220 -230
f1 (ppm)

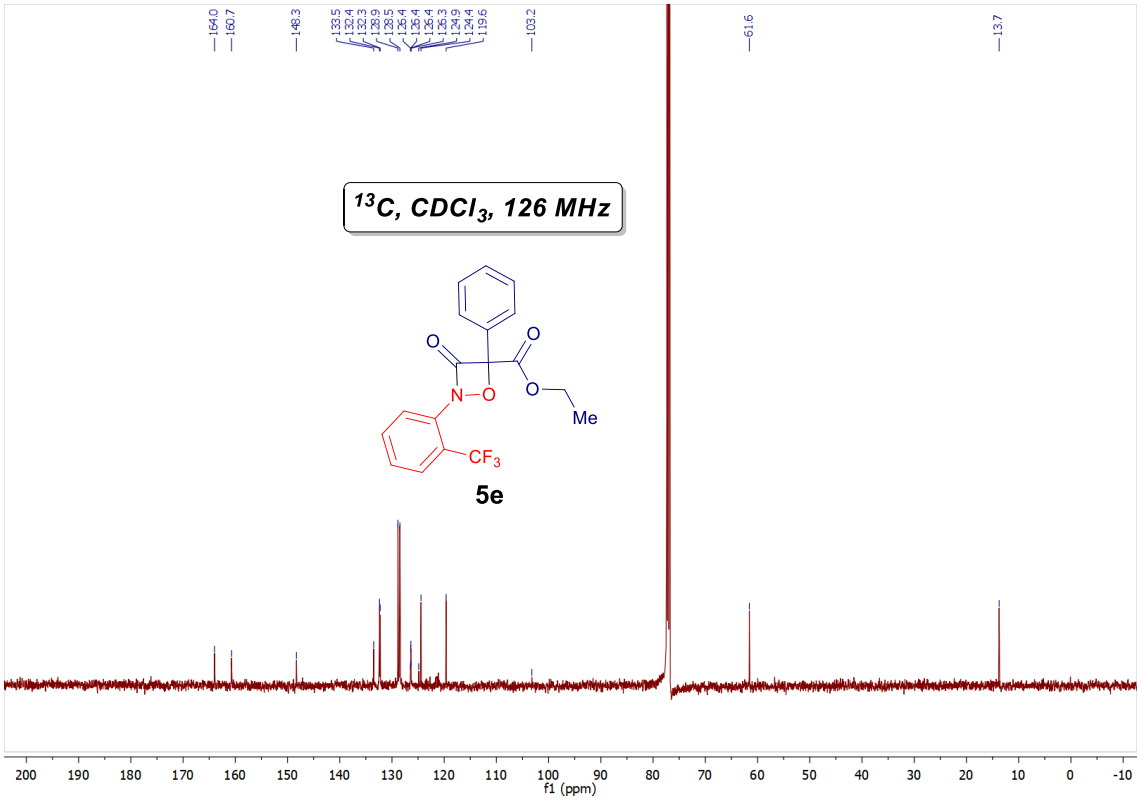
3.6.19. ethyl 4-(4-bromophenyl)-3-oxo-2-phenyl-1,2-oxazetidine-4-carboxylate (5d):

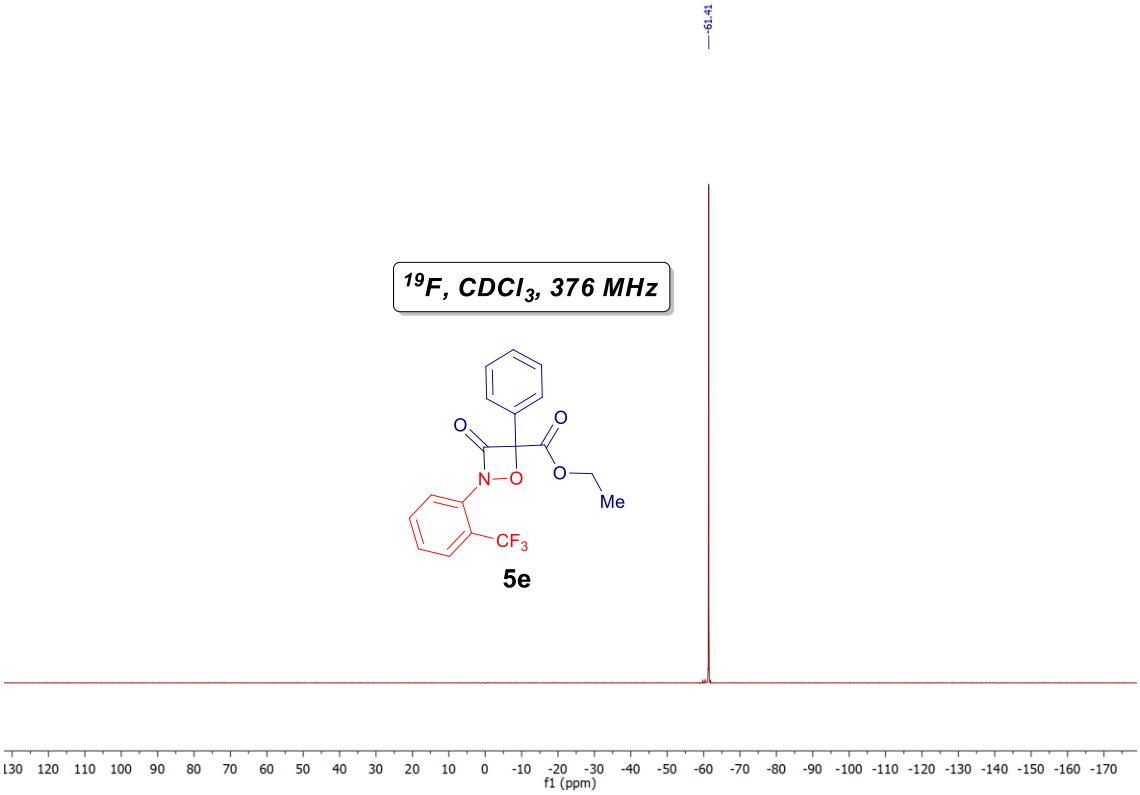




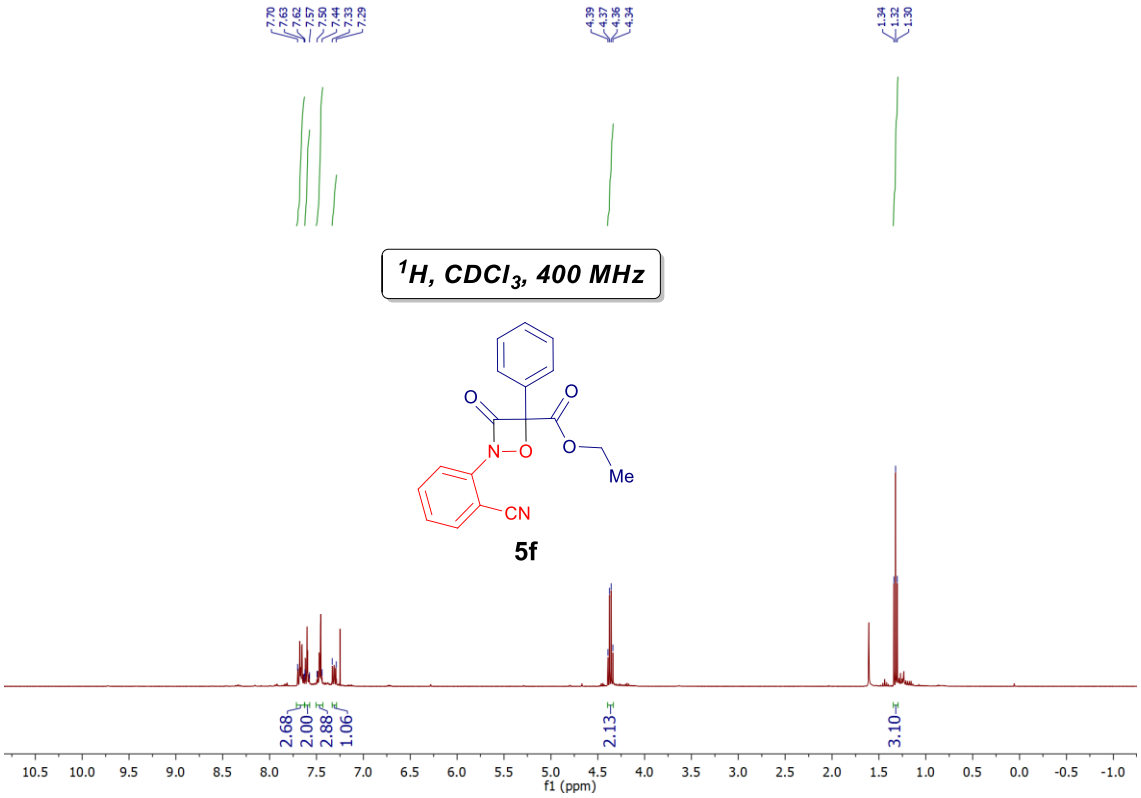
3.6.20. ethyl 3-oxo-4-phenyl-2-(2-(trifluoromethyl)phenyl)-1,2-oxazetidine-4-carboxylate (5e):

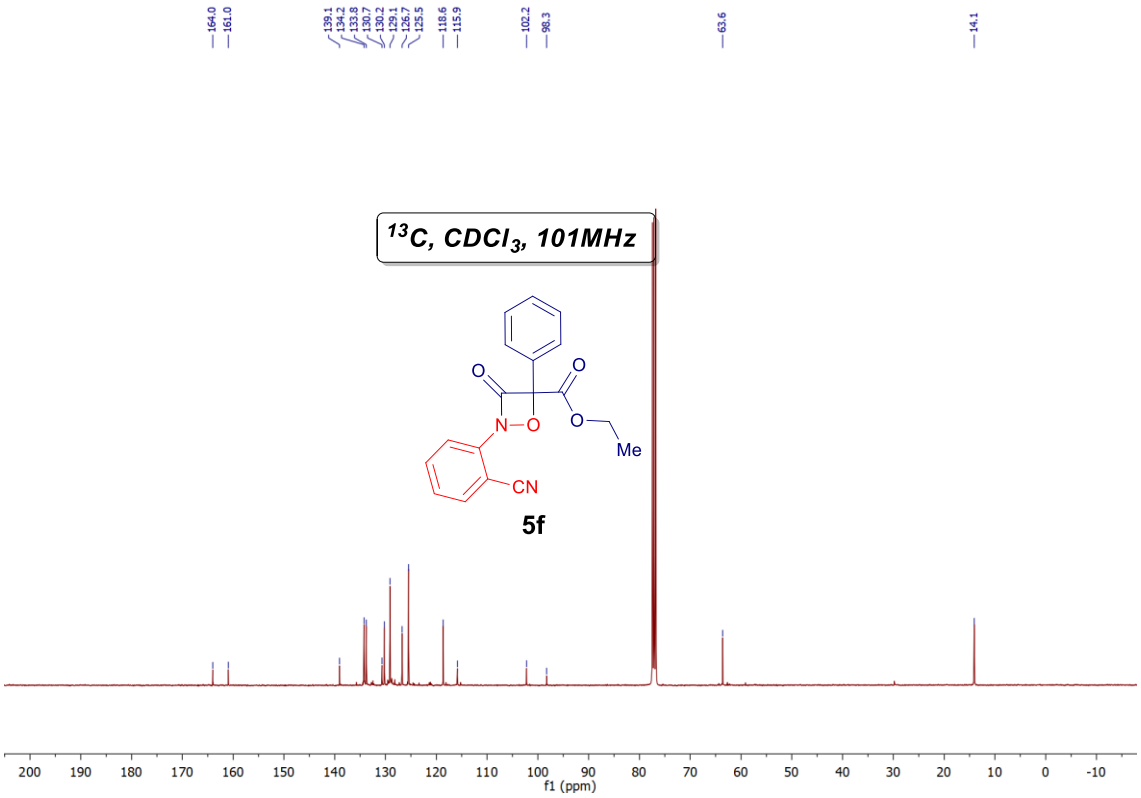




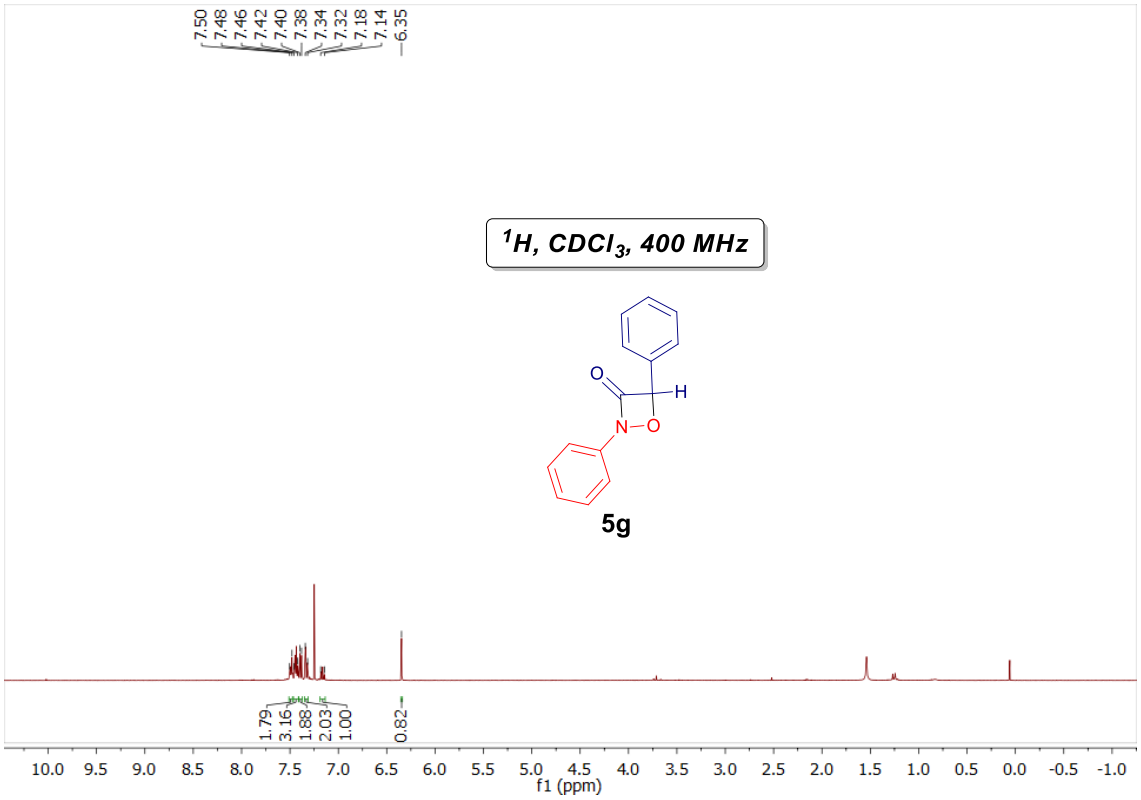


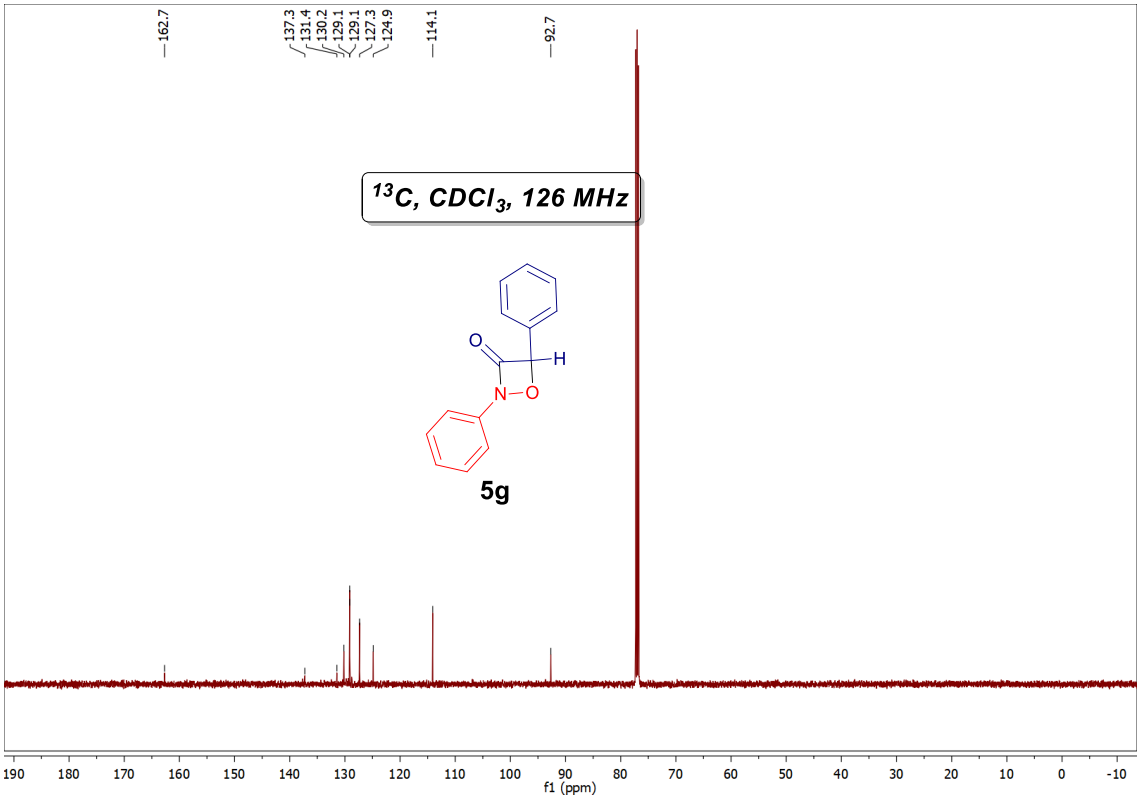
3.6.21. ethyl 2-(2-cyanophenyl)-3-oxo-4-phenyl-1,2-oxazetidine-4-carboxylate (5f):



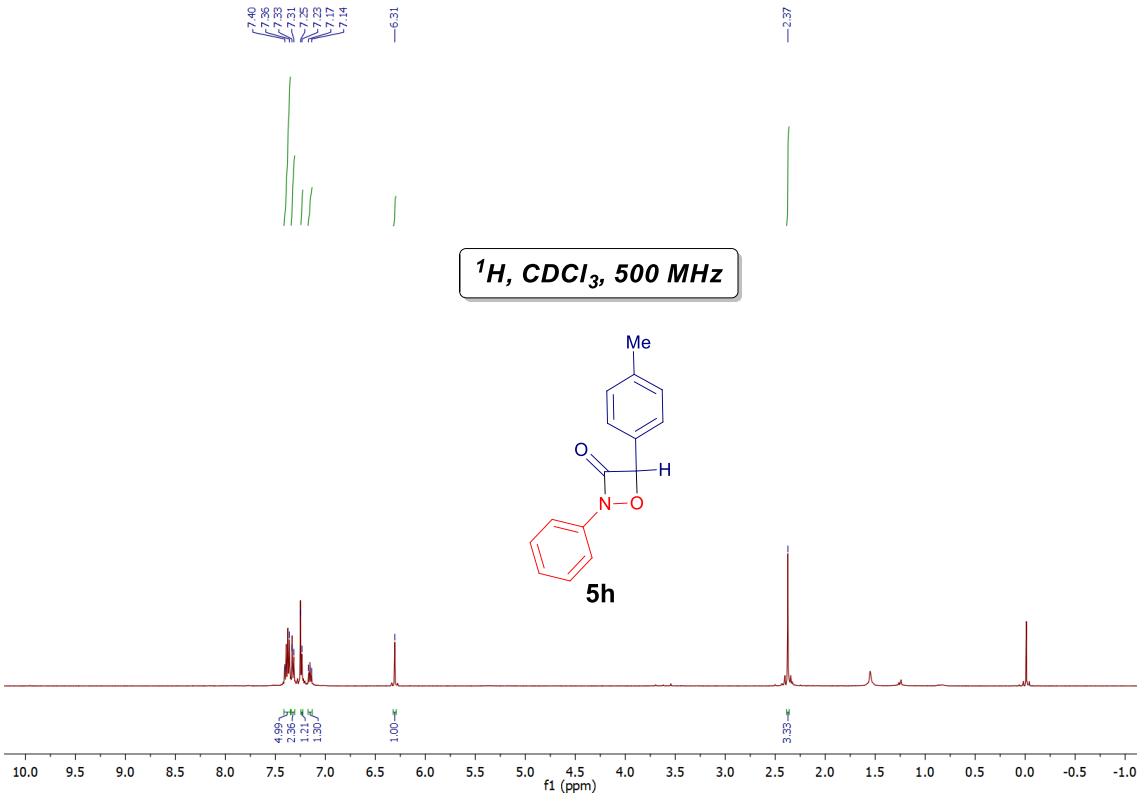


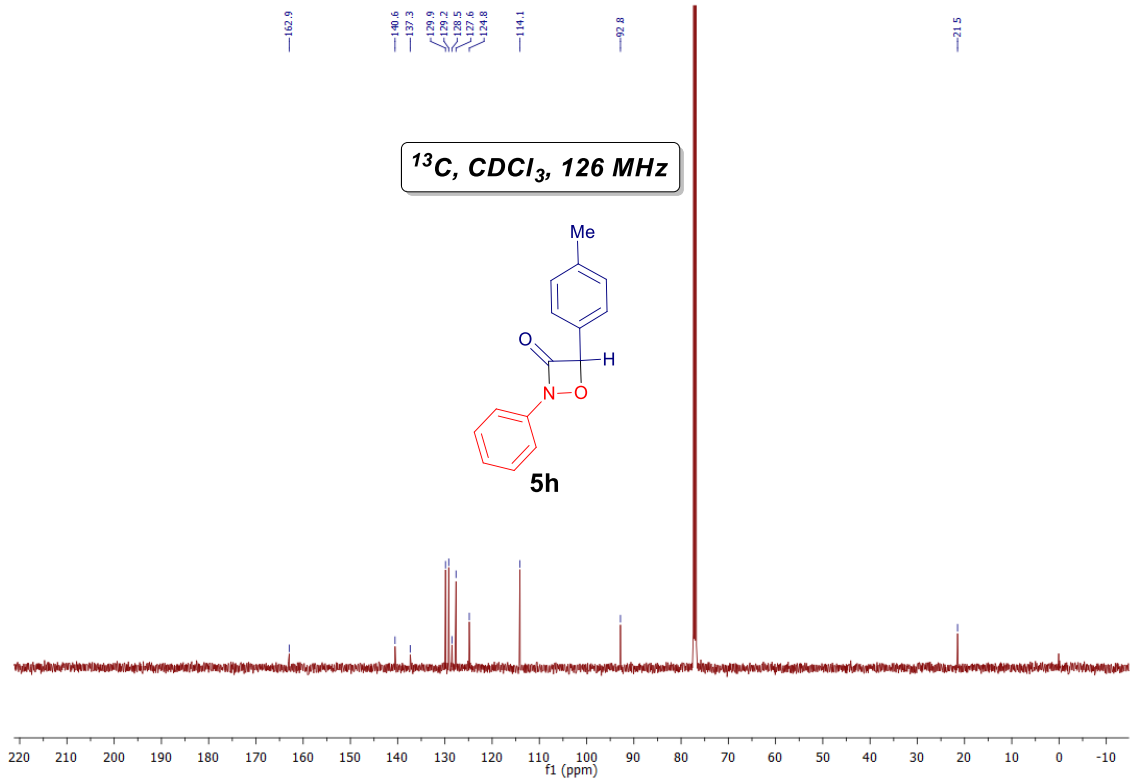
3.6.22. 2,4-diphenyl-1,2-oxazetidin-3-one (5g):



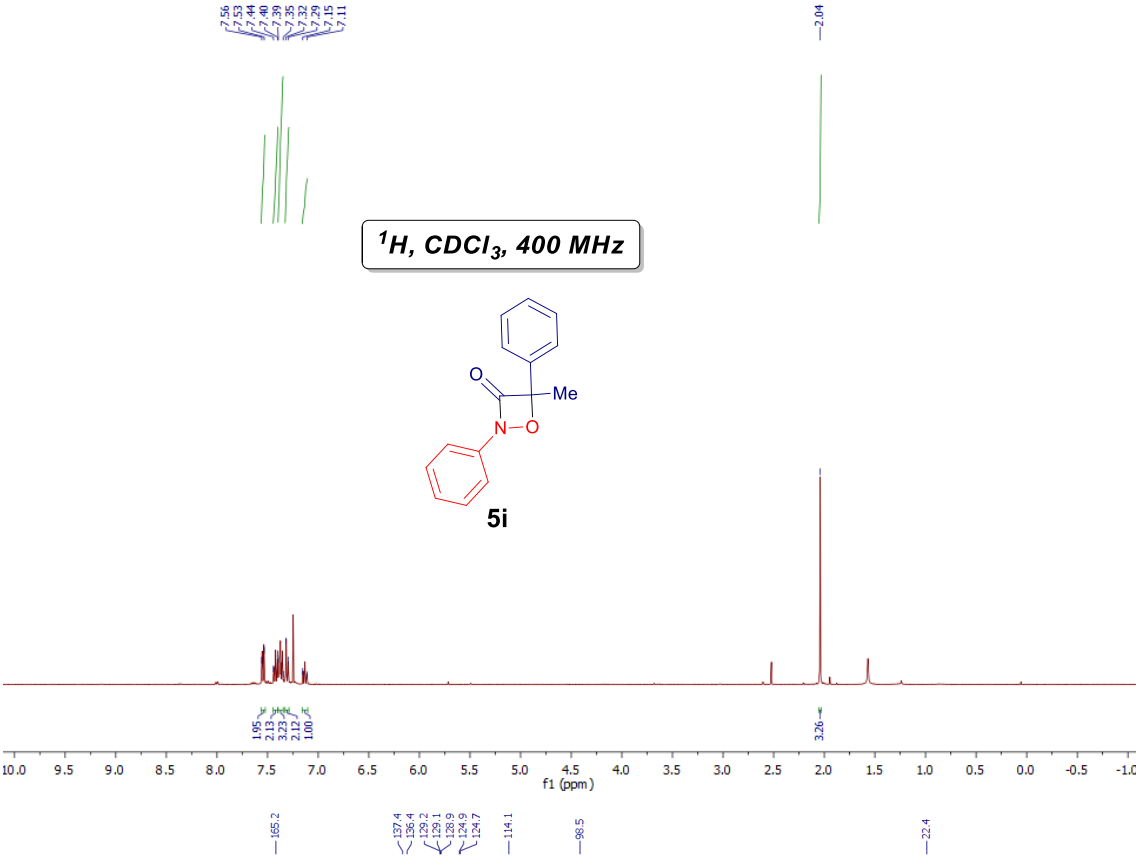

162.7
137.3
131.4
130.2
129.1
129.1
127.3
124.9
114.1
92.7
^{13}C, $CDCl_3$, 126 MHz
O
H
N
O
5g
190
180
170
160
150
140
130
120
110
100
90
80
70
60
50
40
30
20
10
0
-10
f1 (ppm)

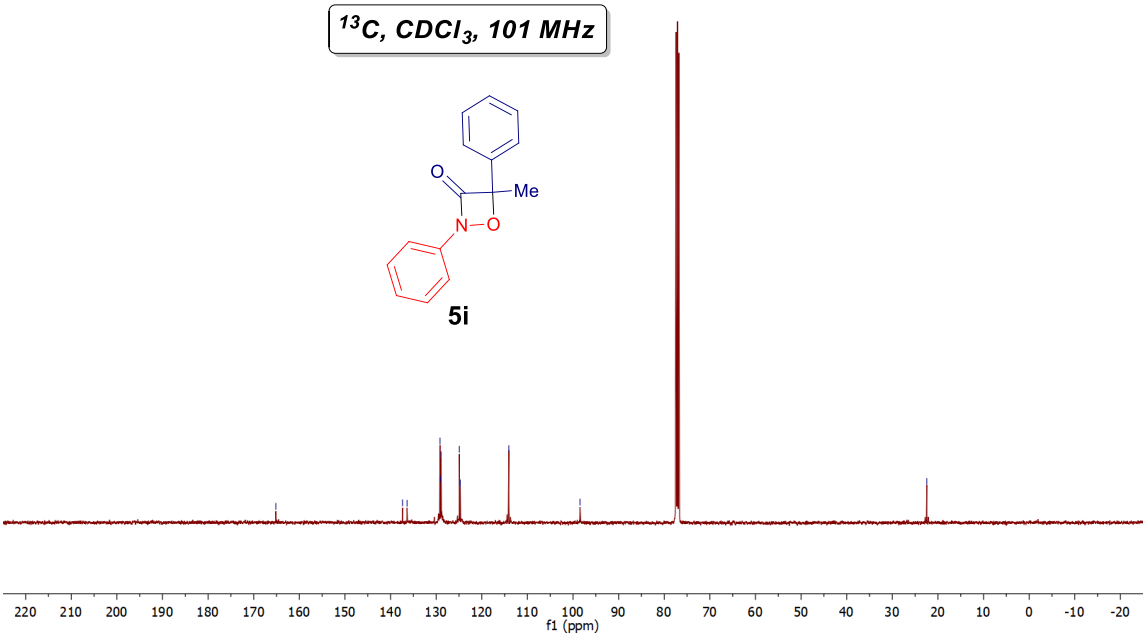
3.6.23. 2-phenyl-4-(*p*-tolyl)-1,2-oxazetidin-3-one (5h):



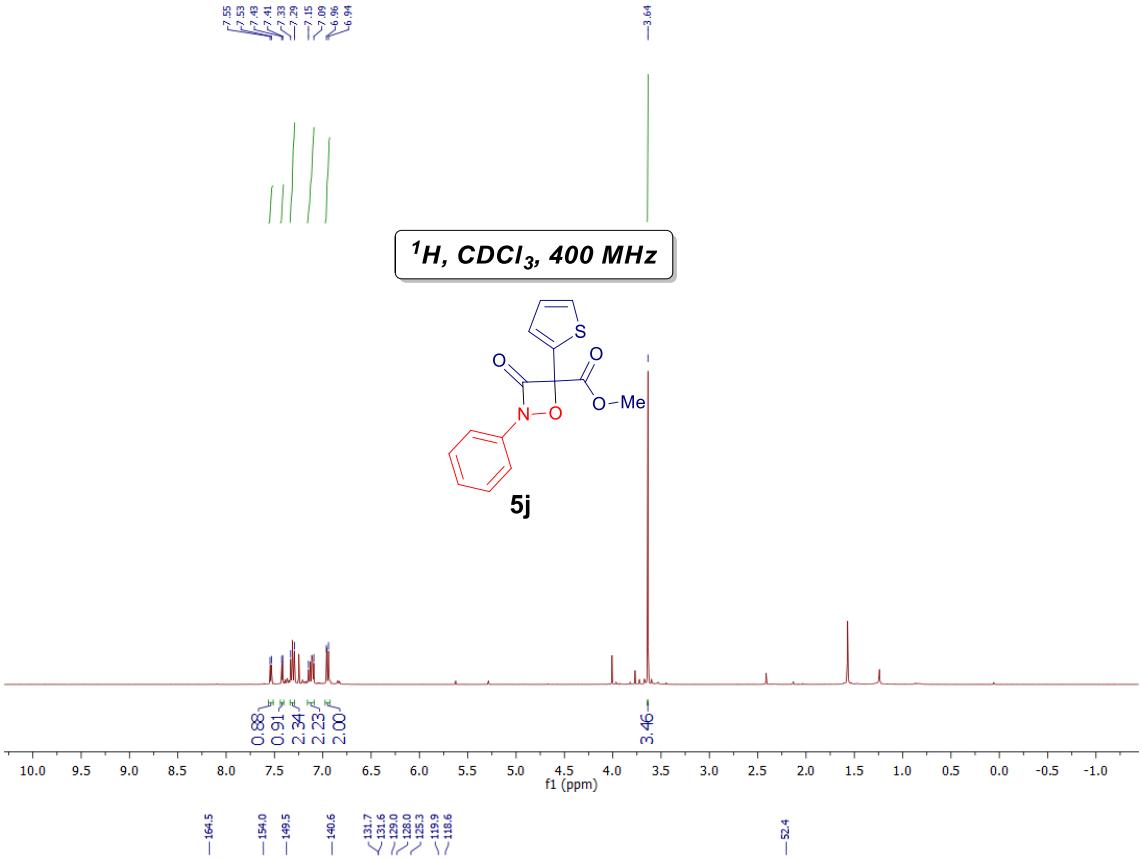


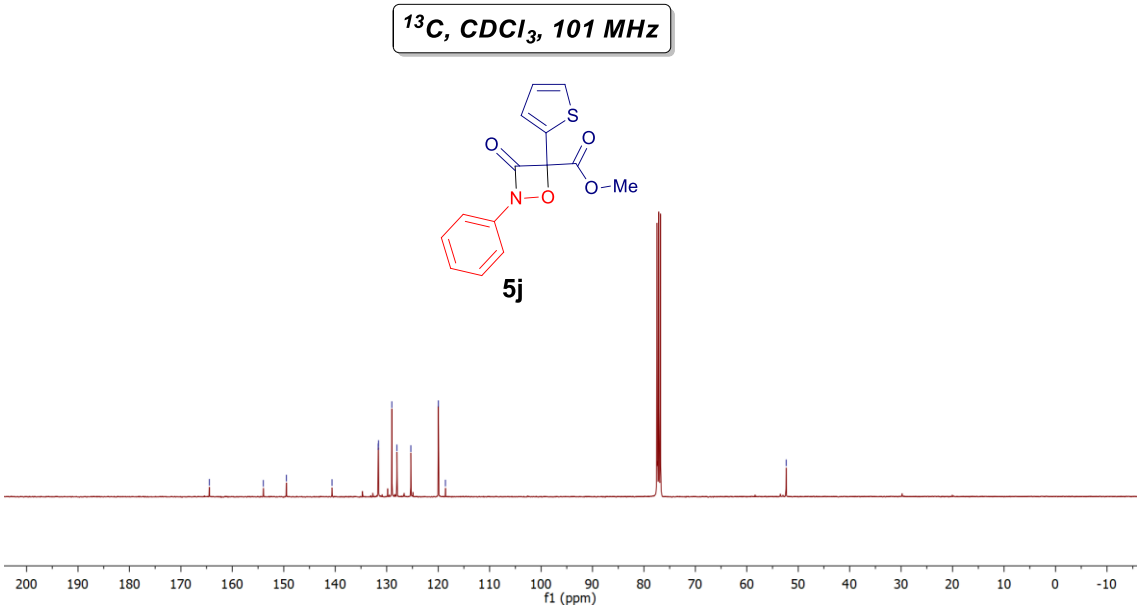
3.6.24. 4-methyl-2,4-diphenyl-1,2-oxazetidin-3-one (5i):



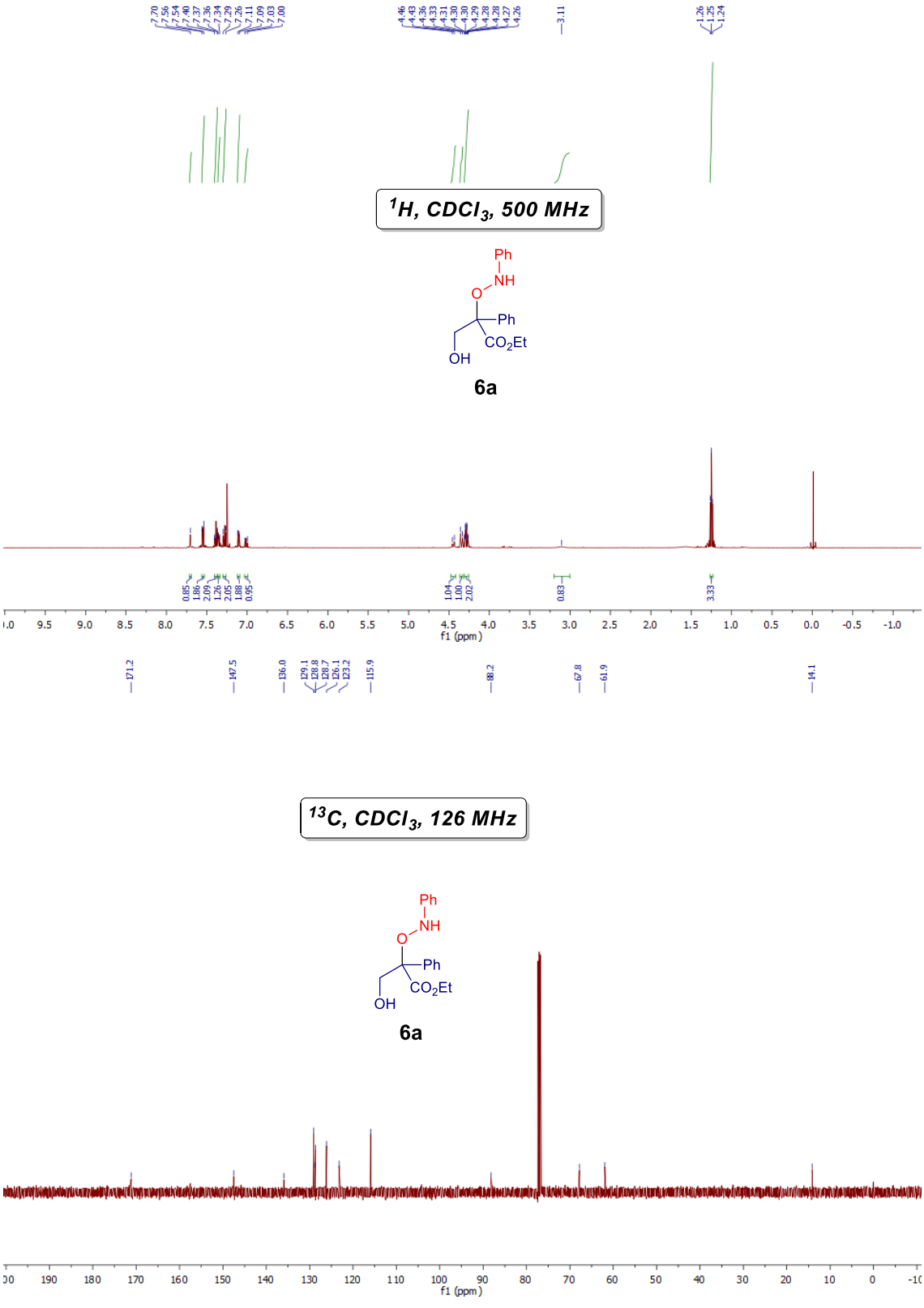


3.6.25. methyl 3-oxo-2-phenyl-4-(thiophen-2-yl)-1,2-oxazetidine-4-carboxylate (5j):

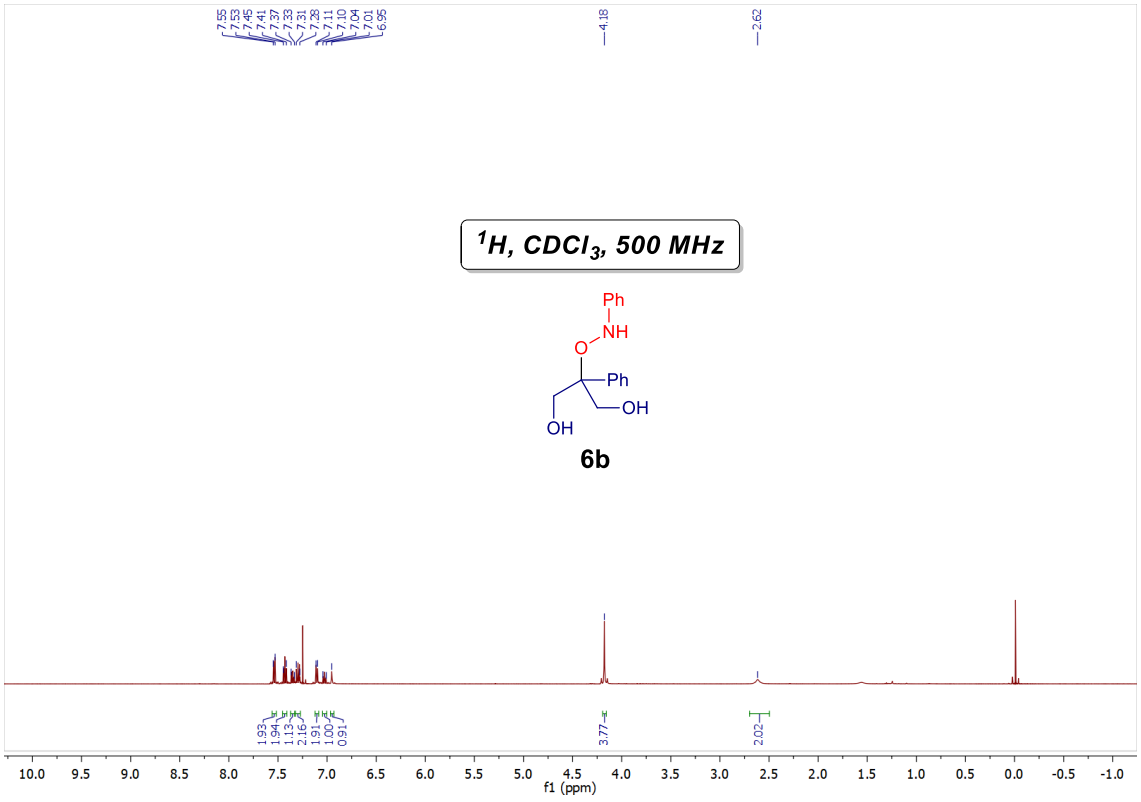


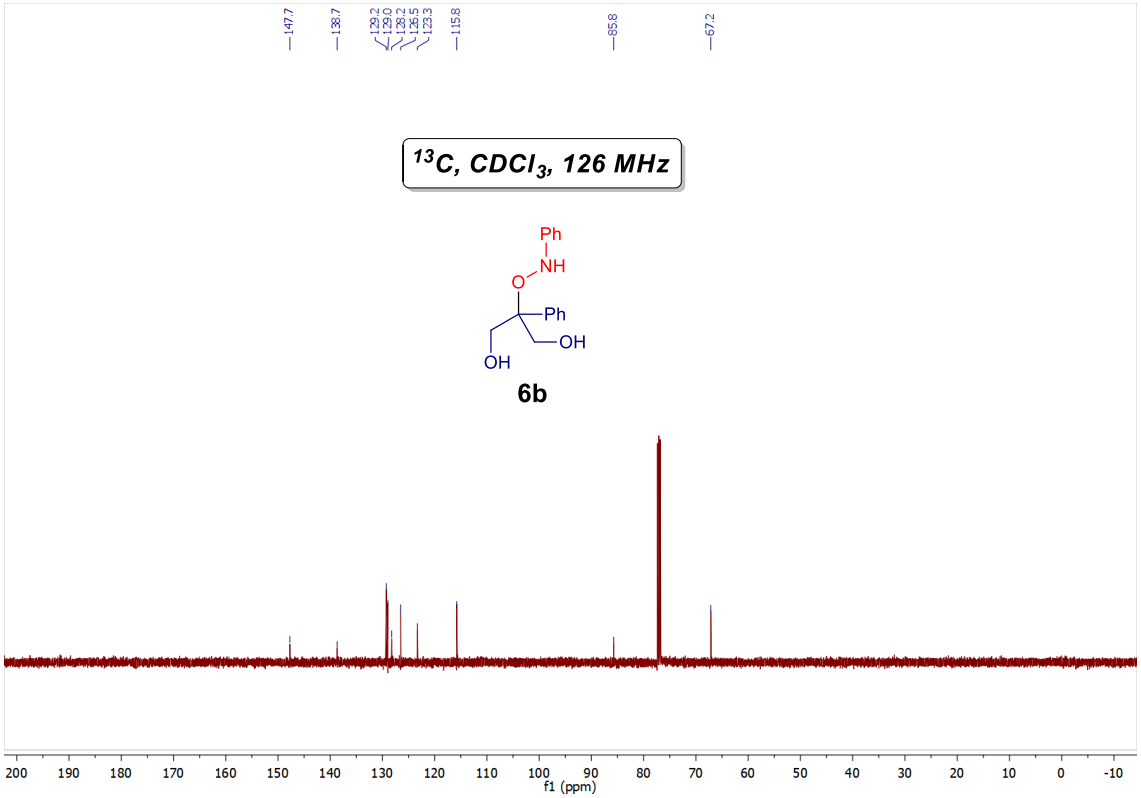


3.6.26. ethyl 3-hydroxy-2-phenyl-2-((phenylamino)oxy)propanoate (6a):

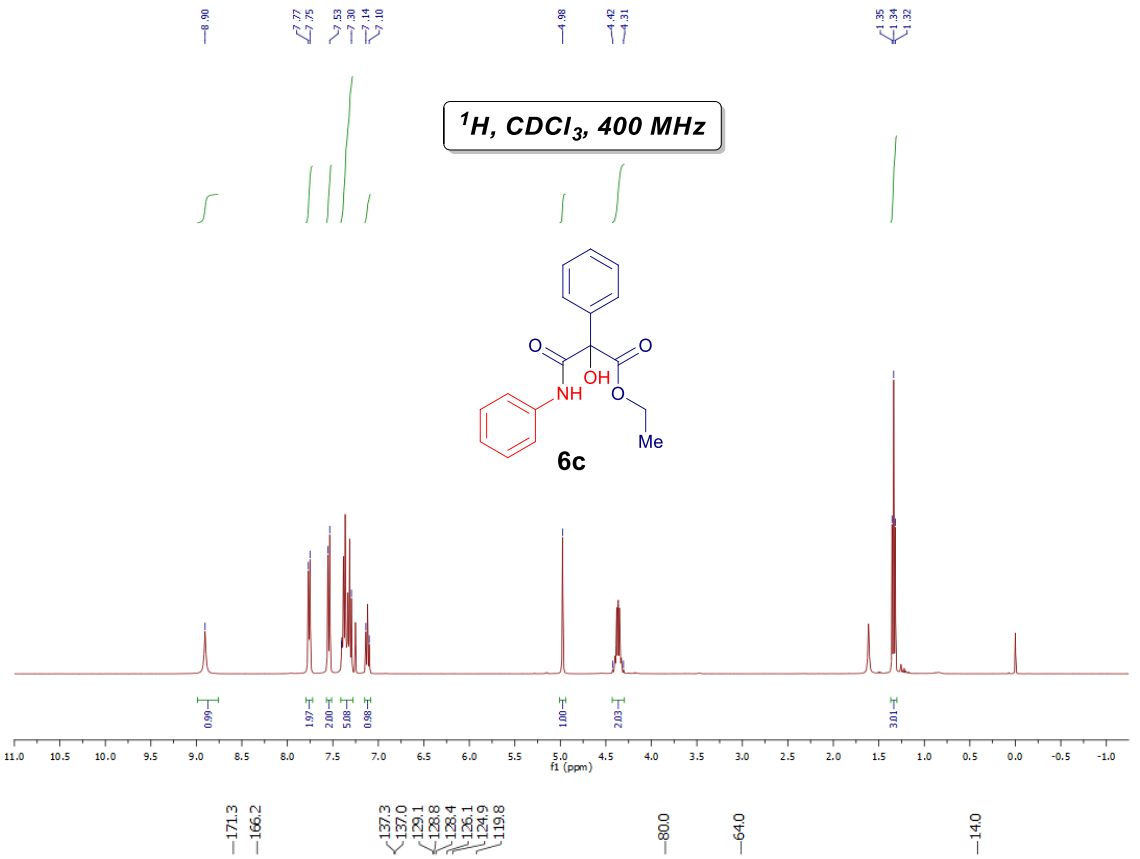


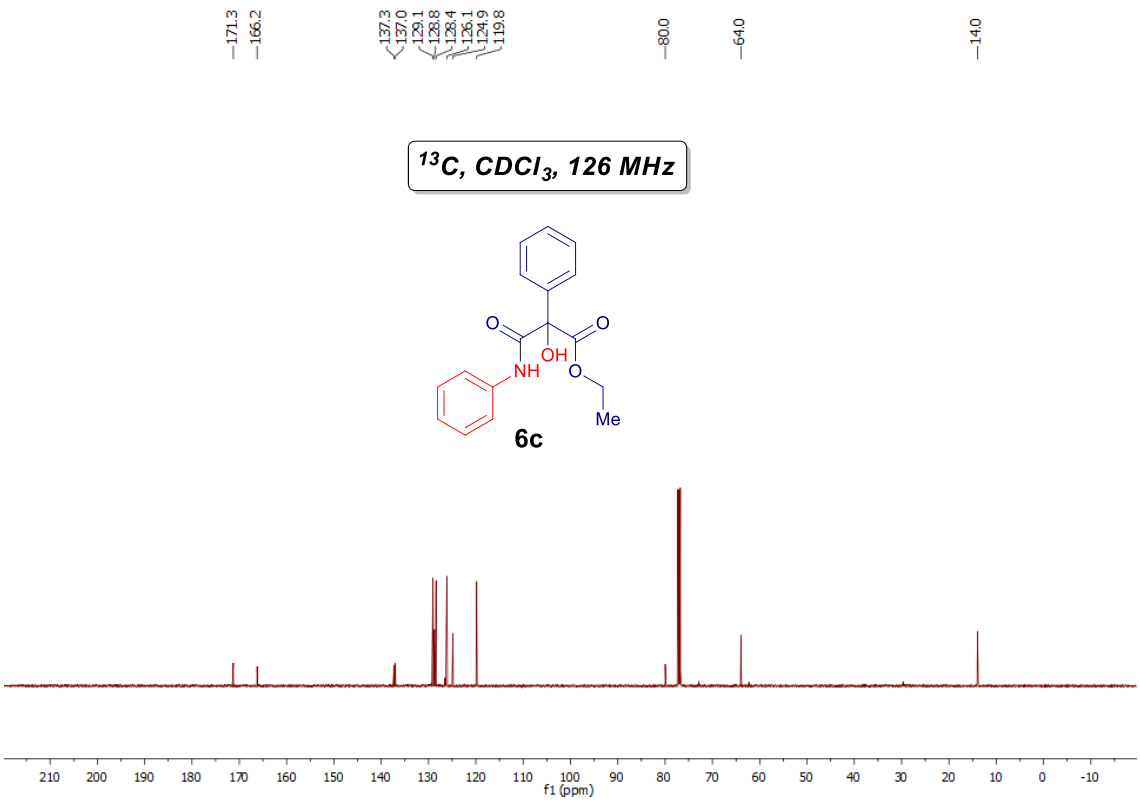
3.6.27. 2-phenyl-2-((phenylamino)oxy)propane-1,3-diol (6b):





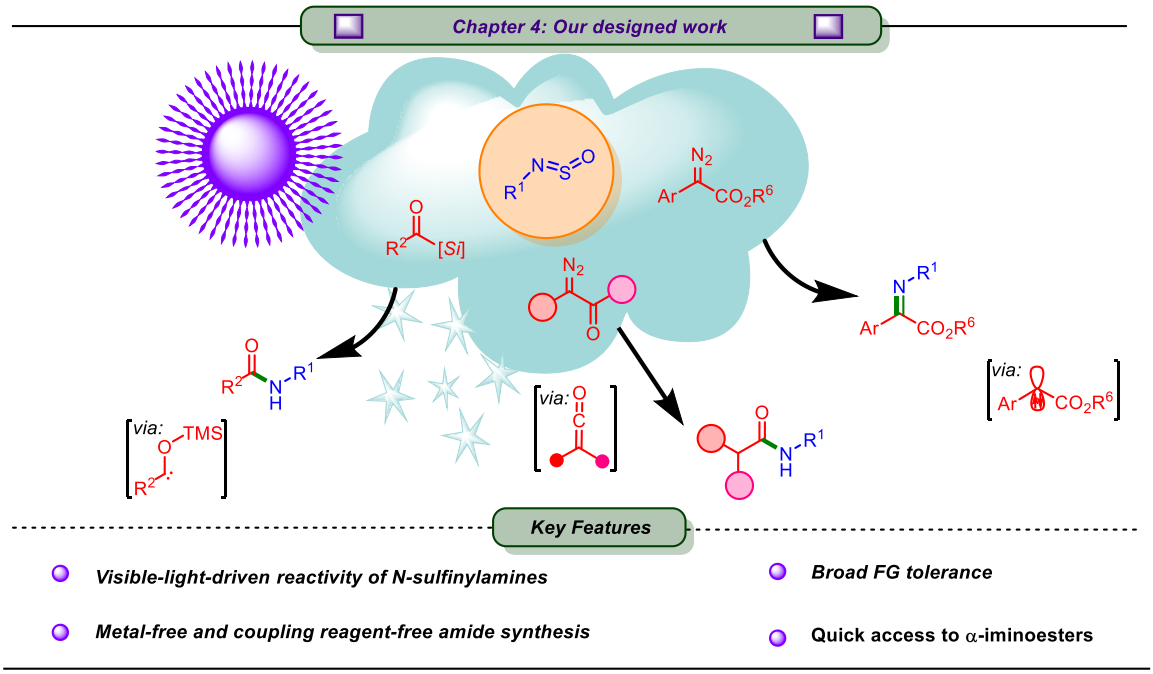
3.6.28. ethyl 2-hydroxy-3-oxo-2-phenyl-3-(phenylamino)propanoate (6c):


8.90
7.77
7.75
7.53
7.30
7.14
7.10
4.98
4.42
4.31
1.35
1.34
1.32
^{1}H, $CDCl_3$, 400 MHz
O
O
OH
NH
O
Me
6c
0.99
1.97
2.00
5.08
0.98
1.00
2.03
3.01
f1 (ppm)


171.3
166.2
137.3
137.0
129.1
128.8
128.4
126.1
124.9
119.8
80.0
64.0
14.0
^{13}C, $CDCl_3$, 126 MHz
O
O
OH
NH
O
Me
6c
f1 (ppm)

Chapter 4

Introducing *N*-Sulfinylamines into Visible-Light-Induced Carbene Chemistry for the Synthesis of Diverse Amides and α-Iminoesters



❖ This work has been submitted for publication.

Author list: **Roy, S.** ‡; Biswas, A. ‡; Paul, H.; Ariyan S.; Chatterjee I.

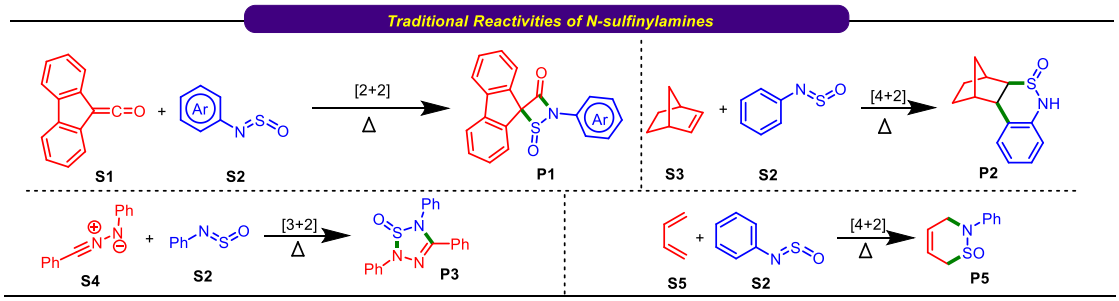
4. Abstract

In this chapter, a rare example of visible-light-mediated diverse reactivity of *N*-Sulfinylamines with different type of carbene precursors has been disclosed. Acylsilanes and aryldiazoacetates have been utilized as nucleophilic and electrophilic carbene precursors into the N=S=O linchpin, to achieve valuable amides and α-iminoesters respectively. On the other hand, diazocarbonyls *in situ* generate ketenes and participate in a visible-light-promoted formal [2 + 2] cycloaddition reaction with N=S=O linchpin followed by release of SO_2 gas to deliver amides. These operationally simple modular method offers a mild, transition metal-free, and coupling reagent-free protocol to fabricate structurally diverse amides and a promptly accessible technique to achieve α-iminoesters, where visible light remains as a key promoter.

4.1. Introduction

After the successful installation of nitrosoarenes into different diazo compounds as a carbene precursor in chapters 3, we wanted to check the reactivity of these carbenes with *N*-sulfinylamines under visible light irradiation.

N-Sulfinylamines have remained noteworthy reagent since 19th century due to its versatile reactivity and straightforward single-step preparation from corresponding amines with thionyl chloride.[1] The physical properties of the *N*-sulfinylamine derivatives make the *S*-center as the positive end and the *N*-center as the negative end of the dipole. Thus, these substances can offer a wide array of six-membered, five-membered, or four-membered rings by virtue of various cycloaddition reactions (Scheme 4.1.1). Additionally, they can react with electrophilic or nucleophilic reagents to render numerous valuable motifs.[2]

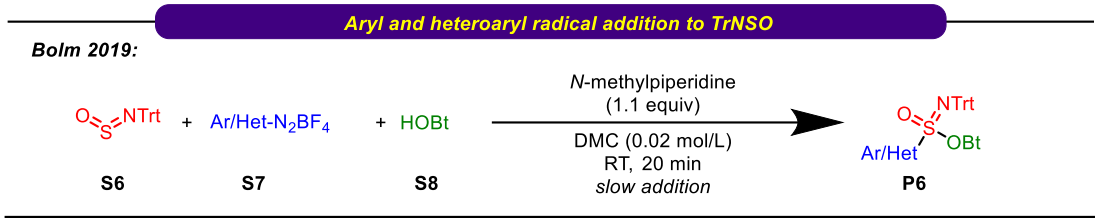


Scheme 4.1.1: Traditional Reactivity of *N*-sulfinylamine Compounds.

Besides its traditional reactivity, last few years have witnessed ample growing interest in harnessing the tuneable reactivity of *N*-sulfinylamines. In this direction, some novel sulfinylamine reagents e.g., *N*-sulfinyltritylamine (Tr-NSO), *N*-triisopropylsilyl sulfinylamine (TIPS-NSO), *N*-sulfinyl-*O*-(tert-butyl)-hydroxylamine (^{t}BuONSO) were prepared and had been widely studied

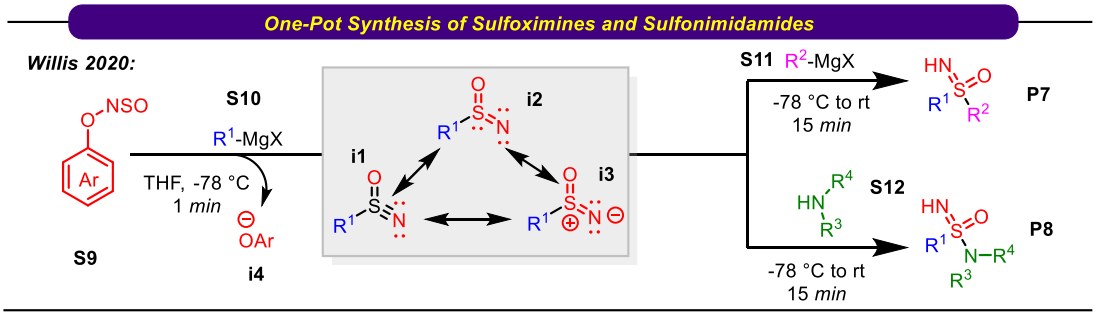
with various organometallic reagents, resulting in important sulfonimidamides, sulfinamides, and sulfonamide derivatives.[3]

In 2019, Bolm et al. were able to disclose a vital method for sulfonimidamide **P6** synthesis by reacting aryldiazonium tetrafluoroborates **S7** as an aryl radical precursor with *N*-tritylsulfinylamine **S6**, and *N*-hydroxybenzotriazole hydrate **S8**. The reaction can be conducted under aerobic conditions and show broad functional group tolerability (Scheme 4.1.2).[5a]



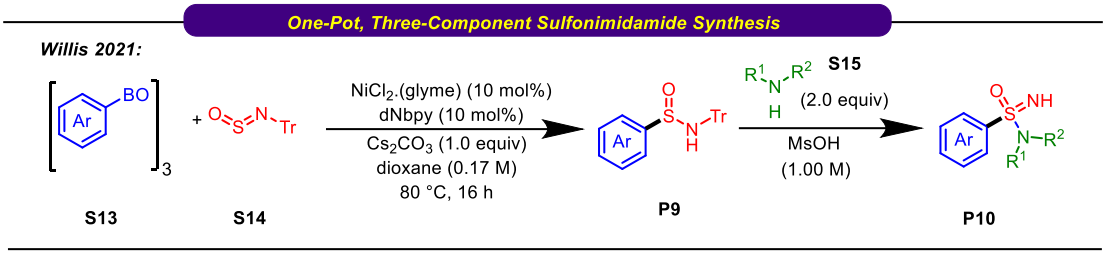
Scheme 4.1.2: Bolm's Reactivity of Aryldiazonium Salts with Trityl Substituted *N*-sulfinylamine.

In 2020, Willis et al. developed a unified, one-pot synthesis of both sulfoximines **P7** and sulfonimidamides **P8** by exploiting the high electrophilicity of sulfinyl nitrenes (**i1**, **i2**, **i3**). These rare reactive intermediates were generated from a novel sulfinylhydroxylamine (R−O−N=S=O) **S9** reagent via an N−O bond fragmentation process. Organometallic reagents like alkyl, (hetero)aryl, and alkenyls (**S10** and **S11**) were used as the first or second reacting components. On the other hand, primary and secondary amines and anilines **S12** were used as the second nucleophile to furnish the desired products (Scheme 4.1.3).[5b]



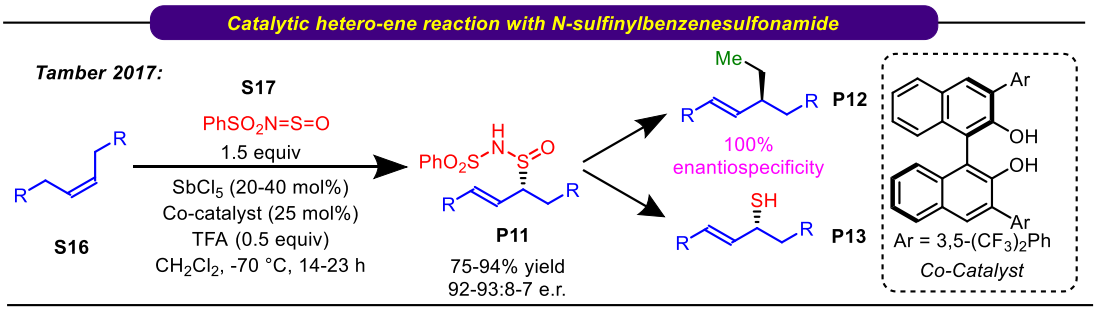
Scheme 4.1.3: Willis's One-Pot Synthesis of Sulfoximines and Sulfonimidamides Using *N*-sulfinylamines Compounds.

In the consecutive years, same group developed a useful protocol by applying a redox-neutral Ni(II)-catalyzed addition of (hetero)aryl boroxines **S13** to *N*-sulfinyltritylamine (Tr-NSO) **S14** to furnish aryl sulfinamides **P9**, which was converted into corresponding sulfonimidamides **P10** in a one-pot sequential operation by reacting with amine derivatives **S15** (Scheme 4.1.4).[4]



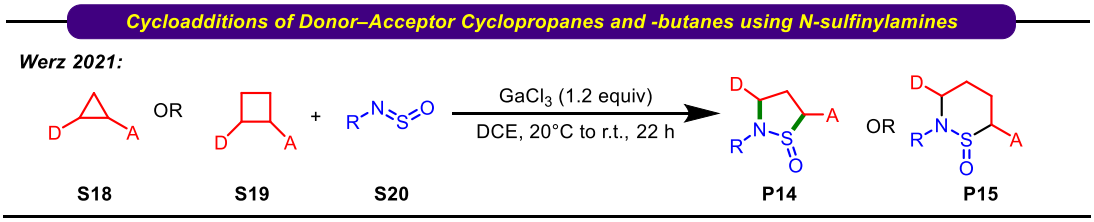
Scheme 4.1.4: Willis's One-Pot Three-Component Sulfonimidamides Using *N*-sulfinylamines Compounds.

Lewis-acid catalysis has been introduced in this direction by Tambar group. In 2017, they have used $SbCl_5$ as Lewis-acid for the enantioselective, regioselective and *E/Z*-selective allylic oxidation of unactivated internal alkenes **S16** via a catalytic hetero-ene reaction with *N*-sulfinylbenzenesulfonamide **S17** (Scheme 4.1.5).[6a]



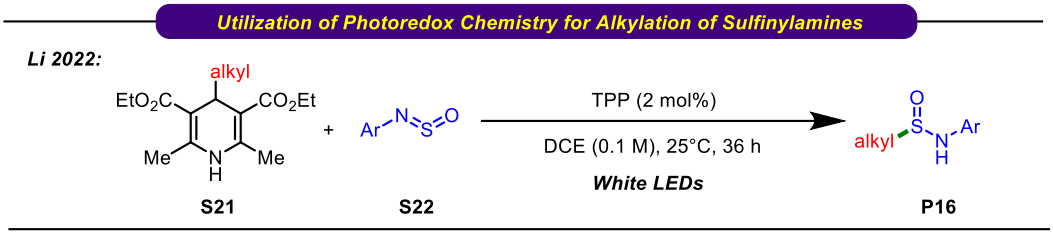
Scheme 4.1.5: Tamber's Catalytic Oxidation of Internal Alkenes Using *N*-Sulfinylbenzenesulfonamide.

In the same line, in 2021, Werz and co-workers exploited the traditional 2π electronic nature of the N=S bond present in *N*-sulfinylamines **S20** by performing [3+2] and [4+2] cycloaddition reactions with donor-acceptor cyclopropane **S18** and cyclobutane **S19** derivatives using $GaCl_3$ as a Lewis-acid (Scheme 4.1.6).[6b]



Scheme 4.1.6: Wertz's [3+2] and [4+2] Cycloaddition Using *N*-Sulfinylanilines, Cyclopropane and Cyclobutates.

Apart from these reports, in recent times, Li et al. have introduced photoredox chemistry to react *N*-sulfinylamines **S22** with C(sp^3)-centered alkyl radicals generated *in situ* from 1,4-dihydropyridine **S21** derivatives to furnish the corresponding sulfinamides **P16** (Scheme 4.1.7).[7]

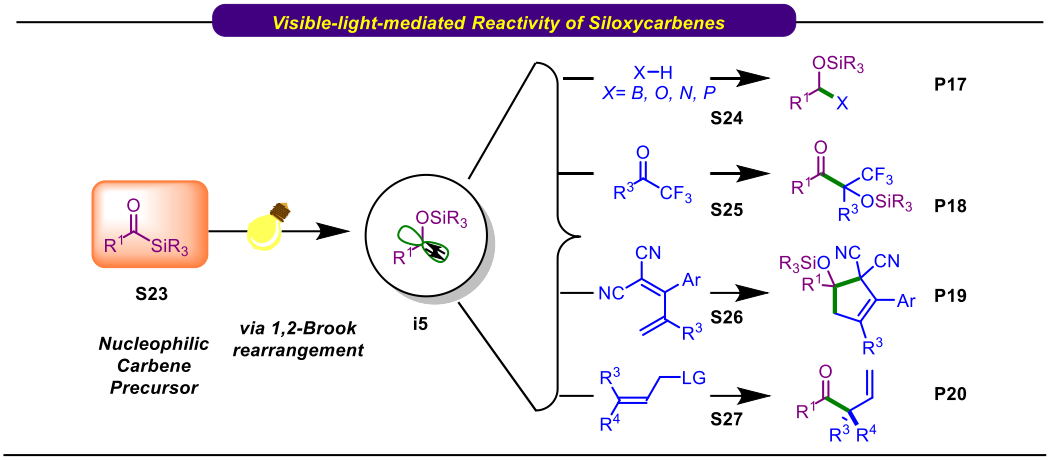


Scheme 4.1.7: Li's introduction of Photoredox Chemistry into *N*-sulfinylamine Compounds.

The reports mentioned above are majorly substrate specific, restricted to the use of hard nucleophiles like organometallic reagents or transition-metal catalysis. However, the utilization of visible light alone in this direction is rare.[7] Therefore, in order to capitalize on this momentum and search for a new reactivity of *N*-sulfinylamines we intend to explore the photoinduced carbene chemistry into N=S=O linchpin.

Over a few decades, carbenes remained an imperative intermediate to introduce various functionalities. In classical organic chemistry, diazo compounds are used as a common source to generate singlet and triplet carbene intermediates or metal carbenoids under thermal or photochemical conditions.[8] Apart from these, modern-day chemistry has delivered ingenious methods by harnessing visible light as a crucial promoter to generate electrophilic carbene intermediates from diazo compounds. Therefore, visible light became an alternative for hazardous transition-metal catalysis due to its operationally simpler, milder, and/or greener reaction conditions.[9]

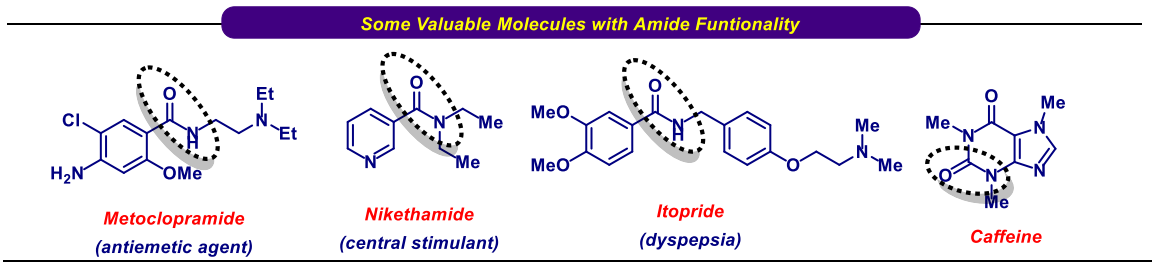
Alike diazo compounds, acylsilanes **S23** are also known as an efficient carbene precursor as they can deliver nucleophilic siloxycarbenes **i5** via 1,2-Brook rearrangement upon photolysis or using high temperature. Since its first synthetic utilization by Brook et al. in 1957,[10] synthetic potential of acylsilanes **S23** in organic chemistry have gained significant interest due to their interesting chemical and physical properties.[11] Although several elegant protocols came across, the reactivity of acylsilanes **S23** was majorly restricted to the use of transition-metal catalysts, organometallic reagents, elevated temperature, high-pressure mercury lamp, etc. Thus, visible light has been introduced in this direction to pursue a milder and greener way.[12] A great effort has been devoted by Glorius, Bolm, Kusama, Shen, Studer, Xuan, Priebbenow, and other research groups, to unfold the visible-light-promoted reactivity of nucleophilic siloxycarbenes derived from acylsilanes producing an ample number of new methods including X−H (B−H, O−H, N−H, P−H) bond insertion, carboxylation, 1,2-carbonyl addition, and various cycloadditions (Scheme 4.1.8).[13]



Scheme 4.1.8: Reactivity of Siloxycarbenes Under Visible Light.

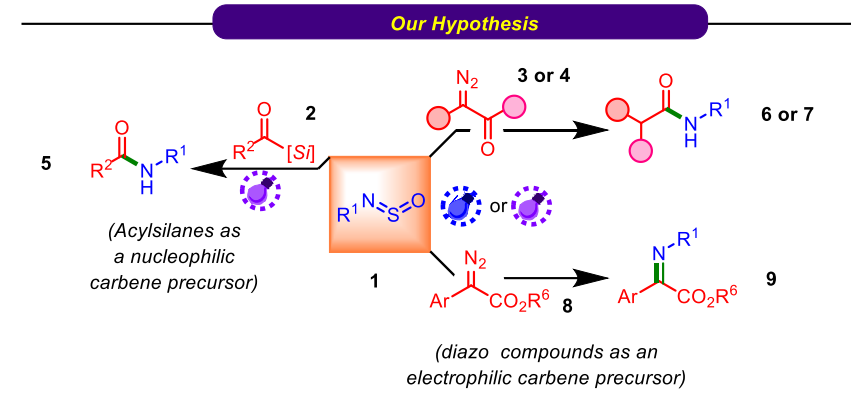
However, the reactivity of visible-light-driven carbene chemistry with *N*-sulfinylamines remained under-explored. Herein, we have disclosed a visible-light-mediated diverse reactivity of *N*-sulfinylamines by reacting with both nucleophilic (acylsilanes) and electrophilic (diazo compounds) carbene precursors, resulting in a wide range of amides and α-iminoesters.

Amides are of fundamental importance in medicinal and process chemistry as they are ubiquitous in proteins, peptides, and crucial drugs (Scheme 4.1.9). Traditional methods for amide synthesis involve the use of stoichiometric amounts of coupling reagents (e.g., EDC, HATU, PyBOP, etc.). Major drawbacks associated with these protocols are the use of elevated temperatures, high cost, and waste generation. Therefore, numerous calls have been made for more efficient methods, and comprehensive reports have come across over the years to bypass the traditional method. However, these reports mainly dealt with the use of metal catalysis (Au, Cu, Pd, etc.).[14] Likewise, α-iminoesters are valuable precursors for synthesizing several natural and unnatural α-amino acid derivatives.[15]



Scheme 4.1.9: Amide Functionality in Different Valuable Motifs.

Therefore, developing an alternative and more sustainable method for amides and α-iminoesters synthesis is always desirable. The present methodology demonstrates a unique advantage over traditional methods to prepare amides and α-iminoester under catalyst-free, coupling reagent-free and mild reaction conditions with shorter reaction time (Scheme 4.1.10).



Scheme 4.1.10: Chapter 4: Our Proposed Working Hypothesis

4.2. Result and Discussion

4.2.1 Optimization of the Reaction Condition for Amide 5

As per our speculation (described in Scheme 10), initial efforts were devoted to conduct the reactions between acylsilane **2a** and *N*-sulfinylaniline **1a** as model substrates under visible light irradiation to form the amide bond without any metal catalyst or coupling reagents.

First, we varied the equivalency of the reactants and reaction time by fixing DCM as a solvent under blue LEDs irradiation, resulting in *N*-phenylbenzamide **5a** in moderate yield (Table 1, entry 4).

4.2.1.1. Chapter 4: Table 1: Miscellaneous Optimization-1[a]

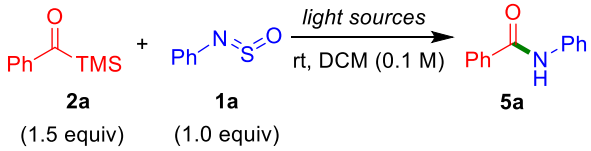


Entry	2a (equiv)	1a (equiv)	time (h)	Yield (%)[b]
1	1	1	10	35
2	1	2	10	32
3	2	1	10	45
4	**1.5**	**1**	**10**	**44**
5	1.5	1	5	30
6	1.5	1	16	47

[a] unless untill mentioned all reactions were carried out in 0.1 mmol scale.
[b] measured by ^{1}H-NMR analysis of the crude reaction mixture using CH_2Br_2 as an internal standard.

Next, in order to find better reaction conditions, we varied several light sources with different wavelengths. Among them, purple LEDs (405 nm) gave the best result with 57% of the isolated yield of *N*-phenylbenzamide **5a** (Table 2, entry 3).

4.2.1.2. Chapter 4: Table 2: Screening of Different Light Sources-1[a]



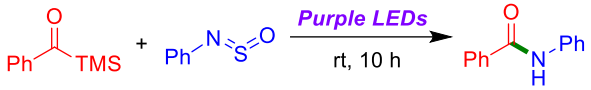
2a (1.5 equiv) **1a** (1.0 equiv) **5a**

Entry	*light sources*	Yield (%)[b]
1	Blue LEDs (450 nm)	44
2	Blue LEDs (420 nm)	50
3	**Purple LEDs (405 nm)**	**57**
4	UV LEDs (365 nm)	22
5	Blue LEDs (strip)	30
6	Green LEDs (strip)	15
7	White LEDs	trace
8	in dark	0

[a] unless untill mentioned all reactions were carried out in 0.1 mmol scale.
[b] measured by ^{1}H-NMR analysis of the crude reaction mixture using CH_2Br_2 as an internal standard.

Solvent can play a crucial role in any organic reaction. Therefore, different solvents and its concentration were varied, which revealed diethyl ether (0.2 M) has more potentiality over others (Table 3, entry 8).

4.2.1.3. Chapter 4: Table 3: Screening of Different Solvents-1[a]



2a (1.5 equiv) **1a** (1.0 equiv) **5a**

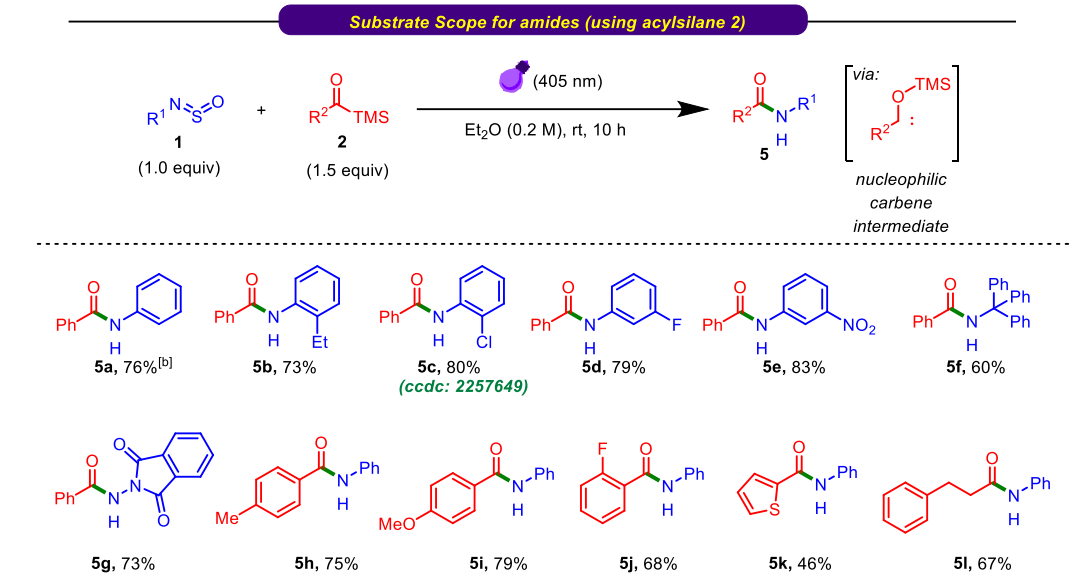
Entry	Solvent (M)	Yield (%)[b]
1	DCM (0.1 M)	57
2	THF (0.1 M)	60
3	Et_2O (0.1 M)	70
4	ACN (0.1 M)	48
5	toluene (0.1 M)	50
6	DMF (0.1 M)	23
7	DCE (0.1 M)	54
8	**Et_2O (0.2 M)**	**82 (76%)**

[a] unless untill mentioned all reactions were carried out in 0.1 mmol scale.
[b] measured by ^{1}H-NMR analysis of the crude reaction mixture using CH_2Br_2 as an internal standard. Isolated yield in bracket.

4.2.2 Substrate Scope Evaluation for Amide 5

With the optimal conditions in hand (Table 3, entry 8), we assessed the robustness of the reaction first by varying electronics on the aryl ring of *N*-sulfinylaniline **1** to achieve the desired amide derivatives (Scheme 4.2.2.1, entries **5b**-**5e**). Next, a variation on *N*-center of *N*-sulfinylamines unfolds that this protocol is not limited to *N*-sulfinylaniline derivatives, as trityl and phthalimide groups were well tolerated under the optimized reaction conditions (Scheme 4.2.2.1, entries **5f** and **5g**).

We then checked the reactivity of acylsilanes **2** by incorporating electron-donating, electron-withdrawing group containing aryl rings, and heterocyclic species to furnish desired amides in good yields (Scheme 4.2.2.1, entries **5h**-**5k**). Moreover, an aliphatic group containing acylsilane also delivered product **5l** in 67% yield.



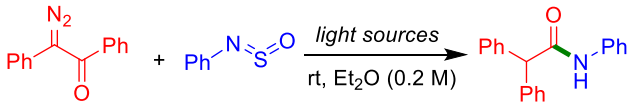
Scheme 4.2.2.1: Substrate Scope Evaluation for Amide **5**.

To check the versatility of this photoinduced amidation reaction, we then moved from acylsilanes **2** to diazo ketones **3** (Table 5), which are well known to form *in situ* ketenes via Wolff rearrangement.[16, 17]

4.2.3 Optimization of the Reaction Condition for Amide 6

In order to find the best-fitted reaction condition, we again investigated the reaction parameters first by choosing diazo ketone **3a** and *N*-sulfinylanilines **1a** as model substrates under different light sources (Table 5). Finally, we found that the amide **6a** formed with 60% yield under blue LEDs (450 nm) irradiation (Table 5, entry 2).

4.2.3.1. Chapter 4: Table 5: Screening of Different Light Source-2[a]



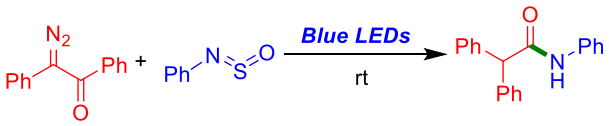
3a (1.5 equiv) **1a** (1.0 equiv) **6a**

Entry	*light sources*	Yield (%)[b]
1	Purple LEDs (405 nm)	45
2	**Blue LEDs (450 nm)**	**60**
3	Blue LEDs (420 nm)	56
4	UV LEDs (365 nm)	28
5	Blue LEDs (strip)	35
6	Green LEDs (strip)	20
7	White LEDs	10
8	in dark	trace

[a] unless untill mentioned all reactions were carried out in 0.1 mmol scale.
[b] measured by ^{1}H-NMR analysis of the crude reaction mixture using CH_2Br_2 as an internal standard.

Thereafter, an extensive screening of solvents, and other reaction parameters suggested that DCM solvent is the most suitable one under blue LEDs irradiation to form amide **6a** within 4 h (Table 6, entry 9).

4.2.3.2. Chapter 4: Table 6: Miscellaneous Optimization-2[a]



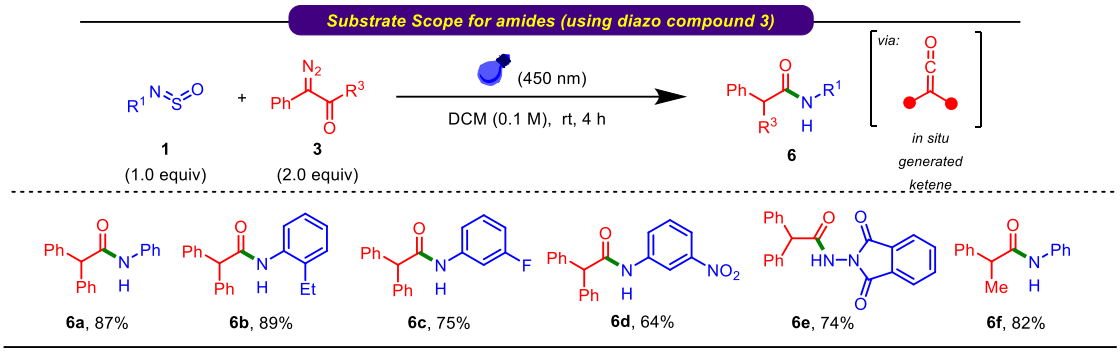
3a **1a** **6a**

Entry	3a (equiv)	1a (equiv)	Solvent (M)	Time	Yield (%)[b]
1	1.5	1	Et_2O (0.2 M)	10 h	60
2	1.5	1	THF (0.2 M)	10 h	54
3	1.5	1	DCM (0.2 M)	10 h	70
4	1.5	1	ACN (0.2 M)	10 h	40
5	1.5	1	toluene (0. 2 M)	10 h	47
6	1.5	1	DCM (0.1 M)	10 h	80
7	2	1	DCM (0.1 M)	10 h	90
8	1	2	DCM (0.1 M)	10 h	40
9	**2**	**1**	**DCM (0.1 M)**	**4 h**	**91 (87%)**
10	2	1	DCM (0.1 M)	16 h	93

[a] unless untill mentioned all reactions were carried out in 0.1 mmol scale.
[b] measured by ^{1}H-NMR analysis of the crude reaction mixture using CH_2Br_2 as an internal standard. Isolated yield in bracket.

4.2.4. Substrate Scope Evaluation for Amide 6

The optimized reaction condition (Table 6, entry 9) was applied to explore the substrate scope. Delightfully, under blue LEDs (450 nm) irradiation, diazo ketones **3** reacted well with various *N*-sulfinylamines **1**, ranging from different aromatic as well as heteroaromatics delivering amides **6** in good yields (Scheme 4.2.4.1, entries **6a-6f**).[18a]



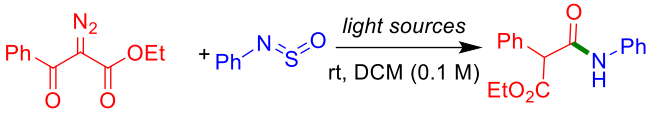
Scheme 4.2.4.1: Substrate Scope Evaluation for Amide **6**.

To test the broadness of this protocol, the reactivity of another class of diazo compounds α-diazo-β-keto esters (or α-diazo-1,3 diketone) **4** were also investigated (Table 7).

4.2.5. Optimization of the Reaction Condition for Amide 7

Here, optimization began by choosing α-diazo-β-keto ester **4a** and *N*-sulfinylaniline **1a**. Therefore, variations in light sources were screened, which discloses that irradiation with purple LEDs was the most effective one to furnish amide **7a** in 55% of isolated yield (Table 7, entry 3).

4.2.5.1. Chapter 4: Table 7: Screening of Different Light Source-3[a]



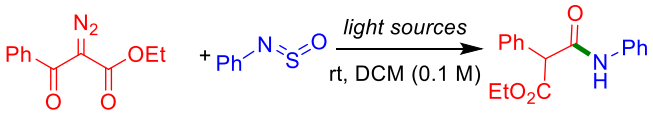
4a (2.0 equiv) **1a** (1.0 equiv) **7a**

Entry	*light sources*	Yield (%)[b]
1	Blue LEDs (450 nm)	45
2	Blue LEDs (420 nm)	47
3	**Purple LEDs (405 nm)**	**55**
4	UV LEDs (365 nm)	40
5	Blue LEDs (strip)	20
6	Green LEDs (strip)	trace
7	White LEDs	trace
8	in dark	0

[a] unless untill mentioned all reactions were carried out in 0.1 mmol scale.
[b] measured by ^{1}H-NMR analysis of the crude reaction mixture using CH_2Br_2 as an internal standard.

Next, other reaction parameters like time, temperature, and equivalency of the reactants were varied to increase the reaction yield. Here, a little higher temperature and longer reaction time gave better outcome (Table 8, entry 5).

4.2.5.2. Chapter 4: Table 8: Miscellaneous Optimization-3[a]



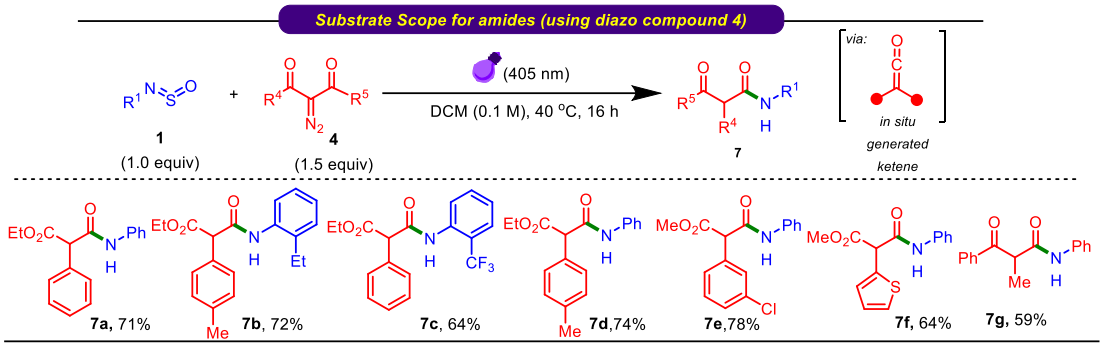
4a **1a** **7a**

Entry	4a (equiv)	1a (equiv)	Temp. (°C)	Time	Yield (%)[b]
1	2	1	rt	10 h	46
2	1.5	1	rt	10 h	46
3	1	2	rt	10 h	28
4	1.5	1	40 °C	10 h	55
5	**1.5**	**1**	**40 °C**	**16 h**	**76 (71%)**
6	1.5	1	40 °C	6 h	40

[a] unless untill mentioned all reactions were carried out in 0.1 mmol scale.
[b] measured by ^{1}H-NMR analysis of the crude reaction mixture using CH_2Br_2 as an internal standard. Isolated yield in bracket.

4.2.6. Substrate Scope Evaluation for Amides 7

By taking the optimal reaction condition in hand, we went out to explore the substrate scope for amide **7**. A diverse range of α-diazo-β-keto esters **4** with different aromatic substituents smoothly reacted with *N*-sulfinylamines **1** to form of α-amido esters (Scheme 4.2.6.1, entries **7a-7e**) in the presence of purple LEDs (405 nm). Moreover, a heteroaryl substituted α-diazo-β-keto esters and α-diazo-1,3 diketone was also tolerable under the optimized reaction conditions to furnish the desired amide **7f** and **7g** (Scheme 4.2.6.1). The synthesis of these α-amido esters is rare, which can hardly be achieved by other traditional methods without using any metal catalyst.[18b, 18c]



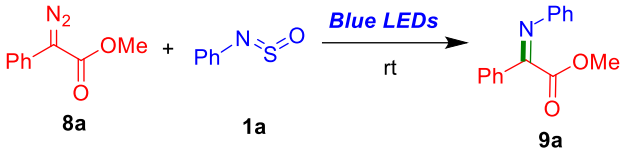
Scheme 4.2.6.1: Substrate Scope Evaluation for Amide **7**.

We next sought to explore the reactivity of *N*-sulfinylamines **1** with electrophilic carbene precursor, i.e., donor/acceptor–substituted diazo compound α-aryldiazoacetate **8** (Table 9).

4.2.7. Optimization of the Reaction Condition for α-Iminoester 9

In order to establish the optimum reaction condition, *N*-sulfinylaniline **1a** and phenyldiazoacetate **8a** were chosen as model substrates and solvents, and reaction time was varied to find the suitable reaction condition. α-Iminoester **9a** was achieved in 73% yield while using blue LED light source in DCM (Table 9, entry 11).

4.2.7.1. Chapter 4: Table 9: Miscellaneous Optimization-4[a]

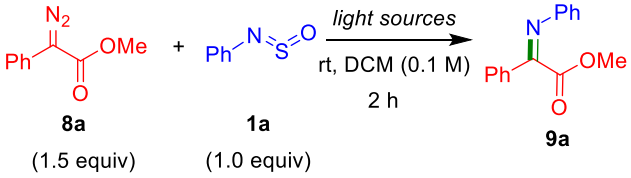


Entry	8a	1a	Solvent (0.1 M)	Time (h)	Yield (%)[b]
1	1	1	DCM	10	48
2	1	1.5	DCM	10	47
3	1.5	1	DCM	10	60
4	1.5	1	DCE	10	56
5	1.5	1	ACN	10	25
6	1.5	1	Toluene	10	45
7	1.5	1	EtOAc	10	30
8	1.5	1	THF	10	28
9	1.5	1	DCM	10	40
10	1.5	1	DCM	6	65
11	**1.5**	**1**	**DCM**	**2**	**73 (67)**

[a] unless untill mentioned all reactions were carried out in 0.1 mmol scale.
[b] measured by ^{1}H-NMR analysis of the crude reaction mixture using CH_2Br_2 as an internal standard. Isolated yield in bracket.

Extensive screening of light sources was then carried out, which reveals the reaction was most suitable under blue LEDs irradiation (Table 10, entry 1).

4.2.7.2. Chapter 4: Table 10: Screening of Different Light Source-4[a]



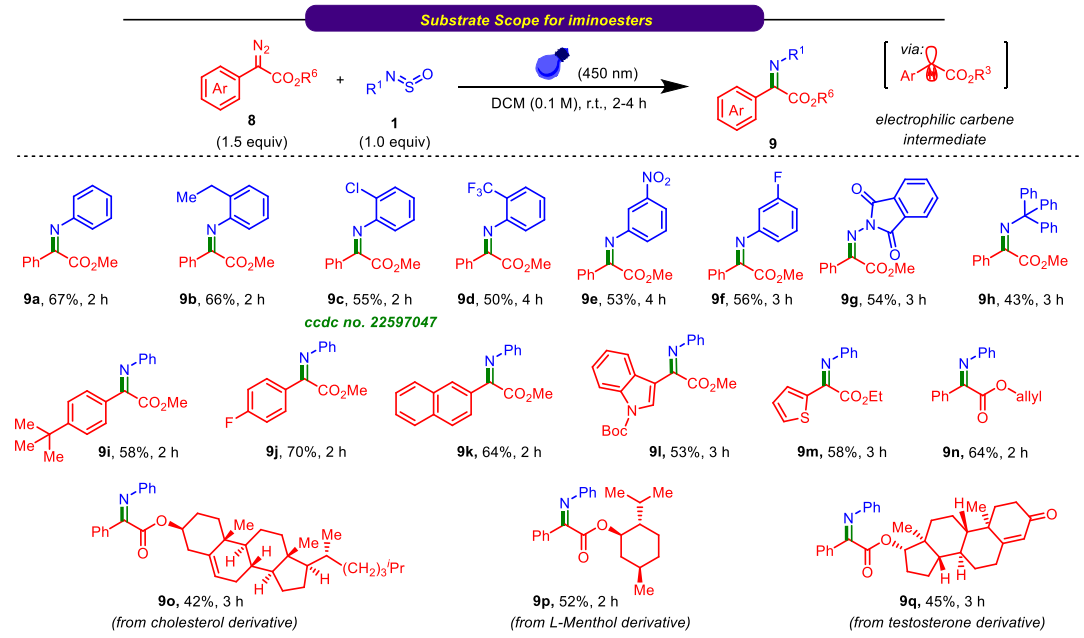
Entry	*light sources*	Yield (%)[b]
1	**Blue LEDs (450 nm)**	**73 (67)**
2	Blue LEDs (420 nm)	62
3	Purple LEDs (405 nm)	55
4	UV LEDs (365 nm)	20
5	Blue LEDs (strip)	35
6	Green LEDs (strip)	15
7	White LEDs	trace
8	in dark	0

[a] unless untill mentioned all reactions were carried out in 0.1 mmol scale.
[b] measured by ^{1}H-NMR analysis of the crude reaction mixture using CH_2Br_2 as an internal standard. Isolated yield in bracket.

4.2.8. Substrate Scope Evaluation for α-iminoesters 9

By fixing table 10, entry 1 as optimal reaction condition we went out to explore the substrate scope for α-iminoesters. To our delight, this transformation tolerated over a broad selection of *N*-sulfinylaniline derivatives **1**, including those with electron-donating, electron-withdrawing substituents, and functional groups like nitro, trifluoromethyl groups producing corresponding α-iminoesters in good yields (Scheme 4.2.8.1, entries **9b-9f**). Moreover, an aliphatic and a heterocyclic group containing *N*-sulfinylamine successfully installed over phenyldiazoacetate **8a** to furnish corresponding α-iminoester **9g** and **9h** in 54% and 43% yield, respectively (Scheme 4.2.8.1).

Encouraged by this observation, we further inspected the scope of α-aryldiazoacetates **8** by varying aryl and heteroaryl partners, producing the desired α-iminoesters in a range of moderate to good yields, 53−70% (Scheme 4.2.8.1, entries **9i-9m**). Subsequently, the variation in the ester part revealed that aryldiazoacetates **8** derived from allyl alcohol, naturally occurring secondary alcohols like cholesterol, menthol, and testosterone derivatives were also compatible with the optimized reaction conditions to furnish target α-iminoesters (Scheme 4.2.8.1, entries **9n-9q**).



Scheme 4.2.8.1: Substrate Scope Evaluation for α-iminoester **9**.

4.2.9. Mechanistic Studies: Experimental

Some preliminary mechanistic investigations were conducted to gain insight the mechanism of this amidation and imination reaction. At the outset, ultraviolet–visible (UV/vis) spectra were recorded for all model substrates (**1a**, **2a**, **3a**, **4a**, and **8a**). A clear absorption band was observed

in the range of 390-420 nm for *N*-sulfinylaniline **1a**, acylsilane **2a**, and α-diazo-β-keto ester **4a**. However, diazo compounds **3a** and **8a** show their λ_{max} value near 440-460 nm (Figure 4.2.9.1).

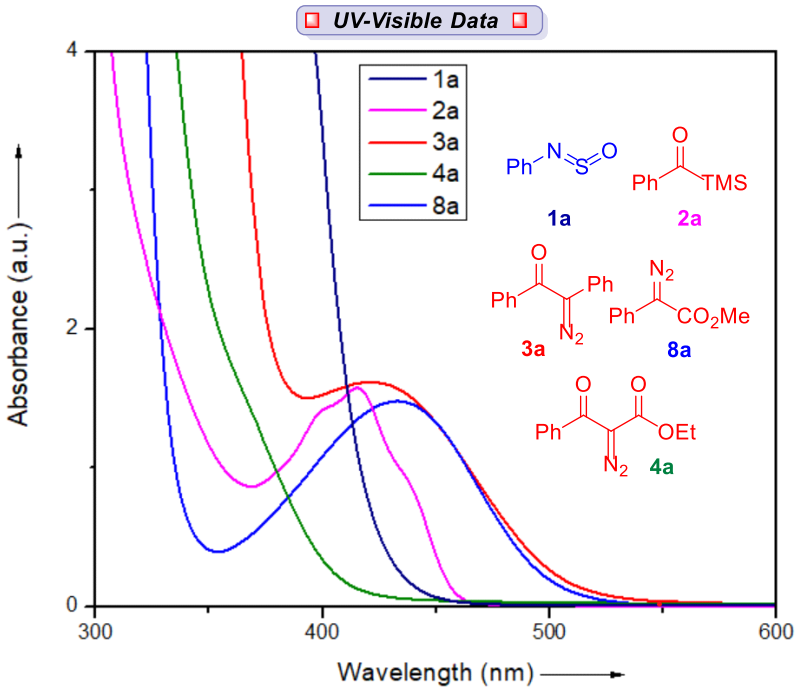
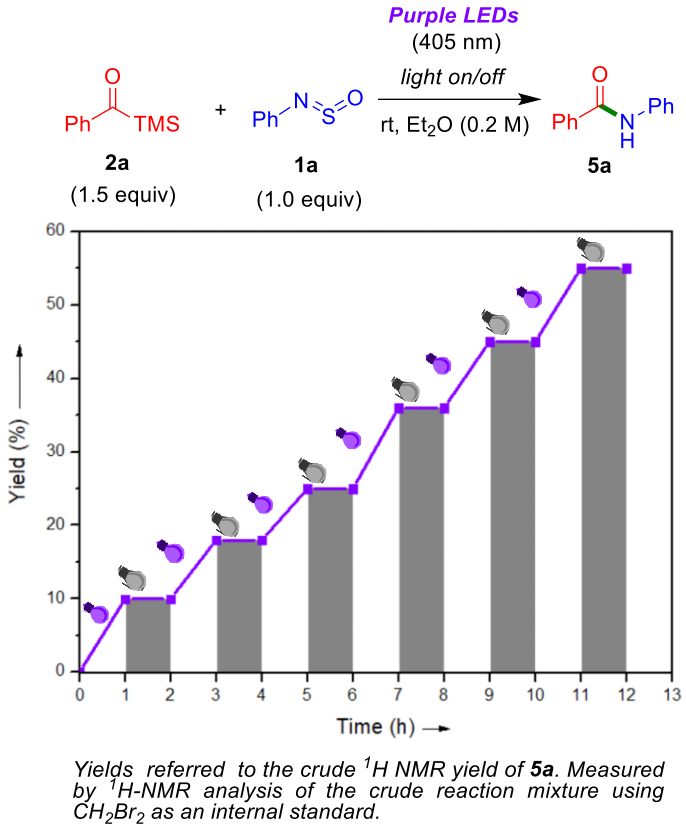


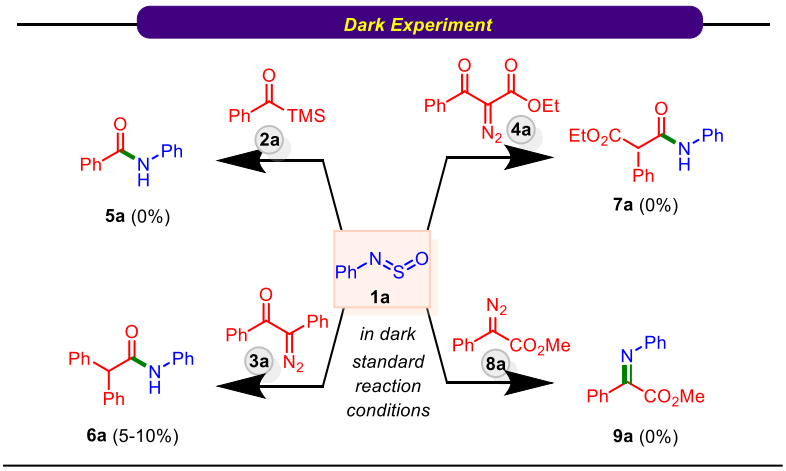
Figure 4.2.9.1: Chapter 4: UV-visible Spectra for different reaction partners.

Light on/off experiment was also carried out to better corroborate the crucial role of visible light in this transformation (Figure 4.2.9.2). Model reactions performed in dark resulted in no desired product (traces for compound **6a**) formations (Scheme 4.2.9.1). These compiled results indicate the necessity of visible light irradiation of the substrates with specific wavelengths.



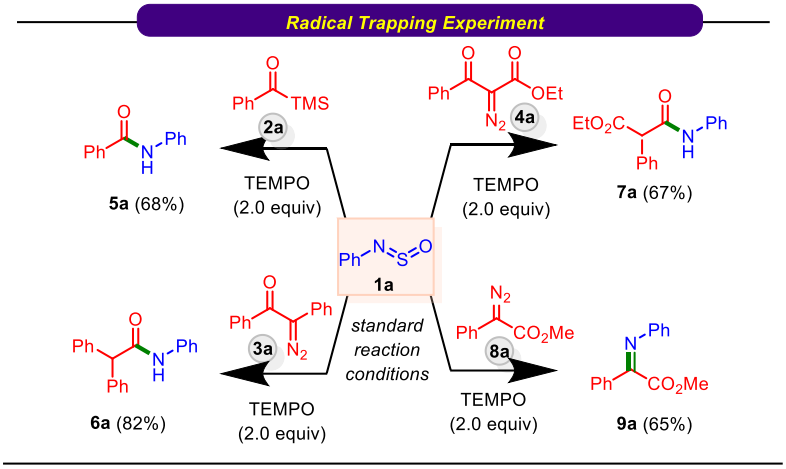
*Yields referred to the crude ^{1}H NMR yield of **5a**. Measured by ^{1}H-NMR analysis of the crude reaction mixture using CH_2Br_2 as an internal standard.*

Figure 4.2.9.2: Chapter4: Light On/Off Experiment.



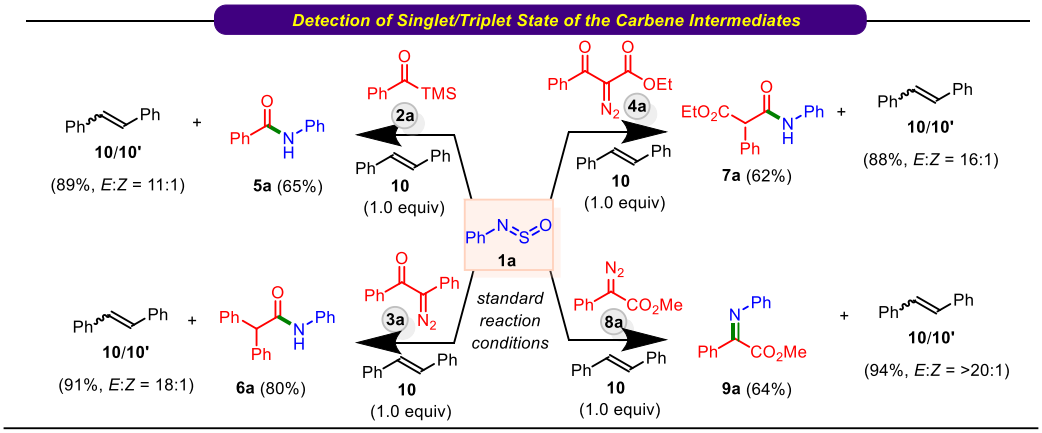
Scheme 4.2.9.1: Chapter 4: Dark Experiments.

The possibility of a radical pathway was excluded as we were unable to detect any TEMPO-adduct and even no significant interference in the reaction yield was observed while using 2 equiv of tetramethylpiperidin-1-yl)oxyl (TEMPO) as a radical trapper (Scheme 4.2.9.2).



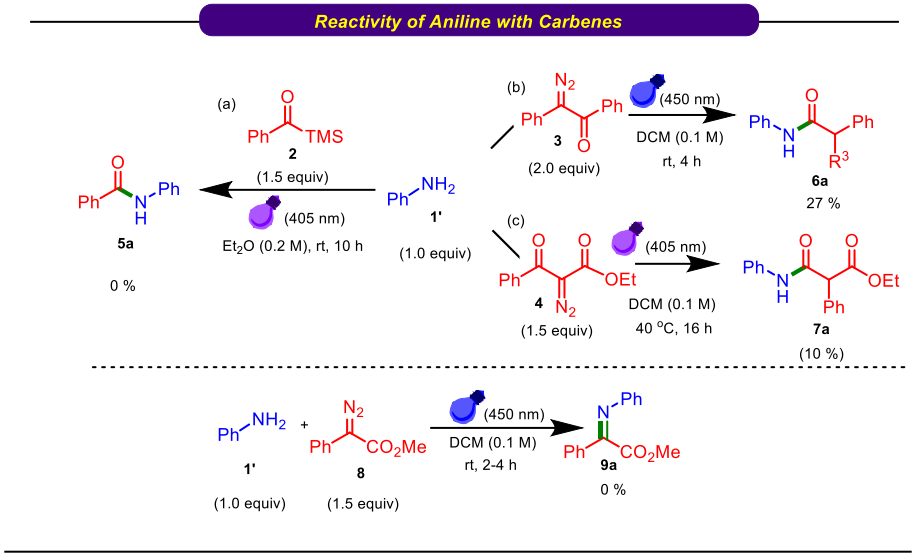
Scheme 4.2.9.2: Radical Trapping Experiments.

The experiments mentioned above indicate that these transformations proceed via a carbene intermediate. Therefore, we wanted to check the singlet/triplet state of the carbene intermediates. In order to do so, 1 equiv of *trans*-stilbene **10** was introduced to the reaction mixtures, which shows no inhibition of the reactions and only a small quantity of the olefin **10** was converted into its *cis*-isomer **10'** (**10**/**10'** recovered 88-94 %; *E*: *Z* = 20:1-11:1). These results showcase that siloxycarbene and other carbene intermediates (from diazo compounds) are more likely proceeds via their singlet (S_1) state.[13c, 13j] However, the triplet (T_1) state is not totally forbidden as a small amount of *trans*-stilbene was converted into its *cis*-isomer (Scheme 4.2.9.3).



Scheme 4.2.9.3: Detection of Singlet/Triplet Experiments.

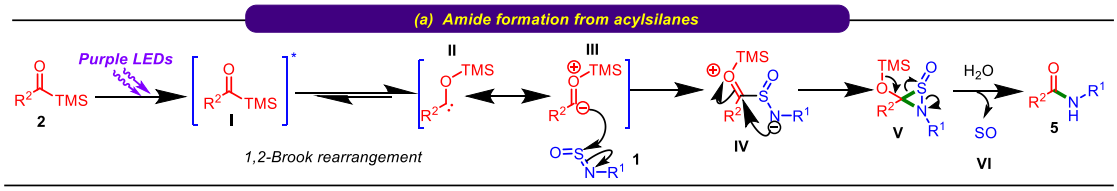
In order to check the reactivity of free amines with different carbene precursors. The reactions were either sluggish or didn't offer any product formation while using $PhNH_2$ instead of PhNSO (Scheme 4.2.9.3).



Scheme 4.2.9.4: Reactivity of Aniline with Carbenes.

4.2.10. Proposed Mechanistic Pathway

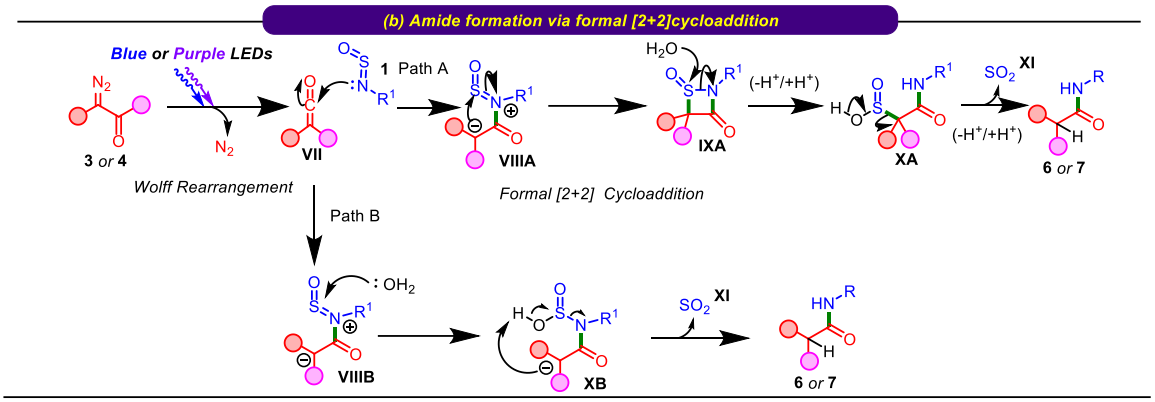
The collective data shown in section 4.2.9 and literature precedence helped us to corroborate the mechanistic elucidation. We propose that the light irradiation on acylsilanes **2** promotes it to its excited state **I**, which readily converted into its siloxycarbene intermediate **II** and/or its resonance form **III** via 1,2-Brook rearrangement.[13] Subsequently, nucleophilic attack to the *S*-center of *N*-sulfinylamine **1** produces intermediate **IV**. In the next step, intermediate **IV** readily got cyclized to form thiaziridine ring **V**. The unstable nature of this thiaziridine ring **V** helps to eliminate sulphur monoxide gas to deliver amide **5** (Scheme 4.2.10.1). A trace amount of water can also facilitate this transformation.



Scheme 4.2.10.1: Mechanism for Amide Formation from Acylsilanes **2**.

A mechanism for the formation of amide **6** or **7** from diazo compounds **3** or **4** is depicted in scheme 4b. Here blue or purple LEDs promote the excitation of the diazo compounds **3** or **4** respectively, which are converted into their corresponding ketene intermediate **VII** via a Wolff rearrangement. The *in situ* generated ketene **VII** undergoes a formal [2 + 2] cycloaddition reaction with *N*-sulfinylamine **1** to form thiazetidin ring **IXA** via path A (detected in HRMS, Figure 4.2.10.1 and 4.2.10.2).[19] Thereafter, the unstable thiazetidin ring **IXA** breaks down in presence of a trace amount of water to construct intermediate **XA**. Finally, a facile release of

sulphur dioxide gas from intermediate **XA** fabricates desired amides **6** or **7** (Scheme 4.2.10.2). Path B reveals an alternative mechanism via direct water attack to intermediate **VIIIB**, which delivers amide products **6** or **7** upon SO_2 gas release from intermediate **XB**.



Scheme 4.2.10.2: Mechanism for Amide Formation from Diazo Compounds **3** or **4**.

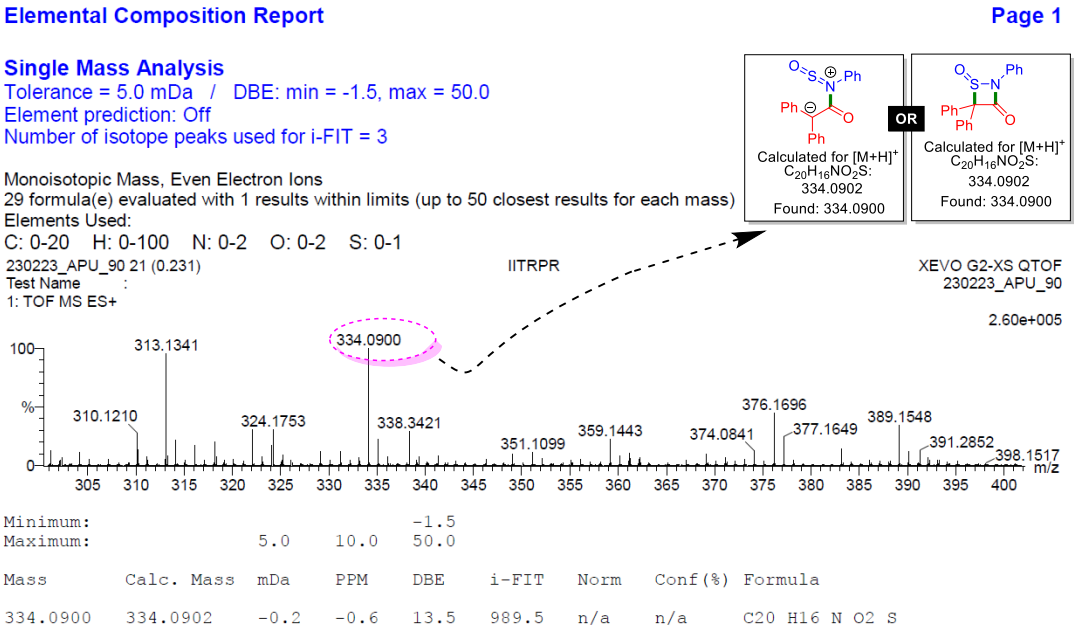


Figure 4.2.10.1: HRMS data for intermediate triphenyl-1,2-thiazetidin-3-one 1-oxide (IXa)

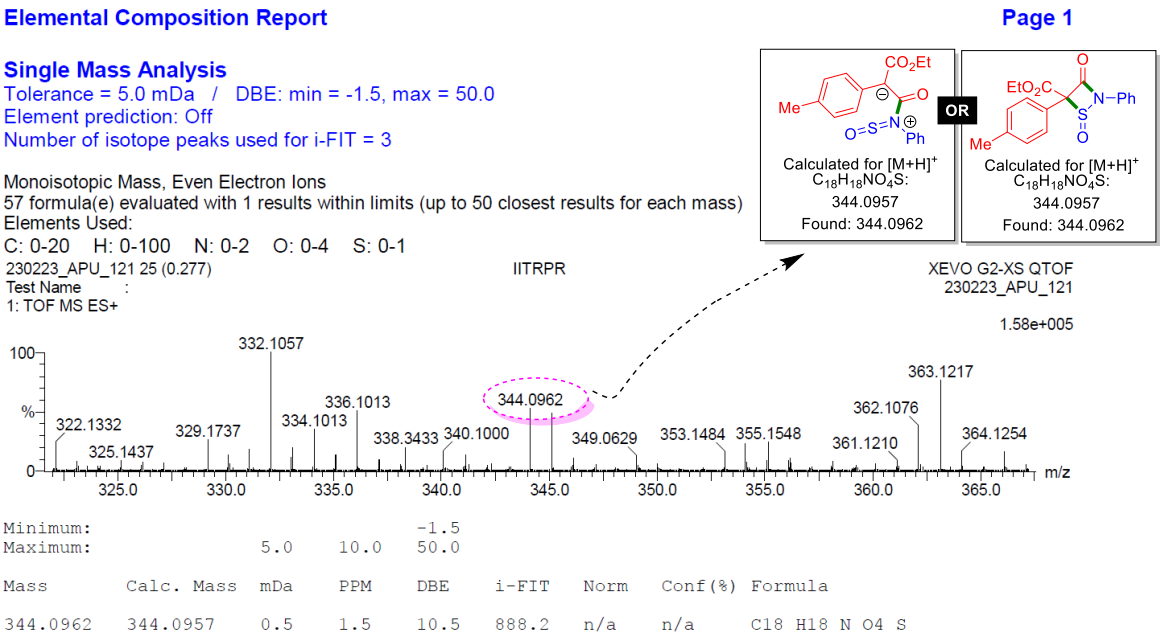
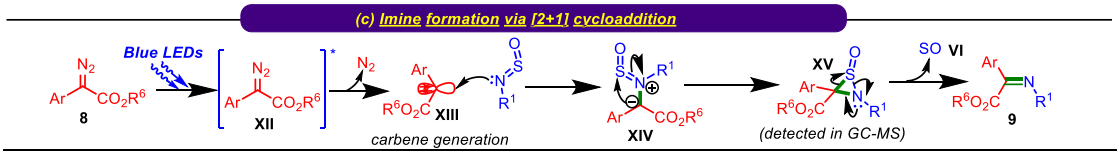


Figure 4.2.10.2: HRMS data for intermediate ethyl-3-oxo-2-phenyl-4-(*p*-tolyl)-1,2-thiazetidine-4-carboxylate 1-oxide (IXb)

On the other hand, formation of α-iminoester **9** is initiated by the excitation of α-aryldiazoacetate **8**.[20] Excited α-aryldiazoacetate **XII** readily unshackles dinitrogen to form carbene intermediate **XIII**. Next, a nucleophilic attack from *N*-sulfinylamine **1** to carbene intermediate **XIII** leads to deliver intermediate **XIV**. Intermediate **XIV** then cyclized to generate an unstable thiaziridine ring **XV** (detected in GC-MS, Figure 4.2.10.3). The decomposition of thiaziridine ring **XV** facilitates the formation of desired α-iminoester **9** by releasing sulphur monoxide gas (Scheme 4.2.10.3). Alternatively, residual water can break down the cyclic intermediate **XV**, resulting in the formation of α-iminoester **9** and sulfinic acid as side product.



Scheme 4.2.10.3: Mechanism for α-Iminoester Formation from Diazo Compounds 8.

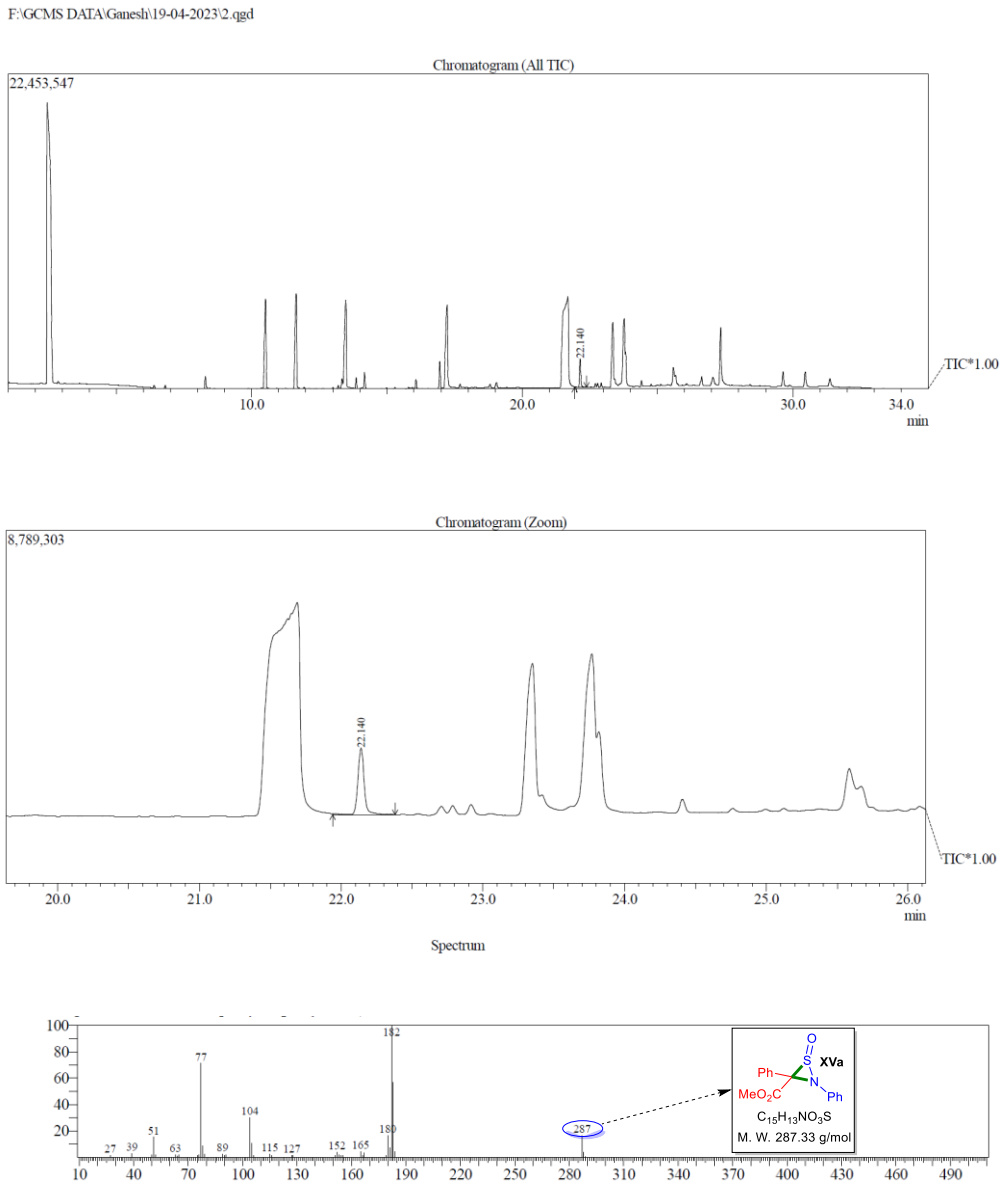
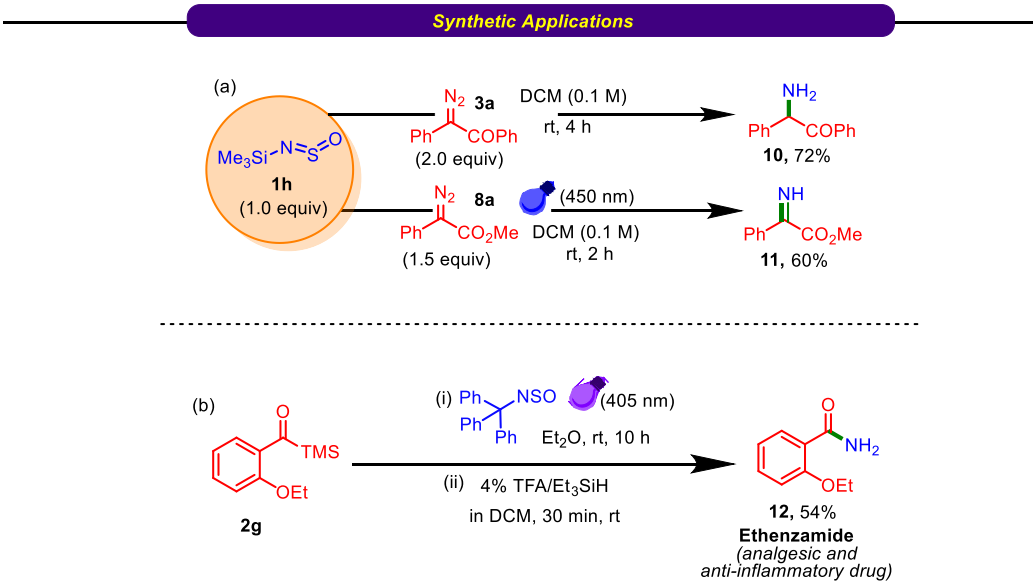


Figure 4.2.10.3: GC-MS data for methyl *C*,*N*-diphenylglycinate 1-oxide (XVa).

4.2.11. Synthetic Applications

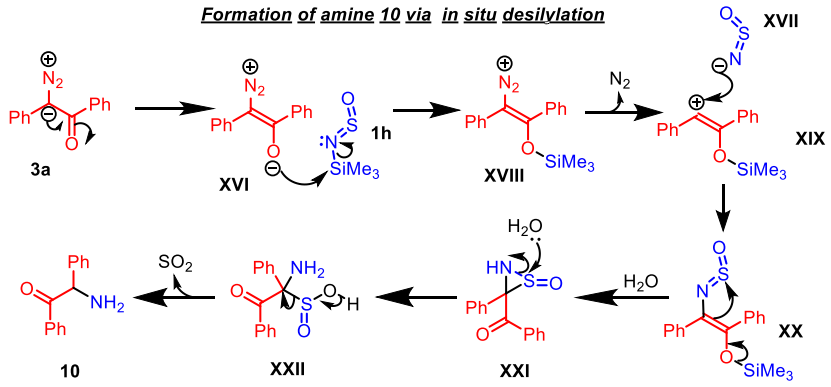
In our efforts to illustrate the synthetic applicability of the developed protocol, the less studied reactivity of *N*-silylsulfinylamine **1h** was checked with diazo compounds **3a** and **8a**.[3f] Delightfully, direct amine installation took place over diazo ketone **3a** when it was treated with *N*-silylsulfinylamine **1h**, furnishing compound **10** in good yield (*N*-centered attack from *N*-silylsulfinylamine take place to the carbene intermediate even before the Wolff rearrangement occurs). Concurrently, unprotected imine product **11** was observed when phenyldiazoacetate **8a** was allowed to react with **1h** (Scheme 4.2.10.4a). Next, a strategically designed reaction between acylsilane **2g** and TrNSO **1f** was carried out, which upon *in situ* sequential trityl deprotection step delivered ethenzamide **12** with 54% yield (Scheme 4.2.10.4b).



Scheme 4.2.10.4: Chapter 4: Synthetic Applications.

4.2.11.1. Mechanistic Pathway for Amine 10:

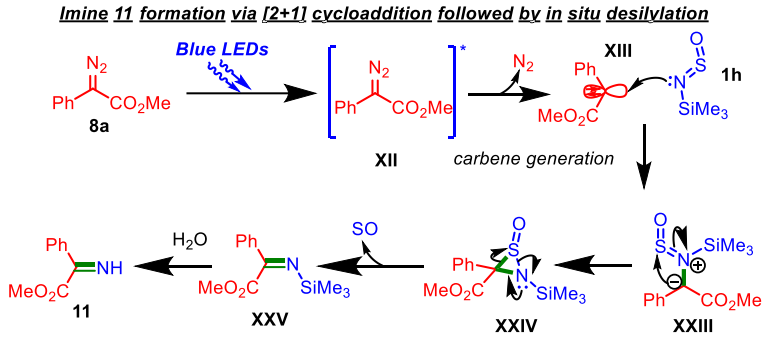
We propose that the reaction starts with a nucleophilic attack from the resonating structure of diazo compound **XVI** towards *N*-silylsulfinylamine **1h** to fabricate intermediate **XVII** and **XVIII**. Next, intermediate **XVIII** unshackles dinitrogen to form the cationic intermediate **XIX**, which was then trapped by the in situ generated species **XVIII** to deliver intermediate **XX**. Now, intermediate **XX** readily got cyclized to form thiaziridine ring **XXI** after desilylation process in presence of water. Finally, the unstable thiaziridine ring **XXI** decomposes in presence of a water molecule to deliver amine **10** after a facile SO_2 gas release from intermediate **XXII** (Scheme 4.2.11.1).



Scheme 4.2.11.1: Mechanism for Amine **10** Formation.

4.2.11.2. Mechanistic Pathway for imine 11:

The formation of unprotected imine **11** follows a similar pathway as mentioned in section 4.2.10 to form α-iminoester **XXV**, which upon a desilylation process in presence of water fabricates product **11** (Scheme 4.2.11.2).



Scheme 4.2.11.2: Mechanism for Imine **11** Formation.

4.3 Conclusion

This chapter accounts for a rarely explored reactivities of *N*-sulfinylamine chemistry, where different kinds of carbene precursors are brought into play to render versatile amide and α-iminoester derivatives through a visible-light-induced manifold. The reaction conditions are mild, benign, easy to set up and scalable. The collective data, including UV-visible spectra, light on/off experiments, and other mechanistic studies, support the proposed mechanism. Further efforts for portraying the synthetic applicability of the developed protocol were carried out by late-stage functionalization of diazo esters derived from naturally occurring secondary alcohols and direct installation of unprotected amines and imines over diazo compounds by utilizing the sporadically explored reactivity of *N*-silylsulfinylamine.

4.4. Experimental Section

4.4.1. General Information:

All reactions were performed in flame-dried glassware under argon atmosphere unless otherwise stated. Liquids and solutions were transferred with syringes. Solvents used were dried and purified by following standard procedures. Technical grade solvents for extraction or chromatography (ethyl acetate, and petroleum ether) were distilled prior to use. $CDCl_3$ was stored over 4Å molecular sieves. Used chemicals were purchased from Sigma-Aldrich, TCI, Alfa-Aesar and Sisco Research Laboratories (SRL) used without further purification. All the liquid chemicals distilled freshly prior to use. Analytical thin-layer chromatography (TLC) was performed on using pre-coated aluminium-backed plates (Merck Kieselgel 60 F254) and visualized by UV radiation, basic aqueous potassium permangante ($KMnO_4$), *p*-anisaldehyde stains and heat as developing agents.

Flash column chromatography was performed on silica gel 60 (40–63 μm, 230–400 mesh, ASTM) from Merck using the indicated solvents. Organic solutions were concentrated under reduced pressure on Heidolph rotary evaporator. NMR spectra were acquired on a JEOL JNM ECS-400 instrument running at 400 MHz for ^{1}H, 101 MHz ^{13}C and 376 MHz for ^{19}F respectively. Chemical shifts (δ) are reported in ppm relative to residual solvent signals ($CHCl_3$, 7.26 ppm for ^{1}H NMR, $CDCl_3$, 77.0 ppm for ^{13}C NMR). Data are reported as follows: chemical shift, multiplicity (br = broad singlet, s = singlet, d = doublet, dd = doublet of doublets, t = triplet, q = quartet, ddd = doublet of doublet of doublet, td = triplet of doublet, m = multiplet), coupling constants (Hz), and integration. 1,2-Dibromomethane was used as an internal standard to calculate NMR yields of products by ^{1}H NMR analysis of the crude mixture. HRMS was recorded on Waters Xevo G2-XS (Q-TOF).

4.4.2. Photoreactor Setup:

Photochemical reactions were carried out in bottom plane irradiated vials in a Hepatochem Photoreactor composed of cooling block and LEDs connected to AC/DC input 100-240 V AC, 50/60 Hz power supply (Figure 1).

Filters used- 450nm, 405nm, and 365nm.

Instrument details available at: https://www.hepatochem.com/photoreactors-leds-accessories/#photoreactors

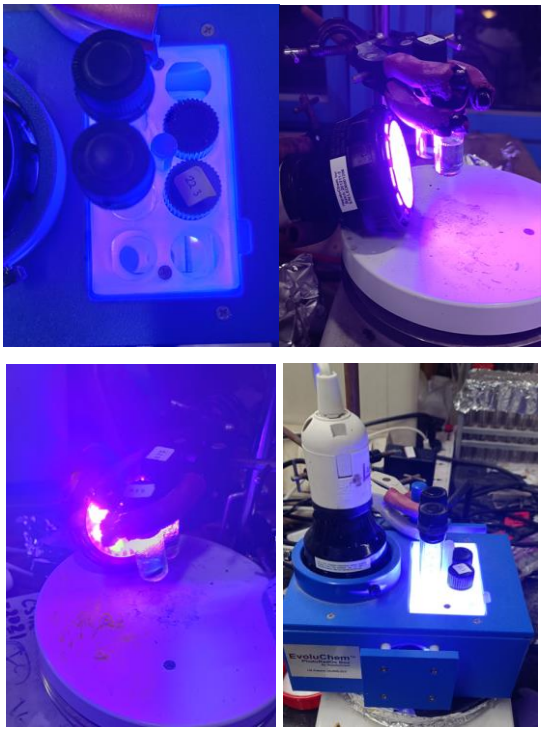


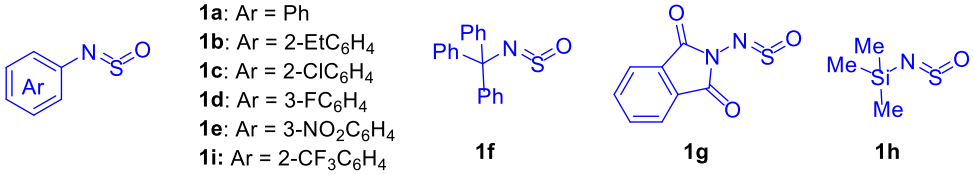
Figure 1: Photochemical reaction set up.

4.4.3. List of substrates prepared:

4.4.3.1. List of *N*-sulfinylamines prepared:

The list of *N*-sulfinylamines prepared according to the previous literatures.[22, 3a]

List of N-sulfinylamines used



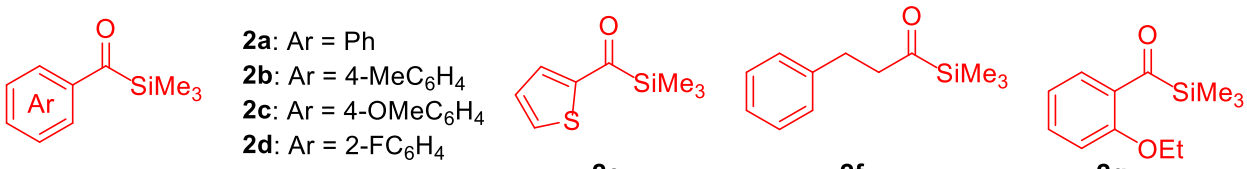
1a: Ar = Ph
1b: Ar = 2-EtC_6H_4
1c: Ar = 2-ClC_6H_4
1d: Ar = 3-FC_6H_4
1e: Ar = 3-$NO_2C_6H_4$
1i: Ar = 2-$CF_3C_6H_4$

1f **1g** **1h**

4.4.3.2. List of acylsilanes prepared:

The list of acylsilanes prepared according to the previous literatures.[23, 13c]

List of acylsilanes used



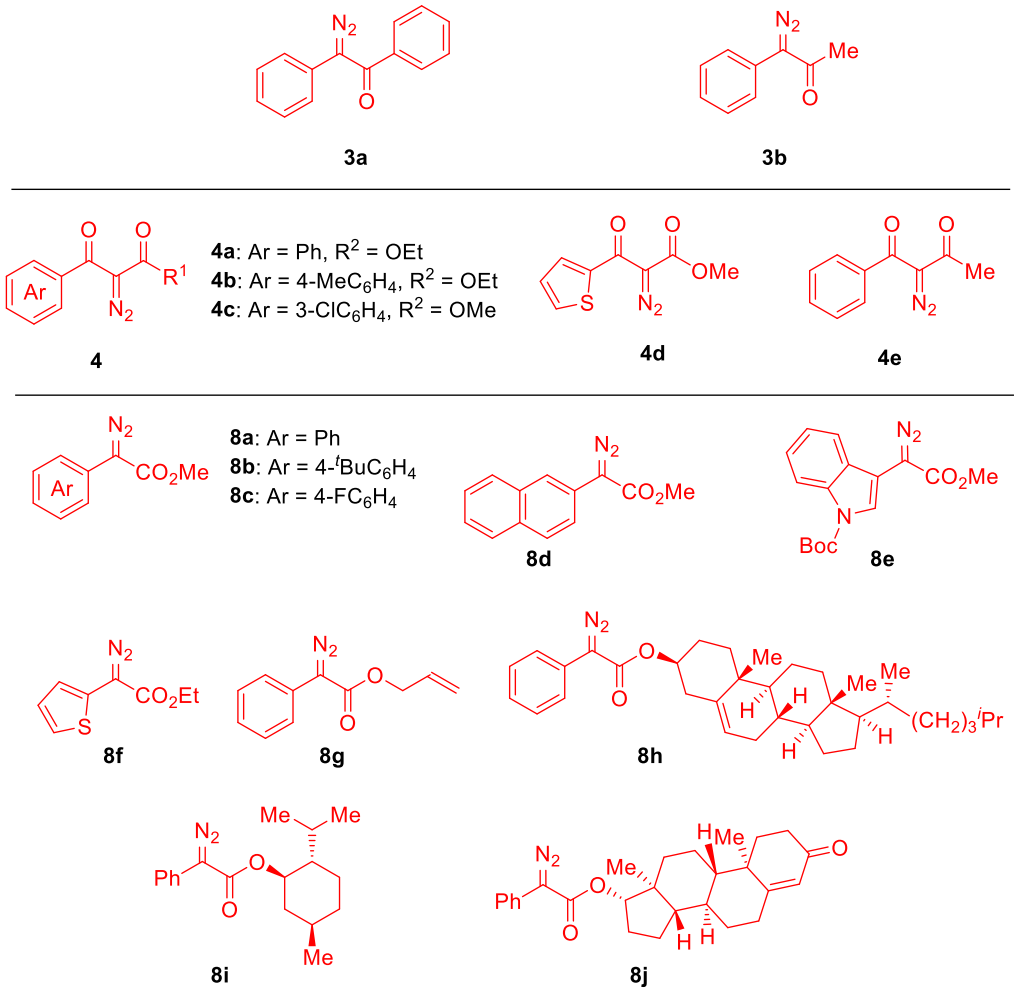
2a: Ar = Ph
2b: Ar = 4-MeC_6H_4
2c: Ar = 4-OMeC_6H_4
2d: Ar = 2-FC_6H_4

2e **2f** **2g**

4.4.3.3. List of diazo compounds prepared:

The list of diazo compounds prepared according to the previous literatures.[24]

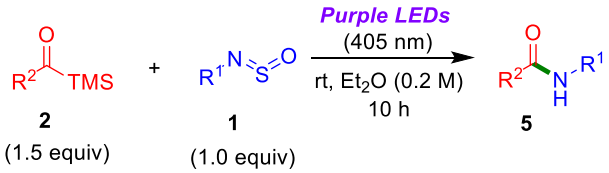
List of diazo compounds used



Scheme 1: List of Substrates Used.

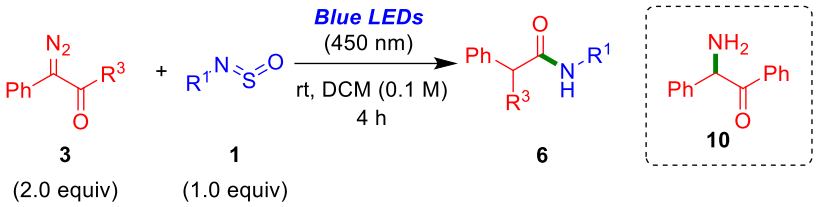
4.4.4. General Procedures:

4.4.4.1. General procedure for the amidation reaction from acylsilanes 2 (GP-1):



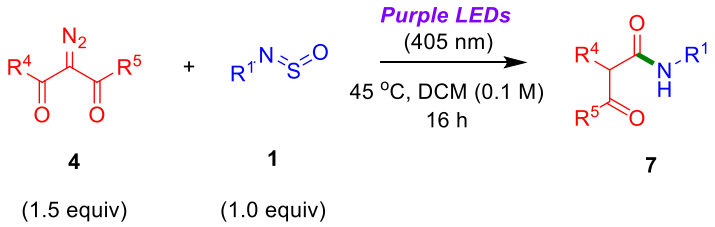
In an oven-dried vial equipped with a teflon-coated stir bar, acylsilane **2** (0.30 mmol, 1.5 equiv) and *N*-sulfinylamines **1** (0.2 mmol, 1.0 equiv) were added. Et_2O (0.2 M, 1.0 ml) was added to the reaction mixture under aerobic conditions and sealed. The vial was then irradiated under purple LEDs for 10 h at room temperature. The solvent was evaporated under reduced pressure. Analytically pure products (**5a-5l**) were obtained by column chromatography on silica gel using petroleum ether and ethyl acetate as eluents.

4.4.4.2. General procedure for the amidation reaction from diazo compounds 3 (GP-2):



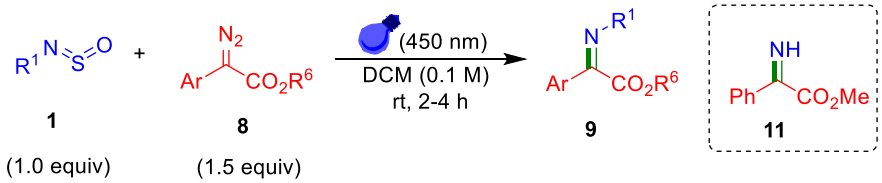
In an oven-dried vial equipped with a teflon-coated stir bar, diazo compound **3** (0.40 mmol, 2.0 equiv) and *N*-sulfinylamines **1** (0.2 mmol, 1.0 equiv) were added. DCM (0.1 M, 2.0 ml) was added to the reaction mixture under aerobic conditions and sealed. The vial was then irradiated under blue LEDs for 4 h at room temperature. The solvent was evaporated under reduced pressure. Analytically pure products (**6a-6f, 10**) were obtained by column chromatography on silica gel using petroleum ether and ethyl acetate as eluents.

4.4.4.3. General procedure for the amidation reaction from diazo compounds 4 (GP-3):



In an oven-dried vial equipped with a teflon-coated stir bar, diazo compound **4** (0.30 mmol, 1.5 equiv) and *N*-sulfinylamines **1** (0.2 mmol, 1.0 equiv) were added. DCM (0.1 M, 2.0 ml) was added to the reaction mixture under aerobic conditions and sealed. The vial was then irradiated under purple LEDs for 16 h at room temperature. The solvent was evaporated under reduced pressure. Analytically pure products (**7a-7g**) were obtained by column chromatography on silica gel using petroleum ether and ethyl acetate as eluents.

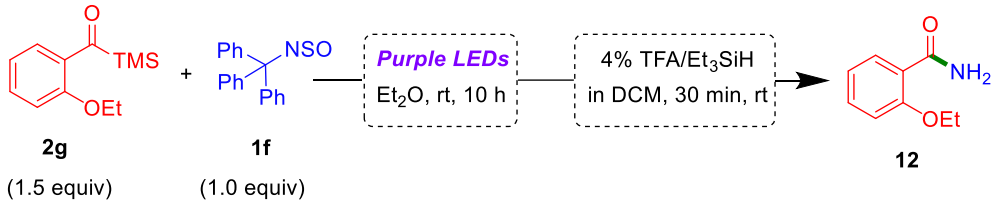
4.4.4.4. General procedure for the imination reaction from diazo compounds 8 (GP-4):



In an oven-dried vial equipped with a teflon-coated stir bar, diazo compound **8** (0.30 mmol, 1.5 equiv) and *N*-sulfinylamines **1** (0.2 mmol, 1.0 equiv) were added. DCM (0.1 M, 2.0 ml) was added to the reaction mixture under aerobic conditions and sealed. The vial was then irradiated under blue LEDs for 16 h at room temperature. The solvent was evaporated under reduced pressure. Analytically pure products (**9a-9q**) were obtained by column chromatography on silica gel using petroleum ether and ethyl acetate as eluents.

Note: Some of the α-iminoesters are unstable and they got decomposed to corresponding α-ketoesters during NMR measurement.

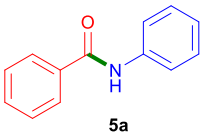
4.4.4.5. General procedure for the ethenzamide 12 (GP-5):



In an oven-dried vial equipped with a teflon-coated stir bar, acylsilane **2g** (0.30 mmol, 1.5 equiv) and *N*-sulfinylamines **1a** (0.2 mmol, 1.0 equiv) were added. Et_2O (0.2 M, 1.0 ml) was added to the reaction mixture under aerobic conditions and sealed. The vial was then irradiated under purple LEDs for 10 h at room temperature. The solvent was evaporated under reduced pressure and added 2 ml 4% TFA/Et_3SiH under aerobic conditions and sealed. The vial was then stirred for 30 min at room temperature. Analytically pure product **12** was obtained by column chromatography on silica gel using petroleum ether and ethyl acetate as eluents.

4.4.5. Result & Characterization:

4.4.5.1. *N*-phenylbenzamide (5a):



5a

$C_{13}H_{11}NO$

M. W. 197.24 g/mol

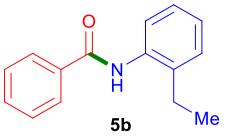
According to **GP-1** compound **5a** was prepared by using **1a** (24 µL, 0.2 mmol, 1.0 equiv) and **2a** (53.0 mg, 0.3 mmol, 1.5 equiv) in 1 ml Et_2O for 10 h at rt under purple LEDs irradiation. Column chromatographic purification (petroleum ether/EtOAc 95:5 to 80:20) afforded **5a** as white solid (30.0 mg, 76%).

For 2 mmol scale reaction compound **5a** was prepared by using **1a** (240.0 µL, 2.0 mmol, 1.0 equiv) and **2a** (530.0 mg, 3.0 mmol, 1.5 equiv) in 10 ml Et_2O for 15 h at rt under purple LEDs irradiation to get 65% (254 mg) isolated yield.

HRMS (ESI): m/z $[M+H]^+$ Calculated for $[C_{13}H_{12}NO]^+$: 198.0919; Found: 198.0913.

^{1}H NMR (400 MHz, $CDCl_3$): 7.92 (br s, 1H), 7.86–7.84 (m, 2H), 7.64–7.62 (m, 2H), 7.55–7.51 (m, 1H), 7.48–7.43 (m, 2H), 7.37–7.33 (m, 2H), 7.16–7.12 (m, 1H). **^{13}C NMR (101 MHz, $CDCl_3$):** 166.0, 138.0, 135.1, 132.0, 129.2, 128.9, 127.1, 124.7, 120.3.

4.4.5.2. *N*-(2-ethylphenyl)benzamide (5b):



5b

$C_{15}H_{15}NO$

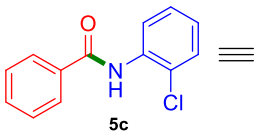
M. W. 225.29 g/mol

According to **GP-1** compound **5a** was prepared by using **1b** (33 µL, 0.2 mmol, 1.0 equiv) and **2a** (53.0 mg, 0.3 mmol, 1.5 equiv) in 1 ml Et_2O for 10 h at rt under purple LEDs irradiation. Column chromatographic purification (petroleum ether/EtOAc 95:5 to 80:20) afforded **5b** as white solid (33.0 mg, 73%).

HRMS (ESI): m/z $[M+H]^+$ Calculated for $[C_{15}H_{16}NO]^+$: 226.1232; Found: 226.1224.

^{1}H NMR (400 MHz, $CDCl_3$): δ 7.95–7.93 (m, 1H), 7.88–7.86 (m, 2H), 7.73 (br s, 1H), 7.58–7.54 (m, 1H), 7.51–7.47 (m, 2H), 7.28–7.24 (m, 2H), 7.18–7.14 (m, 1H), 2.68 (q, *J* = 7.8 Hz, 2H), 1.28 (t, *J* = 7.6 Hz, 3H). **^{13}C NMR (101 MHz, $CDCl_3$):** δ 165.9, 135.2, 132.0, 129.0, 128.7, 127.1, 126.9, 125.8, 123.8, 24.5, 14.1.

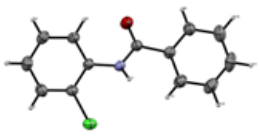
4.4.5.3. *N*-(2-chlorophenyl)benzamide (5c):



5c

$C_{13}H_{10}ClNO$

M. W. 231.68 g/mol



ccdc no. 2257649

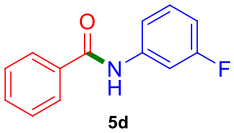
According to **GP-1** compound **5c** was prepared by using **1c** (35 µL, 0.2 mmol, 1.0 equiv) and **2a** (53.0 mg, 0.3 mmol, 1.5 equiv) in 1 ml Et_2O for 10 h at rt under purple LEDs irradiation. Column chromatographic purification (petroleum ether/EtOAc 95:5 to 85:15) afforded **5c** as white solid (37.0 mg, 80%).

HRMS (ESI): m/z $[M+H]^+$ Calculated for $[C_{15}H_{18}N_2O_4F]^+$: 232.0529; Found: 232.0528.

^{1}H NMR (400 MHz, $CDCl_3$): δ 8.57–8.55 (m, 1H), 8.44 (br s, 1H), 7.93–7.90 (m, 2H), 7.60–7.56 (m, 1H), 7.53–7.49 (m, 2H), 7.42–7.40 (m, 1H), 7.35–7.31 (m, 1H), 7.10–7.06 (m, 1H). **^{13}C**

NMR (101 MHz, $CDCl_3$): δ 165.4, 134.8, 134.7, 132.3, 129.1, 129.1, 128.0, 127.2, 124.9, 123.1, 121.6.

4.4.5.4. *N*-(3-fluorophenyl)benzamide (5d):



5d

$C_{13}H_{10}FNO$

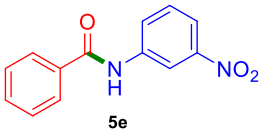
M.W. 215.23 g/mol

According to **GP-1** compound **5d** was prepared by using **1d** (31 µL, 0.2 mmol, 1.0 equiv) and **2a** (53.0 mg, 0.3 mmol, 1.5 equiv) in 1 ml Et_2O for 10 h at rt under purple LEDs irradiation. Column chromatographic purification (petroleum ether/EtOAc 95:5 to 85:15) afforded **5d** as white solid (34.0 mg, 79%).

HRMS (ESI): m/z $[M+H]^+$ Calculated for $[C_{13}H_{11}FNO]^+$: 216.0825; Found: 216.0822.

^{1}H NMR (400 MHz, $CDCl_3$): δ 7.94 (br s, 1H), 7.85–7.83 (m, 2H), 7.64–7.60 (m, 1H), 7.57–7.52 (m, 1H), 7.49–7.45 (m, 2H), 7.32–7.26 (m, 2H), 6.86–6.81 (m, 1H). **^{13}C NMR (101 MHz, $CDCl_3$):** δ 165.9, 163.1 (d, *J* = 245.4 Hz), 139.5 (d, *J* = 10.5 Hz), 134.7, 132.2, 130.3 (d, *J* = 9.6 Hz), 129.0, 127.1, 115.4, 111.4 (d, *J* = 21.1 Hz), 107.8 (d, *J* = 25.9 Hz). **^{19}F NMR (376 MHz, $CDCl_3$):** δ -111.25 (s, 1F)

4.4.5.5. *N*-(3-nitrophenyl)benzamide (5e):



5e

$C_{13}H_{10}N_2O_3$

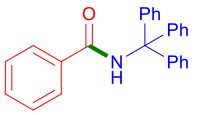
M.W. 242.23 g/mol

According to **GP-1** compound **5e** was prepared by using **1e** (37 µL, 0.2 mmol, 1.0 equiv) and **2a** (53.0 mg, 0.3 mmol, 1.5 equiv) in 1 ml Et_2O for 10 h at rt under purple LEDs irradiation. Column chromatographic purification (petroleum ether/EtOAc 90:10 to 60:40) afforded **5e** as white solid (40.0 mg, 83%).

HRMS (ESI): m/z $[M+H]^+$ Calculated for $[C_{13}H_{11}N_2O_3]^+$: 243.0770; Found: 243.0766.

^{1}H NMR (400 MHz, $CDCl_3$): δ 8.50–8.49 (m, 1H), 8.11–8.08 (m, 1H), 8.05 (br s, 1H), 8.01–7.99 (m, 1H), 7.90–7.87 (m, 2H), 7.61–7.57 (m, 1H), 7.54–7.49 (m, 3H). **^{13}C NMR (101 MHz, $CDCl_3$):** δ 166.1, 148.7, 139.2, 134.1, 132.6, 130.1, 129.1, 127.2, 126.0, 119.2, 115.0.

4.4.5.6. *N*-tritylbenzamide (5f):



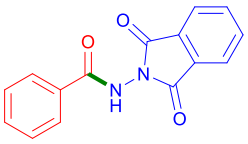
5f
$C_{26}H_{21}NO$
M.W. 363.46 g/mol

According to **GP-1** compound **5f** was prepared by using **1e** (61 mg, 0.2 mmol, 1.0 equiv) and **2a** (53.0 mg, 0.3 mmol, 1.5 equiv) in 1 ml Et_2O for 10 h at rt under purple LEDs irradiation. Column chromatographic purification (petroleum ether/EtOAc 95:5 to 85:15) afforded **5f** as white solid (47.0 mg, 60%).

HRMS (ESI): m/z $[M+H]^+$ Calculated for $[C_{26}H_{22}NO]^+$: 364.1701; Found: 364.1690.

^{1}H NMR (400 MHz, $CDCl_3$): δ 7.80–7.78 (m, 2H), 7.52–7.48 (m, 1H), 7.45–7.40 (m, 2H), 7.33–7.26 (m, 15H). **^{13}C NMR (101 MHz, $CDCl_3$):** δ 166.5, 144.8, 135.4, 131.7, 128.8, 128.2, 127.2, 127.1, 70.9.

4.4.5.7. *N*-(1,3-dioxoisoindolin-2-yl)benzamide (5g):

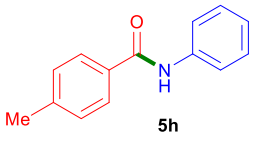


5g
$C_{15}H_{10}N_2O_3$
M.W. 266.26 g/mol

According to **GP-1** compound **5g** was prepared by using **1g** (42 mg, 0.2 mmol, 1.0 equiv) and **2a** (53.0 mg, 0.3 mmol, 1.5 equiv) in 1 ml Et_2O for 10 h at rt under purple LEDs irradiation. Column chromatographic purification (petroleum ether/EtOAc 95:5 to 85:15) afforded **5g** as white solid (47.0 mg, 60%).

^{1}H NMR (400 MHz, $CDCl_3$): δ 9.39 (s, 1H), 7.92–7.87 (m, 4H), 7.79–7.75 (m, 2H), 7.50–7.42 (m, 3H). **^{13}C NMR (101 MHz, $CDCl_3$):** δ 165.3, 158.8, 134.8, 133.7, 131.8, 130.4, 128.9, 128.5, 123.9.

4.4.5.8. 4-methyl-*N*-phenylbenzamide (5h):



5h

$C_{14}H_{13}NO$

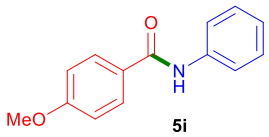
M.W. 211.26 g/mol

According to **GP-1** compound **5h** was prepared by using **1a** (24 µL, 0.2 mmol, 1.0 equiv) and **2b** (58.0 mg, 0.3 mmol, 1.5 equiv) in 1 ml Et_2O for 10 h at rt under purple LEDs irradiation. Column chromatographic purification (petroleum ether/EtOAc 95:5 to 80:20) afforded **5h** as white solid (32.0 mg, 75%).

HRMS (ESI): m/z $[M+H]^+$ Calculated for $[C_{14}H_{14}NO]^+$: 212.1075; Found: 212.1072.

^{1}H NMR (400 MHz, $CDCl_3$): δ 7.82 (br s, 1H), 7.77–7.75 (m, 2H), 7.64–7.62 (m, 2H), 7.38–7.33 (m, 2H), 7.28–7.26 (m, 2H), 7.15–7.11 (m, 1H), 2.41 (s, 3H). **^{13}C NMR (101 MHz, $CDCl_3$):** δ 165.8, 142.5, 138.1, 132.2, 129.6, 129.2, 127.1, 124.5, 120.2, 21.6.

4.4.5.9. 4-methoxy-*N*-phenylbenzamide (5i):



5i

$C_{14}H_{13}NO_2$

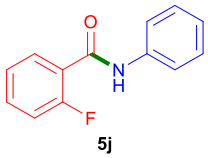
M. W. 227.26 g/mol

According to **GP-1** compound **5i** was prepared by using **1a** (24 µL, 0.2 mmol, 1.0 equiv) and **2c** (62.0 mg, 0.3 mmol, 1.5 equiv) in 1 ml Et_2O for 10 h at rt under purple LEDs irradiation. Column chromatographic purification (petroleum ether/EtOAc 95:5 to 70:30) afforded **5i** as white solid (36.0 mg, 79%).

HRMS (ESI): m/z $[M+H]^+$ Calculated for $[C_{14}H_{14}NO_2]^+$: 228.1025; Found: 228.1021.

^{1}H NMR (400 MHz, $CDCl_3$): δ 7.84–7.82 (m, 2H), 7.78 (br s, 1H), 7.63–7.61 (m, 2H), 7.37–7.33 (m, 2H), 7.14–7.10 (m, 1H), 6.97–6.94 (m, 2H), 3.86 (s, 3H). **^{13}C NMR (101 MHz, $CDCl_3$):** δ 165.3, 162.6, 138.2, 129.2, 129.0, 127.2, 124.5, 120.2, 114.1, 55.6.

4.4.5.10. 2-fluoro-*N*-phenylbenzamide (5j):



5j

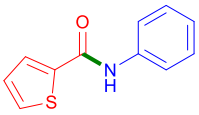
$C_{13}H_{10}FNO$
M. W. 215.23 g/mol

According to **GP-1** compound **5j** was prepared by using **1a** (24 µL, 0.2 mmol, 1.0 equiv) and **2d** (59.0 mg, 0.3 mmol, 1.5 equiv) in 1 ml Et_2O for 10 h at rt under purple LEDs irradiation. Column chromatographic purification (petroleum ether/EtOAc 95:5 to 80:20) afforded **5j** as white solid (29.0 mg, 68%).

HRMS (ESI): m/z $[M+H]^+$ Calculated for $[C_{13}H_{19}FNO]^+$: 216.0825; Found: 216.0833.

^{1}H NMR (400 MHz, $CDCl_3$): δ 8.49 (d, *J* = 14.7 Hz, 1H), 8.14–8.10 (m, 1H), 7.67–7.65 (m, 2H), 7.51–7.46 (m, 1H), 7.38–7.34 (m, 2H), 7.29–7.25 (m, 1H), 7.17–7.12 (m, 2H). **^{13}C NMR (101 MHz, $CDCl_3$):** δ 161.5, 160.4 (d, *J* = 247.3 Hz), 137.8, 133.8 (d, *J* = 9.6 Hz), 132.3, 129.2, 125.2 (d, *J* = 2.9 Hz), 124.9, 121.5 (d, *J* = 11.5 Hz), 120.6, 116.2 (d, *J* = 24.9 Hz). **^{19}F (376 MHz, $CDCl_3$):** -113.12

4.4.5.11. *N*-phenylthiophene-2-carboxamide (5k):



5k

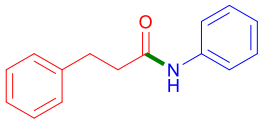
$C_{11}H_9NOS$
M.W. 203.25 g/mol

According to **GP-1** compound **5k** was prepared by using **1a** (24 µL, 0.2 mmol, 1.0 equiv) and **2e** (55.0 mg, 0.3 mmol, 1.5 equiv) in 1 ml Et_2O for 10 h at rt under purple LEDs irradiation. Column chromatographic purification (petroleum ether/EtOAc 95:5 to 80:20) afforded **5k** as colourless oil (19.0 mg, 46%).

HRMS (ESI): m/z $[M+H]^+$ Calculated for $[C_{11}H_{10}NOS]^+$: 204.0483; Found: 204.0478.

^{1}H NMR (400 MHz, $CDCl_3$): δ 7.69 (br s, 1H), 7.62–7.59 (m, 3H), 7.55–7.53 (m, 1H), 7.38–7.34 (m, 2H), 7.16–7.11 (m, 2H). **^{13}C NMR (101 MHz, $CDCl_3$):** δ 160.0, 139.3, 137.6, 130.9, 129.2, 128.5, 128.0, 124.7, 120.3.

4.4.5.12. *N*,3-diphenylpropanamide (5l):



5l

$C_{15}H_{15}NO$

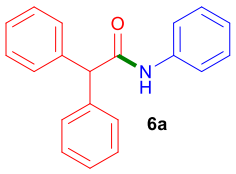
M.W. 225.29 g/mol

According to **GP-1** compound **5l** was prepared by using **1a** (24 µL, 0.2 mmol, 1.0 equiv) and **2f** (62.0 mg, 0.3 mmol, 1.5 equiv) in 1 ml Et_2O for 10 h at rt under purple LEDs irradiation. Column chromatographic purification (petroleum ether/EtOAc 95:5 to 80:20) afforded **5l** as colourless oil (30.0 mg, 67%).

HRMS (ESI): m/z $[M+H]^+$ Calculated for $[C_{15}H_{16}NO]^+$: 226.1232; Found: 226.1226.

^{1}H NMR (400 MHz, $CDCl_3$): δ 7.42–7.40 (m, 2H), 7.31–7.27 (m, 4H), 7.24–7.19 (m, 3H), 7.10–7.06 (m, 1H), 7.01 (br s, 1H), 3.05 (t, *J* = 7.8 Hz, 2H), 2.65 (t, *J* = 7.6 Hz, 2H). **^{13}C NMR (101 MHz, $CDCl_3$):** δ 170.5, 140.7, 137.8, 129.1, 128.8, 128.5, 126.5, 124.4, 120.0, 39.6, 31.7.

4.4.5.13. *N*,2,2-triphenylacetamide (6a):



6a

$C_{20}H_{17}NO$

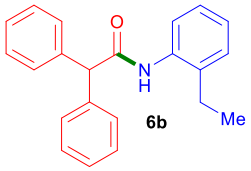
M.W. 287.36 g/mol

According to **GP-2** compound **6a** was prepared by using **1a** (24 µL, 0.2 mmol, 1.0 equiv) and **3a** (88.0 mg, 0.4 mmol, 1.5 equiv) in 2 ml DCM for 4 h at rt under blue LEDs irradiation. Column chromatographic purification (petroleum ether/EtOAc 95:5 to 85:15) afforded **6a** as white solid (49.0 mg, 87%).

HRMS (ESI): m/z $[M+H]^+$ Calculated for $[C_{20}H_{18}NO]^+$: 288.1388; Found: 288.1405.

^{1}H NMR (400 MHz, $CDCl_3$): δ 7.46–7.44 (m, 2H), 7.37–7.26 (m, 13H), 7.10–7.07 (m, 1H), 5.07 (s, 1H). **^{13}C NMR (101 MHz, $CDCl_3$):** δ 170.2, 139.1, 137.7, 129.1, 127.6, 124.6, 119.9, 60.2.

4.4.5.14. *N*-(2-ethylphenyl)-2,2-diphenylacetamide (6b):



6b

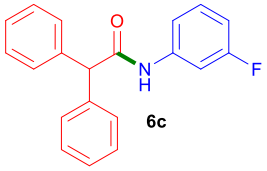
$C_{22}H_{21}NO$
M.W. 315.42 g/mol

According to **GP-2** compound **6b** was prepared by using **1b** (33 µL, 0.2 mmol, 1.0 equiv) and **3a** (88.0 mg, 0.4 mmol, 1.5 equiv) in 2 ml DCM for 4 h at rt under blue LEDs irradiation. Column chromatographic purification (petroleum ether/EtOAc 95:5 to 85:15) afforded **6b** as white solid (56.0 mg, 89%).

HRMS (ESI): m/z $[M+H]^+$ Calculated for $[C_{22}H_{22}NO]^+$: 316.1701; Found: 316.1700.

^{1}H NMR (400 MHz, $CDCl_3$): δ 8.08–8.06 (m, 1H), 7.40–7.31 (m, 9H), 7.23–7.18 (m, 2H), 7.11–7.04 (m, 2H), 5.19 (s, 1H), 2.16 (q, *J* = 7.8 Hz, 2H), 0.87 (t, *J* = 7.6 Hz, 3H). **^{13}C NMR (101 MHz, $CDCl_3$):** δ 170.1, 139.3, 135.0, 133.8, 129.2, 128.8, 128.6, 127.7, 126.9, 125.3, 122.2, 60.5, 24.4, 14.1.

4.4.5.15. *N*-(3-fluorophenyl)-2,2-diphenylacetamide (6c):



6c

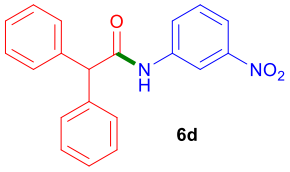
$C_{20}H_{16}FNO$
M.W. 305.35 g/mol

According to **GP-2** compound **6c** was prepared by using **1c** (31 µL, 0.2 mmol, 1.0 equiv) and **3a** (88.0 mg, 0.4 mmol, 1.5 equiv) in 2 ml DCM for 4 h at rt under blue LEDs irradiation. Column chromatographic purification (petroleum ether/EtOAc 95:5 to 85:15) afforded **6c** as white solid (46.0 mg, 61%).

HRMS (ESI): m/z $[M+H]^+$ Calculated for $[C_{20}H_{17}FNO]^+$: 306.1294; Found: 306.1291.

^{1}H NMR (400 MHz, $CDCl_3$): δ 7.50–7.46 (m, 1H), 7.38–7.34 (m, 4H), 7.31–7.27 (m, 6H), 7.23–7.18 (m, 1H), 7.05–7.02 (m, 1H), 6.81–6.77 (m, 1H), 5.07 (s, 1H). **^{13}C NMR (101 MHz, $CDCl_3$):** δ 170.23, 163.00 (d, *J* = 245.2 Hz), 139.13 (d, *J* = 10.8 Hz), 138.78, 130.10 (d, *J* = 9.4 Hz), 129.09, 129.00, 127.74, 114.9 (d, *J* = 3.2 Hz), 111.3 (d, *J* = 21.3 Hz), 107.3 (d, *J* = 26.4 Hz), 60.16. **^{19}F NMR (376 MHz, $CDCl_3$):** -111.19 (s, 1F)

4.4.5.16. *N*-(3-nitrophenyl)-2,2-diphenylacetamide (6d):



6d

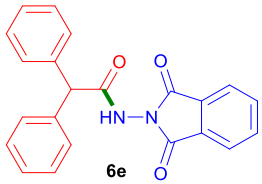
$C_{20}H_{16}N_2O_3$
M.W. 332.35 g/mol

According to **GP-2** compound **6d** was prepared by using **1e** (37.0 mg, 0.2 mmol, 1.0 equiv) and **3a** (88.0 mg, 0.4 mmol, 1.5 equiv) in 2 ml DCM for 4 h at rt under blue LEDs irradiation. Column chromatographic purification (petroleum ether/EtOAc 95:5 to 75:25) afforded **6d** as white solid (42.0 mg, 64%).

HRMS (ESI): m/z $[M+H]^+$ Calculated for $[C_{20}H_{17}N_2O_3]^+$: 333.1239; Found: 333.1232.

^{1}H NMR (400 MHz, $CDCl_3$): 8.29–8.27 (m, 1H), 7.94–7.87 (m, 2H), 7.68 (br s, 1H), 7.45–7.41 (m, 1H), 7.38–7.28 (m, 10H). **^{13}C NMR (126 MHz, $CDCl_3$):** δ 170.8, 148.6, 138.8, 138.5, 129.9, 129.2, 129.0, 127.9, 125.6, 119.2, 114.6, 60.0.

4.4.5.17. *N*-(3-nitrophenyl)-2,2-diphenylacetamide (6e):



6e

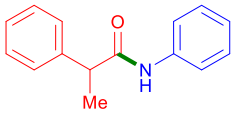
$C_{22}H_{16}N_2O_3$
M.W. 356.38 g/mol

According to **GP-2** compound **6e** was prepared by using **1g** (42.0 mg, 0.2 mmol, 1.0 equiv) and **3a** (88.0 mg, 0.4 mmol, 1.5 equiv) in 2 ml DCM for 4 h at rt under blue LEDs irradiation. Column chromatographic purification (petroleum ether/EtOAc 95:5 to 85:15) afforded **6e** as white solid (53.0 mg, 74%).

HRMS (ESI): m/z $[M+H]^+$ Calculated for $[C_{22}H_{17}N_2O_3]^+$: 357.1239; Found: 357.1263.

^{1}H NMR (400 MHz, $CDCl_3$): 7.89–7.87 (m, 2H), 7.78–7.76 (m, 2H), 7.51 (s, 1H), 7.39–7.34 (m, 6H), 7.32–7.26 (m, 4H), 5.18 (s, 1H). **^{13}C NMR (126 MHz, $CDCl_3$):** δ 170.8, 165.1, 138.1, 134.9, 130.1, 129.2, 129.1, 127.8, 124.1, 57.1.

4.4.5.18. *N*,2-diphenylpropanamide (6f):



6e

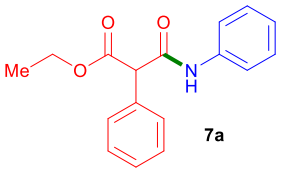
$C_{20}H_{17}NO$
M.W. 225.29 g/mol

According to **GP-2** compound **6f** was prepared by using **1a** (24 µL, 0.2 mmol, 1.0 equiv) and **3b** (64.0 mg, 0.4 mmol, 1.5 equiv) in 2 ml DCM for 4 h at rt under blue LEDs irradiation. Column chromatographic purification (petroleum ether/EtOAc 95:5 to 75:25) afforded **6f** as white solid (37.0 mg, 82%).

HRMS (ESI): m/z $[M+H]^+$ Calculated for $[C_{20}H_{18}NO]^+$: 226.1232; Found: 226.1225.

^{1}H NMR (400 MHz, $CDCl_3$): δ 7.41–7.24 (m, 9H), 7.07–7.03 (m, 2H, including N-H peak), 3.71 (q, *J* = 7.1 Hz, 1H), 1.59 (d, *J* = 7.3 Hz, 3H). **^{13}C NMR (101 MHz, $CDCl_3$):** δ 172.4, 141.0, 137.9, 129.3, 129.0, 127.8, 127.7, 124.4, 119.7, 48.2, 18.7.

4.4.5.19. ethyl 3-oxo-2-phenyl-3-(phenylamino)propanoate (7a):



7a

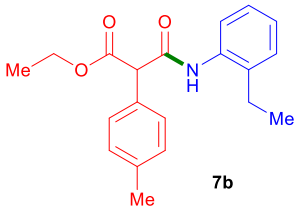
$C_{17}H_{17}NO_3$
M.W. 283.33 g/mol

According to **GP-3** compound **7a** was prepared by using **1a** (24 µL, 0.2 mmol, 1.0 equiv) and **4a** (65.0 mg, 0.3 mmol, 1.5 equiv) in 2 ml DCM for 16 h at rt under purple LEDs irradiation at 45 °C. Column chromatographic purification (petroleum ether/EtOAc 95:5 to 80:20) afforded **7a** as colourless oil (40.0 mg, 71%).

HRMS (ESI): m/z $[M+H]^+$ Calculated for $[C_{17}H_{28}NO_3]^+$: 284.1287; Found: 284.1269.

^{1}H NMR (400 MHz, $CDCl_3$): δ 9.06 (s, 1H), 7.53–7.51 (m, 2H), 7.47–7.45 (m, 2H), 7.39–7.33 (m, 3H), 7.32–7.28 (m, 2H), 7.12–7.07 (m, 1H), 4.62 (s, 1H), 4.32–4.17 (m, 2H), 1.27 (t, *J* = 7.1 Hz, 3H). **^{13}C NMR (101 MHz, $CDCl_3$):** δ 171.5, 165.2, 137.5, 134.1, 129.3, 129.1, 128.6, 128.1, 124.8, 120.1, 62.4, 59.0, 14.1.

4.4.5.20. ethyl 3-((2-ethylphenyl)amino)-3-oxo-2-(*p*-tolyl)propanoate (7b):



7b

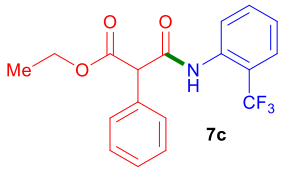
$C_{20}H_{23}NO_3$
M.W. 325.41 g/mol

According to **GP-3** compound **7b** was prepared by using **1b** (33 µL, 0.2 mmol, 1.0 equiv) and **4b** (70.0 mg, 0.3 mmol, 1.5 equiv) in 2 ml DCM for 16 h at rt under purple LEDs irradiation 45 °C. Column chromatographic purification (petroleum ether/EtOAc 95:5 to 80:20) afforded **7b** as colourless oil (47.0 mg, 72%).

HRMS (ESI): m/z $[M+H]^+$ Calculated for $[C_{20}H_{24}NO_5]^+$: 326.1756; Found: 326.1754.

^{1}H NMR (400 MHz, $CDCl_3$): δ 8.86 (br s, 1H), 7.96–7.94 (m, 1H), 7.38–7.36 (m, 2H), 7.20–7.14 (m, 4H), 7.08–7.04 (m, 1H), 4.63 (s, 1H), 4.33–4.17 (m, 2H), 2.53 (q, *J* = 7.3 Hz, 2H), 2.34 (s, 3H), 1.28 (t, *J* = 7.1 Hz, 3H), 1.14 (t, *J* = 7.6 Hz, 3H). **^{13}C NMR (101 MHz, $CDCl_3$):** δ 171.6, 165.5, 138.5, 135.1, 134.3, 131.2, 130.0, 128.7, 128.0, 126.8, 125.2, 122.4, 62.2, 58.9, 24.6, 21.2, 14.2, 14.1.

4.4.5.21. ethyl 3-oxo-2-phenyl-3-((2-(trifluoromethyl)phenyl)amino)propanoate (7c):



7c

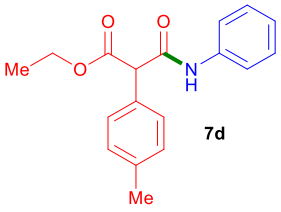
$C_{18}H_{16}F_3NO_3$
M.W. 351.33 g/mol

According to **GP-3** compound **7c** was prepared by using **1i** (41 µL, 0.2 mmol, 1.0 equiv) and **4a** (65.0 mg, 0.3 mmol, 1.5 equiv) in 2 ml DCM for 16 h at rt under purple LEDs irradiation 45 °C.. Column chromatographic purification (petroleum ether/EtOAc 95:5 to 85:15) afforded **7c** as colourless oil (45.0 mg, 64%).

HRMS (ESI): m/z $[M+H]^+$ Calculated for $[C_{18}H_{17}F_3NO_3]^+$: 352.1161; Found: 352.1159.

^{1}H NMR (400 MHz, $CDCl_3$): 9.28 (br s, 1H), 8.20–8.18 (m, 1H), 7.59–7.57 (m, 1H), 7.53–7.51(m, 1H), 7.48–7.45 (m, 2H), 7.42–7.34 (m, 3H), 7.22–7.18 (m, 1H), 4.67 (s, 1H), 4.35–4.18 (m, 2H), 1.27 (t, *J* = 7.1 Hz, 3H). **^{13}C NMR (101 MHz, $CDCl_3$):** δ 170.7, 165.7, 134.9, 133.5, 132.8, 129.4, 128.7, 128.2, 126.1 (q, *J* = 5.4 Hz), 124.7, 123.9 (q, *J* = 271.5 Hz), 124.2, 120.5 (q, *J* = 29.3 Hz), 62.4, 59.3, 14.1. **^{19}F NMR (376 MHz, $CDCl_3$):** -61.01 (s, 3F)

4.4.5.22. ethyl 3-oxo-3-(phenylamino)-2-(*p*-tolyl)propanoate (7d):



7d

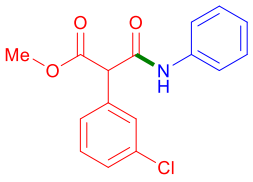
$C_{18}H_{19}NO_3$
M.W. 297.35 g/mol

According to **GP-3** compound **7d** was prepared by using **1a** (24 µL, 0.2 mmol, 1.0 equiv) and **4b** (70.0 mg, 0.3 mmol, 1.5 equiv) in 2 ml DCM for 16 h at rt under purple LEDs irradiation 45 °C. Column chromatographic purification (petroleum ether/EtOAc 95:5 to 80:20) afforded **7b** as colourless oil (44.0 mg, 74%).

HRMS (ESI): m/z $[M+H]^+$ Calculated for $[C_{18}H_{20}NO_3]^+$: 298.1443; Found: 298.1472.

^{1}H NMR (400 MHz, $CDCl_3$): δ 8.97 (br s, 1H), 7.52–7.50 (m, 2H), 7.35–7.33 (m, 2H), 7.31–7.27 (m, 2H), 7.18–7.16 (m, 2H), 7.11–7.07 (m, 1H), 4.59 (s, 1H), 4.29–4.18 (m, 2H), 2.33 (s, 3H), 1.27 (t, *J* = 7.1 Hz, 3H). **^{13}C NMR (101 MHz, $CDCl_3$):** δ 171.5, 165.5, 138.5, 137.6, 131.1, 130.0, 129.1, 128.0, 124.7, 120.1, 62.3, 58.73, 21.2, 14.1.

4.4.5.23. methyl 2-(3-chlorophenyl)-3-oxo-3-(phenylamino)propanoate (7e):



7e

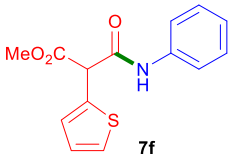
$C_{16}H_{14}ClNO_3$
M.W. 303.74 g/mol

According to **GP-3** compound **7e** was prepared by using **1a** (24 µL, 0.2 mmol, 1.0 equiv) and **4c** (71.0 mg, 0.3 mmol, 1.5 equiv) in 2 ml DCM for 16 h at rt under purple LEDs irradiation 45 °C. Column chromatographic purification (petroleum ether/EtOAc 95:5 to 80:20) afforded **7e** as colourless oil (47.0 mg, 78%).

HRMS (ESI): m/z $[M+H]^+$ Calculated for $[C_{16}H_{15}ClNO_3]^+$: 304.0740; Found:. 304.0736.

^{1}H NMR (400 MHz, $CDCl_3$): δ 9.05 (br s, 1H), 7.53–7.51 (m, 2H), 7.45–7.44 (m, 1H), 7.36–7.28 (m, 5H), 7.14–7.10 (m, 1H), 4.60 (s, 1H), 3.80 (s, 3H). **^{13}C NMR (101 MHz, $CDCl_3$):** δ 171.4, 164.4, 137.3, 135.6, 135.1, 130.5, 129.11, 128.9, 128.4, 126.5, 125.0, 120.2, 58.2, 53.4.

4.4.5.24. methyl 3-oxo-3-(phenylamino)-2-(thiophen-2-yl)propanoate (7f):



7f

$C_{14}H_{13}NO_3S$

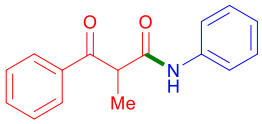
M.W. 275.32 g/mol

According to **GP-3** compound **7f** was prepared by using **1a** (24 µL, 0.2 mmol, 1.0 equiv) and **4d** (63.0 mg, 0.3 mmol, 1.5 equiv) in 2 ml DCM for 16 h at rt under purple LEDs irradiation 45 °C. Column chromatographic purification (petroleum ether/EtOAc 95:5 to 80:20) afforded **7f** as colourless oil (35.0 mg, 64%).

HRMS (ESI): m/z $[M+H]^+$ Calculated for $[C_{14}H_{14}NO_3S]^+$: 276.0694; Found: 276.0693.

^{1}H NMR (400 MHz, $CDCl_3$): δ 8.45 (br s, 1H), 7.50–7.47 (m, 2H), 7.33–7.28 (m, 3H), 7.15 (d, *J* = 4.6 Hz, 1H), 7.13–7.09 (m, 1H), 7.02 (dd, *J* = 5.3, 3.4 Hz, 1H), 4.93 (s, 1H), 3.83 (s, 3H). **^{13}C NMR (101 MHz, $CDCl_3$):** δ 170.5, 164.2, 137.2, 134.7, 129.1, 127.5, 127.4, 126.8, 125.0, 120.1, 54.7, 53.4.

4.4.5.25. 2-methyl-3-oxo-*N*,3-diphenylpropanamide (7g):



7g

$C_{16}H_{15}NO_2$

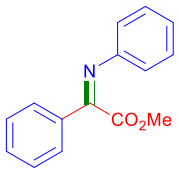
M.W. 253.30 g/mol

According to **GP-3** compound **7g** was prepared by using **1a** (24 µL, 0.2 mmol, 1.0 equiv) and **4e** (56.0 mg, 0.3 mmol, 1.5 equiv) in 2 ml DCM for 16 h at rt under purple LEDs irradiation 45 °C. Column chromatographic purification (petroleum ether/EtOAc 95:5 to 85:15) afforded **7g** as colourless oil (30.0 mg, 59%).

HRMS (ESI): m/z $[M+H]^+$ Calculated for $[C_{16}H_{16}NO_2]^+$: 254.1181; Found:. 254.1177.

^{1}H NMR (400 MHz, $CDCl_3$): δ 8.63 (br s, 1H), δ 8.06–8.04 (m, 2H), 7.65–7.60 (m, 1H), 7.54–7.49 (m, 4H), 7.33–7.29 (m, 2H), 7.12–7.08 (m, 1H), 4.52 (q, *J* = 7.3 Hz, 1H), 1.65 (d, *J* = 6.9 Hz, 3H). **^{13}C NMR (101 MHz, $CDCl_3$):** δ 200.7, 168.1, 137.6, 135.6, 134.4, 129.1, 129.1, 128.8, 124.6, 120.0, 50.1, 18.1.

4.4.5.26. methyl (*Z*)-2-phenyl-2-(phenylimino)acetate (9a):



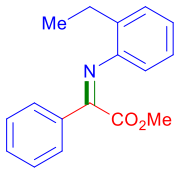
9a
$C_{15}H_{13}NO_2$
M.W. 239.27 g/mol

According to **GP-4** compound **9a** was prepared by using **1a** (24 µL, 0.2 mmol, 1.0 equiv) and **8a** (53.0 mg, 0.3 mmol, 1.5 equiv) in 2 ml DCM for 2 h at rt under blue LEDs. Column chromatographic purification (petroleum ether/EtOAc 99:1 to 95:5) afforded **9a** as yellow oil (32.0 mg, 67%).

HRMS (ESI): m/z $[M+H]^+$ Calculated for $[C_{15}H_{14}NO_2]^+$: 240.1025; Found:. 240.1035.

^{1}H NMR (400 MHz, $CDCl_3$): δ 7.89–7.87 (m, 2H), 7.54–7.45 (m, 3H), 7.36–7.32 (m, 2H), 7.16–7.13 (m, 1H), 6.98–6.96 (m, 2H), 3.63 (s, 3H). **^{13}C NMR (101 MHz, $CDCl_3$):** δ 165.6, 160.1, 150.2, 133.9, 132.0, 129.0, 128.9, 128.1, 125.1, 119.6, 52.0.

4.4.5.27. methyl (*Z*)-2-((2-ethylphenyl)imino)-2-phenylacetate (9b):



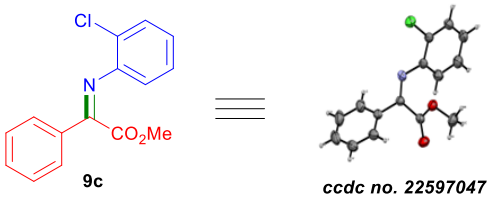
9b
$C_{17}H_{17}NO_2$
M.W. 267.33 g/mol

According to **GP-4** compound **9b** was prepared by using **1b** (33 µL, 0.2 mmol, 1.0 equiv) and **8a** (53.0 mg, 0.3 mmol, 1.5 equiv) in 2 ml DCM for 2 h at rt under blue LEDs. Column chromatographic purification (petroleum ether/EtOAc 99:1 to 95:5) afforded **9b** as yellow oil (35.0 mg, 66%).

HRMS (ESI): m/z $[M+H]^+$ Calculated for $[C_{17}H_{18}NO_2]^+$: 268.1338; Found: 268.1359.

^{1}H NMR (400 MHz, $CDCl_3$): δ 7.94–7.92 (m, 2H), 7.55–7.46 (m, 3H), 7.25–7.23 (m, 1H), 7.16–7.09 (m, 2H), 6.74–6.72 (m, 1H), 3.62 (s, 3H), 2.65 (q, *J* = 7.6 Hz, 2H), 1.21 (t, *J* = 7.8 Hz, 3H). **^{13}C NMR (101 MHz, $CDCl_3$):** δ 165.6, 159.2, 148.4, 135.6, 133.9, 131.8, 128.9, 128.6, 128.1, 126.3, 125.3, 117.6, 52.0, 24.9, 14.1.

4.4.5.28. methyl (*Z*)-2-((2-chlorophenyl)imino)-2-phenylacetate (9c):



9c

$C_{15}H_{12}ClNO_2$

M.W. 273.72 g/mol

ccdc no. 22597047

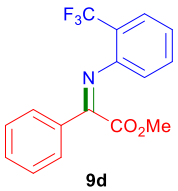
According to **GP-4** compound **9c** was prepared by using **1c** (34 µL, 0.2 mmol, 1.0 equiv) and **8a** (53.0 mg, 0.3 mmol, 1.5 equiv) in 2 ml DCM for 2 h at rt under blue LEDs. Column chromatographic purification (petroleum ether/EtOAc 99:1 to 95:5) afforded **9c** as yellow oil (30.0 mg, 55%).

HRMS (ESI): m/z $[M+H]^+$ Calculated for $[C_{15}H_{13}ClNO_2]^+$: 274.0635; Found:. 274.0628.

^{1}H NMR (400 MHz, $CDCl_3$): δ 7.95–7.92 (m, 2H), 7.56–7.52 (m, 1H), 7.50–7.46 (m, 2H), 7.42–7.40 (m, 1H),

7.22–7.18 (m, 1H), 7.09–7.05 (m, 1H), 6.85–6.83 (m, 1H), 3.63 (s, 3H). **^{13}C NMR (101 MHz, $CDCl_3$):** δ 164.7, 161.2, 147.4, 133.4, 132.4, 129.9, 128.9, 128.4, 127.2, 125.8, 125.6, 119.6, 52.2.

4.4.5.29. methyl (*Z*)-2-phenyl-2-((2-(trifluoromethyl)phenyl)imino)acetate (9d):



9d

$C_{16}H_{12}F_3NO_2$

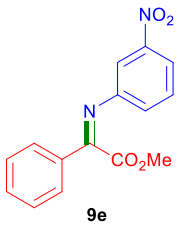
M.W. 307.27 g/mol

According to **GP-4** compound **9d** was prepared by using **1i** (41 µL, 0.2 mmol, 1.0 equiv) and **8a** (53.0 mg, 0.3 mmol, 1.5 equiv) in 2 ml DCM for 4 h at rt under blue LEDs. Column chromatographic purification (petroleum ether/EtOAc 99:1 to 95:5) afforded **9d** as yellow oil (31.0 mg, 50%).

HRMS (ESI): m/z $[M+H]^+$ Calculated for $[C_{16}H_{13}F_3NO_2]^+$: 308.0898; Found:. 308.0905.

^{1}H NMR (400 MHz, $CDCl_3$): δ 7.93–7.91 (m, 2H), 7.67–7.65 (m, 1H), 7.56–7.52 (m, 1H), 7.50–7.44 (m, 3H), 7.23–7.19 (m, 1H), 6.88–6.86 (m, 1H), 3.61 (s, 3H). **^{13}C NMR (101 MHz, $CDCl_3$):** δ 164.6, 160.5, 148.1 (q, J = 1.5 Hz), 133.5, 132.5, 132.4, 128.9, 128.5, 126.5 (q, J = 5.1 Hz), 124.6, 123.8 (q, J = 271.2 Hz), 121.3 (q, J = 30.4 Hz), 119.3, 52.1.

4.4.5.30. methyl (*Z*)-2-((3-nitrophenyl)imino)-2-phenylacetate (9e):



9e

$C_{15}H_{12}N_2O_4$

M.W. 284.27 g/mol

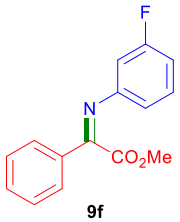
According to **GP-4** compound **9e** was prepared by using **1e** (37 µL, 0.2 mmol, 1.0 equiv) and **8a** (53.0 mg, 0.3 mmol, 1.5 equiv) in 2 ml DCM for 4 h at rt under blue LEDs. Column chromatographic purification (petroleum ether/EtOAc 99:1 to 95:5) afforded **9e** as yellow oil (30.0 mg, 53%).

HRMS (ESI): m/z $[M+H]^+$ Calculated for $[C_{15}H_{13}N_2O_4]^+$: 285.0875; Found: 285.0879.

^{1}H NMR (400 MHz, $CDCl_3$): δ 8.01–7.99 (m, 1H), 7.87–7.85 (m, 2H), 7.83–7.81 (m, 1H), 7.58–7.54 (m, 1H),

7.52–7.46 (m, 3H), 7.27–7.25 (m, 1H), 3.68 (s, 3H). **^{13}C NMR (101 MHz, $CDCl_3$):** δ 164.6, 162.0, 151.1, 148.7, 133.1, 132.7, 129.9, 129.0, 128.4, 125.9, 119.7, 114.8, 52.3.

4.4.5.31. methyl (*Z*)-2-((3-fluorophenyl)imino)-2-phenylacetate (9f):



9f

$C_{15}H_{12}FNO_2$

M.W. 257.26 g/mol

According to **GP-4** compound **9f** was prepared by using **1d** (32 µL, 0.2 mmol, 1.0 equiv) and **8a** (53.0 mg, 0.3 mmol, 1.5 equiv) in 2 ml DCM for 3 h at rt under blue LEDs. Column chromatographic purification (petroleum ether/EtOAc 99:1 to 95:5) afforded **9f** as yellow oil (29.0 mg, 56%).

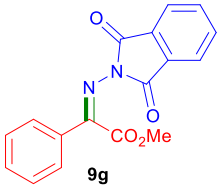
HRMS (ESI): m/z $[M+H]^+$ Calculated for $[C_{15}H_{13}NO_2F]^+$: 258.0930; Found: 258.0950.

^{1}H NMR (400 MHz, $CDCl_3$): δ 7.87–7.85 (m, 2H), 7.55–7.51 (m, 1H), 7.49–7.44 (m, 2H), 7.31–7.25 (m, 1H),

6.87–6.82 (m, 1H), 6.73–6.69 (m, 2H), 3.67 (s, 3H). **^{13}C NMR (101 MHz, $CDCl_3$):** δ 165.1, 163.1 (d, *J* = 246.3 Hz), 160.8, 151.8 (d, *J* = 9.6 Hz), 133.5, 132.3, 130.3 (d, *J* = 9.6 Hz), 128.9, 128.2, 115.2 (d, *J* = 3.8 Hz), 111.8 (d, *J* = 21.1 Hz), 107.3 (d, *J* = 24.0 Hz), 52.1.

^{19}F NMR (376 MHz, $CDCl_3$): -112.29 (s, 1F).

4.4.5.32. methyl (*Z*)-2-((1,3-dioxoisoindolin-2-yl)imino)-2-phenylacetate (9g):



9g

$C_{17}H_{12}N_2O_4$

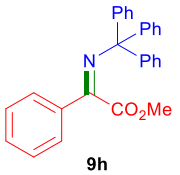
M.W. 308.29 g/mol

According to **GP-4** compound **9g** was prepared by using **1g** (41 mg, 0.2 mmol, 1.0 equiv) and **8a** (53.0 mg, 0.3 mmol, 1.5 equiv) in 2 ml DCM for 3 h at rt under blue LEDs. Column chromatographic purification (petroleum ether/EtOAc 99:1 to 95:5) afforded **9g** as yellow oil (33.0 mg, 54%).

HRMS (ESI): m/z $[M+H]^+$ Calculated for $[C_{17}H_{13}N_2O_4]^+$: 309.0875; Found: 309.0871.

^{1}H NMR (400 MHz, $CDCl_3$): δ 7.92–7.90 (m, 2H), 7.82–7.80 (m, 2H), 7.78–7.76 (m, 2H), 7.55–7.50 (m, 1H), 7.46–7.42 (m, 2H), 3.91 (s, 3H). **^{13}C NMR (101 MHz, $CDCl_3$):** δ 163.8, 162.7, 161.4, 134.8, 132.1, 130.7, 130.2, 128.9, 128.7, 124.1, 53.2.

4.4.5.33. methyl (*Z*)-2-phenyl-2-(tritylimino)acetate (9h):



9h

$C_{28}H_{23}NO_2$

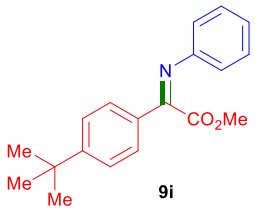
M.W. 405.50 g/mol

According to **GP-4** compound **9h** was prepared by using **1f** (61 mg, 0.2 mmol, 1.0 equiv) and **8a** (53.0 mg, 0.3 mmol, 1.5 equiv) in 2 ml DCM for 3 h at rt under blue LEDs. Column chromatographic purification (petroleum ether/EtOAc 99:1 to 95:5) afforded **9h** as yellow oil (35.0 mg, 43%).

HRMS (ESI): m/z $[M+H]^+$ Calculated for $[C_{28}H_{24}NO_2]^+$: 406.1807; Found: . 406.1801.

^{1}H NMR (400 MHz, $CDCl_3$): δ 7.83–7.81 (m, 2H), 7.47–7.40 (m, 3H), 7.32–7.24 (m, 15H), 3.13 (s, 3H). **^{13}C NMR (101 MHz, $CDCl_3$):** δ 165.6, 157.3, 145.3, 136.4, 130.9, 130.1, 128.5, 127.6, 127.5, 126.8, 92.9, 51.4.

4.4.5.34. methyl (*Z*)-2-(4-(*tert*-butyl)phenyl)-2-(phenylimino)acetate (9i):



9i

$C_{19}H_{21}NO_2$

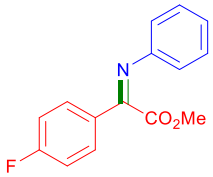
M.W. 295.38 g/mol

According to **GP-4** compound **9i** was prepared by using **1a** (24 µL, 0.2 mmol, 1.0 equiv) and **8b** (69.0 mg, 0.3 mmol, 1.5 equiv) in 2 ml DCM for 3 h at rt under blue LEDs. Column chromatographic purification (petroleum ether/EtOAc 99:1 to 95:5) afforded **9i** as yellow oil (34.0 mg, 54%).

HRMS (ESI): m/z $[M+H]^+$ Calculated for $[C_{19}H_{22}NO_2]^+$: 296.1651; Found: . 296.1645.

^{1}H NMR (400 MHz, $CDCl_3$): δ 7.80–7.77 (m, 2H), 7.49–7.47 (m, 2H), 7.33–7.29 (m, 2H), 7.14–7.10 (m, 1H), 6.95–6.93 (m, 2H), 3.62 (s, 3H), 1.34 (s, 9H). **^{13}C NMR (101 MHz, $CDCl_3$):** δ 165.7, 159.9, 155.6, 150.3, 131.2, 129.0, 127.9, 125.9, 124.9, 119.6, 51.9, 35.12, 31.2.

4.4.5.35. methyl (*Z*)-2-(4-fluorophenyl)-2-(phenylimino)acetate (9j):



9j

$C_{15}H_{12}FNO_2$

M.W. 257.26 g/mol

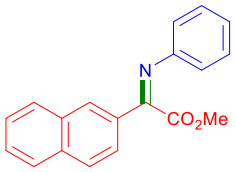
According to **GP-4** compound **9j** was prepared by using **1a** (24 µL, 0.2 mmol, 1.0 equiv) and **8c** (58.0 mg, 0.3 mmol, 1.5 equiv) in 2 ml DCM for 3 h at rt under blue LEDs. Column chromatographic purification (petroleum ether/EtOAc 99:1 to 95:5) afforded **9j** as yellow oil (36.0 mg, 70%).

HRMS (ESI): m/z $[M+H]^+$ Calculated for $[C_{15}H_{13}FNO_2]^+$: 258.0930; Found: 258.0913.

^{1}H NMR (400 MHz, $CDCl_3$): δ 7.89–7.85 (m, 2H), 7.35–7.31 (m, 2H), 7.16–7.12 (m, 3H), 6.95–6.92 (m, 2H), 3.63 (s, 3H). **^{13}C NMR (101 MHz, $CDCl_3$):** δ 165.4, 165.1 (d, J = 253.0 Hz),

158.7, 150.0, 133.2 (d, *J* = 9.6 Hz), 130.4 (d, *J* = 8.6 Hz), 129.0, 125.2, 119.5, 116.0 (d, *J* = 22.0 Hz), 52.1. **^{19}F NMR (376 MHz, $CDCl_3$):** -107.25 (s, 1F).

4.4.5.36. methyl (*Z*)-2-(naphthalen-2-yl)-2-(phenylimino)acetate (9k):



9k

$C_{19}H_{15}NO_2$

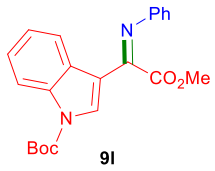
M.W. 289.33 g/mol

According to **GP-4** compound **9k** was prepared by using **1a** (24 µL, 0.2 mmol, 1.0 equiv) and **8d** (68.0 mg, 0.3 mmol, 1.5 equiv) in 2 ml DCM for 2 h at rt under blue LEDs. Column chromatographic purification (petroleum ether/EtOAc 99:1 to 95:5) afforded **9k** as yellow oil (37.0 mg, 64%).

HRMS (ESI): m/z $[M+H]^+$ Calculated for $[C_{19}H_{16}NO_2]^+$: 290.1181; Found: 290.1177.

^{1}H NMR (400 MHz, $CDCl_3$): δ 8.18 (s, 1H), 8.14–8.12 (m, 1H), 7.93–7.86 (m, 3H), 7.59–7.51 (m, 2H), 7.38–7.34 (m, 2H), 7.18–7.14 (m, 1H), 7.02–7.00 (m, 2H), 3.68 (s, 3H). **^{13}C NMR (101 MHz, $CDCl_3$):** δ 165.7, 160.1, 150.3, 135.1, 132.8, 131.3, 129.8, 129.2, 129.0, 128.8, 128.1, 127.9, 126.9, 125.1, 123.8, 119.7, 52.1.

4.4.5.37. *tert*-butyl (*Z*)-3-(2-methoxy-2-oxo-1-(phenylimino)ethyl)-1*H*-indole-1-carboxylate (9l):



9l

$C_{22}H_{22}N_2O_4$

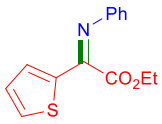
M.W. 378.43 g/mol

According to **GP-4** compound **9l** was prepared by using **1a** (24 µL, 0.2 mmol, 1.0 equiv) and **8e** (94.0 mg, 0.3 mmol, 1.5 equiv) in 2 ml DCM for 3 h at rt under blue LEDs. Column chromatographic purification (petroleum ether/EtOAc 99:1 to 95:5) afforded **9l** as yellow oil (37.0 mg, 64%).

HRMS (ESI): m/z $[M+H]^+$ Calculated for $[C_{22}H_{23}N_2O_4]^+$: 379.1658; Found: 379.1652.

^{1}H NMR (400 MHz, $CDCl_3$): δ 8.55–8.53 (m, 1H), 8.17–8.14 (m, 1H), 7.98 (s, 1H), 7.42–7.38 (m, 1H), 7.36–7.32 (m, 3H), 7.15–7.11 (m, 1H), 6.99–6.97 (m, 2H), 3.61 (s, 3H), 1.69 (s, 9H). **^{13}C NMR (101 MHz, $CDCl_3$):** δ 164.9, 155.0, 150.6, 149.3, 136.0, 131.1, 129.0, 127.5, 125.8, 124.8, 124.2, 123.3, 119.8, 116.5, 115.1, 85.2, 52.1, 28.2.

4.4.5.38. ethyl (*E*)-2-(phenylimino)-2-(thiophen-2-yl)acetate (9m):



9m

$C_{14}H_{13}NO_2S$

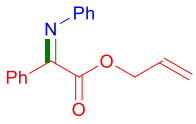
M.W. 259.32 g/mol

According to **GP-4** compound **9m** was prepared by using **1a** (24 µL, 0.2 mmol, 1.0 equiv) and **8f** (59.0 mg, 0.3 mmol, 1.5 equiv) in 2 ml DCM for 3 h at rt under blue LEDs. Column chromatographic purification (petroleum ether/EtOAc 99:1 to 95:5) afforded **9m** as yellow oil (30.0 mg, 58%).

HRMS (ESI): m/z $[M+H]^+$ Calculated for $[C_{14}H_{14}NO_2S]^+$: 260.0745; Found: 260.0740.

^{1}H NMR (400 MHz, $CDCl_3$): δ 7.54–7.53 (m, 1H), 7.45–7.44 (m, 1H), 7.32–7.28 (m, 2H), 7.14–7.09 (m, 2H), 6.96–6.94 (m, 2H), 4.11 (q, *J* = 7.1 Hz, 2H), 0.98 (t, *J* = 7.1 Hz, 3H). **^{13}C NMR (101 MHz, $CDCl_3$):** δ 163.9, 154.4, 149.7, 140.7, 131.6, 131.5, 128.9, 128.0, 125.1, 120.0, 61.8, 13.8.

4.4.5.39. allyl (*Z*)-2-phenyl-2-(phenylimino)acetate (9n):



9n

$C_{17}H_{15}NO_2$

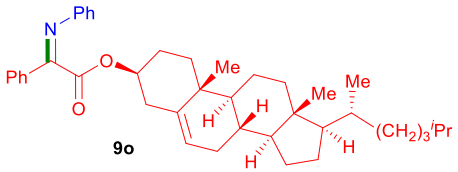
M.W. 265.31 g/mol

According to **GP-4** compound **9n** was prepared by using **1a** (24 µL, 0.2 mmol, 1.0 equiv) and **8g** (61.0 mg, 0.3 mmol, 1.5 equiv) in 2 ml DCM for 2 h at rt under blue LEDs. Column chromatographic purification (petroleum ether/EtOAc 99:1 to 97:3) afforded **9n** as yellow oil (34.0 mg, 64%).

HRMS (ESI): m/z $[M+H]^+$ Calculated for $[C_{17}H_{16}NO_2]^+$: 266.1181; Found: 266.1175.

^{1}H NMR (400 MHz, $CDCl_3$): δ 7.89–7.86 (m, 2H), 7.53–7.49 (m, 1H), 7.48–7.44 (m, 2H), 7.33–7.29 (m, 2H), 7.15–7.10 (m, 1H), 6.96–6.94 (m, 2H), 5.62–5.52 (m, 1H), 5.15–5.10 (m, 2H), 4.53 (dt, *J* = 6.0, 1.4 Hz, 2H). **^{13}C NMR (101 MHz, $CDCl_3$):** δ 164.7, 160.0, 150.2, 133.9, 131.9, 130.8, 130.2, 128.9, 128.8, 128.1, 125.0, 119.7, 66.0.

4.4.5.40. (3*S*,8*S*,9*S*,10*R*,13*R*,14*S*,17*R*)-10,13-dimethyl-17-((*R*)-6-methylheptan-2-yl)-2,3,4,7,8,9,10,11,12,13,14,15,16,17-tetradecahydro-1*H*-cyclopenta[*a*]phenanthren-3-yl (*Z*)-2-phenyl-2-(phenylimino)acetate (9o):



9o

$C_{41}H_{55}NO_2$

M.W. 593.90 g/mol

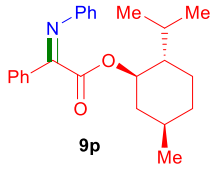
According to **GP-4** compound **9o** was prepared by using **1a** (24 µL, 0.2 mmol, 1.0 equiv) and **8h** (159.0 mg, 0.3 mmol, 1.5 equiv) in 2 ml DCM for 2 h at rt under blue LEDs. Column chromatographic purification (petroleum ether/EtOAc 99:1 to 97:3) afforded **9o** as yellow solid (34.0 mg, 64%).

HRMS (ESI): m/z $[M+H]^+$ Calculated for $[C_{41}H_{56}NO_2]^+$: 594.4311; Found: 594.4315.

^{1}H NMR (400 MHz, $CDCl_3$): δ 7.90–7.88 (m, 2H), 7.53–7.44 (m, 3H), 7.33–7.29 (m, 2H), 7.15–7.11 (m, 1H), 6.97–6.94 (m, 2H), 5.29–5.27 (m, 1H), 4.64 (tt, *J* = 11.4, 5.0 Hz, 1H), 2.05–1.91 (m, 5H), 1.81–1.73 (m, 2H), 1.56–1.48 (m, 4H), 1.46–1.38 (m, 4H), 1.36–1.28 (m, 4H),

1.15–1.06 (m, 5H), 1.03–0.95 (m, 4H), 0.91 (s, 3H), 0.89 (s, 3H), 0.86 (d, *J* = 2.3 Hz, 3H), 0.85 (d, *J* = 2.3 Hz, 3H), 0.65 (s, 3H). **^{13}C NMR (101 MHz, $CDCl_3$):** δ 164.4, 160.6, 150.4, 139.2, 133.9, 131.8, 128.8, 128.8, 128.1, 124.9, 123.1, 119.8, 75.7, 56.7, 56.2, 50.0, 42.4, 39.8, 39.6, 37.6, 36.9, 36.6, 36.3, 35.9, 31.9, 31.9, 28.3, 28.1, 27.4, 24.4, 23.9, 23.0, 22.7, 21.1, 19.3, 18.8, 11.9.

4.4.5.41. (1*R*,2*S*,5*R*)-2-isopropyl-5-methylcyclohexyl (*Z*)-2-phenyl-2-(phenylimino)acetate (9p):



9p

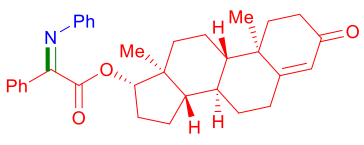
$C_{24}H_{29}NO_2$
M.W. 363.50 g/mol

According to **GP-4** compound **9p** was prepared by using **1a** (24 µL, 0.2 mmol, 1.0 equiv) and **8i** (90.0 mg, 0.3 mmol, 1.5 equiv) in 2 ml DCM for 2 h at rt under blue LEDs. Column chromatographic purification (petroleum ether/EtOAc 100:0 to 99:1) afforded **9p** as yellow solid (38.0 mg, 52%).

HRMS (ESI): m/z $[M+H]^+$ Calculated for $[C_{24}H_{30}NO_2]^+$: 364.2277; Found: 364.2273.

^{1}H NMR (400 MHz, $CDCl_3$): δ 7.87–7.85 (m, 2H), 7.53–7.44 (m, 3H), 7.32–7.28 (m, 2H), 7.13–7.09 (m, 1H), 6.96–6.94 (m, 2H), 4.71 (td, *J* = 11.0, 4.4 Hz, 1H), 1.71–1.66 (m, 1H), 1.60–1.55 (m, 3H), 1.40–1.27 (m, 2H), 1.24–1.18 (m, 2H), 0.96–0.90 (m, 2H), 0.82 (d, *J* = 6.4 Hz, 3H), 0.70 (d, *J* = 6.9 Hz, 3H), 0.56 (d, *J* = 6.9 Hz, 3H). **^{13}C NMR (101 MHz, $CDCl_3$):** δ 164.9, 160.5, 150.2, 134.1, 131.8, 128.9, 128.8, 128.0, 124.8, 119.9, 76.4, 46.5, 40.1, 34.0, 31.4, 25.4, 22.8, 22.0, 20.9, 15.8.

4.4.5.42. (8*R*,9*S*,10*R*,13*S*,14*S*,17*S*)-10,13-dimethyl-3-oxo-2,3,6,7,8,9,10,11,12,13,14,15,16,17-tetradecahydro-1*H*-cyclopenta[*a*]phenanthren-17-yl (*Z*)-2-phenyl-2-(phenylimino)acetate (9q):



9q

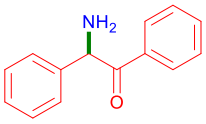
$C_{33}H_{37}NO_3$
M.W. 495.66 g/mol

According to **GP-4** compound **9q** was prepared by using **1a** (24 µL, 0.2 mmol, 1.0 equiv) and **8j** (129.0 mg, 0.3 mmol, 1.5 equiv) in 2 ml DCM for 3 h at rt under blue LEDs. Column chromatographic purification (petroleum ether/EtOAc 99:1 to 97:3) afforded **9q** as yellow oil (45.0 mg, 45%).

HRMS (ESI): m/z $[M+H]^+$ Calculated for $[C_{33}H_{38}NO_3]^+$: 496.2852; Found: 496.2833.

^{1}H NMR (400 MHz, $CDCl_3$): δ 7.87–7.85 (m, 2H), 7.53–7.44 (m, 3H), 7.32–7.28 (m, 2H), 7.13–7.09 (m, 1H), 6.95–6.93 (m, 2H), 5.70 (s, 1H), δ 4.56 (dd, *J* = 9.2, 7.3 Hz, 1H), 2.41–2.34 (m, 2H), 2.31–2.21 (m, 2H), 2.02–1.96 (m, 2H), 1.80–1.76 (m, 2H), 1.70–1.62 (m, 2H), 1.52–1.45 (m, 2H), 1.41–1.35 (m, 2H), 1.14 (s, 3H), 1.03–0.93 (m, 3H), 0.90–0.83 (m, 2H), 0.56 (s, 3H). **^{13}C NMR (101 MHz, $CDCl_3$):** δ 199.6, 170.9, 165.0, 160.4, 150.4, 131.9, 130.0, 128.9, 128.9, 128.1, 124.9, 124.1, 119.8, 84.1, 53.7, 50.0, 42.4, 38.6, 36.1, 35.8, 35.4, 34.0, 32.8, 31.5, 27.0, 23.5, 20.4, 17.4, 14.2.

4.4.5.43. 2-amino-1,2-diphenylethan-1-one (10):



10

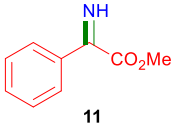
$C_{14}H_{13}NO$

M.W. 211.26 g/mol

According to **GP-2** compound **10** was prepared by using **1h** (27 µL, 0.2 mmol, 1.0 equiv) and **3a** (88.0 mg, 0.3 mmol, 1.5 equiv) in 2 ml DCM for 4 h at rt under blue LEDs. Column chromatographic purification (petroleum ether/EtOAc 99:1 to 98:2) afforded **10** as colourless oil (31.0 mg, 72%).

^{1}H NMR (400 MHz, $CDCl_3$): δ 7.96–7.93 (m, 2H), 7.56–7.52 (m, 1H), 7.48–7.30 (m, 7H), 6.32 (s, 1H). **^{13}C NMR (101 MHz, $CDCl_3$):** δ 191.6, 136.0, 134.4, 133.9, 129.3, 129.3, 129.2, 128.9, 128.6, 62.4.

4.4.5.44. methyl 2-imino-2-phenylacetate (11):



11

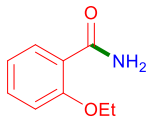
$C_9H_9NO_2$

M.W. 163.18 g/mol

According to **GP-4** compound **11** was prepared by using **1h** (27 µL, 0.2 mmol, 1.0 equiv) and **8a** (53.0 mg, 0.3 mmol, 1.5 equiv) in 2 ml DCM for 2 h at rt under blue LEDs. Column chromatographic purification (petroleum ether/EtOAc 99:1 to 95:5) afforded **11** as yellow oil (31.0 mg, 72%).

^{1}H NMR (400 MHz, $CDCl_3$): δ 7.78–7.75 (m, 2H), 7.52–7.48 (m, 1H), 7.45–7.41 (m, 2H), 4.00 (s, 3H). **^{13}C NMR (101 MHz, $CDCl_3$):** δ 165.9, 162.5, 132.3, 131.1, 128.9, 128.1, 52.3.

4.4.5.45. 2-ethoxybenzamide (12):



12
$C_9H_{11}NO_2$
M.W. 165.19 g/mol

According to **GP-5** compound **12** was prepared by using **2g** (66 µL, 0.3 mmol, 1.5 equiv) and **1a** (61.0 mg, 0.3 mmol, 1.0 equiv) in 2 ml Et_2O for 10 h at rt under purple LEDs. After completion solvent was evaporated under reduced pressure and added 2 ml 4% TFA/Et_3SiH under aerobic conditions and sealed. The vial was then stirred for 30 min at room temperature. Column chromatographic purification (petroleum ether/EtOAc 90:10 to 70:30) afforded **12** as white solid (18.0 mg, 54%).

HRMS (ESI): m/z $[M+H]^+$ Calculated for $[C_9H_{12}NO_2]^+$: 166.0868; Found: 166.0850.

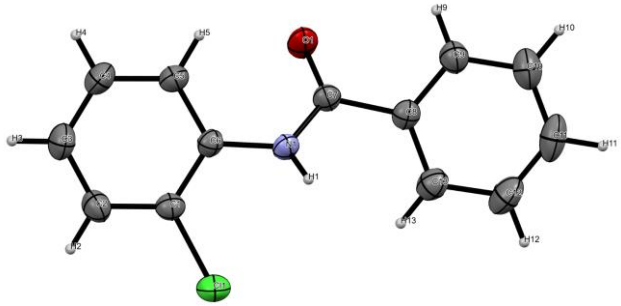
^{1}H NMR (400 MHz, $CDCl_3$): δ 8.22–8.19 (m, 1H), 7.89 (br s, 1H), 7.47–7.43 (m, 1H), 7.08–7.04 (m, 1H), 6.97–6.95 (m, 1H), 5.85 (br s, 1H), 4.20 (q, *J* = 6.9 Hz, 2H), 1.51 (t, *J* = 6.9 Hz, 3H). **^{13}C NMR (101 MHz, $CDCl_3$):** δ 167.3, 157.4, 133.5, 132.7, 121.3, 120.7, 112.4, 64.8, 15.0.

4.4.6. X-ray single crystal data and structure refinement for substrate 5c and 9c:

For the determination of X-ray crystal structures of **5c** and **9c** a single crystal was selected and mounted on Hampton cyoloops. The data was collected at 298K and on a CMOS based Bruker SMART APEX2 area detector diffractometer equipped with an INCOATEC micro-focus source with graphite monochromatic Mo Kα radiation (λ = 0.71073 Å) operation at 50 kV and 30 mA. For the integration of diffraction profiles SAINT program was used. Absorption correction was done applying SADABS program. Using Olex2, the structure was solved with the SHELXT structure solution program using Intrinsic phasing and refined with the SHELXL refinement package applying Least Squares minimization method. All the non-hydrogen atoms in the structure were located the Fourier map and refined anisotropically. The hydrogen atoms were

fixed by HFIX in their ideal positions and refined using riding model with isotropic thermal parameters. The crystal structure (excluding structure factor) has been deposited to Cambridge Crystallographic Data Centre and allocated deposition number for the compound **5c** and **9c** are **CCDC 2257649** and **22597047** respectively.[25]

4.4.6.1. Crystal data and structure refinement for 5c:



Atom colour code: grey = carbon atom, white = hydrogen atom, green = chlorine atom, violet = nitrogen atom, and red = oxygen atom.

Table 11: Fractional Atomic Coordinates ($\times 10^4$) and Equivalent Isotropic Displacement Parameters ($Å^2 \times 10^3$) for ICAPU_150_R_0m. U_{eq} is defined as 1/3 of the trace of the orthogonalised U_{IJ} tensor.

Atom	*x*	*y*	*z*	U(eq)
Cl1	1265.5(5)	1462.6(13)	4195.2(3)	68.2(2)
O1	4339.8(16)	8839(3)	3852.7(7)	65.3(5)
N1	3587.2(15)	4538(3)	4032.4(7)	46.5(4)
C6	3080.3(18)	5056(4)	4601.3(8)	42.9(4)
C8	4605.1(19)	5360(4)	3099.1(9)	47.4(5)
C1	2007.0(19)	3659(4)	4740.9(9)	48.1(5)
C7	4169.3(18)	6413(4)	3695.2(9)	46.2(4)
C5	3633(2)	6867(4)	5040.4(10)	51.8(5)
C2	1501(2)	4036(5)	5300.6(11)	62.1(6)
C13	3955(2)	3377(5)	2740.7(10)	61.4(6)
C4	3111(2)	7241(5)	5595.7(10)	62.1(6)

Table 11: Fractional Atomic Coordinates ($\times 10^4$) and Equivalent Isotropic Displacement Parameters ($Å^2 \times 10^3$) for ICAPU_150_R_0m. U_{eq} is defined as 1/3 of the trace of the orthogonalised U_{IJ} tensor.

Atom	*x*	*y*	*z*	U(eq)
C	2056(2)	5840(5)	5723.3(10)	67.4(6)
C9	5682(2)	6503(5)	2895.7(11)	62.0(6)
C11	5481(3)	3675(6)	1998.9(11)	80.3(9)
C10	6124(3)	5642(6)	2350.1(12)	74.7(7)
C12	4401(3)	2553(6)	2189.1(11)	78.1(8)

Table 13 Anisotropic Displacement Parameters ($Å^2 \times 10^3$) for ICAPU_150_R_0m. The Anisotropic displacement factor exponent takes the form: $-2\pi^2[h^2a^{*2}U_{11}+2hka^*b^*U_{12}+\ldots]$.

Atom	U_{11}	U_{22}	U_{33}	U_{23}	U_{13}	U_{12}
Cl1	62.0(4)	72.4(4)	70.0(4)	-13.7(3)	3.7(3)	-21.0(3)
O1	95.7(12)	31.0(7)	72.5(10)	-5.2(6)	29.3(9)	-6.6(7)
N1	59.7(10)	32.3(8)	48.9(9)	-6.4(7)	12.1(7)	-4.3(7)
C6	50.0(10)	34.9(9)	43.9(10)	-1.3(7)	4.9(8)	5.1(8)
C8	58.9(12)	37.9(10)	45.7(10)	3.2(8)	6.3(9)	6.8(8)
C1	47.9(10)	45.4(11)	50.3(11)	0.0(8)	0.2(8)	0.0(8)
C7	51.5(11)	33.9(10)	53.8(11)	-0.2(8)	8.4(9)	1.1(8)
C5	56.5(12)	44.5(11)	54.7(12)	-6.3(9)	5.1(9)	-4.2(9)
C2	59.5(13)	72.8(15)	55.4(13)	4.9(11)	13.6(10)	-4.2(11)
C13	78.0(15)	56.0(13)	49.7(12)	0.4(10)	0.9(11)	-1.5(11)
C4	77.0(15)	58.1(13)	50.9(12)	-14.2(10)	1.9(11)	1.3(11)
C3	79.6(16)	78.1(16)	46.0(12)	-3.9(11)	14.2(11)	3.5(13)
C9	67.1(14)	63.6(14)	57.0(13)	-0.9(10)	16.0(11)	-1.0(11)
C11	114(2)	84.1(19)	44.6(13)	4.8(12)	18.4(14)	39.3(17)
C10	77.0(16)	88.8(19)	61.3(15)	6.0(13)	24.0(13)	13.7(14)
C12	114(2)	70.0(16)	48.3(13)	-7.9(12)	-5.0(14)	5.3(16)

Table 14 Bond Lengths for ICAPU_150_R_0m.

Atom	Atom	Length/Å		Atom	Atom	Length/Å
Cl1	C1	1.736(2)		C1	C2	1.383(3)

Table 14 Bond Lengths for ICAPU_150_R_0m.						
Atom	**Atom**	**Length/Å**		**Atom**	**Atom**	**Length/Å**
O1	C7	1.226(2)		C5	C4	1.382(3)
N1	C6	1.412(2)		C2	C3	1.368(3)
N1	C7	1.347(2)		C13	C12	1.383(3)
C6	C1	1.389(3)		C4	C3	1.366(3)
C6	C5	1.392(3)		C9	C10	1.375(3)
C8	C7	1.500(3)		C11	C10	1.370(4)
C8	C13	1.387(3)		C11	C12	1.373(4)
C8	C9	1.385(3)				

Table 15 Bond Angles for ICAPU_150_R_0m.							
Atom	**Atom**	**Atom**	**Angle/°**	**Atom**	**Atom**	**Atom**	**Angle/°**
C7	N1	C6	125.83(16)	O1	C7	C8	120.88(17)
C1	C6	N1	119.28(17)	N1	C7	C8	115.64(16)
C1	C6	C5	118.12(17)	C4	C5	C6	120.0(2)
C5	C6	N1	122.58(17)	C3	C2	C1	119.5(2)
C13	C8	C7	122.73(19)	C12	C13	C8	119.4(2)
C9	C8	C7	117.77(18)	C3	C4	C5	120.8(2)
C9	C8	C13	119.46(19)	C4	C3	C2	120.3(2)
C6	C1	Cl1	119.41(15)	C10	C9	C8	120.6(2)
C2	C1	Cl1	119.33(17)	C10	C11	C12	120.4(2)
C2	C1	C6	121.24(19)	C11	C10	C9	119.7(3)
O1	C7	N1	123.48(18)	C11	C12	C13	120.4(3)

Table 16 Torsion Angles for ICAPU_150_R_0m.									
A	**B**	**C**	**D**	**Angle/°**	**A**	**B**	**C**	**D**	**Angle/°**
Cl1	C1	C2	C3	-177.67(18)	C7	C8	C13	C12	178.5(2)
N1	C6	C1	Cl1	-3.7(2)	C7	C8	C9	C10	-179.4(2)

Table 16 Torsion Angles for ICAPU_150_R_0m.

A	B	C	D	Angle/°		A	B	C	D	Angle/°
N1	C6	C1	C2	177.93(19)		C5	C6	C1	Cl1	178.07(15)
N1	C6	C5	C4	-178.41(19)		C5	C6	C1	C2	-0.3(3)
C6	N1	C7	O1	0.8(3)		C5	C4	C3	C2	0.0(4)
C6	N1	C7	C8	-178.88(17)		C13	C8	C7	O1	-145.2(2)
C6	C1	C2	C3	0.7(3)		C13	C8	C7	N1	34.6(3)
C6	C5	C4	C3	0.4(3)		C13	C8	C9	C10	-1.5(3)
C8	C13	C12	C11	0.3(4)		C9	C8	C7	O1	32.7(3)
C8	C9	C10	C11	1.2(4)		C9	C8	C7	N1	-147.6(2)
C1	C6	C5	C4	-0.2(3)		C9	C8	C13	C12	0.7(3)
C1	C2	C3	C4	-0.6(4)		C10	C11	C12	C13	-0.6(4)
C7	N1	C6	C1	145.9(2)		C12	C11	C10	C9	-0.2(4)
C7	N1	C6	C5	-35.9(3)						

Table 17 Hydrogen Atom Coordinates (Å×10^4) and Isotropic Displacement Parameters (Å^2×10^3) for ICAPU_150_R_0m.

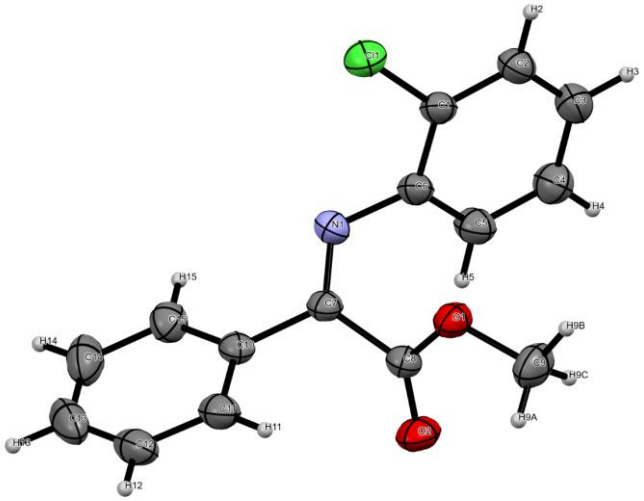
Atom	*x*	*y*	*z*	U(eq)
H1	3518.14	2876.7	3888.15	56
H5	4353.34	7826.25	4960.04	62
H2	787	3069.08	5389.16	75
H13	3225.78	2608.58	2870.03	74
H4	3481.83	8462.53	5886.25	75
H3	1715.07	6113.12	6098.88	81
H9	6109.76	7864.68	3130.1	74
H11	5777.53	3094.91	1629.23	96
H10	6856.37	6392.64	2220.09	90
H12	3966.71	1231.46	1945.72	94

ICAPU_150_R_0m

Table 18: Crystal data and structure refinement for

ICAPU_150_R_0m.	
CCDC NO.	2257649
Empirical formula	$C_{13}H_{10}ClNO$
Formula weight	231.67
Temperature/K	298
Crystal system	monoclinic
Space group	$P2_1/n$
a/Å	10.7547(5)
b/Å	4.8125(2)
c/Å	21.7409(10)
α/°	90
β/°	94.396(2)
γ/°	90
Volume/Å^3	1121.93(9)
Z	4
ρ_{calc}g/cm^3	1.372
μ/mm^{-1}	0.316
F(000)	480.0
Crystal size/mm^3	0.213 × 0.123 × 0.106
Radiation	MoKα (λ = 0.71073)
2Θ range for data collection/°	4.366 to 52.892
Index ranges	$-13 \leq h \leq 13$, $-5 \leq k \leq 6$, $-27 \leq l \leq 27$
Reflections collected	9499
Independent reflections	2295 [R_{int} = 0.0398, R_{sigma} = 0.0327]
Data/restraints/parameters	2295/1/145
Goodness-of-fit on F^2	1.073
Final R indexes [I>=2σ (I)]	R_1 = 0.0451, wR_2 = 0.1143
Final R indexes [all data]	R_1 = 0.0548, wR_2 = 0.1204
Largest diff. peak/hole / e Å^{-3}	0.30/-0.28

4.4.6.2. Crystal data and structure refinement for 9c (22597047):



Atom colour code: grey = carbon atom, white = hydrogen atom, green = chlorine atom, violet = nitrogen atom, and red = oxygen atom.

Table 19 Fractional Atomic Coordinates ($\times 10^4$) and Equivalent Isotropic Displacement Parameters ($Å^2 \times 10^3$) for ICSRY_S14_0ma_a. U_{eq} is defined as 1/3 of the trace of the orthogonalised U_{IJ} tensor.

Atom	*x*	*y*	*z*	U(eq)
Cl1	4945.4(9)	3544.2(4)	7992.8(10)	68.9(3)
O1	6418(2)	4560.6(10)	3688(2)	60.8(5)
O2	8559(2)	5157.0(11)	3499(3)	73.1(6)
N1	7585(3)	4412.2(10)	7232(3)	53.5(6)
C3	7945(4)	2497.8(15)	5380(4)	68.8(8)
C2	6673(4)	2686.2(14)	6262(4)	62.8(8)
C1	6544(3)	3317.7(13)	6830(3)	51.3(6)
C6	7671(3)	3782.2(12)	6516(3)	50.4(6)
C7	7613(3)	4918.8(12)	6288(3)	47.0(6)
C10	7693(3)	5571.0(13)	7088(3)	50.5(6)
C11	7066(3)	6112.6(14)	6244(4)	64.1(8)
C12	7075(4)	6711.9(16)	7032(6)	81.8(10)

Table 19 Fractional Atomic Coordinates (×10^4) and Equivalent Isotropic Displacement Parameters (Å^2×10^3) for ICSRY_S14_0ma_a. U_{eq} is defined as 1/3 of the trace of the orthogonalised U_{IJ} tensor.

Atom	*x*	*y*	*z*	U(eq)
C13	7732(5)	6784(2)	8651(6)	92.9(13)
C4	9072(4)	2945.8(16)	5046(4)	70.9(8)
C5	8941(3)	3581.5(14)	5607(4)	64.1(8)
C14	8380(4)	6261(2)	9492(5)	88.0(11)
C15	8355(3)	5648.3(16)	8727(4)	65.5(8)
C8	7602(3)	4897.0(12)	4329(3)	48.5(6)
C9	6380(4)	4471(2)	1830(4)	83.1(11)

Table 20 Anisotropic Displacement Parameters (Å^2×10^3) for ICSRY_S14_0ma_a. The Anisotropic displacement factor exponent takes the form: $-2\pi^2[h^2a^{*2}U_{11}+2hka^*b^*U_{12}+\ldots]$.

Atom	U_{11}	U_{22}	U_{33}	U_{23}	U_{13}	U_{12}
Cl1	67.1(5)	71.0(5)	69.7(5)	2.5(4)	16.9(4)	-9.2(4)
O1	60.2(11)	74.0(13)	48.3(10)	-1.1(9)	2.8(8)	-21.2(9)
O2	70.9(13)	87.5(15)	61.6(12)	5.9(11)	14.4(10)	-30.8(11)
N1	60.2(14)	47.0(13)	53.4(13)	0.4(10)	3.2(10)	-10.8(10)
C3	87(2)	54.3(17)	64.9(19)	-6.0(15)	3.3(16)	-2.2(16)
C2	74(2)	53.7(17)	60.2(17)	1.8(14)	-0.6(14)	-17.7(14)
C1	58.7(16)	48.3(15)	47.0(14)	7.5(11)	1.3(12)	-7.8(12)
C6	59.8(16)	45.2(14)	46.1(14)	6.4(11)	0.3(11)	-7.2(12)
C7	45.3(13)	48.2(14)	47.7(14)	2.7(11)	5.1(10)	-10.6(11)
C10	47.9(14)	48.7(15)	55.5(15)	-1.5(12)	10.4(11)	-9.8(11)
C11	64.7(18)	54.1(17)	74.4(19)	7.0(15)	16.8(14)	-2.2(13)
C12	88(2)	50.2(18)	109(3)	3.5(19)	41(2)	-0.9(16)
C13	92(3)	65(2)	124(4)	-36(2)	47(3)	-19(2)
C4	70(2)	68(2)	75(2)	-2.1(16)	13.0(16)	2.5(16)
C5	61.0(17)	57.0(18)	75(2)	4.1(15)	11.2(14)	-7.5(14)
C14	83(2)	99(3)	83(2)	-37(2)	11.5(19)	-23(2)
C15	61.4(18)	72(2)	63.5(18)	-9.5(15)	3.1(14)	-11.1(15)
C8	47.4(14)	47.0(14)	51.2(14)	0.8(12)	3.7(11)	-6.5(11)

Table 20 Anisotropic Displacement Parameters ($Å^2×10^3$) for ICSRY_S14_0ma_a. The Anisotropic displacement factor exponent takes the form: $-2\pi^2[h^2a^{*2}U_{11}+2hka^*b^*U_{12}+\ldots]$.

Atom	U_{11}	U_{22}	U_{33}	U_{23}	U_{13}	U_{12}
C9	92(2)	109(3)	48.5(17)	-10.1(17)	0.8(16)	-24(2)

Table 21 Bond Lengths for ICSRY_S14_0ma_a.

Atom	Atom	Length/Å		Atom	Atom	Length/Å
Cl1	C1	1.739(3)		C6	C5	1.387(4)
O1	C8	1.319(3)		C7	C10	1.474(4)
O1	C9	1.452(3)		C7	C8	1.520(4)
O2	C8	1.191(3)		C10	C11	1.390(4)
N1	C6	1.409(3)		C10	C15	1.388(4)
N1	C7	1.271(3)		C11	C12	1.372(5)
C3	C2	1.370(4)		C12	C13	1.371(6)
C3	C4	1.370(4)		C13	C14	1.367(6)
C2	C1	1.373(4)		C4	C5	1.379(4)
C1	C6	1.390(4)		C14	C15	1.389(5)

Table 22 Bond Angles for ICSRY_S14_0ma_a.

Atom	Atom	Atom	Angle/°	Atom	Atom	Atom	Angle/°
C8	O1	C9	115.7(2)	C11	C10	C7	120.9(3)
C7	N1	C6	121.3(2)	C15	C10	C7	120.1(3)
C4	C3	C2	119.6(3)	C15	C10	C11	119.0(3)
C3	C2	C1	120.0(3)	C12	C11	C10	120.6(3)
C2	C1	Cl1	119.5(2)	C13	C12	C11	120.1(4)
C2	C1	C6	121.7(3)	C14	C13	C12	120.3(3)
C6	C1	Cl1	118.8(2)	C3	C4	C5	120.5(3)
C1	C6	N1	120.9(2)	C4	C5	C6	121.0(3)
C5	C6	N1	121.7(2)	C13	C14	C15	120.3(4)
C5	C6	C1	117.2(3)	C10	C15	C14	119.7(3)
N1	C7	C10	120.0(2)	O1	C8	C7	111.9(2)
N1	C7	C8	123.5(2)	O2	C8	O1	125.1(2)

Table 22 Bond Angles for ICSRY_S14_0ma_a.							
Atom	**Atom**	**Atom**	**Angle/°**	**Atom**	**Atom**	**Atom**	**Angle/°**
C10	C7	C8	116.5(2)	O2	C8	C7	123.0(2)

Table 23Torsion Angles for ICSRY_S14_0ma_a.									
A	**B**	**C**	**D**	**Angle/°**	**A**	**B**	**C**	**D**	**Angle/°**
Cl1	C1	C6	N1	4.7(3)	C7	N1	C6	C5	61.0(4)
Cl1	C1	C6	C5	179.0(2)	C7	C10	C11	C12	176.7(3)
N1	C6	C5	C4	174.2(3)	C7	C10	C15	C14	-177.9(3)
N1	C7	C10	C11	-151.4(3)	C10	C7	C8	O1	-126.3(2)
N1	C7	C10	C15	26.5(4)	C10	C7	C8	O2	53.6(4)
N1	C7	C8	O1	55.0(3)	C10	C11	C12	C13	1.3(5)
N1	C7	C8	O2	-125.1(3)	C11	C10	C15	C14	0.0(4)
C3	C2	C1	Cl1	-178.4(2)	C11	C12	C13	C14	0.0(5)
C3	C2	C1	C6	0.8(4)	C12	C13	C14	C15	-1.2(5)
C3	C4	C5	C6	-0.1(5)	C13	C14	C15	C10	1.2(5)
C2	C3	C4	C5	0.7(5)	C4	C3	C2	C1	-1.0(5)
C2	C1	C6	N1	-174.6(2)	C15	C10	C11	C12	-1.2(4)
C2	C1	C6	C5	-0.2(4)	C8	C7	C10	C11	29.9(3)
C1	C6	C5	C4	-0.1(4)	C8	C7	C10	C15	-152.3(2)
C6	N1	C7	C10	-173.3(2)	C9	O1	C8	O2	4.7(4)
C6	N1	C7	C8	5.3(4)	C9	O1	C8	C7	-175.5(3)
C7	N1	C6	C1	-					

Table 23Torsion Angles for ICSRY_S14_0ma_a.									
A	**B**	**C**	**D**	**Angle/°**	**A**	**B**	**C**	**D**	**Angle/°**
				124.9(3)					

Table 24 Hydrogen Atom Coordinates (Å×10^4) and Isotropic Displacement Parameters (Å^2×10^3) for ICSRY_S14_0ma_a.				
Atom	***x***	***y***	***z***	**U(eq)**
H3	8043.1	2068.65	5010.02	83
H2	5895.61	2386.24	6476.34	75
H11	6636.56	6068.21	5136.55	77
H12	6634.55	7069.52	6465.8	98
H13	7736.24	7191.65	9180.43	111
H4	9931.24	2820.3	4437.09	85
H5	9716.46	3879.82	5371.84	77
H14	8840.72	6315.51	10581.94	106
H15	8780.7	5291.51	9310.47	79
H9A	6269.03	4887.63	1273.29	125
H9B	5520.44	4197.59	1498.4	125
H9C	7323.62	4269.36	1490.56	125

ICSRY_S14_0ma_a

Table 1 Crystal data and structure refinement for ICSRY_S14_0ma_a.	
Ccdc no.	22597047
Empirical formula	$C_{15}H_{12}ClNO_2$
Formula weight	273.71
Temperature/K	298
Crystal system	monoclinic
Space group	$P2_1/c$
a/Å	8.655(2)
b/Å	20.496(5)
c/Å	7.7578(17)
α/°	90

β/°	91.798(8)
γ/°	90
Volume/Å^3	1375.4(6)
Z	4
ρ_{calc}g/cm^3	1.322
μ/mm^{-1}	0.274
F(000)	568.0
Crystal size/mm^3	0.231 × 0.123 × 0.089
Radiation	MoKα (λ = 0.71073)
2Θ range for data collection/°	4.708 to 53.01
Index ranges	-10 ≤ h ≤ 10, -25 ≤ k ≤ 25, -9 ≤ l ≤ 7
Reflections collected	12843
Independent reflections	2827 [R_{int} = 0.0609, R_{sigma} = 0.0501]
Data/restraints/parameters	2827/0/173
Goodness-of-fit on F^2	1.046
Final R indexes [I>=2σ (I)]	R_1 = 0.0577, wR_2 = 0.1389
Final R indexes [all data]	R_1 = 0.0811, wR_2 = 0.1527
Largest diff. peak/hole / e Å^{-3}	0.25/-0.25

4.5. References:

1. (a) Gilman, H.; Morris, H. L. The mechanism of reaction between thionylaniline and organomagnesium halides. *J. Am. Chem. Soc.* **1926**, *48*, 2399–2404. (b) Böttinger, C. Effect of thionyl chloride on aniline. *Chem. Ber.* **1878**, *11*, 1407. (c) Michaelis, A.; Herz, R. On the thionylamines, a new series of sulphur-containing compounds. *Chem. Ber*. **1890**, *23*, 3480. (d) Beoke-Goehring, M.; Schwarz, R.; Spiess, W. *Z.* On an isomer of thionylimide and its salts. *Anorg. Allg. Chem.* **1958**, *293*, 294–301. (e) Kresze, G.; Maschke, A.; Albrecht, R.; Bederke, K.; Patzschke, H. P.; Smalla, H.; Trede, A. Organic *N*-Sulfinyl Compounds. *Angew. Chem. Int. Ed.* **1962**, *1*, 89–98. (f) Halasz, S. P. V.; Glemser, Preparation and properties of *N*-heptafloroisopropyl and trifluoroacetyl sulfurdichloride imide and sufuroxido. *Chem. Ber./Recl* **1970**, *103*, 553–560. (g) Wald, L.; Wucherpfennig, W. Synthese von 3,6-Dihydro-2H-1.2-thiazin-1-oxiden. *Liebigs Ann.* **1971**, *746*, 28–31. (h) Porskamp, P.; Zwanenburg, B. A New Synthesis of *N*-Sulfinylamines by Sulfinylation of *N*-Trimethylsilylamines using Sulfur Dioxide. *Synthesis* **1981**, *1981*, 368–369. (i) Kim, Y. H.; Shin, J. M. New facile synthesis of N-sulfinylamine derivatives using N, N′-sulfinylbisimidazole and N-(chlorosulfinyl) imidazole. *Tetrahedron Lett.* **1985**, *26*, 3821–3824. (j) Weinreb, S. M. Synthetic methodology based upon *N*-sulfinyl dienophile [4+ 2]-cycloaddition reactions. *Acc. Chem. Res.* **1988**, *21*, 313–318. (k) Zhizhin, A. A.; Zarubin, D. N.; Ustynyuk, N. A. An imido-transfer reaction of aldehydes with *N*-sulfinylamines using vanadium and molybdenum oxochlorides as catalysts. *Tetrahedron Lett.* **2008**, *49*, 699–702.
2. Davies, T. Q.; Willis, M. C. Rediscovering sulfinylamines as reagents for organic synthesis. *Chem. Eur. J.* **2021**, *27*, 8918–8927.
3. (a) Davies, T. Q.; Hall, A.; Willis, M. C. One-Pot, Three-Component Sulfonimidamide Synthesis Exploiting the Sulfinylamine Reagent *N*-Sulfinyltritylamine, TrNSO. *Angew. Chem. Int. Ed.* **2017**, *56*, 14937–14941. (b) Zhang, Z.-X.; Davies, T. Q.; Willis, M. C. Modular sulfondiimine synthesis using a stable sulfinylamine reagent. *J. Am. Chem. Soc.* **2019**, *141*, 13022−13027. (c) Davies, T. Q.; Tilby, M. J.; Ren, J.; Parker, N. A.; Skolc, D.; Hall, A.; Duarte, F.; Willis, M. C. Harnessing sulfinyl nitrenes: a unified one-pot synthesis of sulfoximines and sulfonimidamides. *J. Am. Chem. Soc.* **2020**, *142*, 15445−15453. (d) Davies, T. Q.; Tilby, M. J.; Skolc, D.; Hall, A.; Willis, M. C. Primary Sulfonamide Synthesis Using the Sulfinylamine Reagent *N*-Sulfinyl-*O*-(*tert-butyl*)hydroxylamine, *t*-BuONSO. *Org. Lett.* **2020**, *22*, 9495−9499. (e) Tummanapalli, S.; Gulipalli, K. C.; Bodige, S.;

Vemula, D.; Endoori, S.; Pommidi, A. K.; Punna, S. K. Direct one step dehydrogenative C−H sulfonimidation of unfunctionalized arenes: A conveneient protocol to emerging medicinal chemistry motifs without prefunctionalized arenes. *Tetrahedron Lett*. **2021**, *73*, 153118. (f) Ding, M.; Zhang, Z.-X.; Davies, T. Q.; Willis, M. C. A silyl sulfinylamine reagent enables the modular synthesis of sulfonimidamides via primary sulfinamides. *Org. Lett.* **2022**, *24*, 1711−1715.

4. Lo, P. K. T.; Willis, M. C. Nickel(II)-Catalyzed Addition of Aryl and Heteroaryl Boroxines to the Sulfinylamine Reagent TrNSO: The Catalytic Synthesis of Sulfinamides, Sulfonimidamides, and Primary Sulfonamides. *J. Am. Chem. Soc*. **2021**, *143*, 15576−15581.
5. Bremerich, M.; Conrads, C. M.; Langletz, T.; Bolm, C. Additions to *N*-Sulfinylamines as an Approach for the Metal-free Synthesis of Sulfonimidamides: *O*-Benzotriazolyl Sulfonimidates as Activated Intermediates. *Angew. Chem. Int. Ed*. **2019**, *58*, 19014–19020.
6. (a) Bayeh, L.; Le, P. Q.; Tambar, U. K. Catalytic allylic oxidation of internal alkenes to a multifunctional chiral building block. *Nature* **2017**, *547*, 196–200. (b) Oliver, G. A.; Loch, M. N.; Augustin, A. U.; Steinbach, P.; Sharique, M.; Tambar, U. K.; Jones, P. G.; Bannwarth, C.; Werz, D. B. Cycloadditions of Donor–Acceptor Cyclopropanes and-butanes using S=N-Containing Reagents: Access to Cyclic Sulfinamides, Sulfonamides, and Sulfinamidines. *Angew. Chem. Int. Ed.*, **2021**, *60*, 25825–25831.
7. Li, L.; Zhang, S.-q.; Chen, Y.; Cui, X.; Zhao, G.; Tang, Z.; Li, G.-x. Photoredox Alkylation of Sulfinylamine Enables the Synthesis of Highly Functionalized Sulfinamides and S(VI) Derivatives. *ACS Catal.* **2022**, *12*, 15334−15340.
8. Selected reviews on metal catalyzed transformations of diazo compounds: (a) Padwa, A. and Hornbuckle, S. F. Ylide formation from the reaction of carbenes and carbenoids with heteroatom lone pairs. *Chem. Rev.* **1991**, *91*, 263. (b) Ye, T. and McKervey, M. A. Organic synthesis with. alpha.-diazo carbonyl compounds. *Chem. Rev.* **1994**, *94*, 1091. (c) Davies, H. M. L. and Beckwith, R. E. J. Catalytic enantioselective C−H activation by means of metal−carbenoid-induced C−H insertion. *Chem. Rev.*, **2003**, *103*, 2861. (d) Zhang, Z. and Wang, J. Recent studies on the reactions of α-diazocarbonyl compounds. *Tetrahedron*, **2008**, *64*, 6577. (e) Davies, H. M. L. and Denton, J. R. Application of donor/acceptor-carbenoids to the synthesis of natural products. *Chem. Soc. Rev.*, **2009**, *38*, 3061. (f) Doyle, M. P.; Duffy, R.; Ratnikov, M. and Zhou, L. Catalytic carbene insertion into C−H bonds. *Chem. Rev.*, **2010**, *110*, 704. (g) Ford, A.; Miel, H.; Ring, A.; Slattery, C. N.; Maguire, A. R. and McKervey, M. A. Modern organic synthesis with α-diazocarbonyl compounds. *Chem. Rev.*, **2015**, *115*, 9981.

9. For recent review articles on photochemical reactions of diazo compounds see: (a) Ciszewski, Ł. W.; Rybicka-Jasińska, K.; Gryko, D. Recent developments in photochemical reactions of diazo compounds. *Org. Biomol. Chem.* **2019**, *17*, 432–448. (b) Yang, Z.; Stivanin, M. L.; Jurberg, I. D.; Koenigs, R. M. Visible light-promoted reactions with diazo compounds: a mild and practical strategy towards free carbene intermediates. *Chem. Soc. Rev.* **2020**, *49*, 6833–6847. (c) Durka, J.; Turkowska, J.; Gryko, D. Lightening diazo compounds? *ACS Sustainable Chem. Eng.* **2021**, *9*, 8895−8918. (d) Empel, C.; Pei, C.; Koenigs, R. M. Unlocking novel reaction pathways of diazoalkanes with visible light. *Chem. Commun.* **2022**, *58*, 2788–2798.
10. Brook, A. G. Triphenylsilyl phenyl ketone. *J. Am. Chem. Soc.* **1957**, *79*, 4373–4375.
11. (a) Zhang, H.-J.; Priebbenow, D. L.; Bolm, C. Acylsilanes: valuable organosilicon reagents in organic synthesis. *Chem. Soc. Rev.* **2013**, *42*, 8540. (b) Priebbenow, D. L. Silicon-Derived Singlet Nucleophilic Carbene Reagents in Organic Synthesis. *Adv. Synth. Catal*. **2020**, *362*, 1927–1946. (c) Zhang, Y.; Chen, J.-J.; Huang, H.-M. Radical Brook rearrangements: concept and recent developments. *Angew. Chem. Int. Ed*. **2022**, *61*, e202205671.
12. Hong, W. P.; Lim, H. N.; Shin, I. Recent progress and perspectives in photo-induced organic reactions of acylsilanes. *Org. Chem. Front*. **2023**, *10*, 819–836.
13. (a) Ishida, K.; Tobita, F.; Kusama, H. Lewis Acid-Assisted Photoinduced Intermolecular Coupling between Acylsilanes and Aldehydes: A Formal Cross Benzoin-Type Condensation. *Chem.–Eur. J.* **2018**, *24*, 543–546. (b) Capaldo, L.; Riccardi, R.; Ravelli, D.; Fagnoni, M. Acyl radicals from acylsilanes: photoredox-catalyzed synthesis of unsymmetrical ketones. *ACS Catal.* **2018**, *8*, 304–309. (c) Ye, J.-H.; Quach, L.; Paulisch, T.; Glorius, F. Visible-light-induced, metal-free carbene insertion into B–H bonds between acylsilanes and pinacolborane. *J. Am. Chem. Soc.* **2019**, *141*, 16227−16231. (d) Vale, J. R.; Valkonen, A.; Afonso, C. A. M.; Candeias, N. R. Synthesis of silacyclopent-2-en-4-ols via intramolecular [2+2] photocycloaddition of benzoyl (allyl) silanes. *Org. Chem. Front*. **2019**, *6*, 3793–3798. (e) Ma, L.; Yu, Y.; Xin, L.; Zhu, L.; Xia, J.; Ou, P.; Huang, X. Visible Light Enabled Formal Cross Silyl Benzoin Reaction as an Access to α-Hydroxyketones. *Adv. Synth. Catal*. **2021**, *363*, 2573–2577. (f) Ye, J.-H.; Bellotti, P.; Paulisch, T. O.; Daniliuc, C. G.; Glorius, F. Visible-Light-Induced Cycloaddition of α-Ketoacylsilanes with Imines: Facile Access to β-Lactams. *Angew. Chem. Int. Ed.* **2021**, *60*, 13671–13676. (g) Stuckhardt, C.; Wissing, M.; Studer, A. Photo click reaction of acylsilanes with indoles. *Angew. Chem. Int. Ed.* **2021**, *60*, 18605. (h) Takeuchi, T.; Aoyama, T.; Orihara, K.; Ishida, K.; Kusama, H. Visible-Light-Induced *In Situ* Generation of Fischer-Type Copper Carbene Complexes from Acylsilanes and Its Application to

Catalytic [4+1] Cycloaddition with Siloxydienes. *Org. Lett.* **2021**, *23*, 9490–9494. (i) Priebbenow, D. L.; Pilkington, R. L.; Hearn, K. N.; Polyzos, A. Fluorinated Ketones as Trapping Reagents for Visible-Light-Induced Singlet Nucleophilic Carbenes. *Org. Lett.* **2021**, *23*, 2783–2789. (j) Fan, Z.; Yi, Y.; Chen, S.; Xi, C. Visible-light-induced catalyst-free carboxylation of acylsilanes with carbon dioxide. *Org. Lett.* **2021**, *23*, 2303−2307. (k) Cai, B. G.; Li, Q.; Li, L.; Xuan, J. Carbon-oxygen bond formation via visible-light-induced O–H insertion between acylsilanes and oximes. *Green Synth. Catal*. **2022**, *3*, 194−197. (l) Reimler, J.; Studer, A. Visible-Light Mediated Tryptophan Modification in Oligopeptides Employing Acylsilanes. *Chem.-Eur. J.* **2021**, *27*, 15392−15395. (m) Bunyamin, A.; Hua, C.; Polyzos, A.; Priebbenow, D. L. Intramolecular photochemical [2+1]-cycloadditions of nucleophilic siloxy carbenes. *Chem. Sci*. **2022**, *13*, 3273–3280. (n) Vale, J. R.; Gomes, R. F.; Afonso, C. A. M.; Candeias, N. R. Functionalized cyclopentenes via the formal [4+1] cycloaddition of photogenerated siloxycarbenes from acyl silanes. *J. Org. Chem*. **2022**, *87*, 8910–8920. (o) Ueda, Y.; Masuda, Y.; Iwai, T.; Imaeda, K.; Takeuchi, H.; Ueno, K.; Gao, M.; Hasegawa, J. and Sawamura, M. Photoinduced copper-catalyzed asymmetric acylation of allylic phosphates with acylsilanes. *J. Am. Chem. Soc.* **2022**, *144*, 2218–2224. (p) Zhou, G.; Shen, X. Synthesis of Cyclopropenols Enabled by Visible-Light-Induced Organocatalyzed [2+1] Cyclization. *Angew. Chem. Int. Ed.* **2022**, *61*, e202115334. (q) Yamaguchi, K.; Shimizu, T.; Miura, A.; Ishida, K.; Kusama, H. Photoinduced Intramolecular Cyclization of Acylsilanes Bearing a Boronate Moiety: Construction of a Highly Strained trans-Fused Bicyclo[3.3.0]octane Skeleton. *Org. Lett*. **2022**, *24*, 5807–5811. (r) Zhu, Z.; Zhang, W.; Zhang, Y.; Liu, S. and Shen, X. Visible-Light-Induced [4+1] Cyclization-Aromatization of Acylsilanes and α, β-Unsaturated Ketones. *CCS Chem*. **2023**, *5*, 325–333.

14. Selected review articles and books on amide synthesis and its utilization: (a) Larock, R. C. Comprehensive Organic Transformations: A Guide to Functional Group Preparations, 2nd ed., Wiley-VCH, New York, **1999**. (b) Montalbetti, C. A. G. N.; Falque, V. M. Synthetic Chemistry: Formation of the Amide Bond, Wiley Encyclopedia of Chemical Biology, Wiley, Weinheim **2008**, pp. 1–17. (c) Valeur, E.; Bradley, M. Amide bond formation: beyond the myth of coupling reagents. *Chem. Soc. Rev*. **2009**, *38*, 606–631. (d) Allen, C. L.; Williams, J. M. J. Metal-catalysed approaches to amide bond formation. *Chem. Soc. Rev*. **2011**, *40*, 3405–3415. (e) Pattabiraman, V. R.; Bode, J. W. Rethinking amide bond synthesis. *Nature* **2011**, *480*, 471–479. (f) Lanigan, R. M.; Sheppard, T. D. Recent developments in amide synthesis: Direct amidation of carboxylic acids and transamidation reactions. *Eur. J. Org. Chem*. **2013**, 7453–7465. (g) Nagaraaj, P.; Vijayakumar, V. Oxidation of amine

α-carbon to amide: a review on direct methods to access the amide functionality. *Org. Chem. Front*. **2019**, *6*, 2570–2599. (h) Lu, B.; Xiao, W.-J.; Chen, J.-R. Recent Advances in Visible-Light-Mediated Amide Synthesis. *Molecules* **2022**, *27*, 517.

15. Selected review articles on α-iminoester synthesis and its applications: (a) Taggi, A. E.; Hafez, A. M.; Lectka, T. α-imino esters: Versatile substrates for the catalytic, asymmetric synthesis of α-and β-amino acids and β-lactams. *Acc. Chem. Res*. **2003**, *36*, 10-19. (b) Ferraris, D.; Young, B.; Cox, C.; Dudding, T.; Drury, W. J.; Ryzhkov, L.; Taggi, A. E.; Lectka, T. Catalytic, enantioselective alkylation of α-imino esters: The synthesis of nonnatural α-amino acid derivatives. *J. Am. Chem. Soc.* **2002**, *124*, 67−77. (c) Metz, A. E.; Kozlowski, M. C. Recent advances in asymmetric catalytic methods for the formation of acyclic α, α-disubstituted α-amino acids. *J. Org. Chem.* **2015**, *80*, 1–7. (d) Sis, B. E.; Zirak, M. α-Imino esters in organic synthesis: recent advances. *Chem. Rev.* **2017**, *117*, 8326−8419.
16. Wolff, L. Ueber diazoanhydride. *Justus Liebigs Ann. Chem.* **1902**, *325*, 129.
17. Selected review articles on photochemical Wolff rearrangement: (a) Kirmse, W. 100 Years of the Wolff Rearrangement. *Eur. J. Org. Chem.* **2002**, 2193−2256. (b) Fuse, S.; Otake, Y.; Nakamura, H. Integrated Micro-Flow Synthesis Based on Photochemical Wolff Rearrangement. *Eur. J. Org. Chem.* **2017**, 6466–6473. (c) Hua, T.-B.; Yang, Q.-Q.; Zou, Y.-Q. Recent advances in enantioselective photochemical reactions of stabilized diazo compounds. *Molecules*, **2019**, *24*, 3191.
18. (a) Ji, X.; Zhang, Z.; Wang, Y.; Han, Y.; Peng, H.; Lia, F.; Liu, L. Catalyst-free synthesis of α, α-disubstituted carboxylic acid derivatives under ambient conditions via a Wolff rearrangement reaction. *Org. Chem. Front.* **2021**, *8*, 6916–6922. (b) Zhang, Z.; Liu, Y.; Ling, L.; Li, Y.; Dong, Y.; Gong, M.; Zhao, X.; Zhang, Y.; Wang, J. Pd-catalyzed carbonylation of diazo compounds at atmospheric pressure: a catalytic approach to ketenes. *J. Am. Chem. Soc.* **2011**, *133*, 4330–4341. (c) Ramakrishna, K.; Sivasankar, C. Synthesis of amido esters and amido phosphonates through carbonylation of diazo compounds followed by nucleophilic addition reaction. *Eur. J. Org. Chem.* **2017**, 4035–4043.
19. (a) Beecken, H.; Korte, F. Cycloaddition of *N*-sulfinylamines to ketenes. *Tetrahedron* **1962**, *18*, 1527. (b) Jian, T.-Y.; He, L.; Tang, C.; Ye, S. N-Heterocyclic Carbene Catalysis: Enantioselective Formal [2+2] Cycloaddition of Ketenes and *N*-Sulfinylanilines. *Angew. Chem. Int. Ed.* **2011**, *50*, 9104–9107.
20. (a) Stoffer, J. O.; Musser, H. R. The photolysis of *N*-sulphinylaniline in the presence of diphenyldiazomethane. *J. Chem. Soc. D* **1970**, 481. (b) Munaretto, L. S.; Santos, C. Y.; Gallo, R. D. C.; Okada, C. Y.; Jr.; Deflon, V. M.; Jurberg, I. D. Visible-Light-Mediated Strategies to Assemble Alkyl 2-Carboxylate-2,3,3-Trisubstituted β-Lactams

and 5-Alkoxy-2,2,4-Trisubstituted Furan-3(2H)-ones Using Aryldiazoacetates and Aryldiazoketones. *Org. Lett.* **2021**, *23*, 9292−9296.

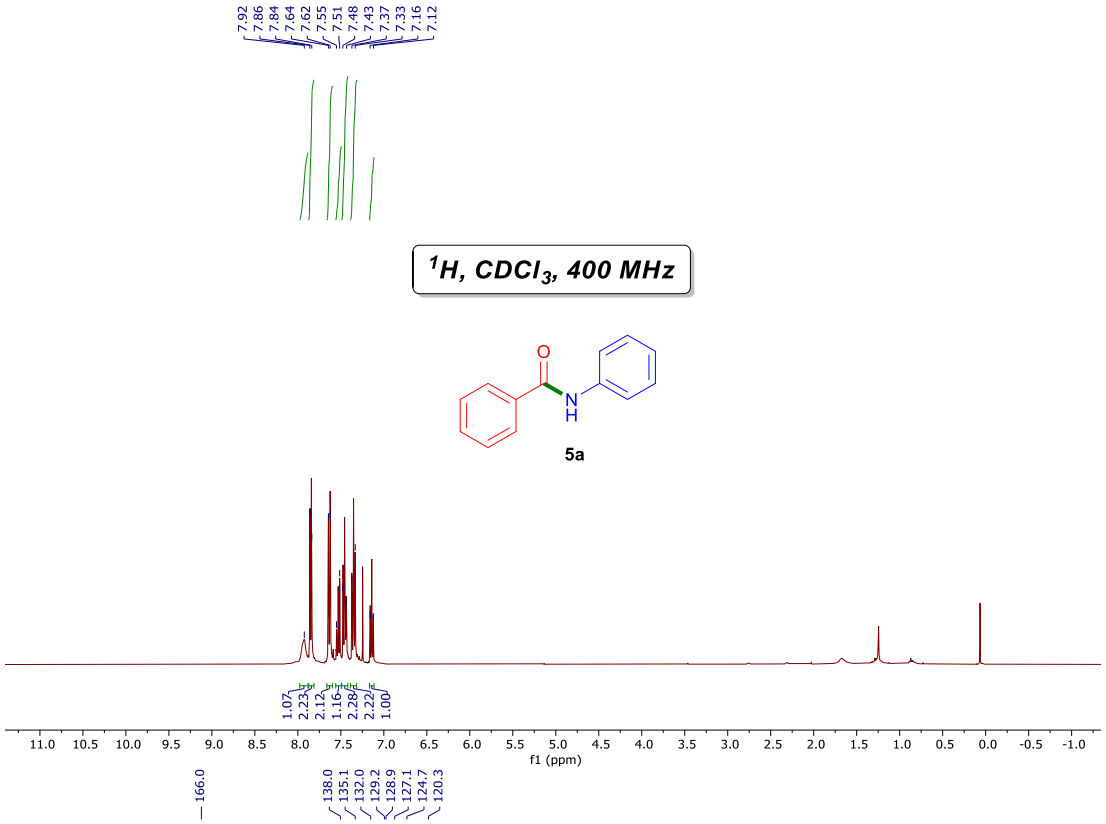
21. (a) Bell, S. I.; Parvez, M.; Weinreb, S. M. Metalation and alkylation of 3, 6-dihydrothiazine 1-oxides prepared via Diels-Alder cycloadditions of *N*-sulfinyl dienophiles. *J. Org. Chem.* **1991**, *56*, 373–377. (b) Ahmed, G. A.; Ismail, N. A.; Yassin, F. A. On the search of the influence of substituents in the structural and vibrational properties of *p*-substituted sulfinylanilines: Study of *p*-trifluoromethylsulfinylaniline. *Relat. Elem.* **1992**, *69*, 253−255.
22. (a) Kresze, G.; Maschke, A.; Albrecht, R.; Bederke, K.; Patzschke, H. P.; Smalla, H.; Trede, A. Organic *N*-Sulfinyl Compounds. *Angew. Chem. Int. Ed. Engl.* **1962**, *1*, 89. (b) Minami, T.; Fukuda, M.; Abe, M.; Agawa, T. Reactions of *N*-Sulfinylamines with Carbodiimides. *Bull. Chem. Soc. Jpn*. **1973**, *46*, 2156. (c) Porskamp, P. A. T. W.; Zwanenburg, B. A New Synthesis of N-Sulfinylamines by Sulfinylation of N-Trimethylsilylamines using Sulfur Dioxide. *Synthesis* **1981**, 368. (d) Butler, R. N.; O'Halloran, G. A.; Burke, L. A. 6π-Cycloadditions of aryl and new heteroaryl *N*-sulphinylamines with 2,3-dimethylbuta-1,3-diene: synthesis, kinetics, substituent effects, theoretical calculations, and reaction mechanism. *J. Chem. Soc., Perkin Trans. 2* **1989**, 1855. (e) Parkes, E.; Woollins, J. D.; Yokelson, H. B.; R. West in Inorganic Syntheses (Ed.: Allcock, H. R.), A WileyInterscience Publication John Wiley & Sons, New York, Chichester, Brisbane, Toronto, Singapore, **1989**, p. 48–49. (f) Bell, S. I.; Parvez, M.; Weinreb, S. M. Metalation and alkylation of 3, 6-dihydrothiazine 1-oxides prepared via Diels-Alder cycloadditions of *N*-sulfinyl dienophiles. *J. Org. Chem.* **1991**, *56*, 373–377. (g) Chemes, D. M.; Cutin, E. H.; Álvarez, R. M.; Robles, N. L.; Oberhammer, H. On the search of the influence of substituents in the structural and vibrational properties of *p*-substituted sulfinylanilines: Study of *p*-trifluoromethylsulfinylaniline. *J. Fluor. Chem.* **2018**, *210*, 94.
23. (a) Linghu, X.; Nicewicz, D. A.; Johnson, J. S. Tandem Carbon−Carbon Bond Constructions via Catalyzed Cyanation/Brook Rearrangement/C-Acylation Reactions of Acylsilanes. *Org. Lett.* **2002**, *4*, 2957–2960. (b) Yu, C.-J.; Li, R.; Gu, P. Intermolecular Schmidt reaction of alkyl azides with acyl silanes. *Tetrahedron Letters* **2016**, *57*, 3568–3570. (c) Deng, X.; Zhou, G.; Tian, J.; Srinivasan, R. Chemoselective Amide-Forming Ligation Between Acylsilanes and Hydroxylamines Under Aqueous Conditions. *Angew. Chem. Int. Ed*. **2021**, *60*, 7024–7029.
24. (a) Keipour, H.; Ollevier, T. Iron-catalyzed carbene insertion reactions of α-diazoesters into Si–H bonds. *Org. Lett*. **2017**, *19*, 5736–5739. (b) Thurow, S.; Fernandes, A. A. G.; Quevedo-Acosta, Y.; de Oliveira, M. F.; de Oliveira, M. G.; Jurberg, I. D. Preparation of Organic Nitrates from Aryldiazoacetates and

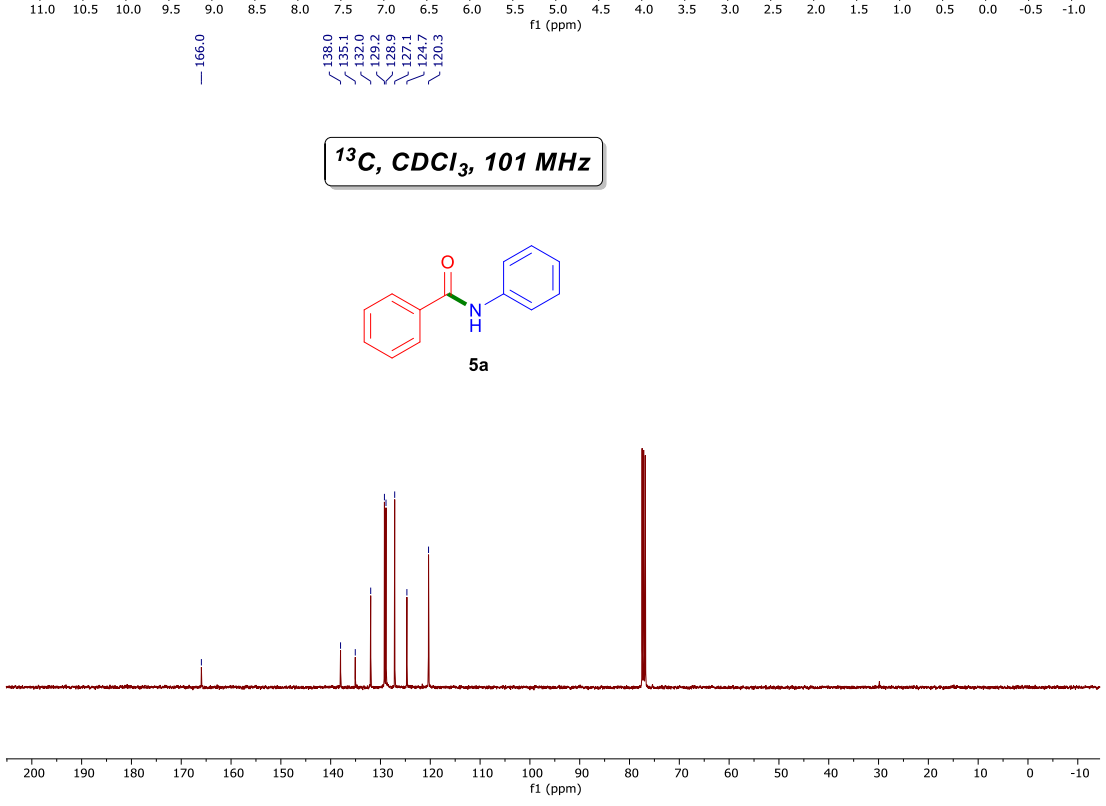
$Fe(NO_3)_3 \cdot 9H_2O$. *Org. Lett.* **2019**, *21*, 6909–6913. (c) Chan, C-M.; Xing, Q.; Chow, Y.-C.; Hung, S.-F.; Yu, W.-Y. Photoredox Decarboxylative C(sp^3)–N Coupling of α-Diazoacetates with Alkyl *N*-Hydroxyphthalimide Esters for Diversified Synthesis of Functionalized *N*-Alkyl Hydrazones. *Org. Lett.* **2019**, *21*, 8037–8043. (d) Davies, H. M. L.; Townsend, R. J. Catalytic asymmetric cyclopropanation of heteroaryldiazoacetates. *J. Org. Chem*. **2001**, *66*, 6595–6603. (e) Jiang, Y.; Chen, X.; Zheng, Y.; Xue, Z.; Shu, C.; Yuan, W.; Zhang, X. Highly Diastereoselective and Enantioselective Synthesis of α-Hydroxy β-Amino Acid Derivatives: Lewis Base Catalyzed Hydrosilylation of α-Acetoxy β-Enamino Esters. *Angew. Chem. Int. Ed.* **2011**, *50*, 7304–7307. (f) Wang, J.; Wang, M.; Chen, K.; Zha, S.; Song, C.; Zhu, J. C–H Activation-Based Traceless Synthesis via Electrophilic Removal of a Directing Group. Rhodium(III)-Catalyzed Entry into Indoles from *N*-Nitroso and α-Diazo-β-keto Compounds. *Org. Lett.* **2016**, *18*, 1178–1181. (g) Liu, Q.; Li, M.; Xiong, R.; Mo, F. Direct Carboxylation of the Diazo Group *ipso*-C(sp^2)–H bond with Carbon Dioxide: Access to Unsymmetrical Diazomalonates and Derivatives. *Org. Lett.* **2017**, *19*, 6756–6759. (h) Marichev, K. O.; Wang, Y.; Carranco, A. M.; Garcia, E. C.; Yu, Z.-X.; Doyle, M. P. Rhodium (II)-catalysed generation of cycloprop-1-en-1-yl ketones and their rearrangement to 5-aryl-2-siloxyfurans. *Chem. Commun.* **2018**, *54*, 9513-9516. (i) Yang, J.; Ke, C.; Zhang, D.; Liu, X.; Feng, X. Enantioselective synthesis of 2, 2, 3-trisubstituted indolines via bimetallic relay catalysis of α-diazoketones with enones. *Org. Lett*. **2018**, *20*, 4536–4539. (j) Rajasekar, S.; Anbarasan, P. A General Proline-Catalyzed Synthesis of 4,5-Disubstituted *N*-Sulfonyl-1,2,3-Triazoles from 1,3-Dicarbonyl Compounds and Sulfonyl Azide. *Chem. Asian J.* **2019**, *14*, 4563–4567.

25. **CCDC 2257649 and 22597047** contains the supplementary crystallographic data for the compound **5c** and **9c** respectively. These data can be obtained free of charge from the Cambridge Crystallographic Data Centre www.ccdc.cam.ac.uk/data_request/cif.

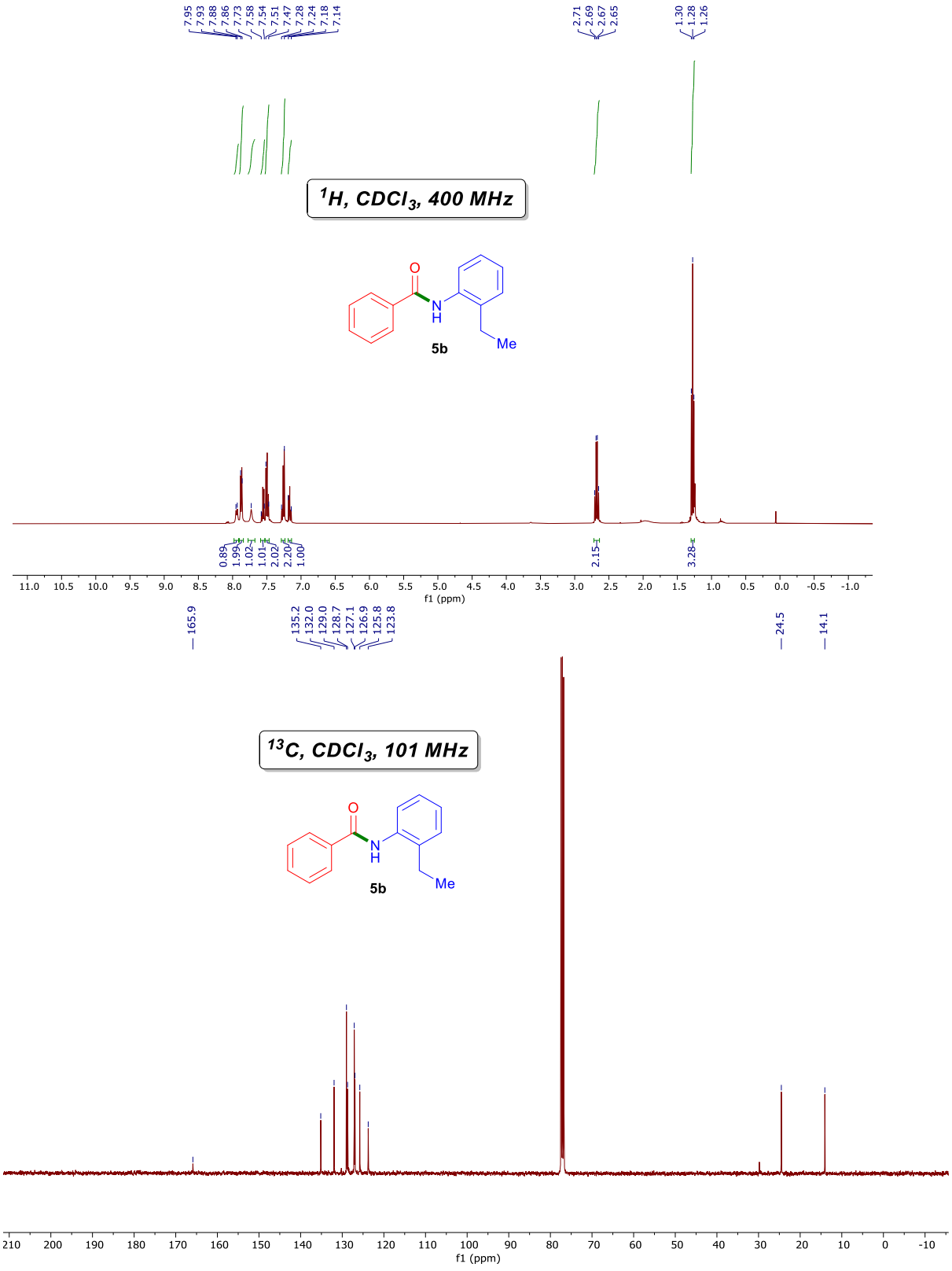
4.6. NMR Spectra:

4.6.1. *N*-phenylbenzamide (5a):

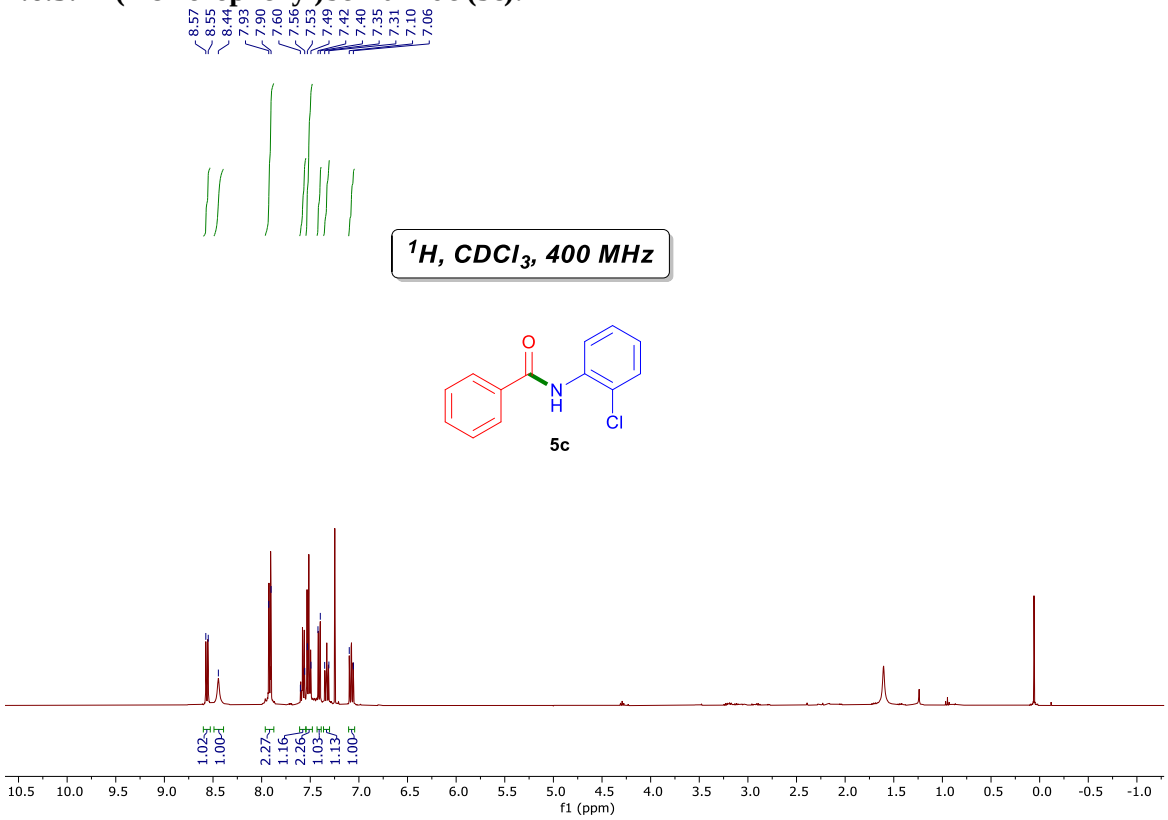


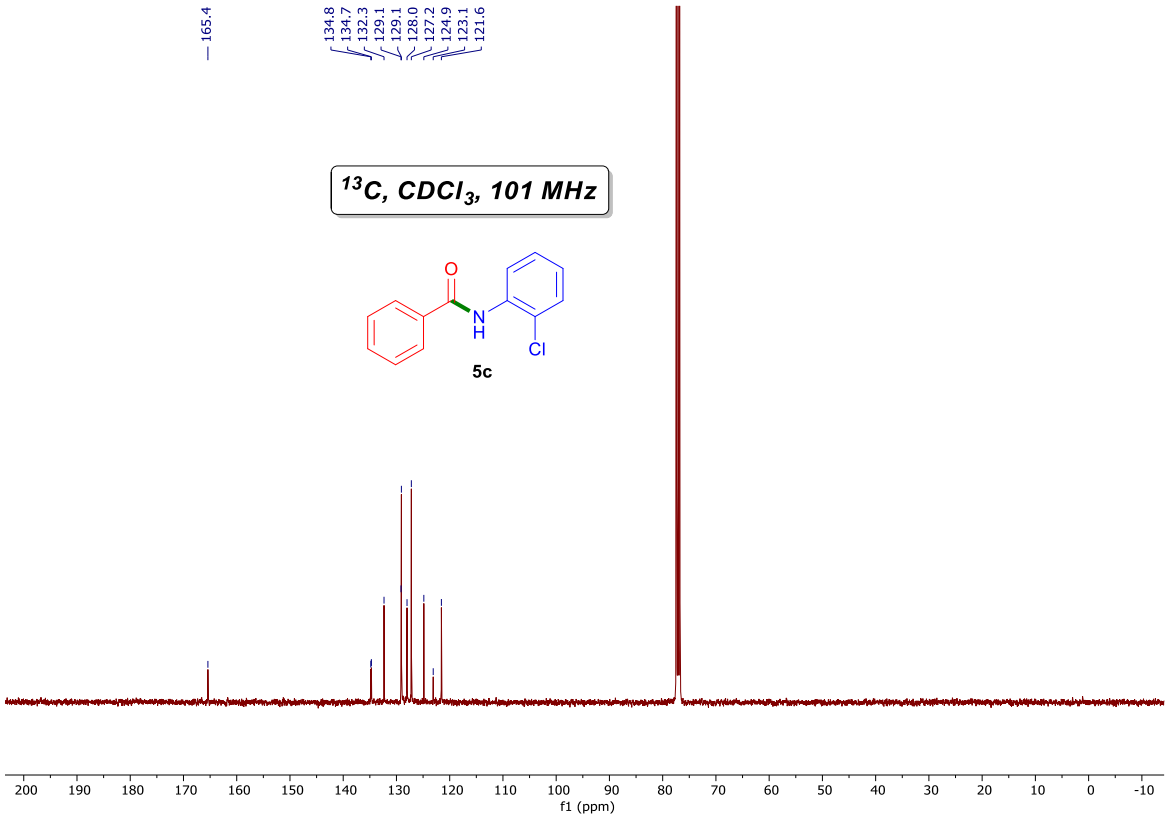


4.6.2. *N*-(2-ethylphenyl)benzamide (5b):

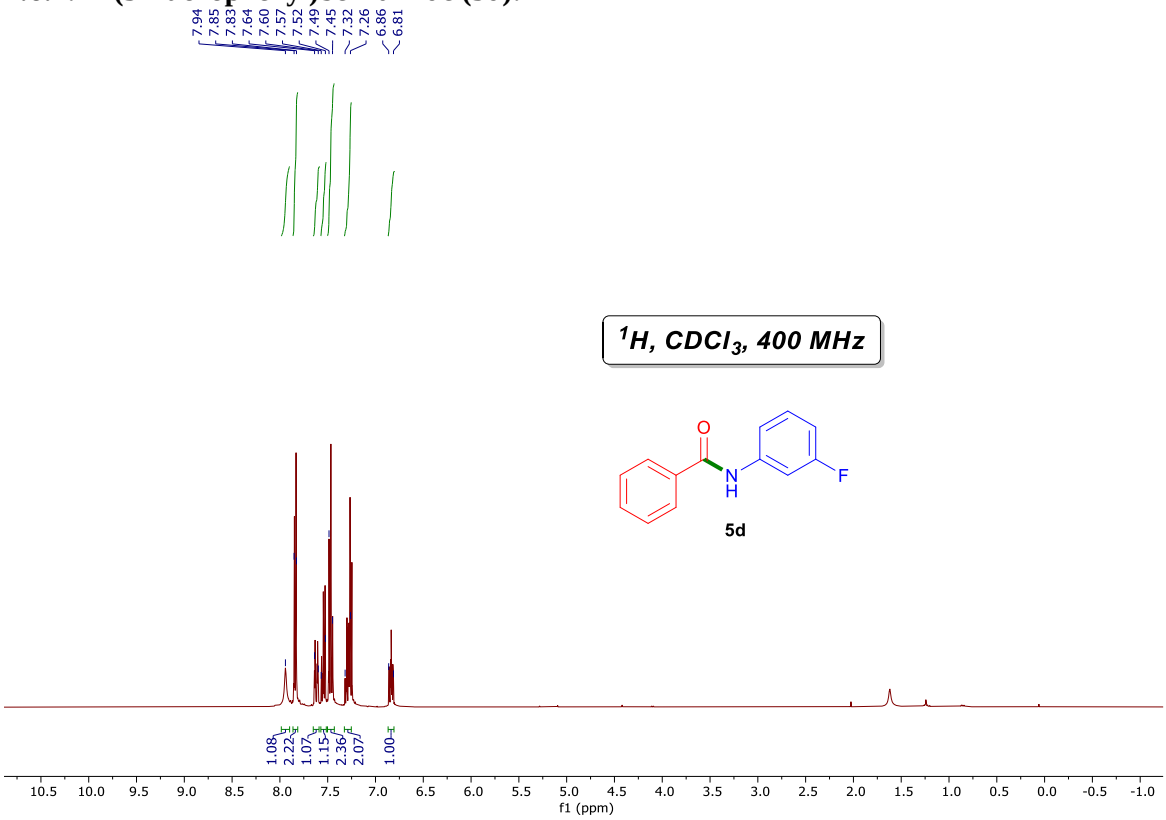


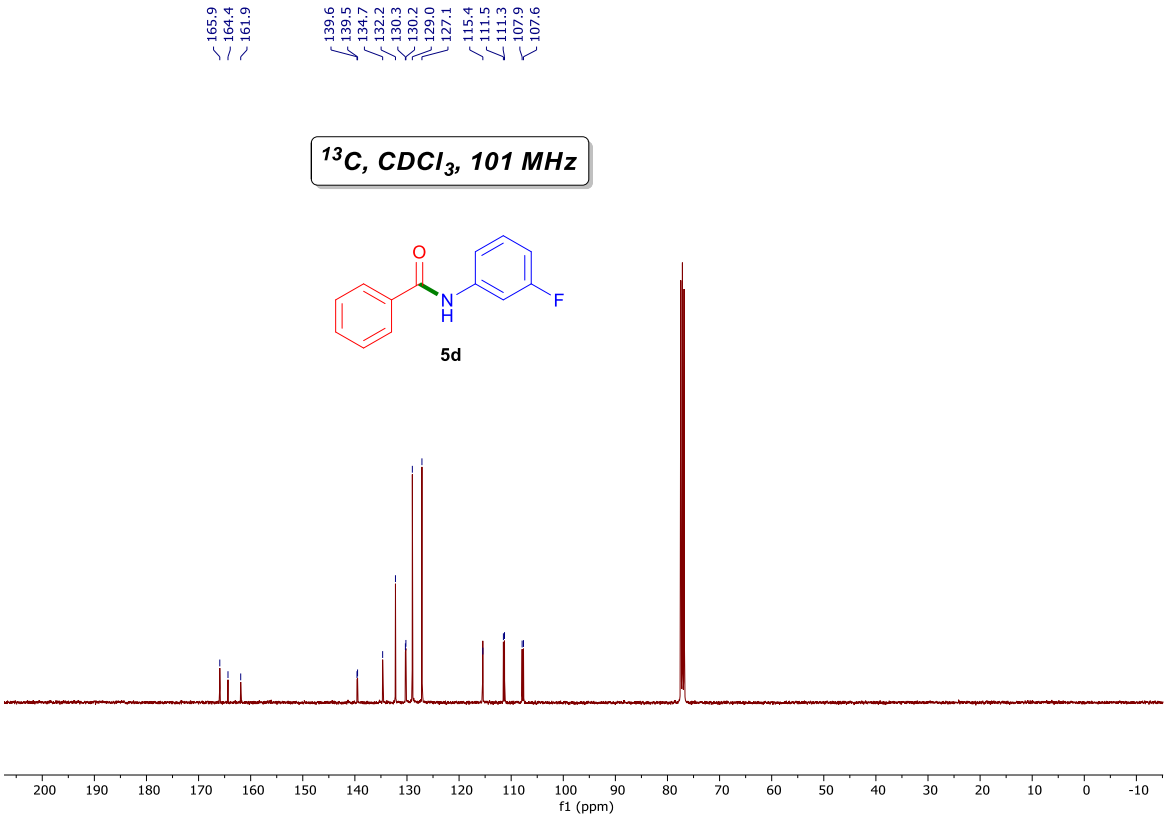
4.6.3. *N*-(2-chlorophenyl)benzamide (5c):

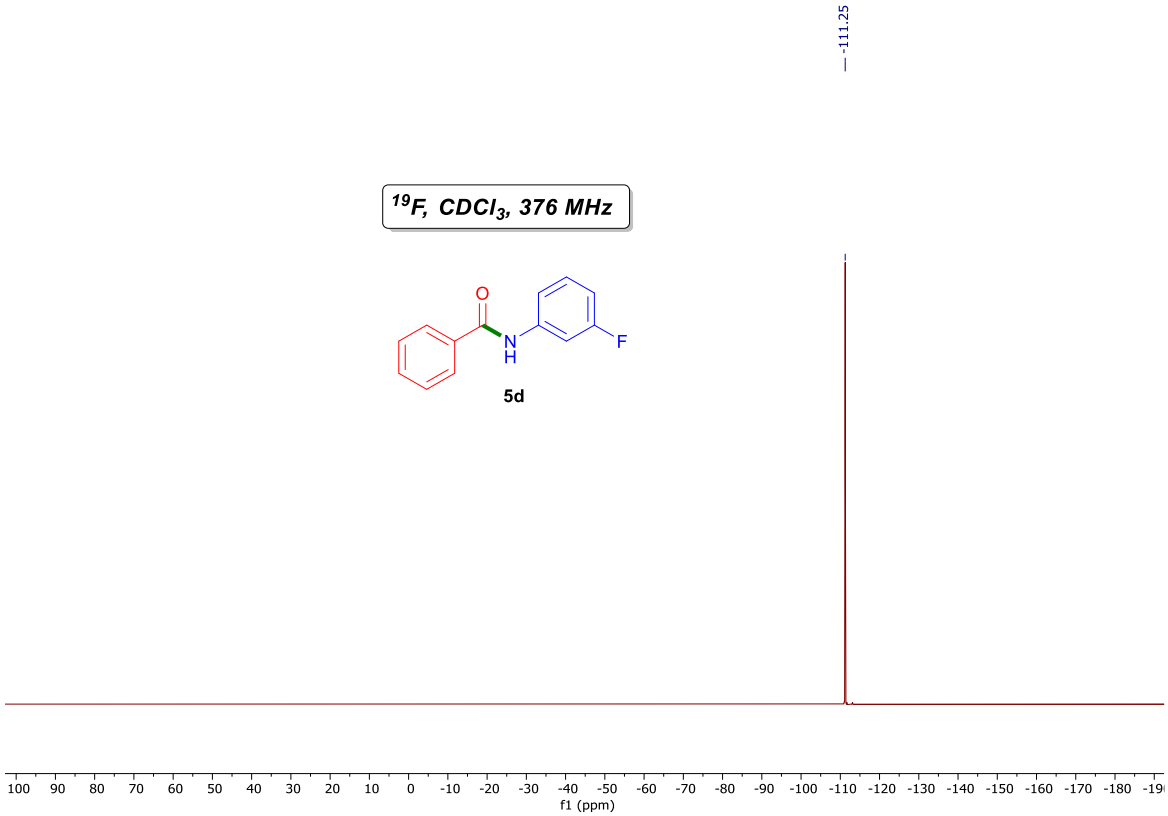




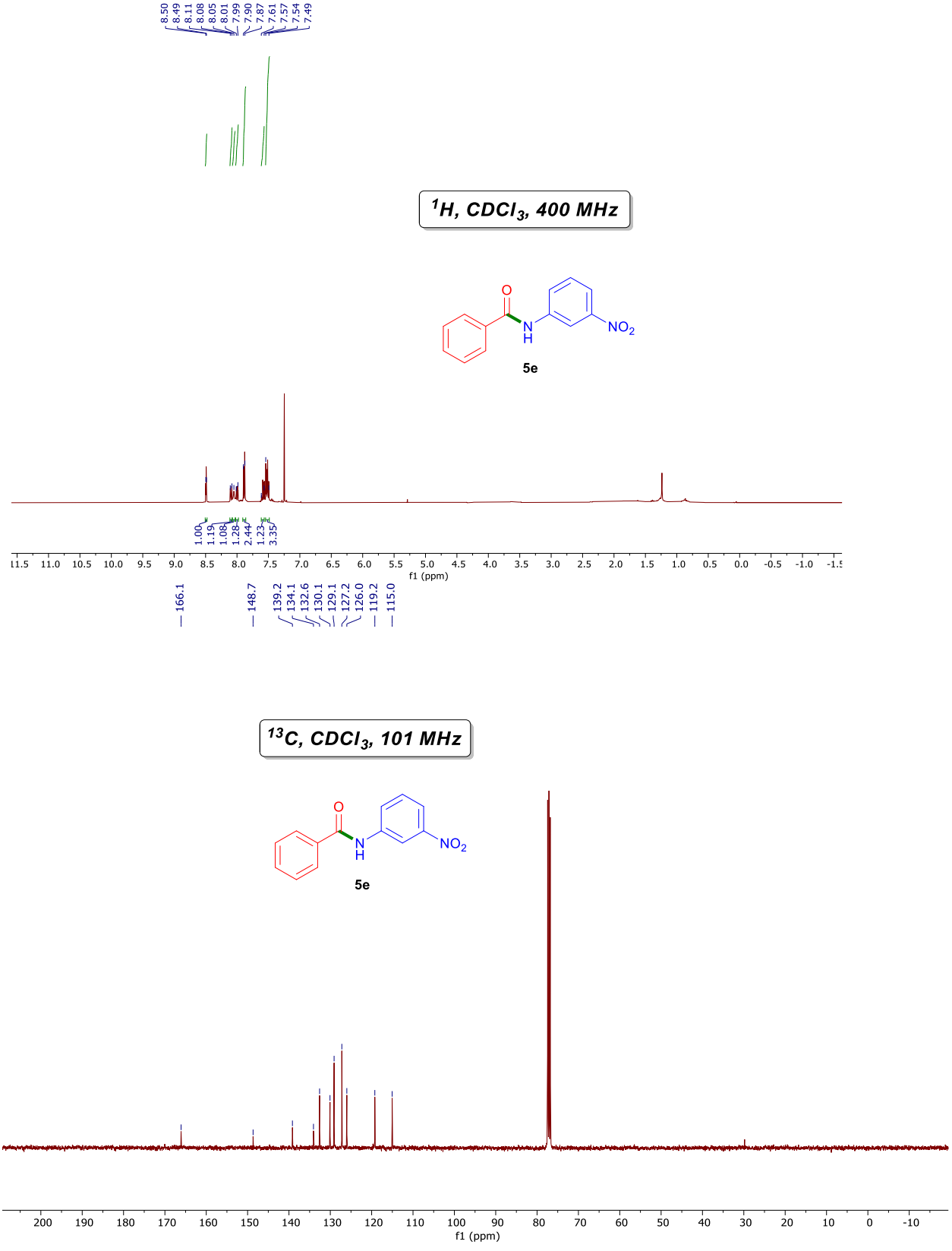
4.6.4. *N*-(3-fluorophenyl)benzamide (5d):



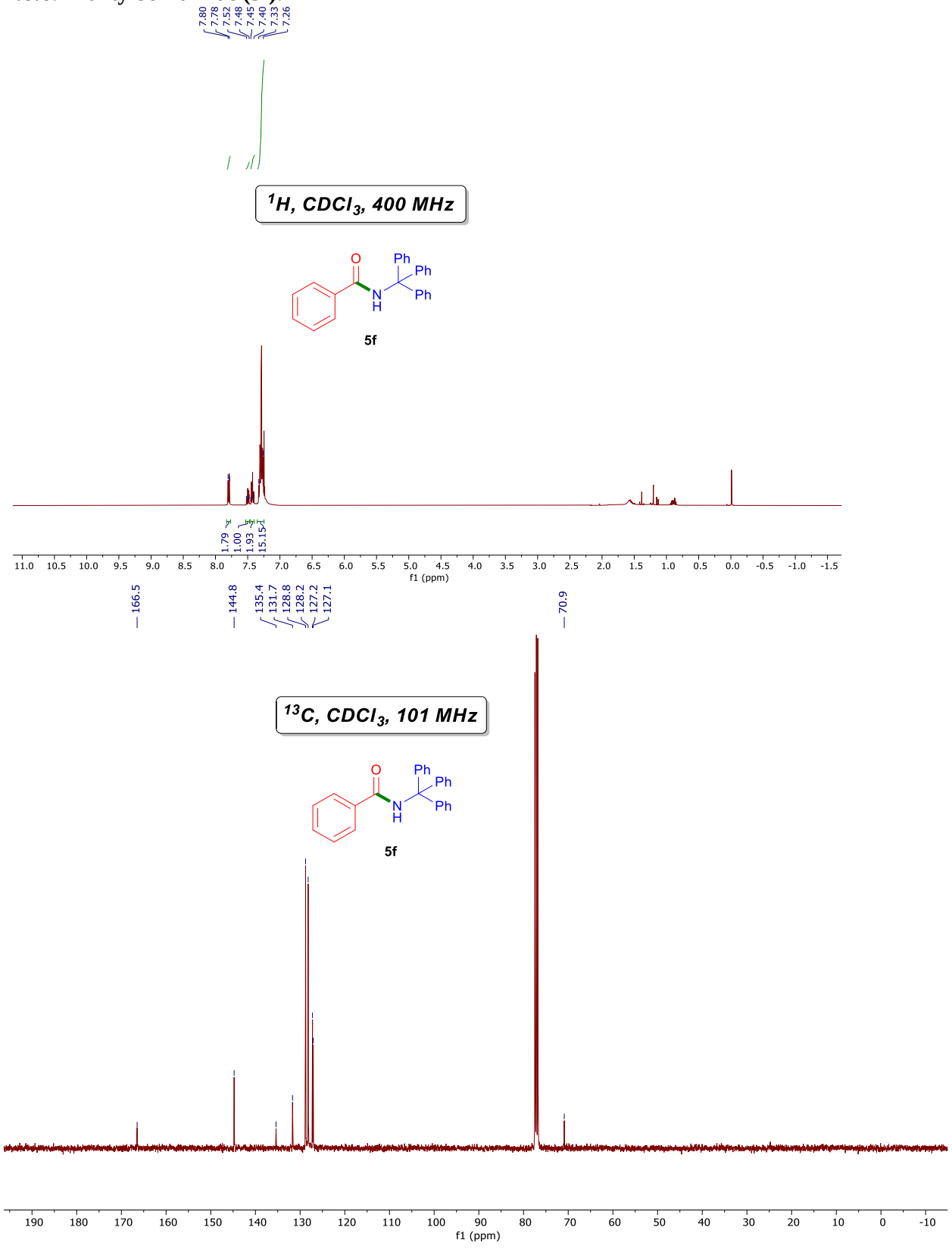



-111.25
^{19}F, $CDCl_3$, 376 MHz
O
N
H
F
5d
100 90 80 70 60 50 40 30 20 10 0 -10 -20 -30 -40 -50 -60 -70 -80 -90 -100 -110 -120 -130 -140 -150 -160 -170 -180
f1 (ppm)

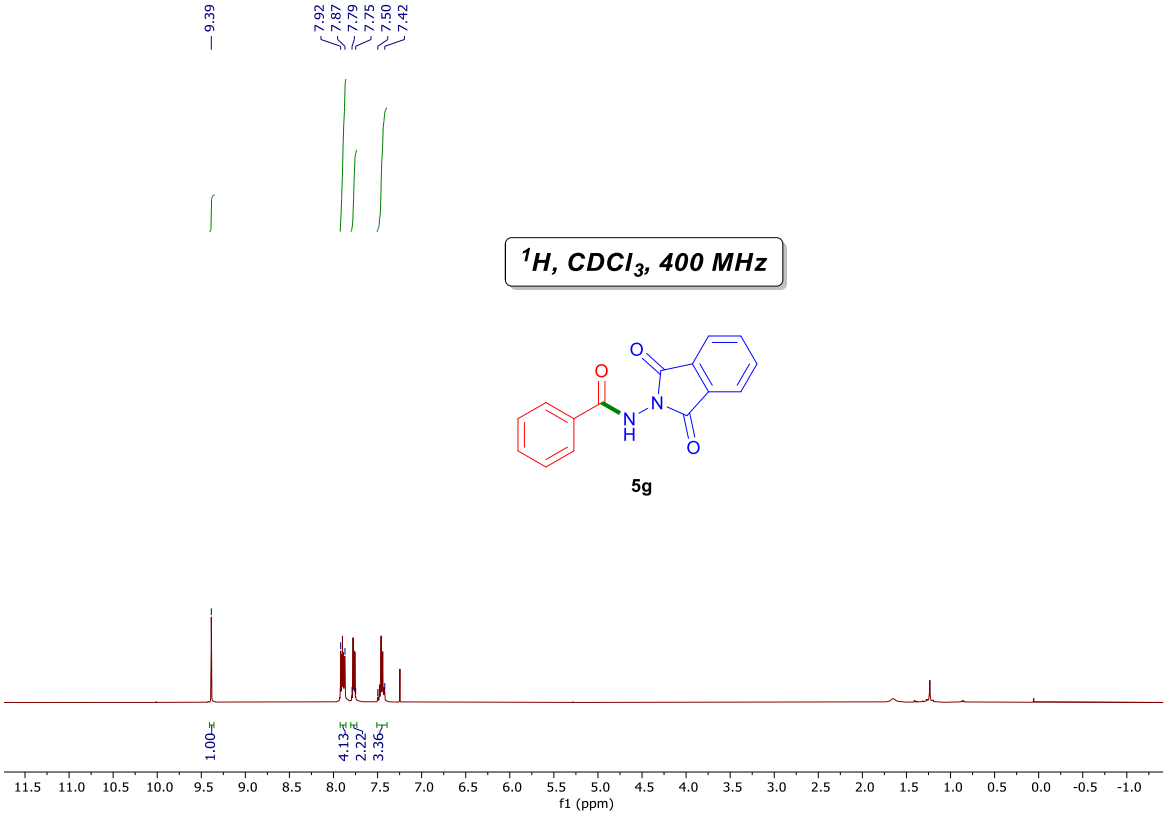
4.6.5. *N*-(3-nitrophenyl)benzamide (5e):



4.6.6. *N*-tritylbenzamide (5f):

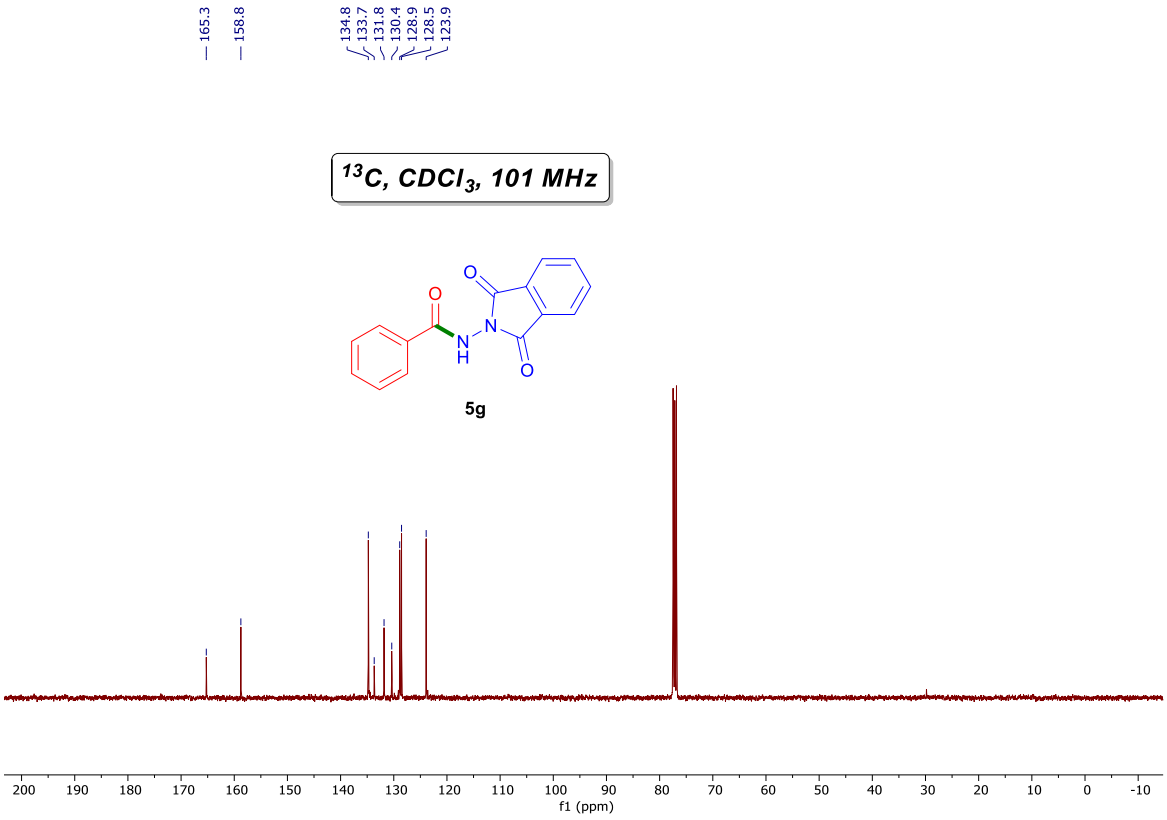


4.6.7. *N*-(1,3-dioxoisoindolin-2-yl)benzamide (5g):



^{1}H, $CDCl_3$, 400 MHz

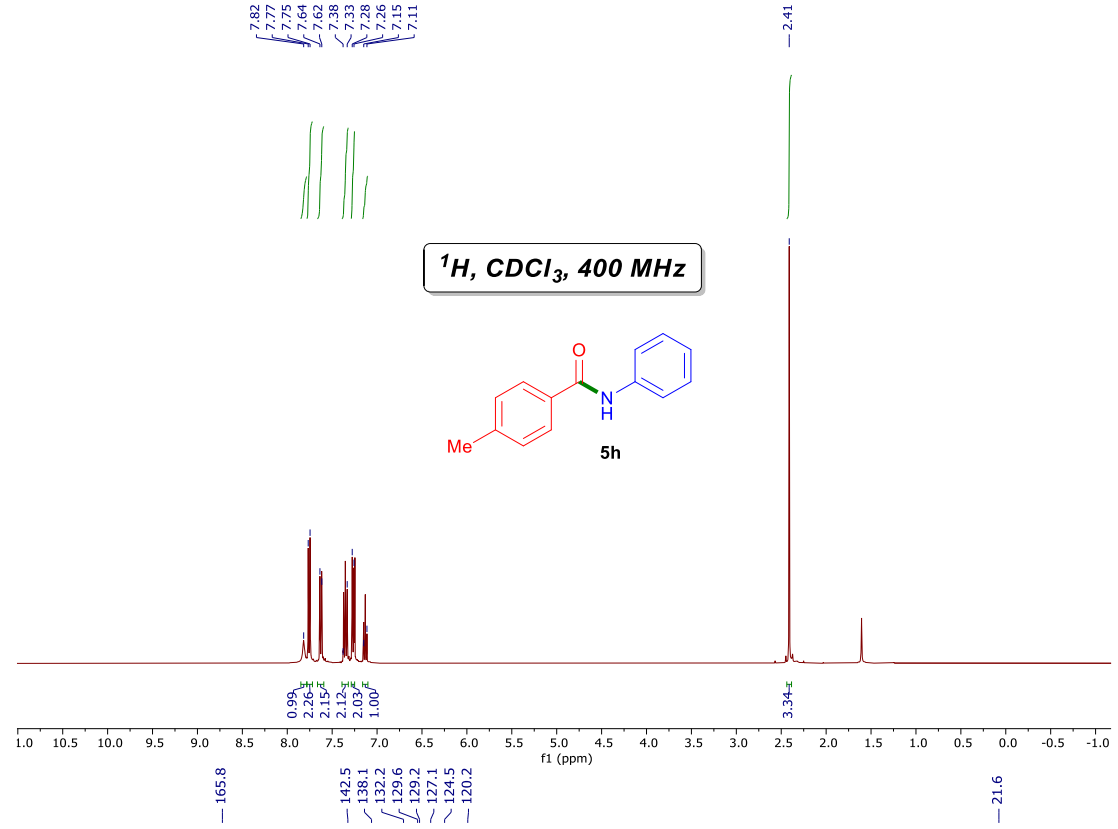
5g

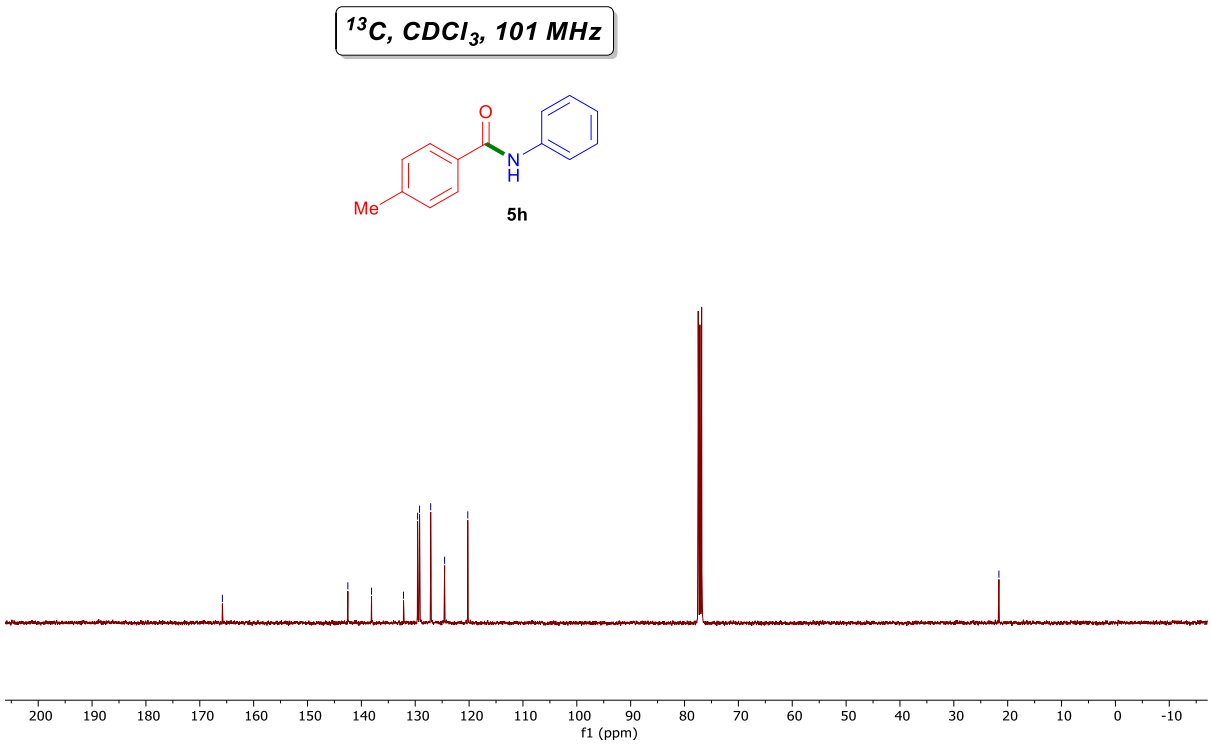


^{13}C, $CDCl_3$, 101 MHz

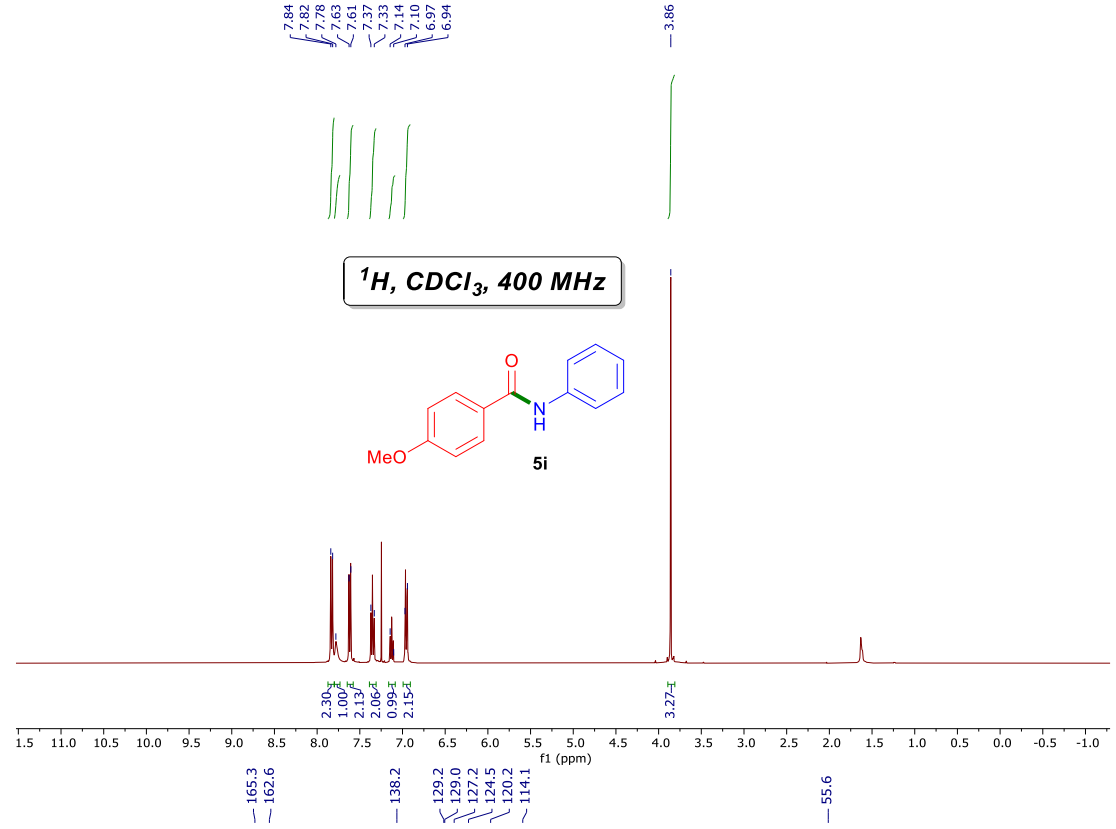
5g

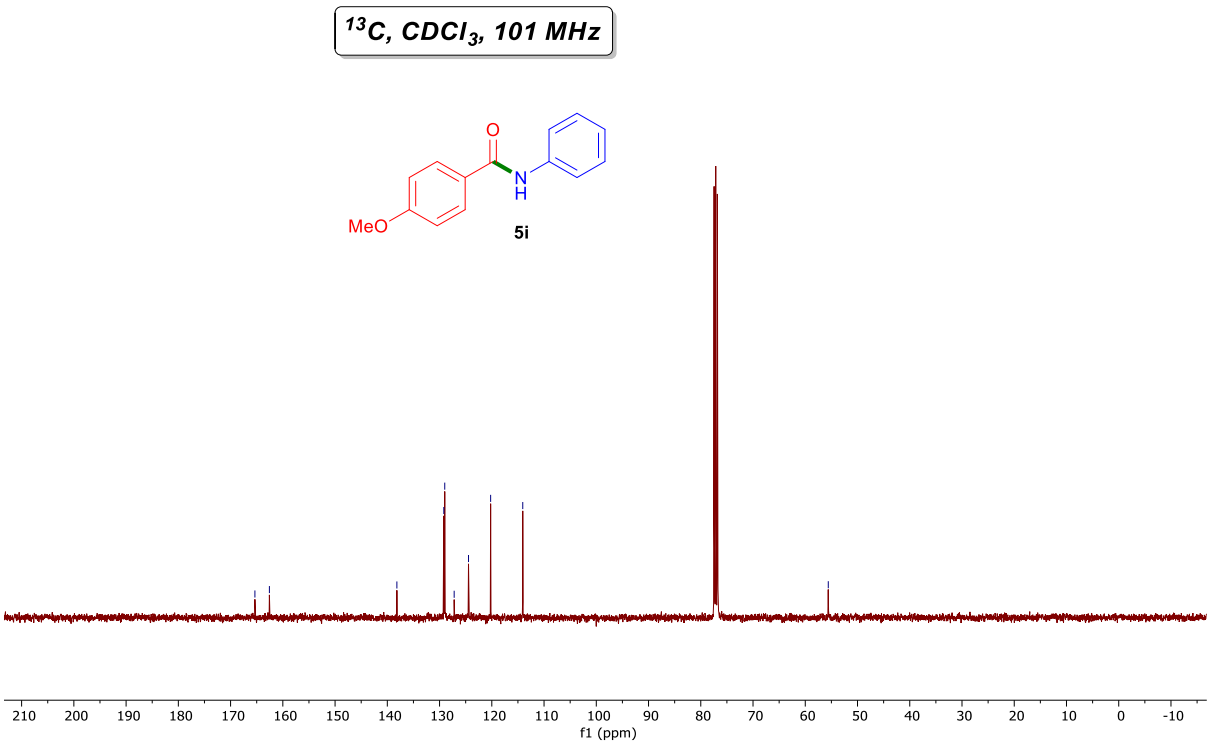
4.6.8. 4-methyl-*N*-phenylbenzamide (5h):



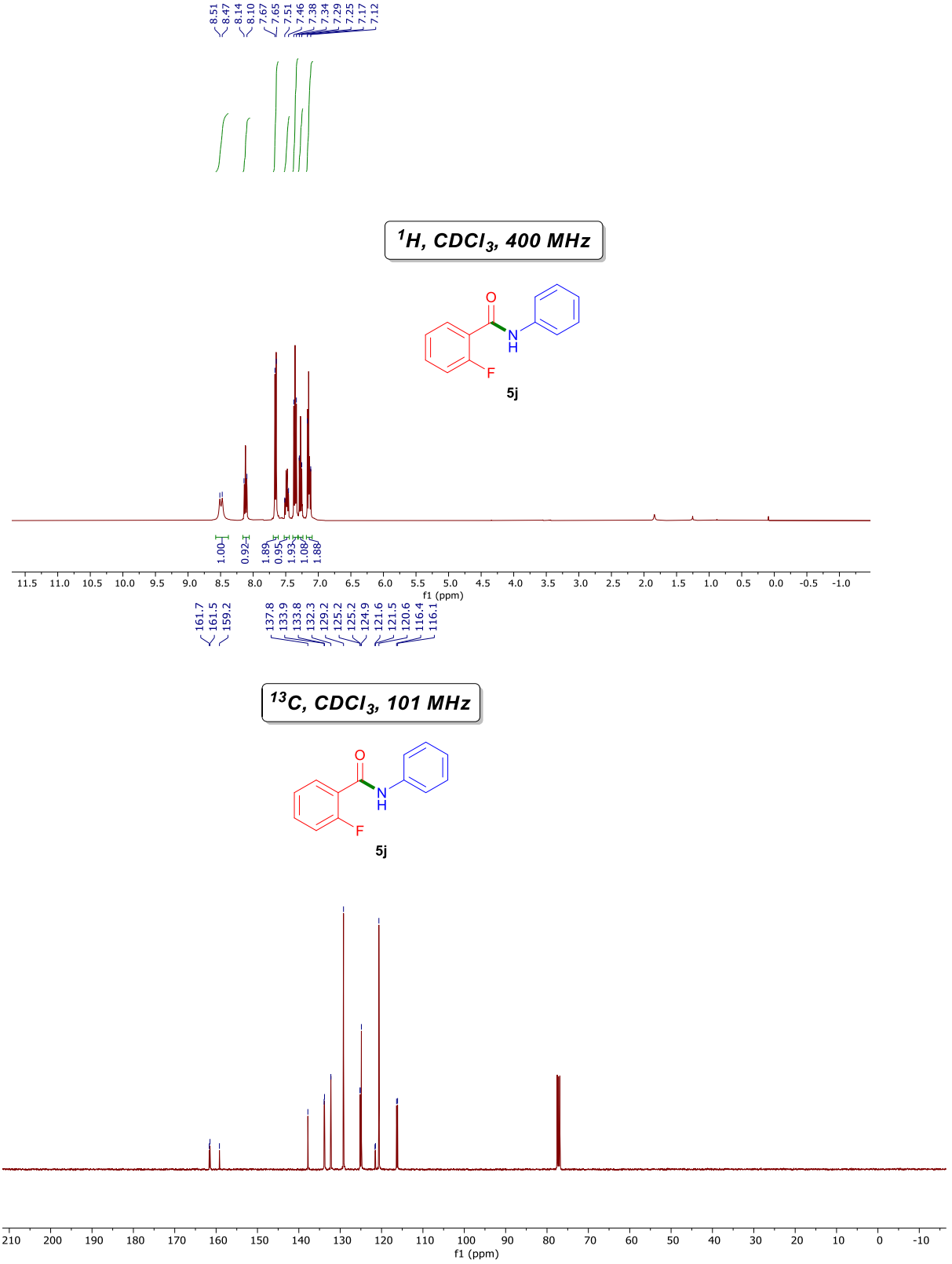


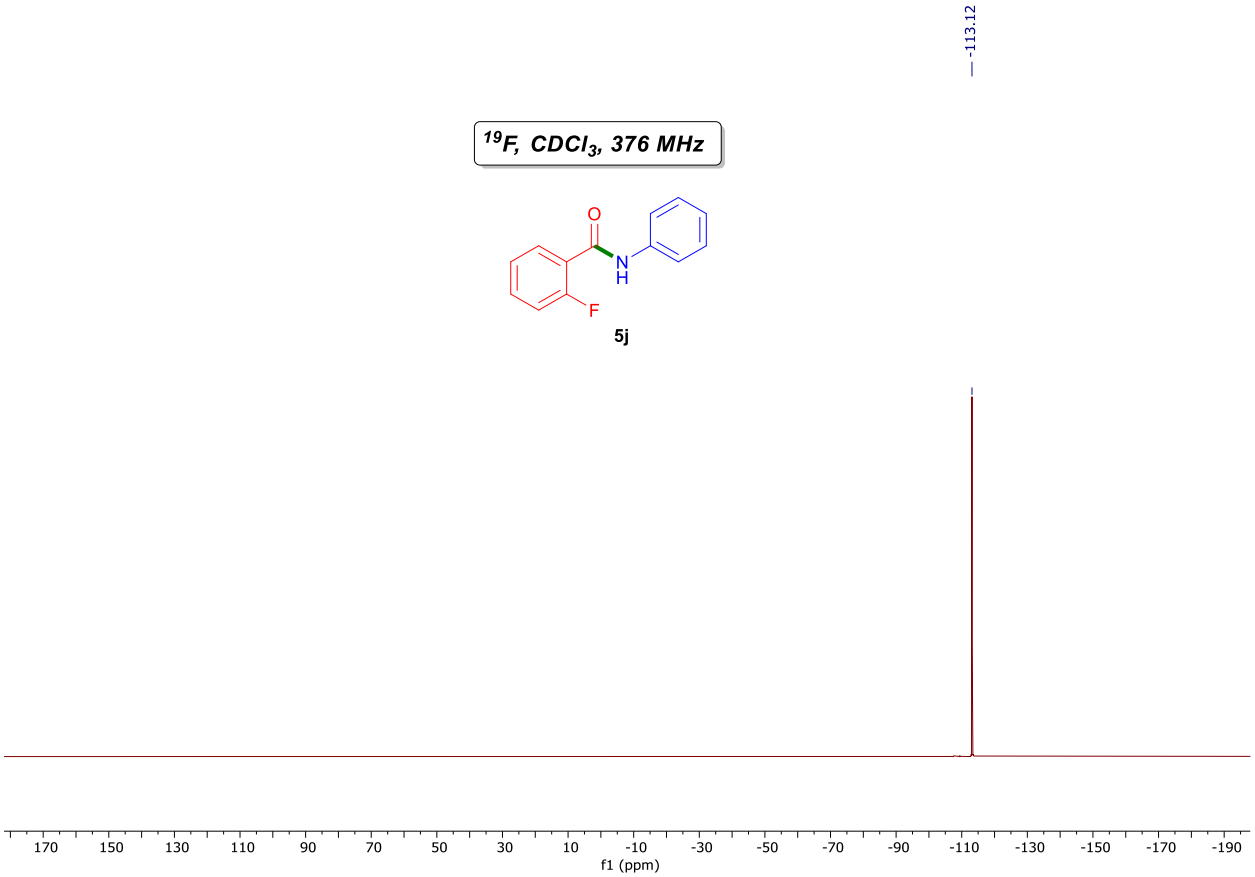
4.6.9. 4-methoxy-*N*-phenylbenzamide (5i):



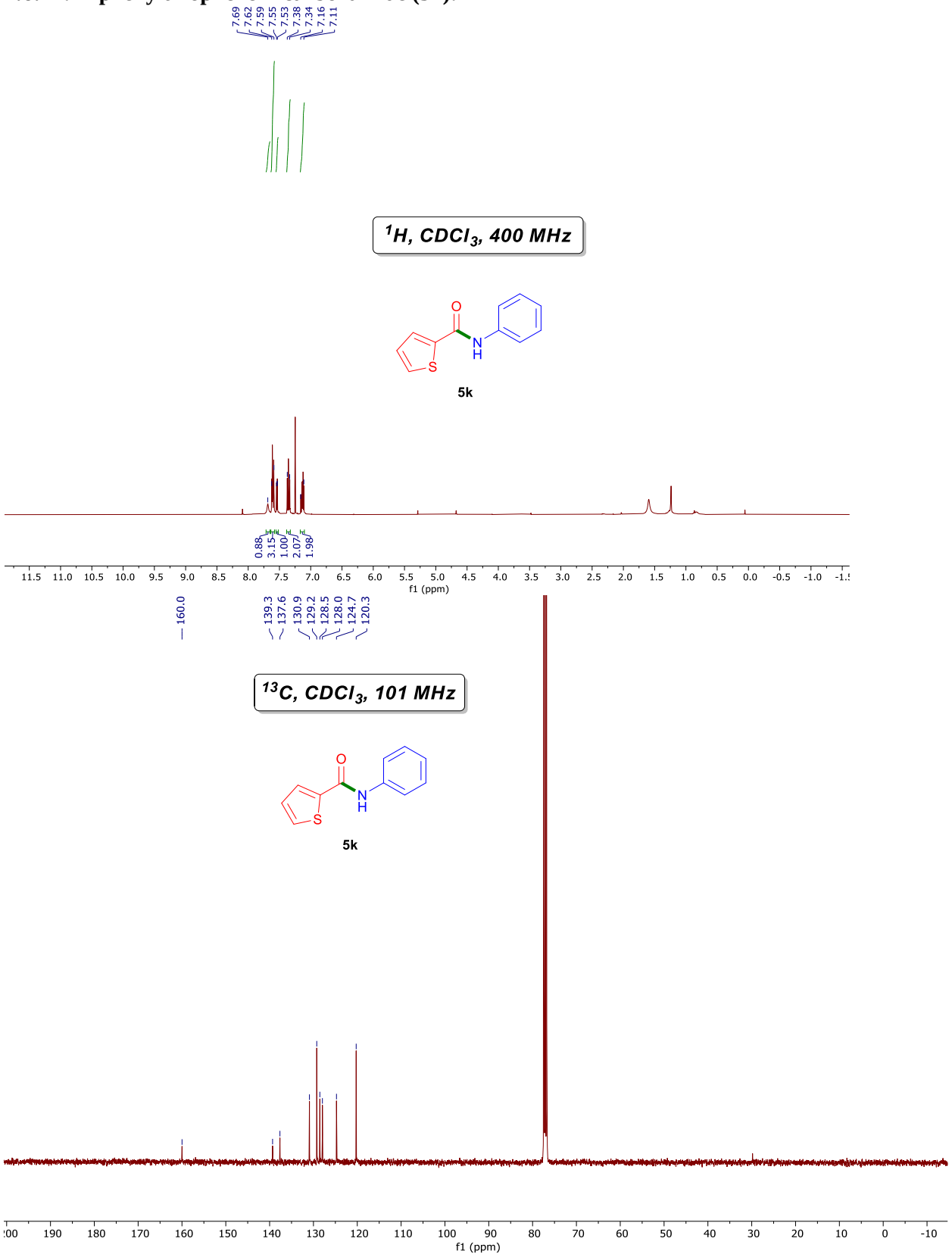


4.6.10. 2-fluoro-*N*-phenylbenzamide (5j):

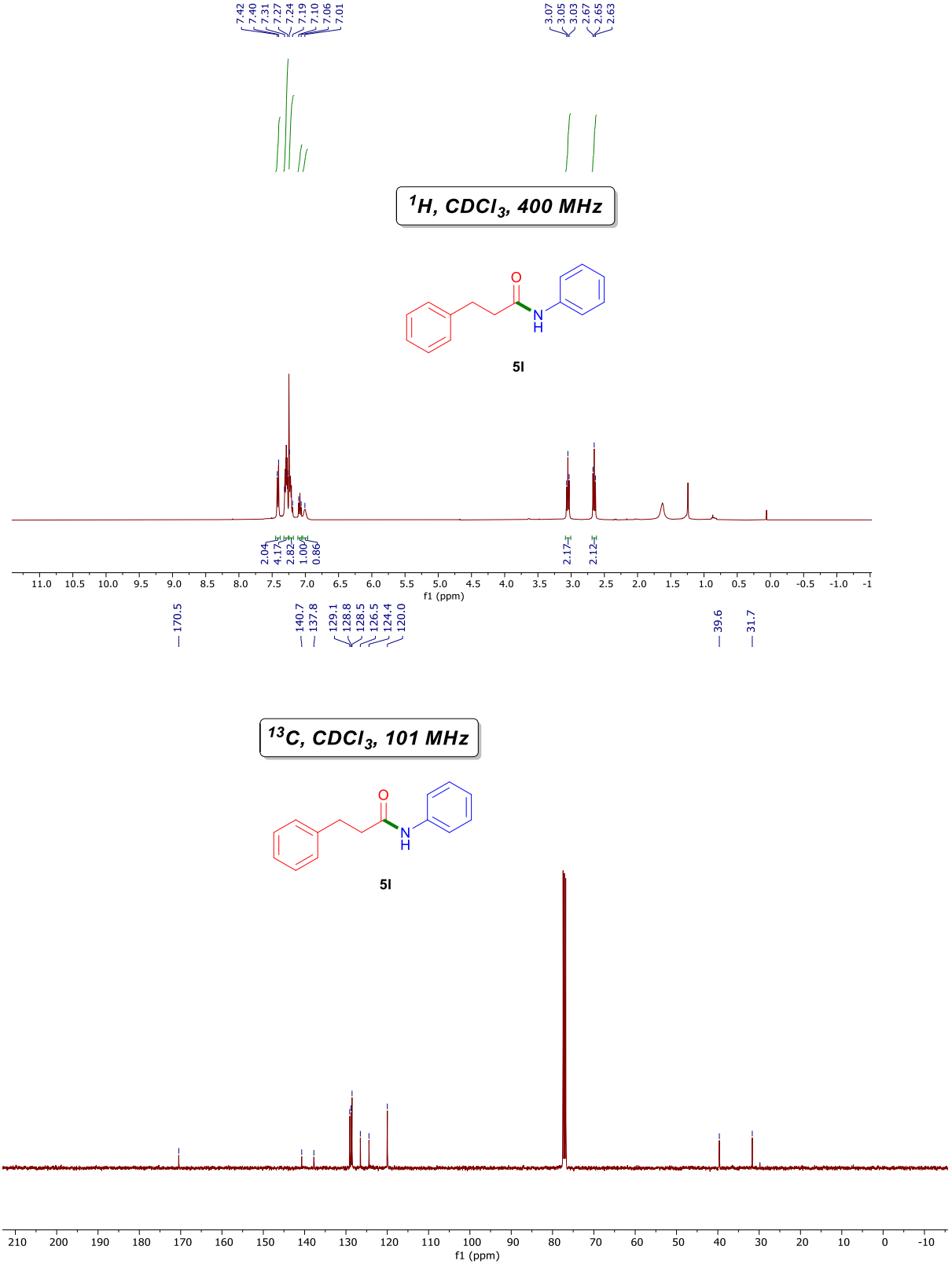



-113.12
^{19}F, $CDCl_3$, 376 MHz
O
N
H
F
5j
170
150
130
110
90
70
50
30
10
-10
-30
-50
-70
-90
-110
-130
-150
-170
-190
f1 (ppm)

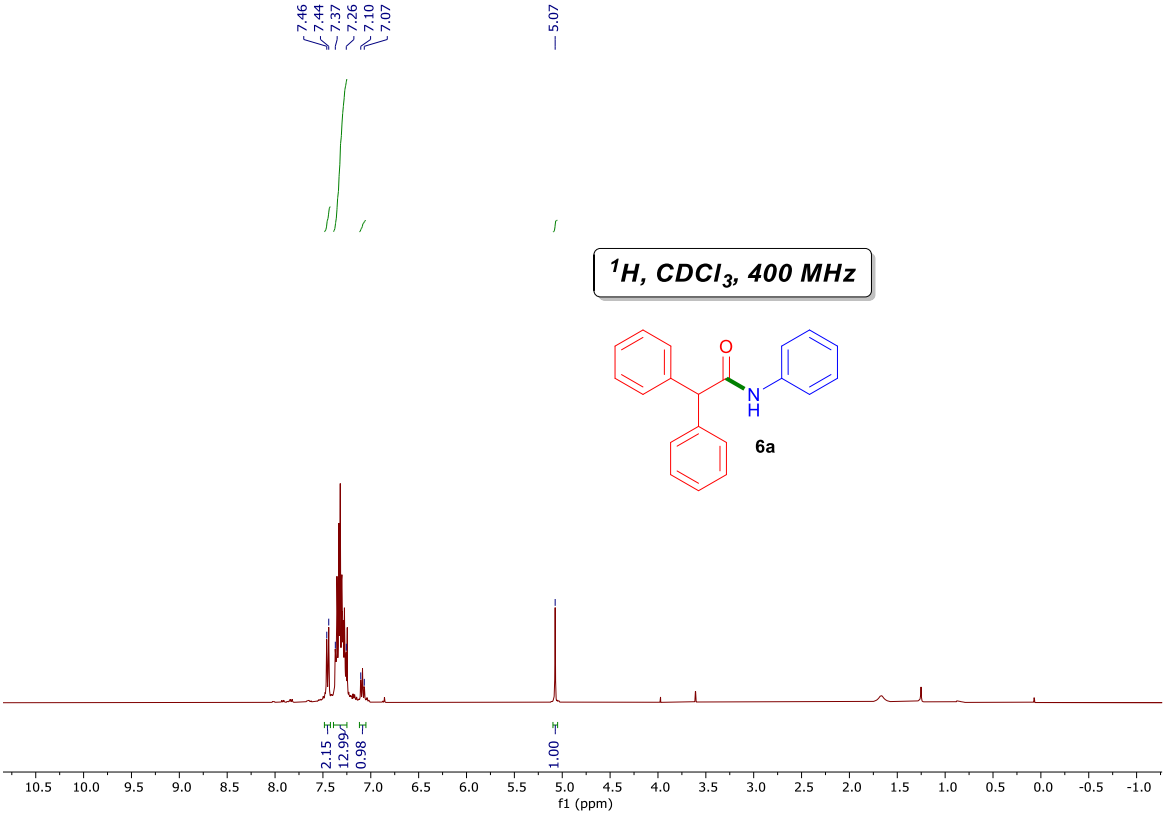
4.6.11. *N*-phenylthiophene-2-carboxamide (5k):

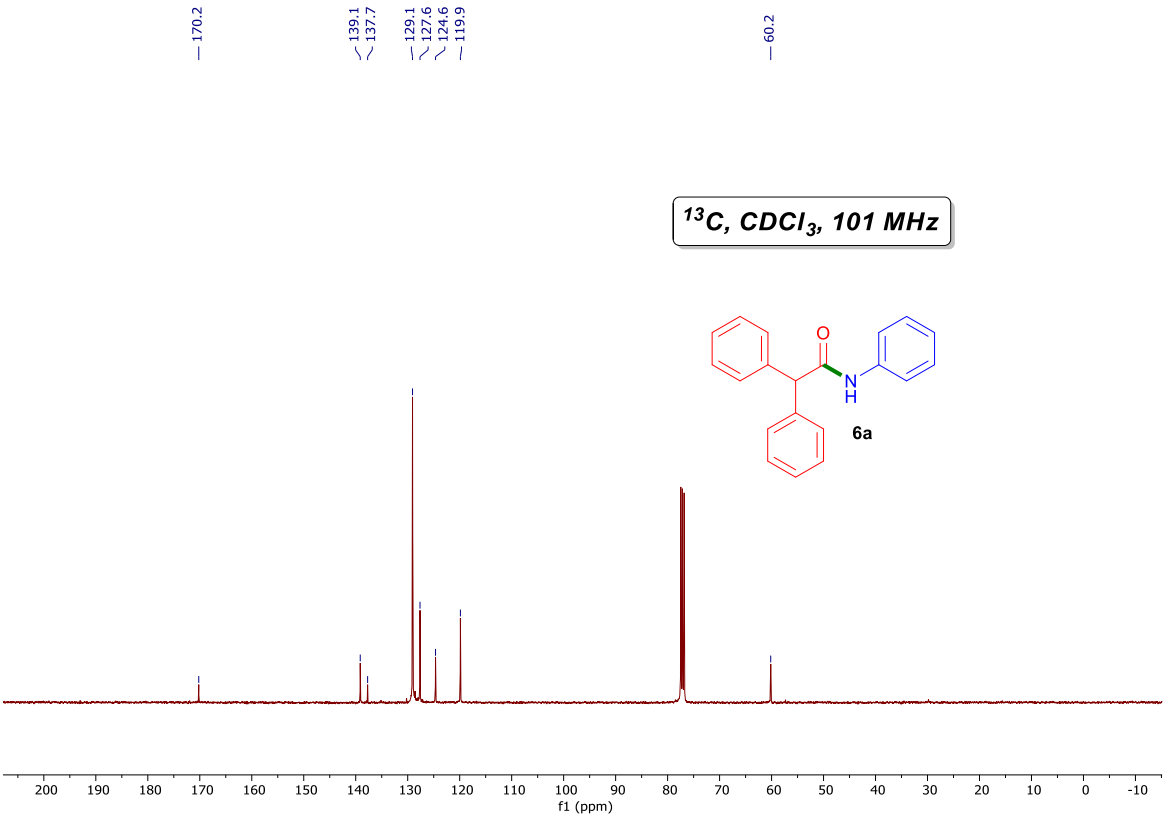


4.6.12. *N*,3-diphenylpropanamide (5l):

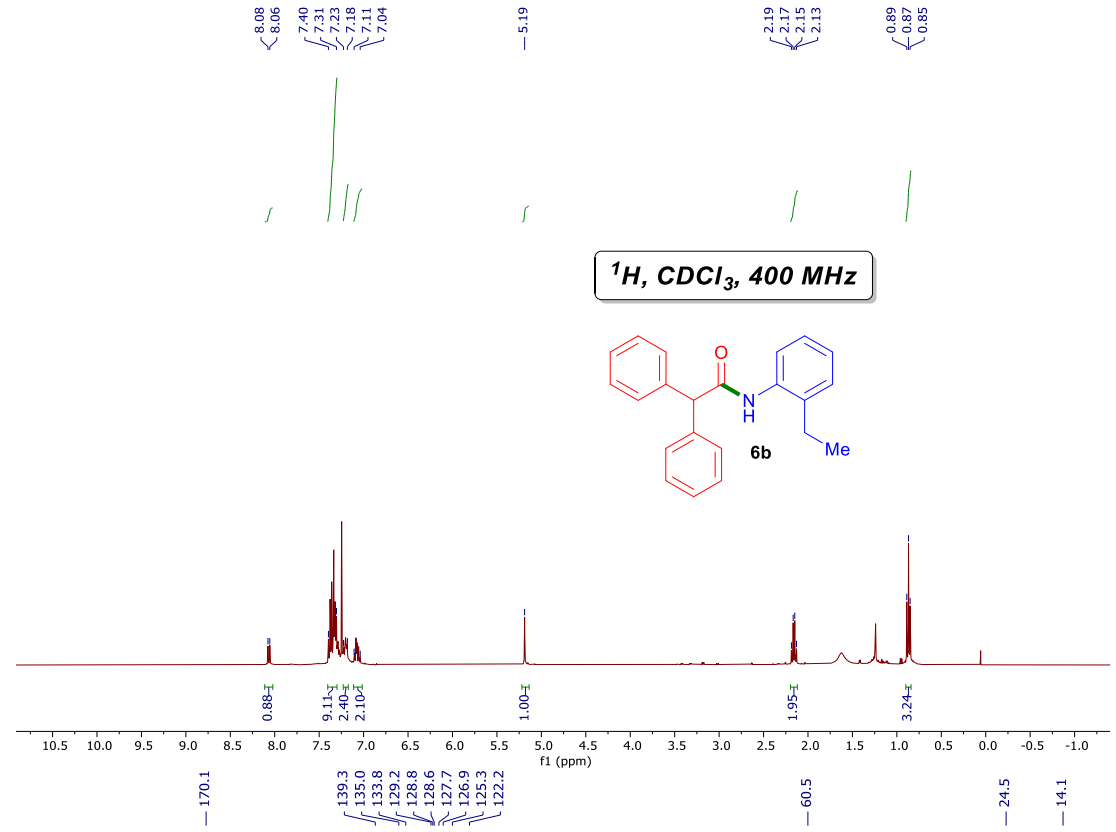


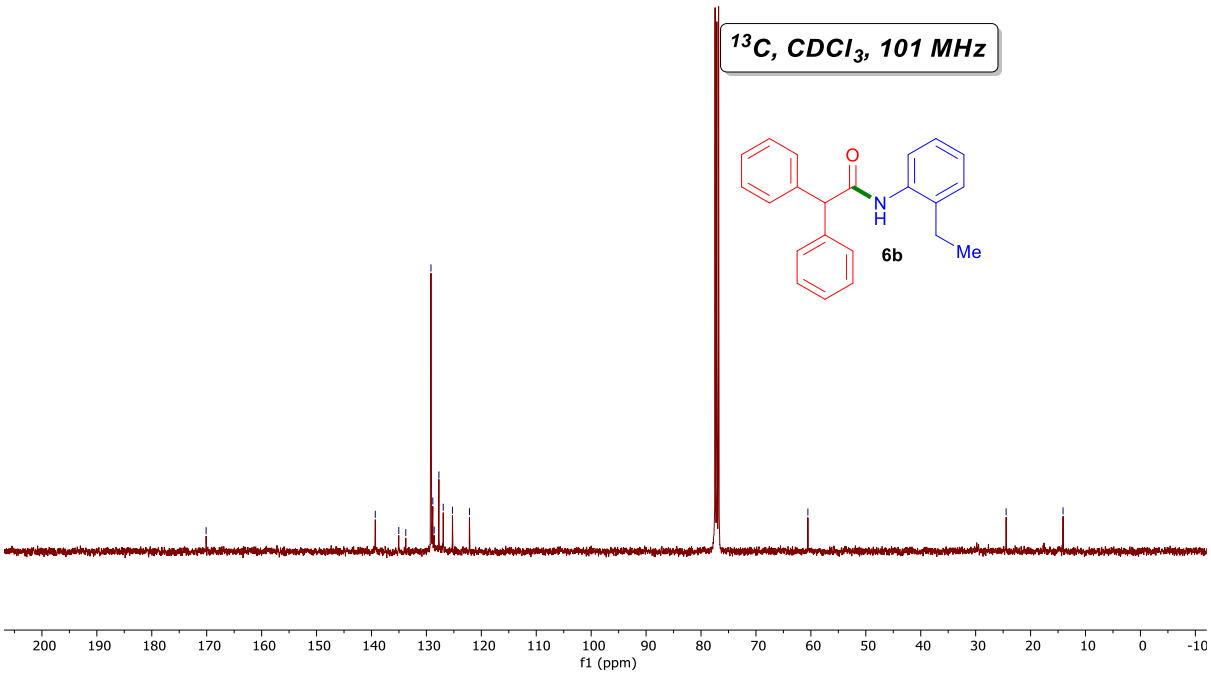
4.6.13. *N*,2,2-triphenylacetamide (6a):



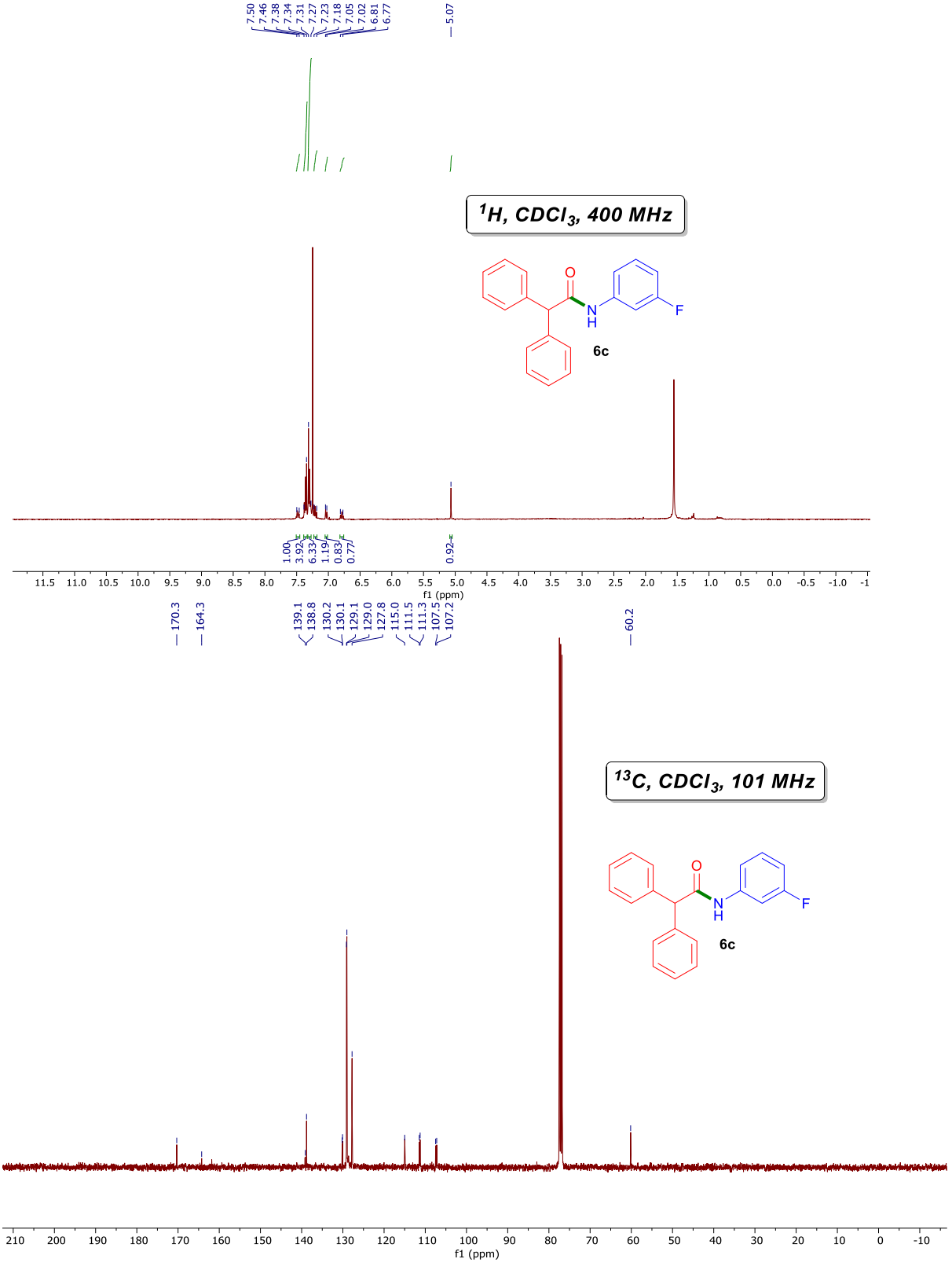


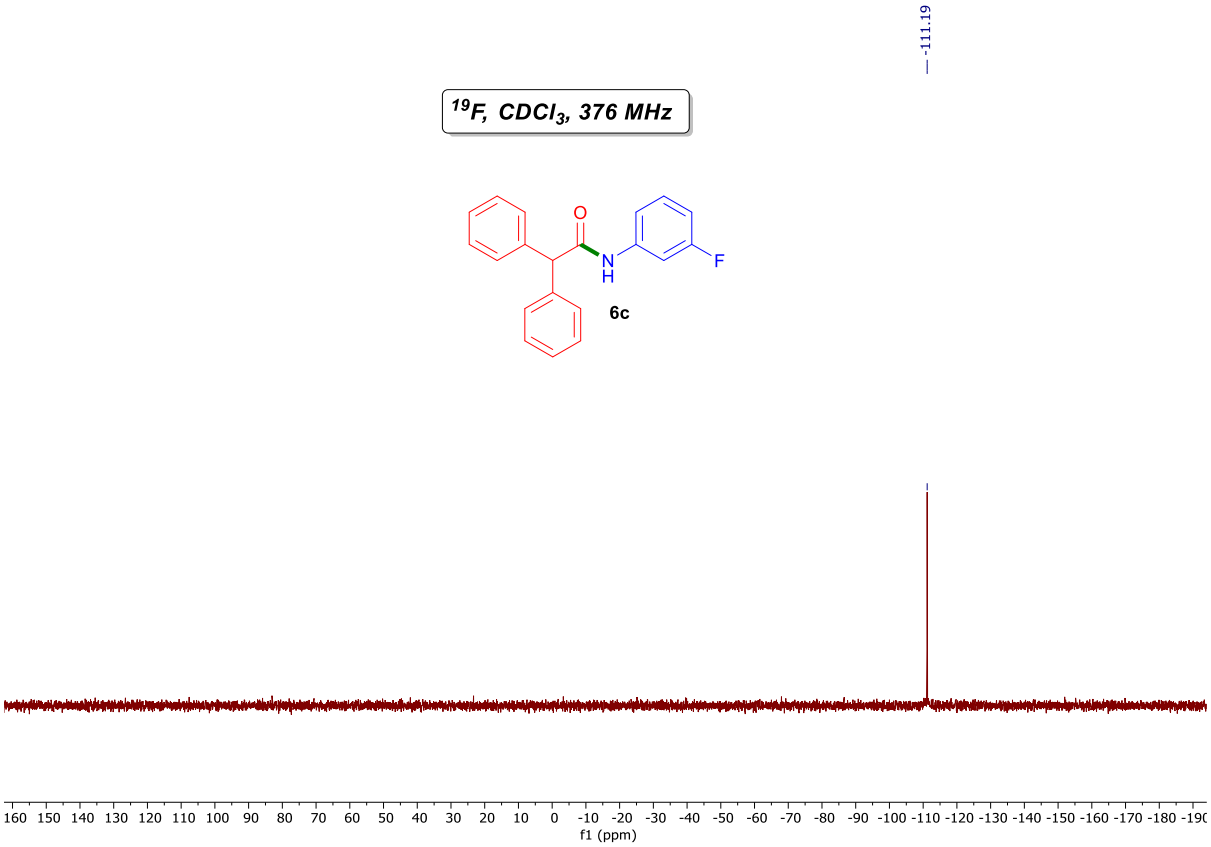
4.6.14. *N*-(2-ethylphenyl)-2,2-diphenylacetamide (6b):



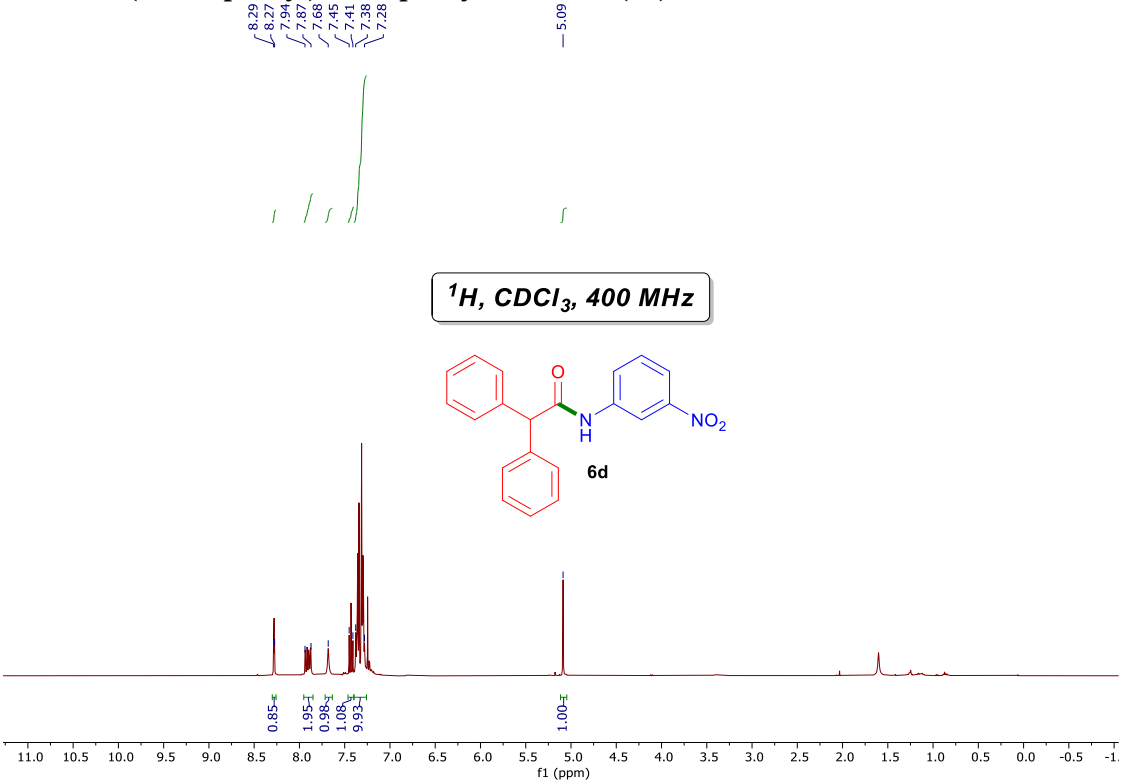


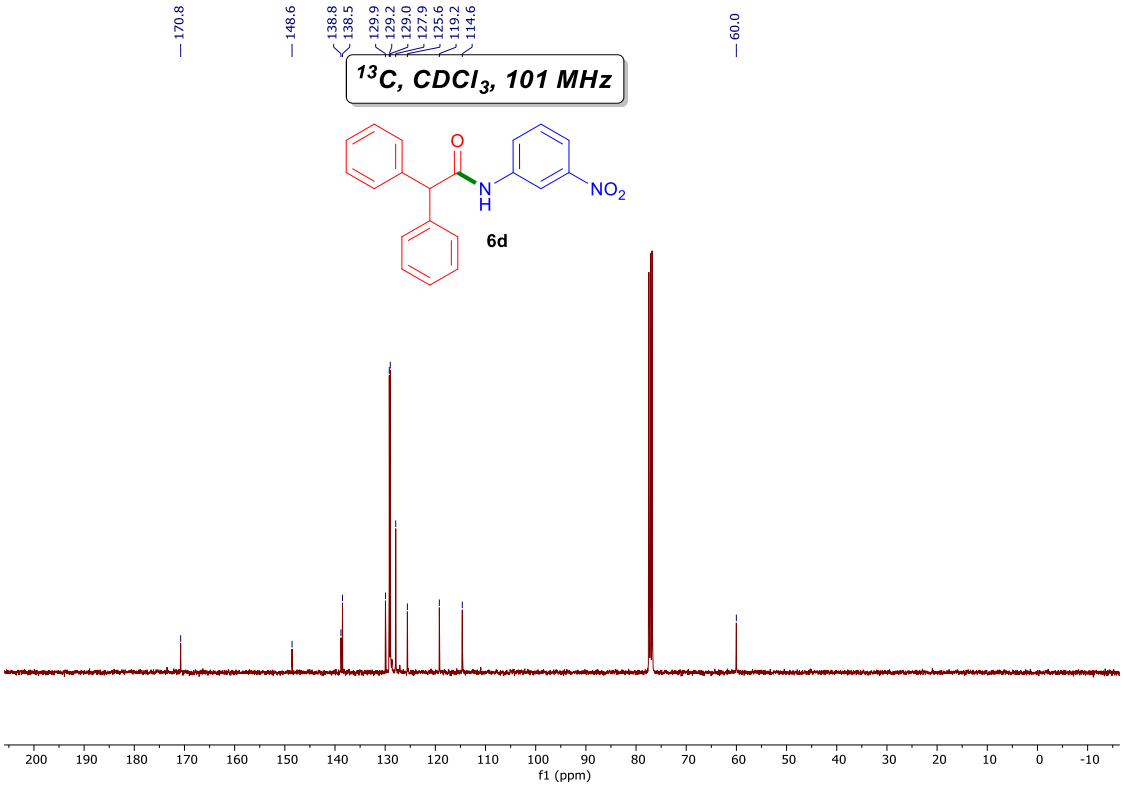
4.6.15. *N*,2,2-triphenylacetamide (6c):



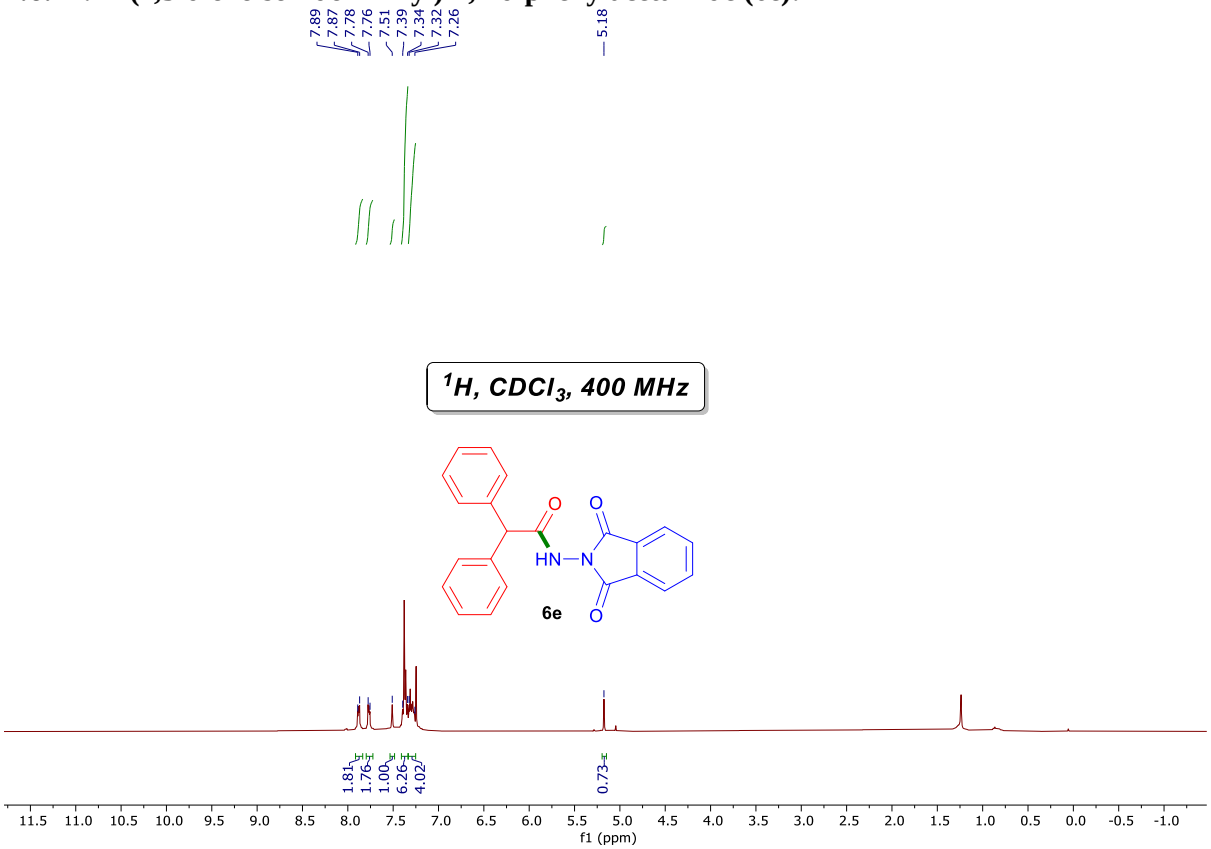

-111.19
^{19}F, $CDCl_3$, 376 MHz
O
N
H
F
6c
160 150 140 130 120 110 100 90 80 70 60 50 40 30 20 10 0 -10 -20 -30 -40 -50 -60 -70 -80 -90 -100 -110 -120 -130 -140 -150 -160 -170 -180 -19(
f1 (ppm)

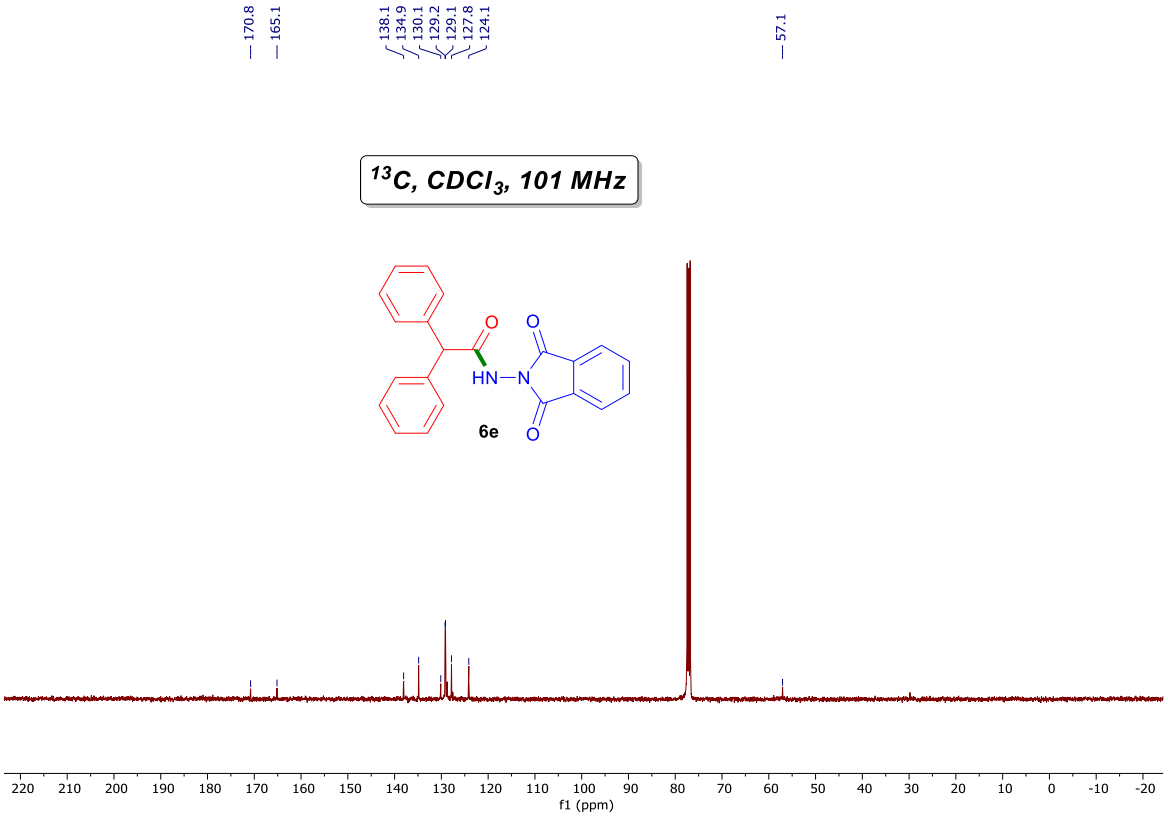
4.6.16. *N*-(3-nitrophenyl)-2,2-diphenylacetamide (6d):



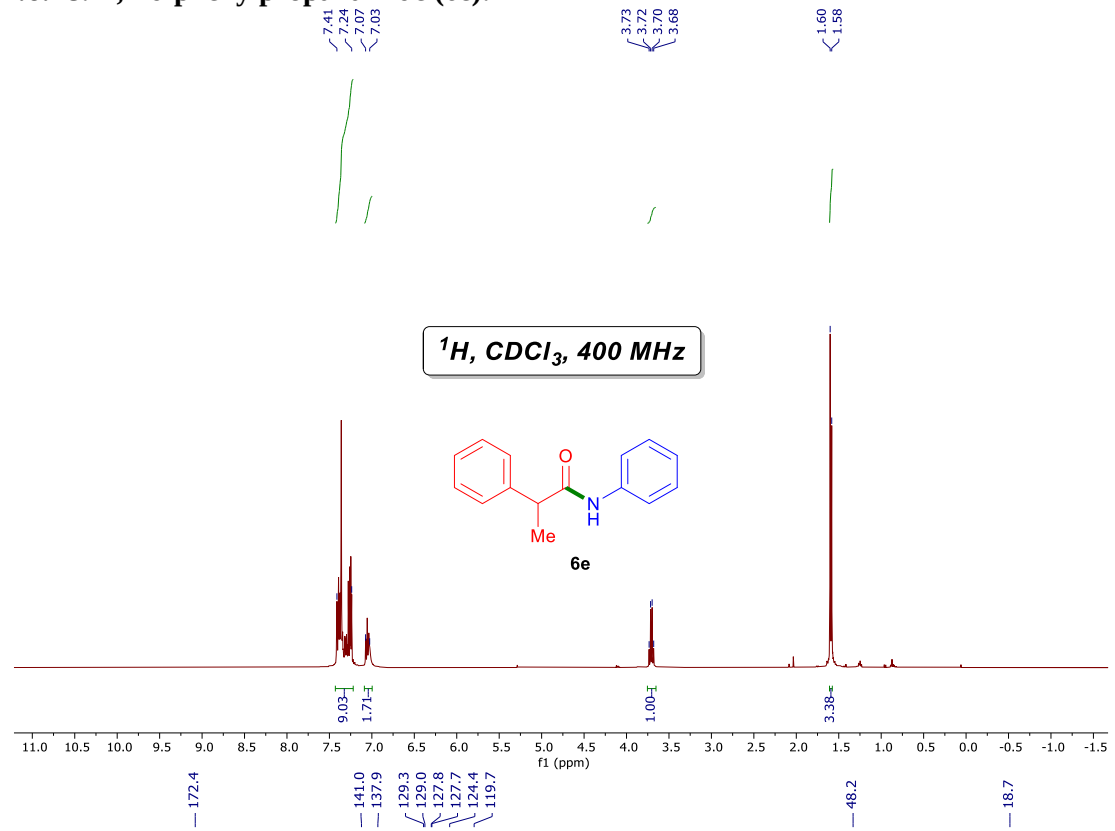


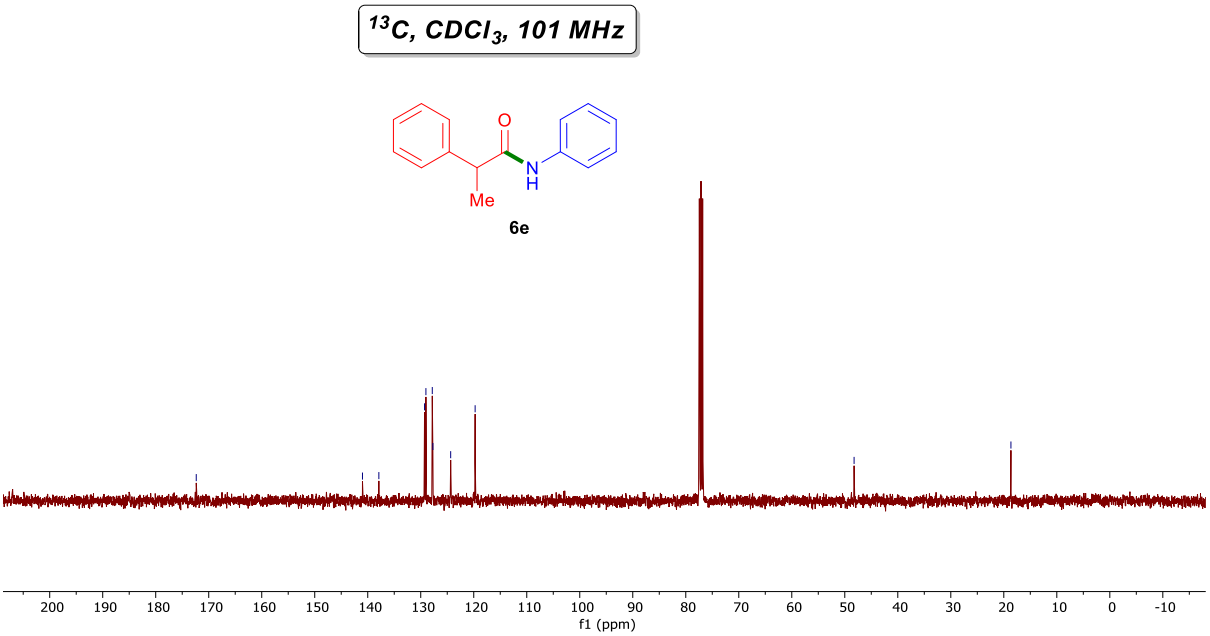
4.6.17. *N*-(1,3-dioxoisoindolin-2-yl)-2,2-diphenylacetamide (6e):



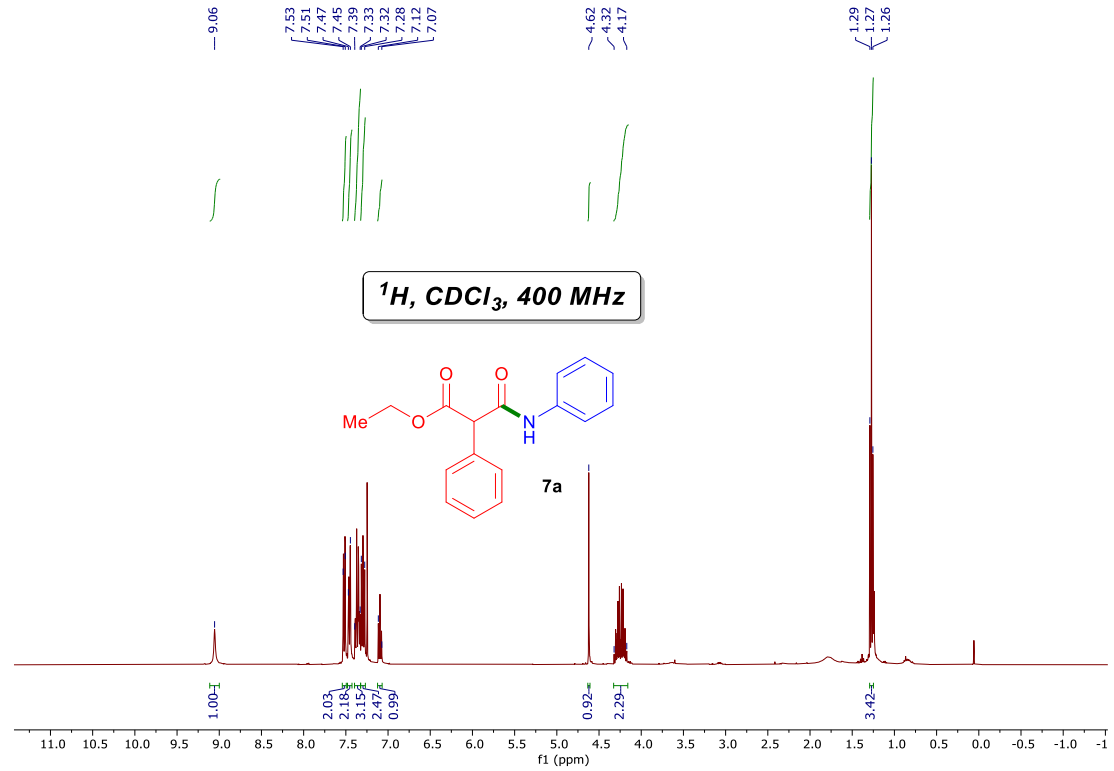


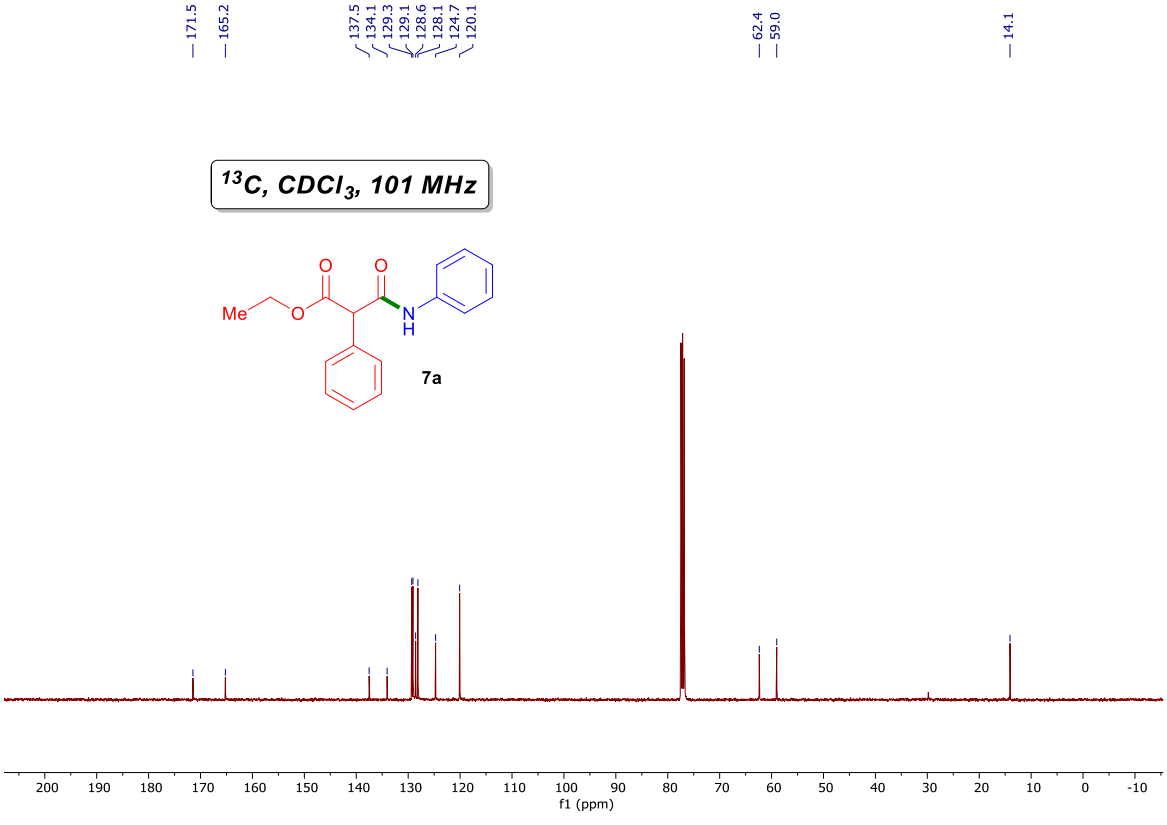
4.6.18. *N*,2-diphenylpropanamide (6e):



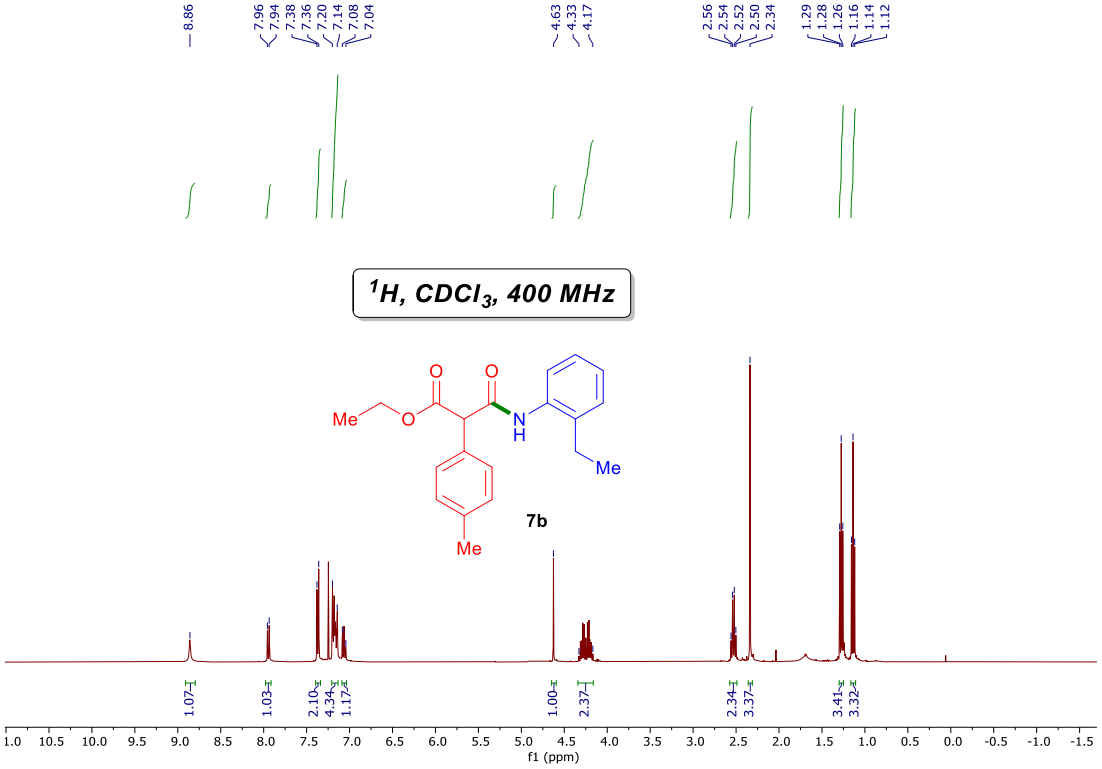


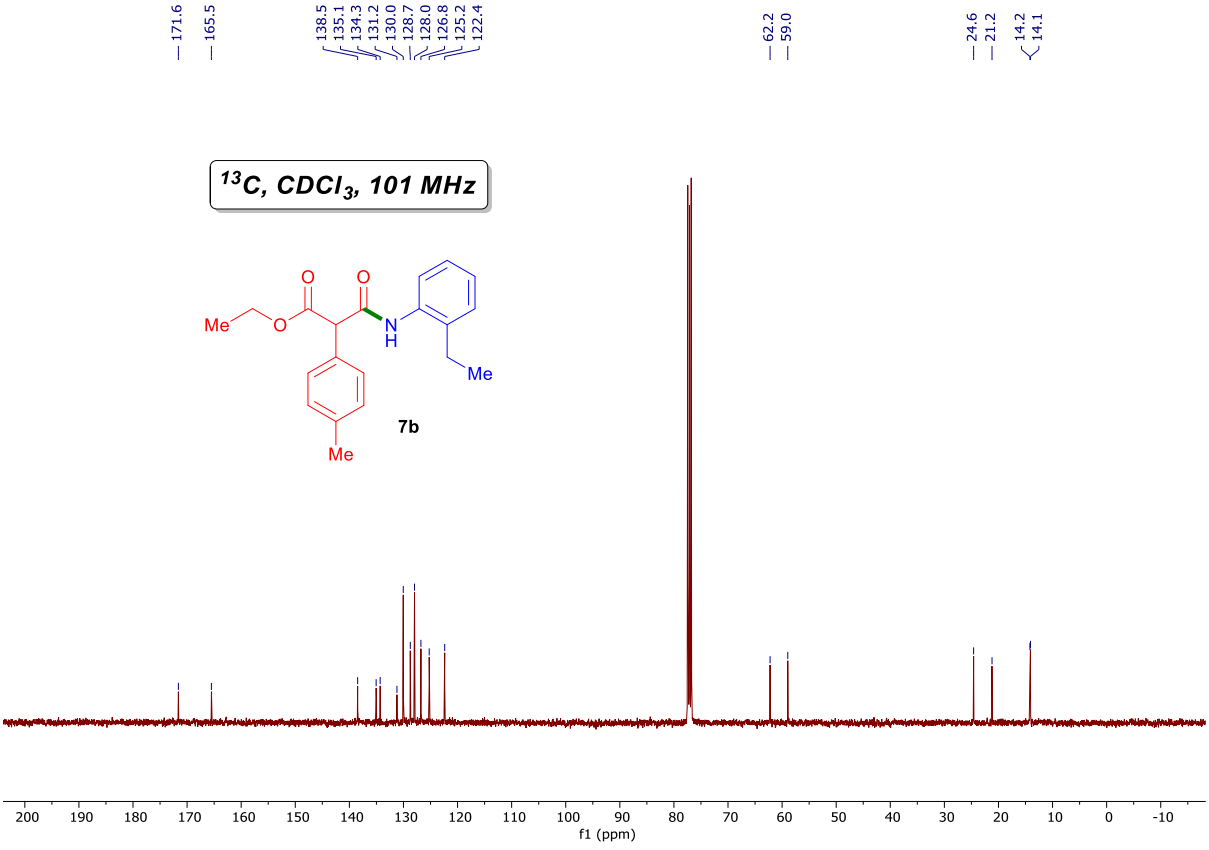
4.6.19. ethyl 3-oxo-2-phenyl-3-(phenylamino)propanoate (7a):



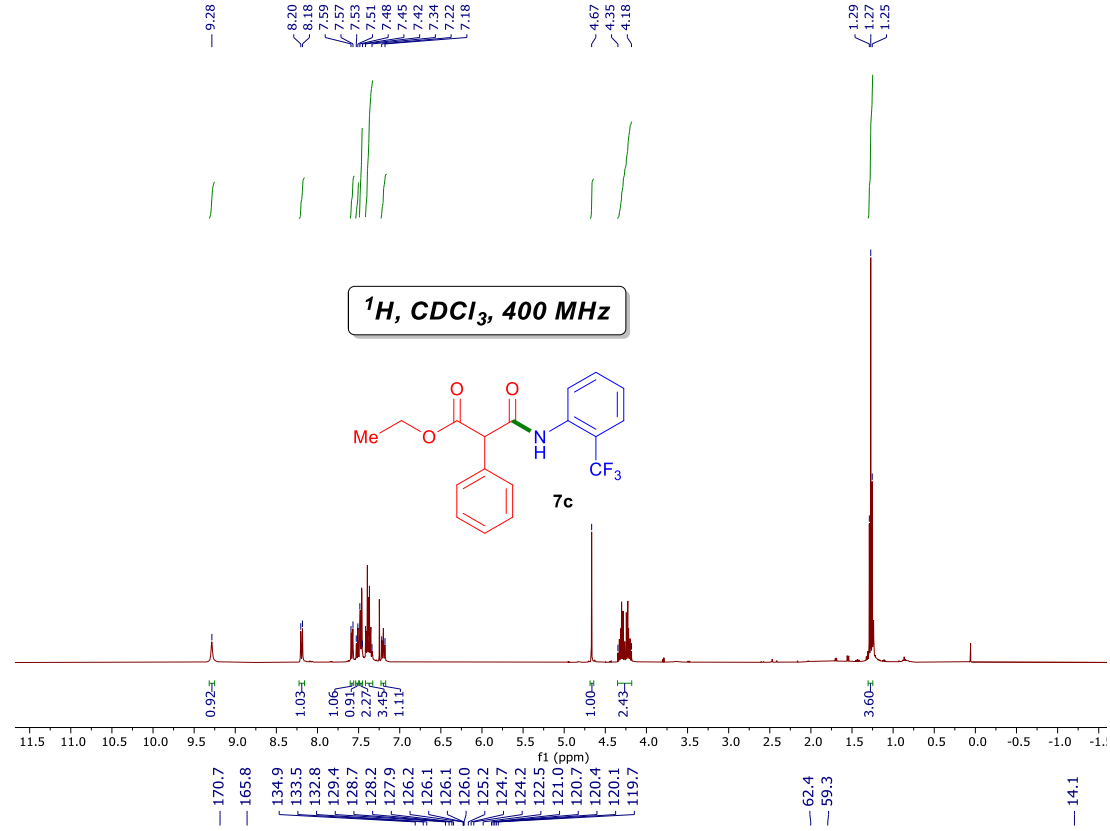


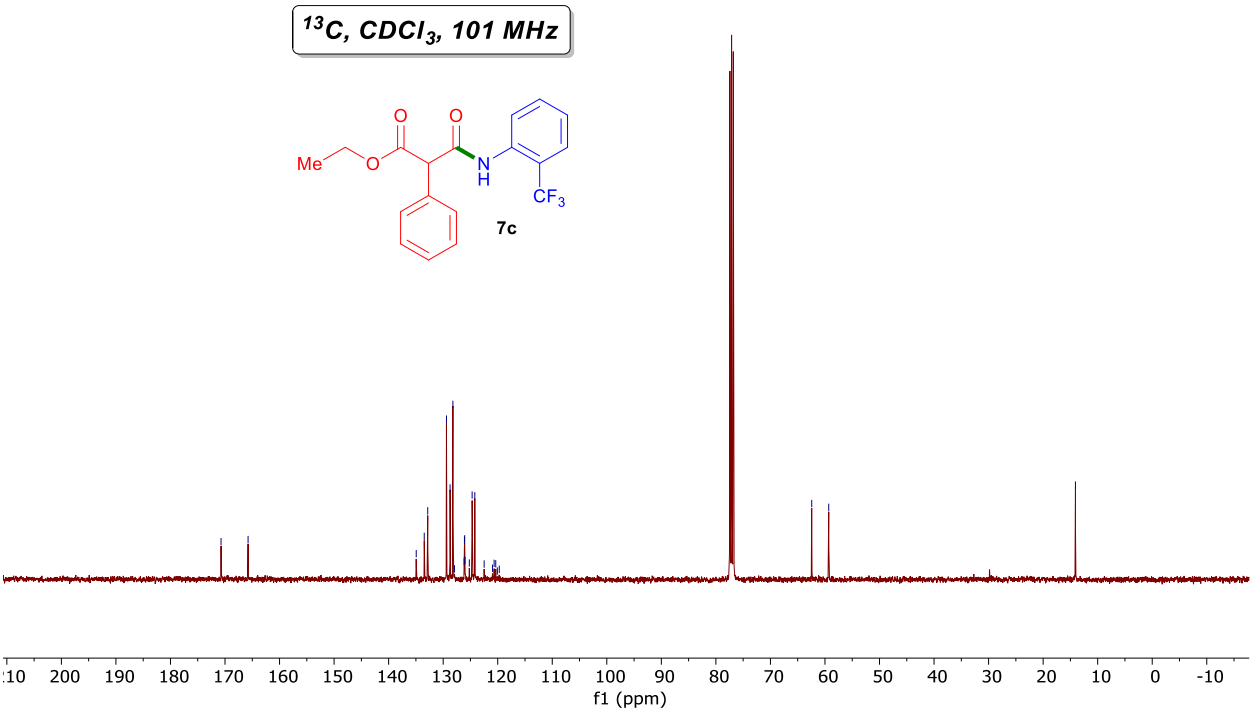
4.6.20. ethyl 3-((2-ethylphenyl)amino)-3-oxo-2-(*p*-tolyl)propanoate (7b):

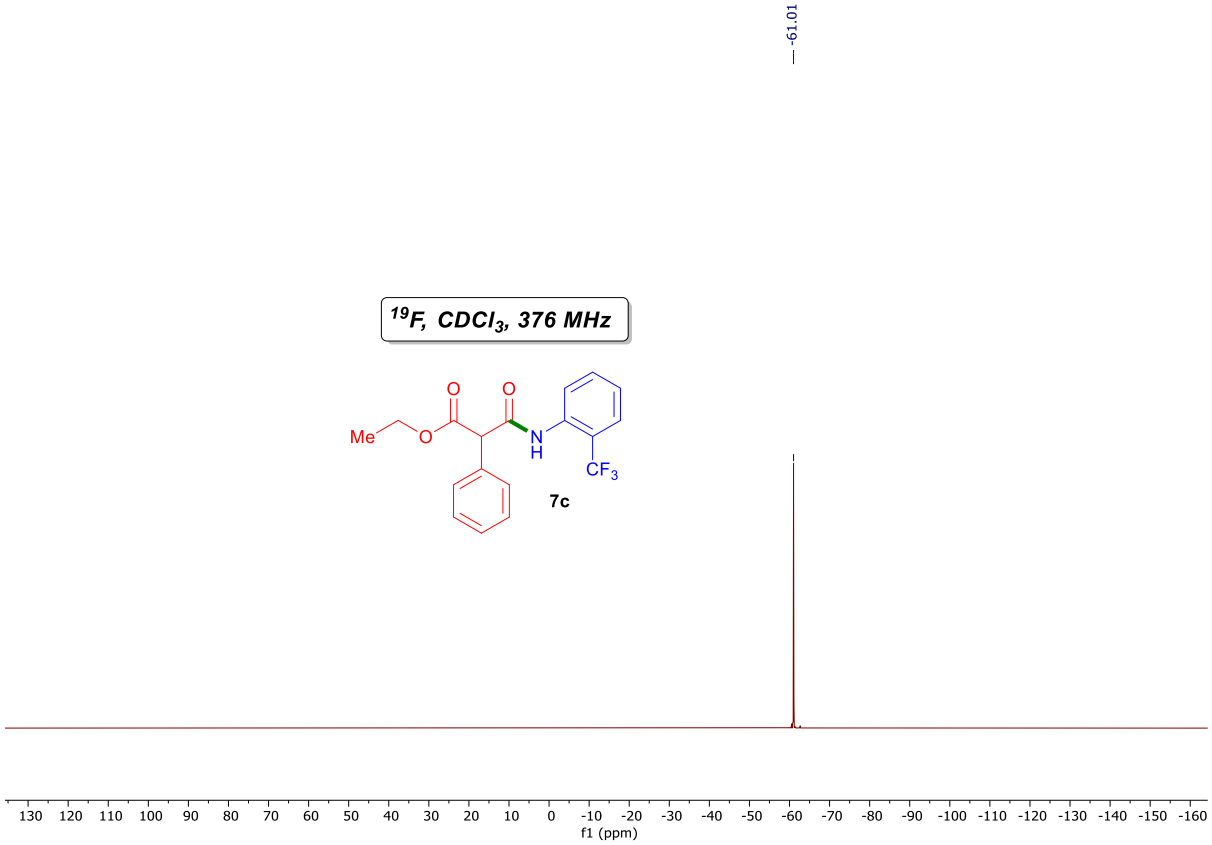




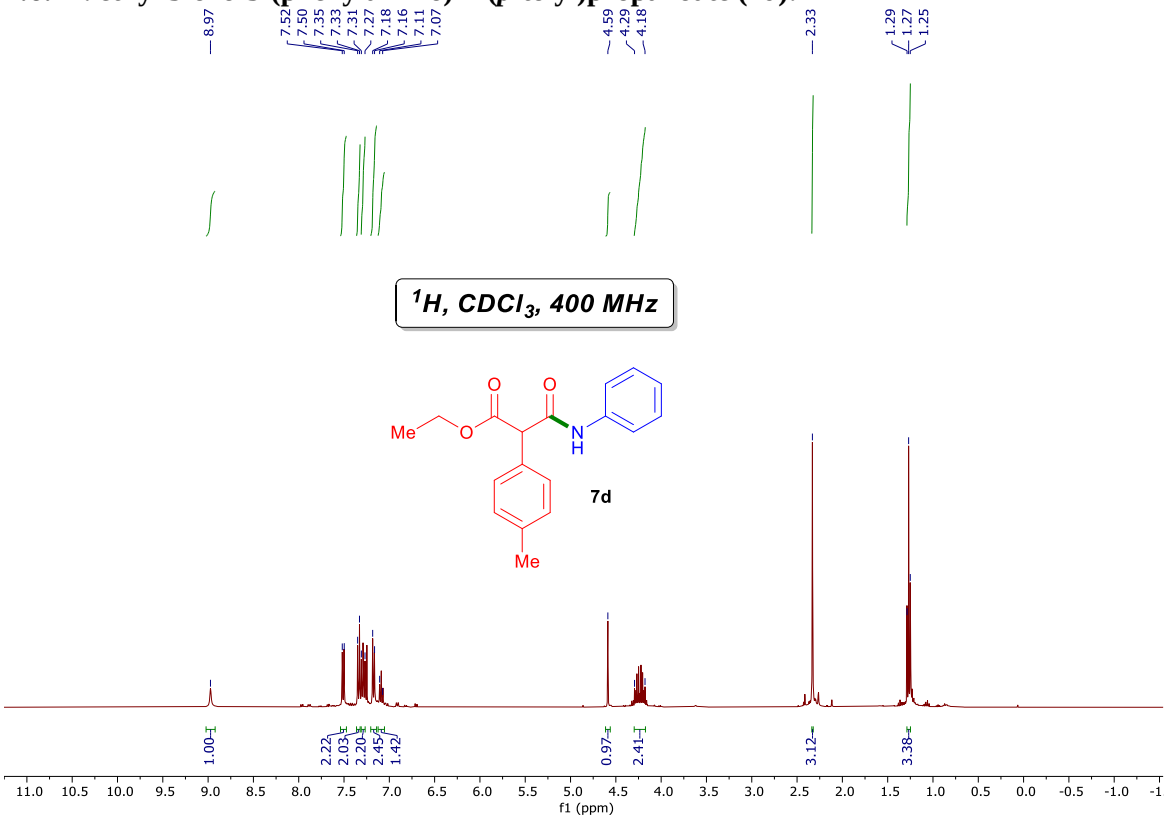
4.6.21. ethyl 3-oxo-2-phenyl-3-((2-(trifluoromethyl)phenyl)amino)propanoate (7c):

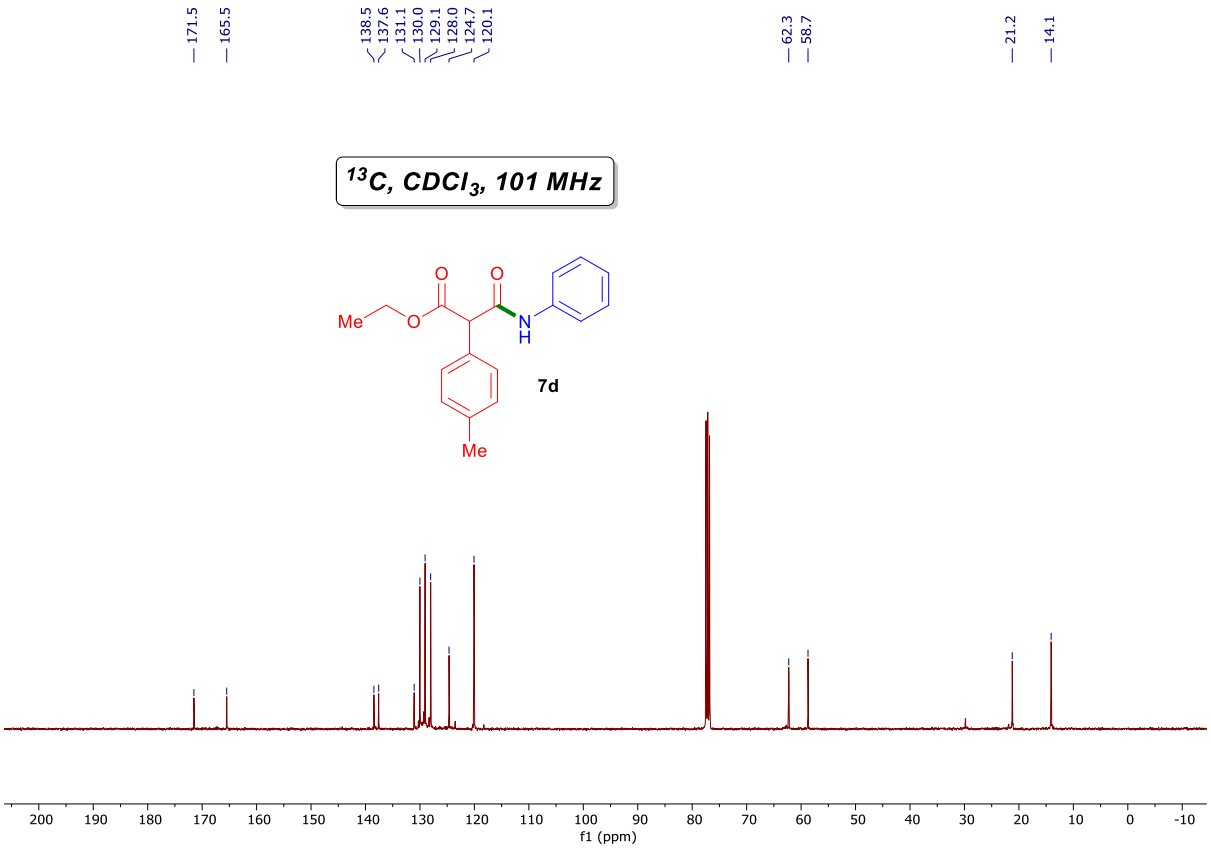




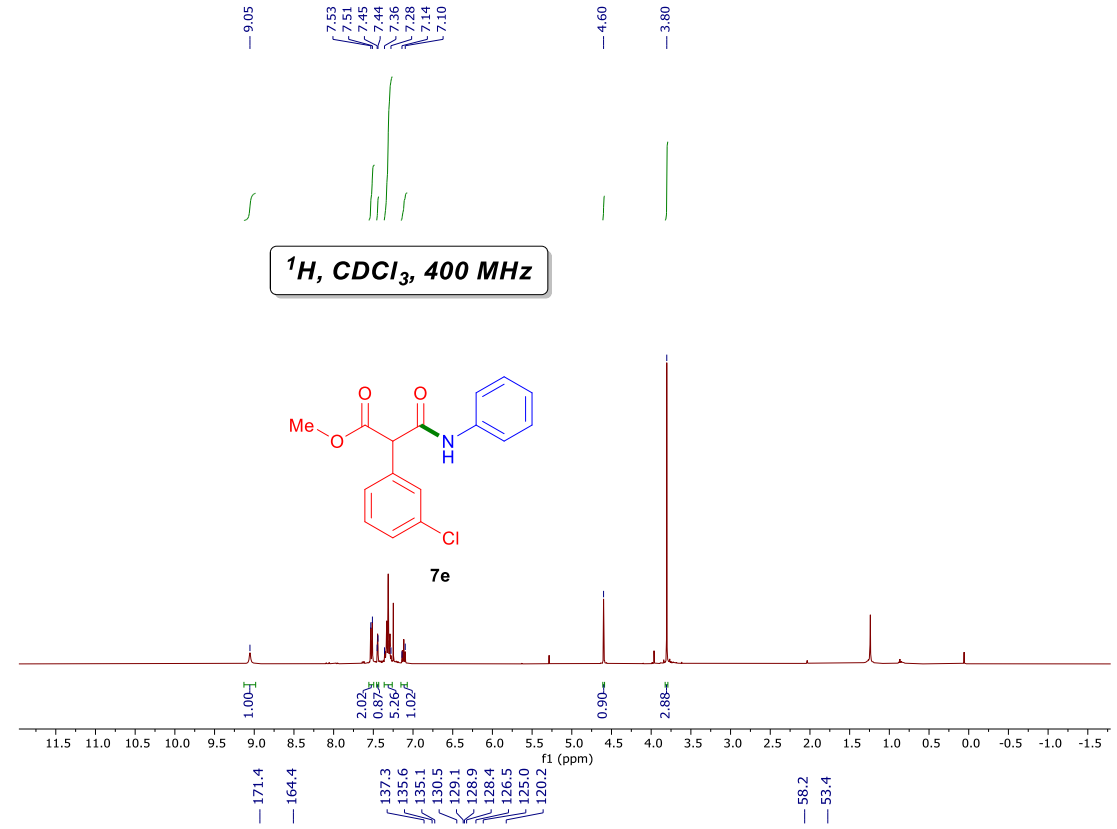

-61.01
^{19}F, $CDCl_3$, 376 MHz
Me
O
O
O
N
H
CF_3
7c
130 120 110 100 90 80 70 60 50 40 30 20 10 0 -10 -20 -30 -40 -50 -60 -70 -80 -90 -100 -110 -120 -130 -140 -150 -160
f1 (ppm)

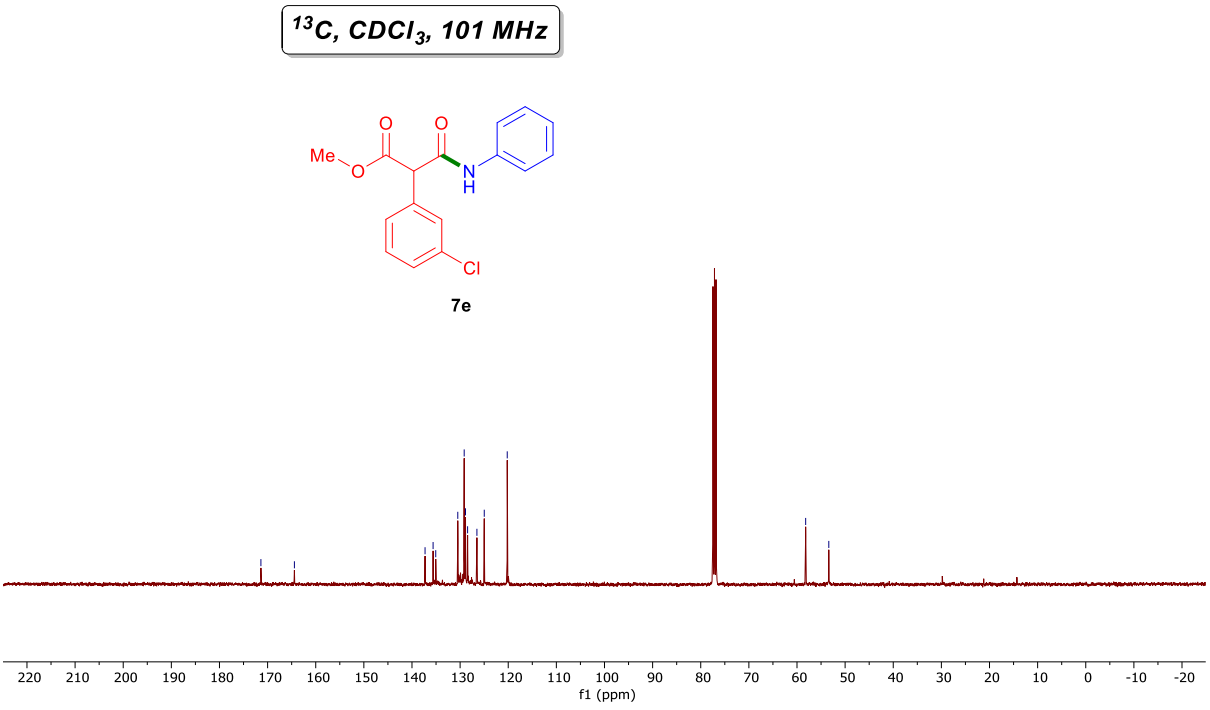
4.6.22. ethyl 3-oxo-3-(phenylamino)-2-(*p*-tolyl)propanoate (7d):



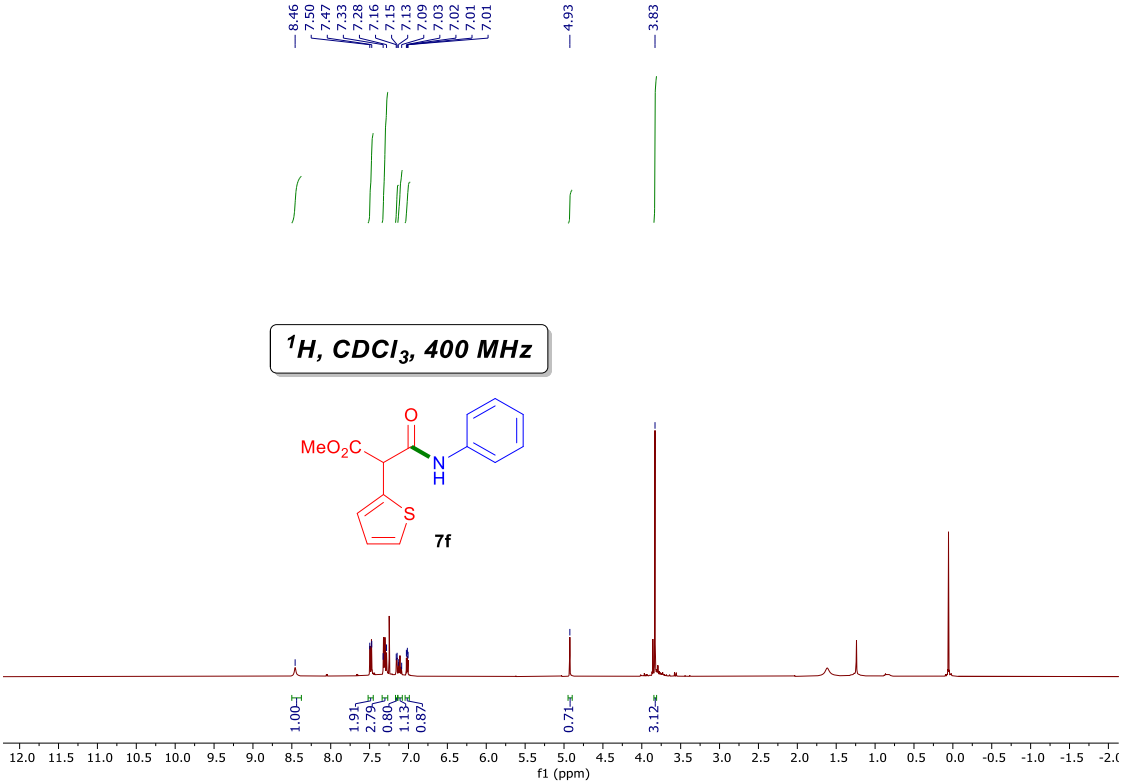


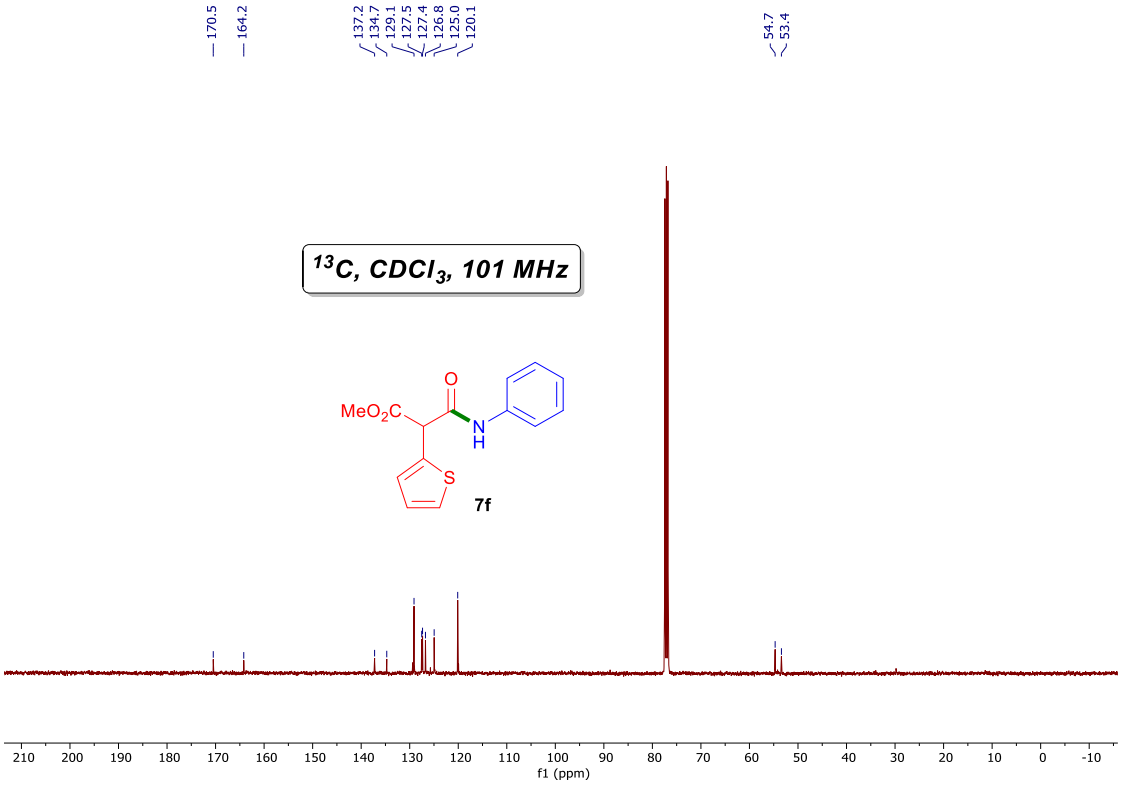
4.6.23. methyl 2-(3-chlorophenyl)-3-oxo-3-(phenylamino)propanoate (7e):



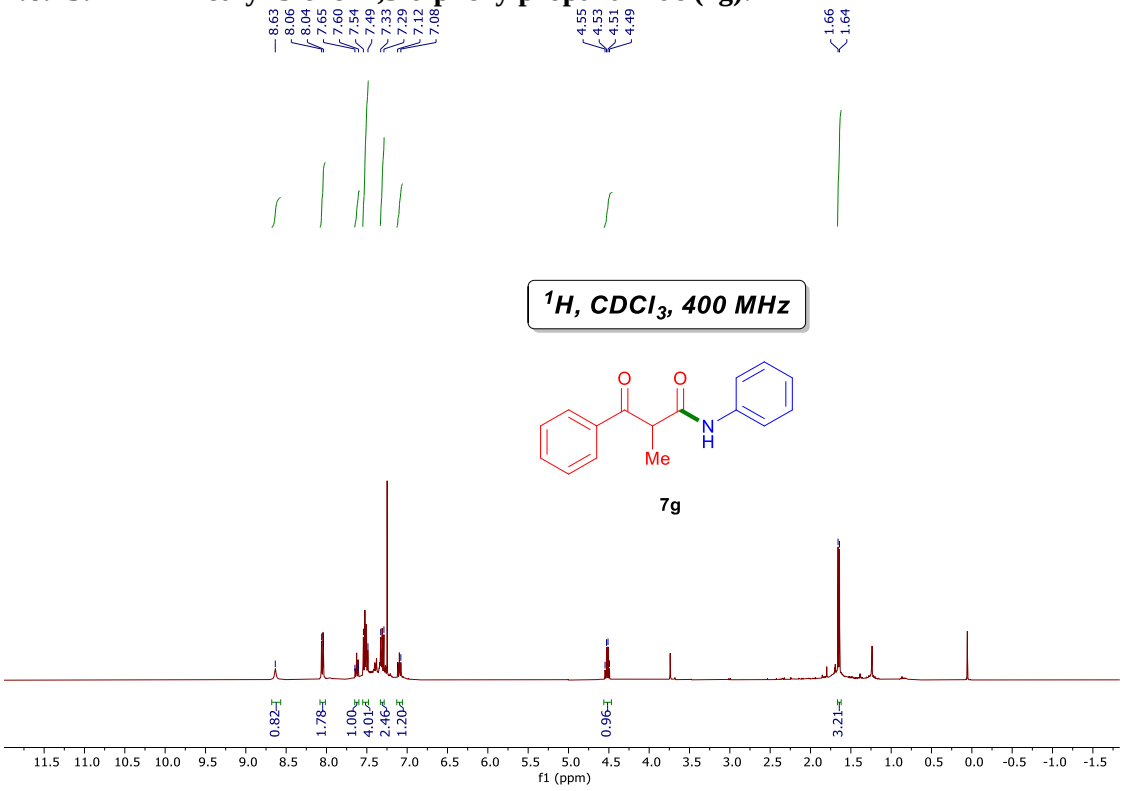


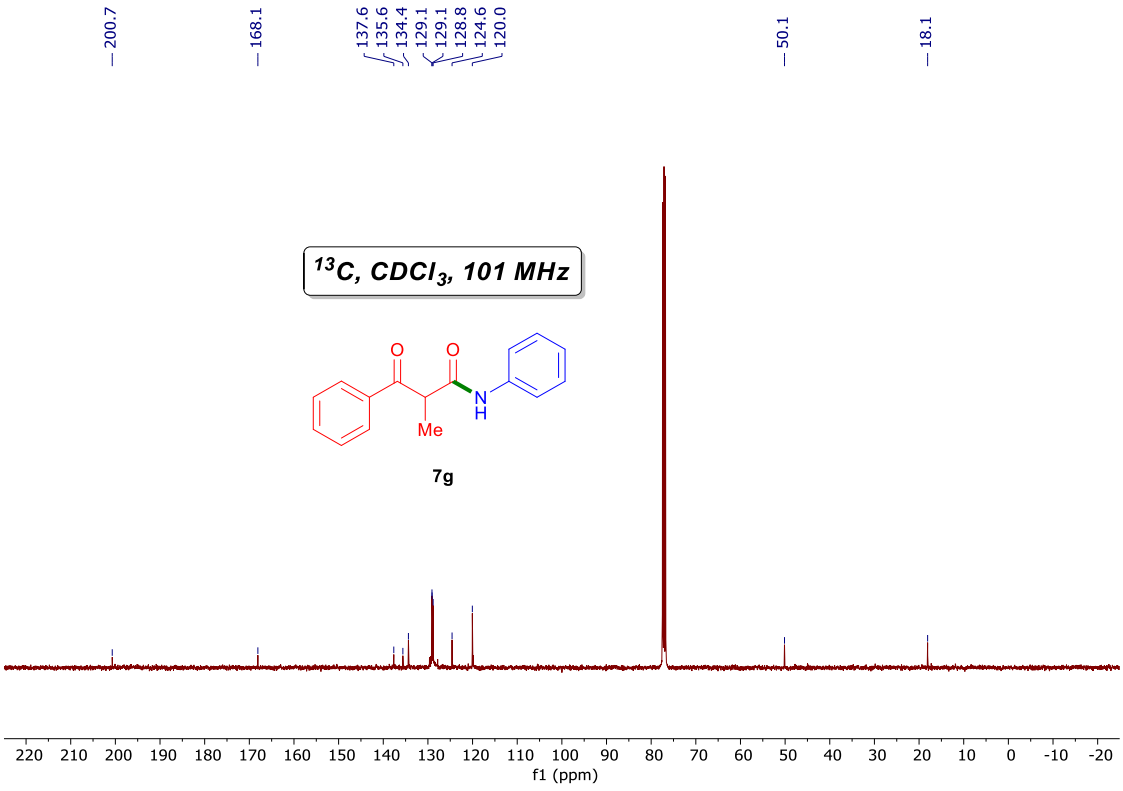
4.6.24. methyl 3-oxo-3-(phenylamino)-2-(thiophen-2-yl)propanoate (7f):



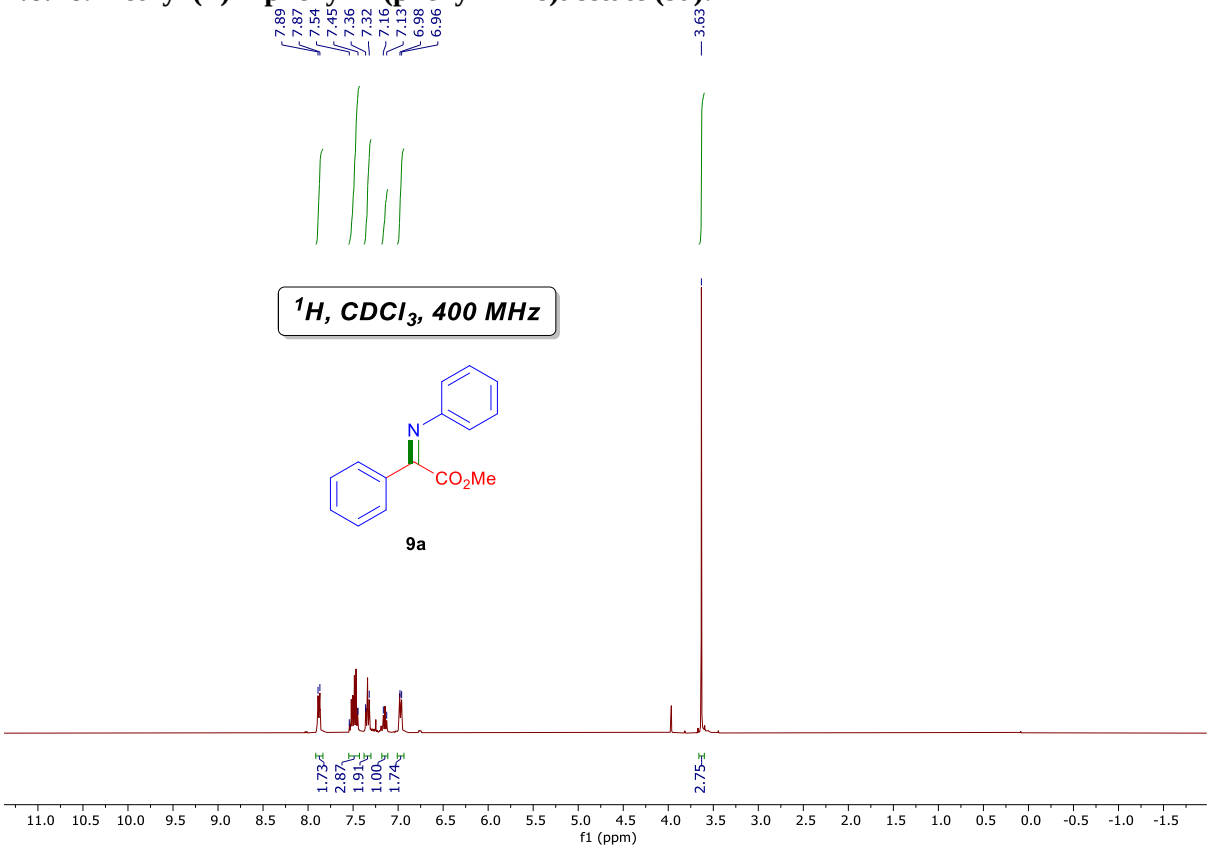


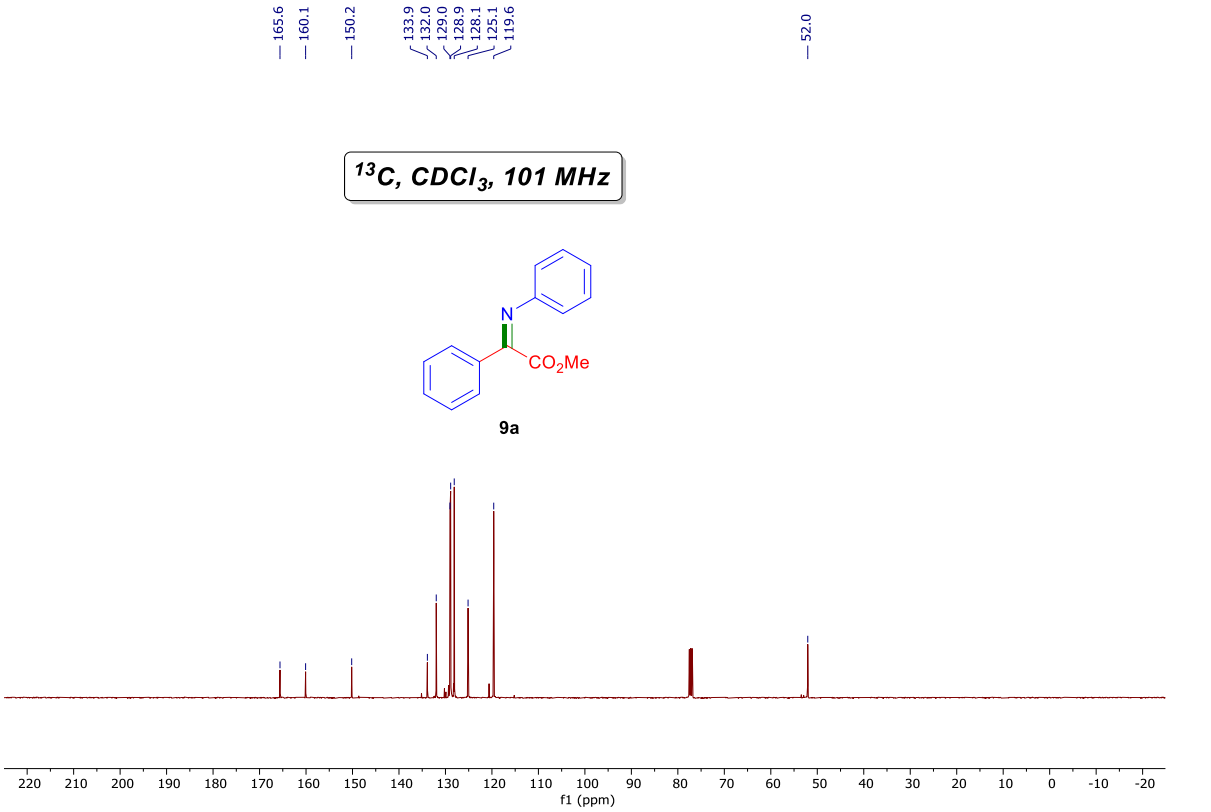
4.6.25. 2-methyl-3-oxo-N,3-diphenylpropanamide (7g):



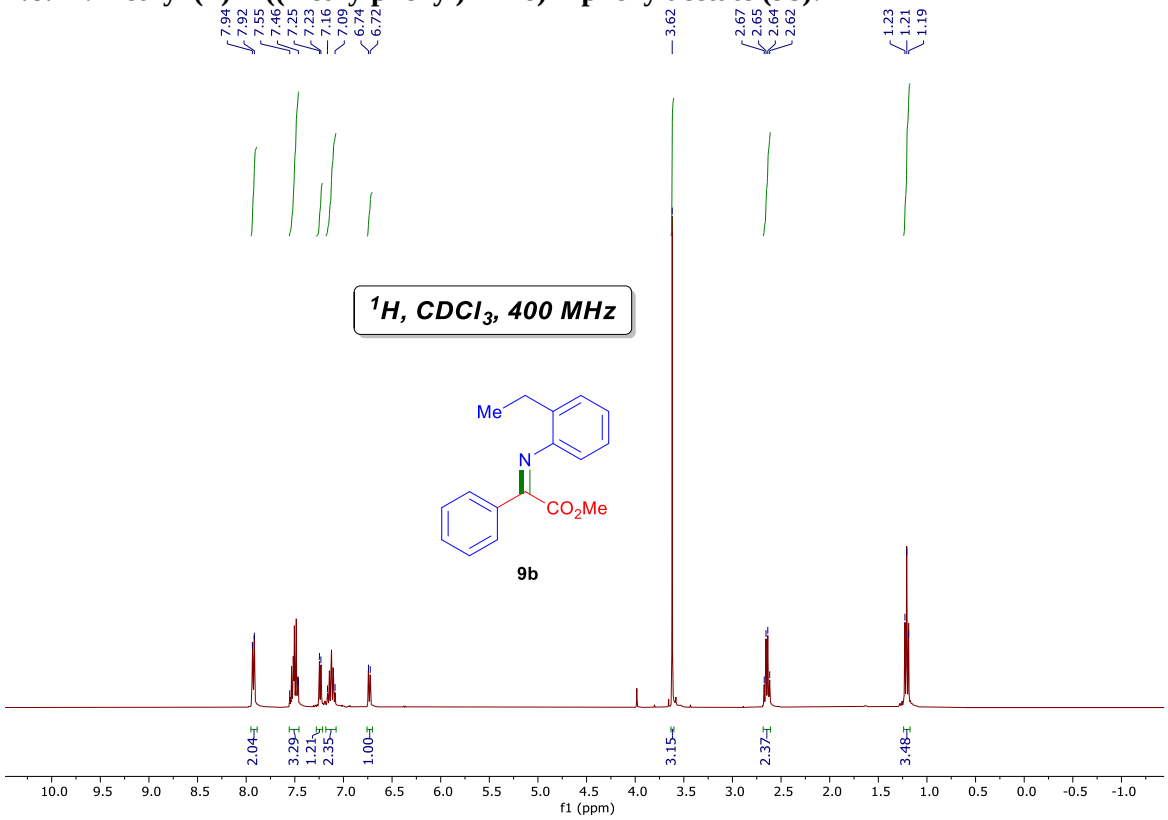


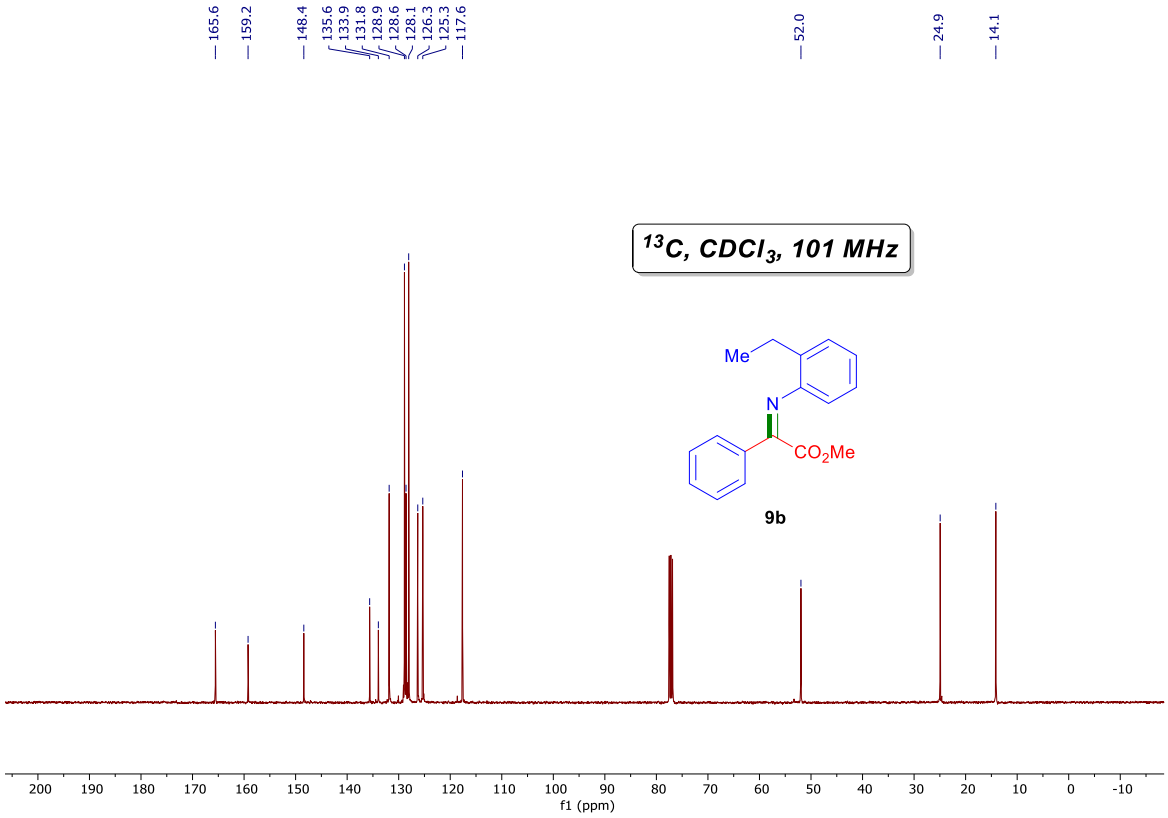
4.6.26. methyl (*Z*)-2-phenyl-2-(phenylimino)acetate (9a):



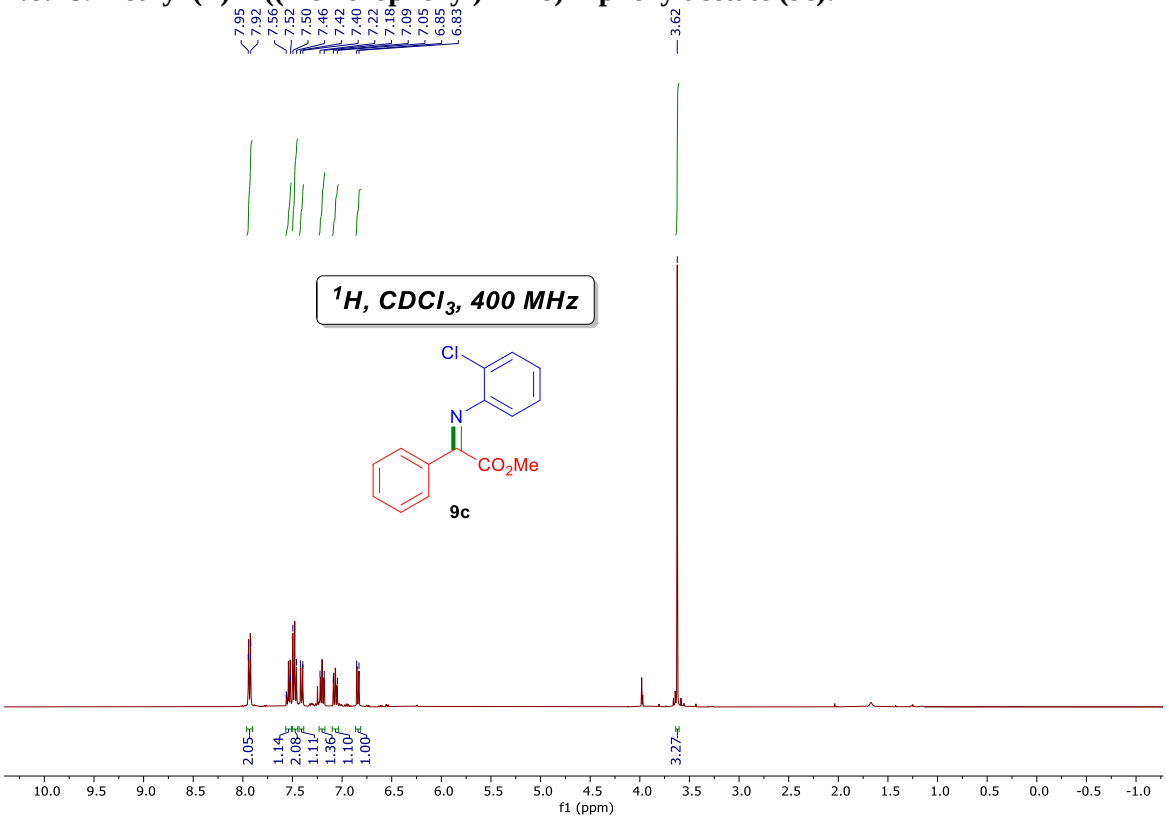


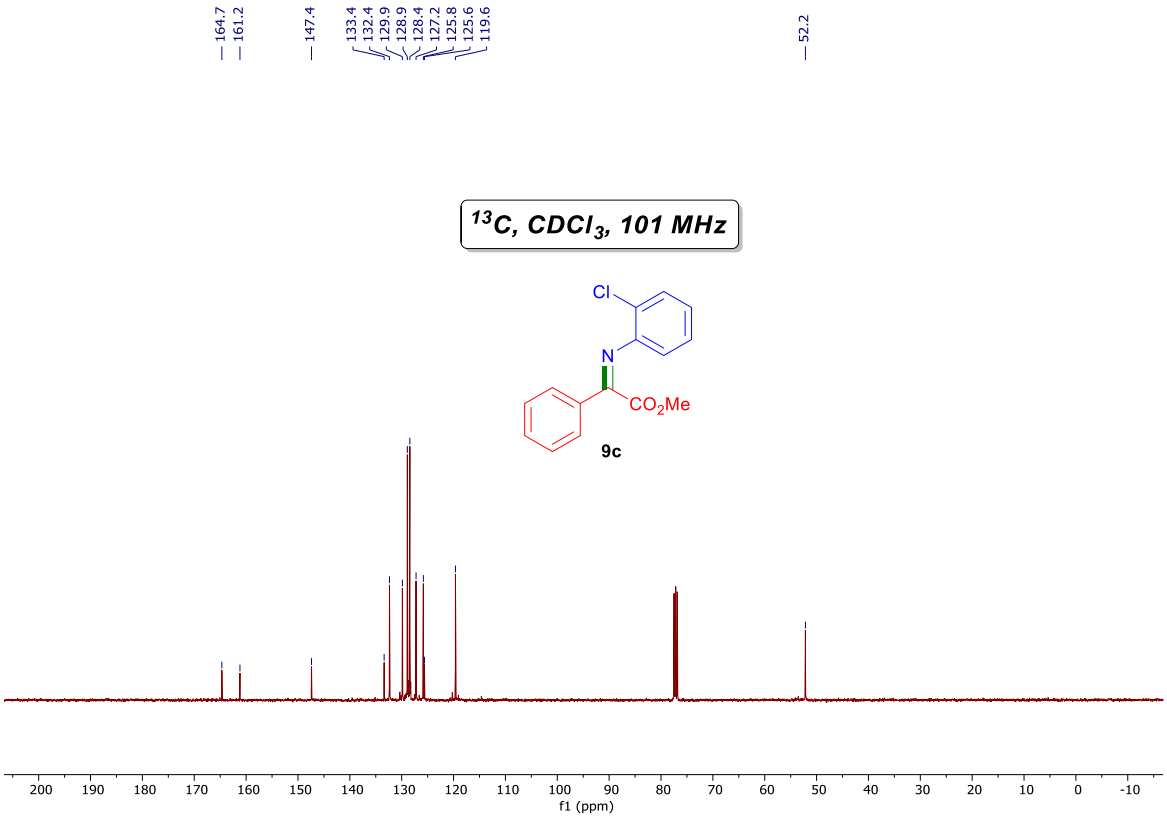
4.6.27. methyl (*Z*)-2-((2-ethylphenyl)imino)-2-phenylacetate (9b):



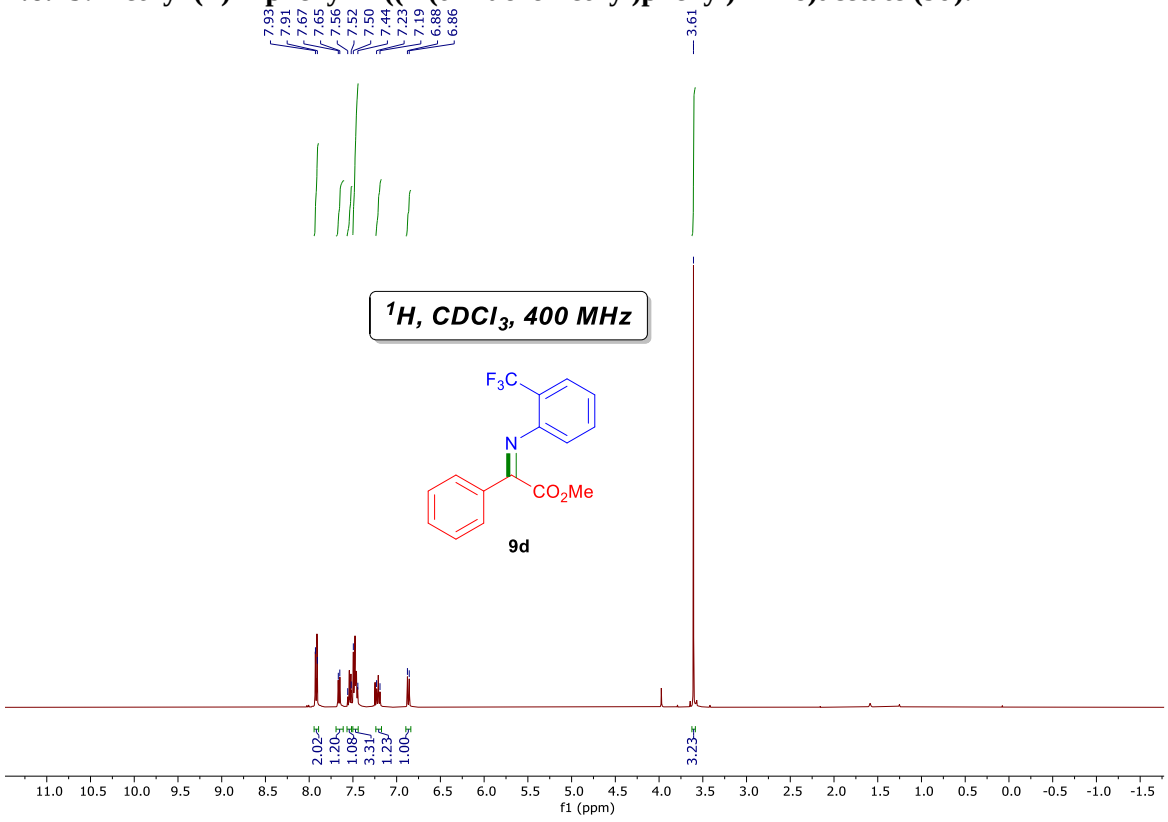


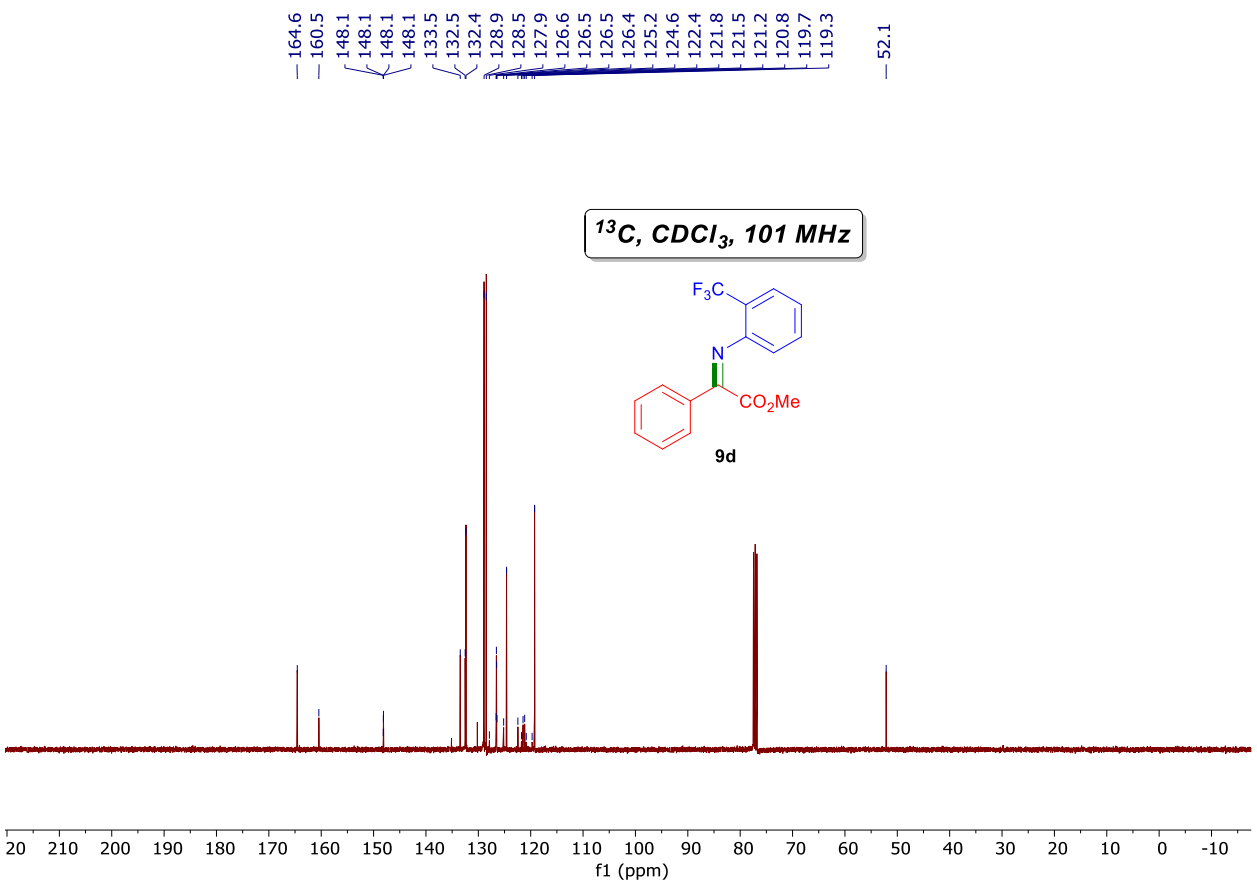
4.6.28. methyl (*Z*)-2-((2-chlorophenyl)imino)-2-phenylacetate (9c):



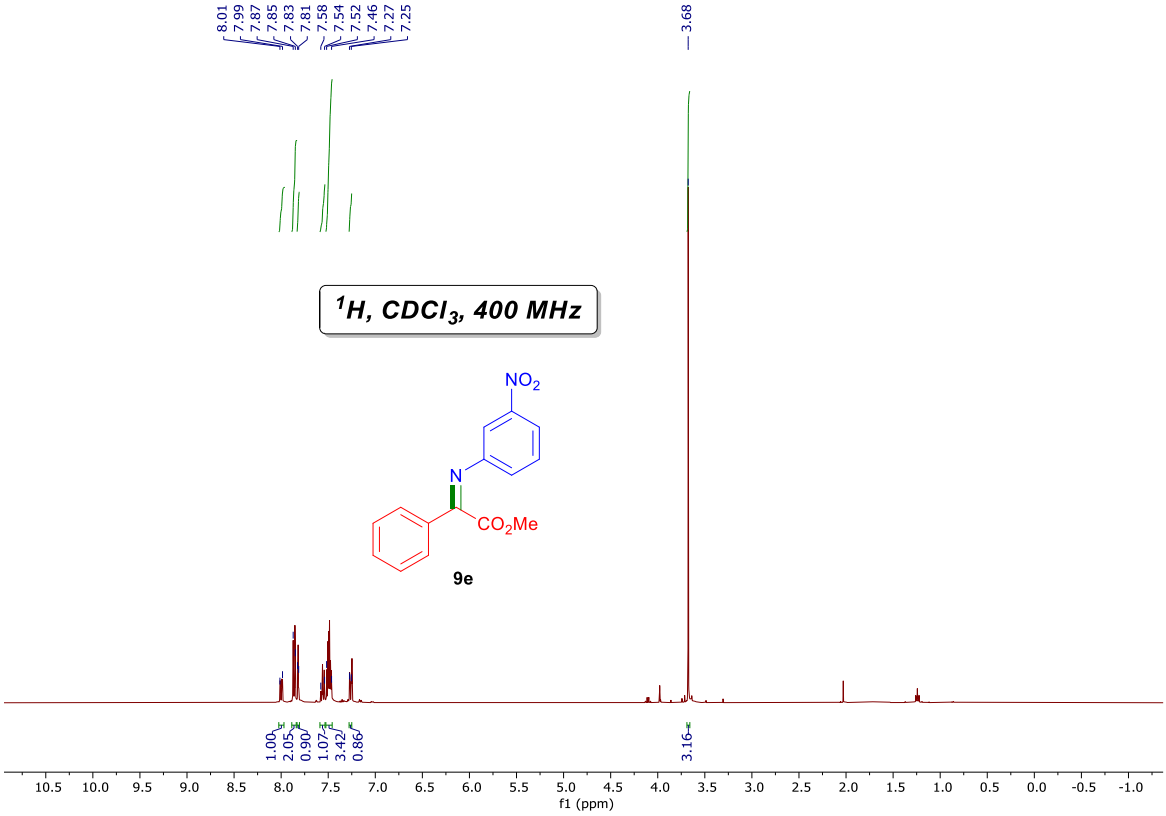


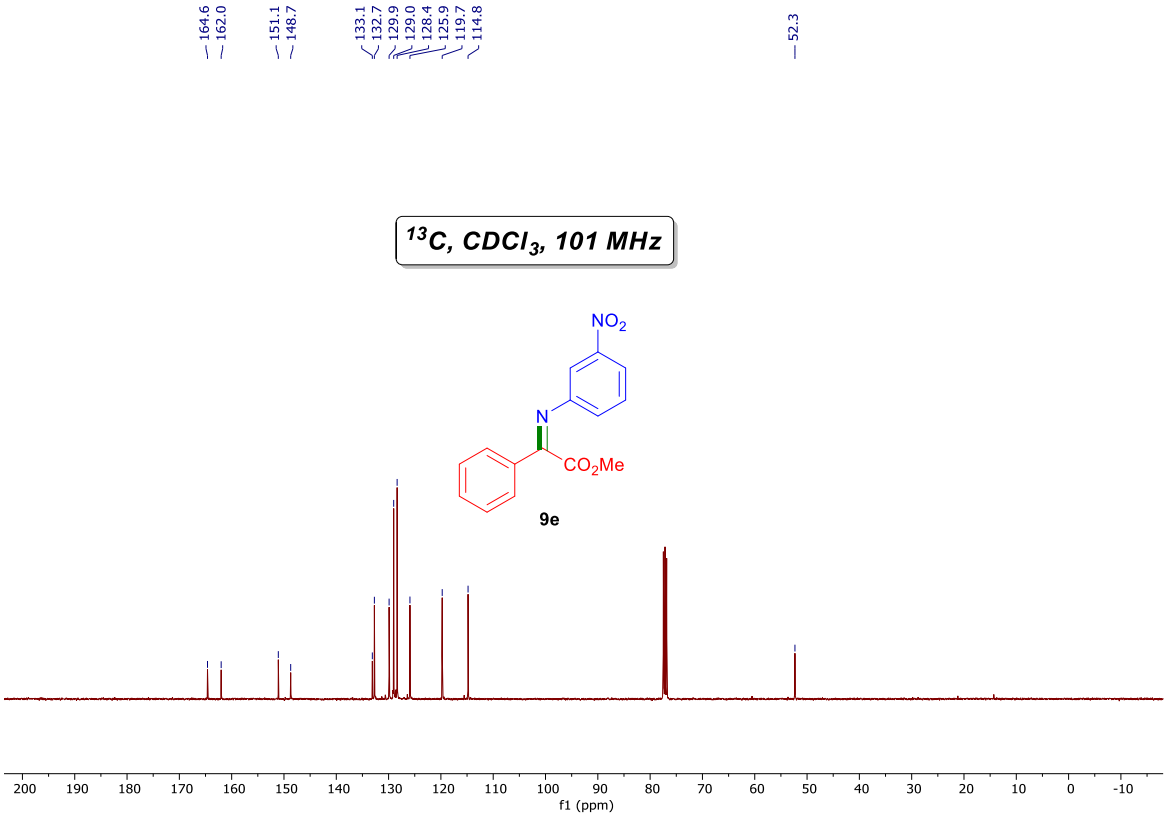
4.6.29. methyl (*Z*)-2-phenyl-2-((2-(trifluoromethyl)phenyl)imino)acetate (9d):



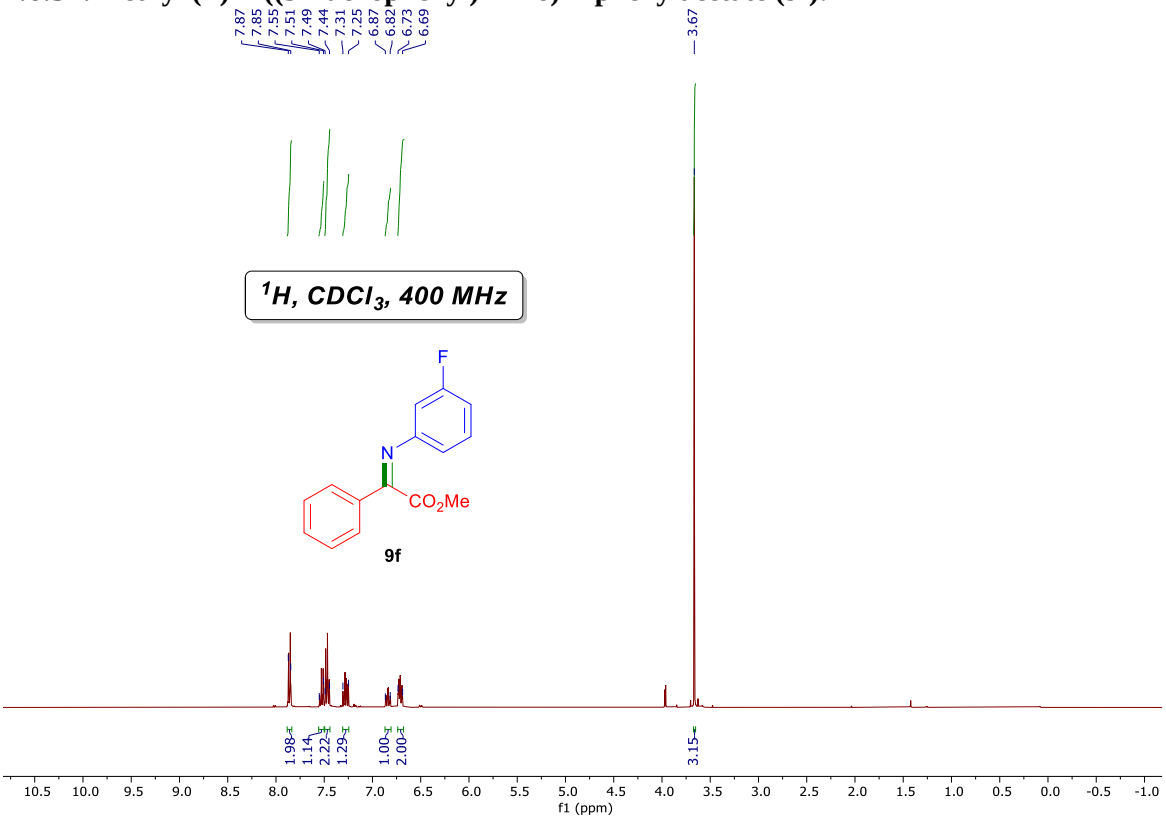


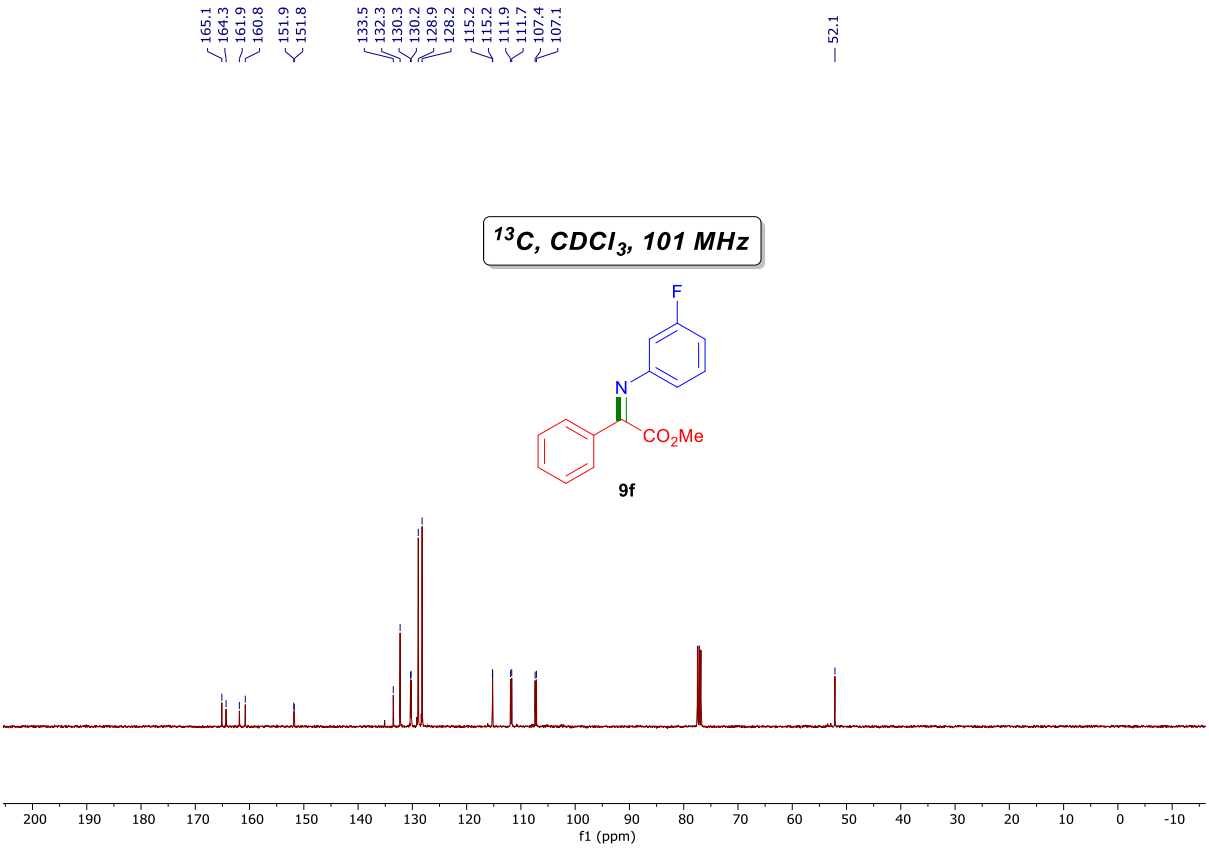
4.6.30. methyl (*Z*)-2-((3-nitrophenyl)imino)-2-phenylacetate (9e):

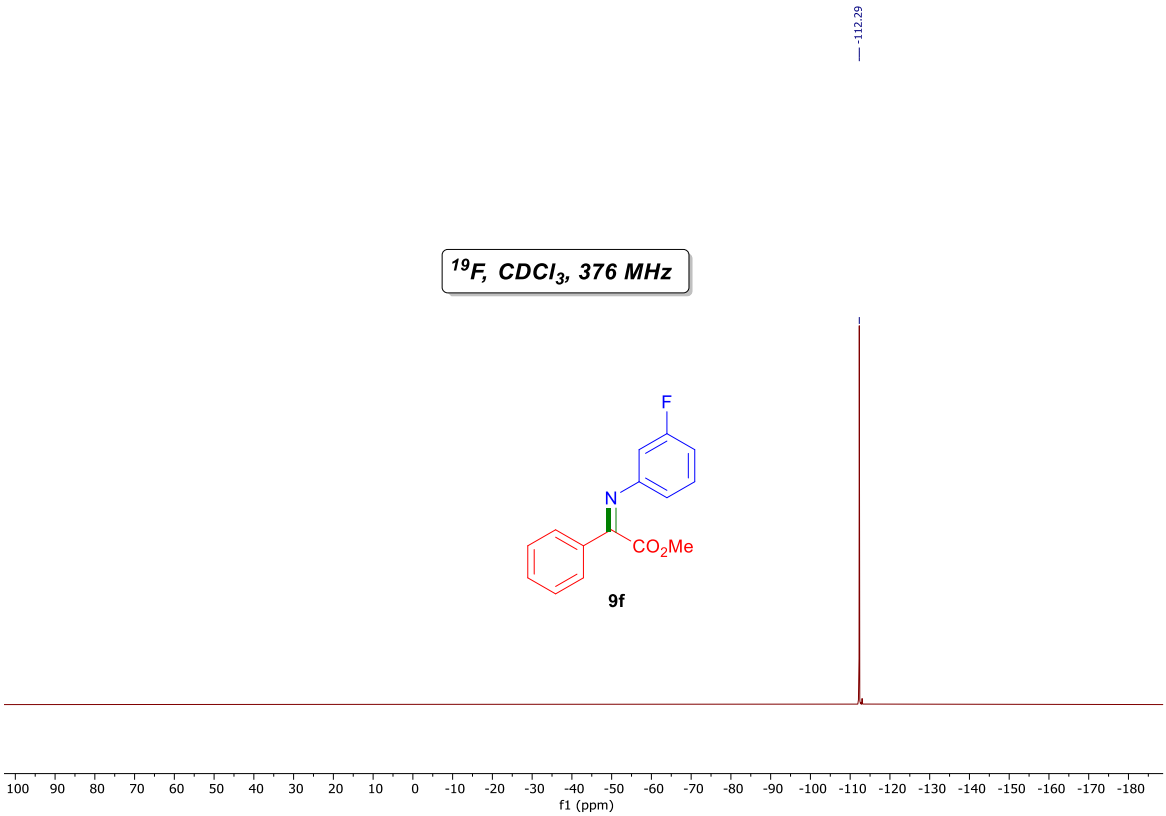




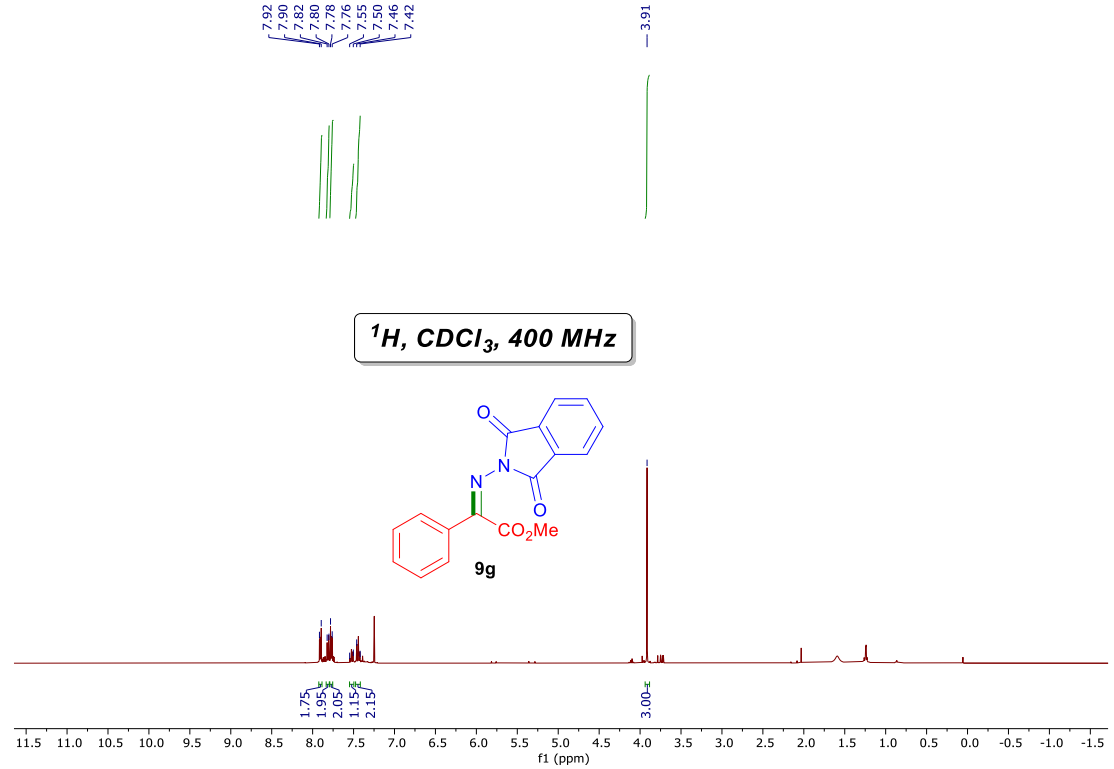
4.6.31. methyl (*Z*)-2-((3-fluorophenyl)imino)-2-phenylacetate (9f):

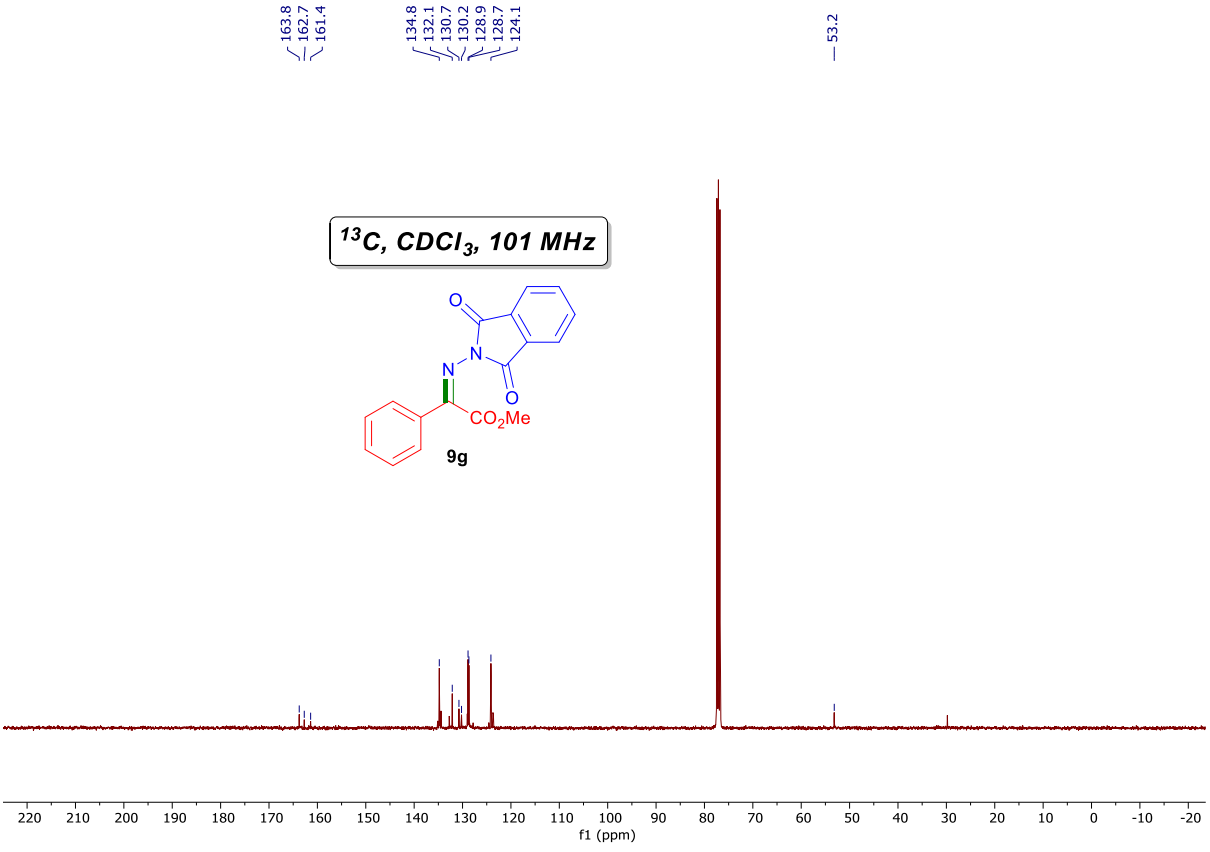




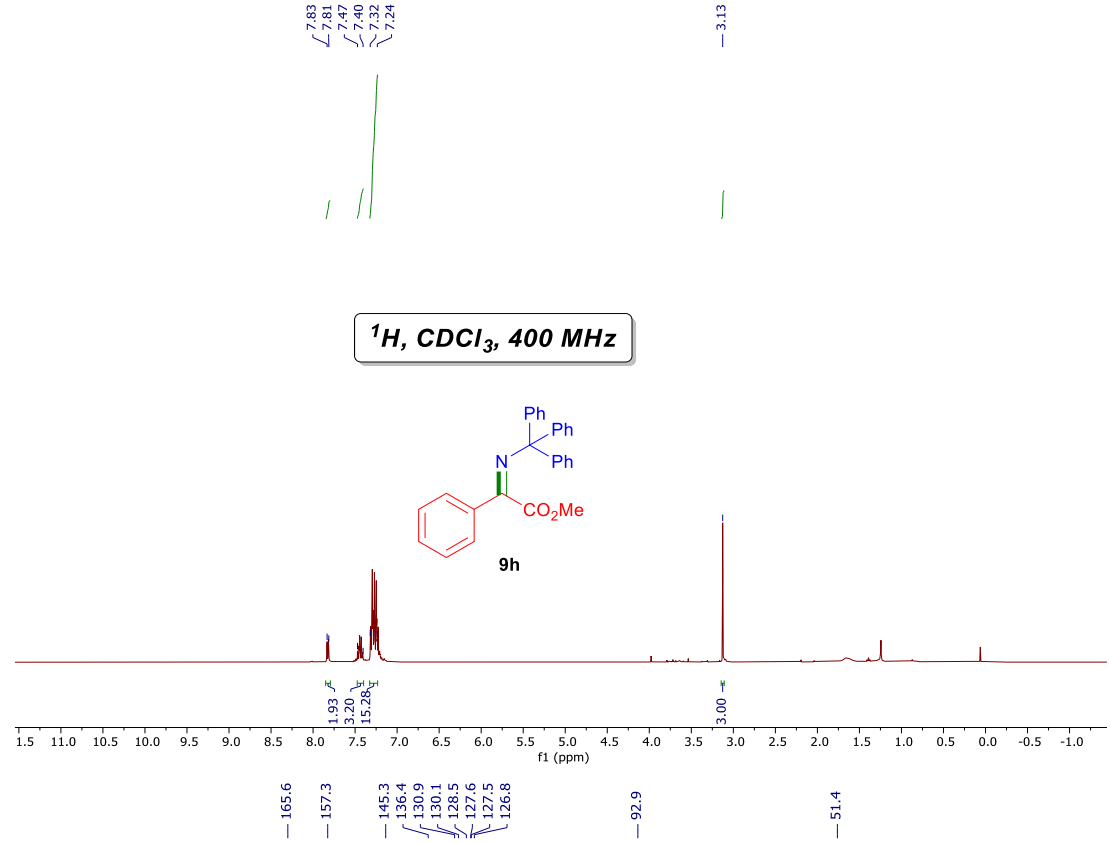

-112.29
^{19}F, $CDCl_3$, 376 MHz
F
N
CO_2Me
9f
100 90 80 70 60 50 40 30 20 10 0 -10 -20 -30 -40 -50 -60 -70 -80 -90 -100 -110 -120 -130 -140 -150 -160 -170 -180
f1 (ppm)

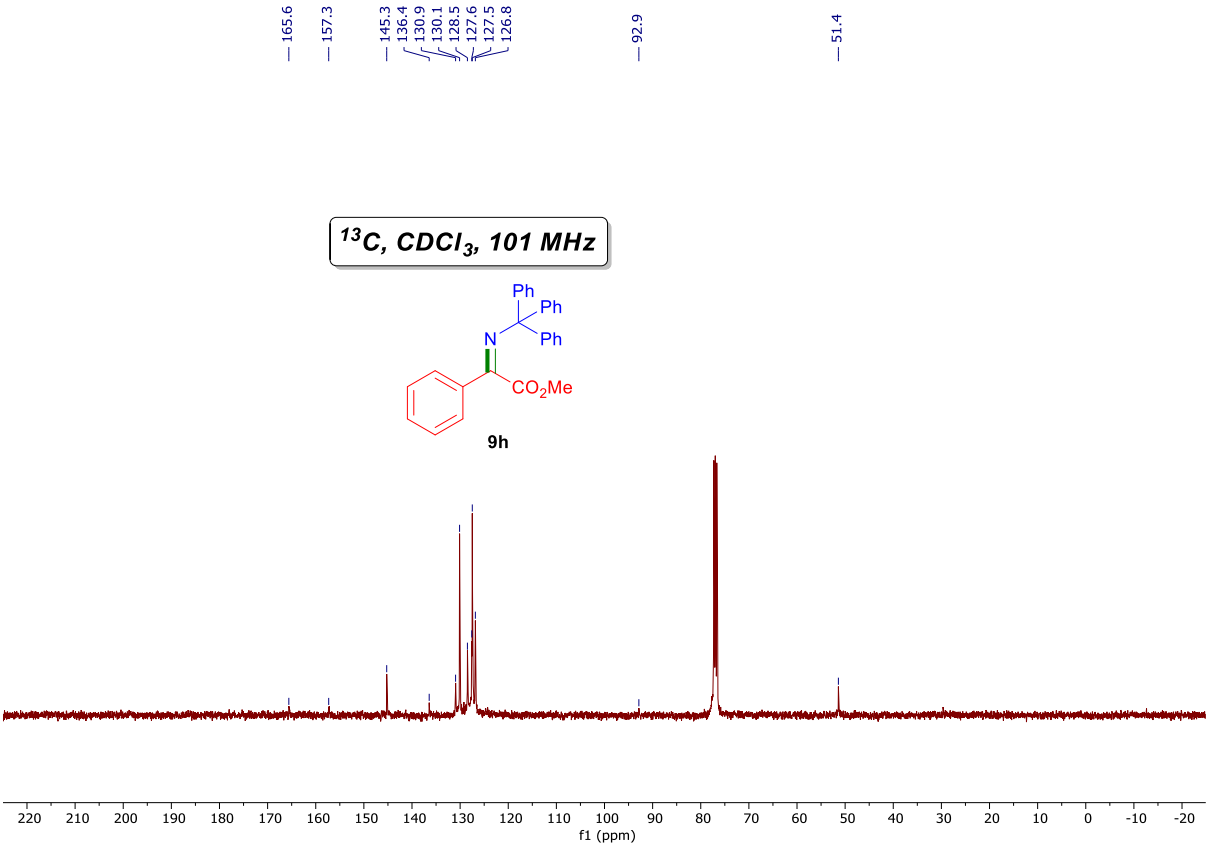
4.6.32. methyl (*Z*)-2-((1,3-dioxoisoindolin-2-yl)imino)-2-phenylacetate (9g):



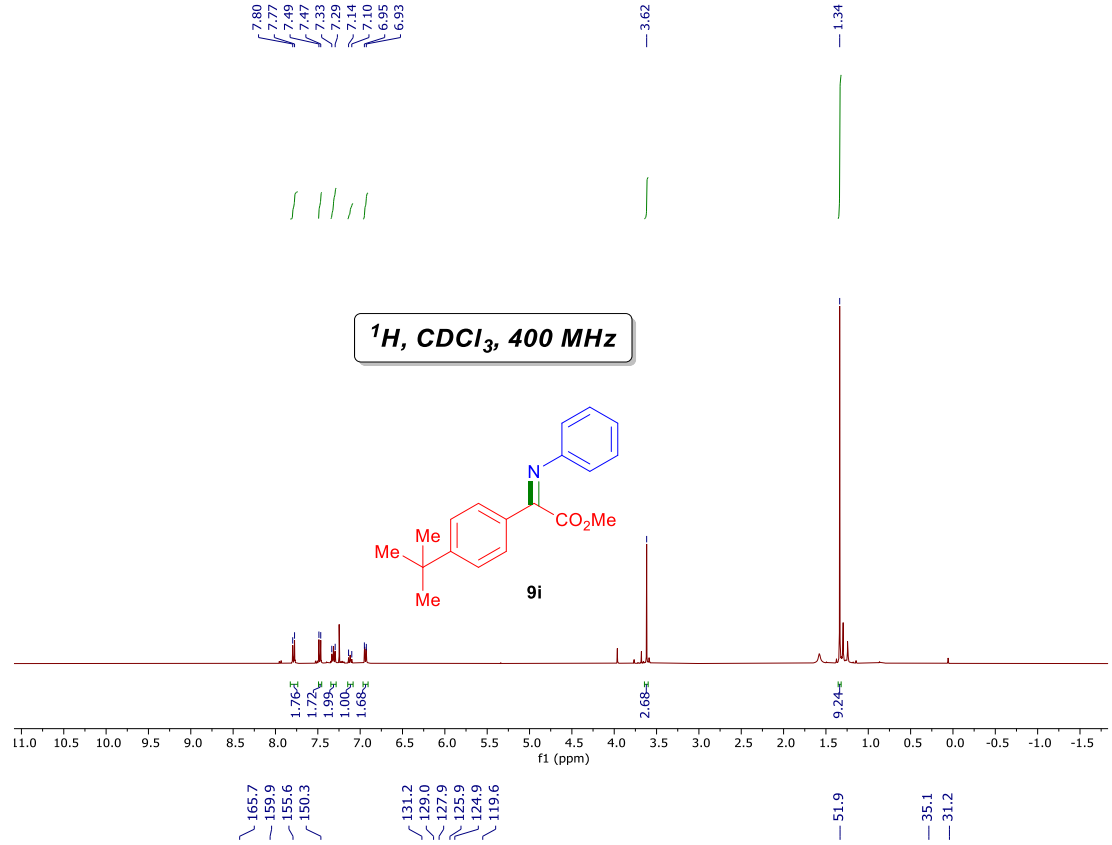


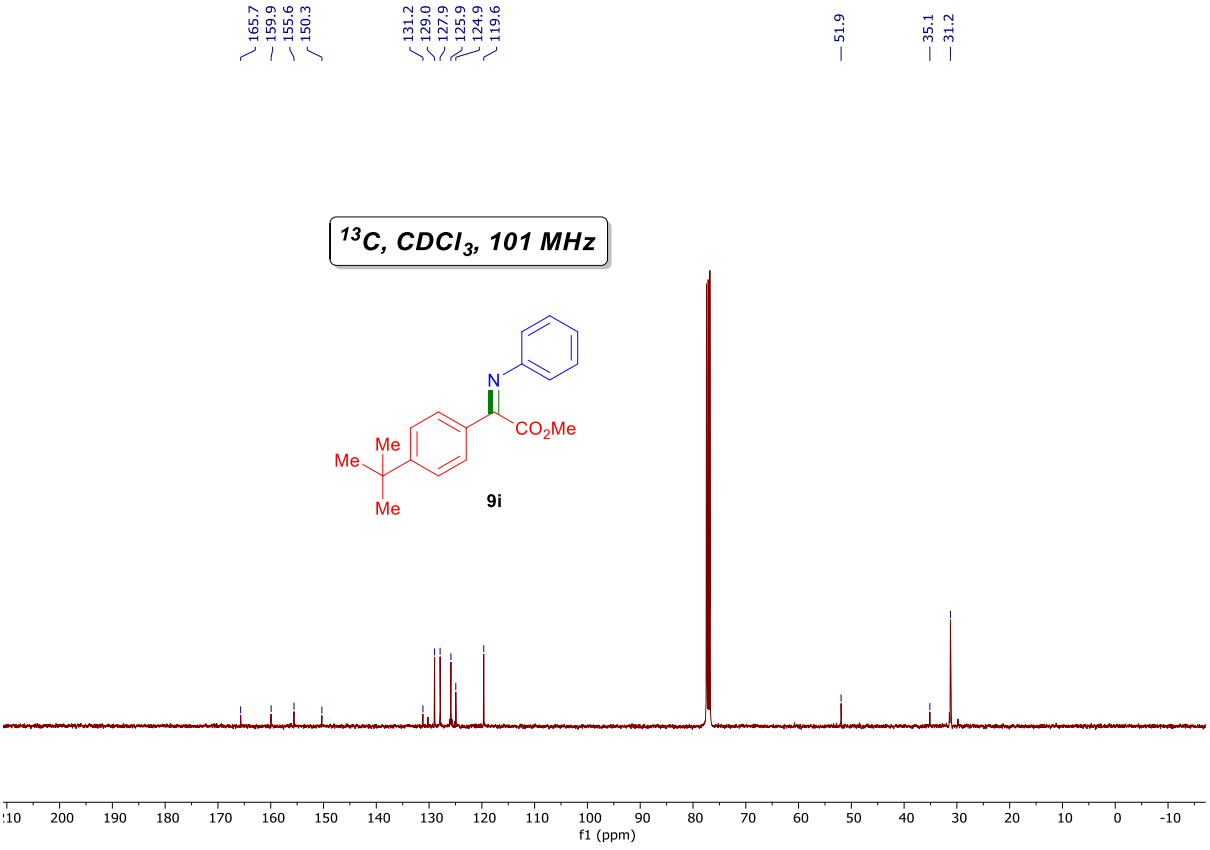
4.6.33. methyl (*Z*)-2-((1,3-dioxoisoindolin-2-yl)imino)-2-phenylacetate (9h):



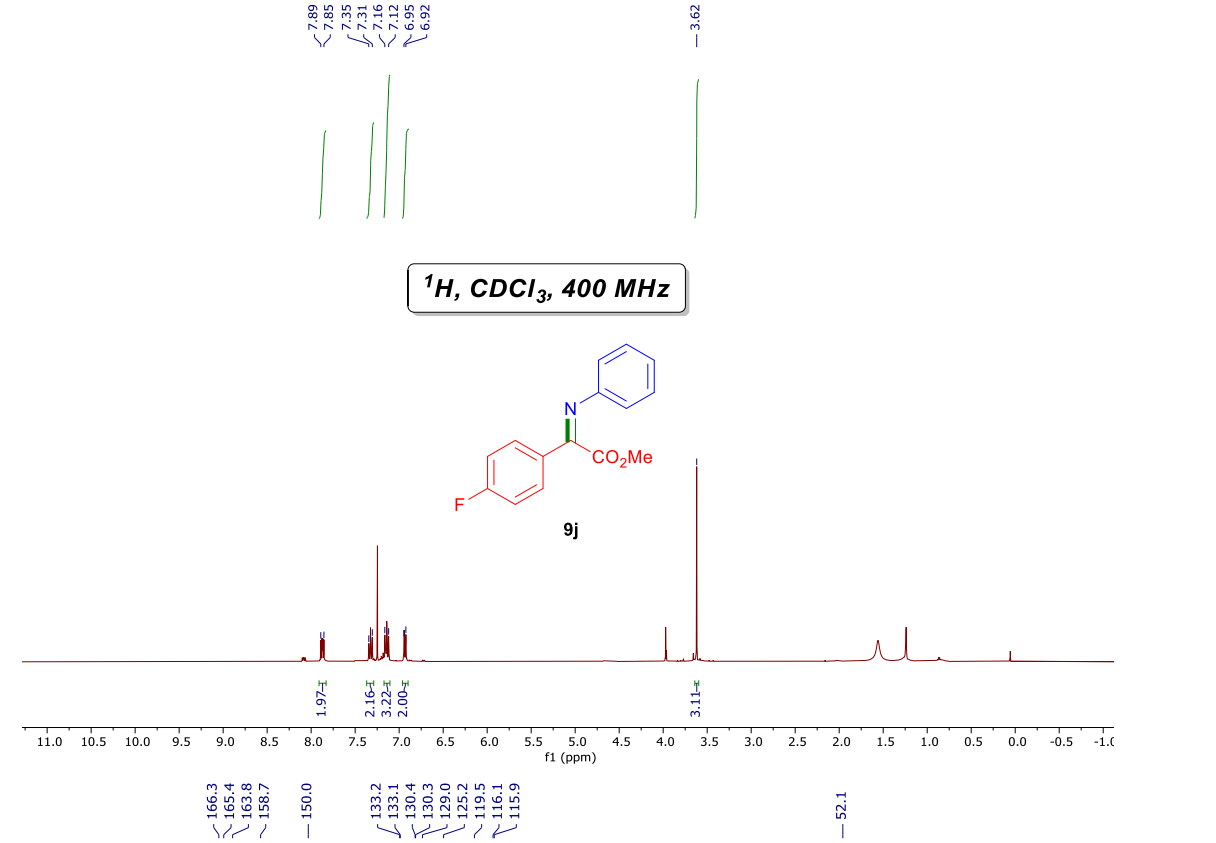


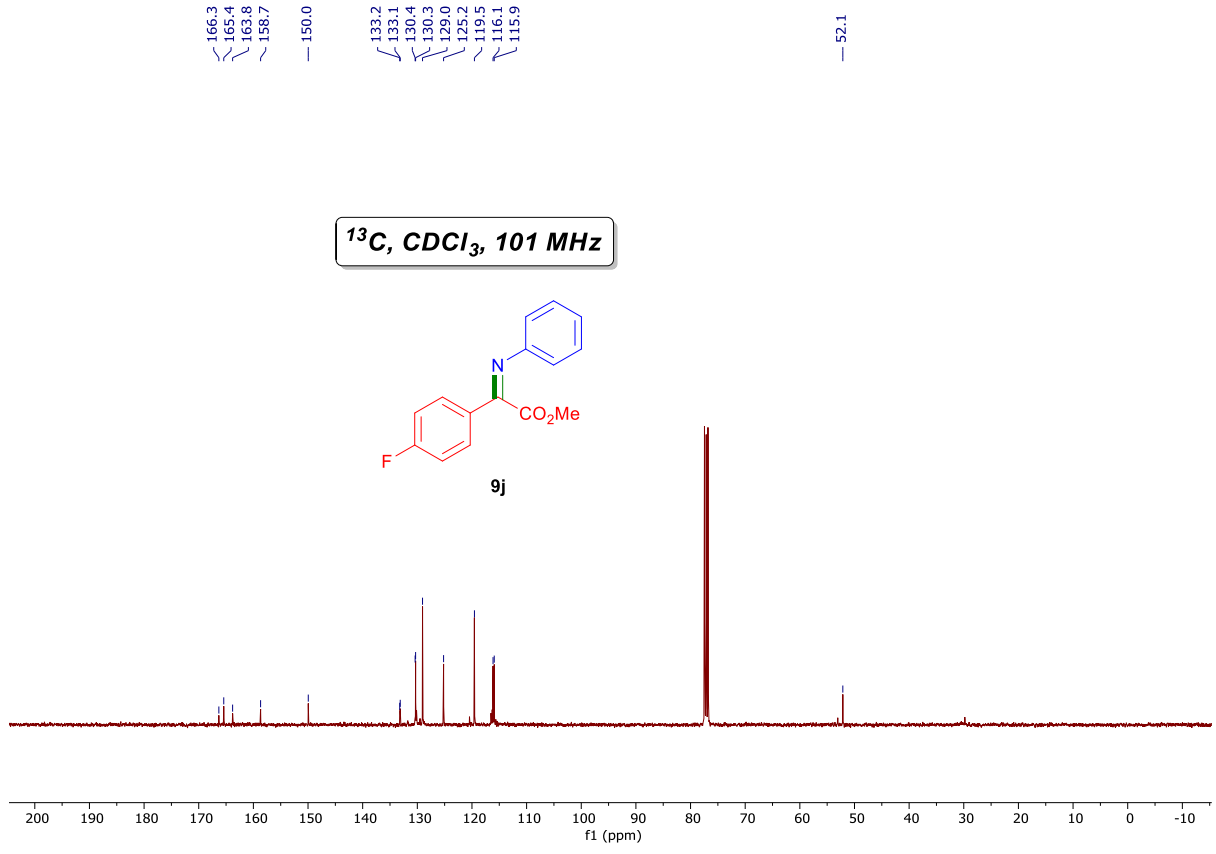
4.6.34. methyl (*Z*)-2-(4-(*tert*-butyl)phenyl)-2-(phenylimino)acetate (9i):

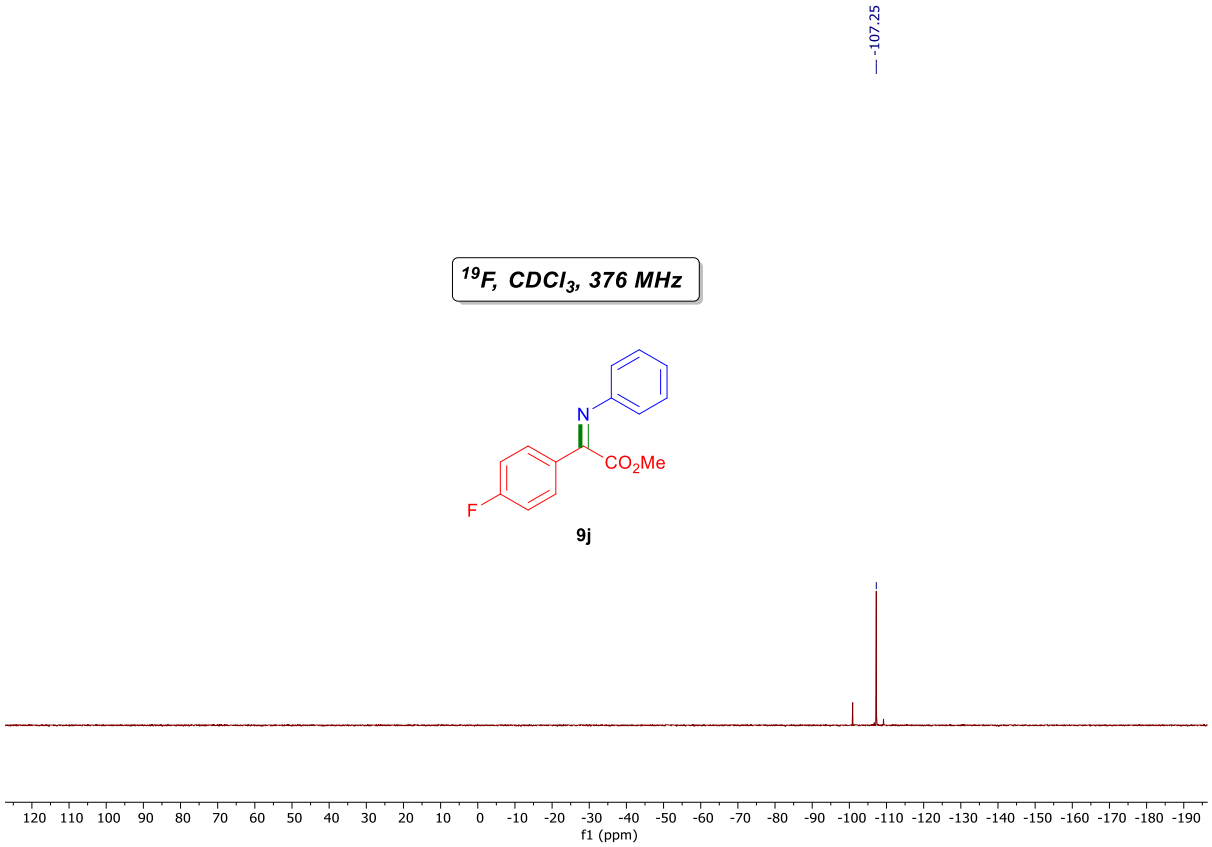




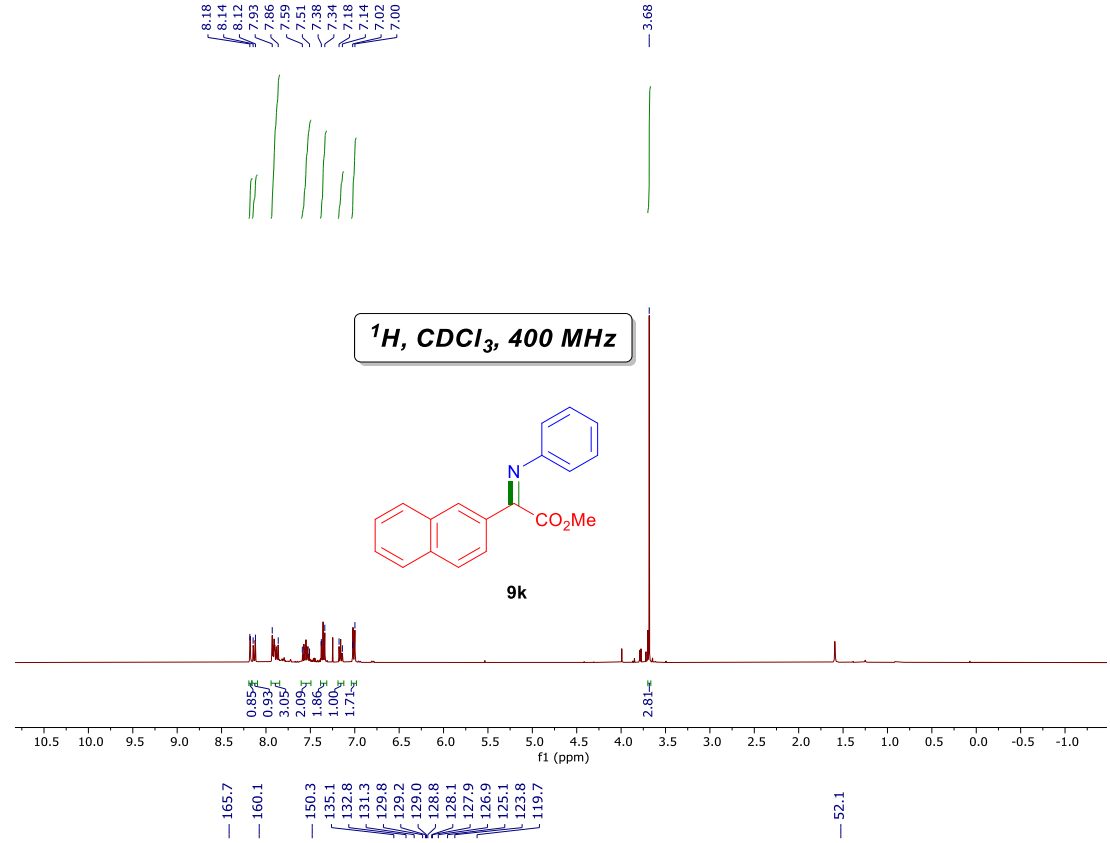
4.6.35. methyl (*Z*)-2-(4-fluorophenyl)-2-(phenylimino)acetate (9j):

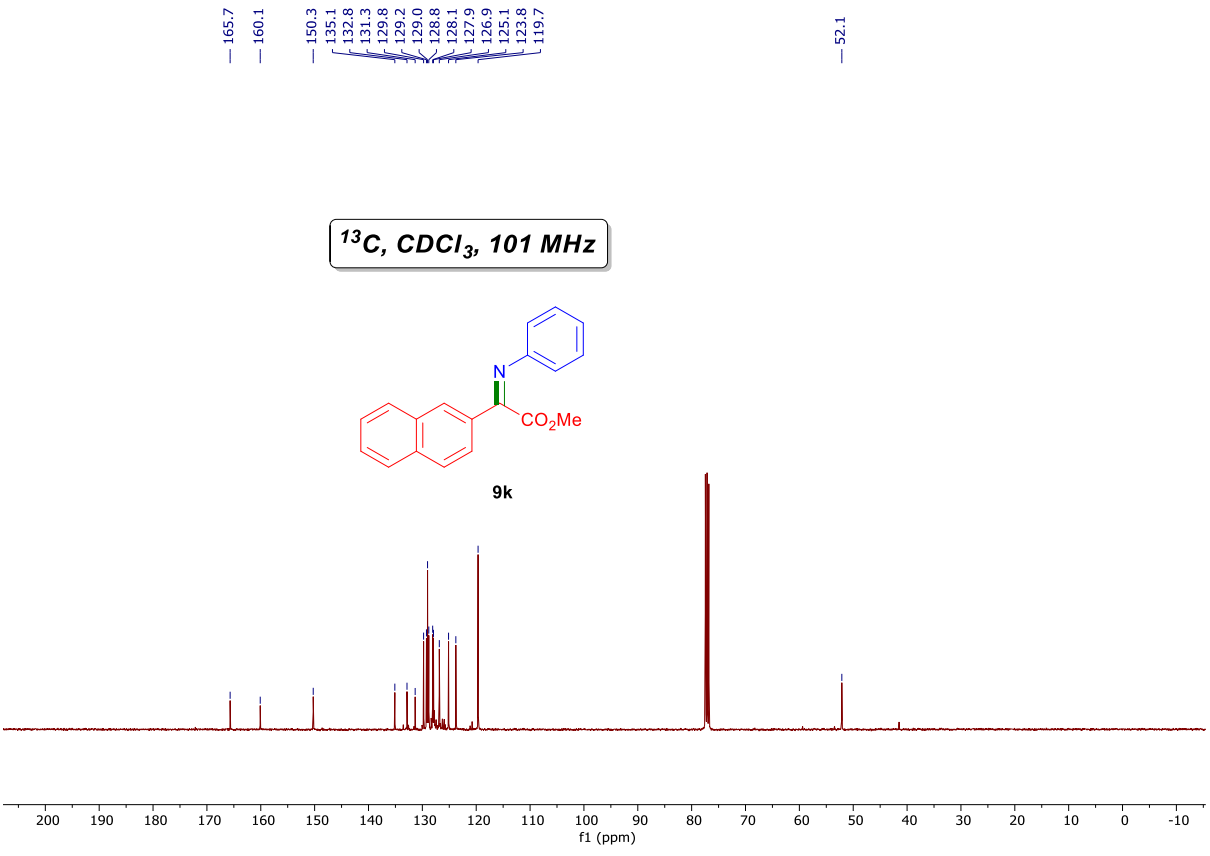




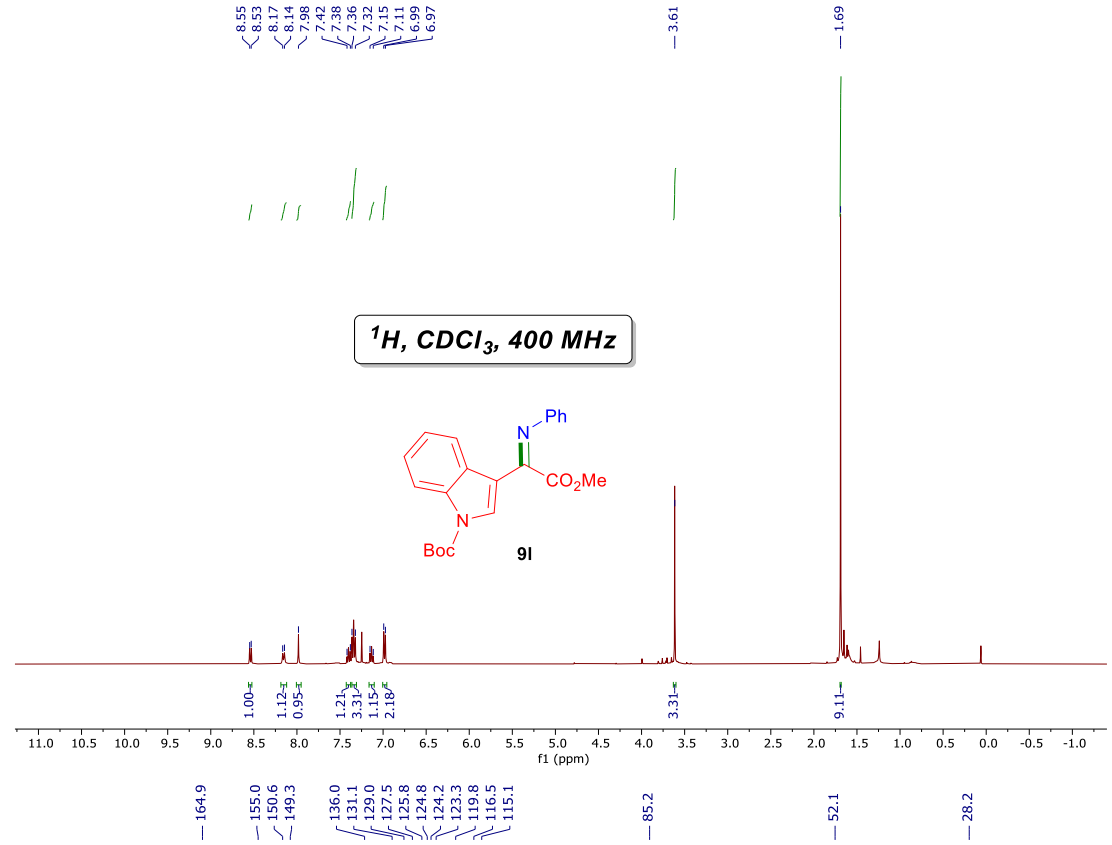

-107.25
^{19}F, $CDCl_3$, 376 MHz
N
CO_2Me
F
9j
120 110 100 90 80 70 60 50 40 30 20 10 0 -10 -20 -30 -40 -50 -60 -70 -80 -90 -100 -110 -120 -130 -140 -150 -160 -170 -180 -190
f1 (ppm)

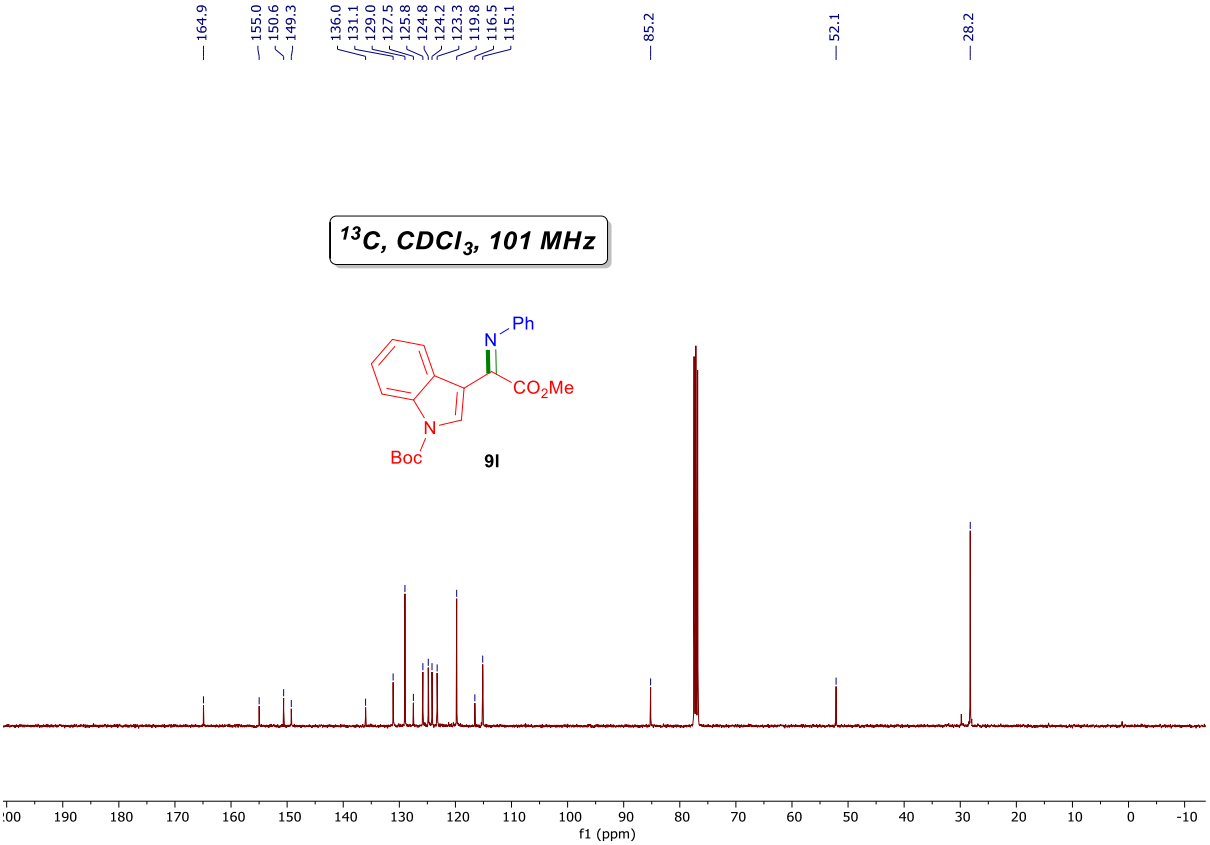
4.6.36. methyl (*Z*)-2-(naphthalen-2-yl)-2-(phenylimino)acetate (9k):



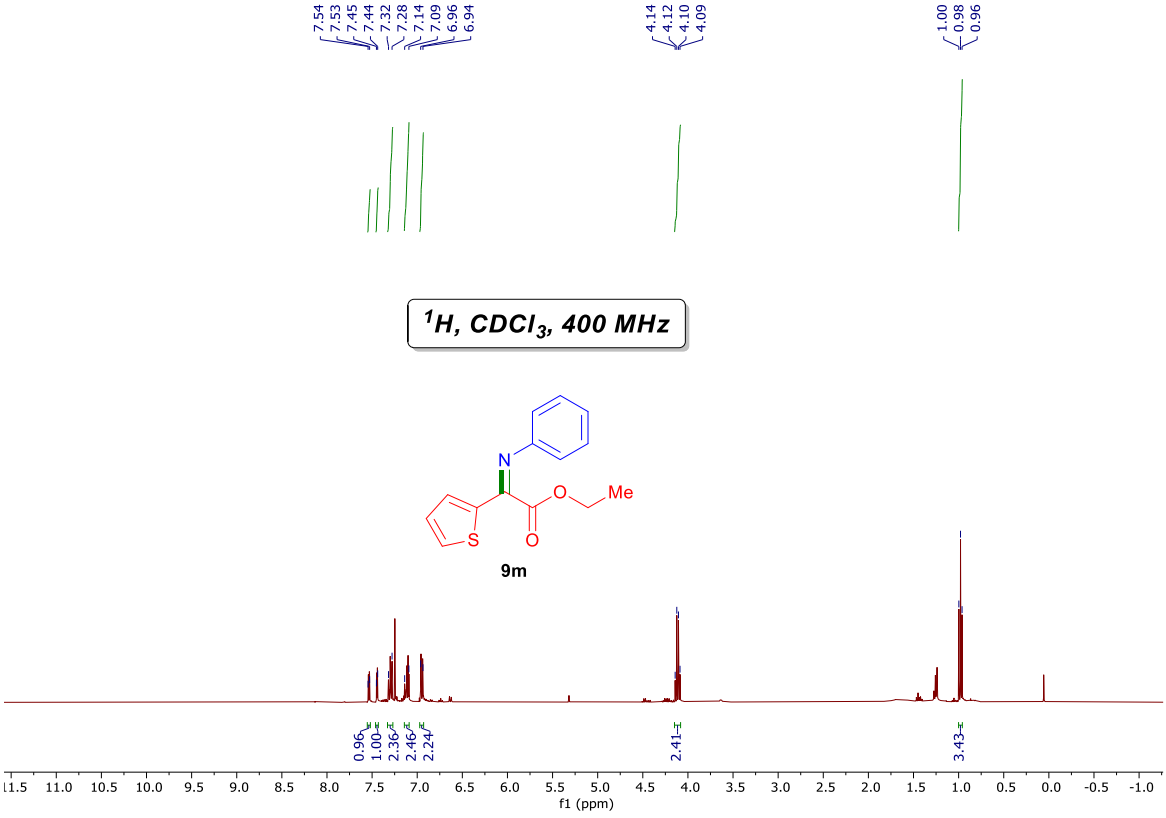


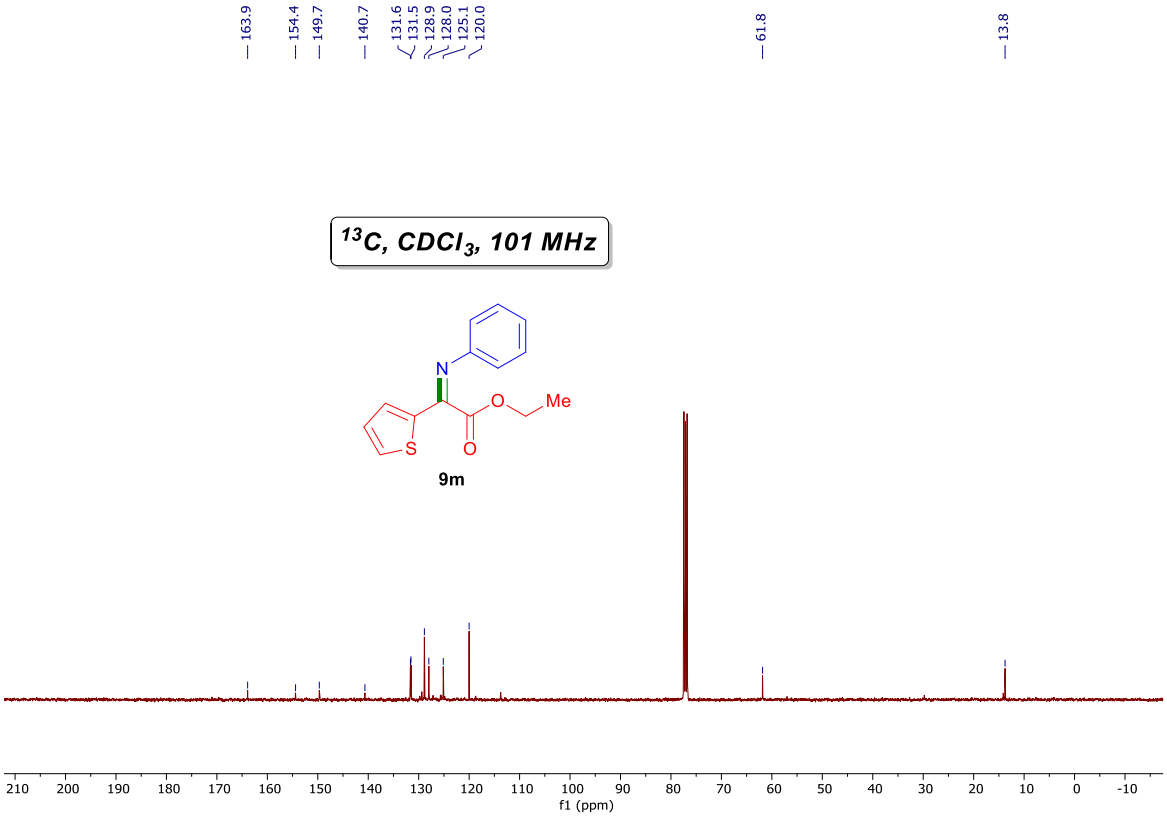
4.6.37. *tert*-butyl (*Z*)-3-(2-methoxy-2-oxo-1-(phenylimino)ethyl)-1*H*-indole-1-carboxylate (9l):



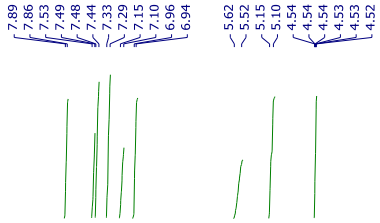


4.6.38. ethyl (*Z*)-2-(phenylimino)-2-(thiophen-2-yl)acetate (9m):

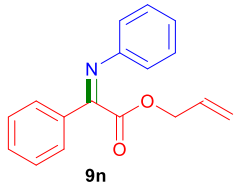




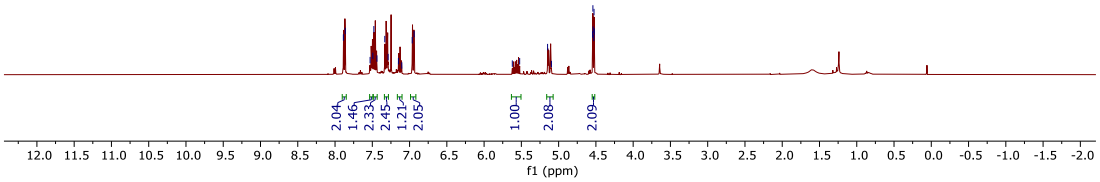
4.6.39. allyl (*Z*)-2-phenyl-2-(phenylimino)acetate (9n):



^{1}H, $CDCl_3$, 400 MHz

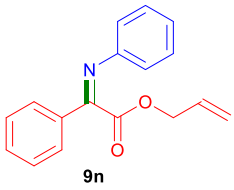


9n

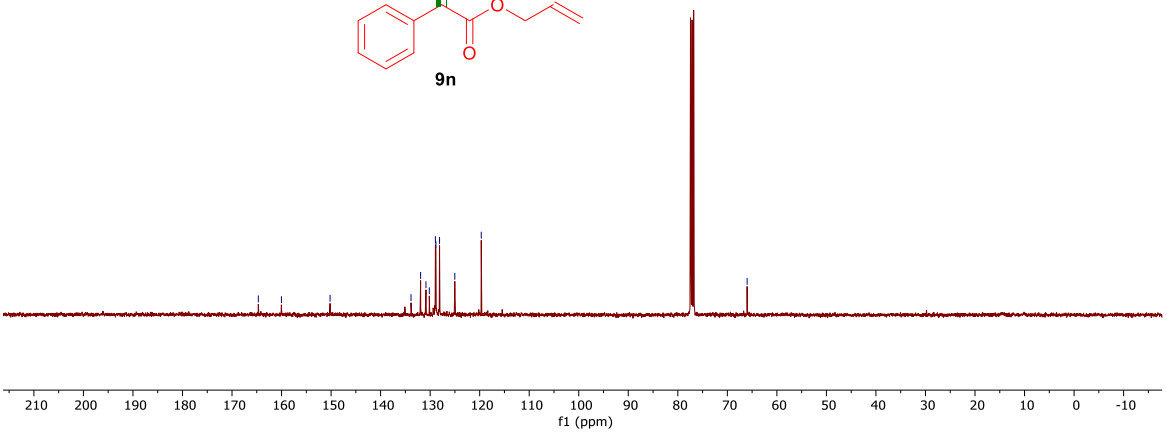




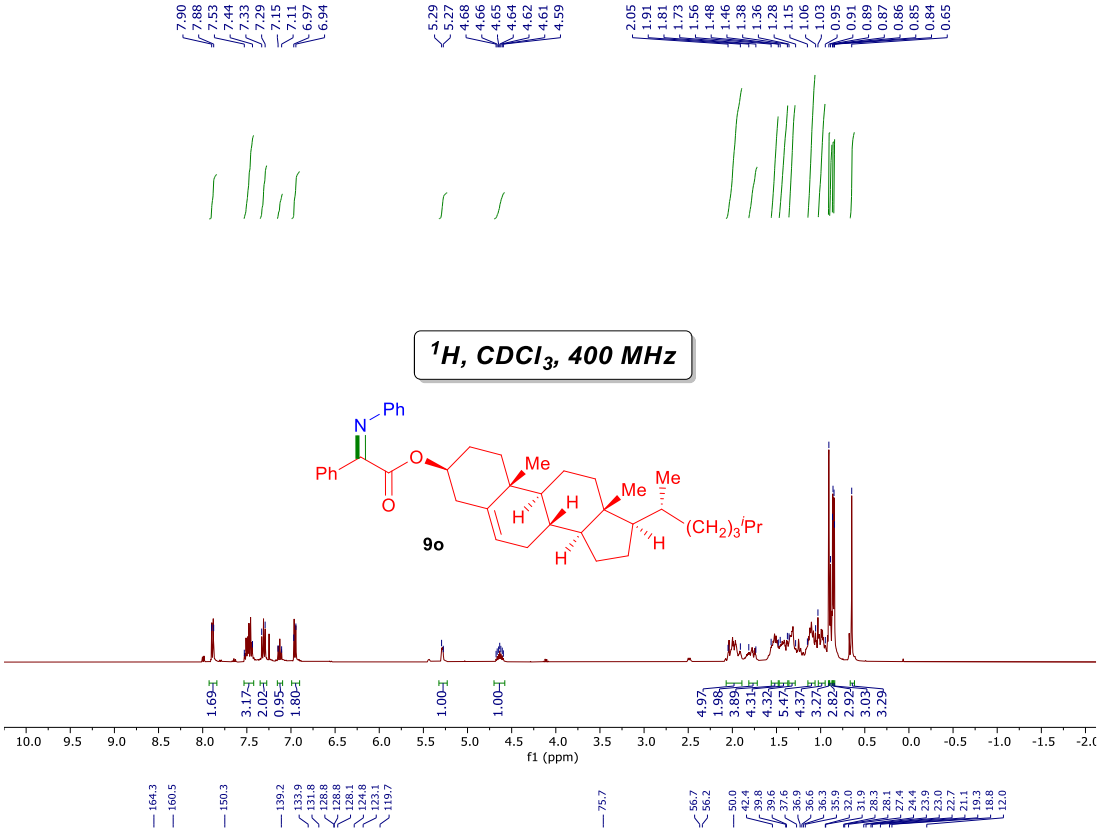
^{13}C, $CDCl_3$, 101 MHz

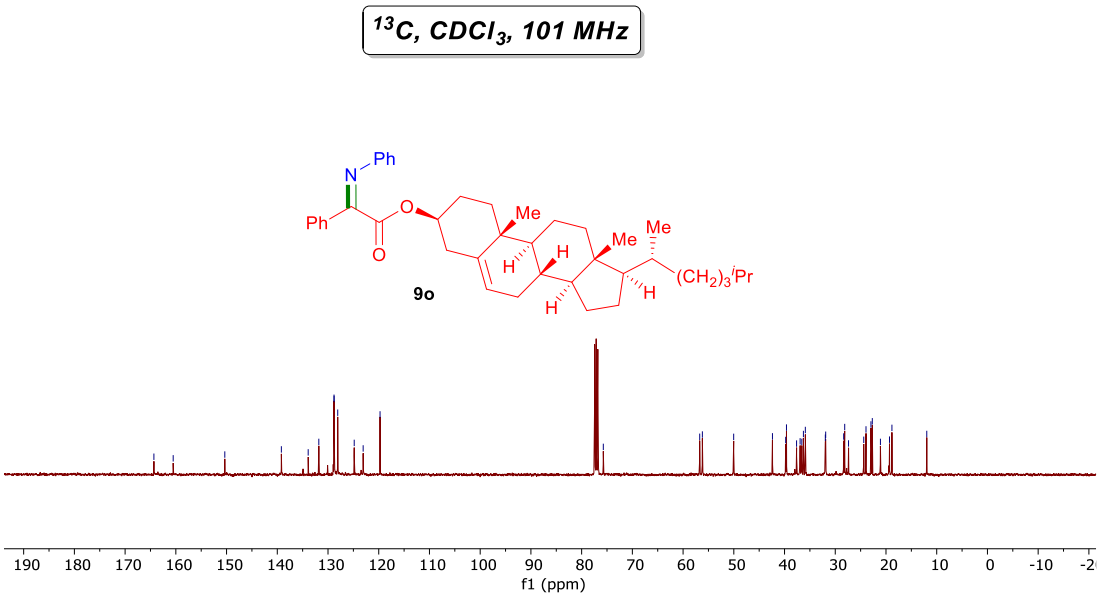


9n

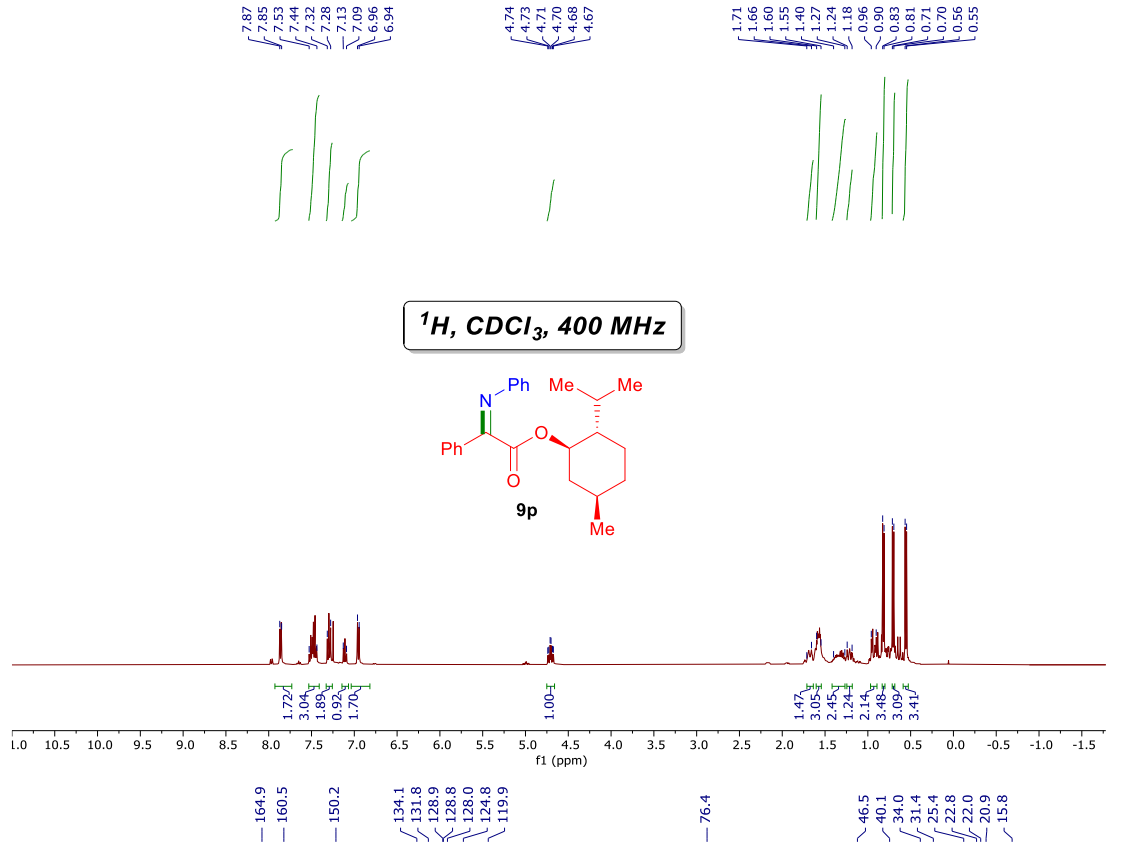


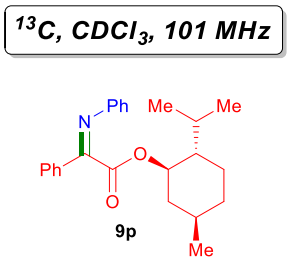
4.6.40. (3*S*,8*S*,9*S*,10*R*,13*R*,14*S*,17*R*)-10,13-dimethyl-17-((*R*)-6-methylheptan-2-yl)-2,3,4,7,8,9,10,11,12,13,14,15,16,17-tetradecahydro-1*H*-cyclopenta[*a*]phenanthren-3-yl (*Z*)-2-phenyl-2-(phenylimino)acetate (9o):

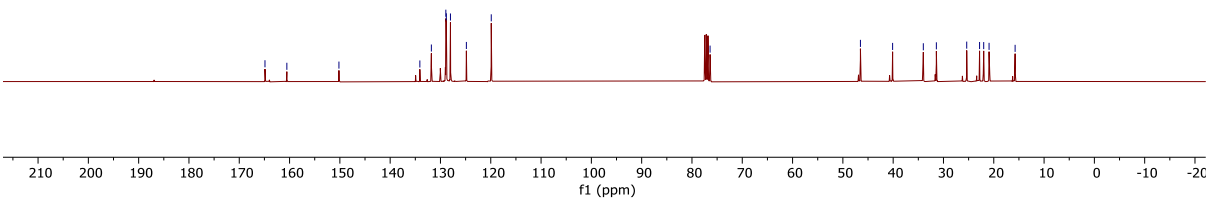




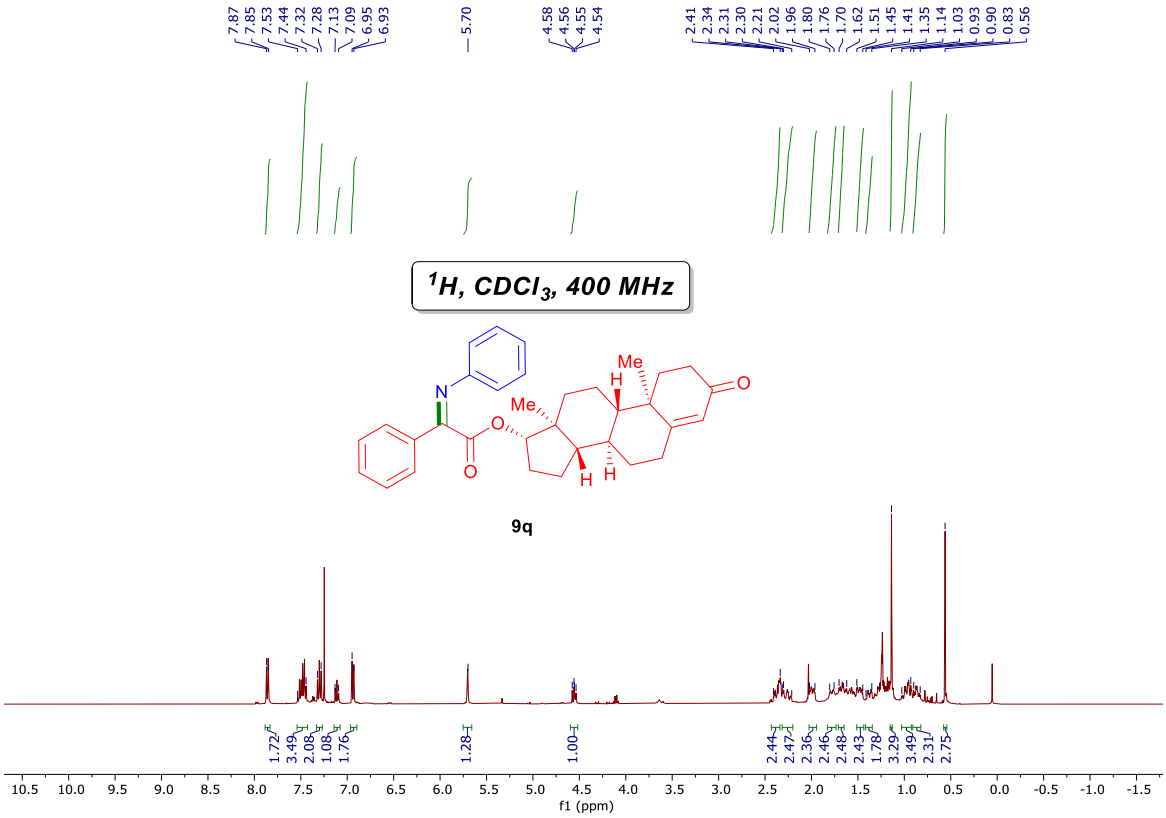
4.6.41. (1*R*,2*S*,5*R*)-2-isopropyl-5-methylcyclohexyl (*Z*)-2-phenyl-2-(phenylimino)acetate (9p):

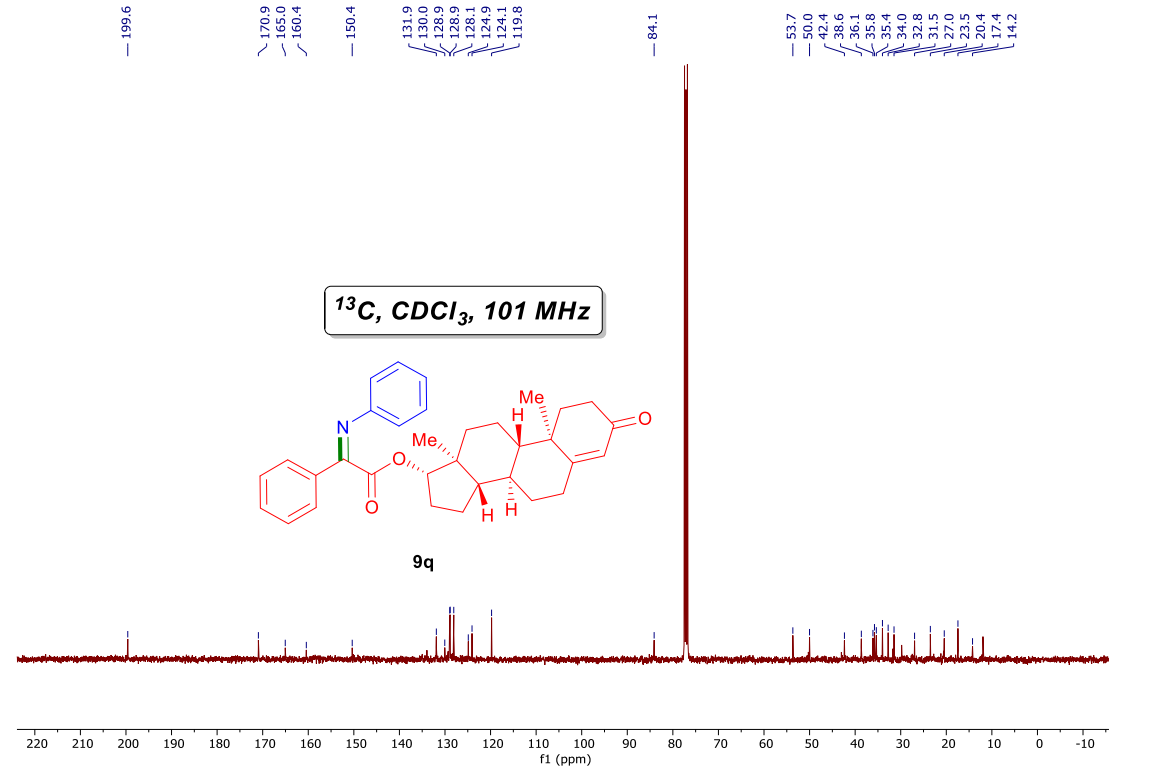




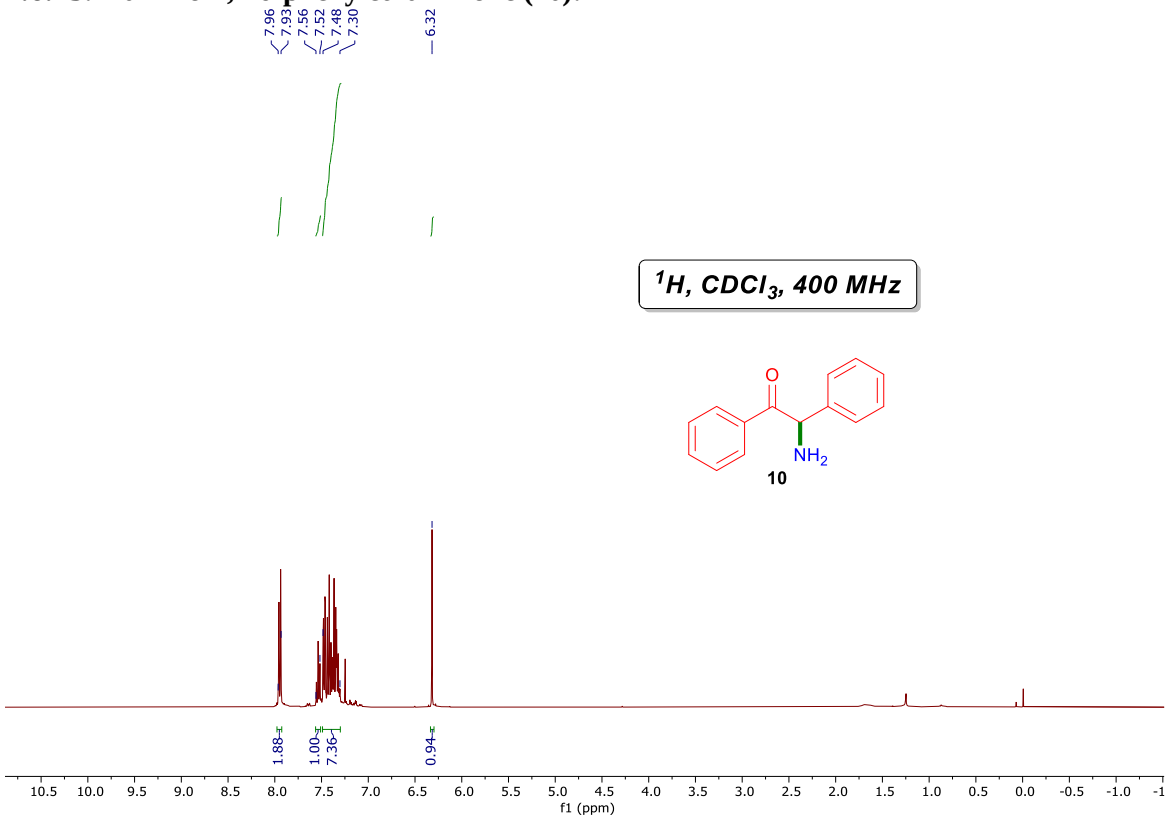


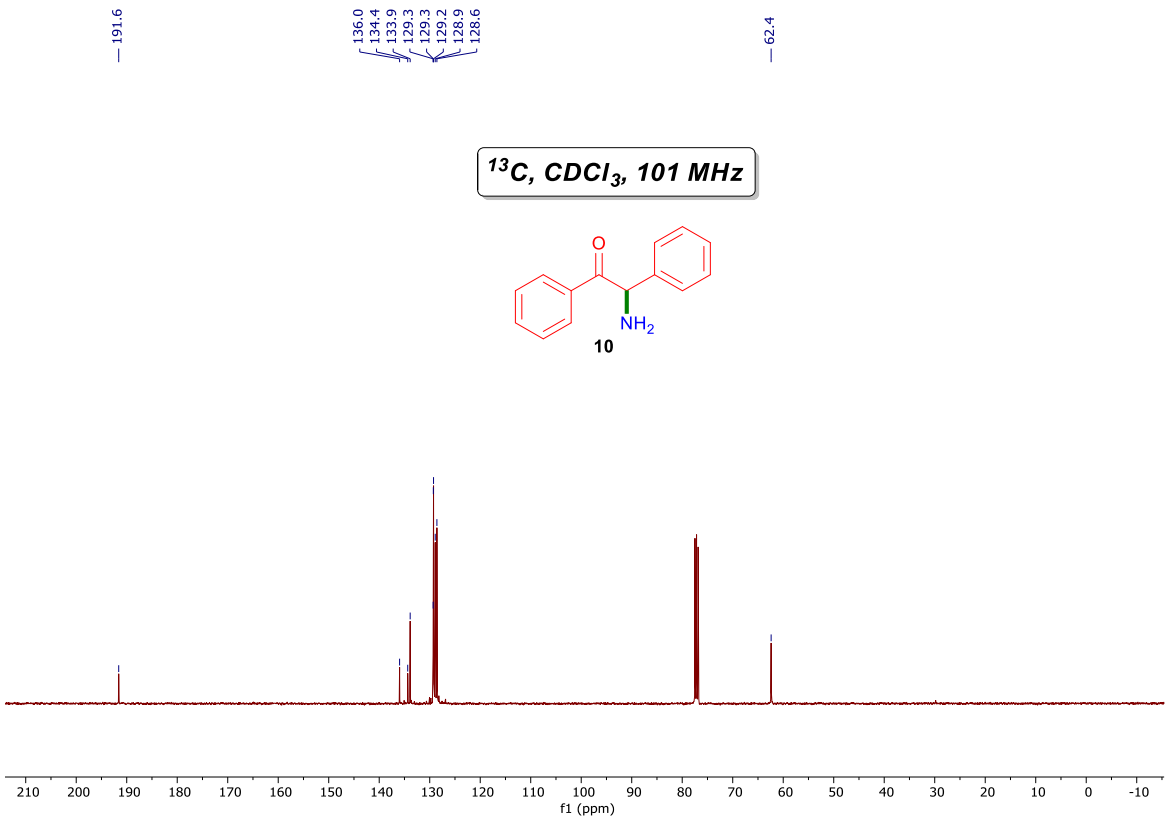
4.6.42. (8*R*,9*S*,10*R*,13*S*,14*S*,17*S*)-10,13-dimethyl-3-*oxo*-2,3,6,7,8,9,10,11,12,13,14,15,16,17-tetradecahydro-1*H*-cyclopenta[*a*]phenanthren-17-yl (*Z*)-2-phenyl-2-(phenylimino)acetate (9q):



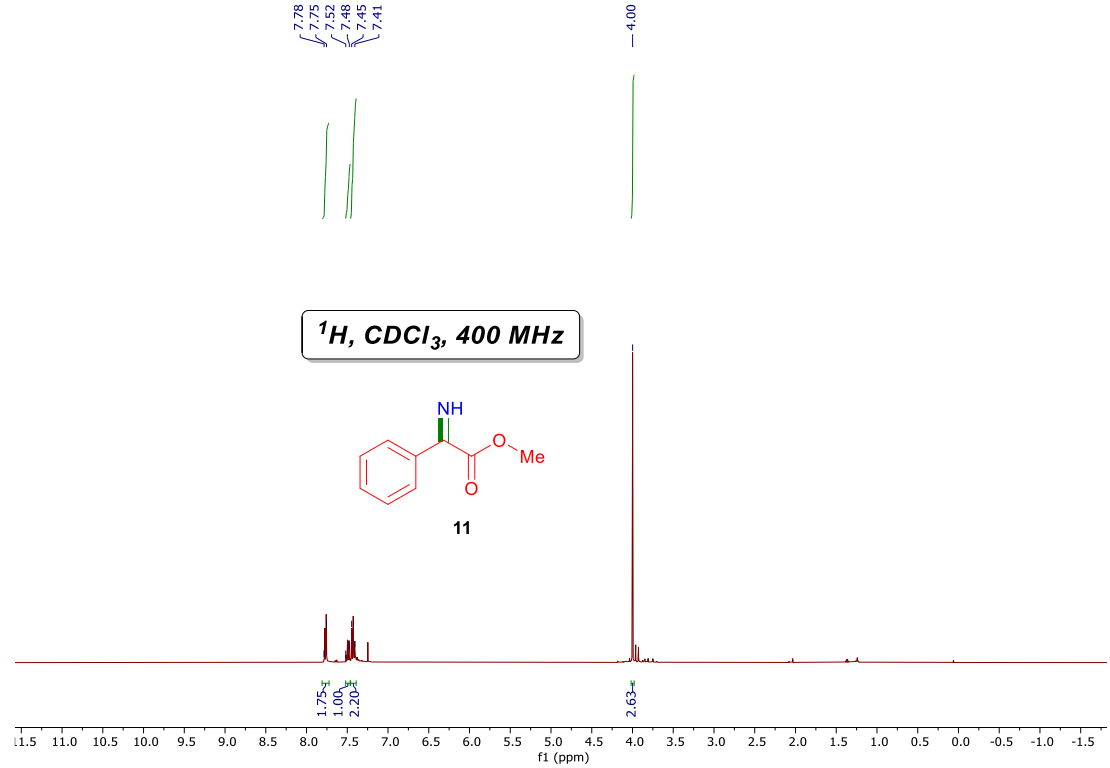


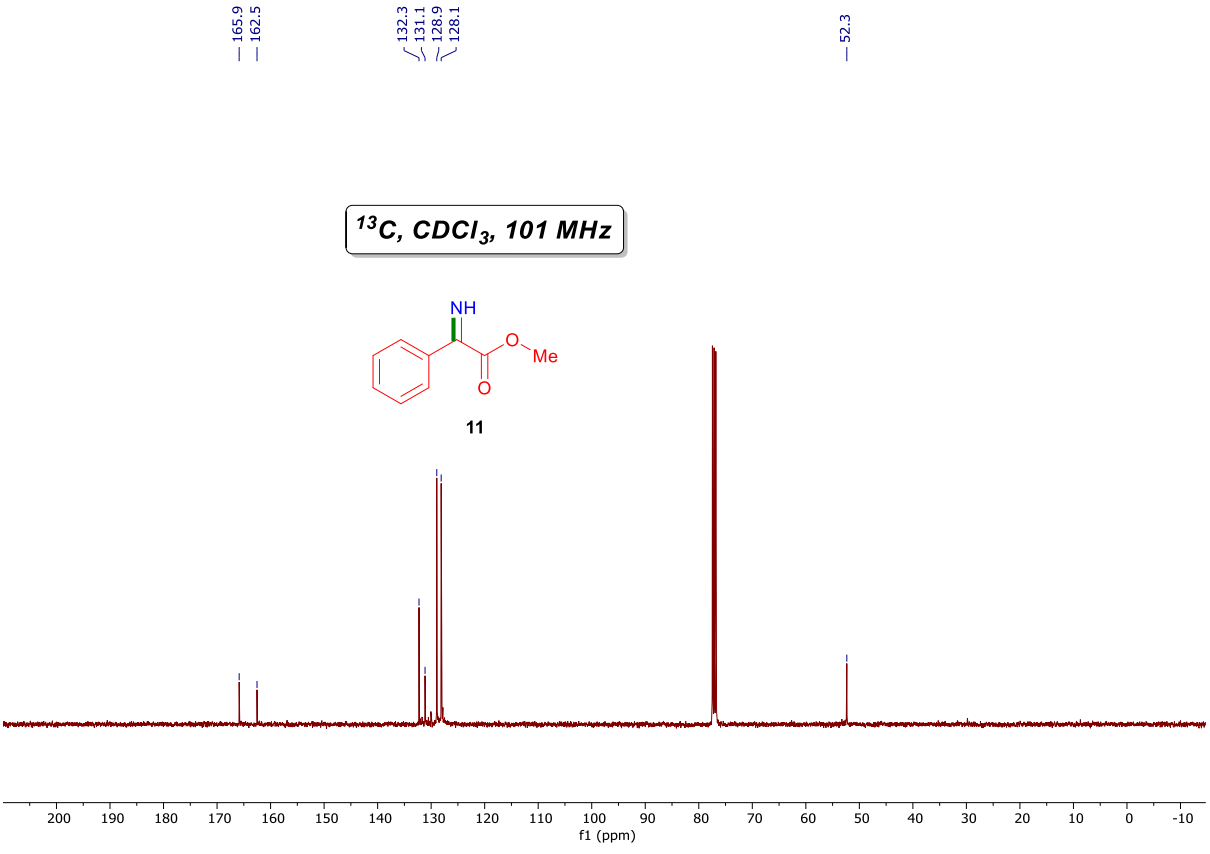
4.6.43. 2-amino-1,2-diphenylethan-1-one (10):



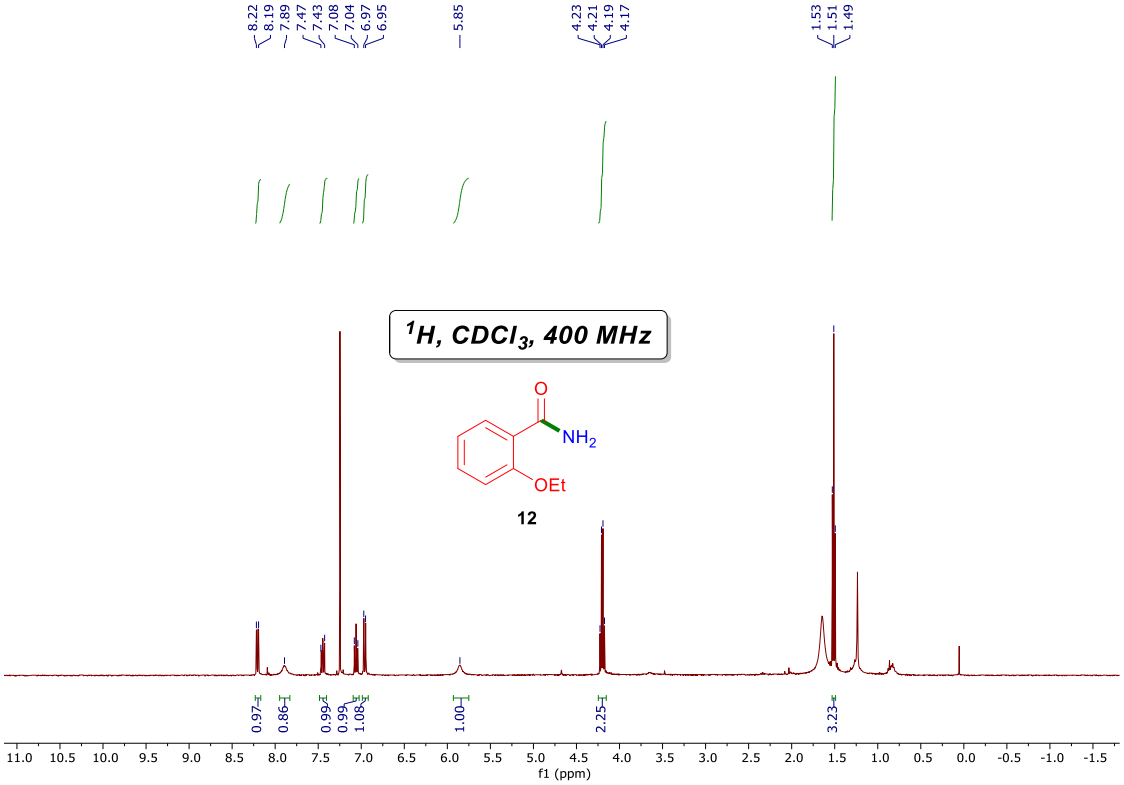


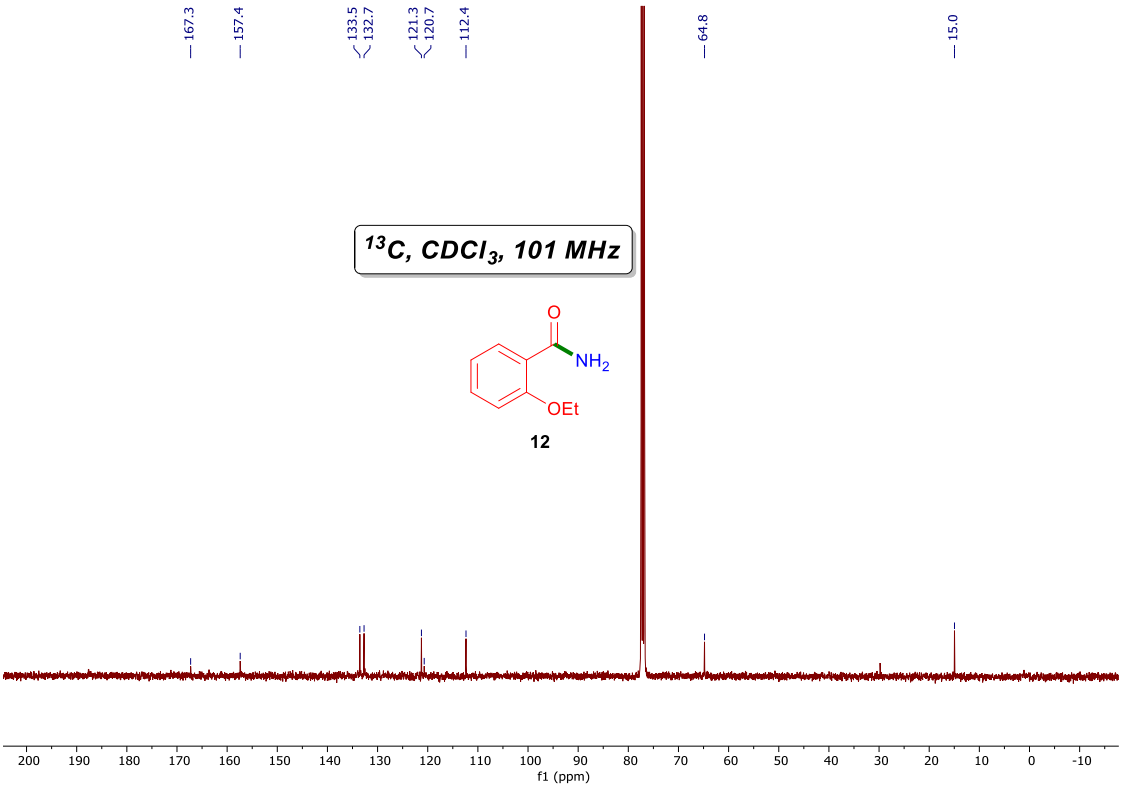
4.6.44. methyl 2-imino-2-phenylacetate (11):





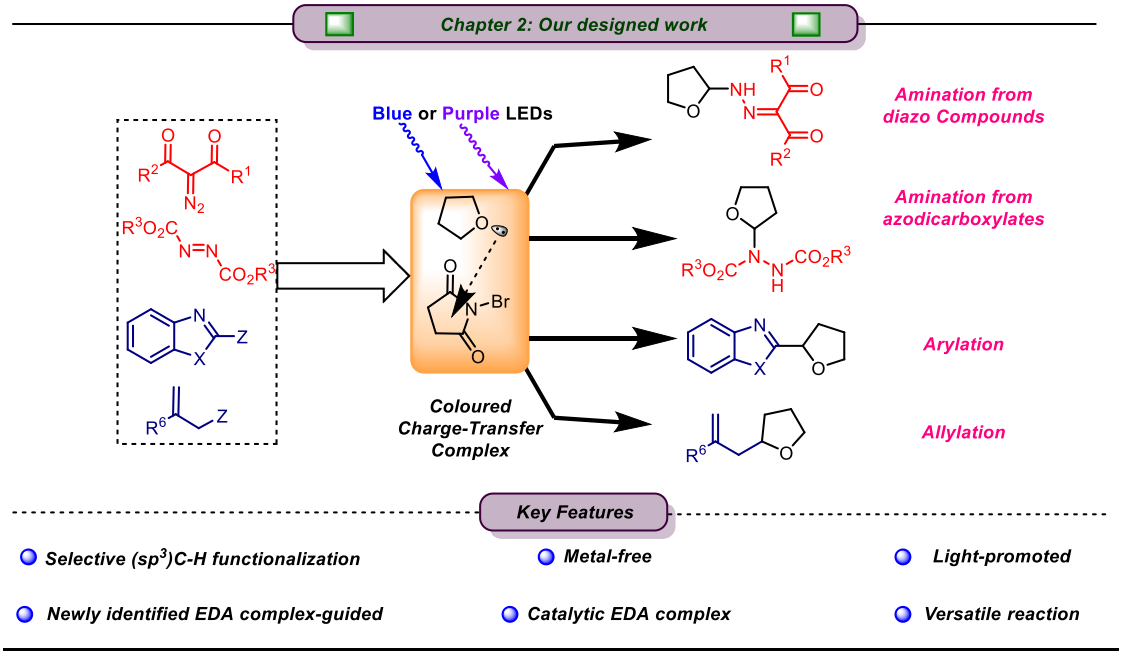
4.6.45. 2-ethoxybenzamide (12):





Chapter 5

Visible-Light-Mediated (sp^3)Cα–H Functionalization of Ethers Enabled by Electron Donor-Acceptor Complex



❖ This work was published in ACS Organic & Inorganic Au (a journal of ACS). Please see the citation as: "Roy, S.; Chatterjee, I. Visible-Light-Mediated (*sp3*)Cα–H Functionalization of Ethers Enabled by Electron Donor-Acceptor Complex. *ACS Org. Inorg. Au* **2022**, *2*, 306–311."

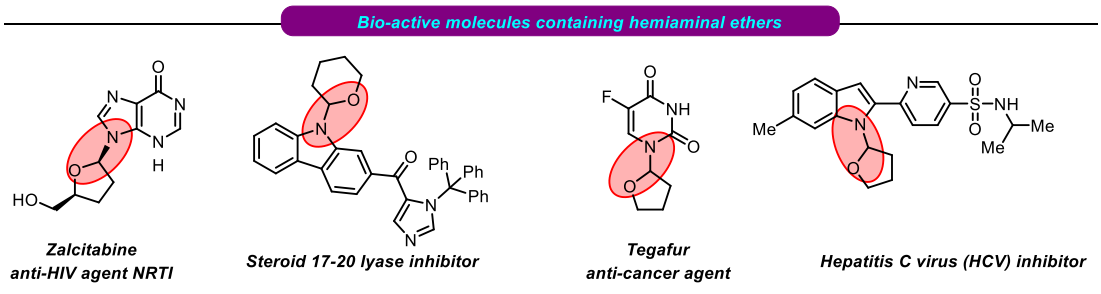
5. Abstract

A synthetically beneficial visible-light mediated protocol has been disclosed to achieve C–H amination of readily available feedstocks cyclic and acyclic ethers. A rarely identified NBS-THF electron donor−acceptor complex served as an initiator to functionalize both α-diazoketones and dialkyl azodicarboxylates. This developed methodology gives an alternative and milder way to construct the C–N bond and can be explored for the formation of C–C bond to perform arylation and allylation reactions.

5.1 Introduction

After the successful exploration of diazo compounds as a carbene precursor in chapter 3 and 4, we sought to explore its *N*-terminal electrophilic reactivity under visible-light-driven arsenal. Visible-light has been served as a robust tool in sustainable synthesis, operative via radical pathways under metal or metal-free conditions, enriching the chemistry of radical-based transformations.[1,2] Photoinduced excitation of organic molecules can drive remarkable transformation those are generally inaccessible via conventional thermal routes. Among light-driven protocols, one of the most valuable techniques is electron donor-acceptor (EDA) complex strategy due to its economic and synthetic utilities in modern-day chemistry.[3-5] Photoexcited EDA complex can break into a radical anion and radical cation, leading to various C–H and C–X bond functionalization.

Likewise, selective (sp^3)Cα–H functionalization of ethers has also gained tremendous attention in recent years. Traditionally, functionalization of (sp^3)Cα–H bonds require external catalysts, additives, elevated temperature, extended reaction time, or excess synthetic oxidant, possessing low functional group tolerability, selectivity, and affords the product moderately.[6-13] Readily available feedstocks like cyclic and acyclic ethers are widely used to form α-oxyalkyl C-radicals that can be trapped by various acceptors. This strategy can be applied over the construction of eminent C−N bonds, offering an elegant synthetic approach to forge *N*–functionalized molecules (Scheme 5.1.1).[14-16]

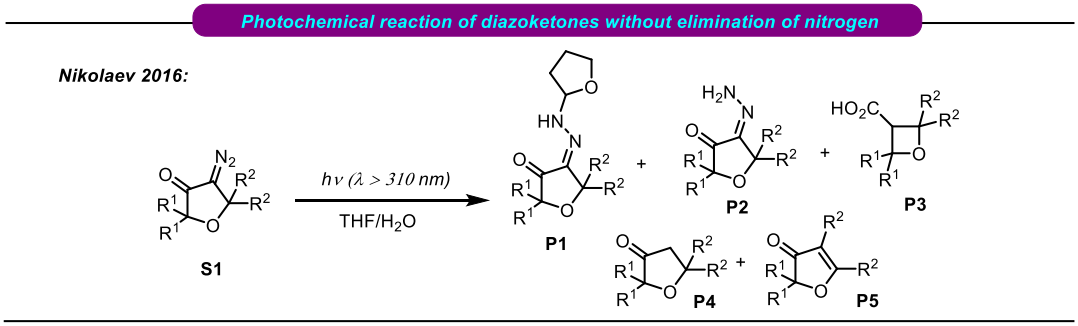


Scheme 5.1.1: Hemiaminal Ethers Present in Different Bio-active Molecules.

Over the years, diazo compounds remained as the prime building block in synthetic chemistry. Several methodologies have been developed by using these compounds as carbene precursors, C-nucleophiles, and 1,3-dipoles in the presence of metal or under photochemical conditions.[17-22] However, we are fascinated to use the diazo compound as *N*-terminal electrophile to forge C–N bond.

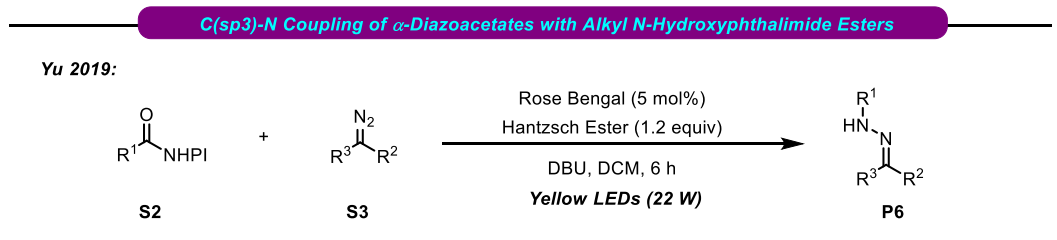
The typical example for this type of reactivity is Japp−Klingemann reaction, where β-ketoesters or acids were allowed to react with aryldiazonium salts, forging hydrazone moiety.[23] In 2006, Takamura and Zhao group reported the use of Grignard reagents as a nucleophile with diazo esters.[24-26] Following this, some valuable reports came into the picture, giving novel access to various hydrazonation reactions.[27-31]

In contrast, Nikolaev et al. demonstrate photosensitizer guided and UV-light mediated insertion of α-C–H bond of tetrahydrofuran (THF) into the terminal *N*-atom of the diazo compound **S1**, suffering from a mixture of products (**P1**-**P5**) with limited substrate scope (Scheme 5.1.2).[32,33]



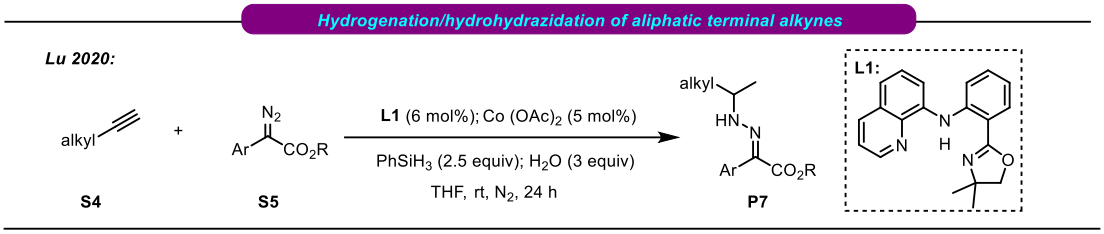
Scheme 5.1.2: Nikolaev's Photochemical Reaction of Diazoketones.

In 2019, photoredox catalysis was introduced by the Yu group to demonstrate a metal-free synthesis of structurally and functionally diverse *N*-alkyl hydrazones **P6** from α-diazoacetates **S3** and alkyl *N*-hydroxyphthalimide esters **S2**. This strategy illustrates a mild retrosynthetic disconnection approach for conventionally inaccessible C(*sp3*)-rich *N*-alkyl hydrazones (Scheme 5.1.3).[34]



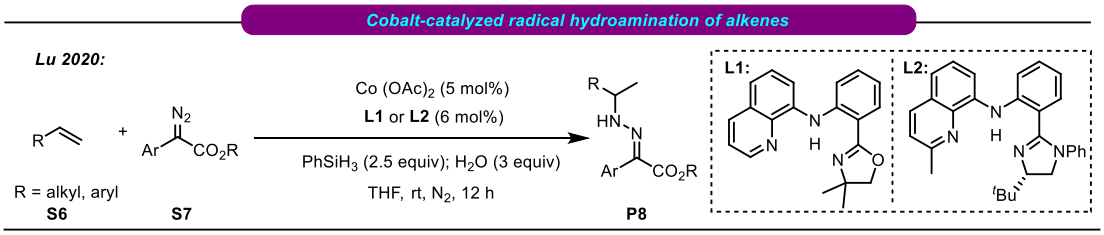
Scheme 5.1.3: Yu's Diversified Synthesis of Functionalized N-Alkyl Hydrazones.

In the same line of hydrohydrazidation reaction, in 2020, Lu et al. reported a mechanistically distinctive double Markovnikov selective and regioselective, sequential semihydrogenation/hydrohydrazidation of aliphatic terminal alkynes **S4** with diazo compounds **S5** to access amine derivatives **P7** under cobalt catalysis. The ligand-cobalt hydride complex plays a dual role for both semihydrogenation of aliphatic terminal alkynes via a unique cobalt-catalyzed Markovnikov-type hydrometalation and hydrohydrazidation of alkenes via a HAT process (Scheme 5.1.4).[35]



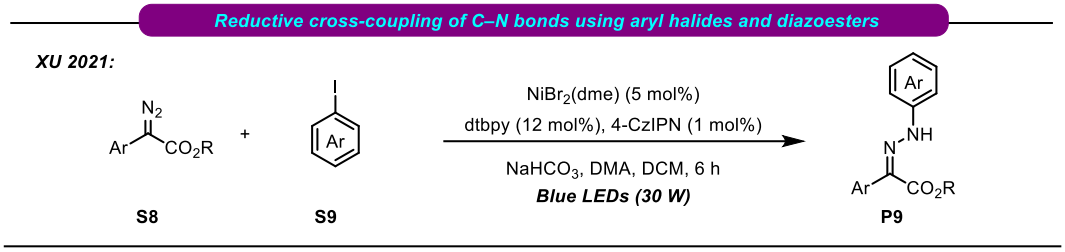
Scheme 5.1.4: Lu's α-C(*sp3*)–H amination of ethereal compounds.

Concurrently, the same group has developed a ligand-promoted cobalt-catalyzed Markovnikov-type hydroamination of alkenes **S6** with diazo compounds **S7**. This mild protocol utilizes *NNN*-tridentate (UNT) ligand, hydrosilanes, and readily available alkenes to construct hydrazones **P8** with broad functional group tolerance (Scheme 5.1.5).[36]



Scheme 5.1.5: Lu's Radical Hydroamination of Olefins.

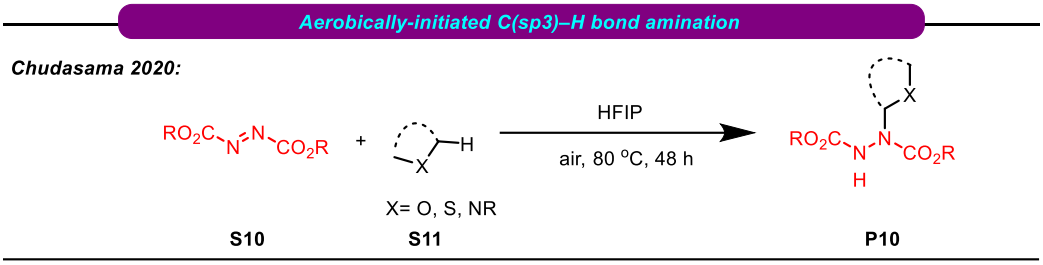
By following this, in 2021, the XU group illustrates a reductive cross-coupling reaction to construct C–N bonds under nickel/photoredox dual catalytic regime. A wide range of aryl hydrazones was obtained under exceptionally mild conditions by using easily available phenyldiazoacetate as a nitrogen source and aryl halides as another reaction partner (Scheme 5.1.6).[37]



Scheme 5.1.6: XU's Protocol to Construct C(*sp2*)–N bonds via dual Ni/photoredox-catalysis.

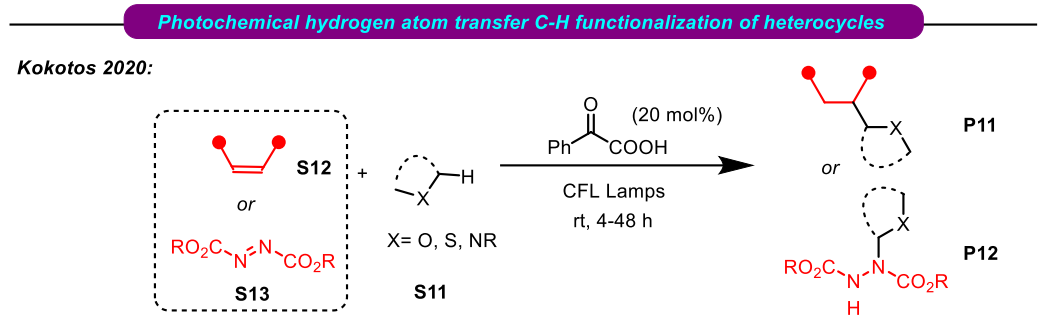
Alike, diazo compounds, dialkyl azodicarboxylates were also employed over radical-based amination reactions.[38-41]

In 2020, Chudasama demonstrated an α-C(*sp3*)–H amination technique over ethereal substrates **S11** by using azodicarboxylates **S10** as nitrogen source, enabled by 1,1,1,3,3,3-Hexafluoroisopropanol (HFIP) under aerobic conditions. A wide range of acetal-azodicarboxylate and ethers responded well to achieve the hemiaminal ethers **P10** with the help of H–bonding ability of HFIP, specifically to the nitrogen atom in azodicarboxylates, resulting in a substantial lowering of the LUMO energy (Scheme 5.1.7).[42]



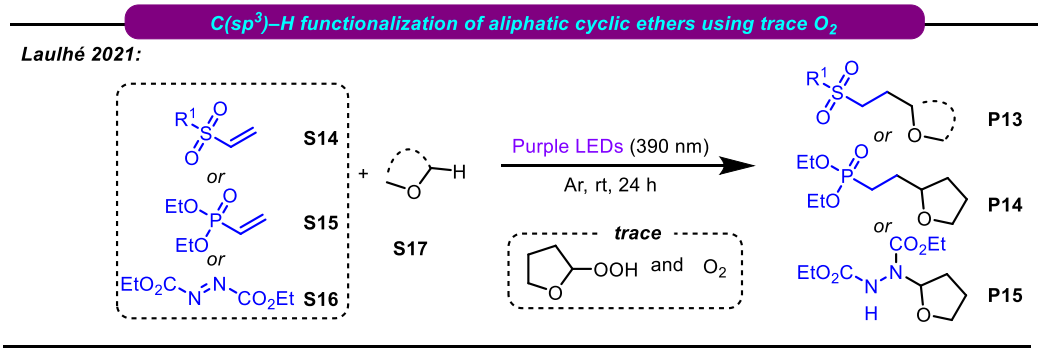
Scheme 5.1.7: Chudasama's α-C(*sp3*)–H Amination of Ethereal Compounds.

In the same year, Kokotos group reported a CFL lamp-promoted, metal-free C–H functionalization of heterocycles **S11** under small organic molecule (phenylglyoxylic acid) catalysis. This C–H bond functionalization method was carried out over various alkenes **S12** or diazo dicarboxylates **S13** leading to desired products **P11** or **P12** in good to high yields (Scheme 5.1.8).[43]



Scheme 5.1.8: Kokotos's Phenylglyoxylic acid Catalyzed C–H Functionalization of Heterocycles.

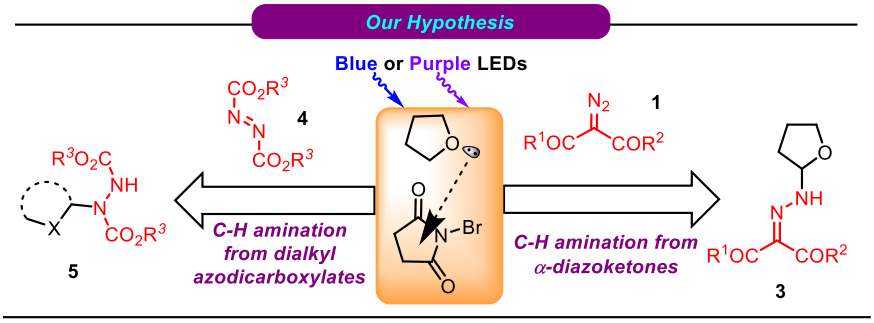
Following this in 2021, Laulhé et al. were able to functionalize the (*sp*3)Cα–H bond of aliphatic cyclic ethers **S17** with different Michael acceptors (**S14-S16**), e. g. vinyl sulfones, vinyl phosphonate esters, DEAD, etc. in the presence of visible light and traces of oxygen and trace amounts of ether peroxides. This environmentally benign and efficient selective C–C bond-forming reaction tolerated broad scopes of vinyl sulfone with various cyclic ethers and provided desired products (**P13-P15**)in good to excellent yields (Scheme 5.1.9).[44]



Scheme 5.1.9: Laulhé's Visible-light-promoted Selective C(sp^3)–H Functionalization of Aliphatic Ethers.

Despite the previous methods mentioned above, there is still considerable room to develop new radical-based C–H amination techniques in an eco-friendly and atom-economical fashion, excluded from any strong oxidants, base, or metal catalysts, and in a cheaper way with sound potential importance. Our literature survey did not offer any report that dealt with EDA-guided, metal-free, photosensitizer, or photocatalyst-free conditions to functionalize (sp^3)Cα–H bonds of ethers by utilizing diazo compounds and dialkyl azodicarboxylates as radical acceptor under visible light irradiation. On our ongoing interest in seeking different reactivities of diazo compounds under photochemical conditions, herein, we devised a catalytic amount of *N*-bromosuccinamide (NBS) as an inexpensive and efficient promoter in (*sp*3)Cα–H bond

functionalization of ethers. This resulted in synthesizing a wide range of hemiaminal ethers where α-diazoketones and dialkyl azodicarboxylates served as an amination reagent (Scheme 5.1.10) guided by catalytic EDA system.[45,46]



Scheme 5.1.10: Chapter 5: Our Hypothesis.

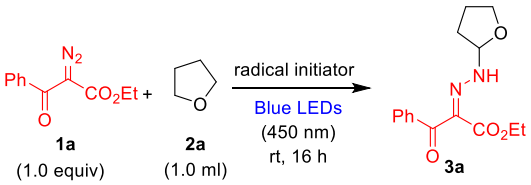
5.2. Result and Discussion

5.2.1 Optimization of the Reaction Condition for Amination from Diazo Compounds.

Based on the previous literature,[32,33] we hypothesized that α-diazo-β-keto compound might act as a good *N*-terminal acceptor. Therefore, we geared our investigation by choosing α-diazo-β-keto ester **1a** as a model substrate in THF (0.5 M) **2a** at room temperature to commence visible-light promoted C–H amination protocol.

In this transformation, THF serve as both solvent and α-oxyalkyl C-radical precursor under aerobic conditions (Table 1, entry 1). However, the formation of no product indicates that a radical initiator must require to trigger this process. Next, we screened several radical initiators (Table 1) amidst NBS (1.0 equiv) gives the best result to furnish aminated product **3a** in 85% yield (Table 1, entry 9). We were pleased to find that using a catalytic amount of NBS (20 mol%) instead of a stoichiometric one doesn't alter the reaction yield significantly (Table 1, entry 10).

5.2.1.1. Chapter5: Table 1: Screening of Radical Initiator[a]

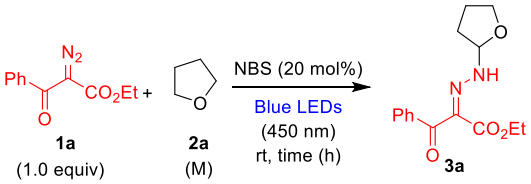


Entry	radical initiator (equiv)	*Z:E*[b]	Yield (%)[b]
1	none	-	0
2	Phenacyl bromide (2.0)	6:1	52
3	Diethyl bromomalonate (2.0)	6:1	47
4	Benzyl bromide (2.0)	5:1	25
5	Bromoacetonitrile (2.0)	4:1	46
6	*N*-Bromosuccinimide (2.0)	6:1	61
7	*N*-Chlorosuccinimide (2.0)	5:1	32
8	*N*-Iodosuccinimide (2.0)	5:1	28
9	*N*-Bromosuccinimide (1.0)	6:1	85
10	***N*-Bromosuccinimide (0.2)**	**6:1**	**82 (78)**

[a] unless untill mentioned all reactions were carried out in 0.1 mmol scale by taking **1a** (1.0 equiv) & corresponding radical initiator in dry and deoxygenated THF. [b] measured by ^{1}H-NMR analysis of the crude reaction mixture using CH_2Br_2 as an internal standard. Isolated yield in bracket.

Variation in the solvent concentration, reaction temperature, and time was also checked (Table 2), suggesting 0.1 (M) THF concentration and 45 ^oC to be the best-fitted one for this transformation (Table 1, entry 1).

5.2.1.2. Chapter5: Table 2: Miscellaneous Optimization[a]

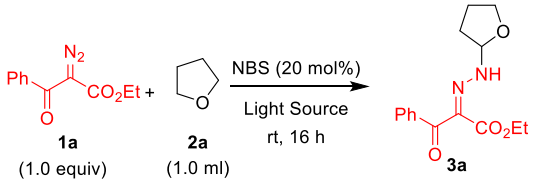


Entry	2a (M)	T (^oC)	time (h)	*Z:E*[b]	Yield (%)[b]
1	**0.1**	**rt**	**16**	**6:1**	**82 (78)**
2	0.1	10	16	6:1	48
3	0.1	45	16	5:1	75
4[c]	0.1	60	16	-	0
5	0.1	rt	24	6:1	77
6	0.1	rt	10	6:1	55
7	0.5	rt	16	5:1	72
8	0.25	rt	16	4:1	75
9	0.05	rt	16	6:1	62

[a] unless untill mentioned all reactions were carried out in 0.1 mmol scale by taking **1a** (1.0 equiv) & 20 mol % NBS in dry and deoxygenated THF. [b] measured by ^{1}H-NMR analysis of the crude reaction mixture using CH_2Br_2 as an internal standard. [c] isolated yield in bracket. [c] Reaction carried out in dark.

Next, the screening of different light sources (Table 3) indicates that blue-LEDs (450 nm) irradiation for 16 h remained more potent over others (Table 3, entry 1). No conversion for the reaction in dark at room temperature suggests light source is essential for this reaction (Table 3, entry 8).

5.2.1.3. Chapter 5: Table 3: Screening of Different Light Source 1[a]



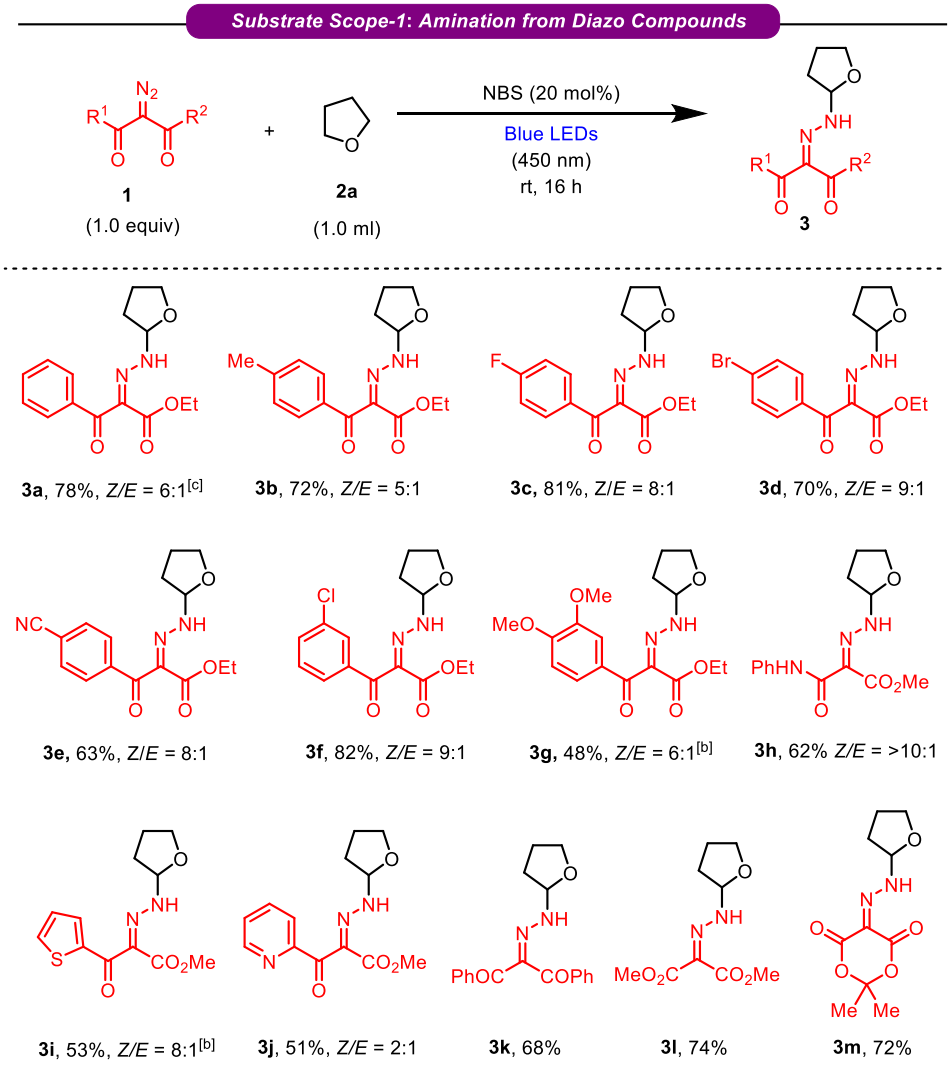
Entry	Light Source	*Z:E*[b]	Yield (%)[b]
1	**Blue LEDs (450 nm)**	6:1	**82 (78)**
2	Blue LEDs (420 nm)	5:1	60
3	Purple LEDs (405 nm)	5:1	51
4	UV LEDs (365 nm)	2:1	32
5	Blue LEDs (strip)	6:1	40
6	Green LEDs (strip)	-	trace
7	White LEDs	-	10
8	in dark	-	0

[a] unless untill mentioned all reactions were carried out in 0.1 mmol scale by taking **1a** (1.0 equiv) & 20 mol % NBS in dry and deoxygenated THF.
[b] measured by ^{1}H-NMR analysis of the crude reaction mixture using CH_2Br_2 as an internal standard. Isolated yield in bracket.

5.2.2 Substrate Scope Evaluation for Amination from Diazo Compounds.

After establishing the optimal reaction conditions (Table 3, entry 1), we investigated the generality of this C–H amination protocol between α-diazo-β-keto compound **1** and THF **2a** (Scheme 5.2.2.1). Under visible light, electron-donating substituent, and electron-withdrawing substitutions on the aryl ring, such as methyl, halogen, and cyano groups with *meta* and *para*-substituted ones, smoothly furnishes the product (Scheme 5.2.2.1, entries **3b**-**3f**) with moderate to good yield and moderate *Z/E* isomeric ratio. Moreover, an aryl ring containing two methoxy substitutions at *meta* and *para* position delivered the desired product **3g** in a 48% yield. Next, amide and heterocycle substituted diazo compounds were investigated, which form the corresponding hydrazones **3h**-**3j**, with moderate yields. Symmetrical acyclic and cyclic α-diazo-β-keto compounds also lead to a facile transformation to achieve compounds **3j**-**3l** in good yield (Scheme 5.2.2.1). Although acceptor/acceptor–diazo compounds react well under these reaction conditions, donor/acceptor–diazo compounds such as α-aryldiazoacetates, α-aryldiazoketones remained incompatible. We reasoned this might be due to under blue LEDs α-aryldiazoacetates are prone to undergo dinitrogen extrusion to generate carbene intermediate, which cannot take part in the reaction.[19-21] Next, several cyclic and acyclic ethers (**2b**-**2f**, see section 5.4.3.3) were

tested as α-oxyalkyl C-radical precursors, but unfortunately, they also remained unreactive under this reaction condition.



Scheme 5.2.2.1: Substrate scope for amination from diazo compounds.[a]

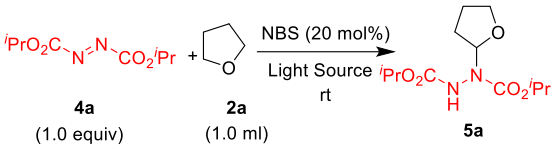
[a] Unless specified, reactions were performed on a 0.1 mmol scale under argon atmosphere by taking freshly distilled and deoxygenated THF. Yields refer to isolated one. *Z/E* ratio was measured by ^{1}H NMR analysis of the crude reaction mixture using dibromomethane as an internal standard. [b] Reactions carried out for 10 h. Reaction performed on a 2.0 mmol scale gives 62% (360 mg) isolated yield of **3a**.

To check the versatility of the developed protocol, we envisioned whether dialkyl azodicarboxylates could act as a radical acceptor to forge the C–N bond.[37-44]

5.2.3. Optimization of the Reaction Condition for Amination from Azodicarboxylates.

Here THF radical was successfully trapped by diisopropylazodicarboxylate **4a**, under blue LEDs irradiation to deliver amine product with moderate yield (Table 4, entry 1). A series of light sources and reaction times were then screened to check the best-fitted one (Table 4). We found purple LEDs are the most efficient to promote this reaction, which gives 91% yield of **5a** within 5 minutes (Table 4, entry 4).

5.2.3.1. Chapter 5: Table 4: Screening of Different Light Source 2[a]



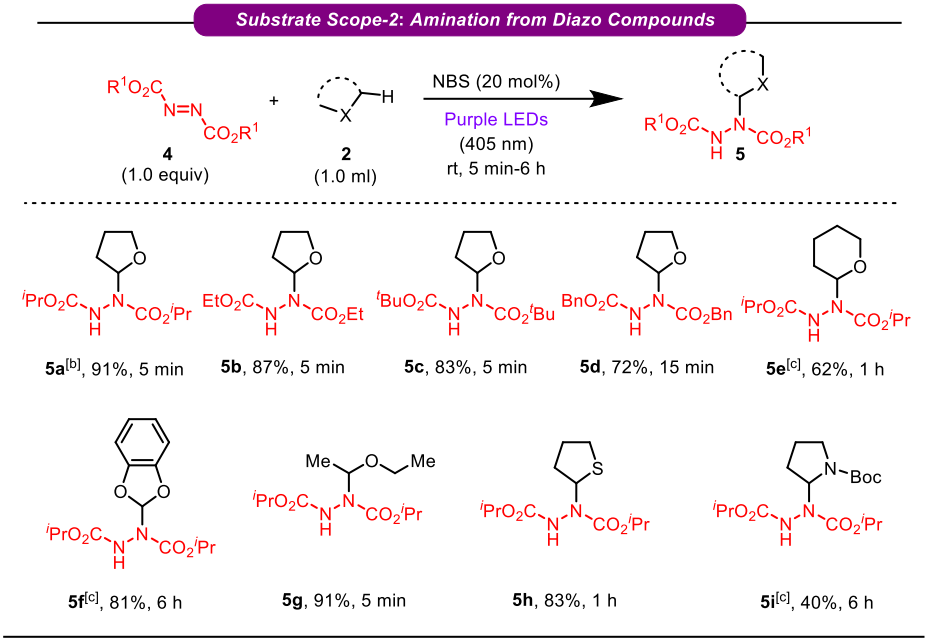
4a (1.0 equiv) **2a** (1.0 ml) **5a**

Entry	Light Source	Time	Yield (%)[b]
1	Blue LEDs (450 nm)	1 h	62
2	Blue LEDs (450 nm)	5 min	77
3	Blue LEDs (420 nm)	5 min	70
4	**Purple LEDs (405 nm)**	**5 min**	**91**
5	UV LEDs (365 nm)	5 min	34
6	Blue LEDs (strip)	1 h	73
7	Green LEDs (strip)	1 h	40
8	White LEDs	1 h	15
9	in dark	1 h	0

[a] unless untill mentioned all reactions were carried out in 0.1 mmol scale by taking **1a** (1.0 equiv) & NBS (20 mol%) in dry and deoxygenated THF. [b] yield refered to isolated one.

5.2.4. Substrate Scope Evaluation for Amination from Azodicarboxylates.

The azodicarboxylates substituted with different alkyl partners furnished the corresponding amines with good yield (Scheme 12, entries **5a**-**5d**). Subsequently, a range of cyclic and acyclic ethers participated in this transformation (Scheme 12, entries **5e**-**5g**). In addition, *S*-heterocycle and *N*-heterocycle were also successfully employed with high efficiency (Scheme 5.2.4.1, entries **5h** and **5i**).



Scheme 5.2.4.1: Substrate scope for amination from azodicarboxylates.[a]

[a] Unless specified reactions were performed on a 0.1 mmol scale under argon atmosphere by taking **4** (1.0 equiv) and **2** (1.0 ml). Yields refer to isolated one. [b] Reaction performed on a 2.0 mmol scale gives 80% (440 mg) isolated yield of **5a**. [c] 10.0 equiv of **2** was used in 0.1 ml benzene.

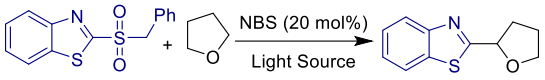
5.2.5. Synthetic Application: Arylation and Allylation reactions.

The general applicability of any developed protocol showcases its usefulness. Gratifyingly, this catalytic protocol also remained potent over some arylation and allylation.

5.2.6. Optimization Study for Arylation and Allylation Reactions.

In order to establish optimal condition for arylation reaction several light sources were screened by choosing aryl sulfone **6a** as a radical acceptor (Table 5), where blue LEDs shows its superiority over others (Table 5, entry 1).

5.2.6.1. Chapter 5: Table 5: Screening of Different Light Source 3[a]



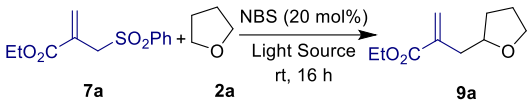
6a (1.0 equiv) + **2a** (1.0 ml) → **8a**

Entry	Light Source	Yield (%)[b]
1	**Blue LEDs (450 nm)**	**73**
2	Blue LEDs (420 nm)	58
3	Purple LEDs (405 nm)	51
4	UV LEDs (365 nm)	32
5	Blue LEDs (strip)	43
6	Green LEDs (strip)	15
7	White LEDs	trace
8	in dark	0

[a] unless untill mentioned all reactions were carried out in 0.1 mmol scale by taking **1a** (1.0 equiv) & NBS (20 mol%) in dry and deoxygenated THF. [b] yield refered to isolated one.

To establish optimal reaction condition for allylation reaction several light sources were screened by choosing allyl sulfone **7a** as a radical acceptor (Table 6), where blue LEDs remains most suitable one to fabricate **9a** with moderate yield (Table 6, entry 1).

5.2.6.2. Chapter 5: Table 6: Screening of Different Light Source 4[a]



7a (1.0 equiv) + **2a** (1.0 ml) → **9a**

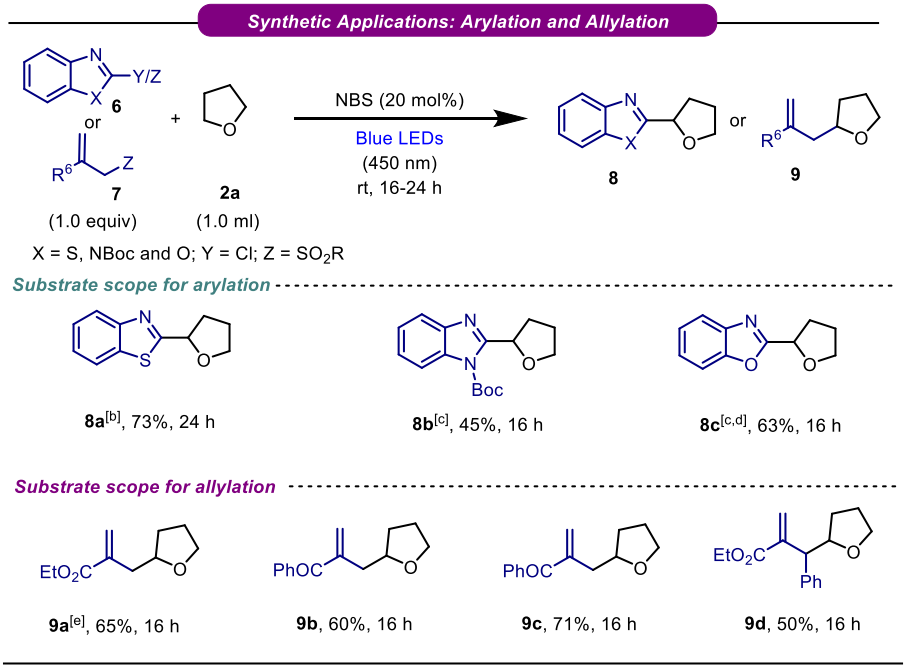
Entry	Light Source	Yield (%)[b]
1	**Blue LEDs (450 nm)**	**65**
2	Blue LEDs (420 nm)	60
3	Purple LEDs (405 nm)	54
4	UV LEDs (365 nm)	40
5	Blue LEDs (strip)	35
6	Green LEDs (strip)	trace
7	White LEDs	trace
8	in dark	0

[a] unless untill mentioned all reactions were carried out in 0.1 mmol scale by taking **1a** (1.0 equiv) & NBS (20 mol%) in dry and deoxygenated THF. [b] yield refered to isolated one.

5.2.7. Substrate Scope Evaluation for Arylation and Allylation Reaction.

In order to explore the substrate scope, various aryl and allyl sulfones were allowed to react under optimal reaction condition which gave desired THF incorporated product via desulfonylation (Scheme 5.2.7.1, entries **8a**, **9a-9d**). Additionally, aryl ring substituted with a halogen atom (e.g. *N*-Boc 2-Chlorobenzimidazole **6b**, 2-Chlorobenzoxazole **6c**, see experimental part, section 5.4.3.4) as a leaving group instead of sulfones, efficiently provides their

corresponding products (Scheme 5.2.7.1, entries **8b** and **8c**). Here sodium acetate was used as an additive to neutralize *in situ* generated hydrochloric acid increasing the reaction yield.[49]



Scheme 5.2.7.1: Substrate scope for amination from azodicarboxylates.[a]

[a] Unless specified, reactions were performed on a 0.1 mmol scale under argon atmosphere by taking **4** (1.0 equiv), freshly distilled and deoxygenated THF. Yields refer to isolated one. [b] Reaction performed on a 2.0 mmol scale gives 59% (240 mg) isolated yield of **8a**. [c] 1.0 equiv NaOAc was used as an additive. [d] Purple LEDs were used instead of Blue LEDs. [e] Reaction performed on a 2.0 mmol scale gives 54% (200 mg) isolated yield of **9a**.

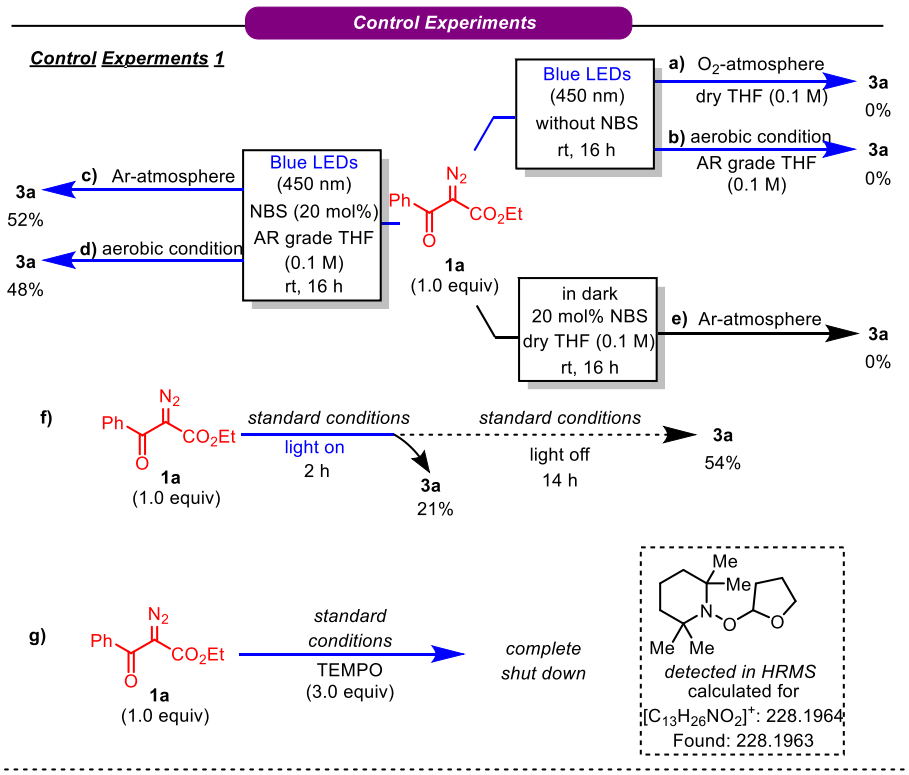
5.2.8. Mechanistic Studies: Experimental

We executed several control experiments to shed light on the plausible reaction pathways of this visible-light-driven transformation. The reaction between **1a** and dry-deoxygenated THF **2a** without NBS, under blue LEDs irradiation and oxygen atmosphere, resulted in no product **3a** formation (Scheme 5.2.8.1a). The result doesn't alter by performing the above reaction under aerobic conditions and using AR grade THF **2a** (Scheme 5.2.8.1b). The yield of **3a** drops significantly on performing the reaction between **1a** and AR grade THF **2a** in the presence of NBS, under argon atmosphere, or aerobic conditions in the presence of blue LEDs (Scheme 5.2.8.1c, 5.2.8.1d). Moreover, reaction under dark conditions did not offer any product formation (Scheme 5.2.8.1e). These results suggest that NBS, blue LEDs irradiation, and entirely inert conditions are necessary to facilitate this transformation. Next, when diisopropyl azodicarboxylate **4a** was allowed to react with dry-deoxygenated THF **2a** under purple LEDs irradiation and

oxygen atmosphere, in absence of NBS gives traces amount of **5a**. However, on increasing the reaction time (5 min to 24 h), a considerable amount of product **5a** (45%) was obtained. Reactions performed by taking AR grade THF **2a** without NBS under aerobic condition and argon atmosphere lead to form 22% and 25% of **5a**, respectively (reaction time 24 h). Similarly, the dark experiment suggested the essentiality of the light source (Scheme 5.2.8.1e).

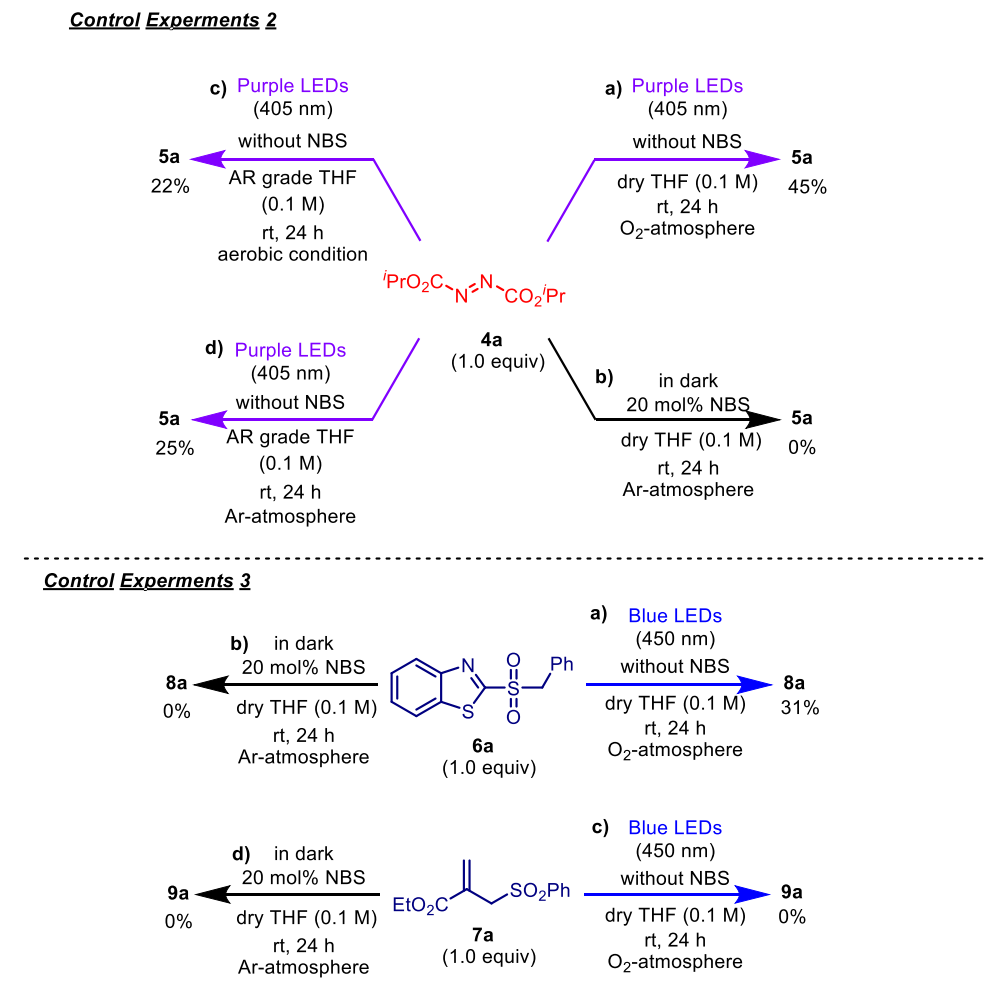
Next, the existence of radical intermediate was tested by adding (2,2,6,6-tetramethylpiperidin-1-yl)oxyl (TEMPO) as a radical-scavenger to the reaction mixture where THF radical **VII** was successfully trapped (detected in HRMS, Figure 5.2.8.1), and the reaction got complete shutdown (Scheme 5.2.8.1g).

To validate whether the reaction proceeds via a radical chain process, we performed a ‘‘light-on/light-off’’ experiment. Irradiating the reaction mixture under blue LEDs for 2 h and then stirring the reaction in dark for 14 h resulted in 54% of **3a** formation (Scheme 5.2.8.1f).



Scheme 5.2.8.1: Chapter 5: Control Experiments 1.

Similar control experiments were conducted over arylation and allylation reaction which doesn’t alter reaction outcome much (Scheme 5.2.8.2)



Scheme 5.2.8.2**:** Chapter 5: Control Experiments 2 and 3.

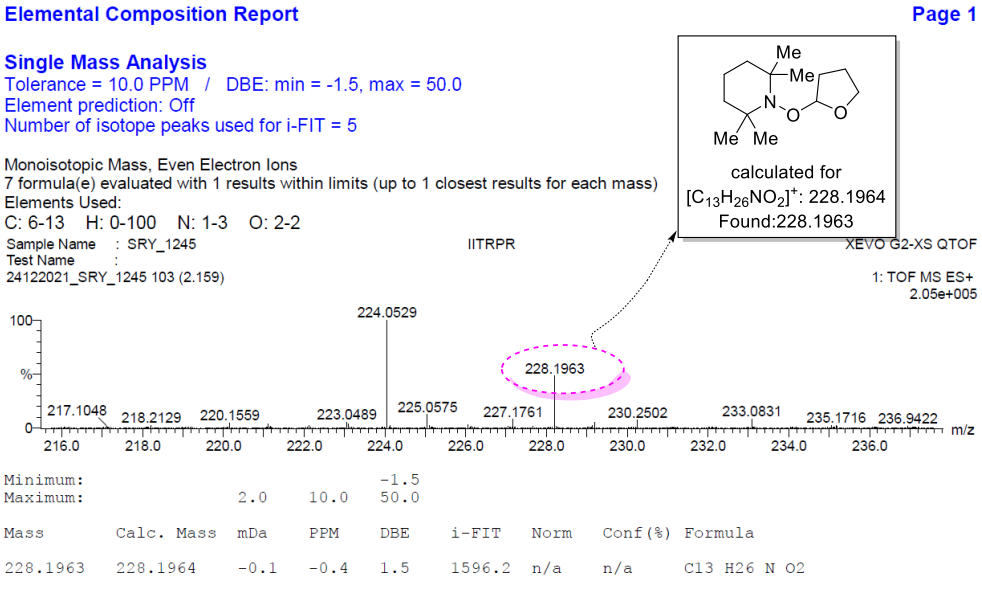


Figure 5.2.8.1: HRMS Data for TEMPO-adduct.

The colored solution of the reaction mixtures encouraged us to check ultraviolet−visible (UV/Vis) spectra. A mixture of diazo compound **1a** and THF **2a** gives an absorbance band near the UV region. Pleasingly, a combination of NBS and THF (dry and deoxygenated) developed a yellow-coloured solution. This solution shows a bathochromic shift in the visible spectral region in its optical absorption spectrum, diagnostic of an EDA complex (samples need to prepare in the glove box to avoid oxygen). In contrast, NBS in acetonitrile doesn't show any coloured solution, and its absorption falls near the UV region. Therefore, a catalytic amount of NBS can act as an acceptor in this system, and THF acts as a donor to form the NBS-THF EDA complex (Figure 5.2.8.2). UV-Visible data for compound **2a**, **4a**, and **6a**, **7a** was also recorded, which further supports NBS-THF EDA complex (Figure 5.2.8.3 and 5.2.8.4).

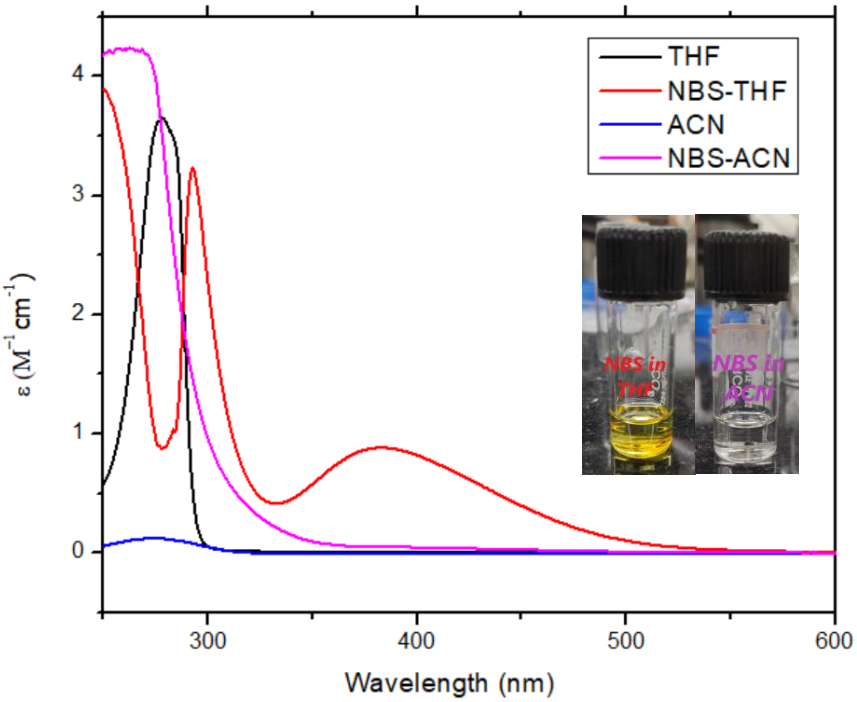


Figure 5.2.8.2: UV-Visible absorption spectra for NBS in CH_3CN and THF.

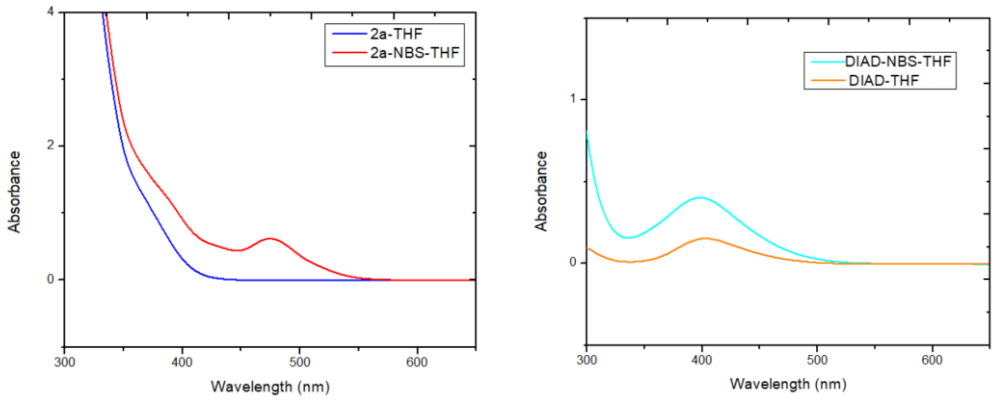


Figure 5.2.8.3: UV-Visible absorption spectra for compound 2a and DIAD.

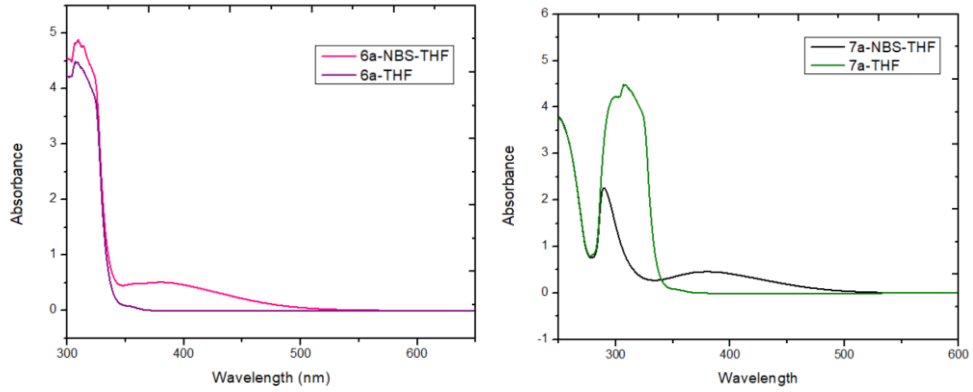


Figure 5.2.8.4: UV-Visible absorption spectra for compound 6a and 7a.

A tool to better corroborate the chain process is to measure the reaction's quantum yield (ϕ) (λ = 405 and 450 nm, using potassium ferrioxalate as the actinometer).[47] We performed this measurement for both the amination reactions and found very high quantum yields (ϕ = 142.97 and 902.41 for the synthesis of **3a** and **5a** respectively, section 5.2.9).

5.2.9. Determination of Quantum Yield:

5.2.9.1. Determination of light intensity of the Blue/Purple LED:

The photon flux was determined by using standard ferrioxalate actinometry.[S12] A 0.15 M solution of ferrioxalate was made by mixing 737 mg of potassium ferrioxalate hydrate in 10 mL of 0.05 M H_2SO_4. A buffered solution of phenanthroline was made by mixing 25 mg of phenanthroline and 5.63 g of sodium acetate in 25 mL of 0.5 M H_2SO_4. Both solutions were kept in the dark. To determine the photon flux, 1.0 mL of the ferrioxalate solution was placed in a cuvette and irradiated for 60.0 seconds at λ = 450/405 nm placing 4 cm away from hepatochem blue/purple

LED lamp. After irradiation, 0.175 mL of the phenanthroline solution was added to the cuvette. The solution was then kept for 1 h to permit the ferrous ions to completely coordinate to the phenanthroline. The absorbance of the solution was determined at 510 nm. A non-irradiated sample was also prepared and the absorbance at 510 nm was determined.

Conversion was calculated using eq. 1

$$mol\ Fe^{2+} = \frac{V.\ \Delta A}{\varepsilon.\ l} \quad \ldots\ldots 1$$

Where V is the total volume (0.001175 L) of the solution after addition of the phenanthroline, ΔA is the difference in absorbance at 510 nm between the irradiated and non-irradiated solutions, l is the path length (1.000 cm), and ε is the molar absorptivity at 510 nm (11,100 L mol^{-1} cm^{-1}).

$$mol\ Fe^{2+} = \frac{0.001175\ \text{L}.\ (0.991-0.429)}{11100\ \text{L.cm}^{-1}\text{.mol}^{-1}.\ 1\ cm}$$

$$= 5.9491\times10^{-8}\ \text{mol (for blue LEDs)}$$

$$mol\ Fe^{2+} = \frac{0.001175\ \text{L}.\ (1.229-0.652)}{11100\ \text{L.cm}^{-1}\text{.mol}^{-1}.\ 1\ cm}$$

$$= 6.1079\times10^{-8}\ \text{mol (for purple LEDs)}$$

The photon flux can be calculated using eq 2.

$$mol\ Fe^{2+}$$

Photon flux = ……2

$$\Phi \ . \ t \ . \ f$$

Where Φ is the quantum yield for the ferrioxalate actinometer (1.01 for a 0.15 M solution at λ = 450 nm), t is the time (60 s), and f is the fraction of light absorbed at λ = 450 nm, $f = 1.000–10^{-A}$.

Calculated $f = 1.000–10^{-A} = 1.000\text{-}10^{-0.991} = 0.8979$.

$$\text{Photon flux} = \frac{5.9491\times10^{-8}}{1.01\times60s\times0.8979}$$

$= 2.04\times10^{-11}$ Einstein s^{-1} (for blue LEDs)

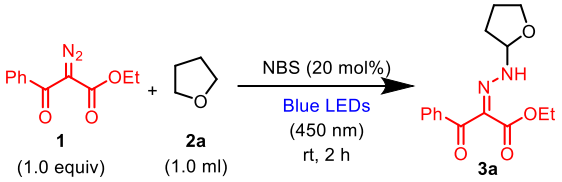
Where Φ is the quantum yield for the ferrioxalate actinometer (1.01 for a 0.15 M solution at λ = 405 nm), t is the time (60 s), and f is the fraction of light absorbed at λ = 405 nm, $f = 1.000–10^{-A}$.

Calculated $f = 1.000–10^{-A} = 1.000\text{-}10^{-1.229} = 0.9409$.

$$\text{Photon flux} = \frac{6.1079\times10^{-8}}{1.01\times60s\times0.9409}$$

$= 1.0712\times10^{-9}$ Einstein s^{-1} (for purple LEDs)

5.2.9.2. Quantum Yield Calculation 1:



In an argon filled glove box, an oven-dried vial equipped with a teflon-coated stir bar, α-diazo-β-keto compound **1a** (22 mg, 0.1 mmol, 1.0 equiv) and *N*-bromosuccinamide (NBS) (4 mg, 0.02 mmol, 0.2 equiv) were added. THF **2a** (0.1 M, 1.0 ml) was added to the reaction mixture and sealed. The vial has been taken out from the glove box and then irradiated under blue LEDs for 2 h. at room temperature. The solvent was evaporated under reduced pressure. Analytically pure product **3a** was obtained by column chromatography on silica gel using petroleum ether and ethyl acetate as eluents. The product revealed 21% isolated yield (2.1×10^{-5} mol). The quantum yield was calculated as follows:

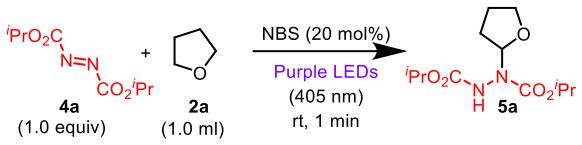
$$\Phi = \frac{mol\ product}{flux.\ t.\ f} \quad \ldots\ldots\ldots\ldots\ldots 3$$

Where, flux is the photon flux determined by ferrioxalate actinometry (2.04×10^{-11} Einstein/s), t is the time (7200 s), and f (> 0.999) is the fraction of light absorbed by NBS-THF at 450 nm under the reaction condition mentioned above.

$$\Phi = \frac{2.1 \times 10^{-5}}{2.04\times10^{-11}\times7200\times1}$$

= 142.97 (for the formation of **3a**)

5.2.9.3. Quantum Yield Calculation 2:



In an argon filled glove box, an oven-dried vial equipped with a teflon-coated stir bar, azodicarboxylate compound 4a (20 µL, 0.1 mmol, 1.0 equiv) and *N*-bromosuccinamide (NBS) (4 mg, 0.02 mmol, 0.2 equiv) were added. THF 2a (0.1 M, 1.0 ml) was added to the reaction mixture and sealed. The vial has been taken out from the glove box and then irradiated under purple LEDs for 1 min at room temperature. The solvent was evaporated under reduced pressure. Analytically pure product 5a was obtained by column chromatography on silica gel using petroleum ether and ethyl acetate as eluents. The product revealed 58% isolated yield (5.8×10^{-5} mol).

The quantum yield was calculated as follows:

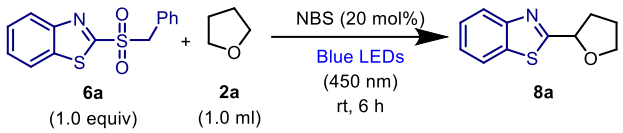
$$\Phi = \frac{mol\ product}{flux.\ t.\ f} \qquad 3$$

Where, flux is the photon flux determined by ferrioxalate actinometry (1.0712×10^{-9} Einstein/s), t is the time (60 s), and f (> 0.999) is the fraction of light absorbed by NBS-THF at 405 nm under the reaction condition mentioned above.

$$\Phi = \frac{5.8 \times 10^{-5}}{1.0712\times10^{-9}\times60\times1}$$

= 902.41 (for the formation of **5a**)

5.2.9.4. Quantum Yield Calculation 3:



In an argon filled glove box, an oven-dried vial equipped with a teflon-coated stir bar, sulfone **6a** (29 mg, 0.1 mmol, 1.0 equiv) and *N*-bromosuccinamide (NBS) (4 mg, 0.02 mmol, 0.2 equiv) were added. THF **2a** (0.1 M, 1.0 ml) was added to the reaction mixture and sealed. The vial has been taken out from the glove box and then irradiated under blue LEDs for 6 h. at room temperature. The solvent was evaporated under reduced pressure. Analytically pure product **8a** was obtained by column chromatography on silica gel using petroleum ether and ethyl acetate as eluents. The product revealed 44% isolated yield (4.4×10^{-5} mol).

The quantum yield was calculated as follows:

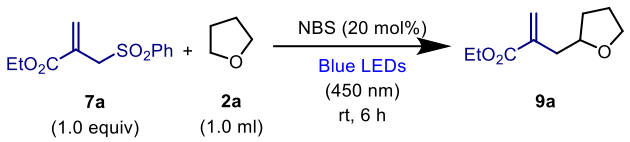
$$\Phi = \frac{mol\ product}{flux.\ t.\ f} \quad \ldots\ldots\ldots\ldots\ldots\ldots 3$$

Where, flux is the photon flux determined by ferrioxalate actinometry (2.04×10^{-11} Einstein/s), t is the time (21600 s), and f (> 0.999) is the fraction of light absorbed by NBS-THF at 450 nm under the reaction condition mentioned above.

$$\Phi = \frac{4.4 \times 10^{-5}}{2.04\times10^{-11}\times21600\times1}$$

= 99.85 (for the formation of 8a)

5.2.9.5. Quantum Yield Calculation 4:



In an argon filled glove box, an oven-dried vial equipped with a teflon-coated stir bar, sulfone **7a** (25 mg, 0.1 mmol, 1.0 equiv) and *N*-bromosuccinamide (NBS) (4 mg, 0.02 mmol, 0.2 equiv) were added. THF **2a** (0.1 M, 1.0 ml) was added to the reaction mixture and sealed. The vial has been taken out from the glove box and then irradiated under blue LEDs for 6 h. at room temperature. The solvent was evaporated under reduced pressure. Analytically pure product **9a** was obtained by column chromatography on silica gel using petroleum ether and ethyl acetate as eluents. The product revealed 43% isolated yield (4.3×10^{-5} mol).

The quantum yield was calculated as follows:

$$\Phi = \frac{mol\ product}{flux.\ t.\ f} \quad \ldots\ldots\ldots\ldots\ldots 3$$

Where, flux is the photon flux determined by ferrioxalate actinometry (2.04×10^{-11} Einstein/s), t is the time (21600 s), and f (> 0.999) is the fraction of light absorbed by NBS-THF at 450 nm under the reaction condition mentioned above.

$$\Phi = \frac{4.3 \times 10^{-5}}{2.04\times10^{-11}\times21600\times1}$$

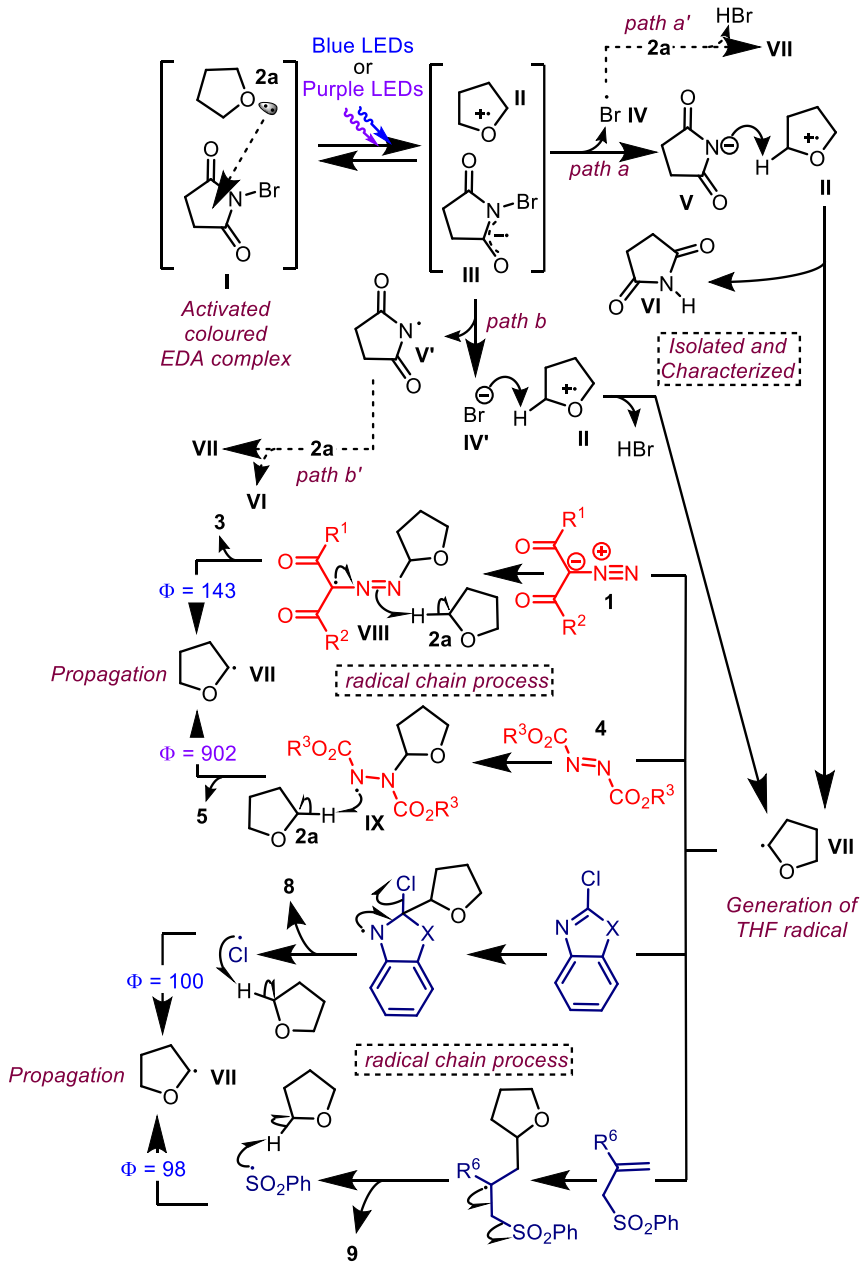
= 97.58 (for the formation of **9a**)

5.2.10. Mechanistic Proposal for the Developed Protocol:

The above results offer compelling evidence to rationalize the mechanism. Based on the mechanistic experiments and literature precedence,[48] we envisioned that the reaction initiated by forming an activated colored NBS-THF EDA complex **I**. Irradiation of this EDA complex **I** by visible lights (Blue or Purple LEDs) facilitates the generation of radical cation **II** and radical anion **III**. Elimination of bromine radical **IV** leads to form anionic species **V**. Intermediate **V** then abstracts one proton from intermediate **II** to deliver the THF radical **VII**. Consequently, the generation of succinimide **VI** also takes place via path a. This crucial radical intermediate **VII** then adds to substrate **1** or **4** to forge the C–N bond and fabricate their respective intermediates **VIII** and **IX**, respectively. Now, intermediate **VIII** and **IX** abstracts a hydrogen atom (HAT) from **2a** to facilitate the radical chain process and furnishes the aminated products (**3** or **5**) as well (Scheme 5). However, as this a radical chain process paths a', b, and b', as described in scheme 5 cannot be discarded as an alternative pathway for the generation of THF radical **VII**. Here, path b represents the formation of bromide ion **IV′** and radical intermediate **V′** from intermediate **III**. Intermediate **IV′** undergoes a deprotonation step with intermediate **II** to generate THF radical **VII**. Similarly, a HAT process between intermediate **V′** or **IV** with **2a** leads to the THF radical **VII** formation via path a' and path b' respectively (Scheme 5.2.10.1).

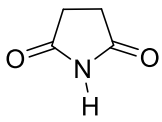
A similar EDA-guided mechanism has been proposed for the arylation and allylation reaction which follows an activated nucleophilic substitution reaction via intermediate **xx** and **xx** following an addition-elimination pathway. The calculated quantum yield (ϕ) for these reactions also supports the radical chain pathway (Scheme 5.2.10.1).

Plausible mechanism



Scheme 5.2.10.1: Chapter 5: Plausible Mechanism.

5.2.10.1. Spectral data in the support of generation of succinimide VI during the reaction:

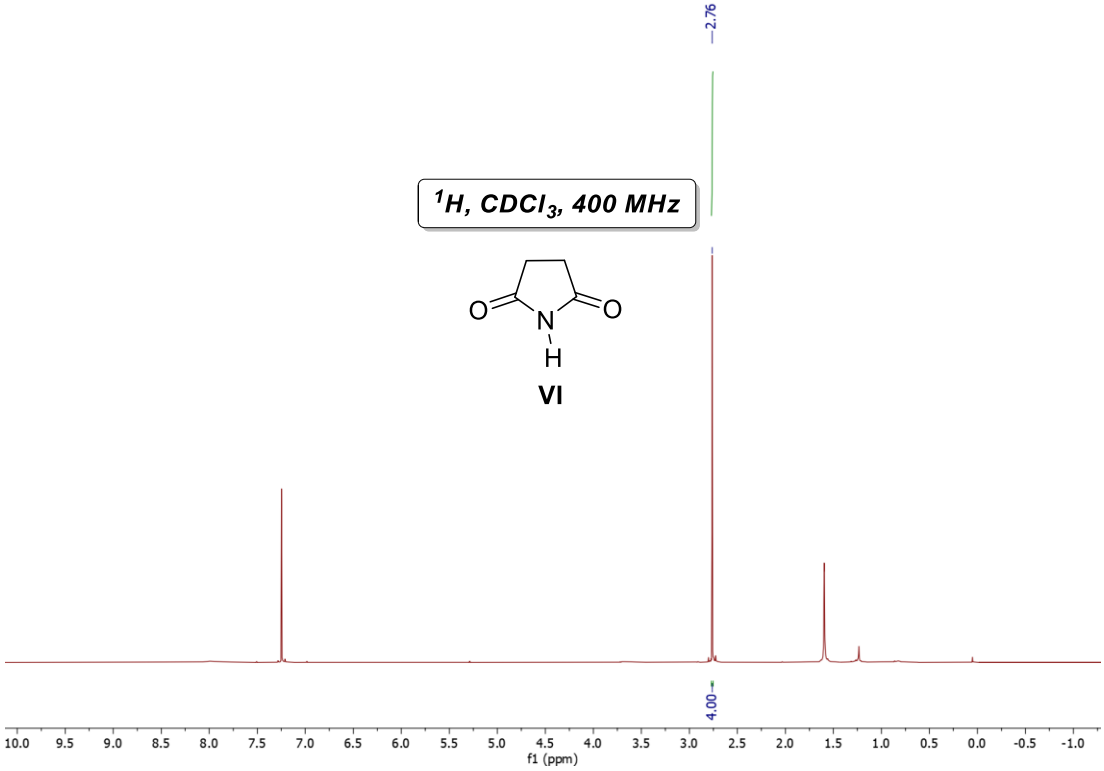


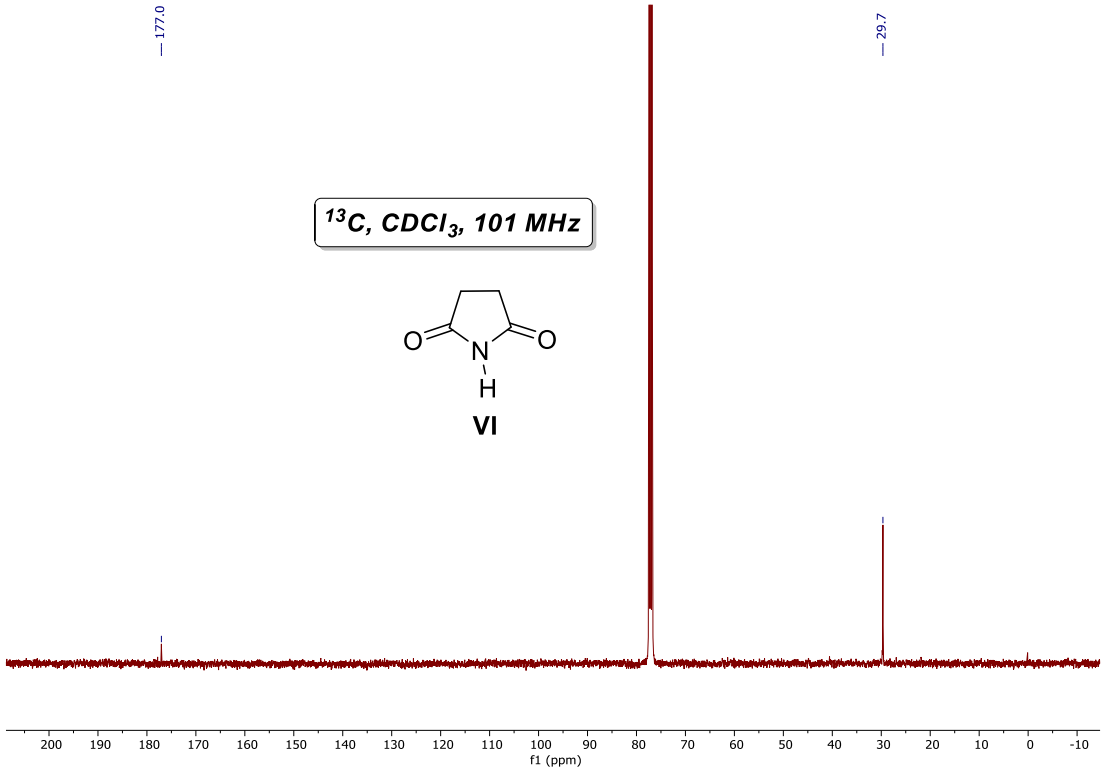
VI

$C_4H_5NO_2$

M. W. 99.08 g/mol

According to **GP-4** or **GP-5** side product **VI** was obtained while preparing compound **3a** or **5a** by using **1a** (22.0 mg, 0.1 mmol, 1.0 equiv) or **4a** (20 µL, 0.1 mmol, 1.0 equiv) and NBS (4.0 mg, 0.02 mmol, 0.2 equiv) in 1 ml THF for 16 h or 5 min at rt. Column chromatographic purification (petroleum ether/EtOAc 90:10 to 50:50) afforded **VI** as white solid (2.0 mg, 20%).





5.3 Conclusion

In summary, this chapter demonstrates a modular method to render a series of amine, C(sp^2)–H, and C(sp^3)–H alkylating products with various ethers. Visible lights were entailed to carry out this metal-free, oxidant-free C–N and C–C bond-forming event. The generation and identification of catalytic NBS-THF electron donor-acceptor (EDA) complex were crucial, permitting direct and selective (sp^3)Cα–H bond functionalization. A radical chain mechanism is proposed based on the literature and our experimental evidence. It is noteworthy that the developed methodology overcomes the significant disadvantages like long reaction time and harsh reaction conditions associated with previous (sp^3)Cα–H bond functionalization techniques.

5.4. Experimental Section

5.4.1. General Information:

All reactions were performed in flame-dried glassware under argon atmosphere unless otherwise stated. Liquids and solutions were transferred with syringes. Solvents used were dried and purified by following standard procedures. Technical grade solvents for extraction or chromatography (ethyl acetate, and petroleum ether) were distilled prior to use. $CDCl_3$ was stored over 4Å molecular sieves. Used chemicals were purchased from Sigma-Aldrich, TCI, Alfa-Aesar and Sisco Research Laboratories (SRL) used without further purification. All the liquid chemicals distilled freshly prior to use. Analytical thin-layer chromatography (TLC) was performed on using pre-coated aluminium-backed plates (Merck Kieselgel 60 F254) and visualized by UV radiation, basic aqueous potassium permangante ($KMnO_4$), *p*-anisaldehyde stains and heat as developing agents.

Flash column chromatography was performed on silica gel 60 (40–63 μm, 230–400 mesh, ASTM) from Merck using the indicated solvents. Organic solutions were concentrated under reduced pressure on Heidolph rotary evaporator. NMR spectra were acquired on a JEOL JNM ECS-400 instrument running at 400 MHz for ^{1}H, 101 MHz ^{13}C and 376 MHz for ^{19}F respectively. Chemical shifts (δ) are reported in ppm relative to residual solvent signals ($CHCl_3$, 7.26 ppm for ^{1}H NMR, $CDCl_3$, 77.0 ppm for ^{13}C NMR). Data are reported as follows: chemical shift, multiplicity (br = broad singlet, s = singlet, d = doublet, dd = doublet of doublets, t = triplet, q = quartet, ddd = doublet of doublet of doublet, td = triplet of doublet, m = multiplet), coupling constants (Hz), and integration. 1,2-Dibromomethane was used as an internal standard to calculate NMR yields of products by ^{1}H NMR analysis of the crude mixture. HRMS was recorded on Waters Xevo G2-XS (Q-TOF).

5.4.2. Photoreactor Setup:

Photochemical reactions were carried out in bottom plane irradiated vials in a Hepatochem Photoreactor composed of cooling block and LEDs connected to AC/DC input 100-240 V AC, 50/60 Hz power supply (Figure 1).

Filters used- 450nm, 405nm, and 365nm.

Instrument details available at: https://www.hepatochem.com/photoreactors-leds-accessories/#photoreactors



Figure 1: Photochemical reaction set up.

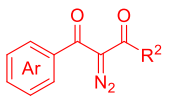
5.4.3. List of substrates prepared:

5.4.3.1. List of diazo compounds prepared:[50-54]

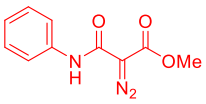
The lists of diazo compounds prepared according to **GP-1–GP-3** are given bellow.

List of successful diazo compounds

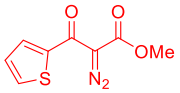
1a: Ar = Ph, R^2 = OEt
1b: Ar = 4-MeC_6H_4, R^2 = OEt
1c: Ar = 4-FC_6H_4, R^2 = OEt
1d: Ar = 4-BrC_6H_4, R^2 = OEt
1e: Ar = 3-ClC_6H_4, R^2 = OMe
1f: Ar = 4-CNC_6H_4, R^2 = OEt
1g: Ar = 3,4-$OMeC_6H_3$, R^2 = OMe



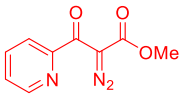
1



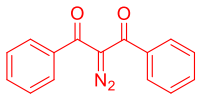
1h



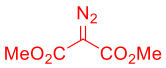
1i



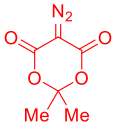
1j



1k

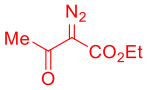


1l

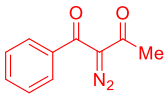


1m

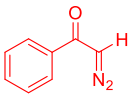
List of unsuccessful diazo compounds



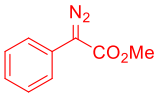
1m



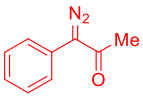
1n



1o



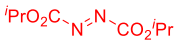
1p



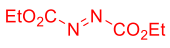
1q

5.4.3.2. List of azodicarboxylates used:

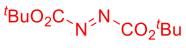
List of azodicarboxylates



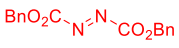
4a



4b

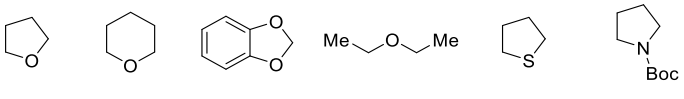


4c



4d

5.4.3.3. List of ethers used:

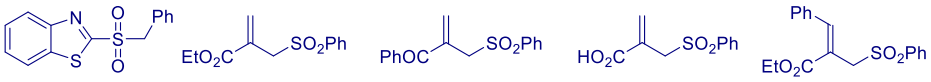


2a **2b** **2c** **2d** **2e** **2f**

5.4.3.4. List of sulfones prepared:

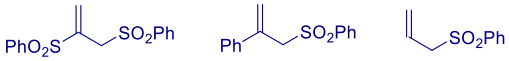
All sulfones were prepared according to the previous literatures.[55-57]

List of succsessful sulfones



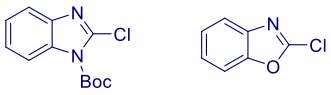
6a **7a** **7b** **7c** **7d**

List unsuccsessful of sulfones



7e **7f** **7g**

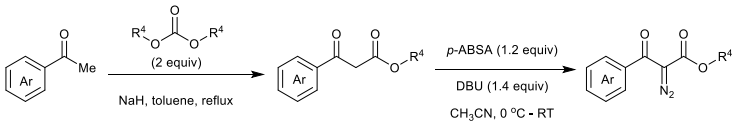
5.4.3.5. List of other aryl substrates used:[58]



6b **6c**

5.4.4. General Procedures:

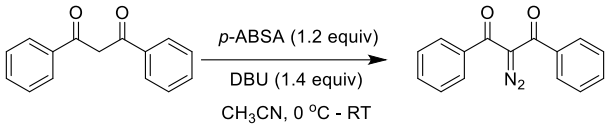
5.4.4.1. General procedure for preparation of α-diazo-β-keto esters (GP-1).[50, 51]



According to previous literature,[50] acetoacetate derivatives were prepared. To a dried 100 mL three-necked flask were added NaH (2.2 g, 60% w/w, 56 mmol), dimethyl carbonate or diethyl carbonate (40 mmol), and toluene (20 mL) under nitrogen. After the reaction mixture was heated to reflux in oil bath, a solution of acetophenone (20 mmol) in toluene (10 mL) was added dropwise over 0.5 h. After the evolution of hydrogen ceased (30-45 min), the reaction was cooled down to room temperature. Glacial acetic acid (6 mL) was added dropwise and a heavy pasty solid was separated. Ice-cold water was slowly added until the solid was dissolved completely. Then, the reaction system was diluted with EtOAc. The organic layer was separated, washed with water (20 mL) and then saturated brine (20 mL) and finally dried over anhydrous Na_2SO_4. After the solvent was evaporated with the aid of rotary evaporator, the residue was purified by flash chromatography on silica gel with EtOAc/hexanes.

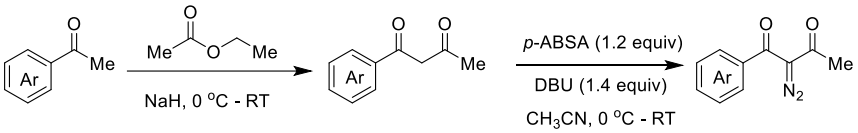
In the next step, according to previous literature,[51] α-diazoesters were prepared. To a solution of acetoacetate derivatives (1 equiv, 5 mmol) and *p*-acetamidobenzenesulfonyl azide (*p*-ABSA) (1.2 equiv, 6 mmol) in anhydrous CH_3CN at 0 °C, triethylamine (Et_3N) (3 equiv, 15 mmol) was added dropwise. After stirring at room temperature for 5 h the reaction mixture was concentrated in vacuo. Water (20 mL) was added. The resulting mixture was extracted with diethyl ether (2 X 20 mL). The combined organic layer was washed with brine (20 mL) and dried over $MgSO_4$. The solvent was removed under reduced pressure, and the residue was purified by a silica gel column chromatography with petroleum ether/ethyl acetate as the eluent to give the entitled diazo compounds.

5.4.4.2. General procedure for preparation of diazoacetophenone (GP-2).[52]



According to previous literature,[52] to a solution of 1,3-diphenylpropanedione (896 mg, 4 mmol) and Et_3N (0.6 mL, 4.2 mmol) in acetonitrile (20 mL), a solution of *p*-ABSA (1200 mg, 5 mmol) in 20 mL acetonitrile was added dropwise with stirring. The reaction mixture was stirred at room temperature overnight. The compound 2-diazo-1,3-diphenylpropane-1,3-dione was purified by column chromatography (silica gel) using PE/EA 20:1 as eluent.

5.4.4.3. General procedure for preparation of α-diazoketones (GP-3):[53, 54]

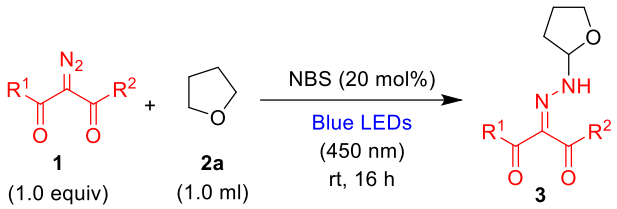


According to previous literature,[53] 1-arylbutane-1,3-diones were prepared. To an oven dried round-bottom flask, substituted aryl ketone (515 mg, 4.3 mmol) and ethyl acetate (20 mL) followed by NaH (17.2 mmol, 60% in dispersions oil) was added at 0 ºC, The resultant reaction mixture was stirred at room temperature for 24 h. Then, it was quenched with saturated NH_4Cl solution, extracted with EtOAc (3 X 25 mL) and the combined layer was dried over Na_2SO_4. The evaporation of solvent under the reduced under pressure followed by purification using column chromatography afforded the products.

According to previous literature,[54]1-arylbutane-1,3-diones were converted into corresponding diazoketones. To an oven-dried round-bottom flask equipped with a magnetic stirring bar 1-

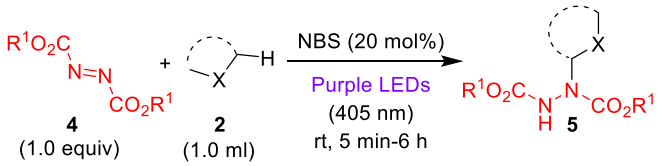
arylbutane-1,3-dione (1 equiv, 10 mmol) and *p*-ABSA (1.2 equiv, 12 mmol) were added, and the system was filled with nitrogen. Acetonitrile was then added, and the reaction mixture was cooled to 0 °C using an ice-bath. Triethylamine (2 equiv, 20 mmol) was added dropwise within 2 min; the reaction mixture was slowly warmed to room temperature, and allowed to stir for 8 h. A white precipitate of *N*-(4-sulfamoylphenyl)acetamide was filtered and washed with dicloromethane (2 X 10 mL). Solvents were evaporated, and diazo compound was purified by column chromatography on silica gel with a 9:1 to 4:1 (v/v) gradient of hexane:ethyl acetate as eluents.

5.4.4.4. General procedure for the amination from diazo compounds (GP-4):



In an argon filled glove box, an oven-dried vial equipped with a teflon-coated stir bar, α-diazo-β-keto compound **1** (0.1 mmol, 1.0 equiv) and *N*-bromosuccinamide (NBS) (0.02 mmol, 0.2 equiv) were added. THF **2a** (0.1 M, 1.0 ml) was added to the reaction mixture and sealed. The vial has been taken out from the glove box and then irradiated under blue LEDs for 16 h. at room temperature. After completion, the crude reaction mixture is used to measure the *Z/E* ratio by ^{1}H NMR. The solvent was evaporated under reduced pressure. Analytically pure products (**3a-3l**) were obtained by column chromatography on silica gel using petroleum ether and ethyl acetate as eluents.

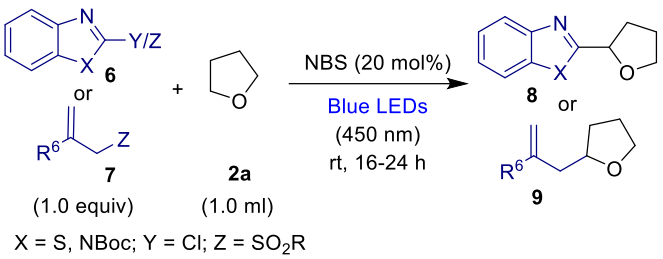
5.4.4.5. General procedure for the amination from azodicarboxylates (GP-5):



In an argon filled glove box, an oven-dried vial equipped with a teflon-coated stir bar, azodicarboxylate **4** (0.1 mmol, 1.0 equiv) and *N*-bromosuccinamide (NBS) (0.02 mmol, 0.2 equiv) were added. Ether **2** (0.1 M, 1.0 ml) was added to the reaction mixture and sealed. The vial has been taken out from the glove box and then irradiated under purple LEDs for 5 min-6 h. at room temperature. After completion, the solvent was evaporated under reduced pressure.

Analytically pure products (**5a-5i**) were obtained by column chromatography on silica gel using petroleum ether and ethyl acetate as eluents.

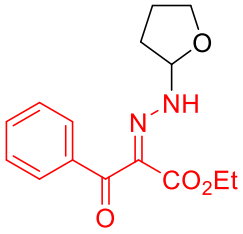
5.4.4.6. General procedure for the arylation and allylation reactions (GP-6):



In an argon filled glove box, an oven-dried vial equipped with a teflon-coated stir bar, arylsulfone **6** or allylsulfone **7** (0.1 mmol, 1.0 equiv) and *N*-bromosuccinamide (NBS) (0.02 mmol, 0.2 equiv) were added. THF **2a** (0.1 M, 1.0 ml) was added to the reaction mixture and sealed. The vial has been taken out from the glove box and then irradiated under Blue LEDs (for compounds **8c** purple LEDs were used instead of blue LEDs) for 16-24 h. at room temperature. After completion, the solvent was evaporated under reduced pressure. Analytically pure products (**8a-8c**, **9a-9d**) were obtained by column chromatography on silica gel using petroleum ether and ethyl acetate as eluents.

5.4.5. Result & Characterization:

5.4.5.1. ethyl (*Z*)-3-oxo-3-phenyl-2-(2-(tetrahydrofuran-2-yl)hydrazono)propanoate (3a):



3a

$C_{15}H_{18}N_2O_4$

M. W. 290.32 g/mol

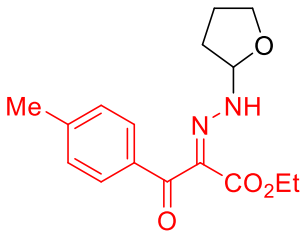
According to **GP-4** compound **3a** was prepared by using **1a** (22.0 mg, 0.1 mmol, 1.0 equiv) and NBS (4.0 mg, 0.02 mmol, 0.2 equiv) in 1 ml THF for 16 h at rt. Column chromatographic purification (petroleum ether/EtOAc 95:5 to 80:20) afforded **3a** as colourless oil (23.0 mg, 78%, *Z/E* = 6:1). (From crude reaction mixture *Z/E* = 6:1).

For 1 mmol scale reaction compound **3a** was prepared by using **1a** (220.0 mg, 0.1 mmol, 1.0 equiv) and NBS (40.0 mg, 0.02 mmol, 0.2 equiv) in 10 ml THF for 20 h at rt to get 65% (190 mg) isolated yield.

HRMS (ESI): m/z $[M+Na]^+$ Calculated for $[C_{15}H_{18}N_2O_4Na]^+$: 313.1164; Found: 313.1165.

^{1}H NMR (400 MHz, $CDCl_3$): 11.07 (d, *J* = 5.5 Hz, 1H), 7.85–7.82 (m, 2H), 7.52–7.48 (m, 1H), 7.42–7.38 (m, 2H), 5.35 (ddd, *J* = 6.9, 6.0, 4.1 Hz, 1H), 4.27 (q, *J* = 7.3 Hz, 2H), 3.94–3.88 (m, 1H), 3.86–3.80 (m, 1H), 2.20–2.11 (m, 1H), 1.92–1.84 (m, 2H), 1.28 (t, *J* = 7.1 Hz, 3H). (Peaks for major isomer) **^{13}C NMR (101 MHz, $CDCl_3$):** δ 190.1, 163.7, 137.8, 132.3, 130.2, 127.9, 126.8, 90.7, 68.3, 61.1, 30.4, 24.9, 14.1. (Peaks for major isomer)

5.4.5.2. ethyl (*Z*)-3-oxo-2-(2-(tetrahydrofuran-2-yl)hydrazono)-3-(*p*-tolyl)propanoate (3b):



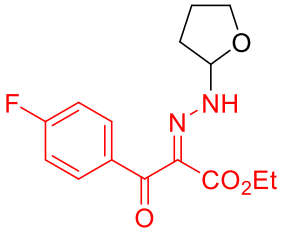
3b
$C_{16}H_{20}N_2O_4$
M. W. 304.35 g/mol

According to **GP-4** compound **3b** was prepared by using **1b** (23.0 mg, 0.1 mmol, 1.0 equiv) and NBS (4.0 mg, 0.02 mmol, 0.2 equiv) in 1 ml THF for 16 h at rt. Column chromatographic purification (petroleum ether/EtOAc 95:5 to 80:20) afforded **3b** as colourless oil (22.0 mg, 72%, *Z*/*E* = 6:1). (From crude reaction mixture *Z*/*E* = 5:1)

HRMS (ESI): m/z $[M+H]^+$ Calculated for $[C_{16}H_{21}N_2O_4]^+$: 305.1501; Found: 305.1501.

^{1}H NMR (400 MHz, $CDCl_3$): δ 10.99 (d, *J* = 6.0 Hz, 1H), 7.77–7.75 (m, 2H), 7.21–7.19 (m, 2H), 5.35 (td, *J* = 6.4, 3.9 Hz, 1H), 4.26 (q, *J* = 7.3 Hz, 2H), 3.96–3.89 (m, 1H), 3.86–3.81 (m, 1H), 2.39 (s, 3H), 2.21–2.12 (m, 1H), 2.08–2.00 (m, 1H), 1.96–1.84 (m, 2H), 1.27 (t, *J* = 7.1 Hz, 3H). (Peaks for major isomer) **^{13}C NMR (101 MHz, $CDCl_3$):** δ 189.7, 163.6, 143.1, 135.0, 130.5, 128.7, 126.9, 90.7, 68.2, 61.1, 30.4, 24.9, 21.7, 14.1. (Peaks for major isomer)

5.4.5.3. ethyl (*Z*)-3-(4-fluorophenyl)-3-oxo-2-(2-(tetrahydrofuran-2-yl)hydrazono)propanoate (3c):



3c

$C_{15}H_{17}FN_2O_4$

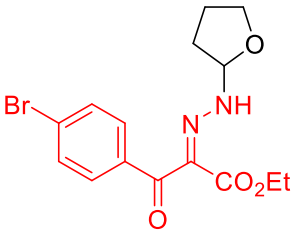
M. W. 308.31 g/mol

According to **GP-4** compound **3c** was prepared by using **1c** (24.0 mg, 0.1 mmol, 1.0 equiv) and NBS (4.0 mg, 0.02 mmol, 0.2 equiv) in 1 ml THF for 16 h at rt. Column chromatographic purification (petroleum ether/EtOAc 99:5 to 85:15) afforded **3c** as colourless oil (25.0 mg, 81%, *Z/E* = 9:1). (From crude reaction mixture *Z/E* = 8:1)

HRMS (ESI): m/z $[M+H]^+$ Calculated for $[C_{15}H_{18}N_2O_4F]^+$: 309.1251; Found: 309.1252.

^{1}H NMR (400 MHz, $CDCl_3$): δ 11.07 (d, *J* = 5.5 Hz, 1H), 7.90–7.85 (m, 2H), 7.09–7.05 (m, 2H), 5.34 (td, *J* = 6.4, 3.9 Hz, 1H), 4.28 (q, *J* = 7.3 Hz, 2H), 3.94–3.89 (m, 1H), 3.87–3.81 (m, 1H), 2.12–2.13 (m, 1H), 2.03 (m, 1H), 1.94–1.86 (m, 2H), 1.29 (t, *J* = 7.1 Hz, 3H). (Peaks for major isomer) **^{13}C NMR (101 MHz, $CDCl_3$):** δ 184.4, 165.3 (d, *J* = 253.5 Hz), 163.5, 133.9 (d, *J* = 2.9 Hz), 132.8 (d, *J* = 9.0 Hz), 126.6, 115.0 (d, *J* = 21.8 Hz), 90.7, 68.3, 61.2, 30.5, 24.9, 14.2. (Peaks for major isomer) **^{19}F NMR: (376 MHz, $CDCl_3$):** δ -106.6. (Peak for major isomer)

5.4.5.4. ethyl (*Z*)-3-(4-bromophenyl)-3-oxo-2-(2-(tetrahydrofuran-2-yl)hydrazono)propanoate (3d):



3d

$C_{15}H_{17}BrN_2O_4$

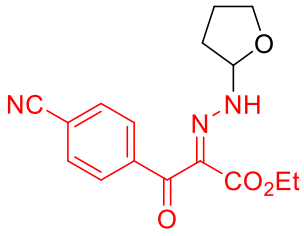
M. W. 369.22 g/mol

According to **GP-4** compound **3d** was prepared by using **1d** (30.0 mg, 0.1 mmol, 1.0 equiv) and NBS (4.0 mg, 0.02 mmol, 0.2 equiv) in 1 ml THF for 16 h at rt. Column chromatographic purification (petroleum ether/EtOAc 95:5 to 85:15) afforded **3d** as colourless oil (26.0 mg, 70%, *Z/E* = 9:1). (From crude reaction mixture *Z/E* = 9:1)

HRMS (ESI): m/z $[M+H]^+$ Calculated for $[C_{15}H_{18}N_2O_4Br]^+$: 369.0450; Found: 369.0448.

^{1}H NMR (400 MHz, $CDCl_3$): δ 11.12 (d, *J* = 5.5 Hz, 1H), 7.71–7.68 (m, 2H), 7.55–7.52 (m, 2H), 5.33 (td, *J* = 6.4, 3.7 Hz, 1H), 4.28 (q, *J* = 7.3 Hz, 2H), 3.94–3.88 (m, 1H), 3.87–3.81 (m, 1H), 2.22–2.13 (m, 1H), 2.06–1.99 (m, 1H), 1.94–1.86 (m, 2H), 1.30 (t, *J* = 7.3 Hz, 3H). (Peaks for major isomer) **^{13}C NMR (101 MHz, $CDCl_3$):** δ 188.8, 163.6, 136.7, 131.8, 131.2, 127.2, 126.4, 90.8, 68.3, 61.2, 30.5, 24.9, 14.1. (Peaks for major isomer)

5.4.5.5. ethyl (*Z*)-3-(4-cyanophenyl)-3-oxo-2-(2-(tetrahydrofuran-2-yl)hydrazono)propanoate (3e):



3e

$C_{16}H_{17}N_3O_4$

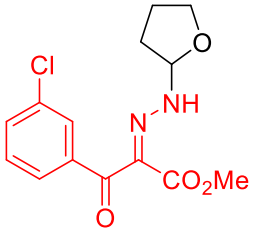
M. W. 315.33 g/mol

According to **GP-4** compound **3e** was prepared by using **1e** (24.0 mg, 0.1 mmol, 1.0 equiv) and NBS (4.0 mg, 0.02 mmol, 0.2 equiv) in 1 ml THF for 16 h at rt. Column chromatographic purification (petroleum ether/EtOAc 90:10 to 70:30) afforded **3e** as colourless oil (20.0 mg, 78%, *Z/E* = 9:1). (From crude reaction mixture *Z/E* = 8:1)

HRMS (ESI): m/z $[M+H]^+$ Calculated for $[C_{16}H_{18}N_3O_4]^+$: 316.1297; Found: 316.1297.

^{1}H NMR (400 MHz, $CDCl_3$): δ 11.31 (d, *J* = 5.4 Hz, 1H), 7.86–7.83 (m, 2H), 7.70–7.67 (m, 2H), 5.31 (ddd, *J* = 10.3, 7.0, 3.7 Hz, 1H), 4.31 (q, *J* = 7.2 Hz, 2H), 3.95–3.89 (m, 1H), 3.87–3.81 (m, 1H), 2.23–2.14 (m, 1H), 2.04–1.97 (m, 1H), 1.93–1.86 (m, 2H), 1.33 (t, *J* = 7.1 Hz, 3H). (Peaks for major isomer) **^{13}C NMR (101 MHz, $CDCl_3$):** δ 188.3, 163.6, 142.2, 131.7, 130.4, 126.0, 118.4, 115.0, 90.9, 68.5, 61.4, 30.5, 24.8, 14.1. (Peaks for major isomer)

5.4.5.6. methyl (*Z*)-3-(3-chlorophenyl)-3-oxo-2-(2-(tetrahydrofuran-2-yl)hydrazono)propanoate (3f):



3f

$C_{14}H_{15}ClN_2O_4$

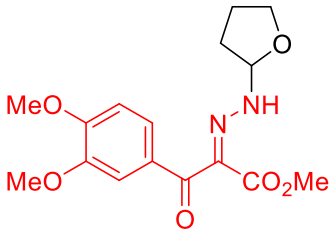
M. W. 310.73 g/mol

According to **GP-4** compound **3f** was prepared by using **1f** (24.0 mg, 0.1 mmol, 1.0 equiv) and NBS (4.0 mg, 0.02 mmol, 0.2 equiv) in 1 ml THF for 16 h at rt. Column chromatographic purification (petroleum ether/EtOAc 95:5 to 80:20) afforded **3f** as colourless oil (25.5 mg, 82%, *Z/E* = 10:1). (From crude reaction mixture *Z/E* = 9:1)

HRMS (ESI): m/z $[M+H]^+$ Calculated for $[C_{14}H_{16}ClN_2O_4]^+$: 311.0799; Found: 311.0798.

^{1}H NMR (400 MHz, $CDCl_3$): δ 11.23 (d, *J* = 4.7 Hz, 1H), 7.78–7.77 (m, 1H), 7.69–7.66 (m, 1H), 7.47–7.44 (m, 1H), 7.35–7.31 (m, 1H), 5.35 (ddd, *J* = 6.7, 5.2, 3.7 Hz, 1H), 3.95–3.91 (m, 1H), 3.90–3.85 (m, 1H), 3.84 (s, 3H), 2.21–2.12 (m, 1H), 2.10–2.02 (m, 1H), 1.92–1.85 (m, 2H). (Peaks for major isomer) **^{13}C NMR (101 MHz, $CDCl_3$):** δ 188.5, 164.0, 139.7, 134.0, 132.0, 130.2, 129.2, 128.3, 125.9, 90.5, 68.5, 52.0, 30.4, 24.8. (Peaks for major isomer)

5.4.5.7. methyl (*Z*)-3-(3,4-dimethoxyphenyl)-3-oxo-2-(2-(tetrahydrofuran-2-yl)hydrazono)propanoate (3g):



3g

$C_{16}H_{20}N_2O_6$

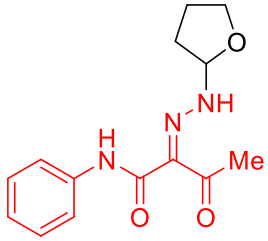
M. W. 336.34 g/mol

According to **GP-4** compound **3g** was prepared by using **1g** (26.0 mg, 0.1 mmol, 1.0 equiv) and NBS (4.0 mg, 0.02 mmol, 0.2 equiv) in 1 ml THF for 16 h at rt. Column chromatographic purification (petroleum ether/EtOAc 99:1 to 95:5) afforded **3g** as colourless oil (16.0 mg, 78%, *Z/E* = 7:1). (From crude reaction mixture *Z/E* = 6:1)

HRMS (ESI): m/z $[M+H]^+$ Calculated for $[C_{16}H_{21}N_2O_6]^+$: 337.1400; Found: 337.1399.

^{1}H NMR (400 MHz, $CDCl_3$): δ 10.96 (d, *J* = 6.0 Hz, 1H), 7.53–7.50 (m, 2H), 6.87–6.83 (m, 1H), 5.36 (td, *J* = 6.6, 4.1 Hz, 1H), 3.93 (s, 3H), 3.92 (s, 3H), 3.88–3.81 (m, 2H), 3.80 (s, 3H), 2.23–2.15 (m, 1H), 2.08–2.00 (m, 1H), 1.99–1.88 (m, 2H). (Peaks for major isomer) **^{13}C NMR (101 MHz, $CDCl_3$):** δ 188.6, 163.9, 153.1, 148.6, 130.1, 126.4, 125.7, 112.3, 109.7, 90.7, 68.1, 56.1, 56.1, 51.9, 30.5, 25.0. (Peaks for major isomer)

5.4.5.8. methyl (*Z*)-3-oxo-3-(phenylamino)-2-(2-(tetrahydrofuran-2-yl)hydrazono)propanoate (3h):



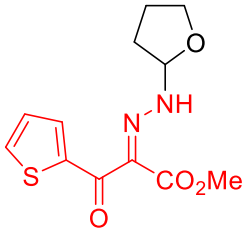
3h
$C_{14}H_{17}N_3O_3$
M. W. 275.30 g/mol

According to **GP-4** compound **3h** was prepared by using **1h** (20.0 mg, 0.1 mmol, 1.0 equiv) and NBS (4.0 mg, 0.02 mmol, 0.2 equiv) in 1 ml THF for 16 h at rt. Column chromatographic purification (petroleum ether/EtOAc 95:5 to 85:15) afforded **3h** as colourless oil (17.0 mg, 62%). (From crude reaction mixture *Z*/*E* = >10:1)

HRMS (ESI): m/z $[M+H]^+$ Calculated for $[C_{14}H_{18}N_3O_3]^+$: 276.1348; Found: 276.1349.

^{1}H NMR (400 MHz, $CDCl_3$): δ 11.35 (s, 1H), 7.57–7.54 (m, 2H), 7.34–7.30 (m, 2H), 7.13–7.09 (m, 1H), 5.44 (td, *J* = 6.5, 3.5 Hz, 1H), 4.02–3.97 (m, 1H), 3.94–3.89 (m, 1H), 2.43 (s, 3H), 2.33–2.24 (m, 1H), 2.20–2.11 (m, 1H), 2.10–1.97 (m, 2H). **^{13}C NMR (101 MHz, $CDCl_3$):** δ 199.7, 162.9, 137.3, 129.1, 126.1, 124.7, 121.0, 91.6, 68.4, 30.6, 26.0, 25.0.

5.4.5.9. methyl (*Z*)-3-oxo-2-(2-(tetrahydrofuran-2-yl)hydrazono)-3-(thiophen-2-yl)propanoate (3i):



3i

$C_{12}H_{14}N_2O_4S$

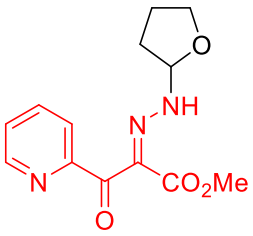
M. W. 282.31 g/mol

According to **GP-4** compound **3i** was prepared by using **1i** (21.0 mg, 0.1 mmol, 1.0 equiv) and NBS (4.0 mg, 0.02 mmol, 0.2 equiv) in 1 ml THF for 10 h at rt. Column chromatographic purification (petroleum ether/EtOAc 99:1 to 95:5) afforded **3i** as colourless oil (15.0 mg, 53%). (From crude reaction mixture *Z/E* = 8:1)

HRMS (ESI): m/z $[M+H]^+$ Calculated for $[C_{12}H_{15}N_2O_4S]^+$: 283.0753; Found: 283.0753.

^{1}H NMR (400 MHz, $CDCl_3$): δ 11.12 (d, *J* = 5.3 Hz, 1H), 7.90 (dd, *J* = 3.8, 1.2 Hz, 1H), 7.60 (dd, *J* = 5.0, 1.3 Hz, 1H), 7.09 (dd, *J* = 4.9, 3.9 Hz, 1H), 5.51 (td, *J* = 6.4, 4.0 Hz, 1H), 4.02–3.96 (m, 1H), 3.93–3.88 (m, 1H), 3.84 (s, 3H), 2.31–2.24 (m, 1H), 2.18–2.09 (m, 1H), 2.06–1.95 (m, 2H). **^{13}C NMR (101 MHz, $CDCl_3$):** δ 180.4, 163.9, 141.5, 134.8, 134.4, 127.4, 126.0, 90.9, 68.3, 52.1, 30.7, 25.0.

5.4.5.10. methyl (*Z*)-3-oxo-3-(pyridin-2-yl)-2-(2-(tetrahydrofuran-2-yl)hydrazono)propanoate (3j):



3j

$C_{13}H_{15}N_3O_4$

M. W. 277.28 g/mol

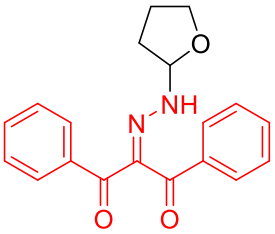
According to **GP-4** compound **3j** was prepared by using **1j** (20.0 mg, 0.1 mmol, 1.0 equiv) and NBS (4.0 mg, 0.02 mmol, 0.2 equiv) in 1 ml THF for 16 h at rt. Column chromatographic purification (petroleum ether/EtOAc 80:20 to 60:40) afforded **3i** as colourless oil (14.0 mg, 51%). (From crude reaction mixture *Z/E* = 2:1)

HRMS (ESI): m/z $[M+H]^+$ Calculated for $[C_{13}H_{15}N_3O_4]^+$: 278.1140; Found: 278.1141.

^{1}H NMR (400 MHz, $CDCl_3$): δ 11.12 (d, *J* = 5.0 Hz, 1H), 8.61–8.60 (m, 1H), 7.85–7.77 (m, 3H), 5.39–5.35 (m, 1H), 3.90–3.86 (m, 1H), 3.85–3.79 (m, 1H), 3.72 (s, 3H), 2.08–2.01 (m, 2H), 1.89–1.82 (m, 2H). (Peaks for major isomer)

^{13}C NMR (101 MHz, $CDCl_3$): δ 189.6, 163.8, 156.0, 148.5, 136.6, 126.6, 125.8, 123.6, 90.8, 68.3, 51.7, 30.4, 24.7. (Peaks for major isomer)

5.4.5.11. 1,3-diphenyl-2-(2-(tetrahydrofuran-2-yl)hydrazono)propane-1,3-dione (3k):



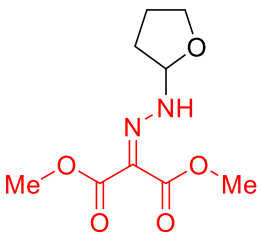
3k
$C_{19}H_{18}N_2O_3$
M. W. 322.36 g/mol

According to **GP-4** compound **3k** was prepared by using **1l** (25.0 mg, 0.1 mmol, 1.0 equiv) and NBS (4.0 mg, 0.02 mmol, 0.2 equiv) in 1 ml THF for 16 h at rt. Column chromatographic purification (petroleum ether/EtOAc 95:5 to 85:15) afforded **3k** as colourless oil (22.0 mg, 68%).

HRMS (ESI): m/z $[M+Na]^+$ Calculated for $[C_{19}H_{18}N_2O_3Na]^+$: 345.1215; Found: 345.1215.

^{1}H NMR (400 MHz, $CDCl_3$): δ 11.78 (d, *J* = 5.3 Hz, 1H), 7.99–7.97 (m, 2H), 7.61–7.59 (d, *J* = 9.4 Hz, 2H), 7.58–7.54 (m, 1H), 7.48–7.44 (m, 3H), 7.37–7.33 (m, 2H), 5.41 (td, *J* = 6.3, 3.7 Hz, 1H), 3.98–3.93 (m, 1H), 3.89–3.84 (m, 1H), 2.26–2.16 (m, 1H), 2.14–2.06 (m, 1H), 1.97–1.89 (m, 2H). **^{13}C NMR (101 MHz, $CDCl_3$):** δ 192.6, 191.8, 138.2, 137.0, 134.0, 132.6, 132.5, 130.6, 128.4, 128.3, 128.1, 91.1, 68.5, 30.6, 24.9.

5.4.5.12. dimethyl 2-(2-(tetrahydrofuran-2-yl)hydrazono)malonate (3l):



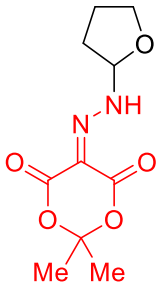
3l
$C_9H_{14}N_2O_5$
M. W. 230.22 g/mol

According to **GP-4** compound **3k** was prepared by using **1k** (16.0 mg, 0.1 mmol, 1.0 equiv) and NBS (4.0 mg, 0.02 mmol, 0.2 equiv) in 1 ml THF for 16 h at rt. Column chromatographic purification (petroleum ether/EtOAc 90:10 to 70:30) afforded **3k** as colourless oil (17.0 mg, 74%).

HRMS (ESI): m/z $[M+Na]^+$ Calculated for $[C_9H_{14}N_2O_5Na]^+$: 253.0800; Found: 253.0800.

^{1}H NMR (400 MHz, $CDCl_3$): δ 11.27 (d, *J* = 5.2 Hz, 1H), 5.45 (td, *J* = 6.5, 3.5 Hz, 1H), 4.00–3.93 (m, 1H), 3.90–3.84 (m, 1H), 3.82 (s, 3H), 3.79 (s, 3H), 2.28–2.19 (m, 1H), 2.11–2.05 (m, 1H), 2.03–1.92 (m, 2H). **^{13}C NMR (101 MHz, $CDCl_3$):** δ 163.7, 163.6, 118.8, 91.1, 68.2, 52.2, 51.9, 30.6, 24.8.

5.4.5.13. 2,2-dimethyl-5-(2-(tetrahydrofuran-2-yl)hydrazono)-1,3-dioxane-4,6-dione (3m):



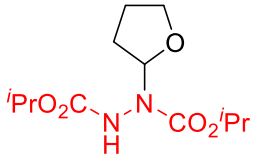
3m
$C_{10}H_{14}N_2O_5$
M. W. 242.23 g/mol

According to **GP-4** compound **3m** was prepared by using **1m** (17.0 mg, 0.1 mmol, 1.0 equiv) and NBS (4.0 mg, 0.02 mmol, 0.2 equiv) in 1 ml THF for 16 h at rt. Column chromatographic purification (petroleum ether/EtOAc 90:10 to 70:30) afforded **3m** as colourless oil (17.5 mg, 72%).

HRMS (ESI): m/z $[M+Na]^+$ Calculated for $[C_{10}H_{14}N_2O_5Na]^+$: 265.0800; Found: 265.0801.

^{1}H NMR (400 MHz, $CDCl_3$): δ 12.12 (s, 1H), 5.60 (td, *J* = 6.2, 3.4 Hz, 1H), 4.08–4.03 (m, 1H), 3.96–3.90 (m, 1H), 2.37–2.21 (m, 2H), 2.10–2.01 (m, 2H), 1.75 (s, 3H), 1.74 (s, 3H). **^{13}C NMR (126 MHz, $CDCl_3$):** δ 160.7, 159.6, 111.8, 105.7, 92.7, 69.3, 31.3, 27.6, 24.6.

5.4.5.14. diisopropyl 1-(tetrahydrofuran-2-yl)hydrazine-1,2-dicarboxylate (5a):



5a

$C_{12}H_{22}N_2O_5$

M. W. 274.31 g/mol

According to **GP-5** compound **5a** was prepared by using **4a** (20 µL, 0.1 mmol, 1.0 equiv) and NBS (4.0 mg, 0.02 mmol, 0.2 equiv) in 1 ml THF for 5 min at rt. Column chromatographic purification (petroleum ether/EtOAc 90:10 to 70:30) afforded **5a** as white solid (25.0 mg, 91%).

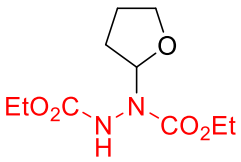
HRMS (ESI): m/z $[M+Na]^+$ Calculated for $[C_{12}H_{22}N_2O_5Na]^+$: 297.1426; Found: 297.1428.

Melting Point: 85–87 °C.

^{1}H NMR (400 MHz, $CDCl_3$): δ 6.29–6.13 (m, 1H), 6.05–5.92 (m, 1H), 5.00–4.90 (m, 2H), 3.99–3.94 (m, 1H), 3.77–3.71 (m, 1H), 2.06–2.02 (m, 1H), 2.00–1.93 (m, 1H), 1.88–1.82 (m, 1H), 1.72–1.69 (m, 1H), 1.25–1.23 (m, 12H). **^{13}C NMR (101 MHz, $CDCl_3$):** δ 156.4, 155.2, 87.3, 70.7, 69.9, 68.7, 28.3, 25.4, 22.1, 22.0.

These data are in accordance with the previous report.[58,59]

5.4.5.15. diethyl 1-(tetrahydrofuran-2-yl)hydrazine-1,2-dicarboxylate (5b):



5b

$C_{10}H_{18}N_2O_5$

M. W. 246.26 g/mol

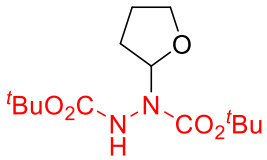
According to **GP-5** compound **5b** was prepared by using **4b** (16 µL, 0.1 mmol, 1.0 equiv) and NBS (4.0 mg, 0.02 mmol, 0.2 equiv) in 1 ml THF for 5 min at rt. Column chromatographic purification (petroleum ether/EtOAc 90:10 to 70:30) afforded **5b** as colourless oil (21.5 mg, 87%).

HRMS (ESI): m/z $[M+Na]^+$ Calculated for $[C_{10}H_{18}N_2O_5Na]^+$: 269.1113; Found: 269.1113.

^{1}H NMR (400 MHz, $CDCl_3$): δ 6.52–6.43 (m, 1H), 6.24–5.98 (m, 1H), 4.21–4.16 (m, 4H), 4.00–3.94 (m, 1H), 3.77–3.72 (m, 1H), 2.07–1.93 (m, 3H), 1.89–1.82 (m, 1H), 1.27–1.24 (m, 6H). **^{13}C NMR (101 MHz, $CDCl_3$):** δ 156.8, 155.6, 87.6, 68.8, 63.0, 62.3, 28.3, 25.4, 14.5, 14.5.

These data are in accordance with the previous report.[58,59]

5.4.5.16. di-*tert*-butyl 1-(tetrahydrofuran-2-yl)hydrazine-1,2-dicarboxylate (5c):



5c

$C_{14}H_{26}N_2O_5$

M. W. 302.37 g/mol

According to **GP-5** compound **5c** was prepared by using **4c** (23 µL, 0.1 mmol, 1.0 equiv) and NBS (4.0 mg, 0.02 mmol, 0.2 equiv) in 1 ml THF for 5 min at rt. Column chromatographic purification (petroleum ether/EtOAc 90:10 to 70:30) afforded **5c** as colourless oil (25.0 mg, 83%).

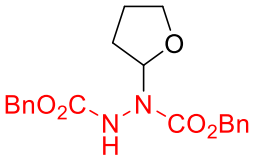
Melting Point: 102-104 °C.

HRMS (ESI): m/z $[M+Na]^+$ Calculated for $[C_{14}H_{26}N_2O_5Na]^+$: 325.1739; Found: 325.1740.

^{1}H NMR (400 MHz, $CDCl_3$): 6.25–6.17 (m, 1H), 5.99–5.90 (m, 1H), 3.98–3.93 (m, 1H), 3.76–3.70 (m, 1H), 2.03–1.81 (m, 4H), 1.45 (s, 18H). **^{13}C NMR (101 MHz, $CDCl_3$):** δ 155.8, 154.4, 87.9, 86.6, 81.5, 81.2, 68.6, 28.2, 25.4.

These data are in accordance with the previous report.[58,59]

5.4.5.17. dibenzyl 1-(tetrahydrofuran-2-yl)hydrazine-1,2-dicarboxylate (5d):



5d

$C_{20}H_{22}N_2O_5$

M. W. 370.40 g/mol

According to **GP-5** compound **5d** was prepared by using **4d** (30.0 mg, 0.1 mmol, 1.0 equiv) and NBS (4.0 mg, 0.02 mmol, 0.2 equiv) in 1 ml THF for 15 min at rt. Column chromatographic purification (petroleum ether/EtOAc 90:10 to 75:25) afforded **5d** as colourless oil (26.5 mg, 72%).

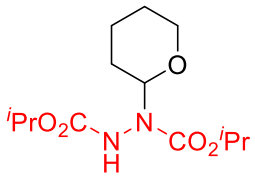
HRMS (ESI): m/z $[M+H]^+$ Calculated for $[C_{20}H_{23}N_2O_5]^+$: 371.1607; Found: 371.1606.

^{1}H NMR (400 MHz, $CDCl_3$): δ 7.36–7.21 (m, 10H), 6.70–6.58 (m, 1H), 6.44–6.02 (m, 1H), 3.97–3.92 (m, 1H), 3.75–3.70 (m, 1H), 2.11–2.03 (m, 2H), 1.98–1.89 (m, 1H), 1.87–1.80 (m, 1H).

^{13}C NMR (101 MHz, $CDCl_3$): δ 156.6, 155.4, 135.7, 135.6, 128.7, 128.6, 128.5, 128.4, 128.3, 128.1, 87.8, 68.8, 68.0, 67.9, 28.2, 25.3.

These data are in accordance with the previous report.[58,59]

5.4.5.18. diisopropyl 1-(tetrahydro-2*H*-pyran-2-yl)hydrazine-1,2-dicarboxylate (5e):



5e

$C_{13}H_{24}N_2O_5$

M. W. 288.34 g/mol

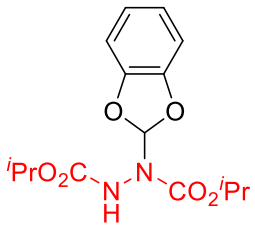
According to **GP-5** compound **5a** was prepared by using **4a** (20 µL, 0.1 mmol, 1.0 equiv), NBS (4.0 mg, 0.02 mmol, 0.2 equiv), and **2b** (98 µL, 1.0 mmol, 10.0 equiv) in 0.1 ml benzene for 1 h at rt. Column chromatographic purification (petroleum ether/EtOAc 90:10 to 70:30) afforded **5e** as colourless oil (18 mg, 62%).

HRMS (ESI): m/z $[M+Na]^+$ Calculated for $[C_{13}H_{24}N_2O_5Na]^+$: 311.1583; Found:. 311.1583.

^{1}H NMR (400 MHz, $CDCl_3$): δ 6.43–6.42 (m, 1H), 5.29–5.05 (m, 1H), 4.97–4.91 (m, 2H), 3.99–3.96 (m, 1H), 3.60–3.54 (m, 1H), 1.90–1.88 (m, 1H), 1.78–1.74 (m, 1H), 1.66–1.59 (m, 3H), 1.48–1.42 (m, 1H), 1.26–1.22 (m, 12H). **^{13}C NMR (101 MHz, $CDCl_3$):** δ 156.2, 155.0, 84.5, 70.6, 69.7, 68.2, 27.9, 25.1, 23.0, 22.1, 22.0.

These data are in accordance with the previous report.[58,59]

5.4.5.19. diisopropyl 1-(benzo[*d*][1,3]dioxol-2-yl)hydrazine-1,2-dicarboxylate (5f):



5f

$C_{15}H_{20}N_2O_6$

M. W. 324.33 g/mol

According to **GP-5** compound **5f** was prepared by using **4a** (20 µL, 0.1 mmol, 1.0 equiv), NBS (4.0 mg, 0.02 mmol, 0.2 equiv), and **2c** (115.0 µL, 1.0 mmol, 10.0 equiv) in 0.1 ml benzene for 6

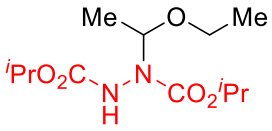
h at rt. Column chromatographic purification (petroleum ether/EtOAc 90:10 to 80:20) afforded **5f** as colourless oil (18 mg, 81%).

HRMS (ESI): m/z $[M+Na]^+$ Calculated for $[C_{15}H_{20}N_2O_6Na]^+$: 347.1219; Found: 347.1219.

^{1}H NMR (400 MHz, $CDCl_3$): δ 7.69 (brs, 1H), 6.82 (s, 4H), 6.23–6.05 (m, 1H), 5.07–4.89 (m, 2H), 1.28–1.16 (m, 12H). **^{13}C NMR (101 MHz, $CDCl_3$):** δ 155.2, 153.1, 146.4, 144.0, 121.8, 120.9, 115.4, 108.0, 71.8, 70.3, 21.9, 21.9.

These data are in accordance with the previous report.[60]

5.4.5.20. diisopropyl 1-(1-methoxypropyl)hydrazine-1,2-dicarboxylate (5g):



5g

$C_{12}H_{24}N_2O_5$

M. W. 276.33 g/mol

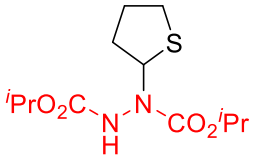
According to **GP-5** compound **5g** was prepared by using **4a** (20 µL, 0.1 mmol, 1.0 equiv) and NBS (4.0 mg, 0.02 mmol, 0.2 equiv) in 1 ml **2d** for 5 min at rt. Column chromatographic purification (petroleum ether/EtOAc 90:10 to 70:30) afforded **5g** as colourless oil (25.0 mg, 91%).

HRMS (ESI): m/z $[M+Na]^+$ Calculated for $[C_{12}H_{24}N_2O_5Na]^+$: 299.1586; Found:. 299.1583.

^{1}H NMR (400 MHz, $CDCl_3$): δ 6.19–6.02 (m, 1H), 5.58–5.41 (m, 1H), 4.97–4.93 (m, 2H), 3.37–3.43 (m, 2H), 1.33–1.31 (m, 3H), 1.26–1.23 (m, 12H), 1.17 (t, *J* = 7.0 Hz, 3H) **^{13}C NMR (101 MHz, $CDCl_3$):** δ 156.2, 155.5, 82.7, 70.3, 69.7, 63.4, 22.1, 18.7, 18.0, 15.1.

These data are in accordance with the previous report.[58,59]

5.4.5.21. diisopropyl 1-(tetrahydrothiophen-2-yl)hydrazine-1,2-dicarboxylate (5h):



5h

$C_{12}H_{22}N_2O_4S$

M. W. 290.37 g/mol

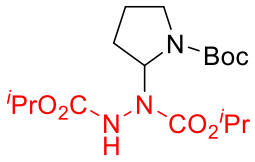
According to **GP-5** compound **5h** was prepared by using **4a** (20 µL, 0.1 mmol, 1.0 equiv) and NBS (4.0 mg, 0.02 mmol, 0.2 equiv) in 1 ml **2e** for 1 h at rt. Column chromatographic purification (petroleum ether/EtOAc 90:10 to 70:30) afforded **5h** as colourless oil (24.0 mg, 82%).

HRMS (ESI): m/z $[M+Na]^+$ Calculated for $[C_{12}H_{22}N_2O_4NaS]^+$: 313.1198; Found:. 313.1198.

^{1}H NMR (400 MHz, $CDCl_3$): δ 6.40–6.24 (m, 1H), 6.15–6.04 (m, 1H), 4.98–4.88 (m, 2H), 3.03–2.98 (m, 1H), 2.79–2.73 (m, 1H), 2.10–1.92 (m, 4H), 1.26–1.22 (m, 12H). **^{13}C NMR (101 MHz, $CDCl_3$):** δ 156.2, 155.0, 70.1, 69.9, 67.2, 34.4, 33.3, 30.2, 22.1, 22.0.

These data are in accordance with the previous report.[58,59]

5.4.5.22. diisopropyl 1-(1-(tert-butoxycarbonyl)pyrrolidin-2-yl)hydrazine-1,2-dicarboxylate (5i):



5i

$C_{17}H_{31}N_3O_6$

M. W. 373.45 g/mol

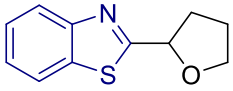
According to **GP-5** compound **5i** was prepared by using **4a** (20 µL, 0.1 mmol, 1.0 equiv), NBS (4.0 mg, 0.02 mmol, 0.2 equiv), and **2f** (171 mg, 1.0 mmol, 10.0 equiv) in 0.1 ml benzene for 6 h at rt. Column chromatographic purification (petroleum ether/EtOAc 90:10 to 50:50) afforded **5i** as colourless oil (15 mg, 40%).

HRMS (ESI): m/z $[M+H]^+$ Calculated for $[C_{17}H_{32}N_3O_6]^+$: 374.2291; Found: 374.2292.

^{1}H NMR (400 MHz, $CDCl_3$): δ 6.34–6.09 (m, 1H), 5.91–5.87 (m, 1H), 4.99–4.91 (m, 2H), 3.45–3.36 (m, 2H), 2.15–2.09 (m, 2H), 1.92–1.85 (m, 1H), 1.79–1.74 (m, 1H), 1.43 (s, 9H), 1.26–1.23 (m, 12H). **^{13}C NMR (101 MHz, $CDCl_3$):** δ 156.5, 154.4, 80.4, 80.3, 70.1, 46.7, 31.3, 28.5, 22.8, 22.2, 22.1, 21.8.

These data are in accordance with the previous report.[61]

5.4.5.23. 2-(tetrahydrofuran-2-yl)benzo[*d*]thiazole (8a):



8a

$C_{11}H_{11}NOS$

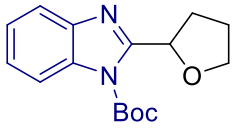
M. W. 205.27 g/mol

According to **GP-6** compound **8a** was prepared by using **6a** (29.0 mg, 0.1 mmol, 1.0 equiv) and NBS (4.0 mg, 0.02 mmol, 0.2 equiv) in 1 ml THF for 24 h at rt. Column chromatographic purification (petroleum ether/EtOAc 99:1 to 90:10) afforded **8a** as colourless oil (15.0 mg, 73%).

HRMS (ESI): m/z $[M+H]^+$ Calculated for $[C_{11}H_{12}NOS]^+$: 206.0640; Found:. 206.0640.

^{1}H NMR (400 MHz, $CDCl_3$): δ 7.97–7.95 (m, 1H), 7.89–7.86 (m, 1H), 7.47–7.43 (m, 1H), 7.37–7.33 (m, 1H), 5.34 (dd, *J* = 7.8, 5.4 Hz, 1H), 4.18–4.12 (m, 1H), 4.03–3.97 (m, 1H), 2.56–2.47 (m, 1H), 2.30–2.23 (m, 1H), 2.06–2.01 (m, 2H). **^{13}C NMR (101 MHz, $CDCl_3$):** δ 176.5, 153.7, 134.8, 126.0, 124.9, 122.9, 121.9, 78.8, 69.6, 33.5, 25.8.

5.4.5.24. *tert*-butyl 2-(tetrahydrofuran-2-yl)-1*H*-benzo[*d*]imidazole-1-carboxylate (8b):



8b

$C_{16}H_{20}N_2O_3$

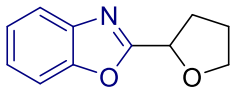
M. W. 288.34 g/mol

According to **GP-6** compound **8b** was prepared by using **6b** (25.0 mg, 0.1 mmol, 1.0 equiv), NBS (4.0 mg, 0.02 mmol, 0.2 equiv), and NaOAc (8.0 mg, 0.1 mmol, 1.0 equiv) in 1 ml THF for 16 h at rt. Column chromatographic purification (petroleum ether/EtOAc 95:5 to 80:20) afforded **8b** as colourless oil (13.0 mg, 45%).

HRMS (ESI): m/z $[M+Na]^+$ Calculated for $[C_{16}H_{20}N_2O_3Na]^+$: 311.1375; Found:. 311.1372.

^{1}H NMR (400 MHz, $CDCl_3$): δ 7.91–7.87 (m, 1H), 7.77–7.73 (m, 1H), 7.33–7.29 (m, 2H), δ 5.71 (dd, *J* = 7.8, 5.0 Hz, 1H), 4.24–4.19 (m, 1H), 4.03–3.97 (m, 1H), 2.50–2.41 (m, 1H), 2.32–2.24 (m, 1H), 2.13–1.95 (m, 2H), 1.70 (s, 9H). **^{13}C NMR (101 MHz, $CDCl_3$):** δ 156.8, 148.8, 142.0, 133.3, 124.8, 124.3, 120.4, 114.9, 85.9, 75.4, 69.3, 31.5, 28.2, 25.5.

5.4.5.25. 2-(tetrahydrofuran-2-yl)benzo[*d*]oxazole (8c):



8c

$C_{11}H_{11}NO_2$

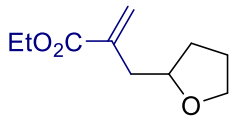
M. W. 189.21 g/mol

According to **GP-6** compound **8c** was prepared by using **6c** (15.0 mg, 0.1 mmol, 1.0 equiv), NBS (4.0 mg, 0.02 mmol, 0.2 equiv), and NaOAc (8.0 mg, 0.1 mmol, 1.0 equiv) in 1 ml THF for 16 h at rt. Column chromatographic purification (petroleum ether/EtOAc 99:1 to 90:10) afforded **8b** as colourless oil (12.0 mg, 63%).

HRMS (ESI): m/z $[M+H]^+$ Calculated for $[C_{11}H_{12}NO_2]^+$: 190.0867; Found: 190.0868.

^{1}H NMR (400 MHz, $CDCl_3$): δ 7.72–7.69 (m, 1H), 7.53–7.51 (m, 1H), 7.35–7.30 (m, 2H), δ 5.20 (t, *J* = 6.6 Hz, 1H), 4.15–4.09 (m, 1H), 4.04–3.98 (m, 1H), 2.43–2.37 (m, 2H), 2.22–2.14 (m, 1H), 2.11–2.01 (m, 1H). **^{13}C NMR (101 MHz, $CDCl_3$):** δ 166.4, 151.0, 140.9, 125.3, 124.5, 120.3, 110.9, 74.0, 69.5, 30.9, 25.9.

5.4.5.26. ethyl 2-((tetrahydrofuran-2-yl)methyl)acrylate (9a):



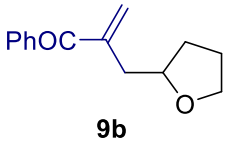
9a
$C_{10}H_{16}O_3$
M. W. 184.23 g/mol

According to **GP-6** compound **9a** was prepared by using **7a** (25.0 mg, 0.1 mmol, 1.0 equiv) and NBS (4.0 mg, 0.02 mmol, 0.2 equiv) in 1 ml THF for 16 h at rt. Column chromatographic purification (petroleum ether/EtOAc 99:1 to 90:10) afforded **9a** as colourless oil (12.0 mg, 65%).

HRMS (ESI): m/z $[M+Na]^+$ Calculated for $[C_{10}H_{16}O_3Na]^+$: 207.0993; Found: 207.0997.

^{1}H NMR (400 MHz, $CDCl_3$): δ 6.22 (d, *J* = 1.4 Hz, 1H), 5.65 (q, *J* = 1.4 Hz, 1H), 4.19 (q, *J* = 7.1 Hz, 2H), 4.05–3.99 (m, 1H), 3.88–3.83 (m, 1H), 3.74–3.69 (m, 1H), 2.51 (dd, *J* = 6.4, 1.0 Hz, 2H), 2.01–1.93 (m, 1H), 1.92–1.79 (m, 2H), 1.53–1.47 (m, 1H), 1.28 (t, *J* = 7.1 Hz, 3H). **^{13}C NMR (101 MHz, $CDCl_3$):** δ 167.2, 137.9, 126.7, 77.6, 67.9, 60.8, 38.0, 31.2, 25.6, 14.3.

5.4.5.27. 1-phenyl-2-((tetrahydrofuran-2-yl)methyl)prop-2-en-1-one (9b):



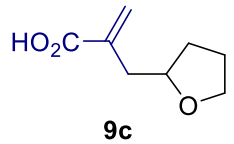
9b
$C_{14}H_{16}O_2$
M. W. 216.28 g/mol

According to **GP-6** compound **9b** was prepared by using **7b** (29.0 mg, 0.1 mmol, 1.0 equiv) and NBS (4.0 mg, 0.02 mmol, 0.2 equiv) in 1 ml THF for 16 h at rt. Column chromatographic purification (petroleum ether/EtOAc 99:1 to 90:10) afforded **9b** as colourless oil (13.0 mg, 60%).

HRMS (ESI): m/z $[M+H]^+$ Calculated for $[C_{14}H_{17}O_2]^+$: 217.1229; Found: 217.1229.

^{1}H NMR (400 MHz, $CDCl_3$): δ 7.77–7.75 (m, 2H), 7.54–7.50 (m, 1H), 7.44–7.40 (m, 2H), 5.94 (q, *J* = 1.2 Hz, 1H), 5.66–5.64 (m, 1H), 4.06–4.00 (m, 1H), 3.88–3.82 (m, 1H), 3.73–3.68 (m, 1H), 2.75 (ddd, *J* = 14.1, 4.9, 1.1 Hz, 1H), 2.63 (ddd, *J* = 14.2, 8.1, 0.9 Hz, 1H), 2.04–1.97 (m, 1H), 1.94–1.81 (m, 2H), 1.57–1.53 (m, 1H). **^{13}C NMR (101 MHz, $CDCl_3$):** δ 198.3, 145.5, 137.9, 132.3, 129.7, 128.3, 127.5, 77.8, 67.8, 38.5, 31.4, 25.7.

5.4.5.28. 2-((tetrahydrofuran-2-yl)methyl)acrylic acid (9c):



9c

$C_8H_{12}O_3$

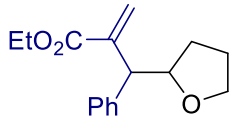
M. W. 156.18 g/mol

According to **GP-6** compound **9c** was prepared by using **7c** (23.0 mg, 0.1 mmol, 1.0 equiv) and NBS (4.0 mg, 0.02 mmol, 0.2 equiv) in 1 ml THF for 16 h at rt. Column chromatographic purification (petroleum ether/EtOAc 99:1 to 85:15) afforded **9c** as colourless oil (11.0 mg, 71%).

HRMS (ESI): m/z $[M+Na]^+$ Calculated for $[C_8H_{12}O_3Na]^+$: 179.0684; Found: . 179.0682.

^{1}H NMR (400 MHz, $CDCl_3$): δ 6.35 (d, *J* = 1.8 Hz, 1H), 5.73 (q, *J* = 1.4 Hz, 1H), 4.10–4.03 (m, 1H), 3.91–3.86 (m, 1H), 3.78–3.73 (m, 1H), 2.56 (dd, *J* = 14.2, 5.0 Hz, 1H), 2.49 (ddd, *J* = 14.2, 7.3, 1.4 Hz, 1H), 2.04–1.96 (m, 1H), 1.94–1.85 (m, 2H), 1.58–1.50 (m, 1H). **^{13}C NMR (101 MHz, $CDCl_3$):** δ 171.3, 137.3, 129.4, 78.0, 68.1, 37.6, 31.0, 25.7.

5.4.5.29. ethyl 2-(phenyl(tetrahydrofuran-2-yl)methyl)acrylate (9d):



9d

$C_{16}H_{20}O_3$

M. W. 260.33 g/mol

According to **GP-6** compound **9d** was prepared by using **7c** (33.0 mg, 0.1 mmol, 1.0 equiv) and NBS (4.0 mg, 0.02 mmol, 0.2 equiv) in 1 ml THF for 16 h at rt. Column chromatographic purification (petroleum ether/EtOAc 99:1 to 90:10) afforded **9d** as colourless oil (13.0 mg, 50%).

HRMS (ESI): m/z $[M+H]^+$ Calculated for $[C_{16}H_{21}O_3]^+$: 261.1491; Found: . 261.1490.

^{1}H NMR (400 MHz, $CDCl_3$): δ 7.28–7.25 (m, 1H), 7.24–7.16 (m, 4H), 7.22–7.16 (m, 2H), 6.40 (d, *J* = 0.7 Hz, 1H), 5.88 (t, *J* = 1.1 Hz, 1H), 4.37–4.31 (m, 1H), 4.15–4.01 (m, 2H), 3.91–3.85 (m, 2H), 3.81–3.76 (m, 1H), 1.88–1.77 (m, 2H), 1.72–1.64 (m, 1H), 1.55–1.48 (m, 1H), 1.19 (t, *J* = 7.1 Hz, 3H). **^{13}C NMR (101 MHz, $CDCl_3$):** δ 167.1, 141.8, 140.4, 128.7, 128.4, 126.9, 124.7, 80.6, 68.4, 60.7, 52.0, 30.8, 25.7, 14.1.

5.5. References:

1. Xuan, J.; He, X.-K.; Xiao, W.-J. Visible light-promoted ring-opening functionalization of three-membered carbo-and heterocycle. *Chem. Soc. Rev.*, **2020**, *49*, 2546–2556.
2. Yu, X.-Y.; Chen, J.-R.; Xiao, W.-J. Visible Light-Driven Radical-Mediated C–C Bond Cleavage/Functionalization in Organic Synthesis. *Chem. Rev.* **2021**, *121*, 506−561.
3. Yuan, Y.-Q.; Majumder, S.; Yang, M.-H.; Guo S-R. Recent advances in catalyst-free photochemical reactions via electron donor-acceptor (EDA) complex process. *Tetrahedron. Lett.* **2020**, *61*, 2713–2716.
4. Yang, Z.; Liu, Y.; Cao, K.; Zhang, X.; Jiang, H.; Li, J. Synthetic reactions driven by electron-donor–acceptor (EDA) complexes. *Beilstein J. Org. Chem.* **2021**, *17*, 771–799.
5. Crisenza, G. E. M.; Mazzarella, D.; Melchiorre, P. Synthetic Methods Driven by the Photoactivity of Electron Donor−Acceptor Complexes. Acceptor Complexes. *J. Am. Chem. Soc.* **2020**, *142*, 5461−5476.
6. Qvortrup, K.; Rankic, D. A.; MacMillan, D. W. C. A General Strategy for Organocatalytic Activation of C−H Bonds via Photoredox Catalysis: Direct Arylation of Benzylic Ethers. *J. Am. Chem. Soc.* **2014**, *136*, 626−629.
7. Jin, J.; MacMillan, D. W. C. Direct α-Arylation of Ethers through the Combination of Photoredox-Mediated C−H Functionalization and the Minisci Reaction. *Angew. Chem., Int. Ed.* **2015**, *54*, 1565−1569.
8. Bhakat, M.; Biswas, P.; Dey, J.; Guin, J. Heteroarylation of Ethers, Amides, and Alcohols with Light and O2. *Org. Lett.* **2021**, *23*, 6886−6890.
9. Huang, X.-J.; Qin, F.-H.; Liu, Y.; Wu, S.-P.; Li, Q.; Wei, W.-T. Acylation/cyclization of 1,6-dienes with ethers under catalyst- and base-free conditions. *Green Chem.* **2020**, *22*, 3952–3955.
10. Wang, X.; Lei, J.; Guo, S.; Zhang, Y.; Ye, Y.; Tang, S.; Sun, K. Radical selenation of C(sp^3)–H bonds to asymmetric selenides and mechanistic study. *Chem. Commun.* **2022**, *58*, 1526–1529.
11. Batra, A.; Singh, P.; Singh, K. N. Recent Advances in Functionalization of α-C(sp^3)–H Centres in Inactivated Ethers through Cross Dehydrogenative Coupling. *Eur. J. Org. Chem.* **2017**, *2017*, 3739–3762.
12. Phillips, A. M. F.; Pombeiro, A. J. L. Recent Developments in Transition Metal-Catalyzed Cross-Dehydrogenative Coupling Reactions of Ethers and Thioethers. *ChemCatChem* **2018**, *10*, 3354– 3383.

13. Batra, A.; Singh, P.; Singh, K. N. Recent Developments in Transition Metal-Free Cross-Dehydrogenative Coupling Reactions for C–C Bond Formation. *Eur. J. Org. Chem.* **2020**, *2020*, 6676–6703.
14. Chen, J.-Y.; Wu, W.; Li, Q.; Wei, W.-T. Visible-Light Induced C(sp^3)–H Functionalization for the Formation of C–N Bonds under Metal Catalyst-Free Conditions. *Adv. Synth. Catal.* **2020**, *362*, 2770–2777.
15. Wang, H.-Z.; Li, J.-Z.; Guo, Z.; Zheng, H.; Wei, W.-T. Visible-Light-Catalyzed N-Radical-Enabled Cyclization of Alkenes for the Synthesis of Five-Membered N-Heterocycles. *ChemSusChem* **2021**, *14*, 4658–4670.
16. Zheng, Y.-N.; Zheng, H.; Li, T.; Wei, W.-T. Recent Advances in Copper-Catalyzed C−N Bond Formation Involving N-Centered Radicals. *ChemSusChem* **2021**, *14*, 5340–5358.
17. Doyle, M. P.; Duffy, R.; Ratnikov, M.; Zhou, L. Catalytic carbene insertion into C−H bonds. *Chem. Rev*. **2010**, *110*, 704.
18. Ford, A.; Miel, H.; Ring, A.; Slattery, C. N.; Maguire, A. R.; McKervey, M. A. Modern Organic Synthesis with α-Diazocarbonyl Compounds. *Chem. Rev.*, **2015**, *115*, 9981.
19. Ciszewski, Ł. W.; Rybicka-Jasińska, K.; Gryko, D. Recent developments in photochemical reactions of diazo compounds. *Org. Biomol. Chem.*, **2019**, *17*, 432–448.
20. Yang, Z.; Stivanin, M. L.; Jurberg, I. D.; Koenigs R. M. Visible light-promoted reactions with diazo compounds: a mild and practical strategy towards free carbene intermediates. *Chem. Soc. Rev.*, **2020**, *49*, 6833–6847.
21. Durka, J.; Turkowska, J.; Gryko, D.; Lightening Diazo Compounds? *ACS Sustainable Chem. Eng.*, **2021**, *9*, 8895−8918.
22. Dasgupta, A.; Richards, E.; Melen R. L. Triarylborane Catalyzed Carbene Transfer Reactions Using Diazo Precursors. *ACS Catalysis* **2022**, *12*, 442–452.
23. Yao, H. C.; Resnick, P. Azo-Hydrazone Conversion. I. The Japp-Klingemann Reaction. *J. Am. Chem. Soc.* **1962**, *84*, 3514.
24. Yasui, E.; Wada, M.; Takamura, N. Novel approach to arylhydrazones, the precursor for Fischer indole synthesis, via diazo esters derived from α-amino acid esters. *Tetrahedron Lett.* **2006**, *47*, 743.
25. Yasui, E.; Wada, M.; Takamura, N. Novel method for synthesis of aryl hydrazones from α-diazo esters: scope and limitations of nucleophiles. *Tetrahedron* **2009**, *65*, 461.
26. Zhang, L.; Meng, X.-H.; Liu, P.; Chen, J.; Zhao, Y.-L. *t*BuLi-Promoted Intermolecular Regioselective Nucleophilic Addition of Arenes to Diazo Compounds as *N*-Terminal

Electrophiles: Efficient Synthesis of Hydrazine Derivatives. *Eur. J. Org. Chem.* **2017**, 2017, 6137.

27. Li, W.; Liu, X.; Hao, X.; Hu, X.; Chu, Y.; Cao, W.; Qin, S.; Hu, C.; Lin, L.; Feng, X. New Electrophilic Addition of α-Diazoesters with Ketones for Enantioselective C−N Bond Formation. *J. Am. Chem. Soc.* **2011**, *133*, 15268.
28. Li, L.; Chen, J.-J.; Li, Y.-J.; Bu, X.-B.; Liu, Q.; Zhao, Y.-L. Activation of α-Diazocarbonyls by Organic Catalysts: Diazo Group Acting as a Strong *N*-Terminal Electrophile. *Angew. Chem., Int. Ed.* **2015**, *54*, 12107.
29. Zheng, J.; Qi, J.; Cui, S. Fe-Catalyzed Olefin Hydroamination with Diazo Compounds for Hydrazone Synthesis. *Org. Lett.* **2016**, *18*, 128.
30. Huo, J.; Xue, Y.; Wang, J. Regioselective copper-catalyzed aminoborylation of styrenes with bis(pinacolato)diboron and diazo compounds. *Chem. Commun.* **2018**, *54*, 12266.
31. Yao, D.; Zhang, J.; Xu, L. C–N Coupling Reactions between Benzophenone Hydrazone and Aryl Chlorides and Boronic Acids. *Chin. J. Org. Chem.* **2020**, *40*, 1673-1679.
32. Rodina, L. L.; Galkina, O. S.; Maas, G.; Platz, M. S.; Nikolaev, V. A. A New Method for C−H Functionalization of Aliphatic Compounds by an Unusual Photochemical Reaction of Diazoketones without Elimination of Nitrogen. *Asian J. Org. Chem.* **2016**, *5*, 691.
33. Rodina, L. L.; Azarova, X. V.; Medvedev, J. J.; Semenok, D. V.; Nikolaev, V. A. Novel photochemical reactions of carbocyclic diazodiketones without elimination of nitrogen - a suitable way to N-hydrazonation of C−H-bonds. *Beilstein J. Org. Chem.* **2018**, *14*, 2250.
34. Chan, C.-M.; Xing, Q.; Chow, Y.-C.; Hung, S.-F.; Yu, W.-Y. Photoredox Decarboxylative C(sp^3)−N Coupling of α-Diazoacetates with Alkyl *N*-Hydroxyphthalimide Esters for Diversified Synthesis of Functionalized *N*-Alkyl Hydrazones. *Org. Lett.* **2019**, *21*, 8037−8043.
35. Wu, X.; Zheng, P.; Li, W.; XU, T. Reductive cross-coupling to access C–N bonds from aryl halides and diazoesters under dual nickel/photoredox-catalyzed conditions. *Org. Chem. Front*., **2021**, *8*, 4118–4123.
36. Shen, X.; Chen, X.; Chen, J.; Sun, Y.; Cheng, Z.; Lu, Z. Ligand-promoted cobalt-catalyzed radical hydroamination of alkenes. *Nat Commun* **2020**, *11*, 783.
37. Chen, J.; Shen, X.; Lu, Z. Cobalt-Catalyzed Markovnikov Selective Sequential Hydrogenation/Hydrohydrazidation of Aliphatic Terminal Alkynes. *J. Am. Chem. Soc.* **2020**, *142*, 14455−14460.

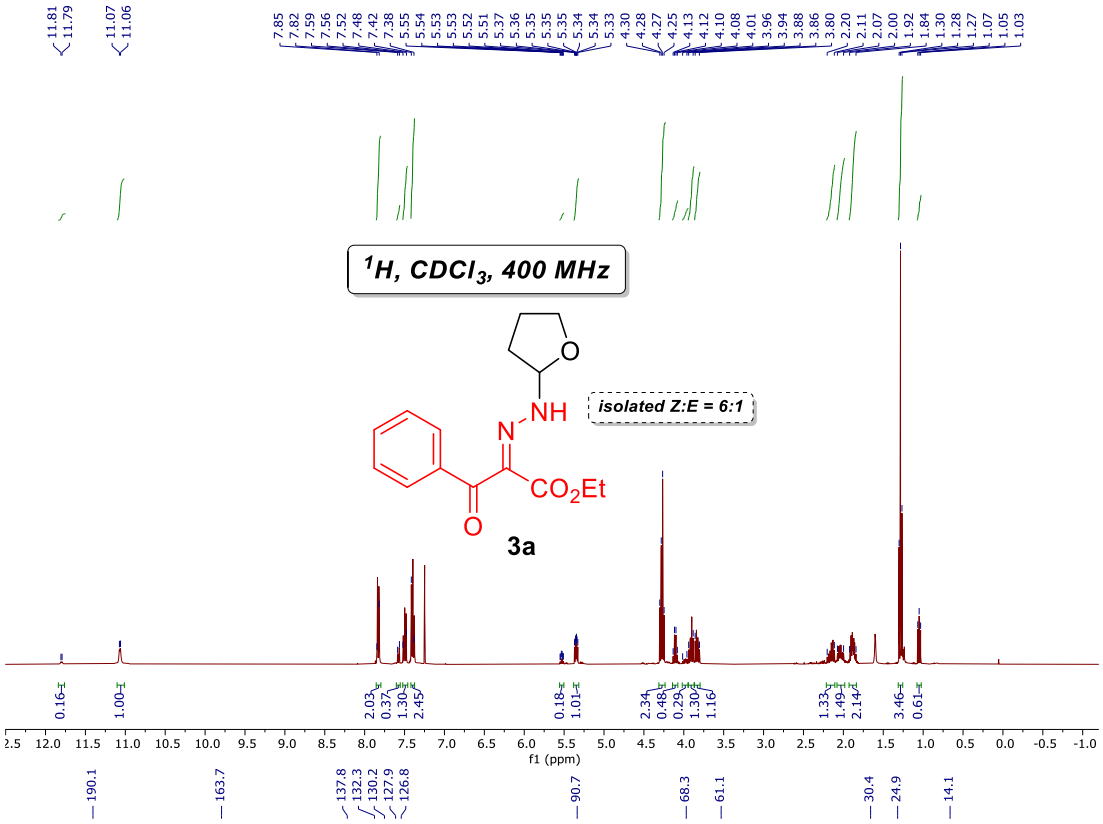
38. Lee, D.; Otte R. D. Transition-Metal-Catalyzed Aldehydic C-H Activation by Azodicarboxylates. *J. Org. Chem.* **2004**, *69*, 3569-3571.
39. Ryu, I.; Tani, A.; Fukuyama, T.; Ravelli, D.; Montanaro, S.; Fagnoni, M.Efficient C–H/C–N and C–H/C–CO–N Conversion via Decatungstate-Photoinduced Alkylation of Diisopropyl Azodicarboxylate. *Org. Lett.* **2013**, *15*, 2554–2557.
40. Bonassi, F.; Ravelli, D.; Protti, S.; Fagnonia, M. Decatungstate Photocatalyzed Acylations and Alkylations in Flow via Hydrogen Atom Transfer. *Adv. Synth. Catal.* **2015**, *357*, 3687–3695.
41. Jin, Y.; Zhang, Q.; Wang, L.; Wang, X.; Meng, C.; Duan, C. Convenient C(sp^3)–H bond functionalisation of light alkanes and other compounds by iron photocatalysis. *Green Chem.* **2021**, *23*, 6984.
42. Shamsabadi, A.; Maruani, A.; Ahmed, N.; Chudasama, V. Aerobically-initiated C(sp^3)–H bond amination through the use of activated azodicarboxylates. *Org. Biomol. Chem*., **2020**, *18*, 6258–6264.
43. Papadopoulos, G. N.; Kokotou, M. G.; Spiliopoulou, N.; Nikitas, N. F.; Voutyritsa, E.; Tzaras, D. I.; Kaplaneris, N.; Kokotos, C. G. Phenylglyoxylic Acid: An Efficient Initiator for the Photochemical Hydrogen Atom Transfer C–H Functionalization of Heterocycles. *ChemSusChem* **2020**, *13*, 5934–5944.
44. Niu, B.; Blackburn, B. G.; Sachidanandan, K.; Cooke, M. V.; Laulhé, S. Metal-free visible-light-promoted C(sp^3)–H functionalization of aliphatic cyclic ethers using trace O_2. *Green Chem.*, **2021**, *23*, 9454–9459.
45. Arceo, E.; Jurberg, I. D.; A´lvarez-Erna´ndez, A.; Melchiorre, P. Photochemical activity of a key donor–acceptor complex can drive stereoselective catalytic a-alkylation of aldehydes. *Nature chemistry* **2013**, *5*, 750–756.
46. Cao, Z.-Y.; Ghosh, T.; Melchiorre, P. Enantioselective radical conjugate additions driven by a photoactive intramolecular iminium-ion-based EDA complex. *Nat Commun* **2018**, *9*, 1–10.
47. Cismesia, M. A.; Yoon, T. P. Characterizing chain processes in visible light photoredox catalysis. *Chem. Sci.* **2015**, *6*, 5426–5434.
48. El-Habeeba, A. A.; Refat M. S. Spectroscopic Studies on the Utility of Charge Transfer Interactions for Determination of Phenytoin Sodium. *Russ J Gen Chem* **2015**, *85*, 939–950.
49. Lipp, A.; Lahm, G.; Opatz, T. Light Induced C−C Coupling of 2-Chlorobenzazoles with Carbamates, Alcohols, and Ethers. *J. Org. Chem.* **2016**, *81*, 4890−4897.
50. Jiang, Y.; Chen, X.; Zheng, Y.; Xue, Z.; Shu, C.; Yuan, W.; Zhang, X. Highly Diastereoselective and Enantioselective Synthesis of α-Hydroxy β-Amino Acid Derivatives:

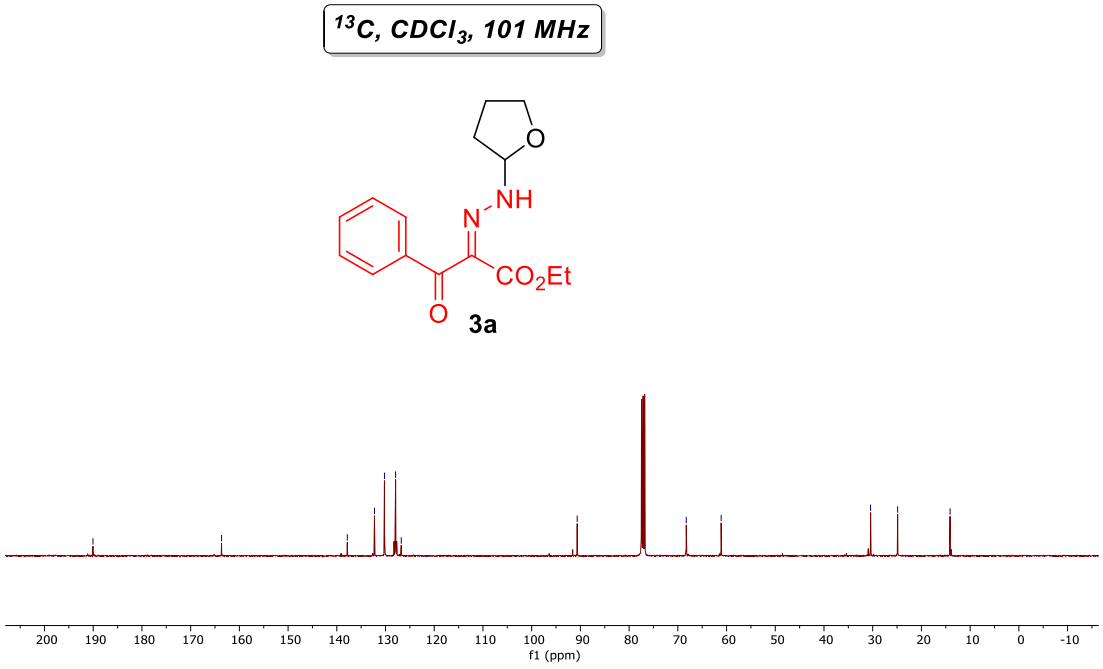
Lewis Base Catalyzed Hydrosilylation of α-Acetoxy β-Enamino Esters *Angew. Chem. Int. Ed.* **2011**, *50*, 7304–7307.

51. Wang, J.; Wang, M.; Chen, K.; Zha, S.; Song, C.; Zhu, J. C–H Activation-Based Traceless Synthesis via Electrophilic Removal of a Directing Group. Rhodium(III)-Catalyzed Entry into Indoles from N-Nitroso and α-Diazo-β-keto Compounds *Org. Lett.* **2016**, *18*, 1178–1181.
52. Liu, Q.; Li, M.; Xiong, R.; Mo, F. Direct Carboxylation of the Diazo Group ipso-C(sp2)–H bond with Carbon Dioxide: Access to Unsymmetrical Diazomalonates and Derivatives *Org. Lett.* **2017**, *19*, 6756–6759.
53. Rajasekar, S.; Anbarasan, P. A General Proline-Catalyzed Synthesis of 4,5-Disubstituted N-Sulfonyl-1,2,3-Triazoles from 1,3-Dicarbonyl Compounds and Sulfonyl Azide *Chem. Asian J.* **2019**, *14*, 4563 –4567.
54. Marichev, K. O.; Wang, Y.; Carranco, A. M.; Garcia, E. C.; Yu, Z.-X.; Doyle, M. P. Rhodium(II)-catalysed generation of cycloprop-1-en-1-yl ketones and their rearrangement to 5-aryl-2-siloxyfurans *Chem. Commun.*, **2018**, *54*, 9513-9516.
55. Day J. J., Neill D. L., Xu S., Xian M. Benzothiazole Sulfinate: A Sulfinic Acid Transfer Reagent under Oxidation-Free Conditions *Org. Lett.* **2017**, *19*, 3819–3822.
56. Liu, H.; Ge, L.; Wang, D.-X.; Chen, N.; Feng C. Photoredox-Coupled F-Nucleophilic Addition: Allylation of gem-Difluoroalkenes *Angew. Chem. Int. Ed.* **2019**, *58*,3918–3922.
57. Lipp, A.; Lahm, G.; Opatz, T. Light Induced C–C Coupling of 2-Chlorobenzazoles with Carbamates, Alcohols, and Ethers *J. Org. Chem.* **2016**, *81*, 4890−4897.
58. Shamsabadi, A.; Maruani, A.; Ahmed, N.; Chudasama, V. Aerobically-initiated C(sp3)–H bond amination through the use of activated azodicarboxylates *Org. Biomol. Chem*., **2020**, *18*, 6258–6264.
59. Papadopoulos, G. N.; Kokotou, M. G.; Spiliopoulou, N.; Nikitas, N. F.; Voutyritsa, E.; Tzaras, D. I.; Kaplaneris, N.; Kokotos, C. G. Phenylglyoxylic Acid: An Efficient Initiator for the Photochemical Hydrogen Atom Transfer C−H Functionalization of Heterocycles *ChemSusChem* **2020**, *13*, 5934–5944.
60. Ryu, I.; Tani, A.; Fukuyama, T.; Ravelli, D.; Montanaro, S.; Fagnoni, M. Efficient C–H/C–N and C–H/C–CO–N Conversion via Decatungstate-Photoinduced Alkylation of Diisopropyl Azodicarboxylate *Org. Lett.* **2013**, *15*, 2554–2557.
61. Cismesia, M. A.; Yoon, T. P. Characterizing chain processes in visible light photoredox catalysis *Chem. Sci.* **2015**, *6*, 5426.
62. An, Q.; Wang, Z.; Chen, Y.; Wang, X.; Zhang, K.; Pan, H.; Liu, W.; Zuo, Z. Cerium-Catalyzed C–H Functionalizations of Alkanes Utilizing Alcohols as Hydrogen Atom Transfer Agents *J. Am. Chem. Soc.* **2020**, *142*, 6216–6226.

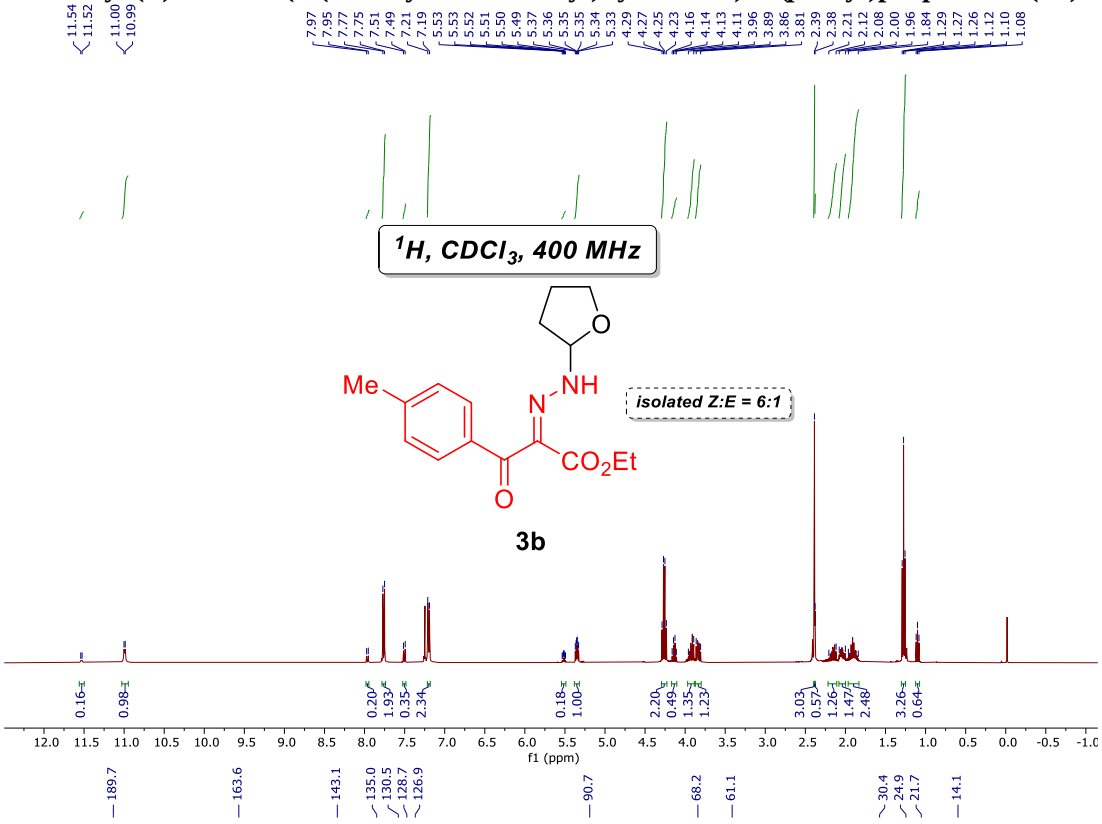
5.6. NMR Spectra:

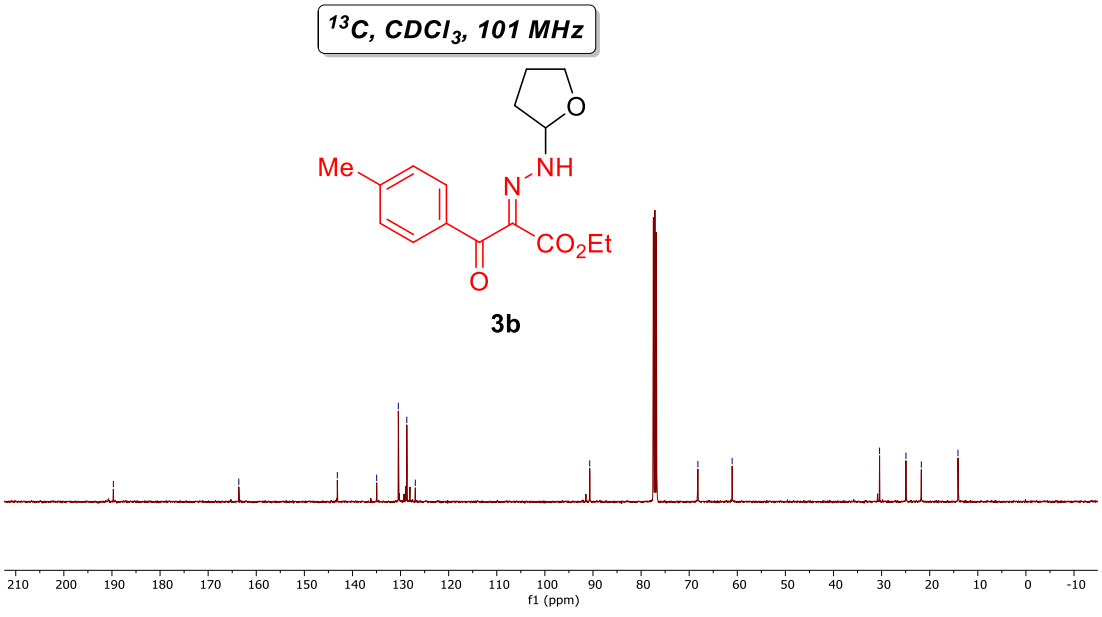
5.6.1. ethyl (*Z*)-3-oxo-3-phenyl-2-(2-(tetrahydrofuran-2-yl)hydrazono)propanoate (3a):



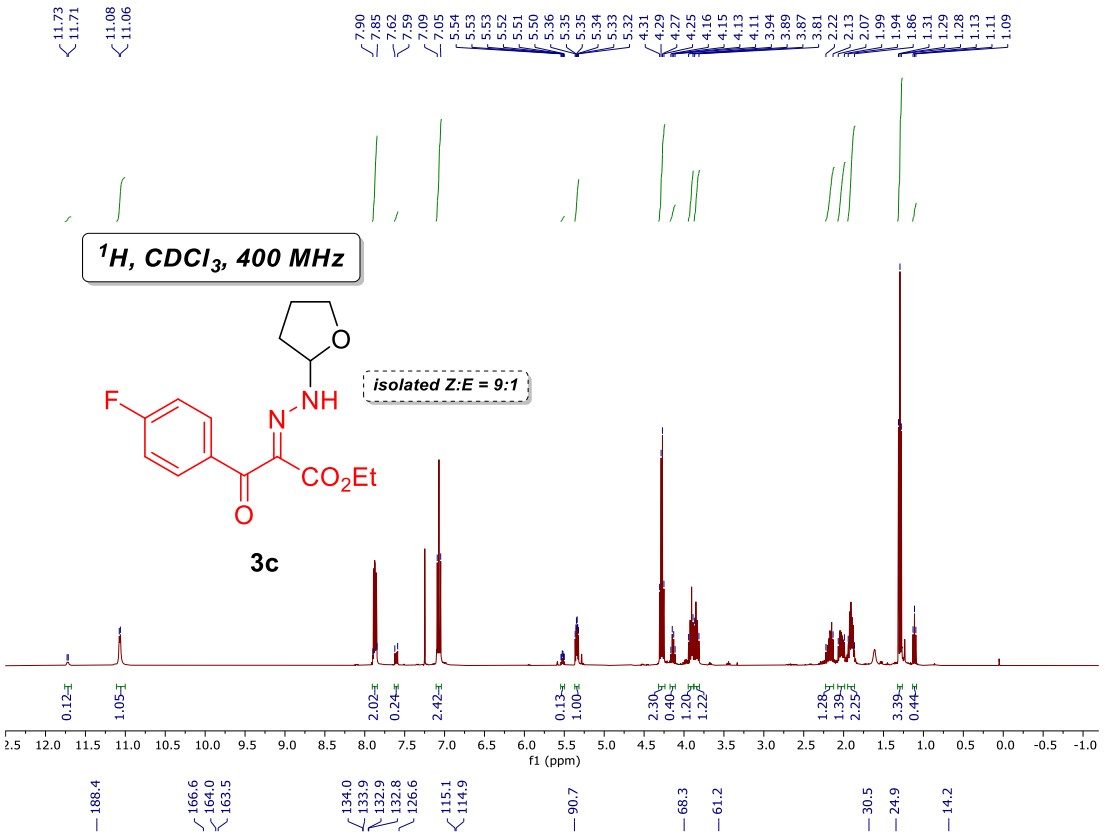


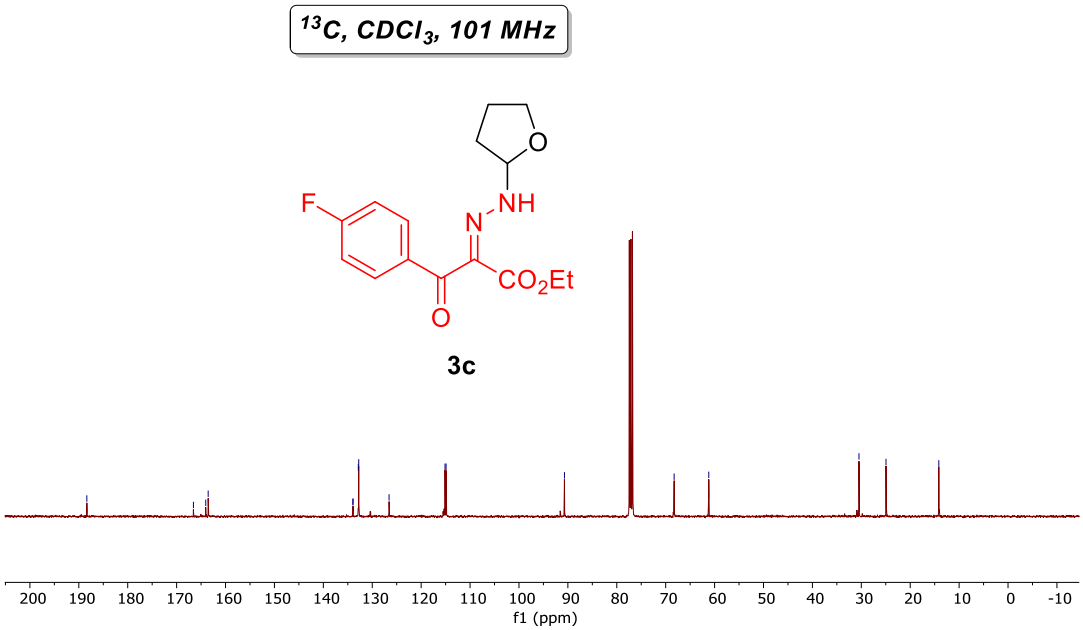
5.6.2. ethyl (*Z*)-3-oxo-2-(2-(tetrahydrofuran-2-yl)hydrazono)-3-(*p*-tolyl)propanoate (3b):

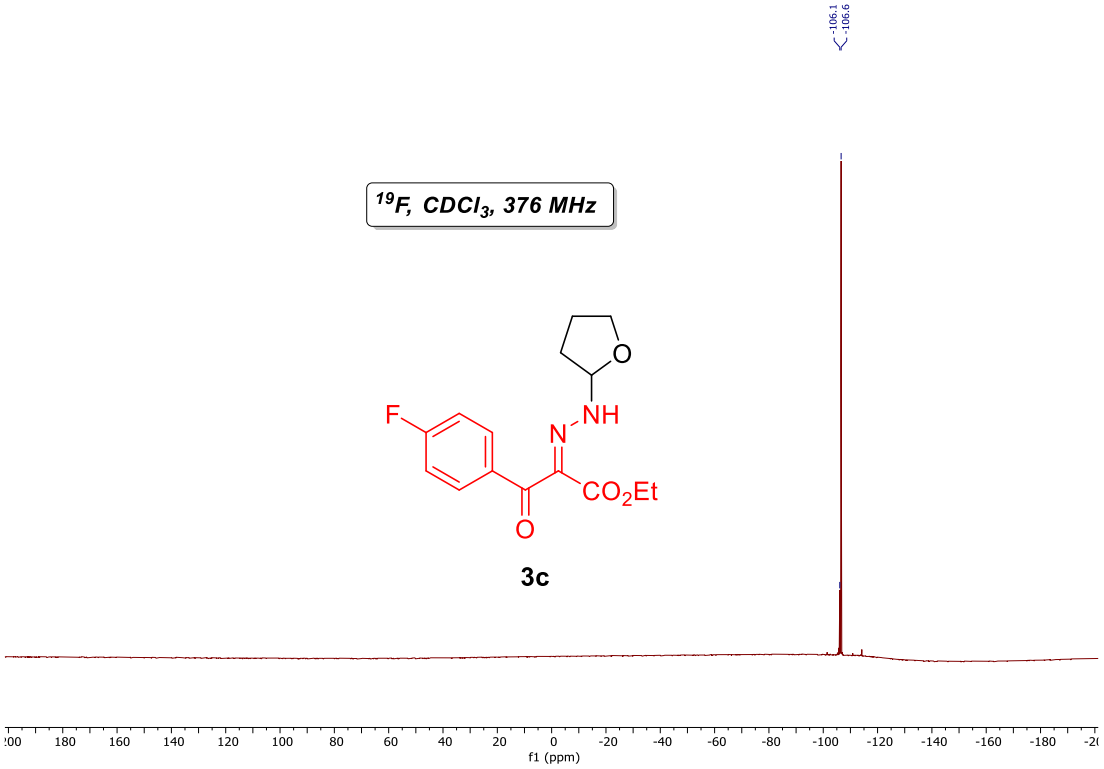




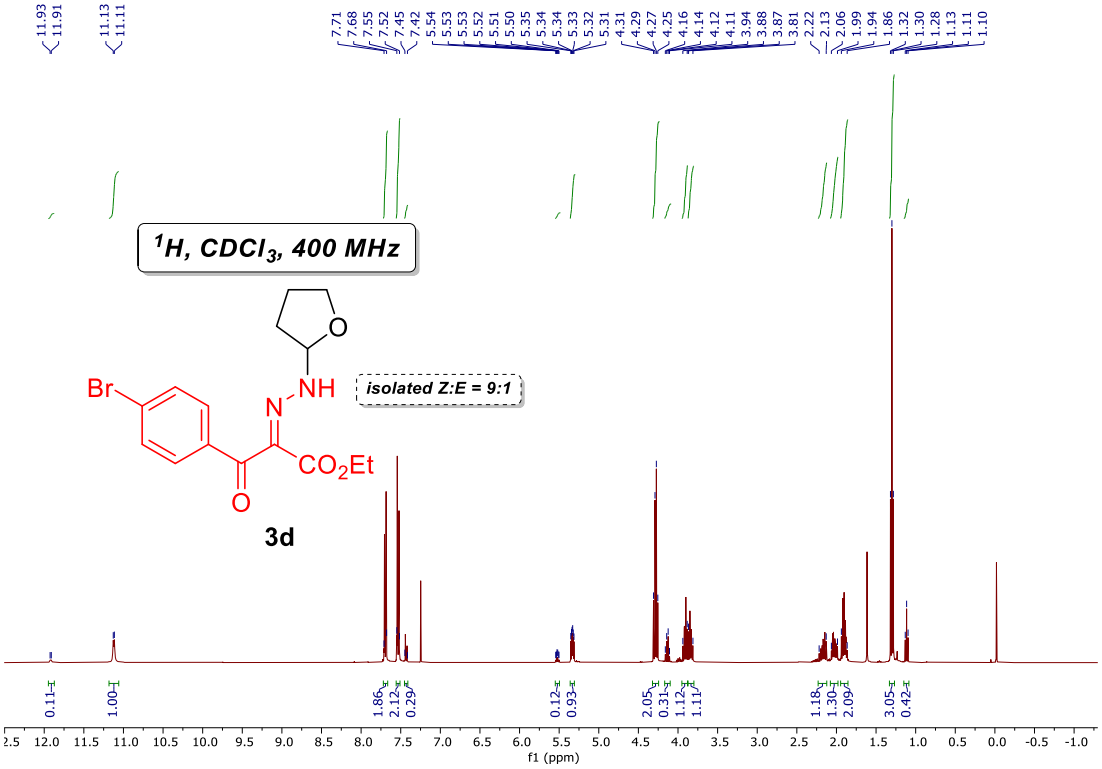
5.6.3. ethyl (*Z*)-3-(4-fluorophenyl)-3-oxo-2-(2-(tetrahydrofuran-2-yl)hydrazono)propanoate (3c):

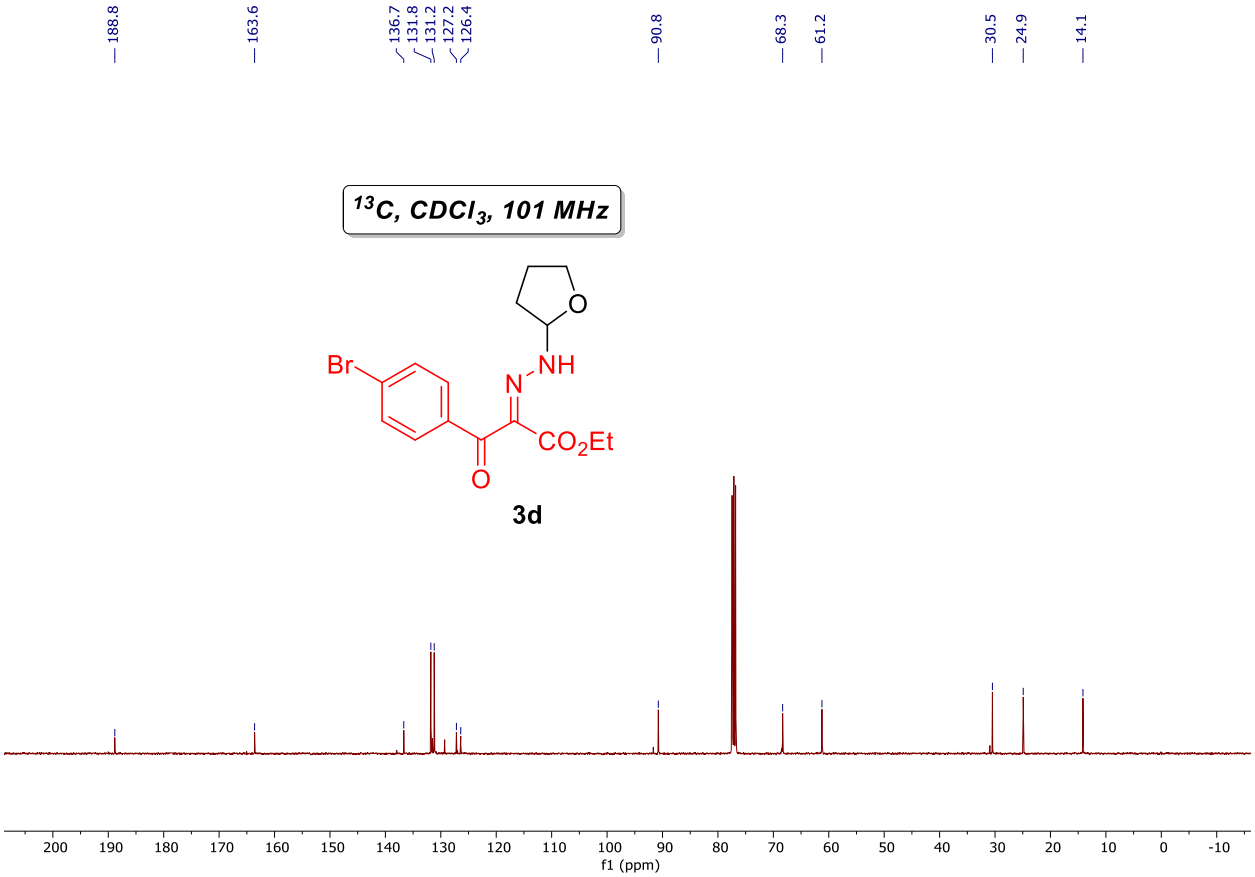




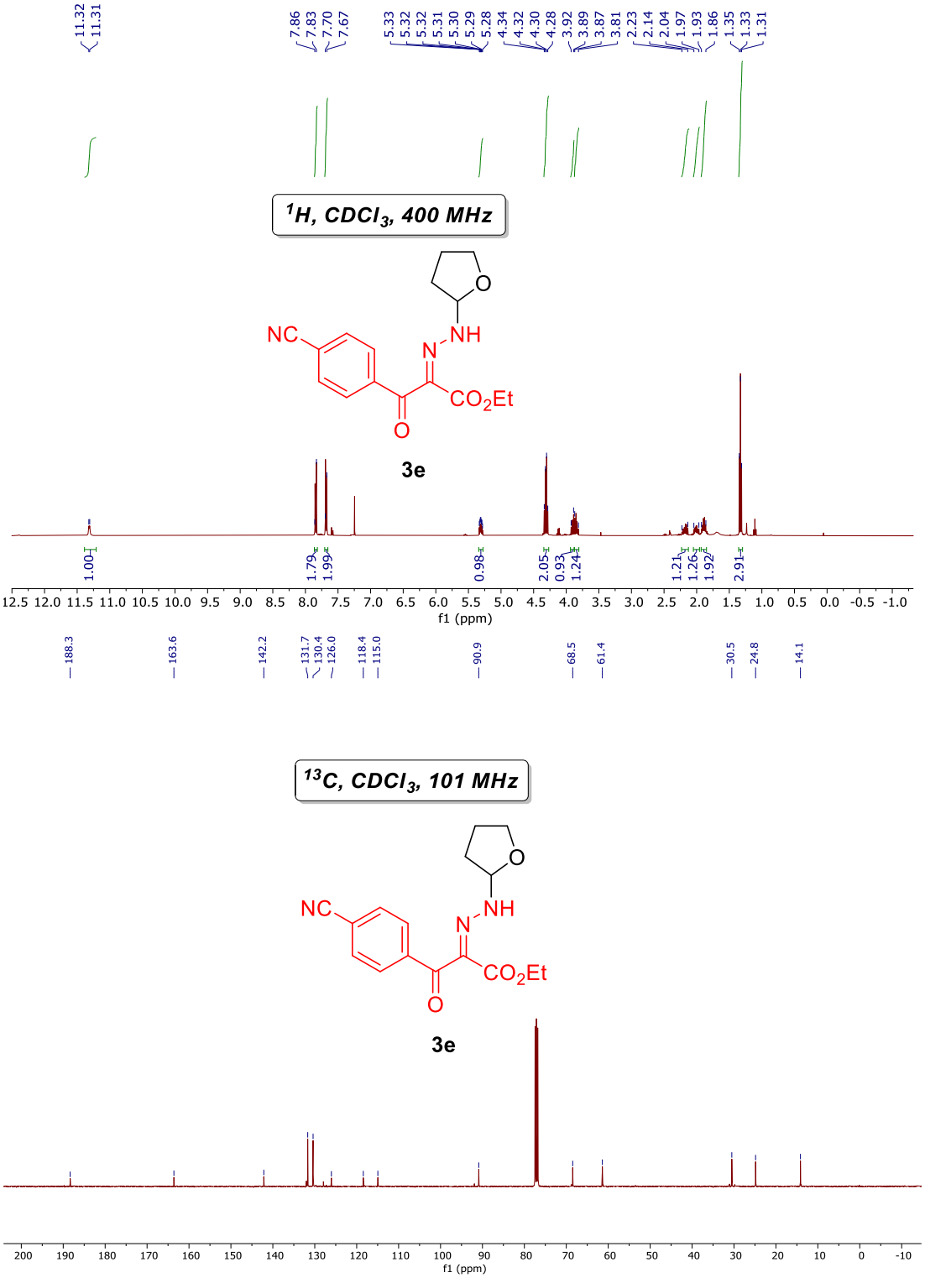


5.6.4. ethyl (*Z*)-3-(4-bromophenyl)-3-oxo-2-(2-(tetrahydrofuran-2-yl)hydrazono)propanoate (3d):

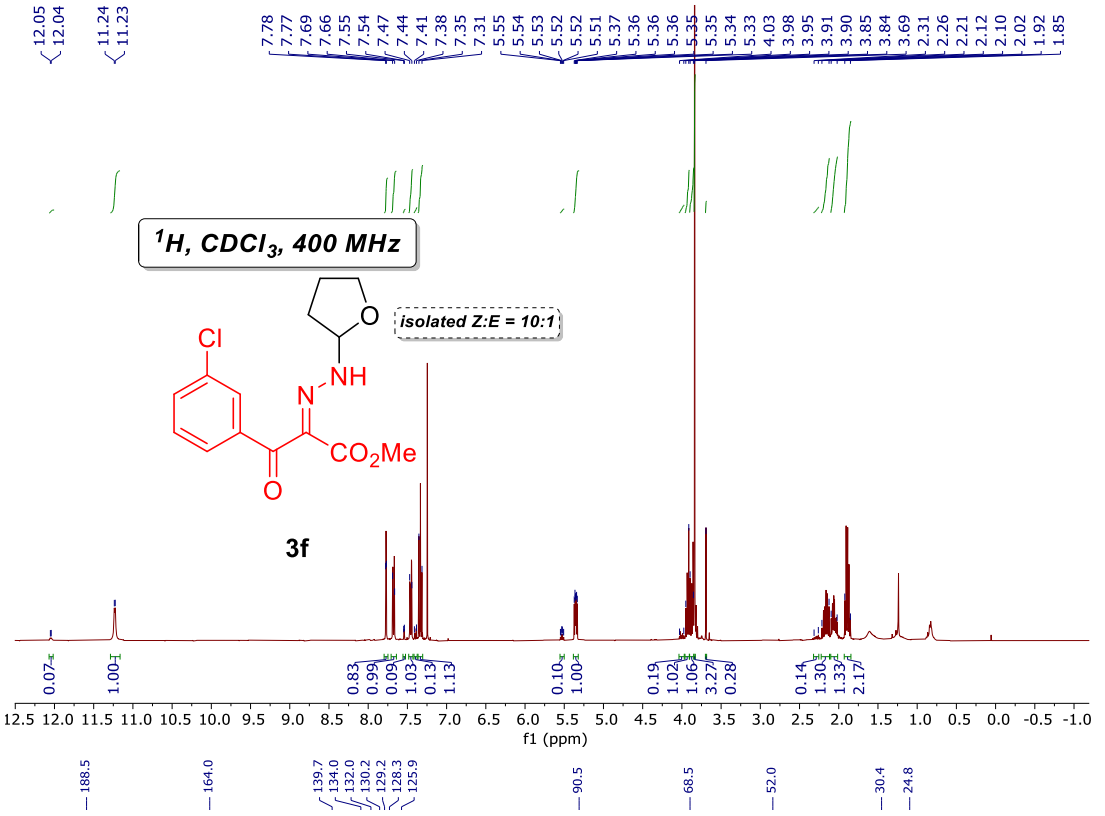


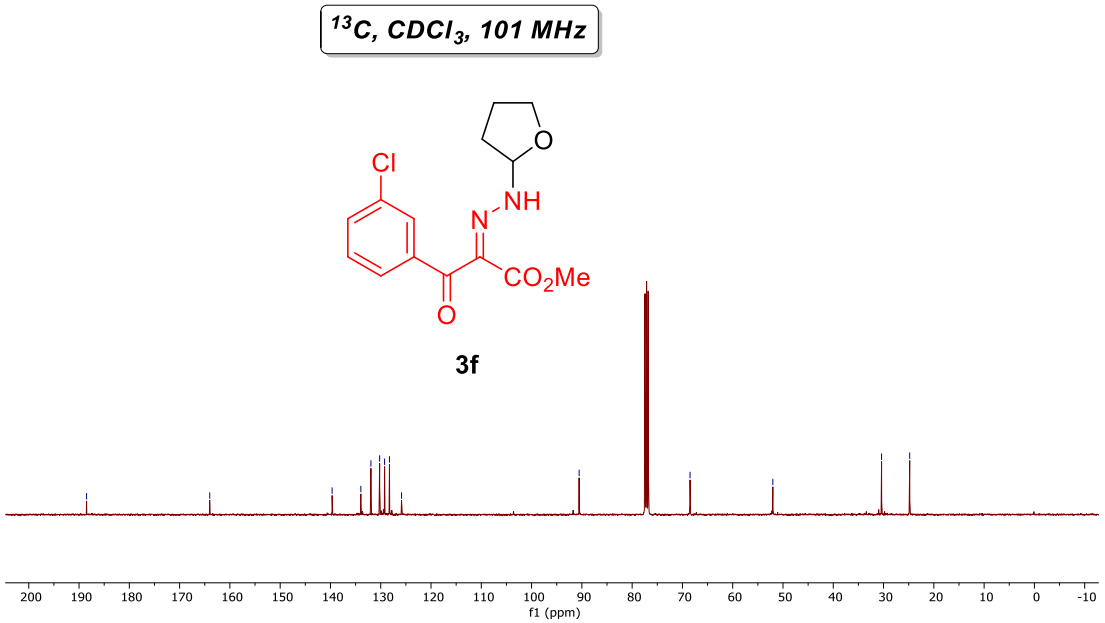

188.8
163.6
136.7
131.8
131.2
127.2
126.4
90.8
68.3
61.2
30.5
24.9
14.1
^{13}C, $CDCl_3$, 101 MHz
Br
N
NH
O
CO_2Et
O
3d
200 190 180 170 160 150 140 130 120 110 100 90 80 70 60 50 40 30 20 10 0 -10
f1 (ppm)

5.6.5. ethyl (*Z*)-3-(4-cyanophenyl)-3-oxo-2-(2-(tetrahydrofuran-2-yl)hydrazono)propanoate (3e):

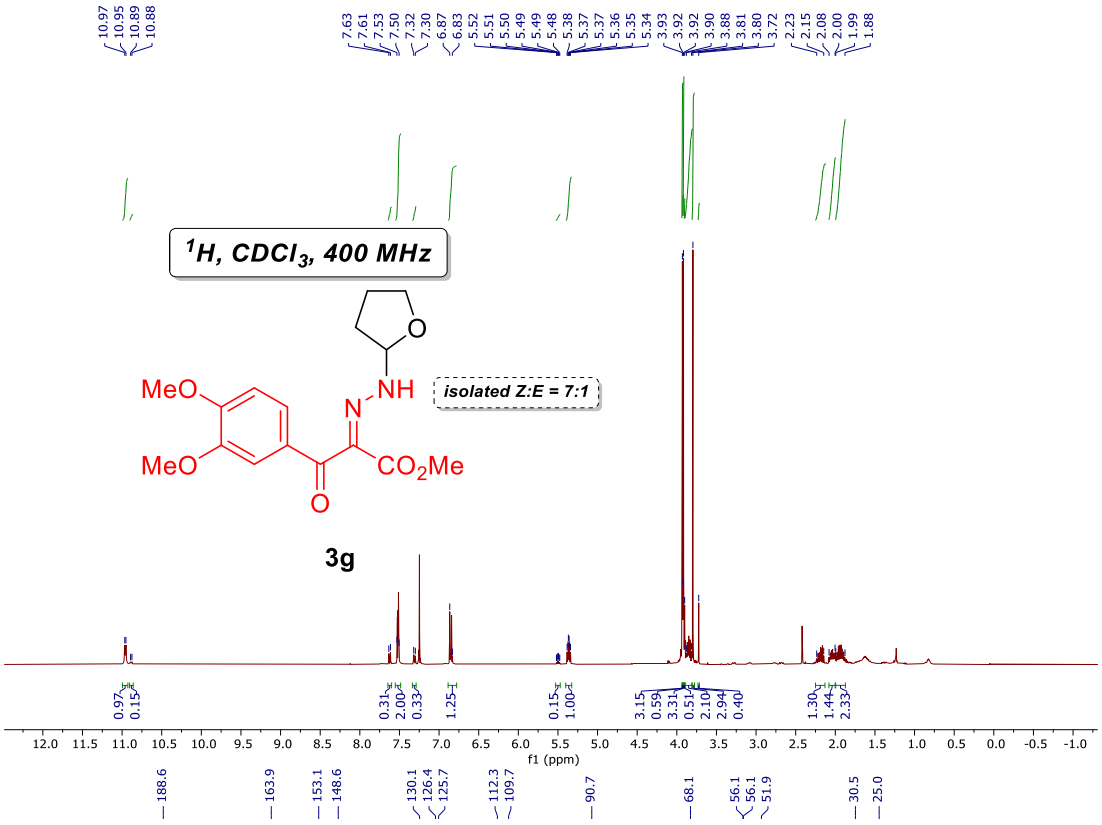


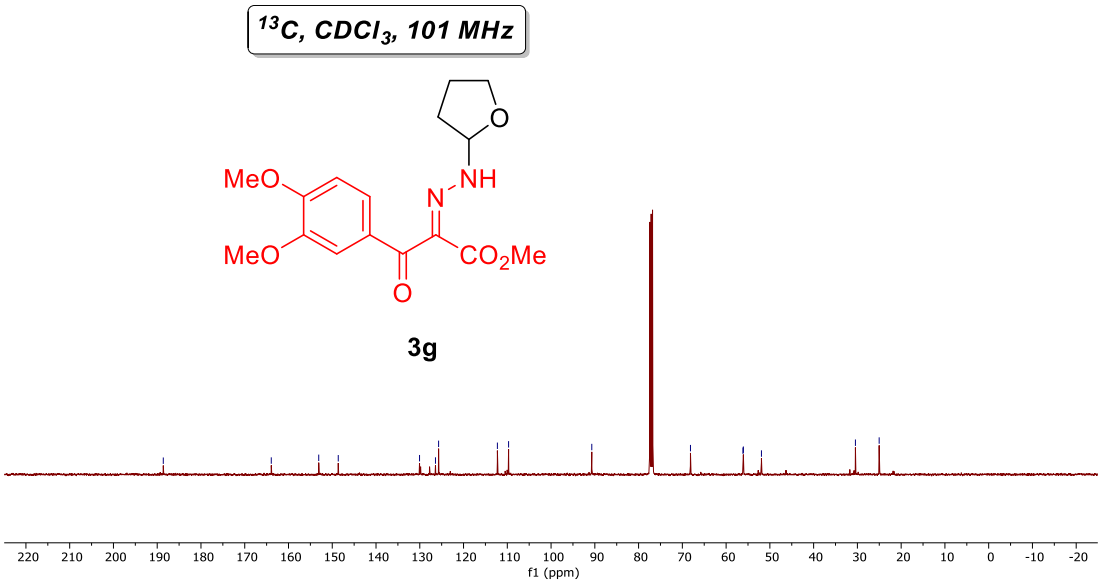
5.6.6. methyl (*Z*)-3-(3-chlorophenyl)-3-oxo-2-(2-(tetrahydrofuran-2-yl)hydrazono)propanoate (3f):



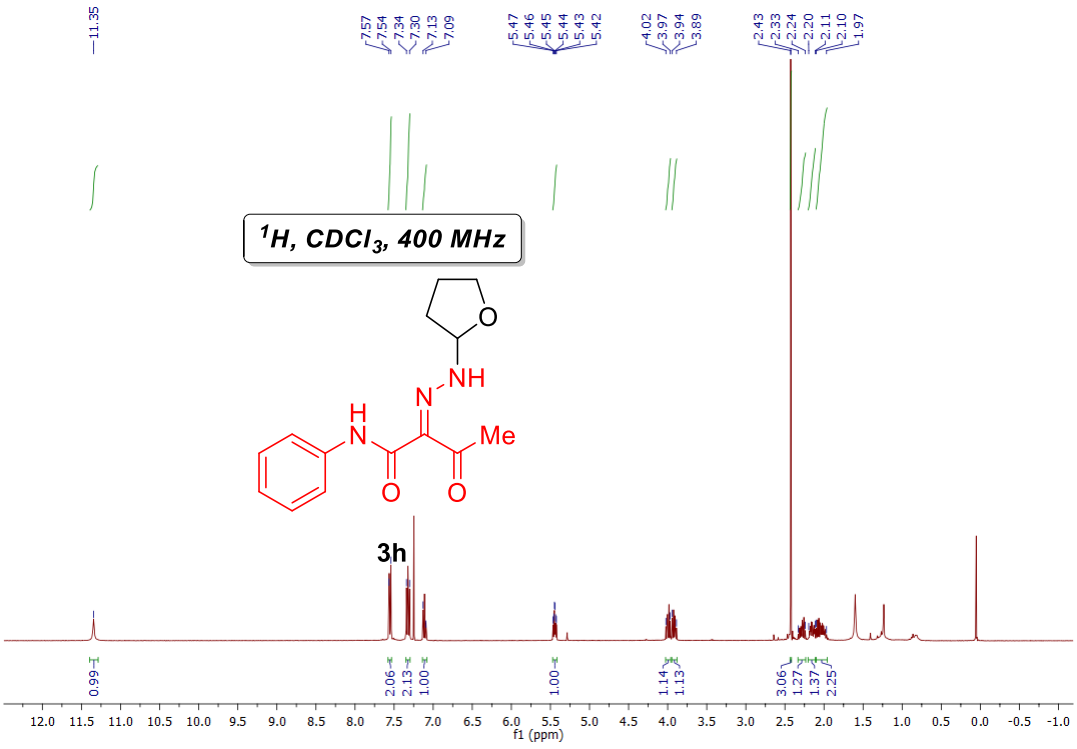


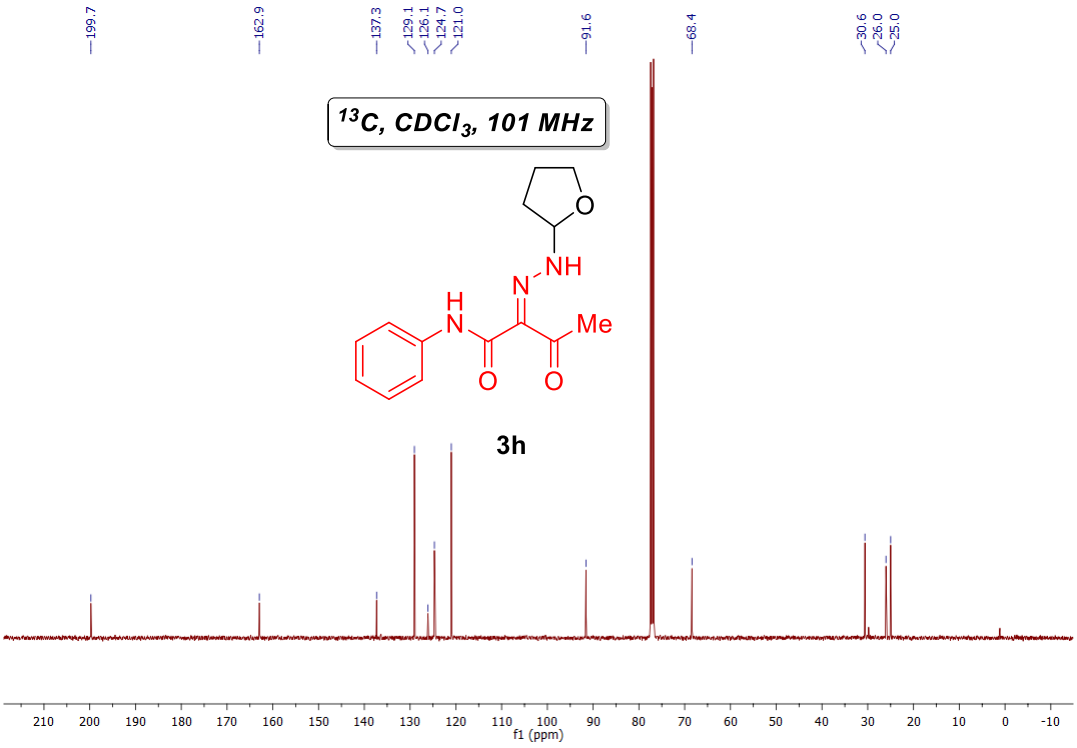
5.6.7. methyl (*Z*)-3-(3,4-dimethoxyphenyl)-3-oxo-2-(2-(tetrahydrofuran-2-yl)hydrazono)propanoate (3g):



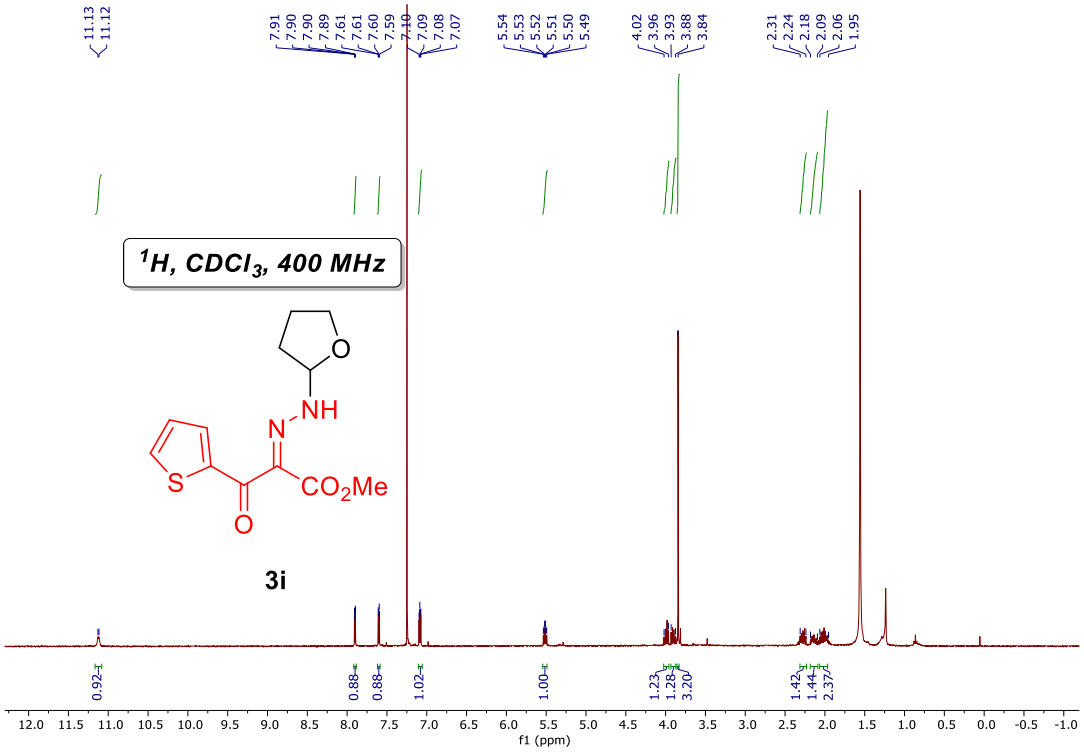


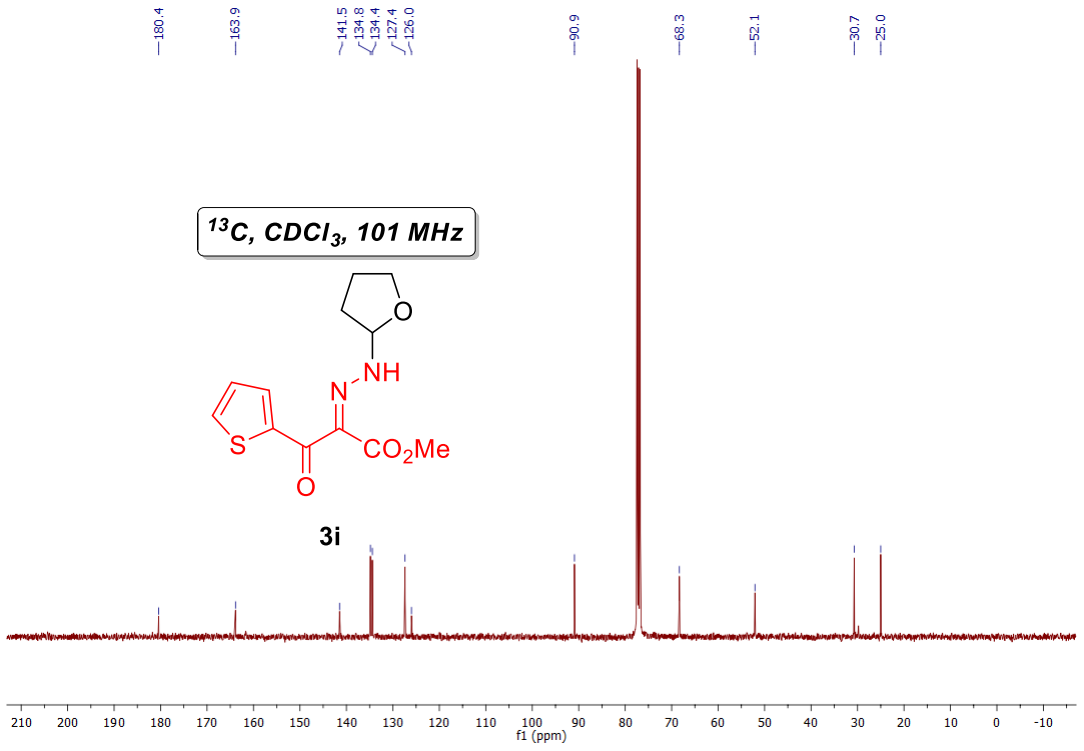
5.6.8. methyl (Z)-3-oxo-3-(phenylamino)-2-(2-(tetrahydrofuran-2-yl)hydrazono)propanoate (3h):



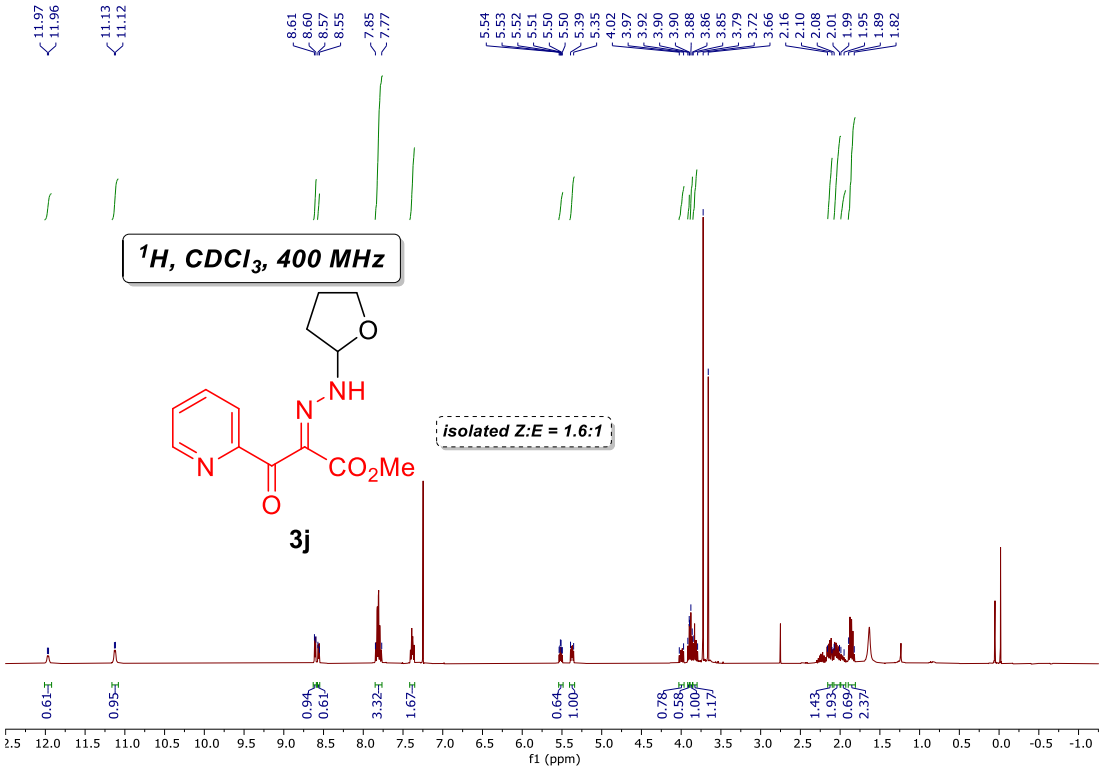


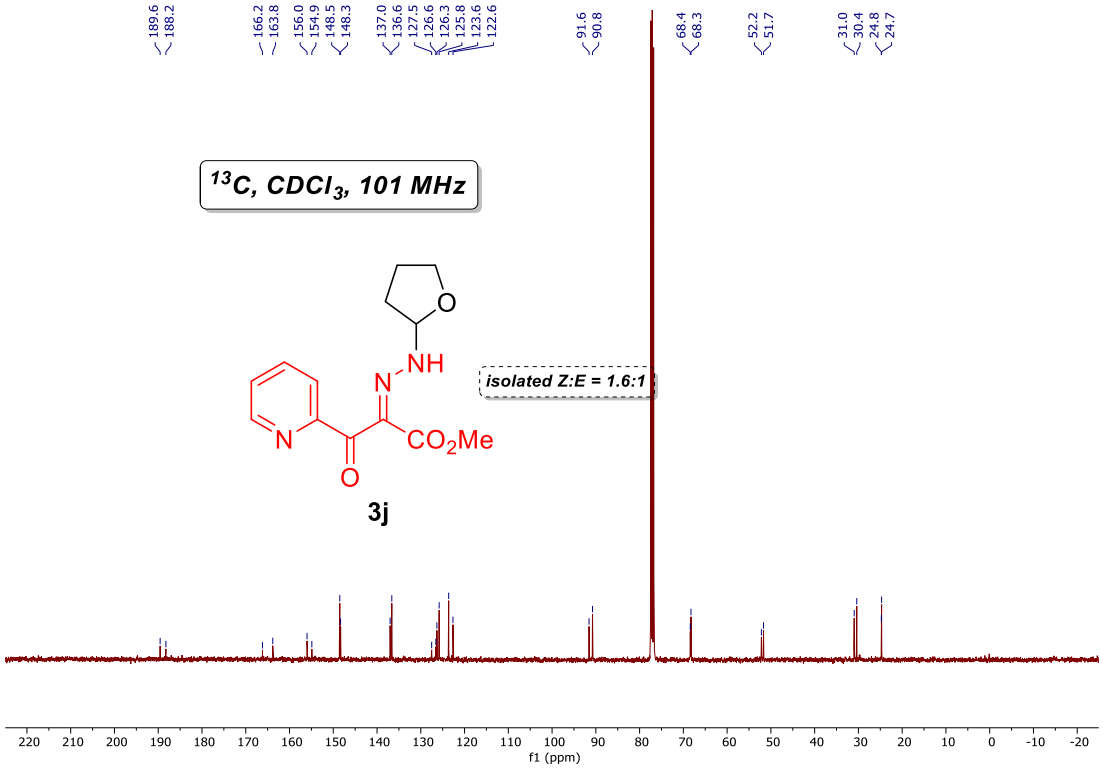
5.6.9. methyl (Z)-3-oxo-2-(2-(tetrahydrofuran-2-yl)hydrazono)-3-(thiophen-2-yl)propanoate (3i):



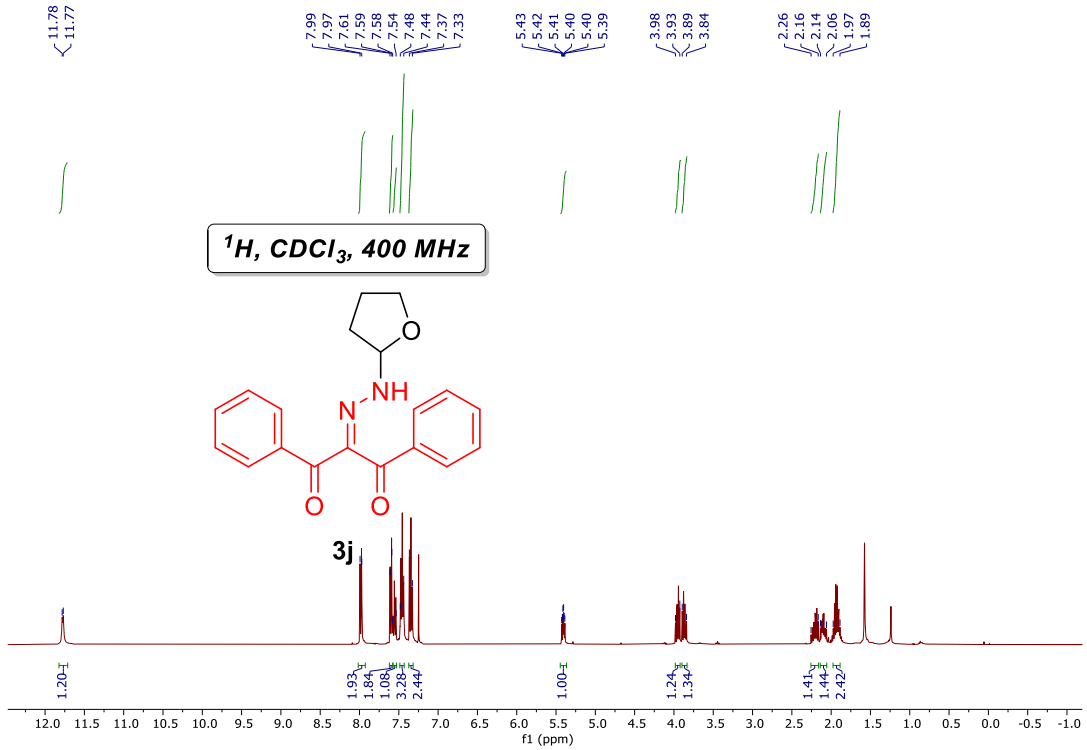


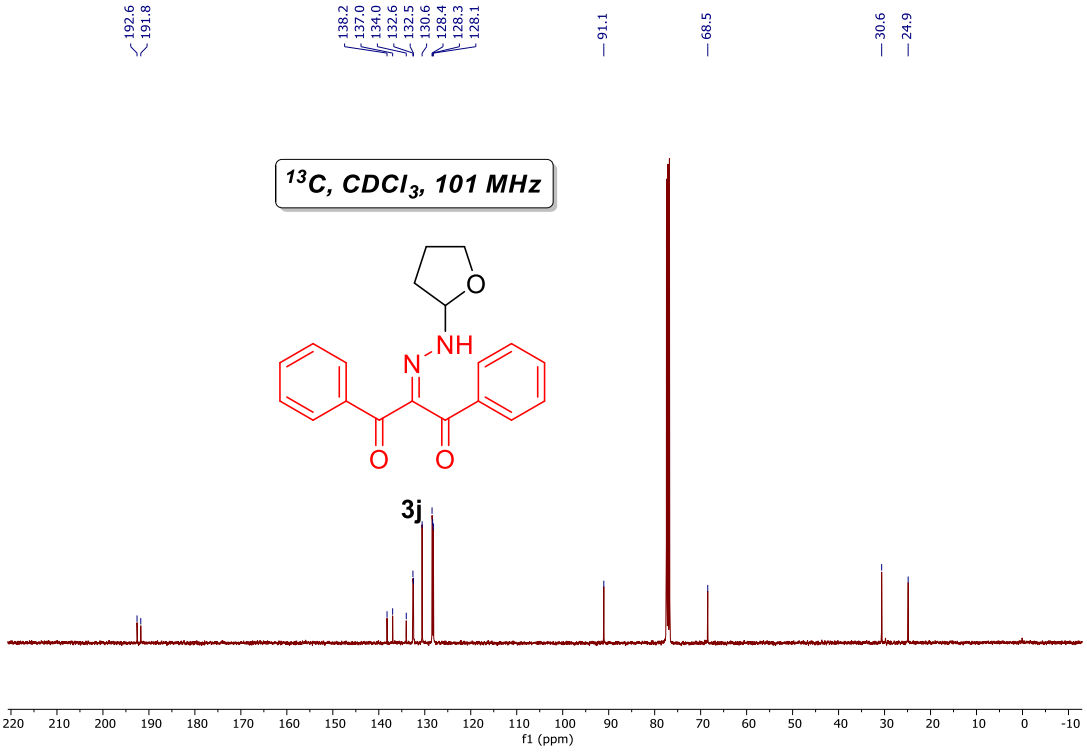
5.6.10. methyl (*Z*)-3-oxo-3-(pyridin-2-yl)-2-(2-(tetrahydrofuran-2-yl)hydrazono)propanoate (3j):



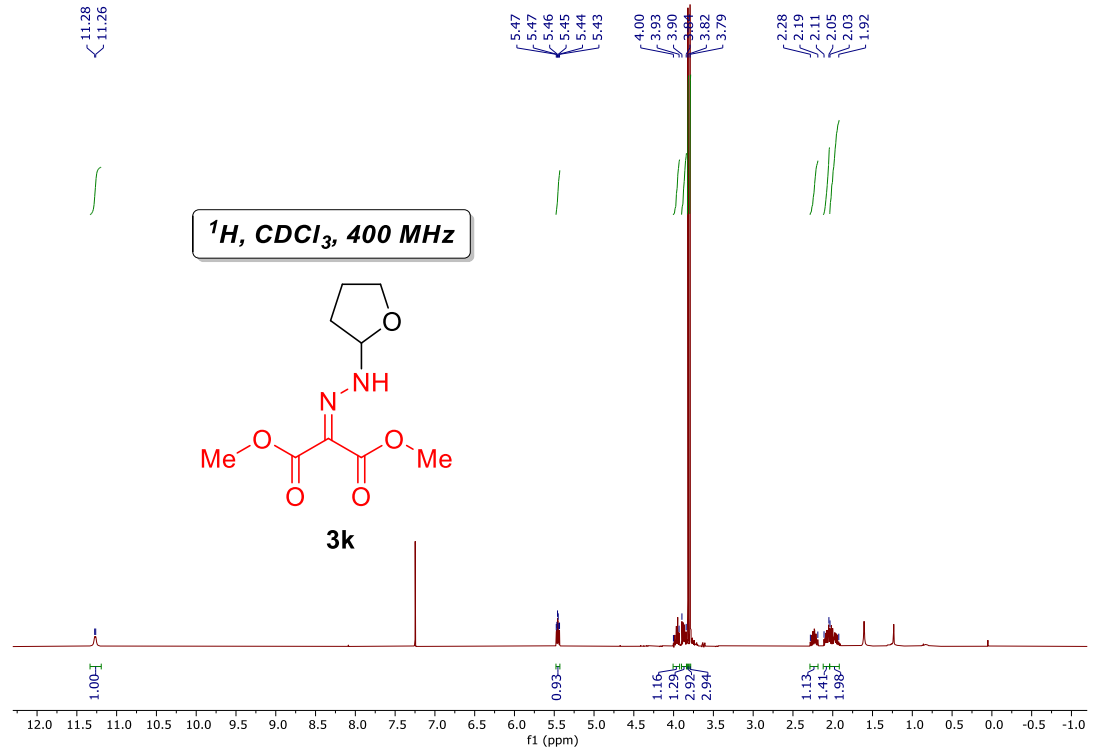


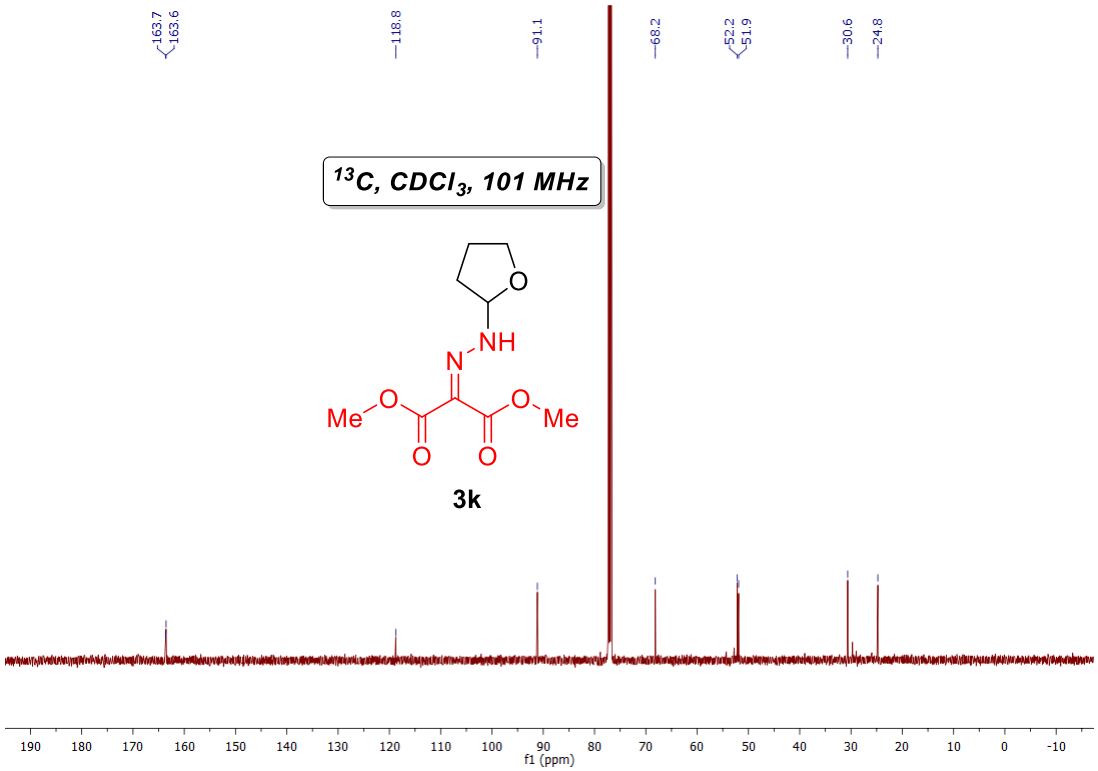
5.6.11. 1,3-diphenyl-2-(2-(tetrahydrofuran-2-yl)hydrazono)propane-1,3-dione (3j):



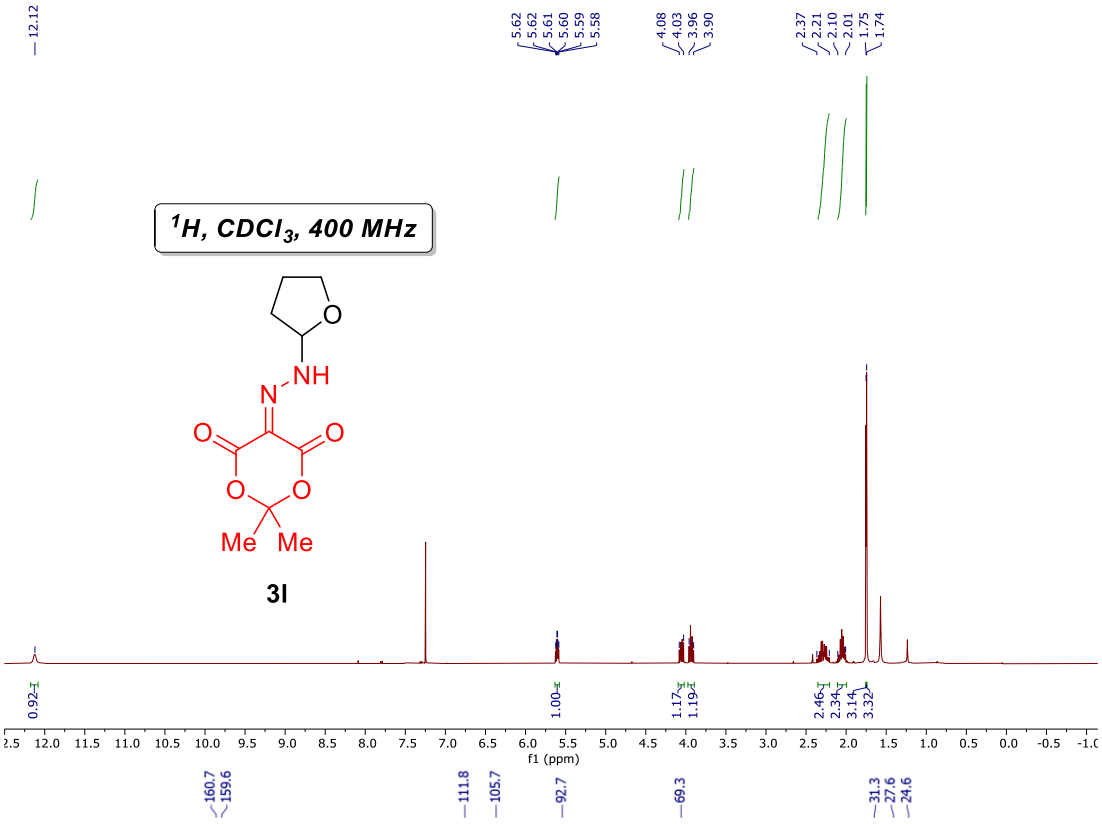


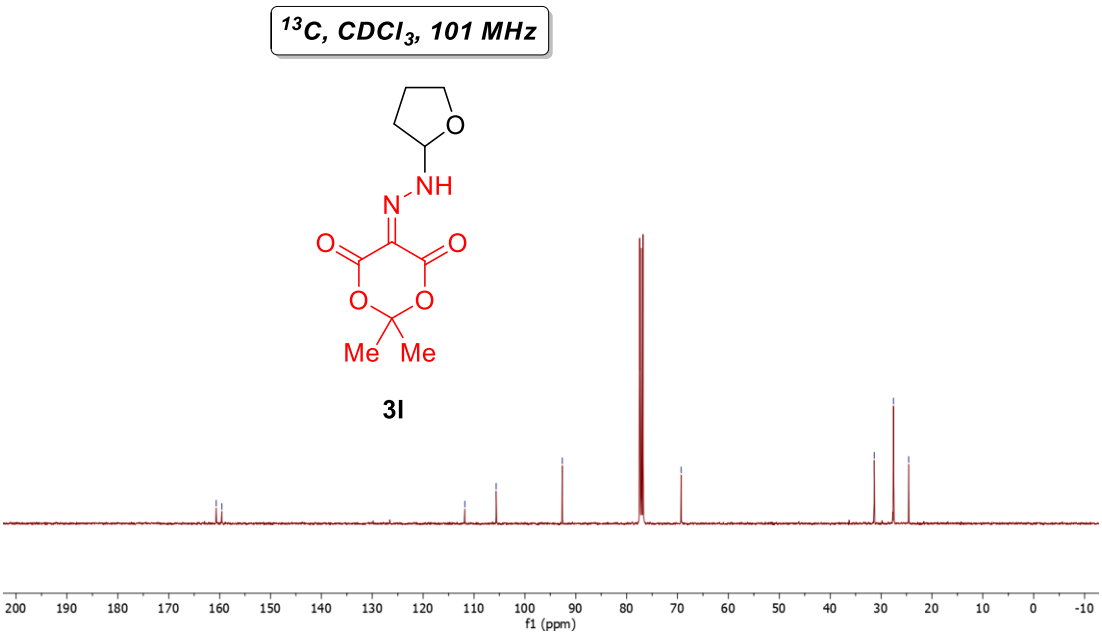
5.6.12. dimethyl 2-(2-(tetrahydrofuran-2-yl)hydrazono)malonate (3k):



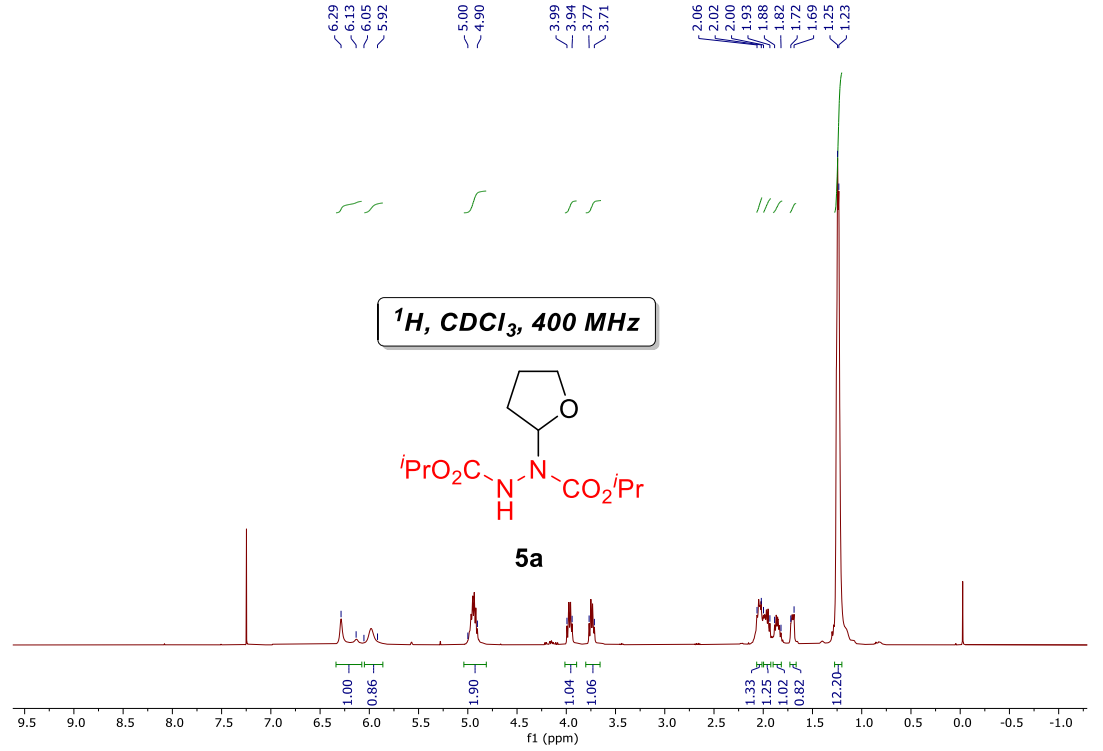


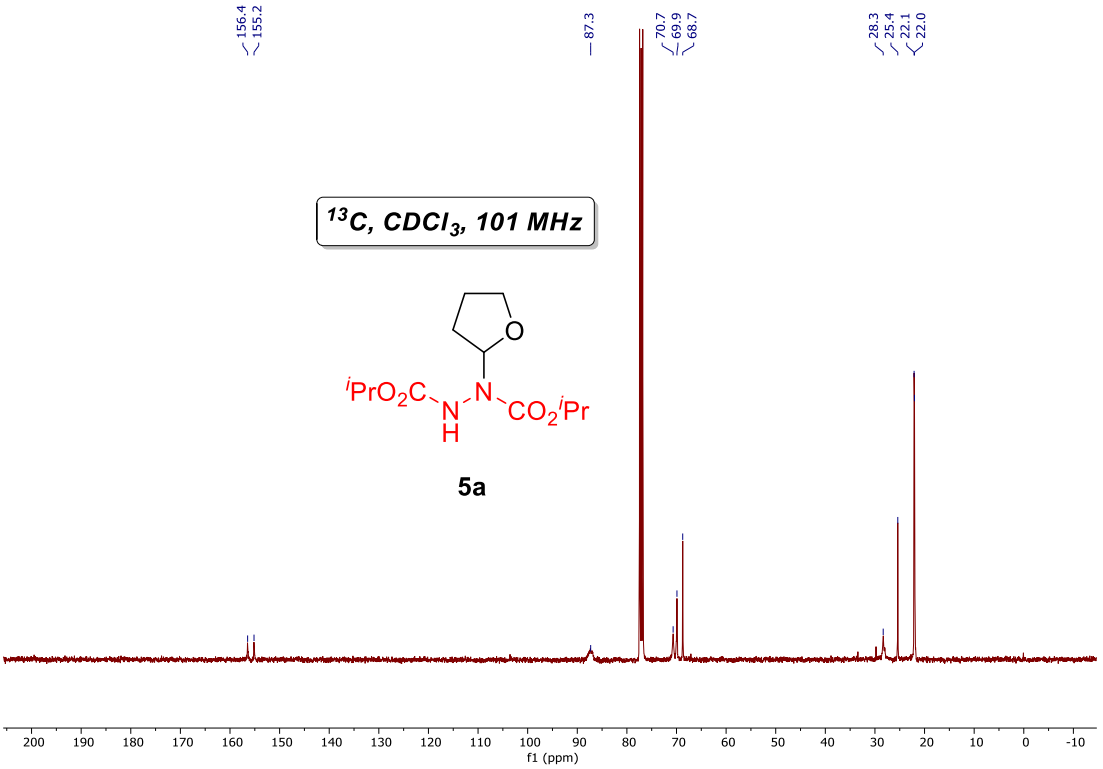
5.6.13. 2,2-dimethyl-5-(2-(tetrahydrofuran-2-yl)hydrazono)-1,3-dioxane-4,6-dione (3l):



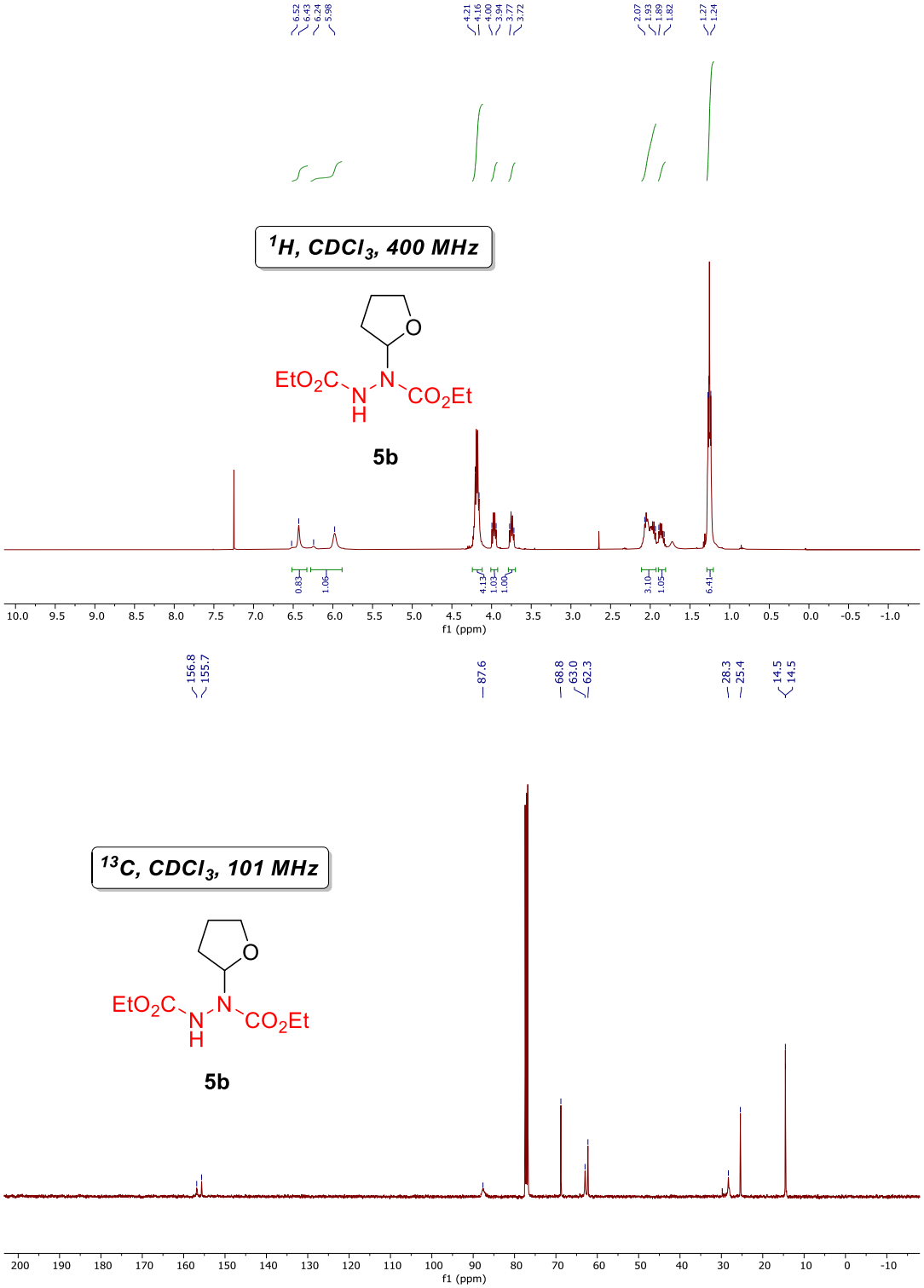


5.6.14. diisopropyl 1-(tetrahydrofuran-2-yl)hydrazine-1,2-dicarboxylate (xx)

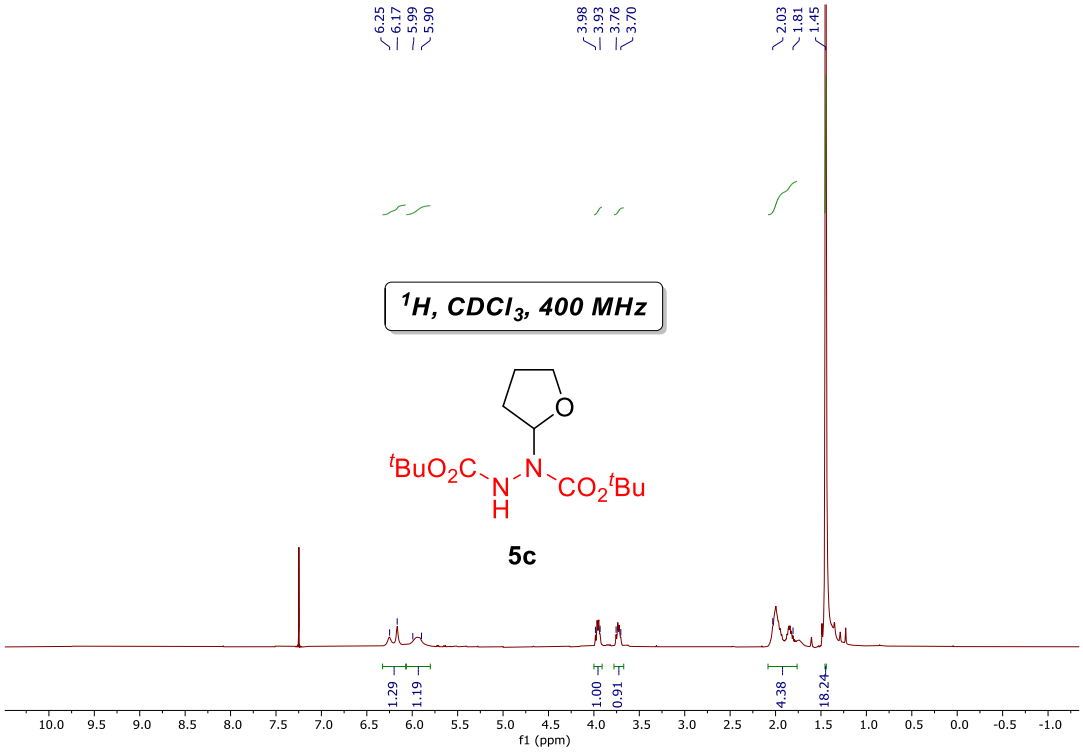


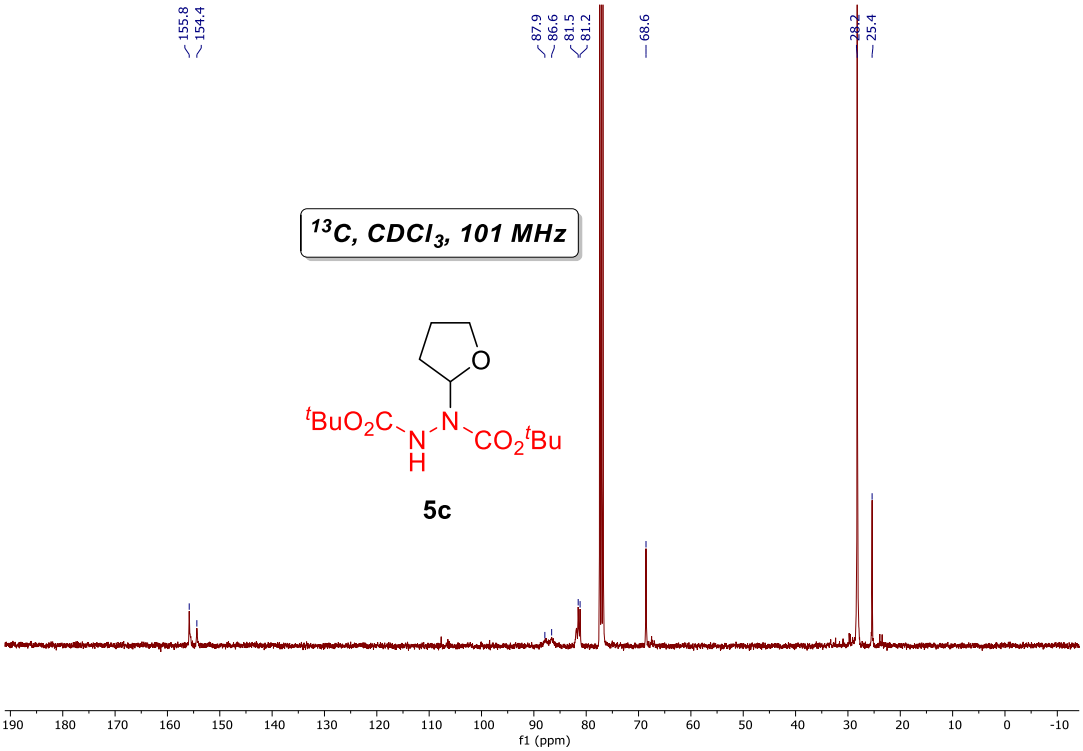


5.6.15. diethyl 1-(tetrahydrofuran-2-yl)hydrazine-1,2-dicarboxylate (5b)

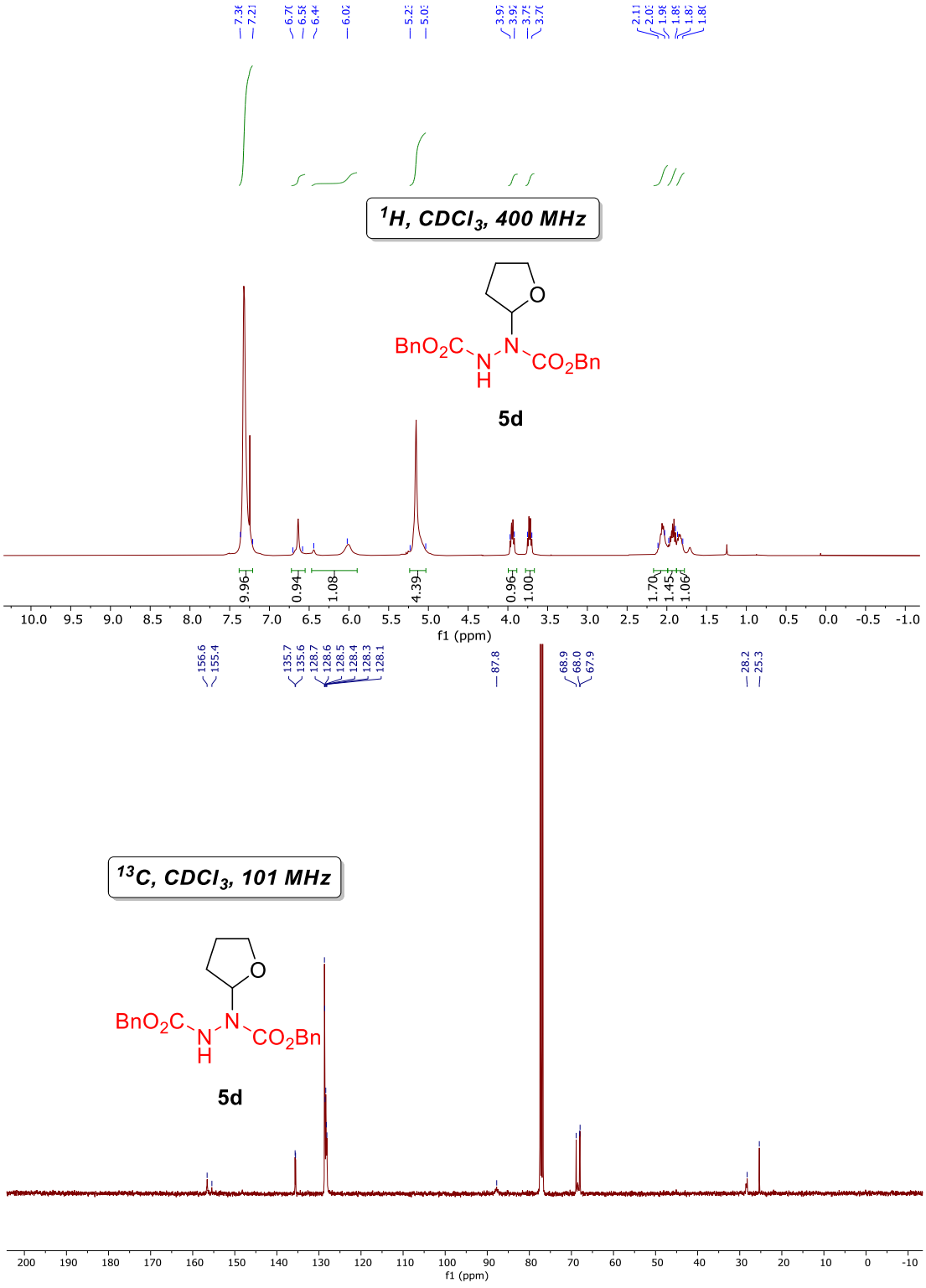


5.6.16. di-*tert*-butyl 1-(tetrahydrofuran-2-yl)hydrazine-1,2-dicarboxylate (5c)

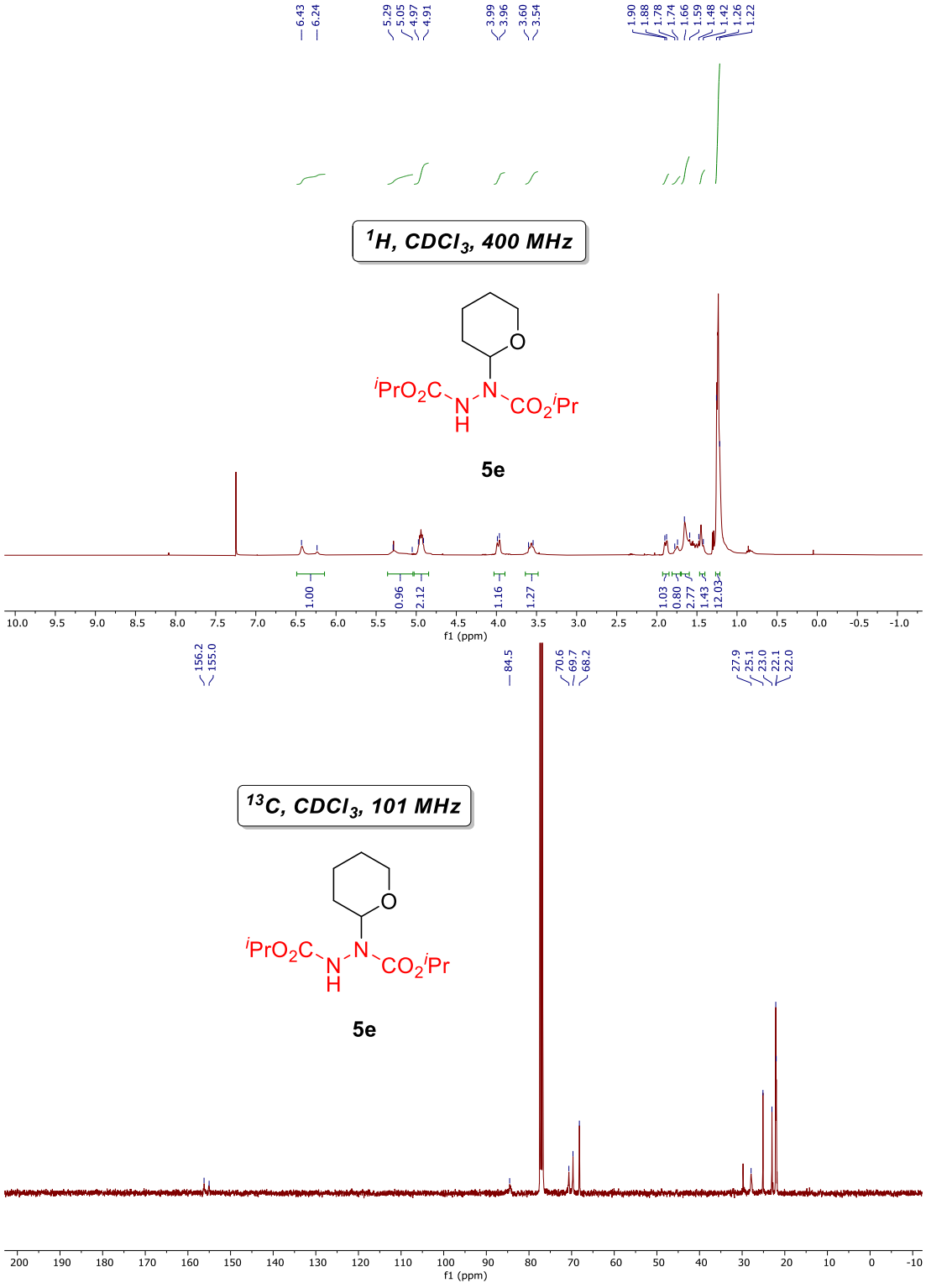




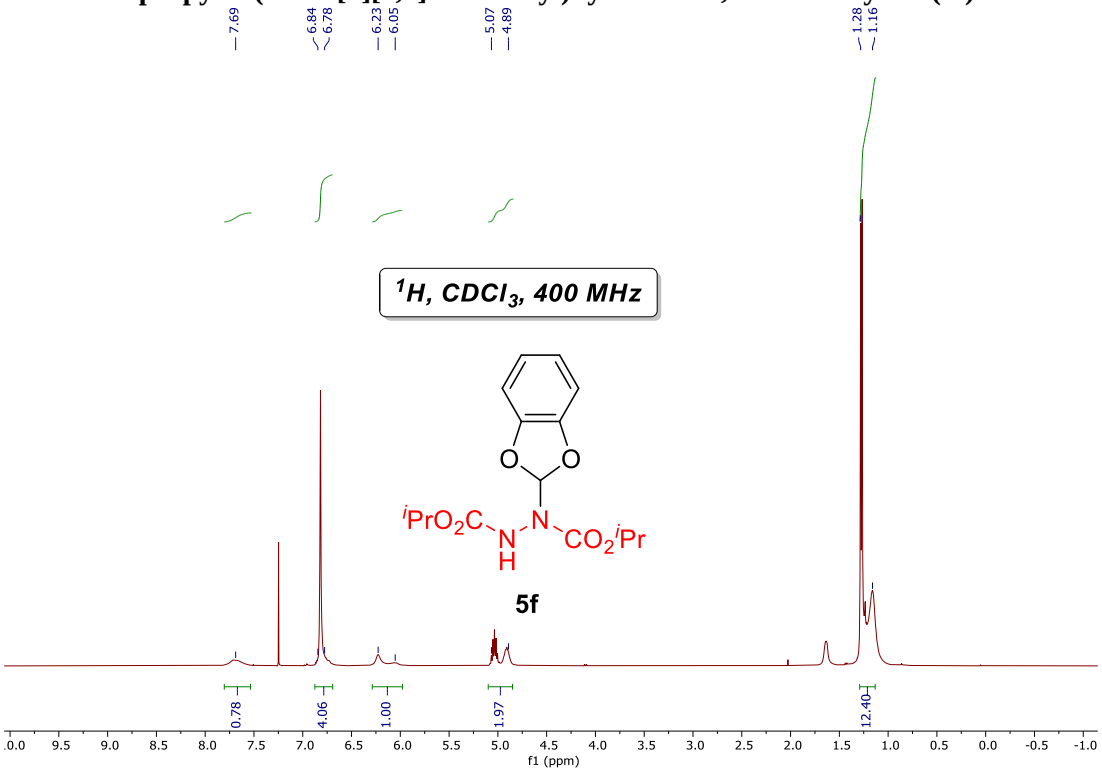
5.6.17. dibenzyl 1-(tetrahydrofuran-2-yl)hydrazine-1,2-dicarboxylate (5d)

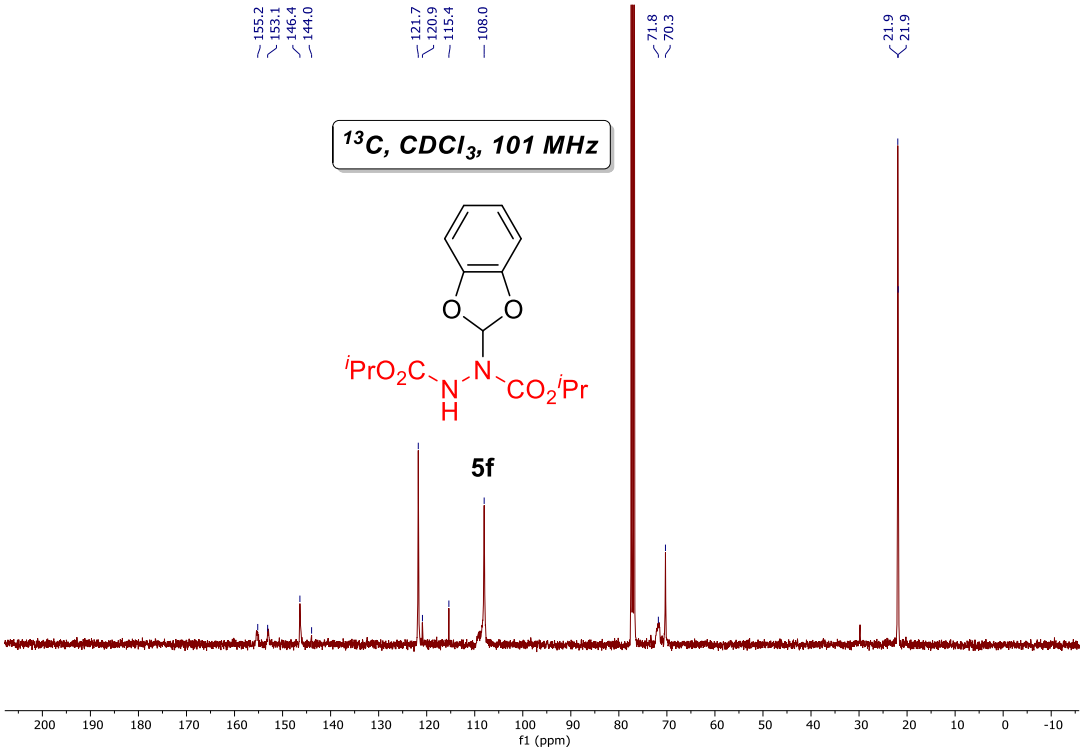


5.6.18. diisopropyl 1-(tetrahydro-2H-pyran-2-yl)hydrazine-1,2-dicarboxylate (5e):

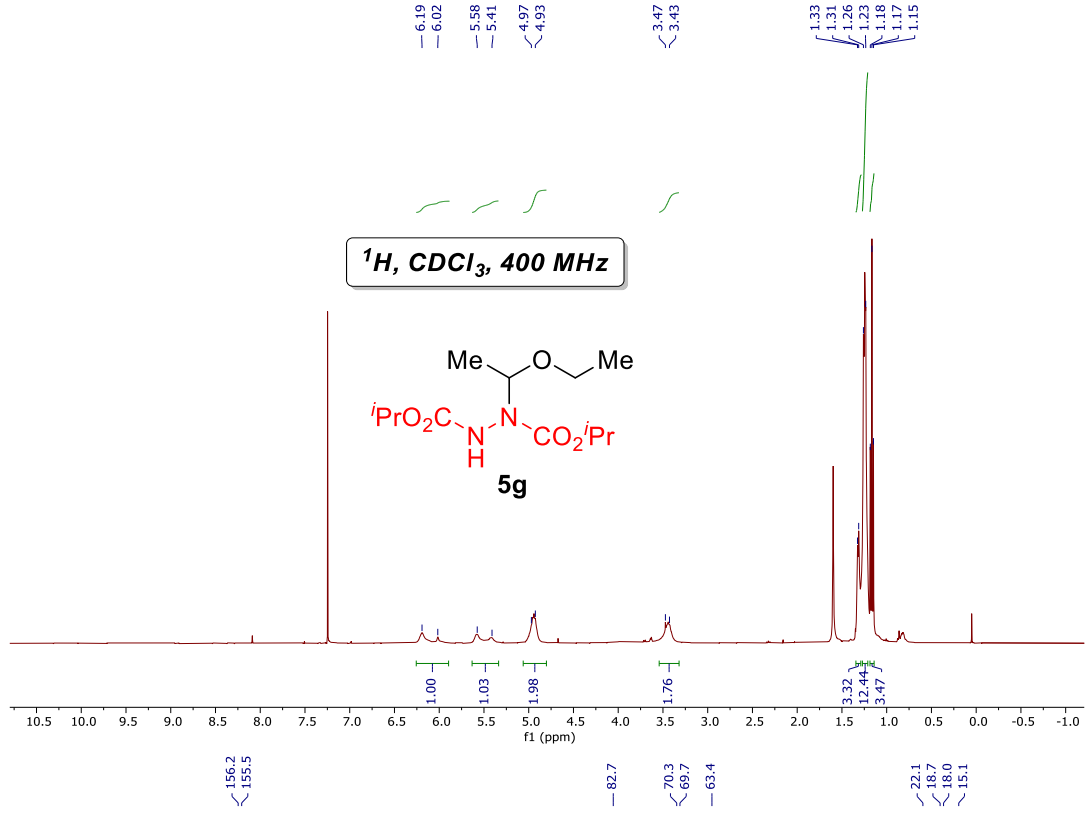


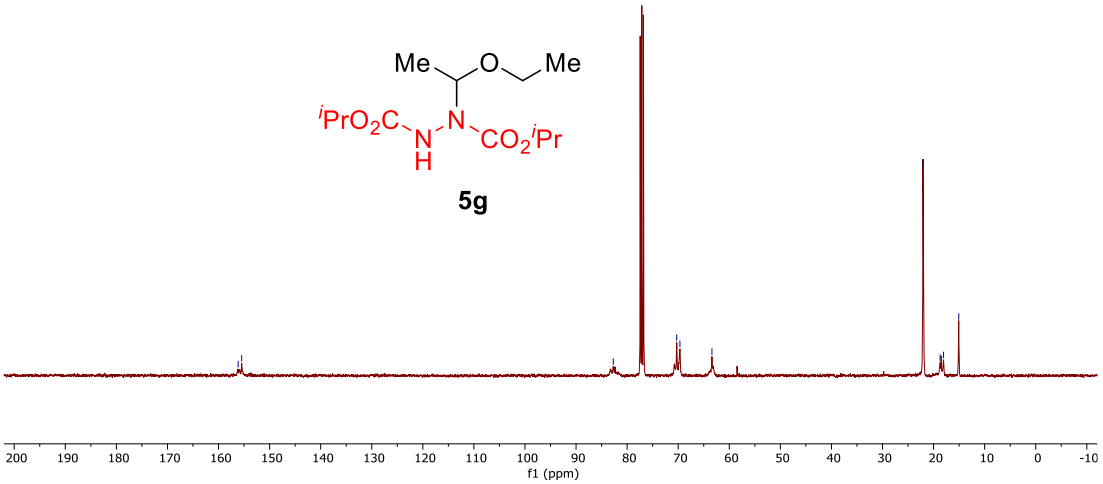
5.6.19. diisopropyl 1-(benzo[*d*][1,3]dioxol-2-yl)hydrazine-1,2-dicarboxylate (5f)



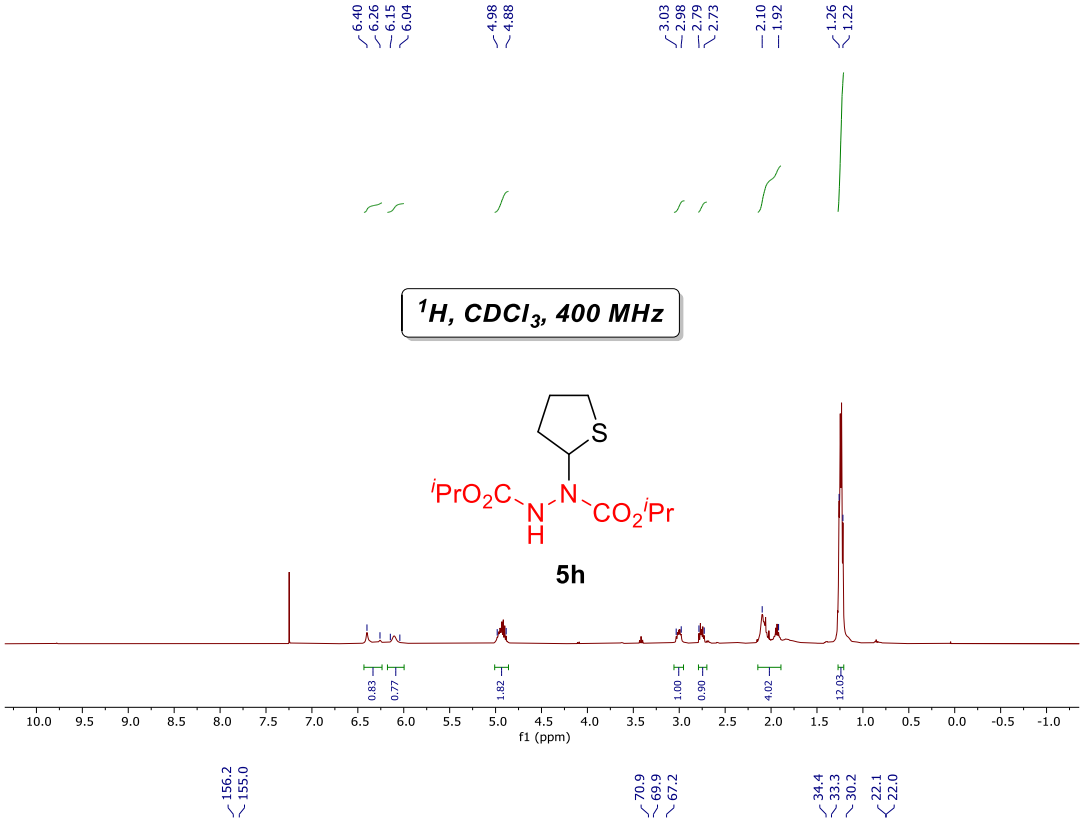


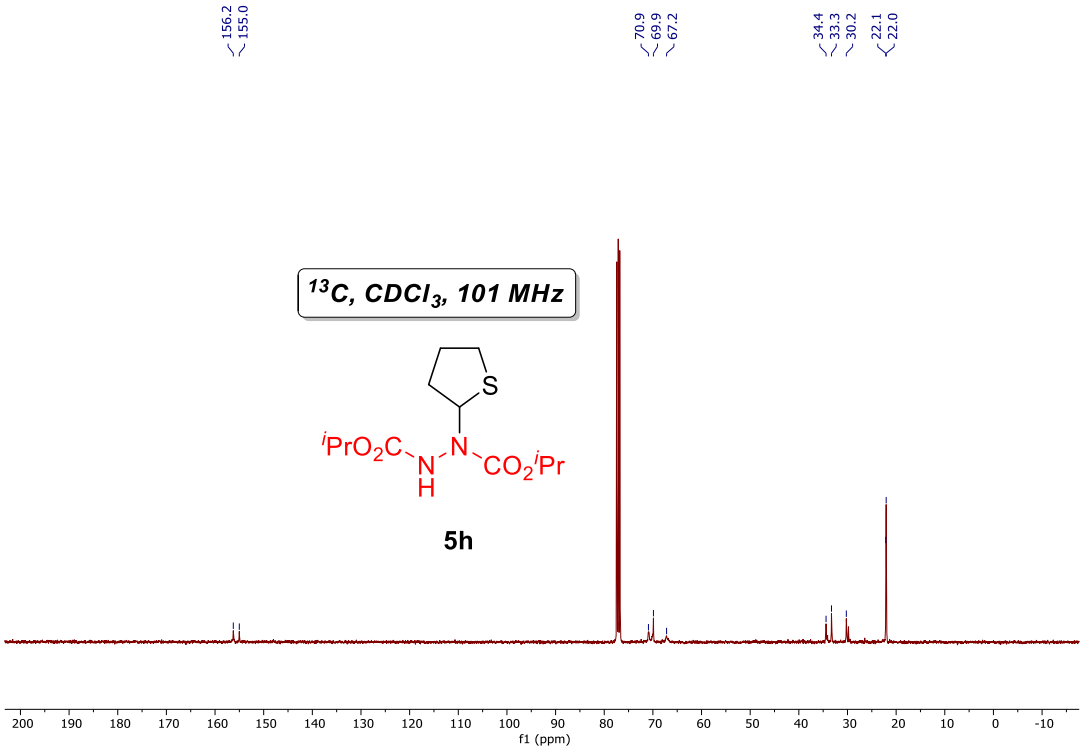
5.6.20. diisopropyl 1-(1-ethoxyethyl)hydrazine-1,2-dicarboxylate (5g)



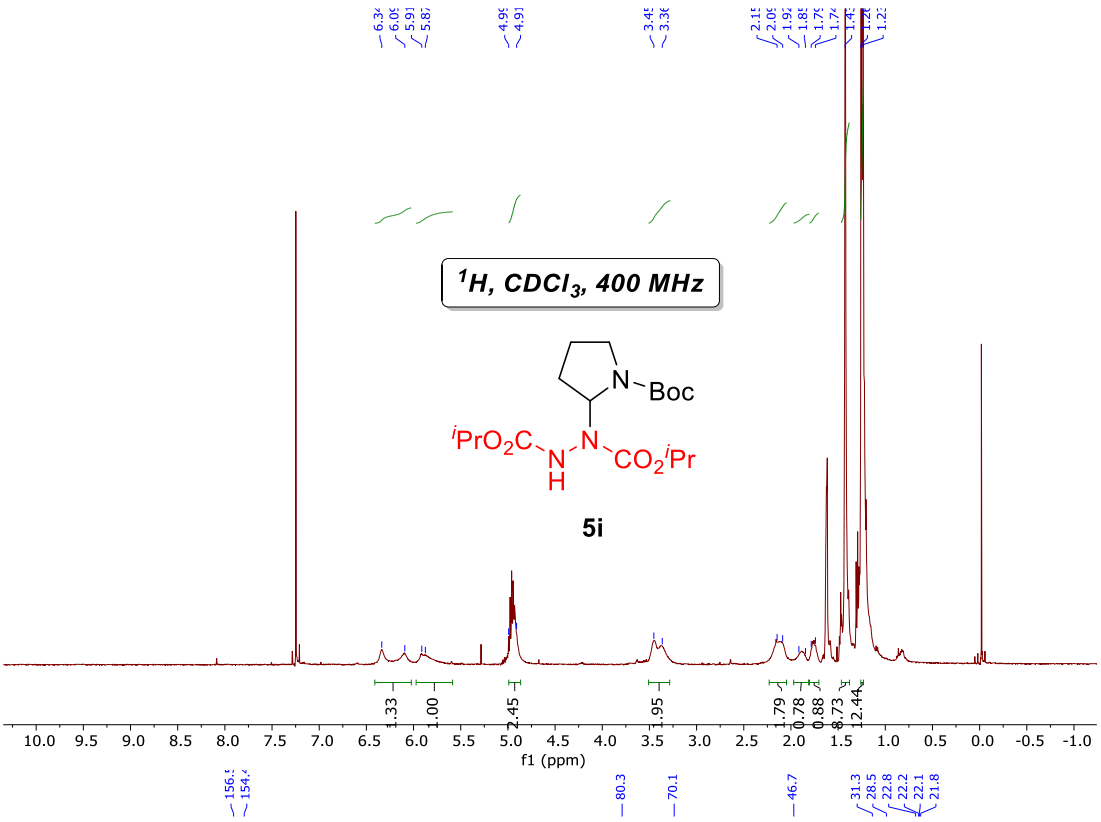


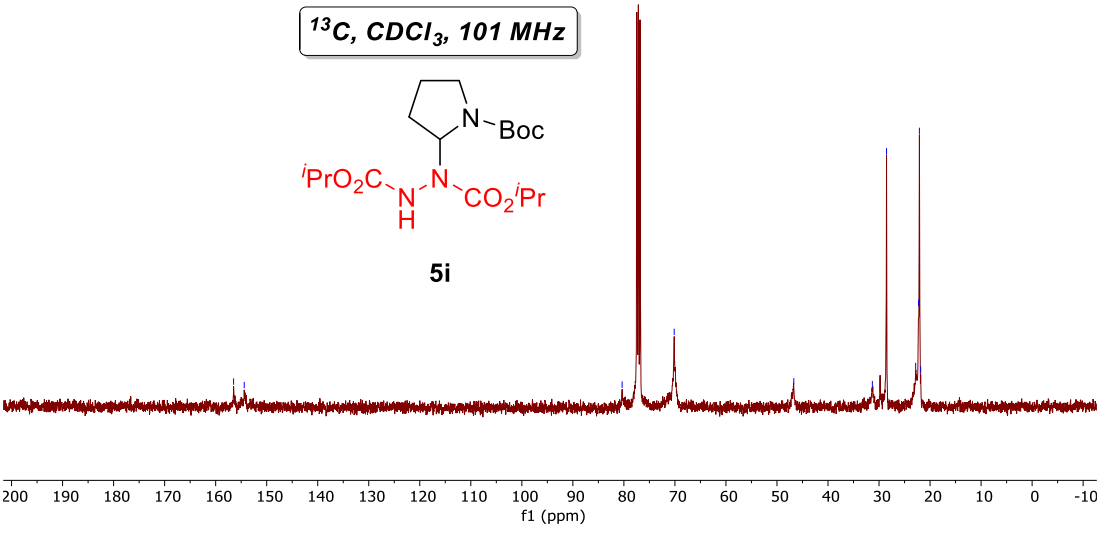
5.6.21. diisopropyl 1-(tetrahydrothiophen-2-yl)hydrazine-1,2-dicarboxylate (5h)



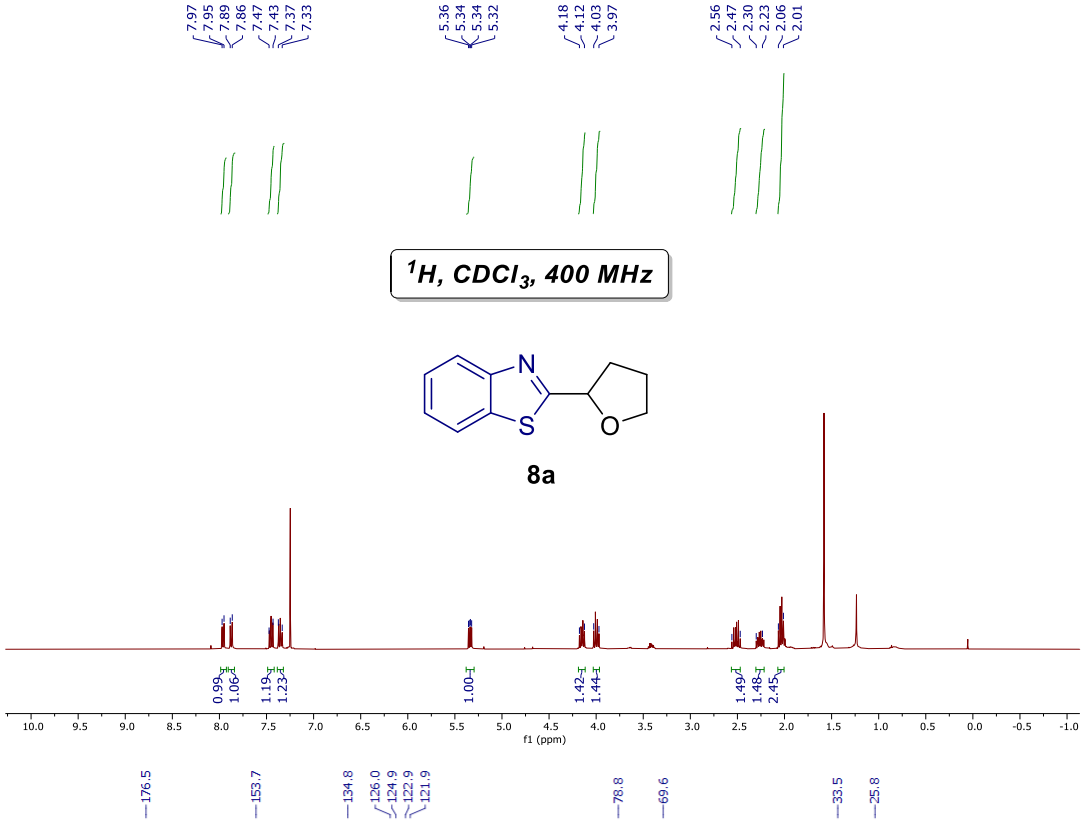


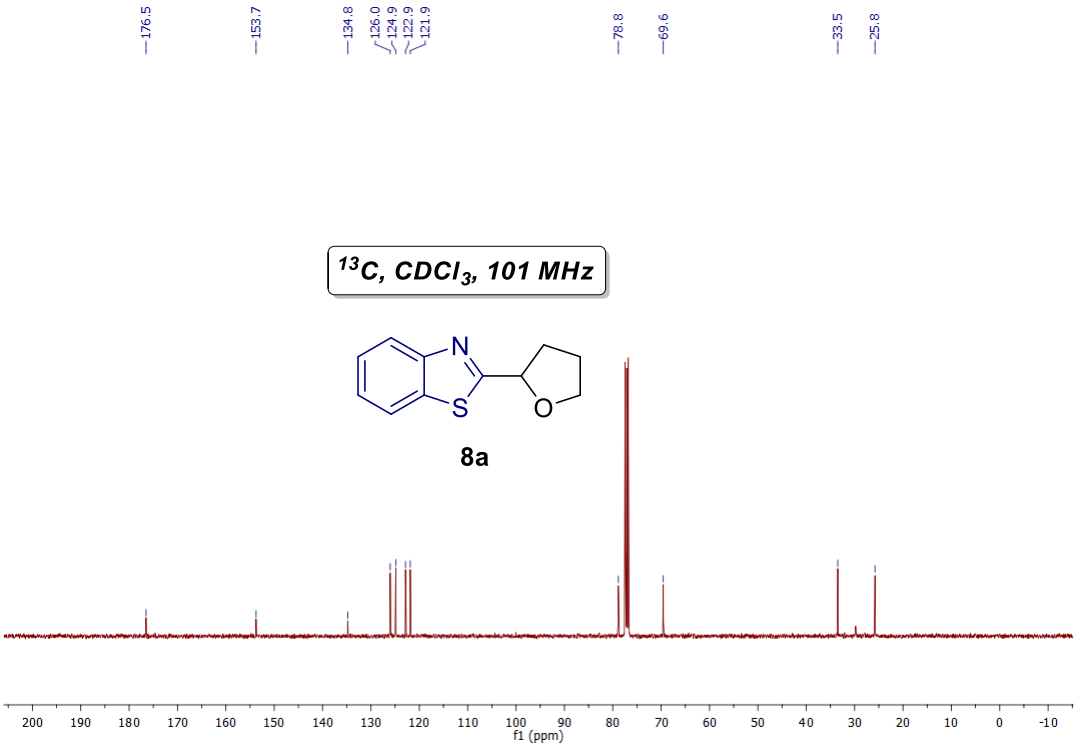
5.6.22. diisopropyl 1-(1-(*tert*-butoxycarbonyl)pyrrolidin-2-yl)hydrazine-1,2-dicarboxylate (5i):



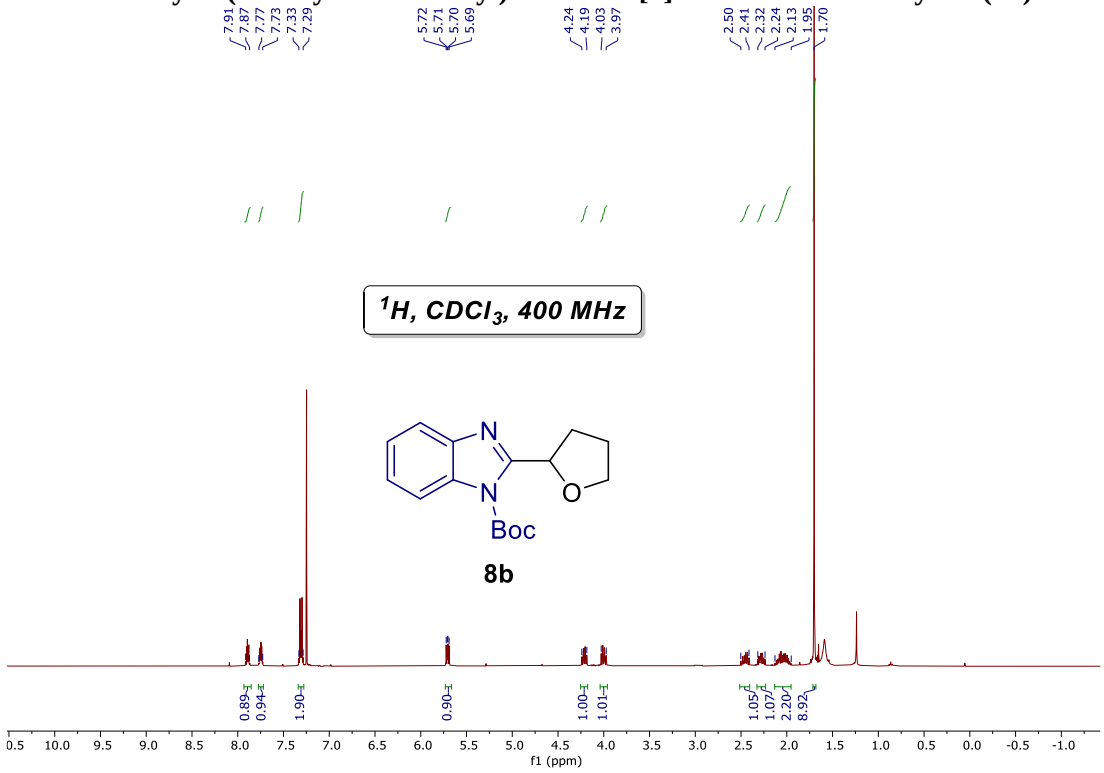


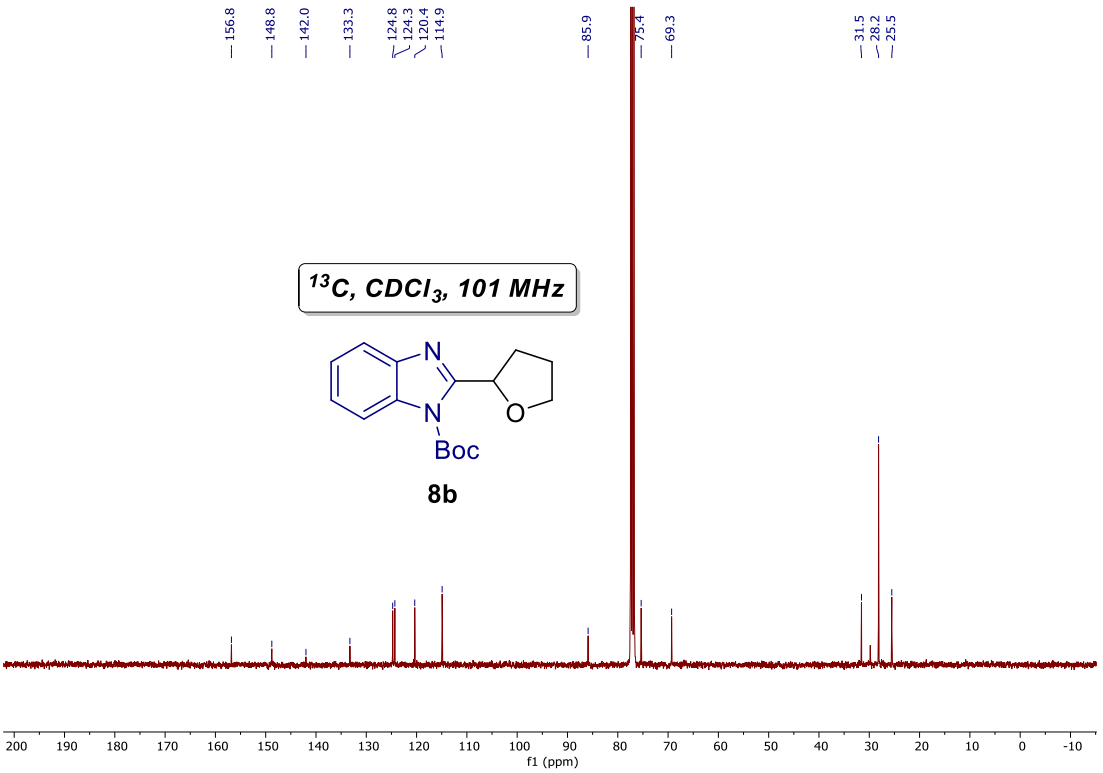
5.6.23. 2-(tetrahydrofuran-2-yl)benzo[*d*]thiazole (8a):



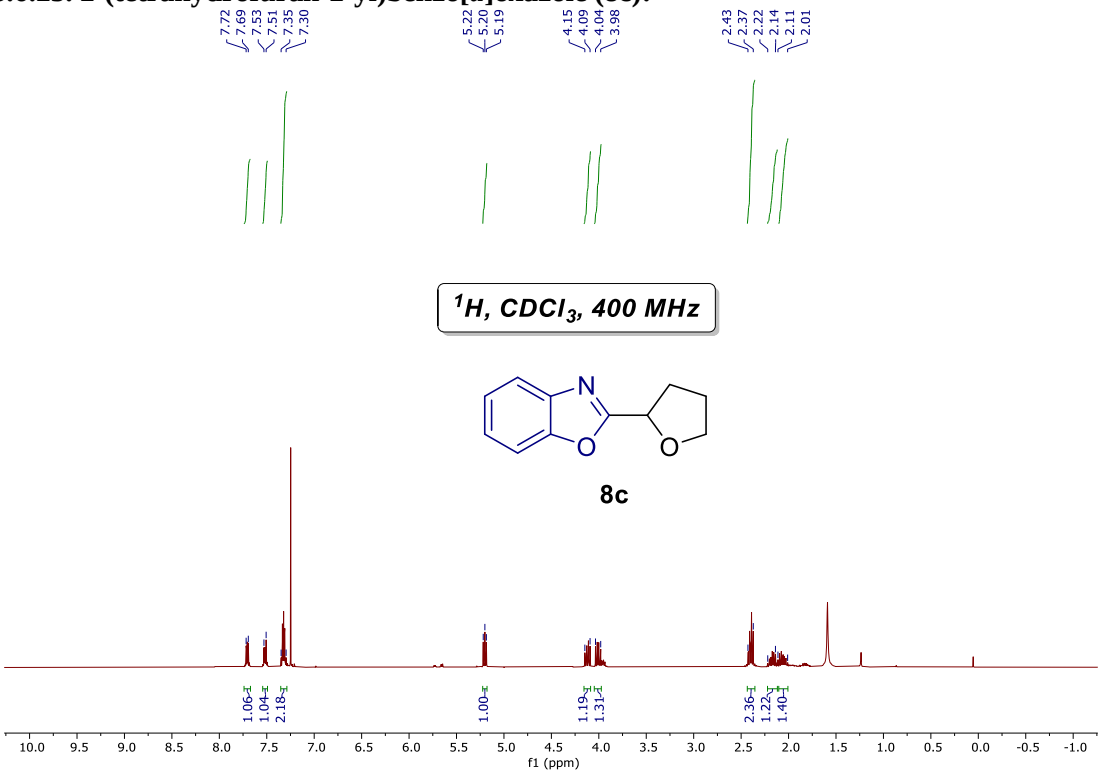


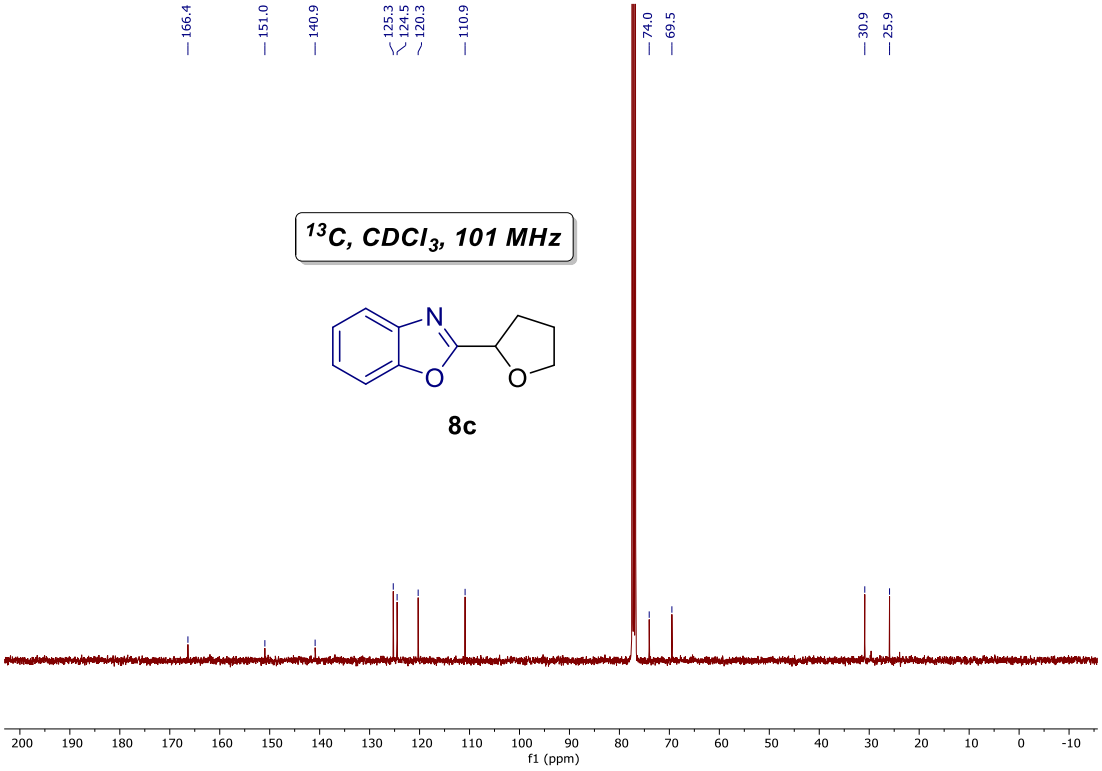
5.6.24. *tert*-butyl 2-(tetrahydrofuran-2-yl)-1*H*-benzo[*d*]imidazole-1-carboxylate (8b):



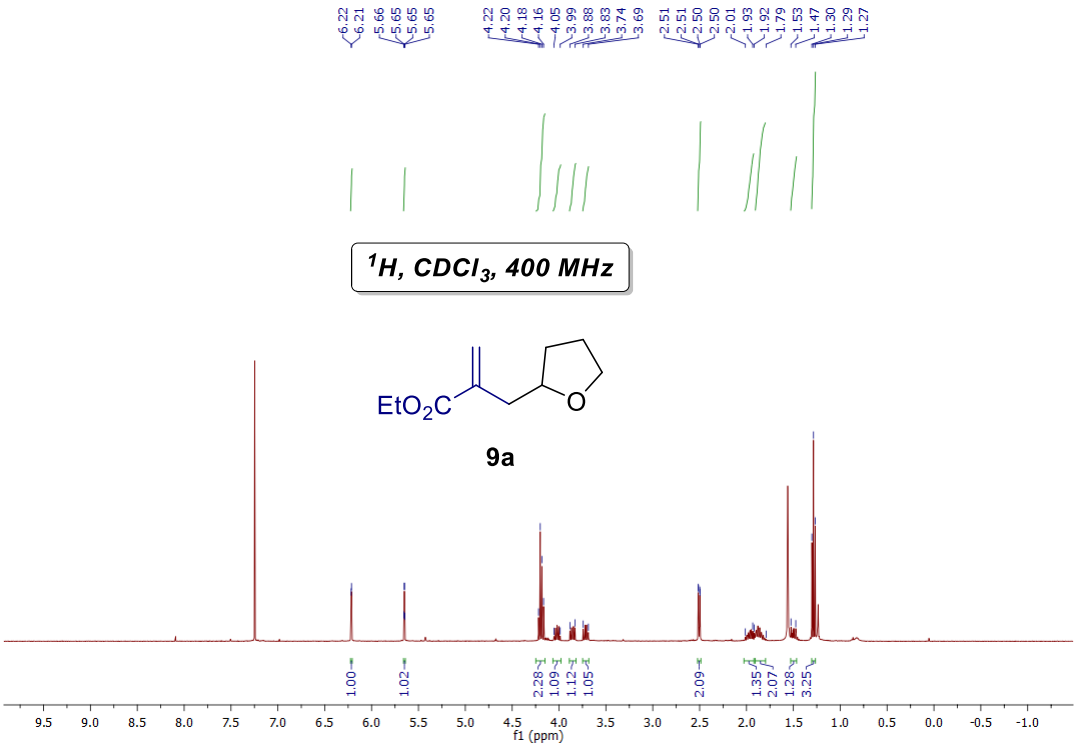


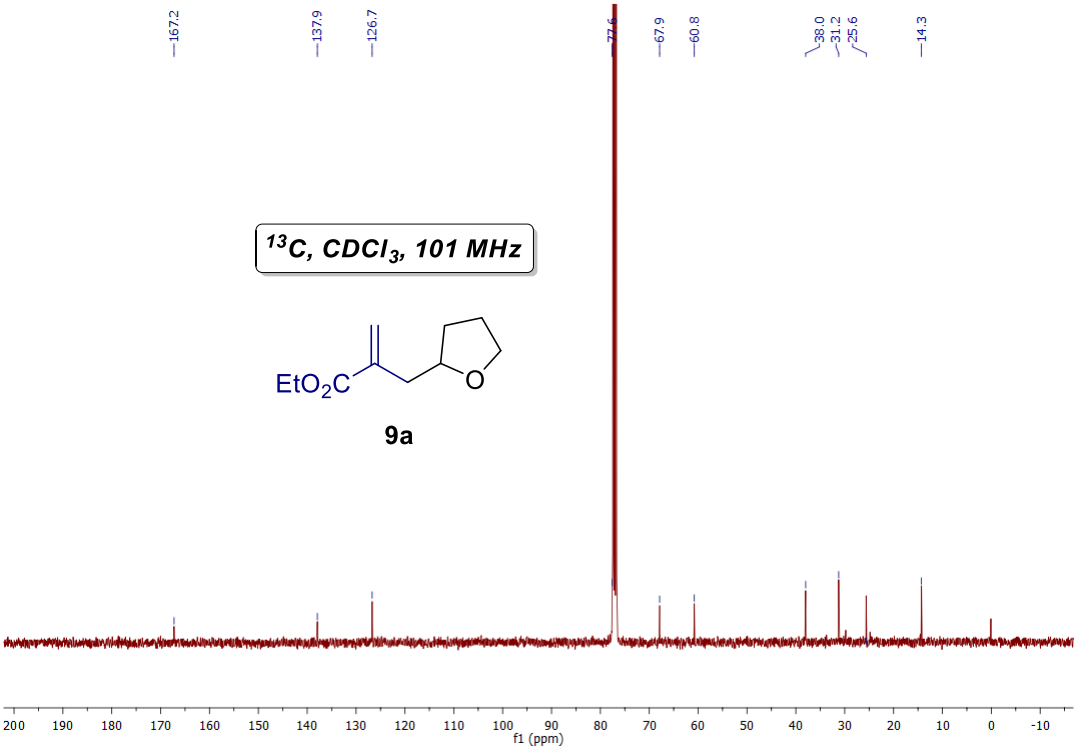
5.6.25. 2-(tetrahydrofuran-2-yl)benzo[*d*]oxazole (8c):



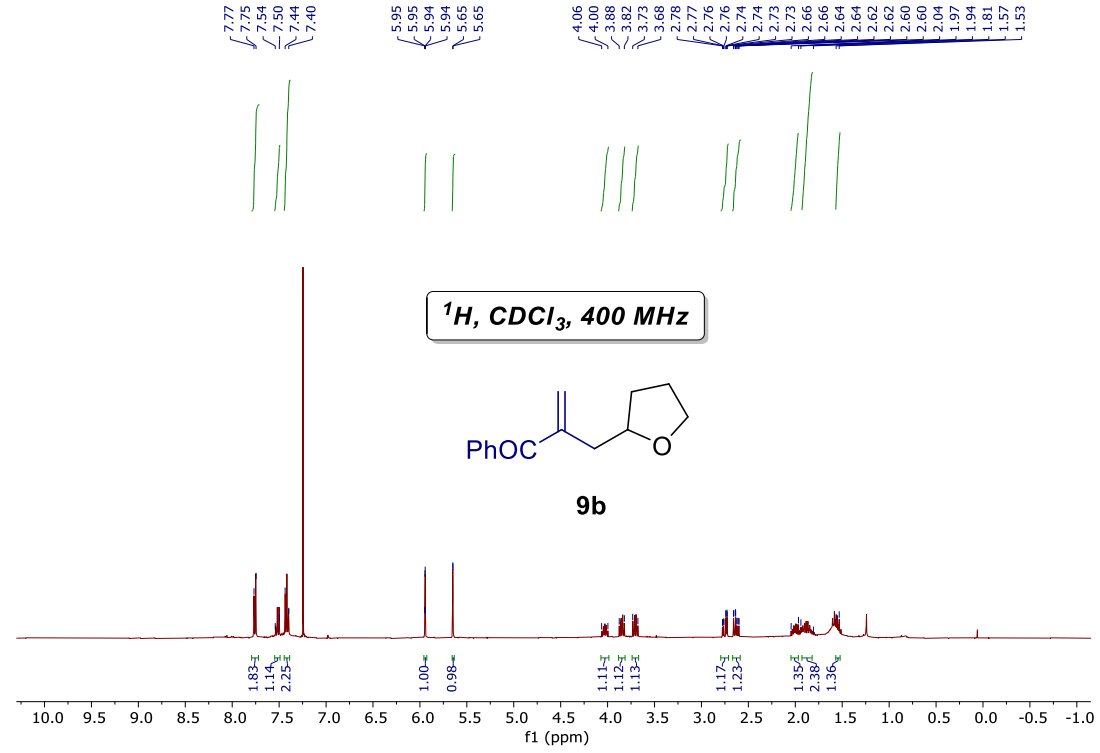


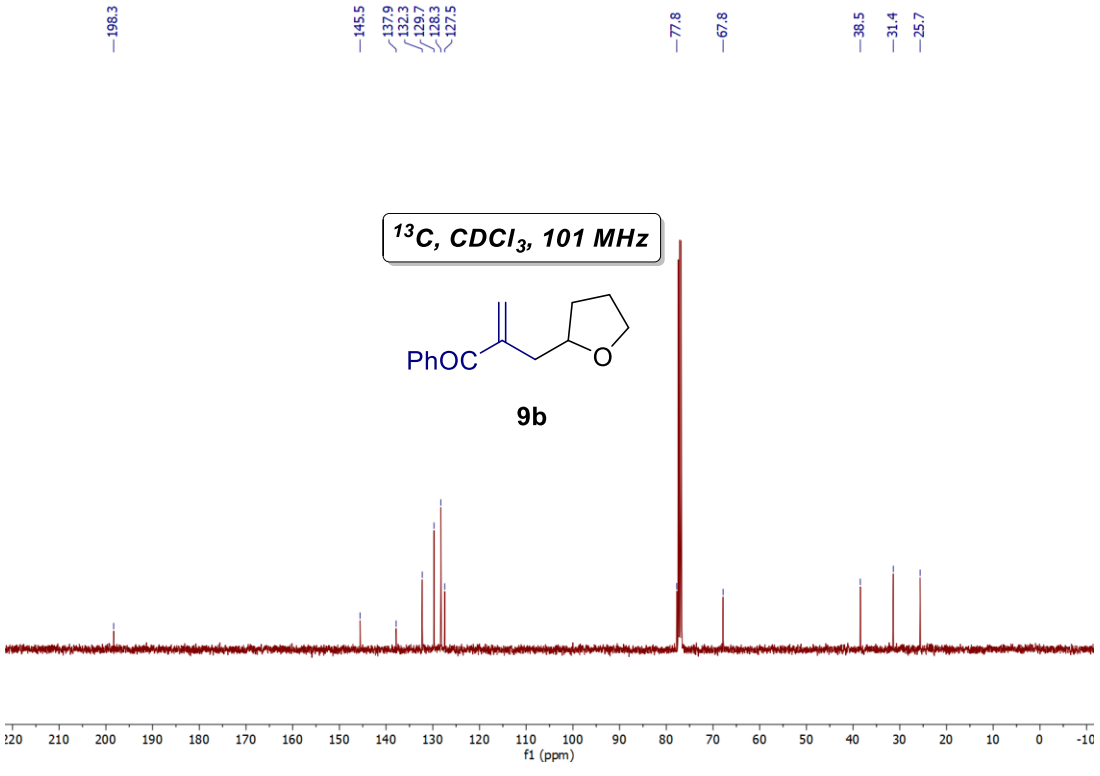
5.6.26. ethyl 2-((tetrahydrofuran-2-yl)methyl)acrylate (9a):



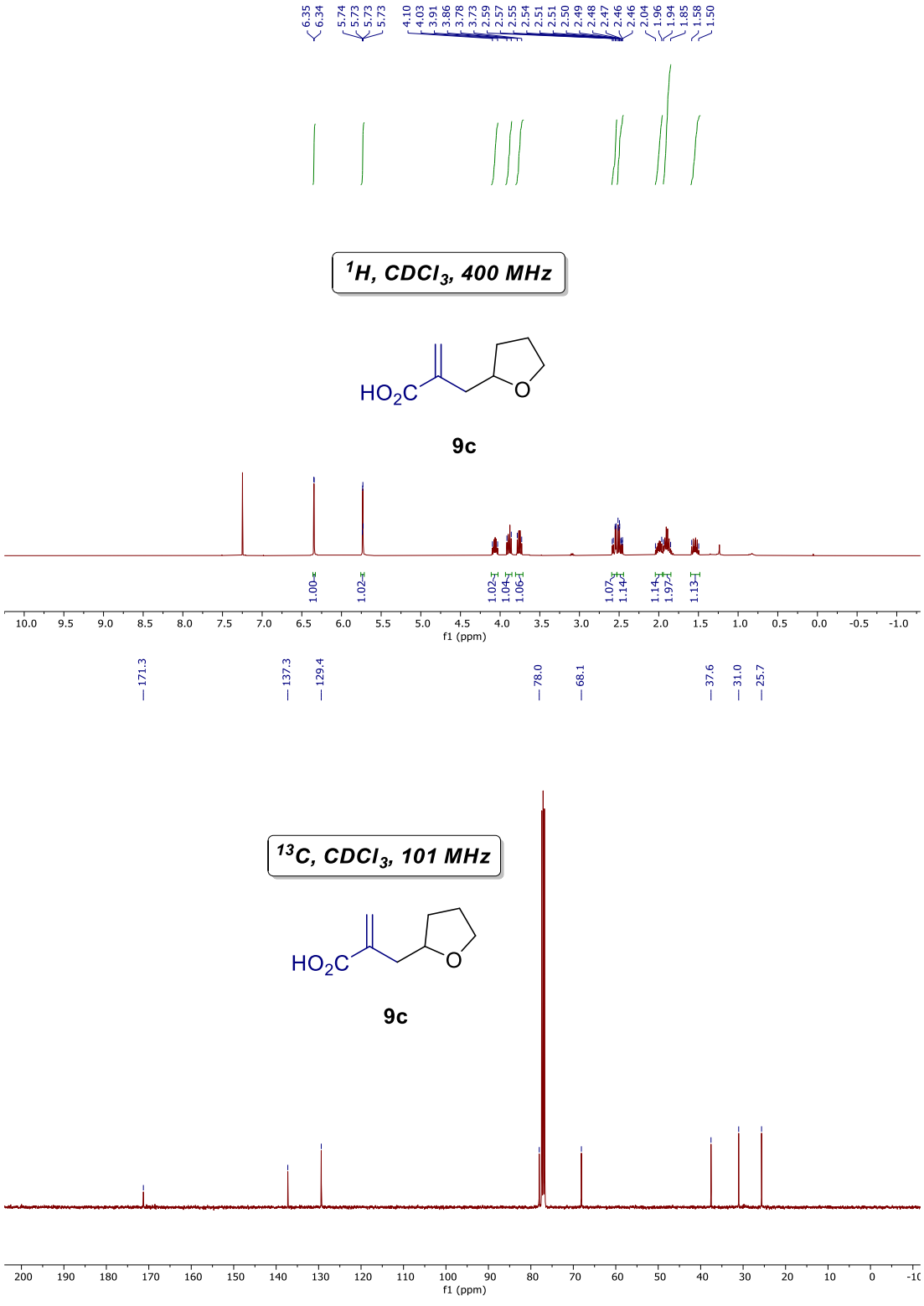


5.6.27. 1-phenyl-2-((tetrahydrofuran-2-yl)methyl)prop-2-en-1-one (9b):

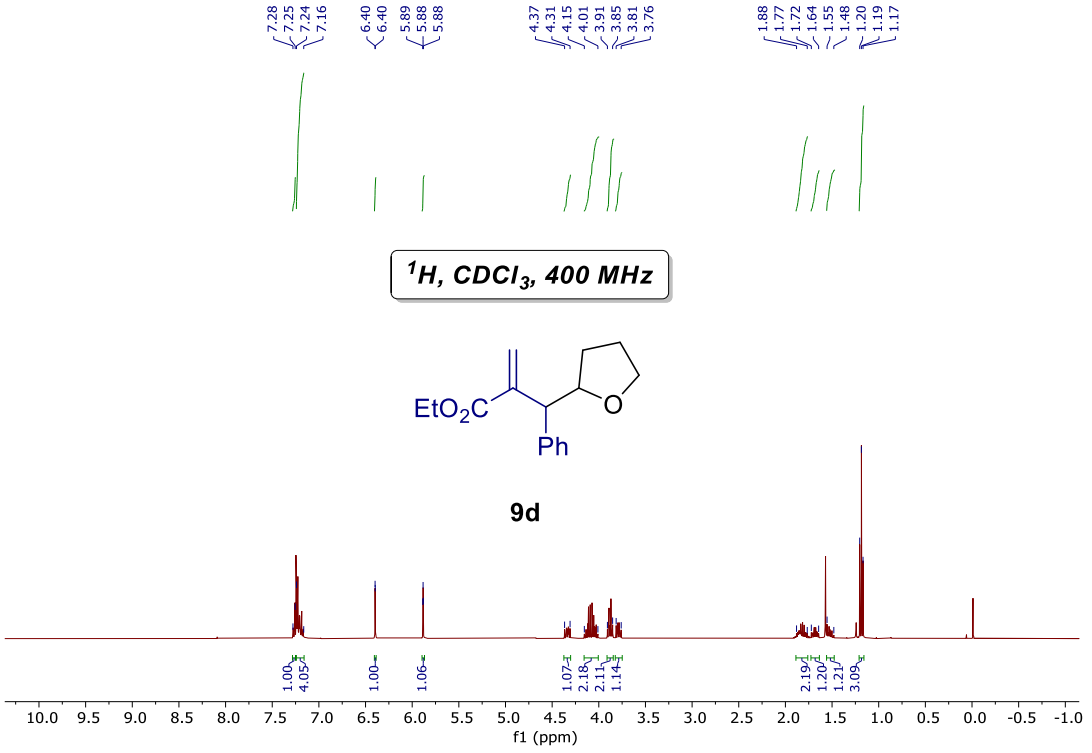


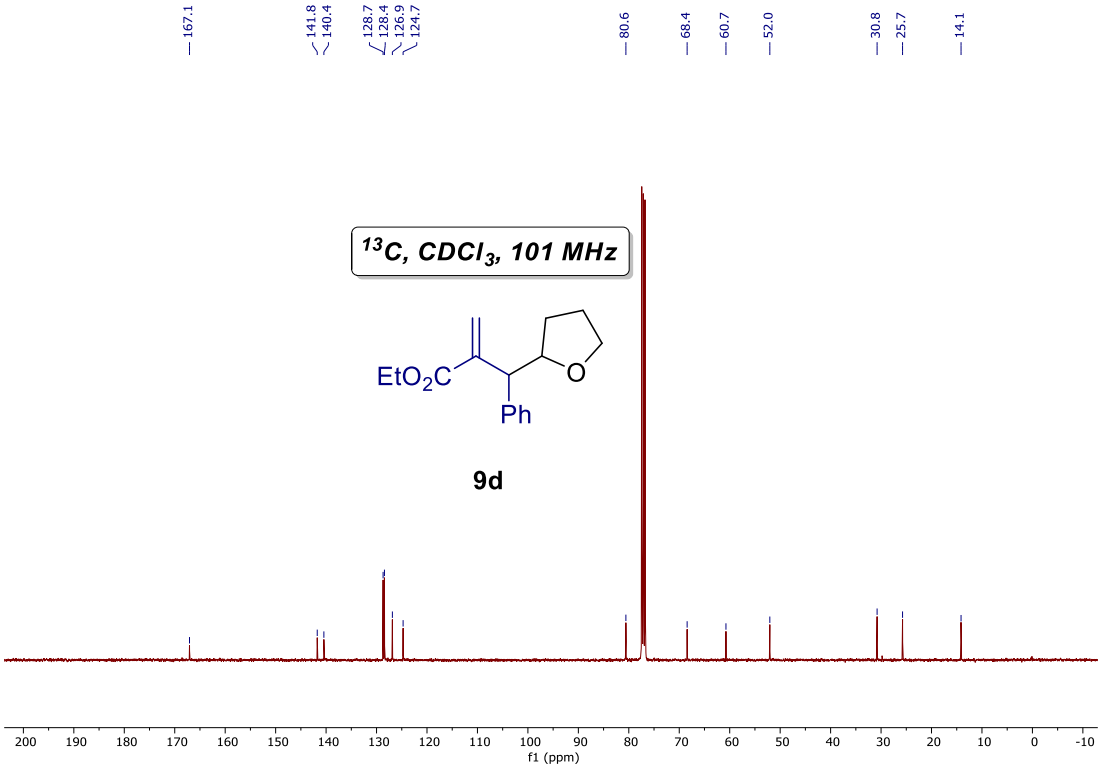


5.6.28. 2-((tetrahydrofuran-2-yl)methyl)acrylic acid (9c):



5.6.29. ethyl 2-(phenyl(tetrahydrofuran-2-yl)methyl)acrylate (9d):



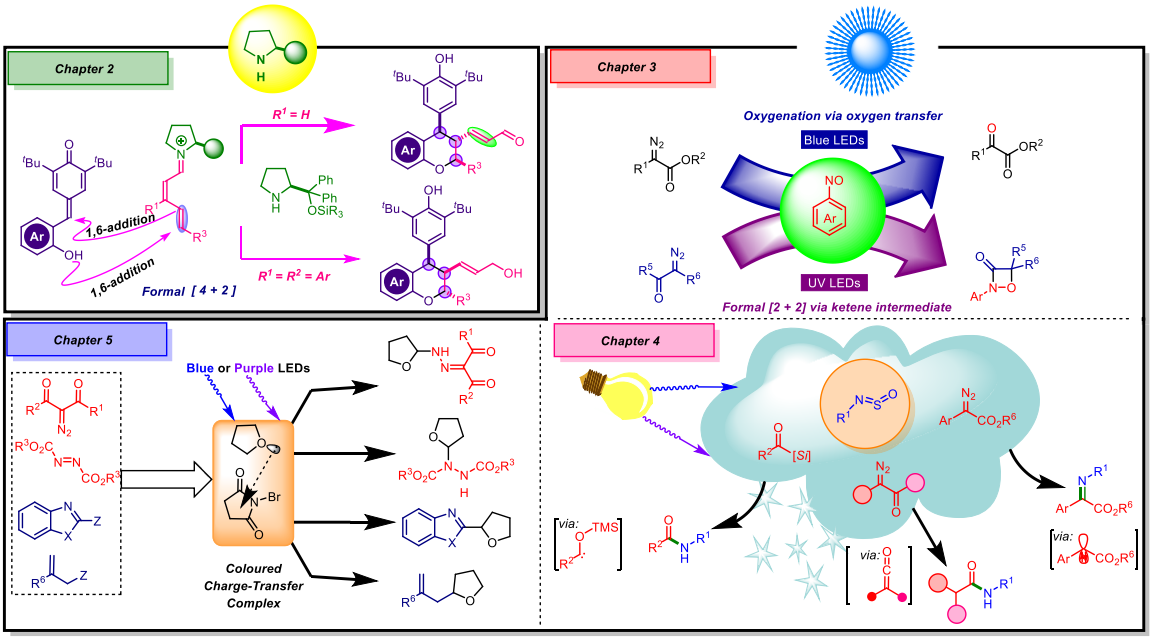


Chapter 6

Conclusion

6.1 Conclusion

The thesis title is "*Organocatalyzed and Photoinduced Synthetic Strategies in Diverse C−C and C−Heteroatom Bond Forming Events*". In this thesis, various distinct methodologies have been discovered in the quest for forging various C−C and C−Heteroatom bonds in a sustainable way by using organocatalysis and photoinduced synthetic techniques. Last three decades have witnessed organocatalysis as a powerful tool to efficiently construct various complex molecular architectures, often via chirality induction. On the other hand, to find a sustainable modern-day synthetic strategy, chemists have introduced visible light in the synthetic organic chemistry arena. Moreover, this chemistry has been well-established in academic laboratories and has engendered industries adopting this benign technology. Like organocatalysis, in recent times, scientists are utilizing visible-light-driven methodologies in crucial steps for the total synthesis of valuable natural products.



Scheme 46: Thesis Summary.

The thesis is majorly divided into five chapters, chapter 1 precisely introduces the area of organocatalysis and photocatalysis with the detailed discussion about the historical advancements, their classifications, basic working principle etc. with literature precedences.

In order to target a privileged scaffold chiral chromans, omnipresent in various natural products and biologically active molecules, we sketched chapter 2 by reacting unbiased *α,β,γ,δ*-unsaturated enals, and *ortho*-hydroxyphenyl-substituted *para*-quinone methides (*p*-QMs) to achieve chiral chromas was achieved with excellent selectivity (up to >20:1 d.r., >99% *ee*) and yield (up to 96%) via an organocatalytic cascade reaction in the presence of chiral secondary

amines. This reaction was initiated by an *oxa*-Michael reaction with exclusive *δ*-site selectivity to a vinylogous unbiased iminium-ion and concluded with a vinylogous dienamine-based 1,6-addition to the *p*-QMs. This work represents a unique example of asymmetric double 1,6-addition. The low reactivity of *δ*-aryl substituted unbiased 2,4-dienals was dramatically influenced using *β, δ*- aryl-substituted 2,4-dienals. Remaining *α, β*-unsaturated enal functionality offered to introduce molecular complexity to the chiral chroman derivatives.

Visible lights were introduced in chapter 3 to showcase a divergent role of photoexcited diazo compounds towards nitrosoarenes to furnish a wide range of α-ketoester and 1,2-oxazetidin-3-one derivatives under catalyst-free, transition-metal-free, and mild reaction conditions. The key to our success was guided by a light-induced formation of carbene intermediate and in situ-generated ketene intermediate. A versatile substrate scope was examined by varying both diazo and nitrosoarene components, which elegantly provided the desired product in moderate to good yield. The synthetic applicability of the developed method was also tested by performing a one-pot synthesis of α-ketoester and converting the cycloadduct into synthetically useful compounds with good yields.

Carbene chemistry was further investigated in chapter 4 to explore the benign reactivity of *N*-sulfinylamine chemistry with different kinds of carbene precursors to render versatile amide and α-iminoester derivatives through a visible-light-induced manifold. The reaction conditions are mild, operationally simple, and easy to set up. The proposed mechanism was supported by collective data, including UV-visible spectra, light on/off experiments, and other mechanistic studies. Further efforts for portraying the synthetic applicability of the developed protocol were carried out by the synthesizing drug molecule ethenzamide, late-stage functionalizations, and direct installation of unprotected amines and imines over diazo compounds by utilizing the sporadically explored reactivity of *N*-silylsulfinylamine.

The *N*-terminal electrophilic character of diazo compounds was disclosed in chapter 5 under visible light irradiation. This modular method rendered a series of amine, C(sp^2)–H, and C(sp^3)–H alkylating products with readily available ethers in absence of any transition-metal or external oxidant. The formation and identification of catalytic NBS-THF electron donor-acceptor (EDA) complex remained crucial, allowing selective (sp^3)Cα–H bond functionalization. A radical chain mechanism was proposed here based on the literature support and our experimental evidence. It is noteworthy that the developed methodology bypasses the major disadvantages like harsh reaction conditions and long reaction time associated with previous (sp^3)Cα–H bond functionalization strategies.

Overall, the research work presented in this thesis illustrates the employment of organocatalysis as an efficient gadget to achieve chiral chromans via a challenging double 1,6 addition. Likewise, a rapidly developing discipline like visible-light-induced transformations was brought into play to shed different undiscovered reactivities of diazo compounds as well as

carbene chemistry, rendering several value-added cyclic and acyclic structural motifs with novel mechanistic aspects. We believe that documented methods in this thesis will motivate the future generation to flourish in these blooming fields more by developing new methodologies for synthesizing several natural products, drug molecules, and the betterment of humankind.

Sourav Roy

Permanent Address: Ashannagar, Pin-741161, Nadia, West Bengal, India

Institute Address: Department of Chemistry, Indian Institute of Technology (IIT) Ropar, Rupnagar, Punjab-140001, India

Email: 2018cyz0013@iitrpr.ac.in and royravsou@gmail.com

Phone: +91-8906008916, +91-7031890856 **Date of Birth:** 14/04/1994

Gender: Male **Physically Disabled:** No

Languages: English (fluent), Hindi (fluent), Bengali (native)

🎓 Education / Qualifications:

Department of Chemistry, Indian Institute of Technology (IIT) Ropar, Punjab, India

Aug 2018 to March 2023 (Anticipated) (CGPA= 8.6): Doctor of Philosophy (PhD) in Synthetic Organic Chemistry with Specialization in organic synthesis, purifications and characterization techniques.

Bidhannagar Govt. College, West Bengal State University, West Bengal, India

Aug 2015 to May 2017 (71.0%): Master of Science (M.Sc.): in Chemistry

Mahadevananda Mahavidyalaya, West Bengal State University, West Bengal, India

July 2011 to Jun 2015 (64.5%): Bachelor of Science (B.Sc.): in Chemistry

🎓 Research Experience:

Department of Chemistry, Indian Institute of Technology (IIT) Ropar, Punjab, India

Aug 2018 to Present: PhD Research Fellow

Title of Thesis: Photodriven and Organocatalytic Diverse Transformations in Synthetic Organic Chemistry

Supervisor: Prof. Dr. Indranil Chatterjee, IIT Ropar, Punjab, India

Year Awarded: 2023 (Probable: March 2023)

- Development of asymmetric organocatalytic double 1,6 additions.
- Explored the unique property diazo compounds in presence of light.
- Exploitation of organocatalysis into photoredox chemistry to construct stereoselective C-C and C-X (X= heteroatom) bonds.

Department of Chemistry, Bidhannagar Govt. College, West Bengal State University, West Bengal, India

Mar 2016 to May 2016: M.Sc. Research Details

Title of Thesis: An Unprecedented Synthetic Route of Pyrrolo Pyrimidinium Ions (02-01-2017 to 10-04-2017)

Supervisor: Dr. Shuvankar Samanta

Year Awarded: 2017

- Worked on the synthesis and development of *N*-heterocyclic molecules.
- Characterized the synthesized molecules via NMR, Mass spectroscopy.

🎓 Teaching Experience:

P.N. DAS College, Palta, West Bengal, India

Aug 2017 to July 2018: Worked as a part time teacher in chemistry.

Department of Chemistry, Indian Institute of Technology (IIT) Ropar, India

Jan 2022 to April 2022: Trained one Master Student during her M.Sc. thesis work in research laboratory.

Jan 2020 to Mar 2020: Teaching Assistant for Undergraduate Students, Laboratory instructor.

Aug 2019 to Mar 2020: Trained one Master Student during his M.Sc. thesis work in research laboratory.

April 2019 to June 2019: Trained one Summer Intern Student during his internship in research laboratory.

🎓 Experimental & Technical Skills:

Synthetic Chemistry:

- Synthesis of organic molecules such as enals, various organocatalyst, *p*-QMs, nitrosoarenes, chromans, ketones, diazo compounds, oxazetidines, azomethane ylides, imines etc.
- Expertise in multistep synthesis as well as multicomponent reactions.
- Handling metal-catalysts, photocatalysts and organocatalysts.
- Running catalytic reactions.
- Having experience to run an industrial project.

Compound Characterization:

- Structural characterization of organic molecules by NMR, Mass Spectrometry (D-Mass & HRMS), SC-XRD.
- Spectroscopic analysis of organic molecules using CV, FTIR, UV-Vis, Fluorescence spectroscopy.

Hands-on Experience:

- Instruments: NMR, HRMS, SC-XRD, UV-Vis spectrometer, Fluorescence spectrometer, Glove Box, HPLC, CV.
- Computational Softwares: Microsoft Office, ChemDraw Ultra, PowerPoint, WinGx.

🎓 **Publications:**

- Pradhan. S.; **Roy, S.**; Ghosh, S.; Chatterjee, I. Regiodivergent Aromatic Electrophilic Substitution Using Nitrosoarenes in Hexafluoroisopropanol: A Gateway for Diarylamines and *p*-Iminoquinone Synthesis. *Adv. Synth. Catal*, **2019**, *361*, 4294-4301.

- **Roy, S.**; Pradhan. S.; Chatterjee, I. Asymmetric Organocatalytic Double 1,6-Addition: Rapid Access to Chiral Chromans with Molecular Complexity. *Org. Chem. Front.*, **2020**, *7*, 1388-1394.

- Pradhan. S.‡; **Roy, S.**‡; Sahoo, B.; Chatterjee, I. Utilization of CO_2 Feedstock for Organic Synthesis by Visible-Light Photoredox Catalysis. *Chem. Eur. J.* **2020**, *7*, 2254-2269. ‡ Equal contributors.

- Kumar, G., **Roy, S.**, Chatterjee. I. Tris(pentafluorophenyl)borane catalyzed C–C and C–heteroatom bond formation. *Org. Biomol. Chem*. **2021**, *19*, 1230-1267.

- **Roy, S**., Kumar, G., Chatterjee I. Photoinduced Diverse Reactivity of Diazo Compounds with Nitrosoarenes *Org. Lett.* **2021**, *23*, 6709–6713.

- **Roy, S.**, Chatterjee I. Visible-Light-Mediated (*sp3*)Cα–H Functionalization of Ethers Enabled by Electron Donor–Acceptor Complex *ACS Org. Inorg. Au* **2022**, *2*, 306–311.

- **Roy, S.** ‡, Paul, H. ‡, Chatterjee I., Light-Mediated Aminocatalysis: The Dual-Catalytic Ability Enabling New Enantioselective Route *Eur. J. Org. Chem*. **2022**, *25*, e202203428. ‡ Equal contributors.

- Ghosh, S.; Qu, Z.-W.; **Roy, S.**; Grimme, S.; Chatterjee, I. Photoredox Catalyzed Single C–F Bond Activation of Trifluoromethyl Ketones: A Solvent Controlled Divergent Access of gem-Difluoromethylene Containing Scaffolds. *Chem. Eur. J.* **2022**, *2022*, e202200446.

- **Roy, S.** ‡; Biswas, A. ‡; Paul, H.; Ariyan S.; Chatterjee I. Introducing N-Sulfinylamines into Visible-Light-Induced Carbene Chemistry for the Synthesis of Diverse Amides and α-Iminoesters. ‡ Equal contributors. *(Manuscript Submitted for Publication)*

- **Roy, S.**; Krishnapriya, A. U., Chakraborty, A.; Kuniyil, R.; Chatterjee, I. Exploiting *N*-Centered Umpolung Reactivity of α-Iminomalonates for the Synthesis of a New Class of *N*-Sulfenylimines and Sulfonamides. *(Manuscript Submitted for Publication).*

Conference Attended and Poster Presentation

- **Tetrahedron Symposium 2022:** Grand Altis Hotel, Lisbon, Portugal.

  Activity: Poster Presentation: Photoinduced Diverse Reactivity of Diazo Compounds with Nitrosoarenes.
- **ICRTGC-2021:** Akal University, India

  Activity: Poster Presentation: Photoinduced Diverse Reactivity of Diazo Compounds with Nitrosoarenes.
- **JNOST-2021:** IISc Bangalore, India

  Activity: Poster Presentation: Asymmetric Organocatalytic Double 1,6-Addition: Rapid Access to Chiral Chromans with Molecular Complexity.
- **ACS-SBQ 2021:** Organic Chemistry Division from the Brazilian Chemical Society.

  Activity: Attended

- **CRIKC-2019:** Department of Chemistry, Indian Institute of Science Education and Research (IISER) Mohali, India

  Activity: Attended

Summary

Highly motivated and aspired researcher with four years of laboratory research experience at IIT Ropar, India. Research Expertise includes organic synthesis, catalytic reactions, photoredox reactions, handling fine chemicals. Highly skilled in organic research and solid understanding in analytical as well as compound characterization techniques. Have a leadership quality and also accustomed to work within multidisciplinary groups. Demonstrated strong verbal/communication and interpersonal skills.